Springer Series in Synergetics

Springer : COMPLEXITY

Sergey G. Abaimov

Statistical Physics of Non-Thermal Phase Transitions

From Foundations to Applications

Springer

Springer Complexity

Springer Complexity is an interdisciplinary program publishing the best research and academic-level teaching on both fundamental and applied aspects of complex systems–cutting across all traditional disciplines of the natural and life sciences, engineering, economics, medicine, neuroscience, social and computer science.

Complex Systems are systems that comprise many interacting parts with the ability to generate a new quality of macroscopic collective behavior the manifestations of which are the spontaneous formation of distinctive temporal, spatial or functional structures. Models of such systems can be successfully mapped onto quite diverse "real-life" situations like the climate, the coherent emission of light from lasers, chemical reaction-diffusion systems, biological cellular networks, the dynamics of stock markets and of the internet, earthquake statistics and prediction, freeway traffic, the human brain, or the formation of opinions in social systems, to name just some of the popular applications.

Although their scope and methodologies overlap somewhat, one can distinguish the following main concepts and tools: self-organization, nonlinear dynamics, synergetics, turbulence, dynamical systems, catastrophes, instabilities, stochastic processes, chaos, graphs and networks, cellular automata, adaptive systems, genetic algorithms and computational intelligence.

The three major book publication platforms of the Springer Complexity program are the monograph series "Understanding Complex Systems" focusing on the various applications of complexity, the "Springer Series in Synergetics," which is devoted to the quantitative theoretical and methodological foundations, and the "SpringerBriefs in Complexity" which are concise and topical working reports, case-studies, surveys, essays and lecture notes of relevance to the field. In addition to the books in these two core series, the program also incorporates individual titles ranging from textbooks to major reference works.

Springer Series in Synergetics

Founding Editor: H. Haken

The Springer Series in Synergetics was founded by Herman Haken in 1977. Since then, the series has evolved into a substantial reference library for the quantitative, theoretical and methodological foundations of the science of complex systems.

Through many enduring classic texts, such as Haken's *Synergetics and Information and Self-Organization*, Gardiner's *Handbook of Stochastic Methods*, Risken's *The Fokker Planck-Equation* or Haake's *Quantum Signatures of Chaos*, the series has made, and continues to make, important contributions to shaping the foundations of the field.

The series publishes monographs and graduate-level textbooks of broad and general interest, with a pronounced emphasis on the physico-mathematical approach.

For further volumes:
http://www.springer.com/series/712

Sergey G. Abaimov

Statistical Physics of Non-Thermal Phase Transitions

From Foundations to Applications

Springer

Sergey G. Abaimov
Advanced Structures, Processes
and Engineered Materials Center
Skolkovo Institute of Science
and Technology
Skolkovo
Russia

ISSN 0172-7389
Springer Series in Synergetics
ISBN 978-3-319-12468-1 ISBN 978-3-319-12469-8 (eBook)
DOI 10.1007/978-3-319-12469-8

Library of Congress Control Number: 2014953779

Springer Cham Heidelberg New York Dordrecht London

Printed on acid-free paper

Springer is part of Springer Science+Business Media (www.springer.com)

“To those summer sunny days,
When world was warm and still,
And unicorn’s four gleamy eyes
Were made of glass and steel,
The running man was hunt in maze
To make a Minotaur’s meal,
But slow, emerald-green waves
Demanded: “Drive the quill!”
A hurt white-crow made mistakes
Against its kind and will,
And near train depot earthquakes
Became a part of cozy home deal.
A life was crazy like a waste
Collecting future regrets’ bill.”

Preface

Statistical physics describes a wide variety of phenomena and systems when interaction forces may have different natures: mechanical, electromagnetic, strong nuclear, etc. The commonality that unites all these systems is that their belonging to statistical physics requires the presence of thermal fluctuations. In this sense these phenomena necessarily include the thermodynamic aspect.

Meanwhile, the second half of the last century may be named the time of the discovery of the so-called complex systems. These systems belong to chemistry, biology, ecology, geology, economics, social sciences, etc. and are generally united by the absence of concepts such as temperature or energy. Instead, their behavior is governed by stochastic laws of nonthermodynamic nature; and these systems can be called nonthermal. Nevertheless, in spite of this principal difference with statistical physics, it was discovered that the behavior of complex systems resembles the behavior of thermodynamic systems. In particular, many of these systems possess a phase transition identical to critical or spinodal phenomenon of statistical physics.

This very analogy has led in recent years to many attempts to generalize the formalism of statistical physics so that it would become applicable and for nonthermal systems also. If we achieved this goal, the powerful, well-developed machinery of statistical physics would help us to explain phenomena such as petroleum clusters, polymerization, DNA mechanism, informational processes, traffic jams, cellular automata, etc. Or, better, we might be able to predict and prevent catastrophes such as earthquakes, snow-avalanches and landslides, failure of engineering structures, economical crises, etc.

However, the formalism of statistical physics is developed for thermodynamic systems; and its direct application to nonthermal phenomena is not possible. Instead, we first have to build analogies between thermal and nonthermal phenomena.

But, what do these analogies include? What are they based on? And even more important question: Why does the behavior of complex systems resemble their thermodynamic analogues?

The answer to the last question is that the analogy exists only in the presence of phase transitions. It is the machinery of a phase transition that is universal, not the systems themselves. In spite of the fact that the behavior of complex systems is governed by nonthermal fluctuations whose nature is quite different from thermal

fluctuations in statistical physics, these fluctuations are, nevertheless, stochastic and scale invariant; and it is the stochastic scale invariance of the system that leads to the universality of phase transitions. Therefore, our attempt to apply the formalism of statistical physics to nonthermal phenomena would be successful only if we mapped the nonthermal fluctuations on their thermal analogues.

This book is devoted to the comparison of thermal and nonthermal systems. As an example of a thermodynamic system we generally discuss an Ising model while the considered nonthermal systems are represented by percolation and damage phenomena. Step-by-step, from the equation of state to the free energy potential, from correlations to the susceptibility, from the mean-field approach to the renormalization group, we compare these systems and find that not only are the rules of behavior similar but also, what is even more important, the methods of solution. We will see that, developing the concept of susceptibility or building the renormalization group, although each time we begin with a particular system considered, the foundation of an approach is always based on the formalism of statistical physics and is, therefore, system independent.

To the purpose of comparison we often sacrifice in this book the specific details of the behavior of particular systems discussed. We cannot claim our study to be complete in the description of rigorous formalism or experimental results of ferromagnetic, percolation, or damage phenomena. Instead, we focus our attention on the intuitive understanding of the basic laws leading to the analogies among these systems. For the same reason and also because we consider our text to be introductory, we cannot claim our list of references to represent all corner-stone studies related to the discussed phenomena. Instead, we are generally referring the reader to the brilliant reviews and references therein.[1]

Also, we should mention that, although in many aspects this book may represent the biased view of its author, we hope that the reader will enjoy, as we do, the mystery of the birth of a new science that has been happening right before our eyes during the last few decades. Since this new science, in our humble opinion, is still at the infantile stage, there are many questions in the book which we cannot answer. However, from our point of view this adds an additional charm to the discussion because it encourages the reader to generate and apply her/his own ideas at the frontiers of science.

Another important aspect of the book is that the comparison with nonthermal systems presents the alternative point of view on thermodynamic phenomena themselves. Not all concepts of statistical physics have their counterparts in complex systems. Thereby, nonthermal phenomena often allow looking at well-known phenomena from quite a different angle to emphasize the omissions in statistical physics itself.

---

[1] The author would appreciate very much to hear about all possible omissions or mistakes by e-mail sgabaimov@gmail.com to the purpose of future corrections. “Needless to say the computer, as a text editing system, should be blamed for all the errors in the book.” (Dietrich Stauffer, in Stauffer, D., Aharony, A.: Introduction to Percolation Theory, 2nd ed. Taylor & Francis, London (1994), rephrased).

This book is based on the course of lectures taught by the author for 5 years at the Department of Theoretical Physics of Moscow Institute of Physics and Technology. The first two chapters represent prerequisites. Statistical physics is often considered to be at the top of theoretical disciplines of a student's curriculum and requires the knowledge of previously studied theoretical mechanics and quantum mechanics. This often prohibits the reader not acquainted with these disciplines to study the applicability of statistical physics to complex phenomena.

However, several years of lecturing statistical physics convinced the author that what is truly required to understand the formalism of phase transitions is the discussion of a limited set of concepts. Chapter 2 presents an attempt to reduce the theoretical formalism of statistical physics to a minimum required to understand further chapters. Therefore, as a prerequisite for this monograph we consider only general physics but not theoretical, quantum, or statistical mechanics. It is our belief that Chap. 2 will be sufficient for the reader, not acquainted earlier with theoretical physics, to understand the following chapters.

The completion of this book has left me indebted to many. I am most grateful to Dr. Yury Belousov, Head of the Department of Theoretical Physics at Moscow Institute of Physics and Technology, for his invaluable support and help in the creation of the monograph and course; and also to my colleagues at the Department of Theoretical Physics for fruitful discussions, especially to Dr. Ilya Polishchuk and Dr. Andrey Mikheyenkov. I am most grateful to Dr. Zafer Gürdal, Director of Advanced Structures, Processes and Engineered Materials Center, Skolkovo Institute of Science and Technology, for his support of the monograph and of the course that I am lecturing at ASPEM. I would like to express my warmest gratitude to Dr. Joseph Cusumano, Department of Engineering Science and Mechanics, Penn State University, for his invaluable support and collaboration in the research of damage phenomena. I am also thankful to Dr. Christopher Coughlin, Springer, for his inestimable support and help in the publication of the monograph.

Sergey Abaimov

Department of Theoretical Physics, Moscow Institute of Physics and Technology

Currently at: Advanced Structures, Processes and Engineered Materials Center, Skolkovo Institute of Science and Technology

Moscow, 2014

Contents

Chapter 1
Fractals

Abstract The power-law dependences in the vicinity of a critical point could often be attributed to the self-similarity and fractal nature of clusters. Therefore, in this chapter, we discuss the basic formalism of fractals. We consider this chapter to be a prerequisite of fractals. Required for further discussions, we consider understanding of both the concept of fractal dimensionality and the origin of fractal power-law dependences. The reader, proficient in these concepts, can skip this chapter.

Since we consider this chapter to be a prerequisite, we only briefly discuss ideas behind the formalism of fractals, providing basic, intuitive understanding. For further study, we refer the reader to brilliant textbooks (Feder 1988; Vicsek 1992; Falconer 2003) and references therein.

Besides the fractals, we also discuss multifractals. Although multifractals with complex geometric support will not be applied directly in the further chapters, we encourage the reader to study their formalism in view of its similarities with the concepts of statistical physics.

1.1 The Concepts of Scale Invariance and Self-Similarity

Although the rapid development and application of the fractal formalism happened in the second half of the twentieth century, the mathematical sets, named later fractals, had been known long before that. So, *the Koch snowflake* (*the Koch star*, *the Koch island*) was created by Helge von Koch in 1904 (von Koch 1904) and another set—*the Sierpinski carpet*—by Wacław Sierpiński in 1916 (Sierpiński 1916). And the well-known, classical Cantor set was discovered by Henry J.S. Smith as early as in 1874 (Smith 1874) and introduced by Georg Cantor in 1883 (Cantor 1883).

However, mathematicians of the beginning of the last century often considered these sets only as "amusing toys" (called them "monsters"); and nobody expected that in several decades the fractals would become widely applicable not only in mathematics but even more so in physics, chemistry, biology, and other sciences.

S. G. Abaimov, *Statistical Physics of Non-Thermal Phase Transitions,*
Springer Series in Synergetics, DOI 10.1007/978-3-319-12469-8_1

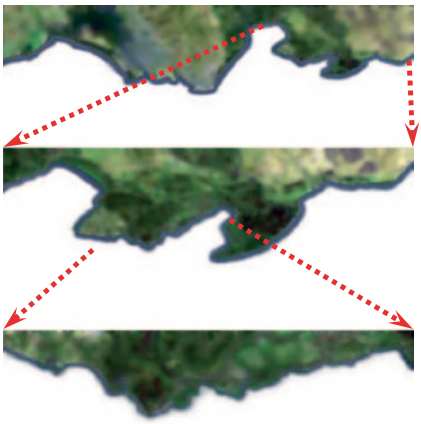

Fig. 1.1 Self-similar structure of the San Francisco Bay coastline.

Fractals began to be "actual" fractals only after Benoit Mandelbrot had published his book (Mandelbrot 1975, 1982). It was one of those occasions when one publication leads to the appearance of a new science. Therefore, in spite of the fact that similar mathematical sets had had a long history in mathematics before, Benoit Mandelbrot is sometimes called "the farther of fractals."

Following Mandelbrot's book, we begin our discussion by considering a map of a shoreline. But in contrast to previous books which have considered the coastlines of Great Britain or Norway, we consider the coastline of San Francisco Bay. Choosing some part of the curve and increasing the scale of the map, we obtain the curve stochastically similar to the initial (Fig. 1.1). A new choice and new scale increase provide again the similar curve, and so on.

The property when a part (*a branch*) of a mathematical set is similar to the whole set is called *scale invariance*. For example, at geological departments of universities students are taught that, photographing a geological object, one should put something beside to demonstrate the scale. Something like a pen, a water bottle, or a hammer (a cigarette pack, which was traditionally on the list, has been excluded by the author). Beside big boulders, a geologist herself/himself could also stay. All this is necessary to distinguish the scale later, on the photograph. Otherwise, it would not be clear what was shot: a mountain or a small piece of rock which one could put in her/his pocket.

If we measure length of a usual curve, the length does not depend on what scale we have used: 1 m scale or 10 cm scale. But the situation would change drastically if we considered not a classical geometrical set but a self-similar set. Let us look at Fig. 1.2.

Initially, we measure our curve by applying etalons with the length ε. There are two such etalons. Therefore, we expect that when we decrease the etalon length thrice, six etalons should be enough to measure the length of the curve. But in reality, it is almost seven etalons. Again, decreasing the length of the etalon

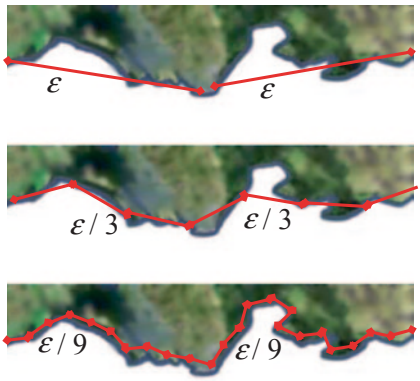

Fig. 1.2 The coastline length measured by etalons of different sizes.

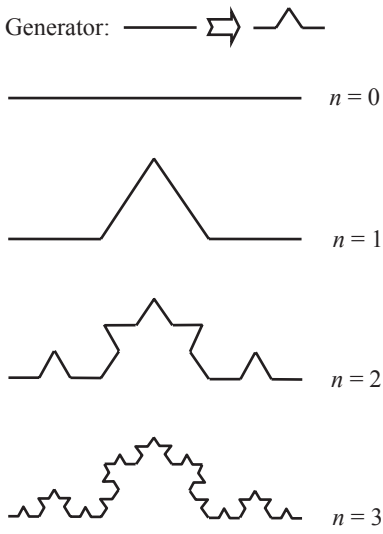

Fig. 1.3 The triadic Koch curve

thrice, we expect the curve length to be less than $3 \cdot 7 = 21$ etalons. In reality, it is 23 etalons.

Why has this happened? Because smaller etalons distinguish smaller map details. As a result, larger etalons go across all coastline meanders while smaller etalons wind, making detours along them. The smaller the etalons, the larger the curve length we obtain in the result of measurements. For infinitesimal etalons $\varepsilon \to +0$, the length of the coastal line would diverge, $L \to +\infty$.

The San Francisco Bay coastline was an example of the stochastic fractal when we could not exactly predict finer details of the increased scale but could foresee them only stochastically. But it is easy to build a deterministic analogue of the coastal line fractal. Let us consider the triadic Koch curve (von Koch 1904) in Fig. 1.3.

As well as for any other fractal, to build the triadic Koch curve we should first construct its initiator and its generator. In case of Fig. 1.3, the line segment of length L_0 will serve as the initiator (iteration $n = 0$). The generator transforms the initiator of iteration $n = 0$ into the structure of iteration $n = 1$. To do that it takes the line segment (*a parent branch*) of length L_0 and breaks it into three thirds $L_0 / 3$ (*daughter branches*). Then the generator replaces the central daughter branch with two other daughter branches at angles 60°. In other words, the parent branch generates $K = 4$ daughter branches, each of which is similar to the parent branch with scale factor $r = 1/3$.

This is how the generator transforms iteration $n = 0$ into iteration $n = 1$. To transform iteration $n = 1$ into iteration $n = 2$, iteration $n = 2$ into iteration $n = 3$, and so on, the generator is applied to each branch of *the parent iteration* to provide branches of *the daughter iteration*. So, in Fig. 1.3 each of the four branches of iteration $n = 1$ is replaced by four branches (in total, 16 daughter branches) of iteration $n = 2$.

Applying the generator n times, we obtain iteration n. We see that infinite iteration $n \to +\infty$ forms a scale-invariant mathematical set. Indeed, in this case each branch is similar to the set in whole, only it is scaled with the scale factor $r = 1/3$. The scale invariance in the case of deterministic (not stochastic) generators is called *self-similarity*. The self-similar iteration $n \to +\infty$ is called *a fractal*.

Strictly speaking, the term "*fractal*" is referred only to the infinite iteration $n \to +\infty$. However, it has become a common practice to refer to finite iteration n as to *iteration n of the fractal*. Sometimes (which is already not correct at all) iteration n is called a fractal. To avoid this confusion, we will call a finite iteration n of a fractal as *a prefractal* while the infinite iteration $n \to +\infty$ we will call *the developed fractal*.

1.2 Measure Versus Dimensionality

What is the measure of the developed triadic Koch curve? To find its length, we again should find the number of etalons covering it.

We are living in the three-dimensional embedding space, $d_0 = 3$, and in the rest of the chapter will measure not only curves but also surfaces, volumes, and more complex sets. Henceforth for etalons, we will not utilize line segments but three-dimensional cubes (boxes) of side ε and volume ε^3. In other words, for etalons we utilize the elements of volume of the embedding space.

To measure, for example, the length of a curve, we should cover this curve by etalons and count the number N of the required etalons (Fig.1.4). This method is called *box counting*. Multiplying the number N of the etalons by the etalon linear size ε, we find the length of the curve: $L = N\varepsilon$.

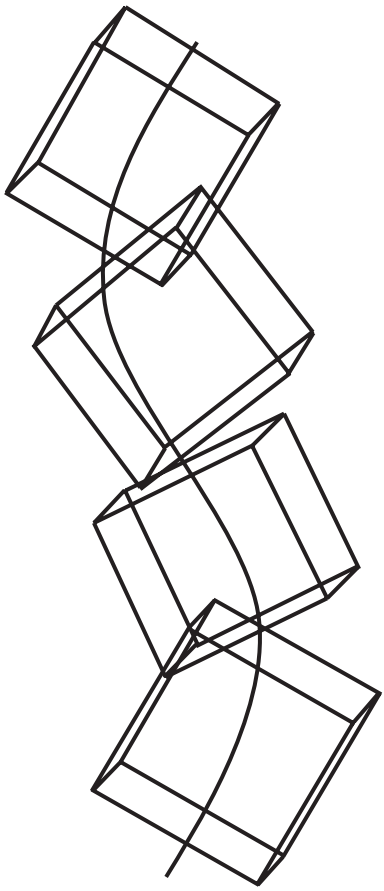

Fig. 1.4 Box counting method

To find the length of the developed triadic Koch curve, we also cover it by etalons. In this case, it is convenient to choose the size of the etalon ε to be equal to the size of the branches of iteration n: $\varepsilon = L_0 r^n$. And we immediately discover that the number of boxes, covering the developed fractal, coincides with the number of boxes covering iteration n. For example, in Fig. 1.5 we have chosen $\varepsilon = L_0 r^1$, and four boxes happen to cover both iteration $n = 1$ and all further iterations.

This property, where the number of boxes covering a particular iteration coincides with the number of boxes covering the whole fractal, is valid only for the simplest formulation of fractal we currently consider. Unfortunately, as we will see later, it is no longer valid for more complex cases, requiring more complex approaches to be developed.

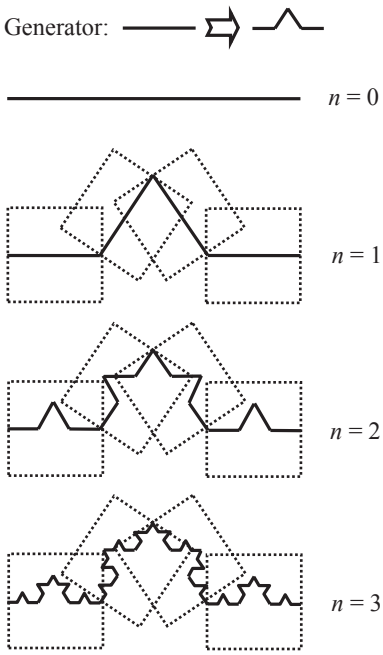

Fig. 1.5 The box counting for the triadic Koch curve

But now, considering the simplest fractal, we see that the number of boxes of size $\varepsilon = L_0 r^n$, covering the developed fractal, coincides with the number of branches of iteration n: $N(\varepsilon) = K^n$. So, the measured length of the curve is $L(\varepsilon) = K^n L_0 r^n = L_0 (4/3)^n$ which clearly depends on the choice of etalon linear size $\varepsilon = L_0 r^n$ (on the choice of iteration n). In the limit $\varepsilon \to +0$ ($n \to +\infty$) the length diverges: $L \to +\infty$.

Why a particular choice of the etalon size changes the results of the measurements? The error in our considerations is not the measure, the error is the dimensionality.

How the dimensionality is defined in mathematics? There are many different approaches: the box counting dimension (Kolmogorov 1958), the Cantor–Minkowski–Bouligand dimension (upper and lower) (Bouligand 1928), and the Hausdorff–Besicovitch dimension (Hausdorff 1918; Besicovitch 1929; Besicovitch and Ursell 1937). To avoid mathematical difficulties, we consider only the simplest examples of fractals when all these dimensions are equal.

The Hausdorff–Besicovitch measure (Hausdorff 1918; Besicovitch 1929; Besicovitch and Ursell 1937) is the limit

$$M_d = \lim_{\varepsilon \to +0} N(\varepsilon) \varepsilon^d, \tag{1.1}$$

where $N(\varepsilon)$ is the number of three-dimensional boxes covering the mathematical set and $d \geq 0$ is some positive (or zero) real number.

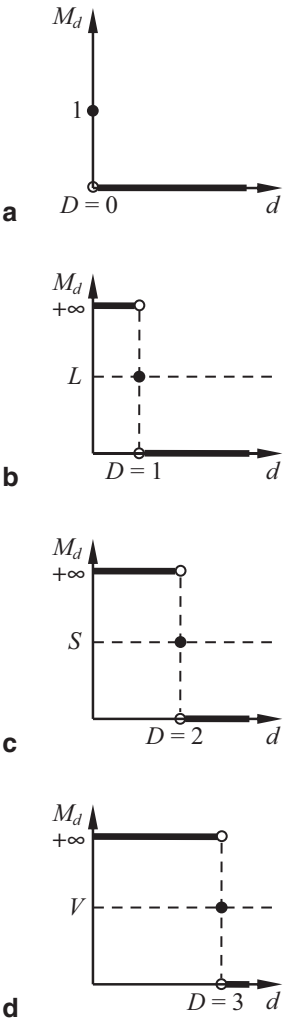

Fig. 1.6 The Hausdorff–Besicovitch measure: **a** For the point, the measure is zero for $d > 0$. **b** For the curve, the measure is infinite for $d < 1$ and zero for $d > 1$. **c** For the surface, the measure is infinite for $d < 2$ and zero for $d > 2$. **d** For the volume, the measure is infinite for $d < 3$ and zero for $d > 3$

Let us apply definition (1.1) to the simplest geometrical sets: a point, a curve, a surface, and a volume. If the mathematical set is a point, only one box covers it. Therefore, the measure is $M_d = \lim\limits_{\varepsilon \to +0} \varepsilon^d = \begin{cases} 1, d = 0 \\ 0, d > 0 \end{cases}$ as it is presented in Fig. 1.6a.

The number of boxes, covering a curve, is obviously (Fig. 1.4) the length of the curve L divided by the size of a box: $N(\varepsilon) = L / \varepsilon$. For the measure this provides

$$M_d = L \lim_{\varepsilon \to +0} \varepsilon^{d-1} = \begin{cases} +\infty, d < 1 \\ L, d = 1 \\ 0, d > 1 \end{cases}.$$

In Fig. 1.6b, we schematically plot infinite value as the top of the axis.

In the case of a surface, the number of covering it boxes is $N(\varepsilon) = S/\varepsilon^2$, where S is the area of this surface. The behavior of the measure $M_d = S \lim\limits_{\varepsilon \to +0} \varepsilon^{d-2} = \begin{cases} +\infty, d < 2 \\ S, d = 2 \\ 0, d > 2 \end{cases}$ is plotted in Fig. 1.6c.

The volume V can be covered by $N(\varepsilon) = V/\varepsilon^3$ boxes. The corresponding measure $M_d = V \lim\limits_{\varepsilon \to +0} \varepsilon^{d-3} = \begin{cases} +\infty, d < 3 \\ V, d = 3 \\ 0, d > 3 \end{cases}$ is presented in Fig. 1.6d.

We see now the common tendencies in the behavior of measure (1.1) for all mathematical sets considered above. With d (where d is just a parameter) increasing from zero to infinity, the measure is always singular (zero or infinity) with the exception of just one point where it is finite. We see that the value of d at this point corresponds to the dimensionality in the sense of common practice. Therefore, we have denoted this value by letter D, representing the actual dimensionality of the mathematical set. The measure $M_{d=D}$ at this point is finite and represents the common sense measure (length of the curve, area of the surface, the value of the volume).

For an arbitrary mathematical set, we define its *dimension* D as the value of d when the Hausdorff–Besicovitch measure is finite (when it passes from infinity to zero). The value $M_{d=D}$ of the measure at this point we define as *the measure of the set*.

But what does it mean that at D the measure M_D is finite (of the order of unity, $M_D \propto \underline{\underline{O}}(1)$)? From (1.1) we see that it means that

$$\lim_{\varepsilon \to +0} N(\varepsilon) = M_D \lim_{\varepsilon \to +0} \frac{1}{\varepsilon^D}, \text{where } M_D \propto \underline{\underline{O}}(1). \tag{1.2a}$$

or, simpler,

$$N(\varepsilon) \propto \frac{1}{\varepsilon^D} \text{when } \varepsilon \to +0. \tag{1.2b}$$

Expressing D from (1.2a), we find

$$D = \lim_{\varepsilon \to +0} \frac{\ln N(\varepsilon) - \ln M_D}{\ln(1/\varepsilon)}. \tag{1.3}$$

But in the limit $\varepsilon \to +0$ the number of boxes is infinite: $N(\varepsilon) \to +\infty$. Therefore, we can neglect $\ln M_D$ in comparison with $\ln N(\varepsilon)$ to find

$$D = \lim_{\varepsilon \to +0} \frac{\ln N(\varepsilon)}{\ln(1/\varepsilon)}. \tag{1.4}$$

Let us consider the general case of a fractal whose generator has K branches and the scale factor r. We choose the size ε of boxes to be equal to the linear size $L_0 r^n$ of branches of prefractal iteration n: $\varepsilon = L_0 r^n$. Then we can cover the developed fractal by $N(\varepsilon) = K^n$ boxes which is the number of branches in this iteration. Substituting these equalities into (1.4), we find

$$D = \lim_{n \to +\infty} \frac{\ln K^n}{\ln(1/(L_0 r^n))} = \frac{\ln K}{\ln(1/r)}. \tag{1.5}$$

For example, for the triadic Koch curve above (with $K = 4$ and $r = 1/3$) we obtain

$$D = \frac{\ln 4}{\ln 3}. \tag{1.6}$$

The dimension is higher than one but is lower than two. In other words, the mathematical set is more "dense" than a usual curve but less dense than a surface.

Now we understand why the length of the coastal line was diverging. This happened because the mathematical set we considered was not one-dimensional. Mathematical sets with noninteger dimensions are called *fractals*.

Since we expect the measure M_D of a fractal to depend on its size L_0 as

$$M_D \propto {L_0}^D, \tag{1.7}$$

we can transform (1.2) into

$$N(\varepsilon) \propto \left(\frac{L_0}{\varepsilon}\right)^D \text{ when } \varepsilon \to +0. \tag{1.8}$$

In all formulae above, we have considered two equivalent limits: $n \to +\infty$ and $\varepsilon = L_0 r^n \to +0$. Rigorously speaking, the limit $n \to +\infty$ is not equivalent to $\varepsilon \to +0$ but to

$$\ln\frac{1}{\varepsilon} = n \ln\frac{1}{r} - \ln L_0 \to +\infty; \tag{1.9}$$

and we have utilized $\varepsilon \to +0$ only due to simpler notation. Although we do not see the difference between (1.9) and $\varepsilon \to +0$, later we will specifically refer to limit (1.9).

Problem 1.2.1

Find dimensions of Cantor sets (Smith 1874; Cantor 1883) presented in the below given figure.

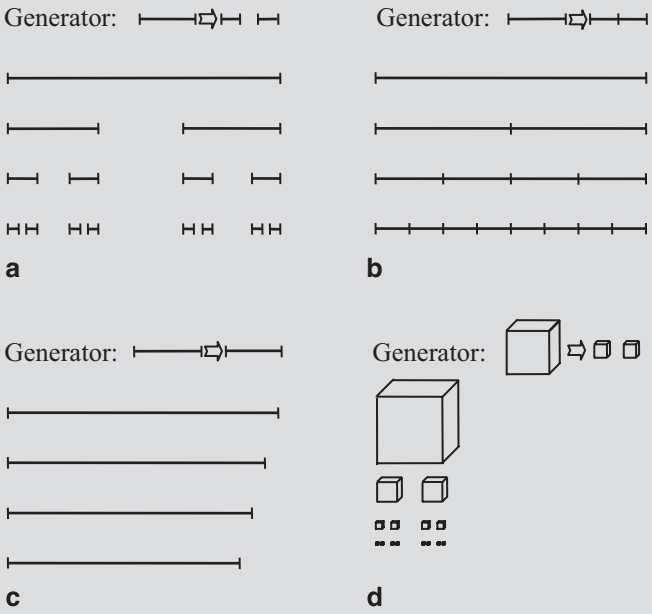

Solution: The Cantor set is generated by breaking a unit line segment into parts and discarding some of them. So, in part a of the figure we build the Cantor fractal with $K = 2$ branches and scale factor $r = 1/3$. In other words, a parent branch is divided into three thirds and the middle third is discarded. In accordance with (1.5) for the dimension of the developed fractal, we find $D = \dfrac{\ln 2}{\ln 3}$.

In the part b of the figure, we consider the Cantor set with $K = 2$ and $r = 1/2$. We divide the init line segment into two halves but do not discard any of them. Thereby, the sum of branches of iteration n is always equivalent to the initiator—the init line segment. In accordance with our expectations, the dimension of the developed fractal is $D = \dfrac{\ln 2}{\ln 2} = 1$; and strictly speaking, this mathematical set is not fractal.

In part c of the figure, we consider the Cantor set with only one daughter branch, $K = 1$, and $r = 0.95$. In other words, the parent branch each time reduces itself by 5% and does not generate other daughter branches. The

dimension $D = \dfrac{\ln 1}{\ln(1/0.95)} = 0$ is zero because the single branch transforms itself step by step into a point.

Although the definition of the Cantor set assumes that the initiator is the unit line segment, in part d of the figure, we consider the initiator to be the unit three-dimensional cube. The generator breaks the cube into 27 daughter cubes with linear scale factor $r = 1/3$ (the linear size decreases thrice). Then the generator keeps only two of the daughter cubes, $K = 2$, at the corners of the parent, discarding the rest. For the dimension of this fractal, we find $D = \dfrac{\ln 2}{\ln 3}$ which equals the dimension of the fractal in the part a of the figure. We see that the dimension of the fractal does not depend on the dimension of the initiator but is determined by the model of the generator.

Problem 1.2.2

Find dimensions of fractals presented in the below given figure.

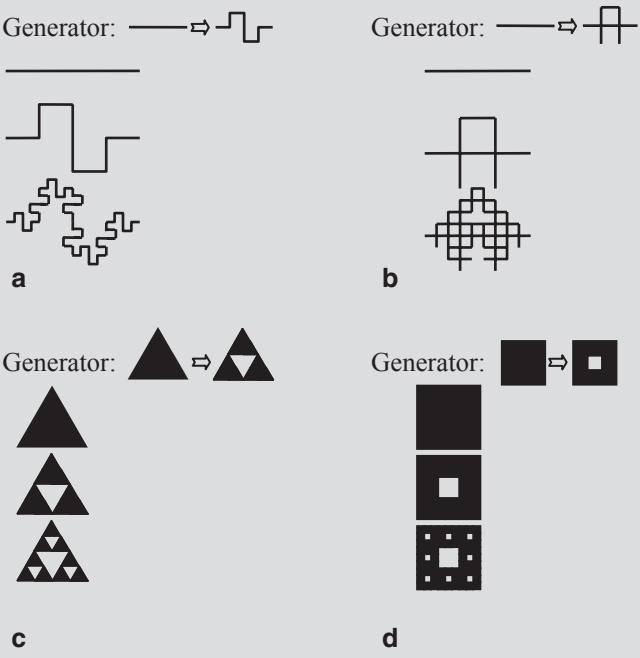

Solution: The part a of the figure represents the prefractal of the quadratic Koch curve (Minkowski sausage). The generator creates $K = 8$ branches with scale factor $r = 1/4$. The fractal dimension is $D = \frac{\ln 8}{\ln 4} = \frac{3}{2}$.

In the case of the Mandelbrot–Given curve (Mandelbrot and Given 1984) the generator has $K = 8$ branches and $r = 1/3$ (part b of the figure). The fractal dimension is $D = \frac{\ln 8}{\ln 3}$.

The Sierpinski gasket (Sierpiński 1915) has $K = 3$ branches with scale factor $r = 1/2$ (part c of the figure). The fractal dimension is $D = \frac{\ln 3}{\ln 2}$.

The Sierpinski carpet (Sierpiński 1916) has $K = 8$ branches with scale factor $r = 1/3$ (part d of the figure). The fractal dimension equals the fractal dimension of the Mandelbrot–Given curve, $D = \frac{\ln 8}{\ln 3}$.

1.3 Self-Similarity (Scale Invariance) as the Origin of the Fractal Dimension

So far, we have determined the fractal dimensions by the box counting method. However, there is another method which we can derive from the concept of the self-similarity itself.

Let us assume that the total developed fractal is covered by $N(\varepsilon)$ cubes of linear size ε (in the upper part of Fig. 1.7 the total developed fractal is covered by four cubes of size ε).

Any developed branch (the lower part of Fig. 1.7) is similar to the fractal in whole but in comparison with the whole fractal it is reduced in size with the linear scale factor r (thrice in Fig. 1.7). If we reduce the boxes with the same scale factor r (boxes with size $\varepsilon r = \varepsilon/3$ in Fig. 1.7), the number $N_{branch}(\varepsilon r)$ of them, covering the developed branch (four in Fig. 1.7), will be equal to the number of initial boxes of size ε, covering the whole fractal.

In other words, let us look at Fig. 1.7 as if we transformed the upper part into the lower part by threefold shrinking of both the fractal and the boxes. Thereby, the fractal transforms into its branch while the boxes become thrice smaller but their number, obviously, does not change.

So, the number $N_{branch}(\varepsilon r)$ of boxes of size εr, covering one fractal branch, equals the number of boxes $N(\varepsilon)$ of size ε, covering the total fractal: $N_{branch}(\varepsilon r) = N(\varepsilon)$. But there are K separate branches in the fractal. Therefore, the fractal in whole can be covered by the number $N(\varepsilon r)$ of boxes of size εr which is K times larger than $N_{branch}(\varepsilon r)$:

$$N(\varepsilon r) = KN(\varepsilon). \tag{1.10}$$

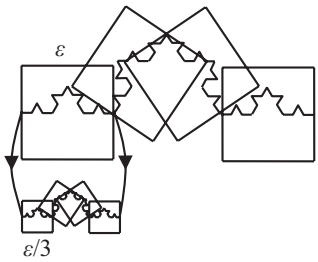

Fig. 1.7 Self-similarity

Again, four big boxes of size ε cover the total fractal in Fig. 1.7; and also four small boxes of size $\varepsilon r = \varepsilon / 3$ cover one branch. Then all $K = 4$ branches can be covered by four times four small boxes which is exactly represented by equality (1.10).

Equality (1.10) is possible only if $N(\varepsilon)$ depends on ε as the power-law (1.2) and (1.8):

$$N(\varepsilon) \propto \frac{const}{\varepsilon^D} \quad (\varepsilon \to +0). \tag{1.11}$$

Substituting (1.11) into (1.10)

$$\frac{const}{(\varepsilon r)^D} = K \frac{const}{\varepsilon^D} \quad (\varepsilon \to +0) \tag{1.12}$$

and expressing D from this equation, we return to the right-hand side of (1.5).

Instead of the developed branches of iteration $n = 1$, we could consider developed branches of an arbitrary iteration n_0. The boxes we now assume to be infinitesimal, $\varepsilon \to +0$, not only in comparison with the size L_0 of the fractal but even in comparison with the size $L_0 r^{n_0}$ of the branches of iteration n_0.

Small boxes can "feel" the fractality of both the total developed fractal and the considered developed branches. Since (due to self-similarity) we assume the dimension of both the developed fractal and the developed branch to be the same, D, for the total fractal, we have a proportionality

$$N(\varepsilon) \propto \left(\frac{L_0}{\varepsilon} \right)^D \quad (\varepsilon \to +0) \tag{1.13}$$

while for a developed branch of iteration n_0 valid is a similar proportionality

$$N_{branch}(\varepsilon) \propto \left(\frac{L_0 r^{n_0}}{\varepsilon} \right)^D \quad (\varepsilon \to +0). \tag{1.14}$$

There are K^{n_0} branches of iteration n_0. Summing their boxes, we should obtain the total number of boxes, covering the fractal:

$$N(\varepsilon) = K^{n_0} N_{branch}(\varepsilon). \tag{1.15}$$

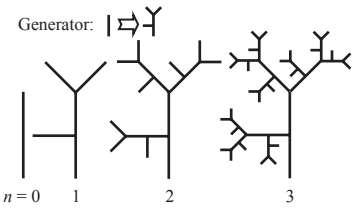

Fig. 1.8 A fractal tree

Substituting now (1.13 and 1.14) into (1.15), we find

$$\left(\frac{L_0}{\varepsilon}\right)^D \propto K^{n_0}\left(\frac{L_0 r^{n_0}}{\varepsilon}\right)^D \quad (\varepsilon \to +0) \text{ or} \tag{1.16a}$$

$$(L_0)^D \propto K^{n_0}(L_0 r^{n_0})^D, \tag{1.16b}$$

where we have cancelled the dependence on ε. The limit $\varepsilon \to +0$ is no longer present in the equation, but the right-hand side still depends on the number of iteration n_0. Considering now the new limit $n_0 \to +\infty$, we see that the proportionality (1.16b) is possible only when the dimension D obeys the right-hand side of equality (1.5).

In this and previous sections, we have considered different fractals and have found their dimensions. Before moving on to a discussion of more complex mathematical sets, we should mention where in nature we can encounter fractals.

The distribution of lakes on the Earth surface is fractal. Fractals are rivers which are, in fact, fractal trees discussed in the following section. Fractals are metal veins in rock. Fractals are the fracture surfaces of damaged solids. Fractals are the statistical properties of earthquakes. Fractals are time dependencies like white and color noises which are self-affine fractals considered below. Fractals are aggregation and surface growth—we can recall here the complex shape of snow-flakes. Fractals are birds' feathers and lung tracheas. Fractals are polymer clusters and the clusters of galaxies. In the following chapters, we will study the fractal behavior of clusters of phases in the vicinity of a point of phase transition.

The reason why so many studies have been and are devoted to fractals is the wide abundance of fractals in nature. Even buying a chocolate bar, it is possible that instead of solid material we find inside the fractal distribution of bubbles. And although it tastes better, there is definitely less chocolate in it than it was suggested by its size.

1.4 Fractal Trees

Fractal trees (Fig. 1.8) represent another kind of fractals. The main difference in comparison with the "usual" fractals is that during generation of daughter branches, we do not discard parent branches but keep them along.

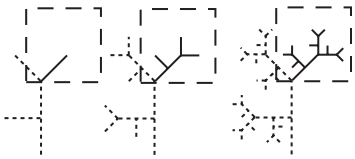

Fig. 1.9 One box covers not only a parent branch but also all its further development

Although it is a common practice to assume the structure of the fractal to be like that of a tree, for the mathematical formalism it is not required. So, all fractals above would become fractal trees if we considered their figures to represent not a succession of iterations but the last iteration. For example, four one-dimensional sets given in the part a of the figure given in Problem 1.2.1 were considered as four successive iterations. If, on the contrary, we considered now these four sets to be one set of iteration $n = 3$, we would obtain the prefractal tree.

How can we find the dimension of a fractal tree? Iteration n contains K^n branches of length $L_0 r^n$, K^{n-1} branches of length $L_0 r^{n-1}$,…, K branches of length $L_0 r$, and one branch of length L_0.

The size of boxes we choose to be $\varepsilon = L_0 r^n$. A branch of length $L_0 r^n$ is covered by one box. A branch of length $L_0 r^{n-1}$ is covered by $(1/r)^d$ boxes, where d is the dimensionality of the fractal initiator (we consider only the simplest geometrical forms for the initiators). So, the initiator in Fig. 1.8 is the init line segment, and $d = 1$. Initiator in part d of the figure in Problem 1.2.1 is the unit cube, and $d = 3$.

Applying this rule to branches of all possible sizes, we find the number of boxes covering each of them. So, the branch of length $L_0 r$ is covered by $(1/r)^{(n-1)d}$ boxes while the branch of length L_0 by $(1/r)^{nd}$ boxes.

To find the total number of boxes of size $\varepsilon = L_0 r^n$, covering the whole developed tree, we should sum all the numbers above:

$$N(\varepsilon) = K^n + K^{n-1}\left(\frac{1}{r}\right)^d + \ldots + K\left(\frac{1}{r}\right)^{(n-1)d} + 1\left(\frac{1}{r}\right)^{nd}. \tag{1.17}$$

Implicitly we have made a very important assumption here that daughter and parent branches are located not far from each other. Indeed, by number (1.17) of boxes, we have definitely covered iteration n. But what about the whole developed tree? Have we covered branches of iterations $n+1, n+2, \ldots$? If daughter branches were located in the vicinity of the parent branch, one box might cover both the parent branch and all its development (Fig. 1.9). In other words, one box will be enough to cover not only one branch of length $L_0 r^n$ but also all its further development. Then (1.17) is applicable not only to iteration n but also to the developed tree. Otherwise, all formulae below will no longer be valid.

Applying geometric progression to (1.17), we find

$$N(\varepsilon) = \frac{K^{n+1} - \left(\frac{1}{r^d}\right)^{n+1}}{K - \frac{1}{r^d}}. \tag{1.18}$$

In the limit $\varepsilon \to +0$ ($n \to +\infty$) the obtained expression depends on the ratio of K to r^{-d}. If $K > r^{-d}$, we find

$$N(\varepsilon) \to \frac{K^{n+1}}{K - \frac{1}{r^d}} \text{ or } D = \frac{\ln K}{\ln(1/r)} > d \tag{1.19}$$

which again corresponds to the right-hand side of (1.5). It, in fact, would be the dimension of the fractal if we had discarded parent branches as before. Discarding parent branches means that we neglect the "trunk and boughs" of the tree and consider only the "canopy of leaves," called, simpler *canopy* or *tip set*. Therefore, (1.19) is often called *the canopy dimension* or *the tip set dimension*.

In the opposite case $K < r^{-d}$ we obtain

$$N(\varepsilon) \to \frac{\left(\frac{1}{r^d}\right)^{n+1}}{\frac{1}{r^d} - K} \text{ or } D = d. \tag{1.20}$$

The case $K = 1/r^d$ requires special attention because geometric progression is no longer applicable. All terms in (1.17) become equal; and we find

$$N(\varepsilon) = K^n + K^n + \ldots + K^n = K^n(n+1) \text{ or } D = \frac{\ln K}{\ln(1/r)} = d. \tag{1.21}$$

Bringing all three equations (1.19–1.21) together, we obtain

$$D = \begin{cases} \dfrac{\ln K}{\ln(1/r)}, \dfrac{\ln K}{\ln(1/r)} > d \\ d, \dfrac{\ln K}{\ln(1/r)} \le d \end{cases}. \tag{1.22}$$

So, the dimension of the fractal tree is still determined by (1.5) but only if it is higher than the dimension d of the initiator. In other words, if the canopy dimension is higher than the dimension of the "trunk." In the opposite case, the dimension of the whole tree becomes equal to the dimension of the initiator. This result is quite expected because the dimension of a mathematical set, fractal or not, cannot be lower than the dimension of its arbitrary subset.

1.5 Self-Affine Fractals

Self-affine fractals present another modification of the "usual" fractals. The difference is that there are several scale factors now, each acting in its own direction.

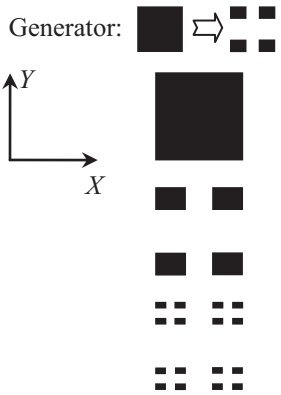

Fig. 1.10 Self-affine fractal

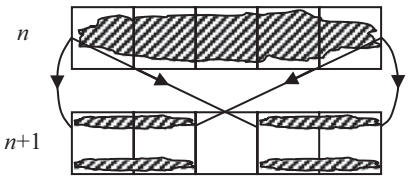

Fig. 1.11 The number of "small" boxes, covering a branch of iteration *n,* is higher than the number of boxes covering its development, because during the branch's development some "holes" appear within it

A classical example of a self-affine fractal is the self-similar time dependence (like Brownian random walk) where a part of the dependence is stochastically similar to the dependence in whole if two separate scale factors are applied: one for the time scale, another for the amplitude of the walk.

Another example of self-affine fractals is presented in Fig. 1.10. The generator creates $K = 4$ daughter branches in the corners of the parent branch. Each daughter branch is generated by the application of two scale factors to the parent branch: $r_x = 1/3$ in the horizontal direction (along *X*-axis) and $r_y = 1/4$ in the vertical direction (along *Y*-axis).

We see that after many iterations, the branches become "stretched": one side is much smaller than another. This complicates the box counting because the set of boxes covering iteration *n,* may no longer correspond to the set of boxes covering the developed fractal.

To discuss this question, let us consider some self-affine fractal in the three-dimensional ($d_0 = 3$) embedding space. In general, this fractal can possess three different scale factors r_x, r_y, r_z which, without loss of generality, we assume to be arranged in increasing order: $r_x \le r_y \le r_z$.

Let us first choose ε to be equal to the smallest side of branches of iteration n, $\varepsilon = r_x^n$, and cover with these boxes iteration n. This number of boxes will then exceed the number of boxes covering the developed fractal because, when a branch of iteration n is further developed, some "holes" appear within it which "small" boxes of size $\varepsilon = r_x^n$ can "feel" (Fig. 1.11). In other words, after the branch's development some boxes, which covered the branch before, will become empty.

Should we then choose the size of boxes to be equal to the largest side of branches of iteration n, $\varepsilon = r_z^n$? Then, clearly, after the branch's development,

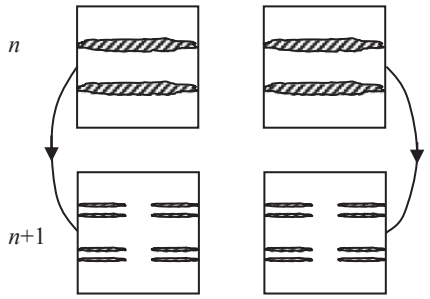

Fig. 1.12 One "big" box of size $\varepsilon = r_z^{\,n}$ can cover several branches of iteration n

none of these boxes will become empty (Fig. 1.12). And now indeed the number of boxes, covering iteration n, corresponds to the number of boxes covering the developed fractal.

But simultaneously, we encounter another difficulty. From Fig. 1.12, we see that one "big" box of size $\varepsilon = r_z^{\,n}$ can cover several branches of this iteration at once. Therefore, the number of boxes $N(\varepsilon)$, covering iteration n, is no longer equal to the number K^n of branches of this iteration. This complicates things because to find now the number of boxes, covering the fractal, we should take into account the relative positions of branches.

To our help, here comes the scale invariance as the method of dimension determination. Let us consider some finite iteration n_0. We consider the developed fractal and the developed branches of this iteration. We choose the size ε of boxes to be infinitesimal in comparison not only with the size L_x, L_y, L_z of the initiator, but also in comparison with the size $L_x r_x^{\,n_0}, L_y r_y^{\,n_0}, L_z r_z^{\,n_0}$ of branches of iteration n_0.

Then, the small boxes "feel" the fractal dimension D of both the developed fractal and the developed branches of iteration n_0. For the total fractal, we have the proportionality

$$N(\varepsilon) \propto \left(\frac{\sqrt[3]{L_x L_y L_z}}{\varepsilon} \right)^D \tag{1.23}$$

while for the developed branch of iteration n_0 we obtain

$$N_{branch}(\varepsilon) \propto \left(\frac{\sqrt[3]{L_x r_x^{\,n_0} L_y r_y^{\,n_0} L_z r_z^{\,n_0}}}{\varepsilon} \right)^D . \tag{1.24}$$

The number $N(\varepsilon)$ of boxes, covering the whole fractal, is K^{n_0} times higher than $N_{branch}(\varepsilon)$:

$$N(\varepsilon) = K^{n_0} N_{branch}(\varepsilon). \tag{1.25}$$

Substituting (1.23 and 1.24) into (1.25), we find

$$\left(\frac{\sqrt[3]{L_x L_y L_z}}{\varepsilon} \right)^D \propto K^{n_0} \left(\frac{\sqrt[3]{L_x r_x^{\,n_0} L_y r_y^{\,n_0} L_z r_z^{\,n_0}}}{\varepsilon} \right)^D . \tag{1.26}$$

Here, we can cancel the dependences on ε, removing the limit $\varepsilon \to +0$ from the proportionality:

$$1 \propto K^{n_0} \left(\sqrt[3]{r_x^{n_0} r_y^{n_0} r_z^{n_0}} \right)^D . \tag{1.27}$$

Introducing the new limit $n_0 \to +\infty$, we see that the proportionality (1.27) is possible only when

$$1 = K \left(\sqrt[3]{r_x r_y r_z} \right)^D . \tag{1.28}$$

This provides the expression for the dimensionality of our self-affine fractal:

$$D = \frac{\ln K}{\ln \frac{1}{\sqrt[3]{r_x r_y r_z}}} . \tag{1.29}$$

1.6 The Geometrical Support of Multifractals

Multifractals are applied to a system when its behavior is described by more complex laws than just simple power-law dependences. The closest analogy would be the application of a Fourier spectrum to a process that is more complex than just a simple harmonic time dependence. Besides, the formalism of multifractals has the closest resemblance with the formalism of statistical physics. That is why, although in further chapters, we consider only the cases of phase transition phenomena described by power-law dependences when the multifractals will not be applied directly, we still encourage the reader to study the rest of this chapter.

Multifractals have been introduced by Benoit Mandelbrot in his works on turbulence (Mandelbrot 1972, 1974, 1982). The multifractals are much more complex than fractals, mathematically and to understand intuitively. Therefore, we will study them step by step, choosing sometimes not the fastest but more illustrative way of discussion.

First, we will consider not multifractals themselves but their geometrical support. *The geometrical support* of a multifractal is a mathematical set represented by infinite iteration of a generator when K branches of the generator have their own scale factors $r_1, \ldots, r_K$.

In other words, we again consider a succession of prefractal iterations leading to the developed set. But, in this case, each of K daughter branches of the generator has its own linear scale factor r_i which the generator applies to reduce the linear size of the daughter branch i relative to the parent branch. Without loss of generality, we assume that all branches are arranged in the increasing order of their scale factors: $r_1 \le \ldots \le r_K$.

Since the simplest fractal we have studied above was the Cantor set, we will utilize it to illustrate all concepts of multifractals. However, the reader should always remember that we consider the one-dimensional generator only for illustrative pur-

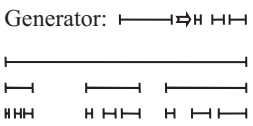

Fig. 1.13 The Cantor set when each of the three daughter branches has its own scale factor

poses while in general the geometrical support can have an arbitrary dimensionality. As an example, in Fig. 1.13 we present the Cantor set with $K = 3$ daughter branches with scale factors $r_1 = 1/9$, $r_2 = 2/9$, and $r_3 = 1/3$.

Let us consider some finite iteration n. Firstly, this iteration contains the smallest branch of size $L_0 r_1^n$ which, during all n applications of the generator, was formed as the first daughter branch of the generator with the scale factor r_1. In future, we will say that this branch was formed "along the path which has passed $\xi_1 = n$ times through the first branch of the generator and has avoided other generator's branches: $\xi_2 = \xi_3 = \ldots = \xi_K = 0$ ".

Secondly, there will be n branches with length $L_0 r_1^{n-1} r_2$ which have been formed along n different paths, passing $\xi_1 = n-1$ times through the first branch of the generator and $\xi_2 = 1$ times through the second branch, avoiding other generator's branches: $\xi_3 = \ldots = \xi_K = 0$.

And so on. For an arbitrary branch of iteration n, we can say that it was formed ξ_1 times through the first branch of the generator,…, ξ_K times—through the K^{th} branch of the generator. Since the generator has worked n times in total, the following equality is always valid:

$$\xi_1 + \xi_2 + \ldots + \xi_K = n. \tag{1.30}$$

For a particular set of numbers $\xi_1, \xi_2, \ldots, \xi_K$, obeying (1.30), there are $\dfrac{n!}{\xi_1! \ldots \xi_K!}$ corresponding branches of length $L_0 r_1^{\xi_1} \ldots r_K^{\xi_K}$ (there are $\dfrac{n!}{\xi_1! \ldots \xi_K!}$ different paths by which these branches have been formed).

Sometimes instead of numbers $\xi_1, \xi_2, \ldots, \xi_K$, we will consider a set of normalized numbers

$$\eta_1 \equiv \frac{\xi_1}{n}, \ldots, \eta_K \equiv \frac{\xi_K}{n}, \tag{1.31}$$

each of which represents the share of a particular generator branch in the path. If $\eta_i = 0$, the path has never passed through branch i. If $\eta_i = 1$, for all n times the path has passed only through branch i. Constraint (1.30) thereby transforms into

$$\eta_1 + \eta_2 + \ldots + \eta_K = 1. \tag{1.32}$$

Sometimes, we will refer to the set of numbers $\xi_1, \xi_2, \ldots, \xi_K$ as to the vector $\vec{\xi}$ just for the simplicity of notation. Similarly, we will refer to the set of numbers $\eta_1, \eta_2, \ldots, \eta_K$ as to the vector $\vec{\eta}$.

How do we find the dimension of such a set? Similar to self-affine fractals, we cannot use boxes with the size equal to the smallest or the largest branch of iteration n. Indeed, let us suppose that we have chosen some finite iteration n. The smallest branch of this iteration has length $L_0 r_1^n$. If we chose boxes to have size equal to this length, $\varepsilon = L_0 r_1^n$, the number of boxes, covering iteration n, would not correspond to the number of boxes, covering the developed set because when branches of iteration n are further developed, some "holes" appear within them. On the contrary, if we chose the size of the boxes to be equal to the length of the largest branch, $\varepsilon = L_0 r_K^n$, the boxes covering iteration n would be the boxes covering the developed set. However, in this case the boxes are so big that they may cover several branches of the iteration n at once, and the number of boxes will not correspond to the number of branches K^n.

Similar to the case of self-affine fractals, to find the dimension of the developed set, we should involve the concept of self-similarity. A developed branch of iteration n_0 is supposed to be similar to the developed set in whole. Therefore, the dimension D of this developed branch equals the dimension of the developed set in whole. If we choose the size of boxes to be infinitesimal in comparison with the size of this branch, the boxes will "feel" the fractality of both the total set and its branch. Then for the total set and for the branch, we obtain

$$N(\varepsilon) \propto \left(\frac{L_0}{\varepsilon}\right)^D, \tag{1.33}$$

$$N_{branch:\vec{\xi}}(\varepsilon) \propto \left(\frac{L_0 r_1^{\xi_1} \ldots r_K^{\xi_K}}{\varepsilon}\right)^D, \tag{1.34}$$

respectively, where

$$\xi_1 + \xi_2 + \ldots + \xi_K = n_0. \tag{1.35}$$

But to find the total number of boxes, covering the whole set, we should sum boxes, covering separate branches:

$$N(\varepsilon) = \sum_{\substack{\xi_1,\ldots,\xi_K=0: \\ \xi_1+\ldots+\xi_K=n_0}}^{n_0} \frac{n_0!}{\xi_1!\ldots\xi_K!} N_{branch:\vec{\xi}}(\varepsilon). \tag{1.36}$$

Substituting (1.33 and 1.34) into (1.36), we find:

$$\left(\frac{L_0}{\varepsilon}\right)^D \propto \sum_{\substack{\xi_1,\ldots,\xi_K=0: \\ \xi_1+\ldots+\xi_K=n_0}}^{n_0} \frac{n_0!}{\xi_1!\ldots\xi_K!}\left(\frac{L_0 r_1^{\xi_1}\ldots r_K^{\xi_K}}{\varepsilon}\right)^D = \frac{L_0{}^D\left(r_1{}^D + \ldots + r_K{}^D\right)^{n_0}}{\varepsilon^D}. \tag{1.37}$$

Cancelling the dependence on ε, we remove the limit $\varepsilon \to +0$ from the equation:

$$1 \propto (r_1{}^D + \ldots + r_K{}^D)^{n_0}. \tag{1.38}$$

In the limit $n_0 \to +\infty$, this proportionality is possible only if

$$r_1{}^D + \ldots + r_K{}^D = 1. \tag{1.39}$$

This is the equation that implicitly determines the dimension of the developed geometrical support.

We have found the dimension by box counting. However, as we saw in Sect. 1.3, the dimension can also be found by the self-similarity of the mathematical set. Let us choose infinitesimal size $\varepsilon \to +0$ for boxes and cover the whole developed geometrical support by them. Let $N(\varepsilon)$ be the total number of boxes required. Then, in accordance with (1.8), the dimension of the set is determined by

$$N(\varepsilon) \propto \frac{1}{\varepsilon^D} \text{ when } \varepsilon \to +0. \tag{1.40}$$

Each branch *i* of iteration $n = 1$, developed further, is similar to the whole set and has the same dimension *D*. Since it is similar to the whole set, it is covered by the same number of boxes, only reduced in size in the same proportion r_i:

$$N_{branch\,i}(\varepsilon r_i) = N(\varepsilon). \tag{1.41}$$

We cannot sum the boxes, covering different branches, because they all have different sizes now. Instead, since ε has been chosen arbitrarily, we can change the variable for every branch separately:

$$N_{branch\,i}(\varepsilon) = N(\varepsilon / r_i). \tag{1.42}$$

In other words, a branch *i* is covered by the same number of boxes of size ε as the number of boxes of size ε / r_i, covering the total set.

Now, since all branches are covered by boxes of the same size ε, summing them, we find the total number of boxes, covering the whole geometrical support:

$$N(\varepsilon) = \sum_{i=1}^{K} N_{branch\,i}(\varepsilon) = \sum_{i=1}^{K} N(\varepsilon / r_i). \tag{1.43}$$

Substituting (1.40) into the left- and right-hand sides of this equation, we return to (1.39).

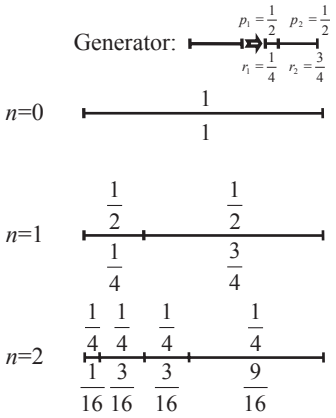

Fig. 1.14 The distribution of gold in rock when gold is distributed equally between two branches

1.7 Multifractals, Examples

1.7.1 Definitions

In the previous section, we studied how to build the geometrical support of a multifractal and found its dimension. In this section, we begin to consider examples of multifractals.

Multifractal is determined as a distribution of measure over branches of the multifractal's geometrical support. The function of measure distribution is fulfilled by the same generator that creates the geometrical support. For this purpose, we assume that initial measure equals 1 and assign measure distribution coefficients $p_1, p_2, ..., p_K$ for each daughter branch of the generator. Then the law of conservation of measure is

$$p_1 + p_2 + \ldots + p_K = 1. \tag{1.44}$$

The role of measure, therefore, can be played by any conserved quantity like probability, mass, etc.

Let us, as a simple example, consider the distribution of gold in the Earth' crust. We know that gold is not distributed uniformly. Instead, the general mass of rock is barren while gold is highly concentrated in gold veins.

As an example, we consider the Cantor set formed by the generator with $K = 2$ branches with scale factors $r_1 = 1/4$ and $r_2 = 3/4$ (Fig. 1.14). Since we have chosen the scale factors to obey the length conservation law $r_1 + r_2 = 1$, the sum of branches' lengths does not change during iterations and represents a rock sample of unit length.

In addition to scale factors for each branch, we introduce measure distribution factors P_1 and P_2. The mass of gold works now as the measure; and we assume that

the initial mass of gold, contained in the initiator, equals 1. Also, we assume that each daughter branch of the generator receives exactly one half of parent's gold: $p_1 = 1/2$ and $p_2 = 1/2$.

In Fig. 1.14, we plot three iterations of the prefractal. The rational number below each branch is the length of this branch. The rational number above the branch is the mass of gold within this branch.

We see that the density of gold (as the ratio of the branch's gold mass to the branch's length) is not uniform along the specimen but is much higher in some branches than in other. However, in multifractals, we do not consider the density of measure. Instead, we introduce *the Lipschitz–Hölder exponent* α (Lipschitz 1877–1880; Hölder 1882) of a branch as

$$\mu = \lambda^{\alpha}, \tag{1.45}$$

where μ is the measure of this branch and λ is the length of this branch.

So, in the case of the example we have considered above, the first branch of iteration $n = 2$ has length 1/16 and measure 1/4. Therefore, its Lipschitz–Hölder exponent is $\alpha = \dfrac{\ln(1/4)}{\ln(1/16)} = \dfrac{1}{2}$. Both the second and third branches of the same iteration have length 3/16 and measure 1/4. So, they both have the same exponents $\alpha = \dfrac{\ln(1/4)}{\ln(3/16)} = \dfrac{2\ln 2}{4\ln 2 - \ln 3}$. Finally, the fourth branch has $\alpha = \dfrac{\ln(1/4)}{\ln(9/16)} = \dfrac{\ln 2}{2\ln 2 - \ln 3}$.

In the example above, we have considered the measure equally distributed between the branches. But it is not necessarily the case. In Fig. 1.15, we present the prefractal with $p_1 = 1/3$ and $p_2 = 2/3$ when the generator transfers one-third of the parent's gold to the first branch and two-thirds to the second. The Lipschitz–Hölder exponents of branches of iteration $n = 2$ are $\alpha = \dfrac{\ln(1/9)}{\ln(1/16)} = \dfrac{\ln 3}{2\ln 2}$, $\alpha = \dfrac{\ln(2/9)}{\ln(3/16)} = \dfrac{2\ln 3 - \ln 2}{4\ln 2 - \ln 3}$, $\alpha = \dfrac{\ln(2/9)}{\ln(3/16)} = \dfrac{2\ln 3 - \ln 2}{4\ln 2 - \ln 3}$, and $\alpha = \dfrac{\ln(4/9)}{\ln(9/16)} = \dfrac{\ln 3 - \ln 2}{2\ln 2 - \ln 3}$.

We see that some branches (second and third) have equal Lipschitz–Hölder exponents. To study the multifractal, we sort its branches into subsets by the values of their Lipschitz–Hölder exponents and then study these subsets separately.

From Figs. 1.14 and 1.15, we see that the first branch of iteration $n = 2$ is formed along the path $\xi_1 = 2, \xi_2 = 0$. The second and third branches (that have the Lipschitz–Hölder exponents equal one to another) correspond to two paths with $\xi_1 = 1, \xi_2 = 1$. Finally, the fourth branch is formed by the path $\xi_1 = 0, \xi_2 = 2$. This simple comparison suggests that equal Lipschitz–Hölder exponents are possessed by the branches that were formed along the paths corresponding to the same set of numbers ξ_1, ξ_2. Later, we will discuss that this is not correct in general because this correspondence is not bijective. But for now, for illustrative purposes, we will assume that the subsets α of branches formed by different values of α are equivalent to subsets $\vec{\xi}$ formed by different sets of numbers ξ_1, ξ_2.

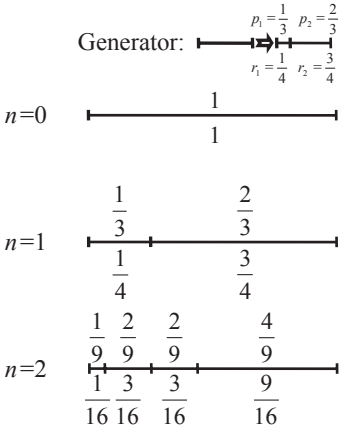

Fig. 1.15 The distribution of gold in the rock when gold is distributed unequally between two branches

1.7.2 The General Case of the Cantor Set

After considering the simplest examples of Figs. 1.14 and 1.15, let us now discuss the general case of the Cantor set (Fig. 1.16) whose generator has K branches with scale factors $r_1,...,r_K$ and measure distribution factors $p_1,...,p_K$, obeying (1.44).

Iteration n of our multifractal contains $\frac{n!}{\xi_1!\ldots\xi_K!}$ branches formed along paths $\xi_1,\ldots,\xi_K$, where

$$\xi_1+\xi_2+\ldots+\xi_K=n. \tag{1.46}$$

Each of these branches has length $r_1^{\xi_1}\ldots r_K^{\xi_K}$ and measure $p_1^{\xi_1}\ldots p_K^{\xi_K}$. Since they all have equal lengths and equal measures, they all have equal Lipschitz–Hölder exponents

$$p_1^{\xi_1}\ldots p_K^{\xi_K}=(r_1^{\xi_1}\ldots r_K^{\xi_K})^{\alpha}, \text{ or} \tag{1.47}$$

$$\alpha=\frac{\xi_1\ln p_1+\ldots+\xi_K\ln p_K}{\xi_1\ln r_1+\ldots+\xi_K\ln r_K}, \text{ or} \tag{1.48}$$

$$\alpha=\frac{\eta_1\ln p_1+\ldots+\eta_K\ln p_K}{\eta_1\ln r_1+\ldots+\eta_K\ln r_K}, \tag{1.49}$$

where we applied the change of variables (1.31).

Generally, we build the subsets of the multifractal by gathering the branches with equal values of α. As we agreed before, we assume that different sets of numbers $\xi_1,\ldots,\xi_K$ bijectively correspond to different α. Although it is not true in general, for now, we assume this equivalence to be present. In other words, as a subset of our

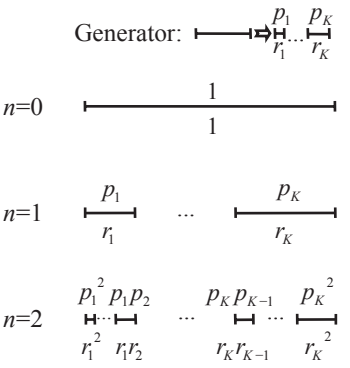

Fig. 1.16 The distribution of measure over the multifractal

multifractal, we consider all branches formed by paths corresponding to a particular vector $\vec{\xi}$ (to a particular vector $\vec{\eta}$ determined by (1.31)).

1.7.3 Dimensions of the Subsets

Let us find the dimension $D(\vec{\eta})$ of a subset $\vec{\eta}$. The size of boxes that we choose to match with the length of the branches of this subset is given by: $\varepsilon = r_1^{\xi_1} \ldots r_K^{\xi_K}$. Then the number of boxes $N_{\vec{\eta}}(\varepsilon)$, covering the subset, is the number $\frac{n!}{\xi_1! \ldots \xi_K!}$ of branches in this subset. For the definition of fractal dimension (1.11) to be valid, it should have the following proportionality:

$$N_{\vec{\eta}}(\varepsilon) = \frac{n!}{\xi_1! \ldots \xi_K!} \propto \frac{1}{\left(r_1^{\xi_1} \ldots r_K^{\xi_K}\right)^{D(\vec{\eta})}}. \tag{1.50}$$

To obtain the dimension, we should apply Stirling's approximation,

$$n! = \left(\frac{n}{e}\right)^n \underline{\underline{O}}(n^\alpha) \approx_{\ln} \left(\frac{n}{e}\right)^n, \tag{1.51}$$

where the notation "$\approx_{\ln}$" means that in the limit $n \gg 1$, we lose all power-law dependences on n in comparison with the exponential dependences on n. We will call this approximation the "*logarithmic accuracy*." Applying (1.51) to (1.50), we find

$$\eta_1^{-\xi_1} \ldots \eta_K^{-\xi_K} \propto \frac{1}{\left(r_1^{\xi_1} \ldots r_K^{\xi_K}\right)^{D(\vec{\eta})}} \text{ or} \tag{1.52}$$

$$D(\vec{\eta}) = \frac{\eta_1 \ln \eta_1 + \ldots + \eta_K \ln \eta_K}{\eta_1 \ln r_1 + \ldots + \eta_K \ln r_K}. \tag{1.53}$$

Let us investigate the dimensionality of the subsets. To find the subset, having maximal fractal dimension, we should find the point $\vec{\eta}^{\max D}$ of a maximum of (1.53) subject to constraint (1.32). We can achieve that by applying the method of Lagrange multipliers. In other words, we should maximize functional

$$\Psi[\vec{\eta}] = \frac{\eta_1 \ln \eta_1 + \ldots + \eta_K \ln \eta_K}{\eta_1 \ln r_1 + \ldots + \eta_K \ln r_K} + a(\eta_1 + \ldots + \eta_K - 1) \tag{1.54}$$

defined on the vector space $\vec{\eta}$. Here, a is the Lagrange multiplier.

To maximize (1.54), we find when its derivatives become zero. Differentiation with respect to a

$$\frac{\partial \Psi}{\partial a} = 0 \tag{1.55}$$

returns us to (1.32). Differentiation with respect to η_i

$$\left.\frac{\partial \Psi}{\partial \eta_i}\right|_{\vec{\eta}^{\max D}} = 0 \tag{1.56}$$

provides

$$\eta_i^{\max D} = r_i^{const}. \tag{1.57}$$

Substituting (1.57) into (1.32) and recalling (1.39), we find

$$\eta_i^{\max D} = r_i^D, \tag{1.58}$$

where D is the dimension of the geometrical support of the multifractal in whole. Utilizing (1.49), we see that (1.58) corresponds to

$$\alpha^{\max D} = \frac{r_1^D \ln p_1 + \ldots + r_K{}^D \ln p_K}{r_1^D \ln r_1 + \ldots + r_K{}^D \ln r_K}. \tag{1.59}$$

Substituting (1.58) into (1.53), we find that the maximal dimension of the subsets equals the dimension of the geometrical support of the multifractal in whole:

$$D(\vec{\eta}^{\max D}) = D. \tag{1.60}$$

Therefore, we could say that the subset with the highest dimension "inherits" the dimensionality of the whole geometrical support.

Problem 1.7.1

Consider the multifractal in the below given figure whose generator has $K = 2$ branches with scale factors r_1, r_2 and measure factors $p_1 = p$ and $p_2 = 1 - p$. Investigate the dependence of the subset dimension on the Lipschitz–Hölder exponent of the subset.

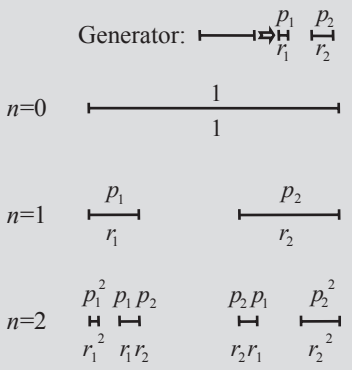

Solution: Let us consider a particular vector $\vec{\eta} = \begin{Vmatrix} \eta_1 \\ 1-\eta_1 \end{Vmatrix}$. Substituting it into (1.53) and (1.49), we find

$$D(\vec{\eta}) = \frac{\eta_1 \ln \eta_1 + (1-\eta_1)\ln(1-\eta_1)}{\eta_1 \ln r_1 + (1-\eta_1)\ln r_2} \tag{1.61}$$

$$\alpha = \frac{\eta_1 \ln p + (1-\eta_1)\ln(1-p)}{\eta_1 \ln r_1 + (1-\eta_1)\ln r_2}. \tag{1.62}$$

Above, in (1.50–1.60), we were working in terms of vectors $\vec{\eta}$ although we should be working in terms of the Lipschitz–Hölder exponents α. But what was difficult in the general case becomes quite simple for the case of our problem when $K = 2$. We need only to express η_1 from (1.62) and substitute it into (1.61) to find the dependence of the subset's dimension on the subset's Lipschitz–Hölder exponent

$$D(\alpha) = \frac{\ln(1-p) - \alpha \ln r_2}{\ln(1-p)\ln r_1 - \ln(p)\ln r_2} \ln \frac{\ln(1-p) - \alpha \ln r_2}{\alpha \ln \frac{r_1}{r_2} + \ln \frac{1-p}{p}} + \frac{\alpha \ln r_1 - \ln p}{\ln(1-p)\ln r_1 - \ln(p)\ln r_2} \ln \frac{\alpha \ln r_1 - \ln p}{\alpha \ln \frac{r_1}{r_2} + \ln \frac{1-p}{p}}. \tag{1.63}$$

To find the maximum of this dependence, we should equate its derivative to zero:

$$\left.\frac{dD}{d\alpha}\right|_{\alpha^{\max D}} = 0. \tag{1.64}$$

For the point $\alpha^{\max D}$ of maximum this provides

$$\alpha^{\max D} = \frac{r_1^{\,D} \ln p + r_2^{\,D} \ln(1-p)}{r_1^{\,D} \ln r_1 + r_2^{\,D} \ln r_2}. \tag{1.65}$$

Substituting (1.65) into (1.63), for the dimension of the subset corresponding to the point $\alpha^{\max D}$ we find

$$D(\alpha^{\max D}) = D, \tag{1.66}$$

where D is the dimension of the geometrical support in whole. The general dependence of the subset's dimension on the Lipschitz–Hölder exponent is given in the below figure for the case $p = 0.9$, $r_1 = r_2 = 1/2$.

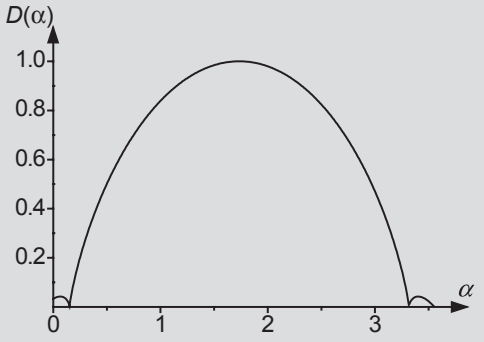

From the above figure, we see that subsets in the vicinity of $\alpha^{\max D}$ have dimensions close to D while other subsets have lower dimensions.

1.7.4 Lengths of the Subsets

To find the total length of the prefractal, we should sum the lengths of all branches of iteration n:

$$L = \sum_{\substack{\xi_1,\ldots,\xi_K=0: \\ \xi_1+\ldots+\xi_K=n}}^{n} \frac{n!}{\xi_1!\ldots\xi_K!} r_1^{\xi_1} \ldots r_K^{\xi_K} = \left(r_1 + \ldots + r_K\right)^n. \tag{1.67}$$

We see that if the length is not conserved, $r_1 + \ldots + r_K < 1$, the total length of the prefractal becomes smaller and smaller from one iteration to another.

For the subset of vector $\vec{\eta}$, the total length of branches is

$$L(\vec{\eta}) = \frac{n!}{\xi_1 ! \ldots \xi_K !} r_1^{\xi_1} \ldots r_K^{\xi_K} \approx_{\ln} \left(\frac{r_1}{\eta_1}\right)^{n\eta_1} \ldots \left(\frac{r_K}{\eta_K}\right)^{n\eta_K}. \tag{1.68}$$

Similar to (1.54), to find the subset with the largest length, we should maximize the following functional:

$$\Psi[\vec{\eta}] = \left(\frac{r_1}{\eta_1}\right)^{n\eta_1} \ldots \left(\frac{r_K}{\eta_K}\right)^{n\eta_K} + a(\eta_1 + \ldots + \eta_K - 1), \tag{1.69}$$

where a is the Lagrange multiplier.

Maximization with respect to a,

$$\frac{\partial \Psi}{\partial a} = 0, \tag{1.70}$$

returns us to constraint (1.32). Maximization with respect to $\vec{\eta}$,

$$\left.\frac{\partial \Psi(\vec{\eta})}{\partial \vec{\eta}}\right|_{\vec{\eta}^{\max L}} = 0, \tag{1.71}$$

provides

$$\eta_i^{\max L} = \frac{r_i}{\sum_{i=1}^{K} r_i}. \tag{1.72}$$

The corresponding Lipschitz–Hölder exponent is

$$\alpha^{\max L} = \frac{r_1 \ln p_1 + \ldots + r_K \ln p_K}{r_1 \ln r_1 + \ldots + r_K \ln r_K}. \tag{1.73}$$

At the point of maximum $\vec{\eta}^{\max L}$, the length of the corresponding subset is equal with logarithmic accuracy to the total length of the prefractal:

$$L(\vec{\eta}^{\max L}) \approx_{\ln} L. \tag{1.74}$$

Since the length (1.67) of the whole prefractal is the sum of the subsets' lengths,

$$L = \sum_{\substack{\xi_1, \ldots, \xi_K = 0: \\ \xi_1 + \ldots + \xi_K = n}}^{n} L(\vec{\eta}), \tag{1.75}$$

about equality (1.74) it is said that *the length of the prefractal is equal to its maximal term*.

Critical here are the words "with logarithmic accuracy" because the subsets, adjacent to the subset with maximal length, have comparable lengths. Indeed, let us consider the "adjacent" subset:

$$\vec{\xi}_0 = \vec{\xi}^{\max L} + \begin{Vmatrix} +1 \\ -1 \\ \vdots \end{Vmatrix}. \tag{1.76}$$

In other words, the paths corresponding to this chosen subset are the same as for $\vec{\eta}^{\max L}$ with the exception that we go one time less through the second branch of the generator and one time more through the first branch. The total length of the new subset,

$$L(\vec{\eta}_0) = \frac{n!}{(\xi_1^{\max L}+1)!(\xi_2^{\max L}-1)!\ldots\xi_K^{\max L}!} r_1^{\xi_1^{\max L}+1} r_2^{\xi_2^{\max L}-1} \ldots r_K^{\xi_K^{\max L}}, \tag{1.77}$$

differs from the largest length of the subset $\vec{\eta}^{\max L}$,

$$L(\vec{\eta}^{\max L}) = \frac{n!}{\xi_1^{\max L}!\,\xi_2^{\max L}!\ldots\xi_K^{\max L}!} r_1^{\xi_1^{\max L}} r_2^{\xi_2^{\max L}} \ldots r_K^{\xi_K^{\max L}}, \tag{1.78}$$

by multiplier

$$\frac{L(\vec{\eta}_0)}{L(\vec{\eta}^{\max L})} = \frac{\xi_2^{\max L}}{(\xi_1^{\max L}+1)}\frac{r_1}{r_2} = \frac{\eta_2^{\max L}}{\left(\eta_1^{\max L}+\dfrac{1}{n}\right)}\frac{r_1}{r_2} = \left(1+\frac{\sum_{i=1}^{K} r_i}{nr_1}\right)^{-1} \approx \tag{1.79}$$

$$= 1 - \frac{\sum_{i=1}^{K} r_i}{nr_1} \to 1 \text{ when } n \to +\infty.$$

We see that the subsets, adjacent to $\vec{\eta}^{\max L}$, indeed have similar lengths. Therefore, beside $L(\vec{\eta}^{\max L})$ there are many other terms of the order of $L(\vec{\eta}^{\max L})$ in equality (1.74) which we do not see explicitly. This has happened because equality (1.74) is valid only with logarithmic accuracy.

The logarithmic accuracy means that we neglect all power-law dependences on n in comparison with the exponential dependence on n. Therefore, equality (1.74) is valid with the accuracy of a power-law multiplier:

$$L = L\left(\vec{\eta}^{\max L}\right) \underline{\underline{O}}\left(n^{\phi}\right). \tag{1.80}$$

In other words, the sign $\approx_{\ln}$ disguises the presence of $\underline{\underline{O}}(n^{\phi})$ similar terms, showing only one of them. In fact, in the limit $n \to +\infty$ there could be infinite (!) number of terms of the order of $L(\vec{\eta}^{\max L})$ in (1.74). And we would still put only one of them in the left-hand side of (1.74)!

In the vicinity of the point $\vec{\eta}^{\max L}$ of maximum, we can expand (1.68) in small parameter $\Delta\vec{\eta} = \vec{\eta} - \vec{\eta}^{\max L}$. As a result, we find that the lengths of the subsets in the vicinity of the maximum obey the Gaussian distribution:

$$L(\vec{\eta}) = (r_1 + \ldots + r_K)^n e^{-\frac{n}{2}\sum_{i=1}^{K} \frac{\Delta\eta_i^2}{r_i / \sum_{j=1}^{K} r_j}}. \tag{1.81}$$

The width of the Gaussian "bell" is very small:

$$\delta\eta_i \propto \frac{1}{\sqrt{n}} \to 0 \text{ when } n \to +\infty. \tag{1.82}$$

It corresponds to

$$\delta\xi_i \propto \frac{n}{\sqrt{n}} = \sqrt{n} \to +\infty \text{ when } n \to +\infty \tag{1.83}$$

which represents the standard deviation of an arbitrary component of $\vec{\xi}$. In other words, there are $\underline{\underline{O}}(\sqrt{n})$ different values of ξ_i under the "bell" of the maximum. Considering all components of $\vec{\xi}$ together, there are $\left(\underline{\underline{O}}\left(\sqrt{n}\right)\right)^K \propto \underline{\underline{O}}\left(n^{K/2}\right)$ different subsets which all have lengths comparable with $L(\vec{\eta}^{\max L})$. Therefore, we can refine (1.80) as

$$L = L\left(\vec{\eta}^{\max L}\right)\underline{\underline{O}}\left(n^{K/2}\right). \tag{1.84}$$

Problem 1.7.2

For the multifractal from Problem 1.7.1, prove the Gaussian distribution to be valid for the lengths of subsets.

Solution: The total length of branches for a subset formed along paths $\vec{\eta} = \begin{Vmatrix} \eta_1 \\ 1-\eta_1 \end{Vmatrix}$ is

$$L(\vec{\eta}) \approx_{\ln} \left(\frac{r_1}{\eta_1}\right)^{n\eta_1} \left(\frac{r_2}{1-\eta_1}\right)^{n(1-\eta_1)}, \tag{1.85}$$

where η_1 is connected with α by (1.62). Expressing η_1 from (1.62) and substituting it into (1.85), we find the dependence of the logarithm of $L(\vec{\eta})$ on α :

$$\ln L(\alpha) \approx -n\frac{\ln(1-p)-\alpha\ln r_2}{\alpha\ln\frac{r_1}{r_2}+\ln\frac{1-p}{p}}\ln\left(\frac{1}{r_1}\frac{\ln(1-p)-\alpha\ln r_2}{\alpha\ln\frac{r_1}{r_2}+\ln\frac{1-p}{p}}\right)-$$

$$-n\frac{\alpha\ln r_1-\ln p}{\alpha\ln\frac{r_1}{r_2}+\ln\frac{1-p}{p}}\ln\left(\frac{1}{r_2}\frac{\alpha\ln r_1-\ln p}{\alpha\ln\frac{r_1}{r_2}+\ln\frac{1-p}{p}}\right). \qquad (1.86)$$

The logarithm is the monotonically increasing function. Therefore, $L(\alpha)$ will be maximal when its logarithm is maximal:

$$\left.\frac{\partial\ln L(\alpha)}{\partial\alpha}\right|_{\alpha^{\max L}}=0. \qquad (1.87)$$

Differentiating, we find the point of maximum

$$\alpha^{\max L}=\frac{r_1\ln p+r_2\ln(1-p)}{r_1\ln r_1+r_2\ln r_2}. \qquad (1.88)$$

Substituting (1.88) into (1.86), we find that the length of the set, corresponding to the point of maximum, equals with logarithmic accuracy the length of the total prefractal:

$$\ln L(\alpha^{\max L})\approx n\ln(r_1+r_2)\ \text{ or }\ L(\alpha^{\max L})\approx_{\ln}(r_1+r_2)^n=L. \qquad (1.89)$$

Let us now expand (1.86) in the vicinity of the point $\alpha^{\max L}$ of maximum:

$$\ln L(\alpha)=\ln L(\alpha^{\max L})+\left.\frac{\partial\ln L(\alpha)}{\partial\alpha}\right|_{\alpha^{\max L}}(\alpha-\alpha^{\max L})$$

$$+\frac{1}{2}\left.\frac{\partial^2\ln L(\alpha)}{\partial\alpha^2}\right|_{\alpha^{\max L}}(\alpha-\alpha^{\max L})^2+\ldots \qquad (1.90)$$

In accordance with (1.87), the first derivative here is zero. The second derivative we find as follows:

$$\left.\frac{\partial^2\ln L(\alpha)}{\partial\alpha^2}\right|_{\alpha^{\max L}}=-n\frac{1}{r_1r_2}\left(\frac{\left(r_1\ln r_1+r_2\ln r_2\right)^2}{(r_1+r_2)\left(\ln(1-p)\ln r_1-\ln p\ln r_2\right)}\right)^2. \qquad (1.91)$$

Substituting (1.91) into (1.90) and exponentiating this equality, we find that the distribution of the subsets' lengths in the vicinity of maximum is Gaussian:

$$L(\alpha) \approx L e^{-\frac{n}{2}\frac{1}{\eta_1 r_2}\left(\frac{(r_1 \ln r_1 + r_2 \ln r_2)^2}{(r_1+r_2)(\ln(1-p)\ln r_1 - \ln p \ln r_2)}\right)^2 \left(\alpha - \alpha^{\max L}\right)^2}. \tag{1.92}$$

Let us also find derivative $\frac{dD(\alpha)}{d\alpha}$ at the point $\alpha^{\max L}$. Differentiating (1.63) and substituting (1.88), we find

$$\left.\frac{\partial D(\alpha)}{\partial \alpha}\right|_{\alpha^{\max L}} = -\frac{\ln(r_1+r_2)\ln r_1 - \ln(r_1+r_2)\ln r_2}{\ln(1-p)\ln r_1 - \ln p \ln r_2}. \tag{1.93}$$

1.7.5 Measures of the Subsets

We have discussed the dimensionality and the lengths of different subsets. Now, let us consider the measures of the subsets. First, we check that the total measure of the multifractal is conserved. Summing the measure over all subsets, we find that the measure of iteration *n* still equals 1:

$$M = \sum_{\substack{\xi_1,\ldots,\xi_K=0: \\ \xi_1+\ldots+\xi_K=n}}^{n} \frac{n!}{\xi_1!\ldots\xi_K!} p_1^{\xi_1}\ldots p_K^{\xi_K} = \left(p_1+\ldots+p_K\right)^n = 1. \tag{1.94}$$

The measure of a subset $\vec{\eta}$ is

$$M(\vec{\eta}) = \frac{n!}{\xi_1!\ldots\xi_K!} p_1^{\xi_1}\ldots p_K^{\xi_K} \approx_{\ln} \left(\frac{p_1}{\eta_1}\right)^{n\eta_1}\ldots\left(\frac{p_K}{\eta_K}\right)^{n\eta_K}. \tag{1.95}$$

To find the subset with the highest measure, we should maximize the following functional

$$\Psi[\vec{\eta}] = \left(\frac{p_1}{\eta_1}\right)^{n\eta_1}\ldots\left(\frac{p_K}{\eta_K}\right)^{n\eta_K} + a(\eta_1+\ldots+\eta_K-1), \tag{1.96}$$

where *a* is the Lagrange multiplier. Maximization provides

$$\eta_i^{\max M} = p_i \tag{1.97}$$

which corresponds to

$$\alpha^{\max M} = \frac{p_1 \ln p_1 + \ldots + p_K \ln p_K}{p_1 \ln r_1 + \ldots + p_K \ln r_K}. \tag{1.98}$$

We see that at the point $\vec{\eta}^{\max M}$ of maximal measure, the number of branches is inversely proportional to the measure of branches,

$$\frac{n!}{\xi_1^{\max M}!\ldots\xi_K^{\max M}!} \approx_{\ln} \frac{1}{p_1^{\xi_1^{\max M}}\ldots p_K^{\xi_K^{\max M}}}, \tag{1.99}$$

to provide the unit value of measure for this subset.

In accordance with (1.97), the highest measure is possessed by the subset whose paths have been chosen in accordance with the probabilities of the measure distribution. The measure of this subset with logarithmic accuracy equals the measure of the total prefractal:

$$M(\vec{\eta}^{\max M}) \approx_{\ln} M = 1. \tag{1.100}$$

Since the measure (1.94) of the whole set is the sum of subsets' measures,

$$M = \sum_{\substack{\xi_1,\ldots,\xi_K=0: \\ \xi_1+\ldots+\xi_K=n}}^{n} M(\vec{\eta}), \tag{1.101}$$

it is said that *the measure of the prefractal is equal to its maximal term*. Again, equality (1.100) is valid only with logarithmic accuracy, and there are other subsets with the measure of the same order.

Expanding (1.95) in small difference $\Delta\vec{\eta} = \vec{\eta} - \vec{\eta}^{\max M}$, we again find the Gaussian distribution:

$$M(\vec{\eta}) = e^{-\frac{n}{2}\sum_{i=1}^{K}\frac{\Delta\eta_i^2}{p_i}}. \tag{1.102}$$

The width of the maximum is again

$$\delta\eta \propto \frac{1}{\sqrt{n}} \to 0, \tag{1.103}$$

$$\delta\xi \propto \sqrt{n} \to +\infty, \tag{1.104}$$

so for equality (1.100), the logarithmic accuracy means that there are $\underline{\underline{O}}\left(n^{K/2}\right)$ different subsets under the "bell" of the maximum, each of which has measure of the order of $M(\vec{\eta}^{\max M})$:

$$M = M(\vec{\eta}^{\max M})\underline{\underline{O}}\left(n^{K/2}\right). \tag{1.105}$$

Problem 1.7.3

For the multifractal from Problem 1.7.1, prove the Gaussian distribution to be valid for the measures of subsets.

Solution: The total measure of a subset formed along paths $\vec{\eta} = \begin{Vmatrix} \eta_1 \\ 1-\eta_1 \end{Vmatrix}$ is

$$M(\vec{\eta}) \approx_{\ln} \left(\frac{p}{\eta_1}\right)^{n\eta_1} \left(\frac{1-p}{1-\eta_1}\right)^{n(1-\eta_1)}, \tag{1.106}$$

where η_1 is connected with α by (1.62). Expressing η_1 from (1.62) and substituting into (1.106), we find the dependence of the logarithm of $M(\vec{\eta})$ on α:

$$\ln M(\alpha) \approx -n\frac{\ln(1-p)-\alpha\ln r_2}{\alpha\ln\frac{r_1}{r_2}+\ln\frac{1-p}{p}}\ln\left(\frac{1}{p}\frac{\ln(1-p)-\alpha\ln r_2}{\alpha\ln\frac{r_1}{r_2}+\ln\frac{1-p}{p}}\right)-$$

$$-n\frac{\alpha\ln r_1-\ln p}{\alpha\ln\frac{r_1}{r_2}+\ln\frac{1-p}{p}}\ln\left(\frac{1}{1-p}\frac{\alpha\ln r_1-\ln p}{\alpha\ln\frac{r_1}{r_2}+\ln\frac{1-p}{p}}\right). \tag{1.107}$$

To find the maximum of $M(\alpha)$, we differentiate its logarithm:

$$\left.\frac{\partial\ln M(\alpha)}{\partial\alpha}\right|_{\alpha^{\max M}} = 0 \tag{1.108}$$

and find the point of maximum:

$$\alpha^{\max M} = \frac{p\ln p+(1-p)\ln(1-p)}{p\ln r_1+(1-p)\ln r_2}. \tag{1.109}$$

Substituting (1.109) into (1.107), we find that the measure of the set, corresponding to the point $\alpha^{\max M}$ of maximum, equals with logarithmic accuracy unity:

$$\ln M(\alpha^{\max M}) \approx 0 \text{ or } M(\alpha^{\max M}) \approx_{\ln} 1, \tag{1.110}$$

where unity is the measure of the total prefractal.

Finally, we expand (1.107) in the vicinity of the point $\alpha^{\max M}$ of the maximum:

$$\ln M(\alpha) = \ln M(\alpha^{\max M}) + \left.\frac{\partial \ln M(\alpha)}{\partial \alpha}\right|_{\alpha^{\max M}} (\alpha - \alpha^{\max M}) + \frac{1}{2}\left.\frac{\partial^2 \ln M(\alpha)}{\partial \alpha^2}\right|_{\alpha^{\max M}} (\alpha - \alpha^{\max M})^2 + \ldots \quad (1.111)$$

The first derivative (1.108) is zero. The second derivative we find as follows:

$$\left.\frac{\partial^2 \ln M(\alpha)}{\partial \alpha^2}\right|_{\alpha^{\max M}} = -n\left(\frac{\left(p\ln r_1 + (1-p)\ln r_2\right)^2}{\ln(1-p)\ln r_1 - \ln p \ln r_2}\right)^2 \left(\frac{1}{p} + \frac{1}{1-p}\right). \quad (1.112)$$

Exponentiating equality (1.111), we prove the distribution of subsets' measures in the vicinity of the maximum to be Gaussian:

$$M(\alpha) = e^{-\frac{n}{2}\left(\frac{\left(p\ln r_1 + (1-p)\ln r_2\right)^2}{\ln(1-p)\ln r_1 - \ln p \ln r_2}\right)^2 \left(\frac{1}{p} + \frac{1}{1-p}\right)\left(\alpha - \alpha^{\max M}\right)^2}. \quad (1.113)$$

Finally, let us find the derivative $\frac{dD(\alpha)}{d\alpha}$ at the point $\alpha^{\max M}$ of the maximum. Differentiating (1.63) and substituting (1.109) into it, we find

$$\left.\frac{\partial D(\alpha)}{\partial \alpha}\right|_{\alpha^{\max M}} = 1. \quad (1.114)$$

We see that for multifractal from Problem 1.7.3, the subset $\alpha^{\max M}$ with the highest measure corresponds to the point at which (1.114) is valid. But will this be true for the general case?

To answer this question, in the general case of the Cantor set with K branches, we should differentiate expression (1.53):

$$dD(\vec{\eta}) = d\left(\frac{\eta_1 \ln \eta_1 + \ldots + \eta_K \ln \eta_K}{\eta_1 \ln r_1 + \ldots + \eta_K \ln r_K}\right). \quad (1.115)$$

However, we should remember that variables $\eta_1,\ldots,\eta_K$ are not independent but obeying constraint (1.32). Let us express η_K as a function of $\eta_1,\ldots,\eta_{K-1}$,

$$\eta_K = 1 - \sum_{i=1}^{K-1} \eta_i, \quad (1.116)$$

and substitute it into (1.115):

$$dD(\vec{\eta}) = d\left(\frac{\sum_{i=1}^{K-1}\eta_i \ln\eta_i + \left(1-\sum_{i=1}^{K-1}\eta_i\right)\ln\left(1-\sum_{i=1}^{K-1}\eta_i\right)}{\sum_{i=1}^{K-1}\eta_i \ln r_i + \left(1-\sum_{i=1}^{K-1}\eta_i\right)\ln r_K}\right). \tag{1.117}$$

Differentiating, we find

$$dD(\vec{\eta}) = \frac{\left\{\sum_{i=1}^{K-1}(\ln\eta_i - \ln\eta_K)d\eta_i\right\}\left\{\sum_{i=1}^{K}\eta_i \ln r_i\right\}}{\left\{\sum_{i=1}^{K}\eta_i \ln r_i\right\}^2} - \frac{\left\{\sum_{i=1}^{K}\eta_i \ln\eta_i\right\}\left\{\sum_{i=1}^{K-1}(\ln r_i - \ln r_K)d\eta_i\right\}}{\left\{\sum_{i=1}^{K}\eta_i \ln r_i\right\}^2}. \tag{1.118}$$

At the point $\vec{\eta}^{\max M}$, this expression transforms into

$$dD(\vec{\eta}^{\max M}) = \frac{\sum_{i=1}^{K-1}(\ln p_i - \ln p_K)d\eta_i - \alpha^{\max M}\sum_{i=1}^{K-1}(\ln r_i - \ln r_K)d\eta_i}{\sum_{i=1}^{K} p_i \ln r_i}. \tag{1.119}$$

Similarly, the differential of the Lipschitz–Hölder exponent (1.49),

$$d\alpha = d\left(\frac{\sum_{i=1}^{K-1}\eta_i \ln p_i + \left(1-\sum_{i=1}^{K-1}\eta_i\right)\ln p_K}{\sum_{i=1}^{K-1}\eta_i \ln r_i + \left(1-\sum_{i=1}^{K-1}\eta_i\right)\ln r_K}\right), \tag{1.120}$$

equals

$$d\alpha = \frac{\left\{\sum_{i=1}^{K-1}(\ln p_i - \ln p_K)d\eta_i\right\}\left\{\sum_{i=1}^{K}\eta_i \ln r_i\right\}}{\left\{\sum_{i=1}^{K}\eta_i \ln r_i\right\}^2} - \frac{\left\{\sum_{i=1}^{K}\eta_i \ln p_i\right\}\left\{\sum_{i=1}^{K-1}(\ln r_i - \ln r_K)d\eta_i\right\}}{\left\{\sum_{i=1}^{K}\eta_i \ln r_i\right\}^2} \tag{1.121}$$

At the point $\vec{\eta}^{\max M}$, we find

$$d\alpha(\vec{\eta}^{\max M}) = \frac{\sum_{i=1}^{K-1}(\ln p_i - \ln p_K)d\eta_i - \alpha^{\max M}\sum_{i=1}^{K-1}(\ln r_i - \ln r_K)d\eta_i}{\left\{\sum_{i=1}^{K} p_i \ln r_i\right\}}. \tag{1.122}$$

We see that (1.122) is equal to (1.119). Therefore, for the general case of the Cantor set, the point $\vec{\eta}^{\max M}$ of the highest measure is indeed determined by the equation

$$\left.\frac{\partial D(\alpha)}{\partial \alpha}\right|_{\alpha^{\max M}} = 1. \tag{1.123}$$

A somewhat similar situation we have already seen for the case of the point $\vec{\eta}^{\max D}$ of the highest dimension (1.58–1.60); only in that case the point was determined by equation

$$\left.\frac{\partial D(\alpha)}{\partial \alpha}\right|_{\alpha^{\max D}} = 0. \tag{1.124}$$

1.7.6 Analogy with Statistical Physics

Let us look one more time at the measure of a branch $p_1^{\xi_1} \ldots p_K^{\xi_K}$. We can rewrite this expression as

$$e^{-\xi_1 \ln \frac{1}{p_1}} \ldots e^{-\xi_K \ln \frac{1}{p_K}}. \tag{1.125}$$

This expression closely resembles Gibbs probability in statistical physics, especially if we consider each branch to be a particular microstate and introduce *effective temperatures*

$$\Theta_1 = \ln^{-1} \frac{1}{p_1}, \ldots, \Theta_K = \ln^{-1} \frac{1}{p_K}. \tag{1.126}$$

Then the measure of a subset $\vec{\eta}$ becomes the partial partition function (see Chap. 2)

$$M(\vec{\eta}) = \frac{n!}{\xi_1! \ldots \xi_K!} e^{-\frac{\xi_1}{\Theta_1}} \ldots e^{-\frac{\xi_K}{\Theta_K}} \tag{1.127}$$

while the measure of the whole prefractal—the total partition function

$$M = \sum_{\substack{\xi_1, \ldots, \xi_K = 0: \\ \xi_1 + \ldots + \xi_K = n}}^{n} \frac{n!}{\xi_1! \ldots \xi_K!} e^{-\frac{\xi_1}{\Theta_1}} \ldots e^{-\frac{\xi_K}{\Theta_K}}. \tag{1.128}$$

After the introduction of this similarity with statistical physics, all approaches of the next chapter become applicable. For example, we can introduce the action of the free energy of a multifractal as the minus logarithm of the partial partition function:

$$A_{\{\{\vec{\eta}\}\}} \equiv -\ln M(\vec{\eta}) = -\ln \frac{n!}{\xi_1!\ldots\xi_K!} e^{-\frac{\xi_1}{\Theta_1}} \ldots e^{-\frac{\xi_K}{\Theta_K}}. \qquad (1.129)$$

Obviously, minimization of the action functional leads us to the subset $\vec{\eta}^{\max M}$ with the highest measure.

All other methods of Chap. 2 can be easily generalized for the case of multifractals as well; however, we will not present the formulae here, leaving their development to the reader.

1.7.7 Subsets $\vec{\eta}$ Versus Subsets α

At the end of this section, we discuss the question why the subsets in terms of the Lipschitz–Hölder exponents α do not correspond to the subsets in terms of vectors $\vec{\eta}$. The simplest example would be a multifractal whose generator has coinciding scale factors, $r_i = r_j$, and coinciding measure distribution factors, $p_i = p_j$, for two different branches, $i \neq j$. Going l times through the i^{th} branch and m times through the j^{th} branch of the generator, we would create the same Lipschitz–Hölder exponent as if we were going m times through the i^{th} branch and l times through the j^{th} branch of the generator. The Lipschitz–Hölder exponent is the same but the vectors $\vec{\eta}$ are different. Therefore, the connection between α and $\vec{\eta}$ is not bijective—many vectors $\vec{\eta}$ can correspond to the same value of α.

The example above is trivial; and, having such a multifractal, we could analytically unite subsets of different vectors $\vec{\eta}$, corresponding to the same value of α, into one subset. However, there are trickier situations. Let us consider a generator with $p_i = 1/4$, $p_j = 1/9$, $r_i = 1/2$, and $r_j = 1/3$. For an arbitrary iteration n we consider a branch that has been formed by path $\ldots,\xi_i = 1,\ldots,\xi_j = 0,\ldots$ The measure of this branch is $\ldots\left(\frac{1}{4}\right)^1\ldots\left(\frac{1}{9}\right)^0\ldots$ and the length is $\ldots\left(\frac{1}{2}\right)^1\ldots\left(\frac{1}{3}\right)^0\ldots$ The Lipschitz–Hölder exponent of this branch (taking into account only the known multipliers) is $\alpha = 2$.

Now, let us consider another path $\ldots,\xi_i = 0,\ldots,\xi_j = 1,\ldots$ The measure of the branch is $\ldots\left(\frac{1}{4}\right)^0\ldots\left(\frac{1}{9}\right)^1\ldots$ while its length is $\ldots\left(\frac{1}{2}\right)^0\ldots\left(\frac{1}{3}\right)^1\ldots$ The Lipschitz–Hölder exponent of this branch is again $\alpha = 2$. And the connection between α and $\vec{\eta}$ is again not bijective.

We have built subsets in terms of different vectors $\vec{\eta}$ only because this provided preliminary intuitive understanding of multifractals. In reality, following the definition of a multifractal, we had to build subsets in terms of different Lipschitz–Hölder exponents α.

1.7.8 Summary

Summarizing, in this section we have considered several examples of multifractals. Also, we have introduced the concept of the Lipschitz–Hölder exponent whose values allowed us to divide the total set into subsets. We have studied the properties of these separate subsets and found the distributions of subsets' dimensions, lengths, and measures.

Now, we see that the properties of multifractals are determined by the "clash" of two phenomena: the geometry of daughter branches and the measure distribution among the daughter branches. The larger the size of a branch, the lower is its Lipschitz–Hölder exponent. The higher the measure of a branch, the higher is its Lipschitz–Hölder exponent. This "tug of war" over the value of the Lipschitz–Hölder exponent leads to the separation of the mathematical set into fractal subsets with different properties.

Also, we saw that there is no bijective connection between vectors $\vec{\eta}$ and Lipschitz–Hölder exponents α. It could be convenient to work with vectors $\vec{\eta}$; however, to study the multifractal, we will have to transform finally subsets $\vec{\eta}$ into subsets α.

Of course, this is only a matter of definition—to investigate the properties of subsets α instead of subsets $\vec{\eta}$. But, again, the reader should always remember that, generally speaking, the subsets of multifractals are always determined by different values of the Lipschitz–Hölder exponents α. If one builds subsets by different vectors $\vec{\eta}$, she/he, rigorously speaking, is investigating not multifractals.

1.8 The General Formalism of Multifractals

In the previous section, we considered several examples of multifractals and began to understand intuitively what the multifractals are. In this section, we study the general formalism.

We consider a developed multifractal and cover it by boxes of size ε. For example, we can divide the embedding space into cells of volume ε^{d_0}, where d_0 is the dimension of the embedding space. Then we count only those boxes that have caught something from the set and disregard empty boxes.

We will enumerate nonempty boxes by index i. Integrating the measure over each box, we denote the measure, contained by box i, as μ_i. Since the measure is conserved, we always have

$$M = \sum_{i=1}^{N(\varepsilon)} \mu_i = 1, \tag{1.130}$$

where $N(\varepsilon)$ is the number of nonempty boxes, covering the multifractal.

For each box *i,* we introduce *the Lipschitz–Hölder exponent* α_i by the following definition:

$$\mu_i = \varepsilon^{\alpha_i}. \tag{1.131}$$

Let us divide the initial mathematical set into subsets, corresponding to different values of the Lipschitz–Hölder exponent. In other words, having found for each box *i* its Lipschitz–Hölder exponent α_i, we gather into a subset α all boxes whose Lipschitz–Hölder exponents α_i correspond to the given value α. Then, in accordance with (1.131), the boxes of the subset α contain all the same measure $\mu_{i\in\alpha} = \varepsilon^{\alpha}$.

Firstly, we should understand how many different subsets are there. Let us imagine that we investigate the properties of the multifractal experimentally. So, we literally divide the embedding space into cells and experimentally calculate the measure within each box. How then we unite boxes into subsets? For example, if the Lipschitz–Hölder exponent of one box is $\alpha = 1.00000$ while the Lipschitz–Hölder exponent of another box is $\alpha = 1.00001$, do these boxes belong to one subset or to two different subsets?

If we are working experimentally, we generally divide the range of possible values of α into a set of intervals (bins). Each interval then represents a particular subset whose boxes possess the Lipschitz–Hölder exponents with values from this interval. Further, we assume that the number of intervals is a power-law dependence $\underline{\underline{O}}\left(\ln^{\varphi}\frac{1}{\varepsilon}\right)$ on $\ln\frac{1}{\varepsilon}$ in the limit (1.9).

The whole set is covered by $N(\varepsilon)$ boxes while only some of them are boxes, covering the subset α . If we denote the number of boxes, covering the subset α, by $N_\alpha(\varepsilon)$, then the total number $N(\varepsilon)$ of boxes should equal the sum of numbers of boxes, covering different subsets:

$$N(\varepsilon) = \sum_{\alpha} N_\alpha(\varepsilon). \tag{1.132}$$

Following the box counting method (1.8), the dimension of the whole multifractal is determined by

$$N(\varepsilon) \propto \frac{1}{\varepsilon^{D}} \tag{1.133}$$

while the dimension of a subset α is determined by

$$N_\alpha(\varepsilon) \propto \frac{1}{\varepsilon^{D(\alpha)}}. \tag{1.134}$$

Only this time, we will look at these proportionalities from a different point of view. These proportionalities are valid in the limit $\varepsilon \to +0$ or, more rigorously, in the limit (1.9):

$$\ln\frac{1}{\varepsilon} \to +\infty. \tag{1.135}$$

"Tossing" ε into the exponents, we rewrite proportionalities (1.133 and 1.134) as

$$N(\varepsilon) \propto e^{D\ln\frac{1}{\varepsilon}}, \tag{1.136}$$

$$N_\alpha(\varepsilon) \propto e^{D(\alpha)\ln\frac{1}{\varepsilon}}. \tag{1.137}$$

In the right-hand sides of these proportionalities, we see exponential dependencies on $\ln\frac{1}{\varepsilon}$ which is infinite in the limit $\ln\frac{1}{\varepsilon} \to +\infty$. The exponential dependence on an infinite parameter suggests the applicability of logarithmic accuracy:

$$N(\varepsilon) = e^{D\ln\frac{1}{\varepsilon}} \underline{\underline{O}}\left(\ln^{\varphi}\frac{1}{\varepsilon}\right) \approx_{\ln} e^{D\ln\frac{1}{\varepsilon}}, \tag{1.140}$$

$$N_\alpha(\varepsilon) = e^{D(\alpha)\ln\frac{1}{\varepsilon}} \underline{\underline{O}}\left(\ln^{\varphi}\frac{1}{\varepsilon}\right) \approx_{\ln} e^{D(\alpha)\ln\frac{1}{\varepsilon}}. \tag{1.141}$$

However, an equality valid with logarithmic accuracy is not equivalent to a proportionality. A proportionality means that only a constant of proportionality is omitted:

$$f(\varepsilon) = const \cdot g(\varepsilon) \propto g(\varepsilon), \tag{1.142}$$

while an equality valid with logarithmic accuracy means that omitted is a power-law dependence:

$$f(\varepsilon) = g(\varepsilon)\underline{\underline{O}}\left(\ln^{\varphi}\frac{1}{\varepsilon}\right) \approx_{\ln} g(\varepsilon). \tag{1.143}$$

What should we choose for further discussions: strict proportionalities (1.136 and 1.137) or more general equalities (1.140 and 1.141)? If we considered the mathematically rigorous division of the multifractal into subsets (when $\alpha = 1.00000$ and $\alpha = 1.00001$ always meant two different subsets), then we could apply rigorous proportionality dependences (1.136 and 1.137). However, instead, we have divided the range of possible values of α into a set of intervals. The width of these intervals was, in fact, arbitrary; we only require that the number of the intervals should be a power-law dependence $\underline{\underline{O}}\left(\ln^{\varphi}\frac{1}{\varepsilon}\right)$ on $\ln\frac{1}{\varepsilon}$.

Why did not we specify more detailed information about the procedure of how we choose the length of intervals of α? Because this information is not required for the formalism to work. Indeed, suppose we choose intervals twice larger than before, what would happen? Instead of $N_\alpha(\varepsilon)$ boxes, there are now $\tilde{N}_\alpha(\varepsilon) = 2N_\alpha(\varepsilon)$

boxes corresponding to the subset α. But this does not influence equality (1.141) because the multiplier 2 will be neglected by the logarithmic accuracy:

$$\tilde{N}_\alpha(\varepsilon) = 2e^{D(\alpha)\ln\frac{1}{\varepsilon}} \underline{\underline{O}}\left(\ln^\varphi \frac{1}{\varepsilon}\right) \approx_{\ln} e^{D(\alpha)\ln\frac{1}{\varepsilon}}. \tag{1.144}$$

Even if we chose the length of the intervals $\underline{\underline{O}}\left(\ln^\varphi \frac{1}{\varepsilon}\right)$ times larger (infinite (!) number of times larger in the limit (1.135)), the logarithmic accuracy would still disguise the difference!

We see now that the logarithmic accuracy is the corner stone of the whole formalism. It allows us to choose the width of the intervals of α almost arbitrarily. It allows us to neglect all complex power-law dependencies in comparison with the exponential dependencies. It allows us to equate sums to their maximal terms. And so on. Without logarithmic accuracy, the general formalism could be impossible. And this is true not only for multifractals but also for many other systems as we will see in the following chapters.

Summarizing, since the choice of the width of the intervals of α was arbitrary, we cannot apply strict mathematical proportionality (1.137). Instead, we have to utilize less strict (1.141):

$$N_\alpha(\varepsilon) = e^{D(\alpha)\ln\frac{1}{\varepsilon}} \underline{\underline{O}}\left(\ln^\varphi \frac{1}{\varepsilon}\right) \approx_{\ln} e^{D(\alpha)\ln\frac{1}{\varepsilon}} \text{ or} \tag{1.145}$$

$$N_\alpha(\varepsilon) \approx_{\ln} \frac{1}{\varepsilon^{D(\alpha)}}. \tag{1.146}$$

However, the loss of strictness will be only to our benefit because it simplifies all further formulae.

Let us see how. The subset $\alpha^{\max D}$ with the highest dimension is, obviously, determined by

$$\left.\frac{\partial D(\alpha)}{\partial \alpha}\right|_{\alpha^{\max D}} = 0 \tag{1.147}$$

which is analogous to (1.124). But in accordance with (1.132), $N(\varepsilon)$ is the sum of $N_\alpha(\varepsilon)$. Substituting (1.140) and (1.146) into (1.132), we find

$$\frac{1}{\varepsilon^D} \approx_{\ln} \sum_\alpha \frac{1}{\varepsilon^{D(\alpha)}} \text{ or } e^{D\ln\frac{1}{\varepsilon}} \approx_{\ln} \sum_\alpha e^{D(\alpha)\ln\frac{1}{\varepsilon}}. \tag{1.148}$$

The left- and the right-hand sides of this equality are "fast" exponential dependences on $\ln\frac{1}{\varepsilon} \to +\infty$ while the number of significant terms in the sum $\sum_\alpha$, over

which the sum gathers its main value, is a power-law dependence on $\ln\frac{1}{\varepsilon}$. Therefore, we can approximate the sum by its maximal term and neglect the power-law dependence on $\ln\frac{1}{\varepsilon}$:

$$\frac{1}{\varepsilon^D} \approx_{\ln} \max_\alpha \frac{1}{\varepsilon^{D(\alpha)}} \text{ or } e^{D\ln\frac{1}{\varepsilon}} \approx_{\ln} \max_\alpha e^{D(\alpha)\ln\frac{1}{\varepsilon}}. \tag{1.149}$$

Since the maximal term is provided by (1.147), we find

$$\frac{1}{\varepsilon^D} \approx_{\ln} \frac{1}{\varepsilon^{D(\alpha^{\max D})}} \text{ or } e^{D\ln\frac{1}{\varepsilon}} \approx_{\ln} e^{D(\alpha^{\max D})\ln\frac{1}{\varepsilon}}. \tag{1.150}$$

Taking the logarithm of this equation, we prove that the highest dimension among the subsets belongs to the subset, determined by condition (1.147), and equals the dimension D of the whole multifractal:

$$D(\alpha^{\max D}) \approx D. \tag{1.151}$$

For the total measure of the whole multifractal we find

$$M = \sum_\alpha M(\alpha) = 1. \tag{1.152}$$

Since all boxes of a subset α possess the same value of measure $\mu_{i\in\alpha} = \varepsilon^\alpha$, the measure of the whole subset α is

$$M(\alpha) = N_\alpha(\varepsilon)\varepsilon^\alpha \approx_{\ln} \varepsilon^{\alpha - D(\alpha)}. \tag{1.153}$$

The subset $\alpha^{\max M}$ with the highest measure is determined by

$$\left.\frac{\partial \ln M(\alpha)}{\partial \alpha}\right|_{\alpha^{\max M}} = 0 \text{ or } \left.\frac{dD(\alpha)}{d\alpha}\right|_{\alpha^{\max M}} = 1 \tag{1.154}$$

which is analogous to (1.123).

From (1.153), we see that the subsets' measures $M(\alpha)$ depend exponentially on $\ln\frac{1}{\varepsilon}$ while the number of significant terms in the sum (1.152), over which the sum gathers its unity value, is a power-law dependence on $\ln\frac{1}{\varepsilon}$ (recall (1.101–1.105)). Neglecting all power-law dependencies, the total sum (1.152) is equal with logarithmic accuracy to its maximal term:

$$M \approx_{\ln} M(\alpha^{\max M}). \tag{1.155}$$

Since $M = 1$, (1.155) states that

$$1 \approx_{\ln} N_{\alpha^{\max M}}(\varepsilon)\varepsilon^{\alpha^{\max M}} \quad \text{or} \tag{1.156a}$$

$$1 \approx_{\ln} \varepsilon^{\alpha^{\max M} - D(\alpha^{\max M})} = e^{\left\{D(\alpha^{\max M}) - \alpha^{\max M}\right\} \ln \frac{1}{\varepsilon}}. \tag{1.156b}$$

In the limit (1.135) this is possible only if

$$N_{\alpha^{\max M}}(\varepsilon) \approx_{\ln} \varepsilon^{-\alpha^{\max M}} \quad \text{and} \tag{1.157a}$$

$$\alpha^{\max M} \approx D(\alpha^{\max M}). \tag{1.157b}$$

Next, we find the second derivative of $M(\alpha)$ at the point $\alpha^{\max M}$ of the maximum by differentiating (1.153):

$$\left.\frac{\partial^2 \ln M(\alpha)}{\partial \alpha^2}\right|_{\alpha^{\max M}} \approx \left.\frac{\partial^2 D(\alpha)}{\partial \alpha^2}\right|_{\alpha^{\max M}} \ln \frac{1}{\varepsilon}. \tag{1.158}$$

Substituting the first derivative (1.154) and the second derivative (1.158) into the expansion of $\ln M(\alpha)$,

$$\begin{aligned} \ln M(\alpha) = \ln M(\alpha^{\max M}) &+ \left.\frac{\partial \ln M(\alpha)}{\partial \alpha}\right|_{\alpha^{\max M}} \left(\alpha - \alpha^{\max M}\right) \\ &+ \frac{1}{2} \left.\frac{\partial^2 \ln M(\alpha)}{\partial \alpha^2}\right|_{\alpha^{\max M}} \left(\alpha - \alpha^{\max M}\right)^2 + \ldots, \end{aligned} \tag{1.159}$$

and exponentiating, we return to the Gaussian distribution:

$$M(\alpha) \propto e^{\frac{1}{2}\left.\frac{\partial^2 D(\alpha)}{\partial \alpha^2}\right|_{\alpha^{\max M}} \ln \frac{1}{\varepsilon}\left(\alpha - \alpha^{\max M}\right)^2}. \tag{1.160}$$

The width of the maximum is

$$\delta\alpha \propto \frac{1}{\sqrt{\ln \frac{1}{\varepsilon}}} \tag{1.161}$$

which is very small in the limit (1.135).

Let us now calculate *Gibbs–Shannon entropy* (Gibbs 1876, 1878; Shannon 1948) of the multifractal:

$$S^{MF} \equiv -\sum_{i=1}^{N(\varepsilon)} \mu_i \ln \mu_i. \tag{1.162}$$

We should mention that in contrast to the previous section as microstates, we consider here not the separate branches of the prefractal but separate nonempty boxes covering the developed multifractal.

Substituting (1.131) into the logarithm in (1.162), we find

$$S^{MF} = \ln\left(\frac{1}{\varepsilon}\right) \sum_{i=1}^{N(\varepsilon)} \mu_i \alpha_i. \tag{1.163}$$

The obtained equality represents averaging of the Lipschitz–Hölder exponent with the measure distribution:

$$S^{MF} = \ln\left(\frac{1}{\varepsilon}\right) \langle \alpha \rangle_\mu, \tag{1.164}$$

where

$$\langle \alpha \rangle_\mu \equiv \sum_{i=1}^{N(\varepsilon)} \mu_i \alpha_i. \tag{1.165}$$

Let us rewrite the definition of averaging (1.165) as the sum not over boxes but over subsets:

$$\langle \alpha \rangle_\mu = \sum_{\alpha} N_\alpha(\varepsilon) \varepsilon^\alpha \alpha. \tag{1.166}$$

Here, the first two dependencies under the sign of the sum, $N_\alpha(\varepsilon) \approx_{\ln} e^{D(\alpha)\ln\frac{1}{\varepsilon}}$ and $\varepsilon^\alpha = e^{-\alpha \ln\frac{1}{\varepsilon}}$, are very "fast" dependencies on α because of the parameter $\ln\frac{1}{\varepsilon}$ in the exponent. The product $N_\alpha(\varepsilon)\varepsilon^\alpha$ of these dependencies is the measure $M(\alpha)$ of the subset α which has the very narrow maximum (1.160).

In contrast, the third dependence α is rather "slow" in comparison with the other dependencies. Therefore, the product $N_\alpha(\varepsilon)\varepsilon^\alpha$ acts for this "slow" dependence as a δ-function. All the more so that in accordance with (1.152), the sum $\sum_{\alpha} N_\alpha(\varepsilon)\varepsilon^\alpha$ is normalized to unity. So, we expect the averaged α to be equal to the point of maximum $\alpha^{\max M}$:

$$\langle \alpha \rangle_\mu \approx \alpha^{\max M}. \tag{1.167}$$

Let us now prove this statement. The width of the maximum is provided by (1.161). Sum (1.166) gathers its main value under the "bell" of the maximum; and we can neglect other terms. Under the "bell" of the maximum, the "slow" dependence α equals

$$\alpha = \alpha^{\max M} + \underline{\underline{O}}\left(1/\sqrt{\ln 1/\varepsilon}\right). \tag{1.168}$$

Substituting it into (1.166), we find

$$\langle\alpha\rangle_\mu = \left\{\alpha^{\max M} + \underline{\underline{O}}\left(1/\sqrt{\ln 1/\varepsilon}\right)\right\}\sum_\alpha N_\alpha(\varepsilon)\varepsilon^\alpha = \alpha^{\max M} + \underline{\underline{O}}\left(1/\sqrt{\ln 1/\varepsilon}\right) \tag{1.169}$$

which proves (1.167) in the limit (1.135).

Substituting (1.167) into (1.164), for the entropy of the multifractal we find:

$$S^{MF} = \ln\left(\frac{1}{\varepsilon}\right)\alpha^{\max M}. \tag{1.170}$$

1.9 Moments of the Measure Distribution

Next, we introduce *the moments* of the measure distribution:

$$M_q(\varepsilon) \equiv \sum_{i=1}^{N(\varepsilon)} \mu_i{}^q. \tag{1.171}$$

In other words, we sum over all (nonempty) boxes the q^{th}-power of box' measure (Sinai 1972; Bowen 1975; Ruelle 1978). Here, q should be considered to be just a parameter whose values might not correspond to a physical property of the system.

For the zeroth moment ($q = 0$) from (1.171), we find

$$M_0(\varepsilon) \equiv \sum_{i=1}^{N(\varepsilon)} 1 = N(\varepsilon) \approx_{\ln} \frac{1}{\varepsilon^D} \tag{1.172}$$

while for the first moment ($q = 1$):

$$M_1(\varepsilon) \equiv \sum_{i=1}^{N(\varepsilon)} \mu_i = 1. \tag{1.173}$$

We assume that all moments depend exponentially on $\ln\dfrac{1}{\varepsilon}$, similar to dependencies (1.140 and 1.141):

$$M_q(\varepsilon) \propto \varepsilon^{(q-1)\Delta_q}. \tag{1.174}$$

Parameters Δ_q here are called *the q^{th}-order generalized dimensions* (Grassberger 1983; Hentschel and Procaccia 1983; Grassberger and Procaccia 1983). The reader should understand that these parameters may not correspond to any physical dimensions really present in the system. Therefore, we have utilized letter Δ instead of letter D to emphasize this.

The multiplier $(q-1)$ in the exponent of (1.174) is just a matter of definition and was introduced to guarantee that for the case of the first moment ($q=1$) equality (1.173), representing the law of conservation of measure, will be always valid. Besides, if we distribute measure evenly over a classical nonfractal set (like a surface), measure μ_i is the same for all boxes, $\mu_i = \dfrac{1}{N(\varepsilon)}$, while q^{th}-moment (1.171) transforms into $M_q(\varepsilon) = \dfrac{N(\varepsilon)}{N^q(\varepsilon)} = N^{1-q}(\varepsilon)$. Substituting (1.2b) into this equality, $M_q(\varepsilon) \propto \varepsilon^{(q-1)D}$, and comparing the result with (1.174), we see that the multiplier $(q-1)$ has also been chosen for the purpose that all q^{th}-order generalized dimensions coincide with the dimension of the classical set with evenly distributed measure.

Comparing (1.174) with (1.172), we see that

$$\Delta_0 = D. \tag{1.175}$$

The moments introduced by (1.171) are often called also the *generating functions*, or *partition functions*, or *statistical sums*. There are so many names due to the importance of the role played by these quantities.

Indeed, let us transform sum (1.171) over boxes into the sum over the subsets α :

$$M_q(\varepsilon) = \sum_{\alpha} N_\alpha(\varepsilon)\varepsilon^{q\alpha}. \tag{1.176}$$

This expression is very similar to the partition function of the canonical ensemble:

$$Z^{CE} = \sum_{E} g_E e^{-E/T^{res}}, \tag{1.177}$$

Indeed, if we thought of boxes as of microstates and of Lipschitz–Hölder exponent α—as of the negative energy of these microstates, then the subset α would seem to play the role of a group of microstates, corresponding to the given value of energy. And $N_\alpha(\varepsilon)$ would be g_E—the statistical weight of energy level E (the number of microstates corresponding to the given value of energy) while parameter q—the inverse temperature of the system.

Due to this analogy, the moments are often called the partition functions. However, the reader should clearly understand the difference between (1.176) and (1.177). In statistical physics, $e^{-E/T^{res}}$ represents the probability of a microstate while $\varepsilon^{q\alpha}$ is not the measure of a microstate but the q^{th}-power of that measure. Therefore, although the mathematics is very similar, the concepts behind it are not.

Since all moments depend exponentially on $\ln\frac{1}{\varepsilon}$, we expect that sum (1.176) is equal to its maximal term:

$$M_q(\varepsilon) \approx_{\ln} N_{\alpha^{\max M_q}(q)}(\varepsilon)\varepsilon^{q\alpha^{\max M_q}(q)}, \tag{1.178}$$

where the point of maximum $\alpha^{\max M_q}(q)$ is determined by

$$\left.\frac{\partial(N_\alpha(\varepsilon)\varepsilon^{q\alpha})}{\partial\alpha}\right|_{\alpha^{\max M_q}} = 0 \text{ or } \left.\frac{\partial\ln(N_\alpha(\varepsilon)\varepsilon^{q\alpha})}{\partial\alpha}\right|_{\alpha^{\max M_q}} = 0. \tag{1.179}$$

Substituting (1.146) into (1.179), we find equality

$$\left.\frac{\partial\ln\varepsilon^{q\alpha-D(\alpha)}}{\partial\alpha}\right|_{\alpha^{\max M_q}} = 0 \text{ or } \left.\frac{\partial D(\alpha)}{\partial\alpha}\right|_{\alpha^{\max M_q}} = q \tag{1.180}$$

which determines the point $\alpha^{\max M_q}(q)$ of the maximum.

For the q^{th}-moment we have introduced the q^{th}-order generalized dimension (1.174). Substituting (1.178) and (1.146) into (1.174), we find the connection between the subsets' dimensions $D(\alpha)$ and the generalized dimensions Δ_q:

$$q\alpha^{\max M_q}(q) - D(\alpha^{\max M_q}) = (q-1)\Delta_q. \tag{1.181}$$

Differentiating the left-hand side of this equality, we find

$$\begin{aligned}&\frac{d}{dq}\left\{q\alpha^{\max M_q}(q) - D(\alpha^{\max M_q})\right\}\\ &= \alpha^{\max M_q} + q\frac{d\alpha^{\max M_q}}{dq} - \left.\frac{\partial D(\alpha)}{\partial\alpha}\right|_{\alpha^{\max M_q}}\frac{d\alpha^{\max M_q}}{dq} = \alpha^{\max M_q},\end{aligned} \tag{1.182}$$

where in the last equality we have cancelled two last terms in accordance with (1.180). Therefore, $\alpha^{\max M_q}$ can be found as the derivative of the right-hand side of (1.181):

$$\alpha^{\max M_q}(q) = \frac{d}{dq}\left\{(q-1)\Delta_q\right\}. \tag{1.183}$$

If we know the dependence $\Delta_q(q)$, we substitute it into (1.183) to find the dependence $\alpha^{\max M_q}(q)$. Inverting, in turn, the last functional dependence $q(\alpha^{\max M_q})$ and

substituting it into (1.181), we find the dependence $D(\alpha)$. So, knowing $\Delta_q(q)$, we can find $D(\alpha)$. And vice versa, knowing $D(\alpha)$, we can find $\Delta_q(q)$. Both dependences can be investigated experimentally, and having found one of them, we immediately obtain another (Halsey et al. 1986).

For the first moment from (1.181), we find

$$\alpha^{\max M_1}(1) = D(\alpha^{\max M_1}) \tag{1.184}$$

which coincides with (1.157b). Substituting $q = 1$ into (1.183), we obtain

$$\alpha^{\max M_1}(1) = \Delta_1. \tag{1.185}$$

Let us now find the generalized dimensions with the aid of self-similarity. We consider an arbitrary case of a multifractal whose generator has K branches with scale factors $r_1,...,r_K$ and measure distribution factors $p_1,...,p_K$.

We cover the whole developed set with boxes of infinitesimal size ε. Let $N(\varepsilon)$ be the total number of boxes required.

Next, we consider a branch i of the first iteration $n = 1$. Further development of this branch is similar to the set in whole and can be covered by the same number of boxes but with the reduced size εr_i:

$$N_{branch\,i}(\varepsilon r_i) = N(\varepsilon). \tag{1.186}$$

The share of measure, inherited by the branch, is p_i. This means that the distribution of measure for further development of this branch is similar to the measure distribution of the whole multifractal, only the branch starts with measure p_i in contrast to 1 in the case of the total set (the generator creates the same distribution but with the different initial value). So, each box of size εr_i, covering the branch, possesses measure p_i times lower than the corresponding box of size ε, covering the whole multifractal:

$$\mu(\varepsilon r_i) = p_i \mu(\varepsilon). \tag{1.187}$$

For the q^{th}-moment of the whole multifractal, covered by boxes of size ε, we have

$$M_q(\varepsilon) \equiv \sum_{j=1}^{N(\varepsilon)} \mu_j{}^q(\varepsilon) \tag{1.188}$$

while for the branch i valid is

$$M_q^{branch\,i}(\varepsilon r_i) \equiv \sum_{j=1}^{N_{branch\,i}(\varepsilon r_i)} \mu_j{}^q(\varepsilon r_i) = \sum_{j=1}^{N(\varepsilon)} (p_i \mu_j(\varepsilon))^q = p_i{}^q M_q(\varepsilon), \tag{1.189}$$

where we have utilized (1.186) and (1.187).

Since ε has been chosen arbitrarily, we can change the variable:

$$M_q^{branch\,i}(\varepsilon) = p_i{}^q M_q(\varepsilon / r_i). \tag{1.190}$$

Then, because after the change of the variable all branches are covered by boxes of the same size ε, summing (1.190) over all branches, we find the q^{th}-moment of the whole multifractal, covered by boxes of size ε:

$$M_q(\varepsilon) = \sum_{i=1}^{K} M_q^{branch\,i}(\varepsilon) = \sum_{i=1}^{K} p_i{}^q M_q(\varepsilon / r_i). \tag{1.191}$$

Substituting (1.174) into this equation, we find (Hentschel and Procaccia 1983; Halsey et al. 1986)

$$1 = \sum_{i=1}^{K} p_i{}^q r_i^{-(q-1)\Delta_q} \tag{1.192}$$

which provides implicitly the dependence of Δ_q on q. 0^{th}-moment ($q = 0$) returns us to (1.39) while for the first-moment ($q = 1$) from (1.192), we obtain only the trivial equality (1.44).

Knowing the dependence $\Delta_q(q)$, we can find the dependence $D(\alpha)$, as it was described above.

References

Abaimov, S.G.: Statistical Physics of Complex Systems, 2nd ed. Synergetics, Moscow (2013) (in Russian) (From Past to Future, vol. **57**, URSS)

Besicovitch, A.S.: On linear sets of points of fractional dimension. Math. Ann. **101**(1), 161–193 (1929)

Besicovitch, A.S., Ursell, H.D.: Sets of fractional dimensions. J. Lond. Math. Soc. **12**(1), 18–25 (1937)

Bouligand, G.: Ensembles impropres et nombre dimensionnel. Bull. Sci. Math. **52**, 320–344, 361–376 (1928) (Series 2)

Bowen, R.: Equilibrium States and the Ergodic Theory of Anosov Diffeomorphisms, vol. 470. Springer, New York (1975) (Lecture Notes in Mathematics)

Bunde, A., Havlin, S. (eds.): Fractals in Science. Springer, Berlin (1994)

Bunde, A., Havlin, S. (eds.): Fractals and Disordered Systems, 2nd ed. Springer. Berlin (1996)

Cantor, G.: Ueber unendliche, lineare punktmannichfaltigkeiten. Math. Ann. **21**, 545–591 (1883)

Falconer, K.: Fractal Geometry: Mathematical Foundations and Applications, 2nd ed. Wiley, Chichester (2003)

Feder, J.: Fractals. Physics of Solids and Liquids. Springer, New York (1988)

Gibbs, J.W.: On the equilibrium of heterogeneous substances. Trans. Conn. Acad. **3**, 108 (1876)

Gibbs, J.W.: On the equilibrium of heterogeneous substances. Trans. Conn. Acad. **3**, 343 (1878)

Grassberger, P.: Generalized dimensions of strange attractors. Phys. Lett. A **97**(6), 227–230 (1983)

Grassberger, P., Procaccia, I.: Measuring the strangeness of strange attractors. Physica D **9**(1–2), 189–208 (1983)
Halsey, T.C., Jensen, M.H., Kadanoff, L.P., Procaccia, I., Shraiman, B.I.: Fractal measures and their singularities: The characterization of strange sets. Phys. Rev. A **33**(2), 1141–1151 (1986)
Hausdorff, F.: Dimension und äußeres maß. Math. Ann. **79**(1–2), 157–179 (1918)
Hentschel, H.G.E., Procaccia, I.: The infinite number of generalized dimensions of fractals and strange attractors. Physica D **8**(3), 435–444 (1983)
Hölder, O.: Beiträge zur Potentialtheorie. University of Tübingen (1882)
von Koch, H.: Sur une courbe continue sans tangente, obtenue par une construction géométrique élémetaire. Ark. Mat. Astr. Phys. **1**, 681–702 (1904)
Kolmogorov, A.: A new invariant for transitive dynamical systems. Doklady Akademii Nauk SSSR **119**, 861 (1958)
Lipschitz, R.: Lehrbuch der Analysis. Grundlagen der Analysis, vol. **1–2**. Verlag von Max Cohen & Sohn (Fr. Cohen), Bonn (1877–1880)
Mandelbrot, B.B.: Possible refinement of the lognormal hypothesis concerning the distribution of energy dissipation in intermittent turbulence. In: Rosenblatt, M., Van Atta, C. (eds.) Statistical Models and Turbulence, vol. **12**, pp. 333–351. Springer, New York (1972) (Lecture Notes in Physics)
Mandelbrot, B.B.: Intermittent turbulence in self-similar cascades: Divergence of high moments and dimension of the carrier. J. Fluid Mech. **62**(02), 331–358 (1974)
Mandelbrot, B.B.: Fractals: Form, Chance and Dimension. W.H. Freeman & Co, San Francisco (1975)
Mandelbrot, B.B.: The Fractal Geometry of Nature. W.H. Freeman & Co, San Francisco (1982)
Mandelbrot, B.B., Given, J.A.: Physical properties of a new fractal model of percolations clusters. Phys. Rev. Lett. **52**, 1853 (1984)
Ruelle, D.: Thermodynamic Formalism, vol. **5**. Encyclopedia of Mathematics and its Applications. Addison-Wesley, Reading (1978)
Shannon, C.E.: A mathematical theory of communication. Bell Sys. Tech. J. **27**, 379–423, 623–656 (1948)
Sierpiński, W.: Sur une courbe dont tout point est un point de ramification. C.R. Hebd. Sea. Acad. Sci., Paris **160**, 302–305 (1915)
Sierpiński, W.: Sur une courbe *cantor*ienne qui contient une image biunivoque et continue de toute courbe donnée. C.R. Hebd. Sea. Acad. Sci., Paris **162**, 629–632 (1916)
Sinai, Y.G.: Gibbs Measures in Ergodic Theory. Russ. Math. Surv. **27**, 21 (1972)
Smith, H.J.S.: On the integration of the discontinuous functions. Proc. Lond. Math. Soc. **6**, 140–153 (1874) (Series 1)
Vicsek, T.: Fractal Growth Phenomena, 2nd ed. World Scientific, Singapore (1992)

Chapter 2
Ensemble Theory in Statistical Physics: Free Energy Potential

Abstract In this chapter, we discuss the basic formalism of statistical physics. Also, we consider in detail the concept of the free energy potential.

Similar to Chap. 1, this chapter is a prerequisite. As required for further discussions, we consider understanding of the free energy concept, its connection with the probability of fluctuations,

$$W_{fluctuation}^{ensemble} = e^{\frac{\Psi^{equilibrium} - \Psi_{fluctuation}}{T^{res}}}, \tag{2.1}$$

and with the partial partition function,

$$\Psi_{fluctuation} = -T^{res} \ln Z_{fluctuation}. \tag{2.2}$$

The reader who is proficient in these concepts may skip this chapter.

Since the purpose of this chapter is to refresh in memory the class studied by students only 1 or 2 quarters ago, we generally avoid rigorous discussions or mathematical proofs. Instead, we illustrate the formalism by simple examples and multiple figures. This provides intuitive understanding of all concepts discussed in the following chapters and simultaneously introduces terminology utilized in the following discussions.

For the reader not familiar with statistical physics, we recommend to follow thoroughly all the formulae below because the chapter has been developed to serve as a "guide" to basic concepts of statistical physics. Although we consider the discussions presented here to be sufficient for understanding of the following results, for further study we refer the reader to brilliant textbooks, e.g., Landau and Lifshitz (1980).

2.1 Basic Definitions

Statistical physics studies systems with high number of degrees of freedom. A classical example is a gas, 1 mol of which contains $N_A \propto 6 \cdot 10^{23}$ particles, where N_A is *the Avogadro constant*. This is important because many results in statistical

S. G. Abaimov, *Statistical Physics of Non-Thermal Phase Transitions,*
Springer Series in Synergetics, DOI 10.1007/978-3-319-12469-8_2

physics are valid only when the number of degrees of freedom is infinite: $N \to +\infty$. This limit is called *the thermodynamic limit of infinite number of degrees of freedom* or, simply, *the thermodynamic limit*.

A system is called *an ideal system* if its particles or degrees of freedom do not interact with each other. For example, *an ideal gas* is a gas with noninteracting, noncolliding particles.

However, the above definition is not completely correct because such a gas would never reach the state of thermal equilibrium. For example, if initially half of the gas particles have velocities 10 m/s while the other half have 20 m/s, and particles do not interact or collide, the gas will keep the velocities of its particles unchanged and we will never see the Maxwell–Boltzmann distribution.

Therefore, to reach the state of thermal equilibrium, there must always be present some (maybe weak but nonzero) interaction among the degrees of freedom. For example, we can modify the definition of ideal gas to be a gas whose particles can collide, but these events are extremely rare. So, observing the system for a long period of time, we will see how it evolves toward an equilibrium state. On the contrary, for short time intervals we can neglect particle collisions as improbable events and consider the system to be completely without particle interactions. Therefore, the possibility to consider the system ideal significantly depends on the duration of the time interval during which we intend to investigate the system's behavior.

Besides the interactions of particles or degrees of freedom with each other, we consider their interactions with *external fields*. An example is a magnetic system in a nonzero magnetic field h. We will always consider external fields to be supported as constant and not depending on the state of the system considered.

Constant external field is an example of *boundary conditions* imposed on a system. Other examples may include systems maintained at constant volume, pressure, temperature, etc. In particular, *an isolated system* is a system with prohibited energy and particle exchange, and maintained at constant volume: $E, V, N = const$.

If a property of a system can fluctuate for the given set of boundary conditions, we call this property the system's *fluctuating parameter*. For example, for a system maintained at constant temperature, its energy can fluctuate and is, therefore, a fluctuating parameter. If pressure is also maintained constant, another fluctuating parameter is the system's volume.

In the case when a phase transition is present in the system, the phases are distinguished by the values of fluctuating parameters. For example, for the gas–liquid phase transition at constant pressure, two phases are distinguished by the values of the volume; while for a ferromagnetic system the role of a parameter distinguishing phases is played by the system's magnetization. Such fluctuating parameters are often called *order parameters* because they describe the appearance of an order in a system below its critical point. We will discuss this definition in more detail in the following chapters.

If the property of a system is proportional to the number N of degrees of freedom in the system, we call this property *the extensive parameter* (e.g., energy, entropy, heat capacity, volume, magnetization, etc.). On the contrary, if the property of a system is not proportional to N, we call this property *the intensive parameter* (e.g., temperature, pressure, chemical potential, specific heat capacity, specific magnetization, etc.).

The last definition we should introduce is the definition of *an ensemble*. Let us investigate a particular system. If we observe the system's behavior, we see that it evolves, jumping from one state into another. If we consider, for example, gas particles when they follow their trajectories, the gas as a whole will keep moving from its current state into the next, into the next, into the next, and so on.

But instead of observing the behavior of one particular system, we can build an ensemble of systems. All systems in the ensemble are identical and differ from one another only by their initial conditions. In other words, instead of observing a chain of states $\{\ \}_1 \to \{\ \}_2 \to \{\ \}_3 \to \dots$ for one particular system, we can consider the ensemble of systems which initially are in states $\{\ \}_1, \{\ \}_2, \{\ \}_3, \dots$ *The ergodic hypothesis* claims that these two modeling techniques of the system's behavior are equivalent.

2.2 Energy Spectrum

Firstly we consider an isolated system whose Hamiltonian does not depend on time explicitly. For such a system, we find a discrete or continuous energy spectrum of *microstates* $\{E\}$ as eigenfunctions of the Hamiltonian operator. For simplicity, we consider in this chapter only discrete energy spectra although all our formulae are valid for the case of continuous spectra as well.

We make no assumptions about the structure of the spectrum, requiring only for the dependence of the spectrum density to be exponential on the number of degrees of freedom $N \to +\infty$ in the system. This requirement is valid for the majority of systems and, as we will see below, is in fact, crucial for the formalism of statistical physics.

Each eigenvalue E of the Hamiltonian (as a possible value of the system's energy) is called *an energy level*. Generally for an ideal system, many eigenfunctions $\{E\}$ correspond to the same Hamiltonian eigenvalue E. Then this energy level E is called *degenerate* while the number of microstates $\{E\}$ belonging to this eigenvalue E is called *the degeneracy g_E of this energy level*. This is schematically presented in Fig. 2.1a where microstates $\{E\}$ (shown as horizontal lines to the right) are combined into energy levels E_i (shown as horizontal lines to the left) with degeneracies g_{E_i}.

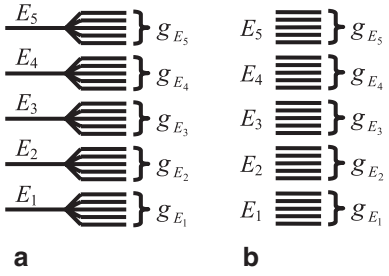

Fig. 2.1 A schematic representation of an energy spectrum. **a** Microstates are combined into energy levels E_i with degeneracies g_{E_i}. **b** Microstates are combined into groups with energies E_i and statistical weights g_{E_i}

Problem 2.2.1

Find the energy spectrum for the Ising model without spin interactions. For simplicity, assume that the model consists only of $N = 3$ spins.

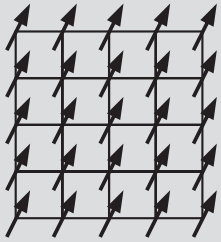

Solution: The Ising model (Ising 1925) is described in detail in Chap. 3. Here we present only the brief description of the Ising model without spin interactions which will be utilized as an example for the rest of this chapter. The model is built on the base of an absolutely rigid lattice whose geometry is currently not important. At each lattice site, a spin (a magnetic moment μ) is located. As it is known from quantum mechanics, the spin of an electron can have only two projections $\pm\frac{1}{2}$ on an axis of an external magnetic field h. In the Ising model, a spin also can have only two projections on the axis of the magnetic field h. But now these projections are chosen to be ± 1 where the multiplier 1/2 has been lost for the purpose of convenience.

Generally, we consider the lattice with N spins, where N is infinite in the thermodynamic limit: $N \to +\infty$. Let index i enumerate the sites of the lattice. If the spin at site i has projection $\sigma_i = +1$ on the axis of magnetic field, then its energy is $-\mu h$. For projection $\sigma_i = -1$, we have energy $+\mu h$. The Hamiltonian of the system equals the sum of the spin energies:

$$\mathrm{H}_{\{\sigma\}} = -\mu h \sum_{i=1}^{N} \sigma_i . \tag{2.3}$$

As we see from (2.3), the Ising model without spin interactions is nothing more than a *two-level system,* where each degree of freedom is allowed to have only two values of energy: $\varepsilon = \pm \mu h$. As an example, we utilize here the Ising model but not the two-level system with the purpose to acquaint the reader with the former.

The formulation of the model above has been oversimplified. Nevertheless, it corresponds to the rigorous formulation; we only need to put "caps" of quantum operators over the Hamiltonian and over the spins:

$$\hat{\mathrm{H}} = -\mu h \sum_{i=1}^{N} \hat{\sigma}_i. \tag{2.4}$$

Microstates $\{\sigma\}$, as the eigenfunctions of Hamiltonian (2.4), correspond to the realizations of different spin orientations on the lattice. In other words, prescribing for each spin its orientation (along the field, $\sigma_i = +1$, or against the field, $\sigma_i = -1$), we are forming a particular microstate $\{\sigma\}$ of the system.

In the case of $N = 3$ (which corresponds to the formulation of our problem), there are only eight microconfigurations $\{\sigma\}$ of spin orientations on the lattice: $\{\uparrow\uparrow\uparrow\}$, $\{\uparrow\uparrow\downarrow\}$, $\{\uparrow\downarrow\uparrow\}$, $\{\downarrow\uparrow\uparrow\}$, $\{\uparrow\downarrow\downarrow\}$, $\{\downarrow\uparrow\downarrow\}$, $\{\downarrow\downarrow\uparrow\}$, and $\{\downarrow\downarrow\downarrow\}$, where the symbol "$\uparrow$" denotes a spin oriented "up" (along the field) while the symbol "$\downarrow$" denotes a spin oriented "down" (against the field). These microconfigurations correspond to the following microstates: $\{E = -3\mu h\}$, $\{E = -\mu h\}$, $\{E = -\mu h\}$, $\{E = -\mu h\}$, $\{E = \mu h\}$, $\{E = \mu h\}$, $\{E = \mu h\}$, and $\{E = 3\mu h\}$.

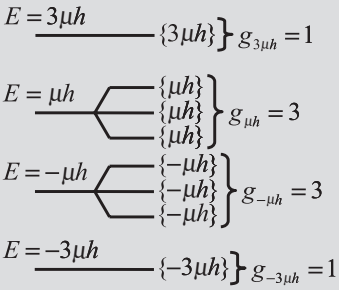

Therefore, the energy spectrum of the system consists of four energy levels. Only one microstate $\{\uparrow\uparrow\uparrow\}$ (which we have denoted as $\{-3\mu h\}$) corresponds to energy level $E = -3\mu h$. Therefore, this level is not degenerate: $g_{-3\mu h} = 1$.

Three microstates $\{\uparrow\uparrow\downarrow\}$, $\{\uparrow\downarrow\uparrow\}$, and $\{\downarrow\uparrow\uparrow\}$ (which we have denoted as $\{-\mu h\}$) correspond to energy level $E = -\mu h$, and this level has triple degeneracy: $g_{-\mu h} = 3$. And so on.

Problem 2.2.2

Find the energy spectrum for the Ising model without spin interactions. Consider the model consisting of $N = 5$ spins.

Problem 2.2.3

Find the energy spectrum for the Ising model without spin interactions. Consider the case of the model with an arbitrary number of spins N.

Solution: *Magnetization* of the system in a microstate $\{\sigma\}$ is introduced as the sum of magnetic moments over the lattice:

$$M_{\{\sigma\}} \equiv \mu \sum_{i=1}^{N} \sigma_i. \tag{2.5}$$

Dividing the magnetization by the number of spins and by the value of the magnetic moment μ, we obtain *specific magnetization*:

$$m_{\{\sigma\}} \equiv \frac{1}{N} \sum_{i=1}^{N} \sigma_i \equiv \frac{M}{N\mu}. \tag{2.6}$$

It is easy to see that in the case of the Ising model without spin interactions the energy of the system depends on its magnetization bijectively: knowing energy, we can find magnetization and vice versa:

$$\mathrm{H}_{\{\sigma\}} = -hM_{\{\sigma\}} = -\mu hNm_{\{\sigma\}}. \tag{2.7}$$

For convenience, we also introduce two more parameters: the number of spins along the field, $N_{\uparrow}$, and the number of spins against the field, $N_{\downarrow}$. The magnetization is, obviously, proportional to the difference between these two numbers,

$$M_{\{\sigma\}} = \mu(N_{\uparrow} - N_{\downarrow}), \tag{2.8}$$

while the sum of these numbers equals the total number of spins on the lattice,

$$N = N_{\uparrow} + N_{\downarrow}. \tag{2.9}$$

Therefore, if we know the energy of the system or its magnetization, we can bijectively find the numbers of spins along and against the field:

$$N_{\uparrow} = \frac{1}{2}\left(N - \frac{E}{\mu h}\right), N_{\downarrow} = \frac{1}{2}\left(N + \frac{E}{\mu h}\right) \tag{2.10}$$

or

$$N_{\uparrow} = N\frac{1+m}{2}, N_{\downarrow} = N\frac{1-m}{2}. \tag{2.11}$$

Vice versa, if we know $N_{\uparrow}$ and $N_{\downarrow}$, we know the energy of the system

$$E = -\mu h(N_{\uparrow} - N_{\downarrow}). \tag{2.12}$$

This expression corresponds to the value of energy of a particular energy level. From (2.12) it is easy to see that two adjacent energy levels are separated by one spin "flip":

$$|\Delta E| = 2\mu h, \tag{2.13}$$

where "2" comes from that a spin with one orientation disappears while a spin with the opposite orientation appears.

To find the degeneracy of energy level E, we should find how many microstates $\{\sigma\}$ correspond to numbers $N_\uparrow$ and $N_\downarrow$, given by (2.10) and (2.11). In other words, for the given values of $N_\uparrow$ and $N_\downarrow$, we have to find the number of microconfigurations by which $N_\uparrow$ of N spins could be oriented along the field while the rest of spins would be oriented against the field:

$$g_E = \frac{N!}{N_\uparrow! N_\downarrow!}. \tag{2.14}$$

As we will see later, one of the most important mathematical formulae in statistical physics is Stirling's approximation

$$N! = \left(\frac{N}{e}\right)^N \underline{\underline{O}}(N^\alpha), \tag{2.15}$$

where $\underline{\underline{O}}(N^\alpha)$ is the power-law dependence on N. In the thermodynamic limit, $N \to +\infty$, the power-law dependence $\underline{\underline{O}}(N^\alpha)$ on N is much "slower" than the "fast," exponential dependence $(N/e)^N$. Further, we will often utilize the notation "$\approx_{\ln}$" of *the logarithmic accuracy* meaning that in the thermodynamic limit, $N \to +\infty$, we neglect all "slow" power-law multipliers in comparison with the "fast," exponential dependencies on N. In particular, for Stirling's approximation we have

$$N! \approx_{\ln} \left(\frac{N}{e}\right)^N. \tag{2.16}$$

Applying (2.16) to (2.14), for the energy level degeneracy we find

$$g_E = \left(\frac{N}{N_\uparrow}\right)^{N_\uparrow} \left(\frac{N}{N_\downarrow}\right)^{N_\downarrow} \underline{\underline{O}}(N^\alpha) \approx_{\ln} \left(\frac{N}{N_\uparrow}\right)^{N_\uparrow} \left(\frac{N}{N_\downarrow}\right)^{N_\downarrow} = \left(\frac{1+m}{2}\right)^{-N\frac{1+m}{2}} \left(\frac{1-m}{2}\right)^{-N\frac{1-m}{2}}. \tag{2.17}$$

Equation (2.17) is the typical representative of the degeneracy dependence on the number of degrees of freedom N in the system. Firstly, we see that both exponents, $N_\uparrow = N\frac{1+m}{2}$ and $N_\downarrow = N\frac{1-m}{2}$, are proportional to N, and,

therefore, the degeneracy of energy levels indeed depends exponentially on N. Secondly, $N/N_{\uparrow}$ and $N/N_{\downarrow}$ are intensive parameters (not proportional to N), and the singularity of the thermodynamic limit, $N \to +\infty$, is absent in them.

Therefore, we can conclude that the typical behavior of the energy-level degeneracy on the value of energy is presented by a "tendency" when something finite is raised to the "singular" power proportional to N.

And it is not important whether this dependence is increasing or decreasing with the increase of energy. For example, for the Ising model, the lowest energy level, when all spins are along the field, is not degenerate. Neither degenerate is the highest energy level, when all spins are against the field. Between these two extremes, the degeneracy initially grows with the increase of energy but then decreases back to unity. For both cases, what is important is that the dependence is exponential on N, when we can neglect all power-law dependences.

The spectrum presented in Fig. 2.1a corresponds to the case of an ideal system. If we consider a nonideal system (which cannot be converted into the ideal by variables' change), the interactions among the degrees of freedom destroy the strict degeneracy when the energy levels "blur," spreading their microstates all over the spectrum and mixing them with other energy levels. The sketch of the resulting spectrum is presented in Fig. 2.1b.

As we will see later, statistical mechanics very successfully "manipulates" the degeneracy of energy levels. Therefore, and for the spectrum of a nonideal system, we would like to introduce something analogous to the strict quantum degeneracy.

Let us unite closely located microstates $\{E\}$ (microstates $\{E\}$ with close values of energy) into groups with the averaged values of energy E_i, where g_{E_i} is the number of microstates in the group (Fig. 2.1b). We would like to call the quantity g_{E_i}, by analogy, the degeneracy. However, this term is reserved for the strict degeneration in quantum mechanics. Therefore, the special term, *the statistical weight,* is introduced, which sometimes is abbreviated as "*the stat-weight*." In future, it will not be important for us whether we refer to the strict degeneracy in the sense of quantum mechanics or to the statistical weight as the number of microstates with close values of energy in the group. In both cases, we will refer to g_{E_i} by the term "statistical weight" without attributing it to the particular structure of the spectrum.

Students who begin to study statistical mechanics after such rigorous disciplines as theoretical or quantum mechanics are often confused by the fact that microstates are combined into groups "at will." How many microstates do we unite into a particular group? Why cannot we make groups 2, 10, 100 times larger? We will obtain the answer to this question later. Now we only mention that the formalism of statistical physics "works" in such a way that it is not important how many microstates we unite into a particular group. In fact, the whole mechanism of statistical physics operates only because this combining can be performed arbitrarily.

2.3 Microcanonical Ensemble

A microcanonical ensemble (or *MCE*) is an ensemble of identical isolated systems (Fig. 2.2). The isolation boundary condition means that there are neither heat exchange $\delta Q^{\leftarrow} = 0$, nor work of external forces $\delta W^{\leftarrow} = 0$, nor particle exchange $\delta \Pi^{\leftarrow} = 0$.

Microstates $\{E, p\}$ of the considered system are the eigenfunctions of the system's Hamiltonian with the value of energy E corresponding to the condition of the system's isolation, $E = const$. Here, by p we have denoted some set of internal parameters distinguishing microstates with the same value of energy E. For example, for the Ising model from Problem 2.2.1, which consists of $N = 3$ spins and is isolated with energy $-\mu h$, there are only three microstates, $\{\uparrow\uparrow\downarrow\}$, $\{\uparrow\downarrow\uparrow\}$, and $\{\downarrow\uparrow\uparrow\}$, corresponding to this value of energy. The parameter p here denotes spin orientations on the lattice and can be equal, for example, to $\uparrow\uparrow\downarrow$.

Isolating our system, we allow it to "visit" microstates with the given value of energy and prohibit "visiting" other microstates. *Strict isolation* means isolation strictly on one energy level (Fig. 2.3a) or strictly in one group of microstates (Fig. 2.3b).

But in nature no system with dense energy spectrum could be strictly isolated. There is always some uncertainty ΔE of isolation, which can include several energy levels (Fig. 2.4a) or several groups of microstates (Fig. 2.4b), if, of course, the energy spectrum is dense enough.

Similar to uncertainty of uniting microstates into groups, the uncertainty of the system's isolation does not influence the formalism of statistical physics. Let us discuss in detail why it is so.

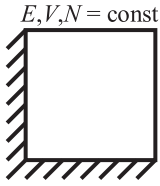

Fig. 2.2 An isolated system

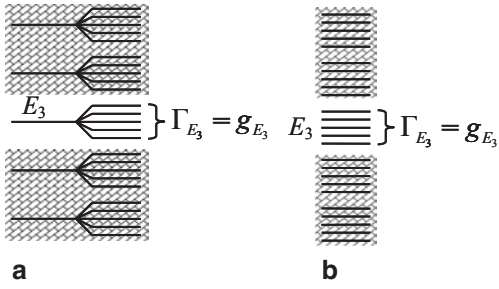

Fig. 2.3 The strict isolation on one energy level (**a**) or in one group of microstates (**b**)

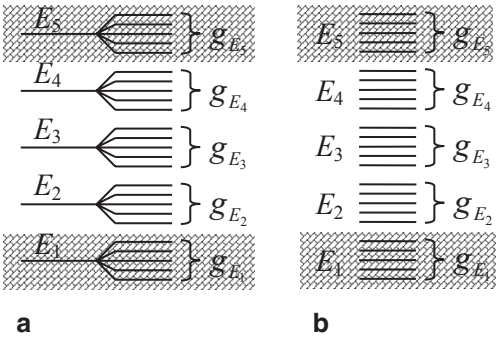

Fig. 2.4 The nonstrict isolation on three energy levels (**a**) or in three groups of microstates (**b**)

Firstly, we need to introduce a new term, *the statistical weight of an ensemble,* or, using slang, *the ensemble stat-weight*. What the statistical weight of a group of microstates is we already know: It is the number of microstates in the group. For the MCE, we utilize a similar definition—*the statistical weight of the MCE*, Γ^{MCE}, is the number of microstates which the system visits with nonzero probabilities. In other words, it is the number of microstates corresponding to the isolation conditions.

In the case of the strict isolation on one energy level E (in one group of microstates), the statistical weight of the MCE is the statistical weight g_E of this energy level (of this group of microstates):

$$\Gamma^{MCE} = g_E. \tag{2.18}$$

If the nonstrict isolation allows the system to visit k energy levels (groups) with close values of energy, the statistical weight of the MCE equals the sum of statistical weights of these levels (groups):

$$\Gamma^{MCE} = g_{E_1} + \ldots + g_{E_k}. \tag{2.19}$$

Let $w_{\{E,p\}}$ be the probability distribution to observe the system in a microstate $\{E,p\}$ in the ensemble. If, for example, we consider a quantum system, this probability distribution is provided by the diagonalized statistical operator (quantum density matrix) $w_{\{E,p\}} \equiv \rho_{\{E,p\},\{E,p\}}$.

Liuville's theorem (Gibbs 1902) suggests that in equilibrium all microstates of the MCE are equiprobable:

$$w^{MCE}_{\{\tilde{E},p\}} = \left\{ \begin{array}{c} \dfrac{1}{\Gamma^{MCE}}, \tilde{E} = E \\ 0, \tilde{E} \neq E \end{array} \right\} = \frac{\delta_{\tilde{E},E}}{\Gamma^{MCE}}, \tag{2.20}$$

where E is the energy of isolation. Here we should again emphasize that distribution of probabilities (2.20) is equilibrium. For nonequilibrium cases, we are free to consider any arbitrary distribution of probabilities $w_{\{E,p\}}$. We will discuss this question in detail later.

Problem 2.3.1

Find the probability distribution of microstates for the Ising model without spin interactions when there are $N = 3$ spins in the model. Consider the model to be strictly isolated with energy $E = -\mu h$.

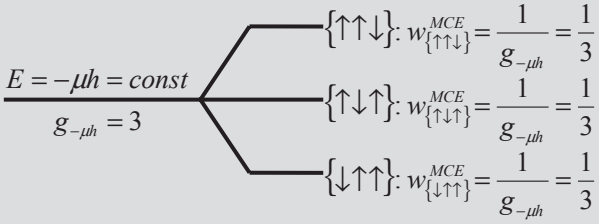

Solution: The strict isolation with energy $E = -\mu h$ means that two spins are oriented along the field, $N_\uparrow = 2$, while one spin is against the field, $N_\downarrow = 1$. The statistical weight of the ensemble is 3, and the probability distribution of microstates is illustrated in the figure.

Entropy is a frequent subject of discussions in the scientific and popular literature because its growth breaks the symmetry of the time axis. Sometimes in the popular literature, entropy is treated as having "magical" properties. Later we will see that all the "magic" belongs to the formalism of statistical physics while there is nothing "magical" in the growth of entropy as a parameter directly related to the probability distribution.

There are many ways to introduce the concept of entropy into the formalism. As the main axiom, we utilize the following definition of entropy:

$$S[w_{\{\}}] \equiv -\sum\nolimits_{\{\}} w_{\{\}} \ln w_{\{\}}, \tag{2.21}$$

which follows from an even more general definition

$$S \equiv -\mathrm{Tr}\left(\hat{\rho} \ln \hat{\rho}\right), \tag{2.22}$$

when the statistical operator (quantum density matrix) is diagonal and its diagonal elements form the distribution of probabilities,

$$w_{\{\}} \equiv \rho_{\{\},\{\}}. \tag{2.23}$$

Let us take a closer look at definition (2.21). Firstly, we see that the entropy is a functional defined on the function space of all possible probability distributions $w_{\{\}}$. Secondly, if $f_{\{\}}$ is some system's parameter related to microstates $\{\}$, e.g., specific magnetization (2.6), its averaged value should be provided by

$$\langle f \rangle_{w_{\{\}}} \equiv \sum_{\{\}} w_{\{\}} f_{\{\}}. \tag{2.24}$$

Therefore, from definition (2.21) we conclude that the entropy is the averaged minus logarithm of the probability distribution:

$$S \equiv \left\langle -\ln w_{\{\}} \right\rangle_{w_{\{\}}}. \tag{2.25}$$

For the first time, definition (2.21) appeared in Gibbs' works (Gibbs 1876, 1878) while later it received further development in Shannon's studies (Shannon 1948) when it was applied to informational processes. Therefore, in statistical physics definition (2.21) is called *Gibbs entropy* while in the theory of complex systems (when there are no thermal fluctuations in a system) it is called *Gibbs–Shannon entropy*. We utilize this definition as a formalism axiom due to its universality—it is applicable to any ensemble, any set of microstates, and any probability distribution $w_{\{\}}$, both equilibrium and nonequilibrium. Therefore, definition (2.21) is always applicable in contrast to other approaches that require more detailed descriptions. The reader can find formulae, similar to (2.21), in many books devoted to nonthermal complex systems which are not described by the formalism of statistical physics. Even more, definition (2.21) was the very starting point that encouraged looking at complex systems from the statistical physics point of view.

For the case of nondiagonal statistical operator (quantum density matrix), a more general definition (2.22) is applied which is called *von Neumann entropy* (von Neumann 1932, 1955).

We already know probability distribution (2.20) of the MCE. To find *the entropy of the MCE,* we should substitute this distribution into entropy functional (2.21):

$$S^{MCE} \equiv -\sum_{\{E,p\}} w^{MCE}_{\{E,p\}} \ln w^{MCE}_{\{E,p\}}. \tag{2.26}$$

Let us, firstly, utilize the limit

$$\lim_{x \to +0} x \ln x = 0 \tag{2.27}$$

for the terms of the sum corresponding to zero probabilities. Secondly, since the remaining terms are all equal one to another, we find,

$$S^{MCE} = -\Gamma^{MCE} \frac{1}{\Gamma^{MCE}} \ln \frac{1}{\Gamma^{MCE}} = \ln \Gamma^{MCE}, \tag{2.28}$$

that the entropy of the ensemble equals the logarithm of the ensemble statistical weight (the logarithm of the number of microstates in which the system "lives"). This equality is called *Boltzmann's entropy*. We see that this definition of the entropy is less universal than (2.21) because it corresponds only to the equilibrium distribution of probabilities (2.20) in the ensemble.

Now let us return to the question why the accuracy of isolation ΔE does not influence the formalism of statistical physics. But firstly, what is generally the accuracy of isolation? For a gas, we can assume that ΔE corresponds to energy of several particles. For the Ising model, to flips of several spins. In this case, the system is

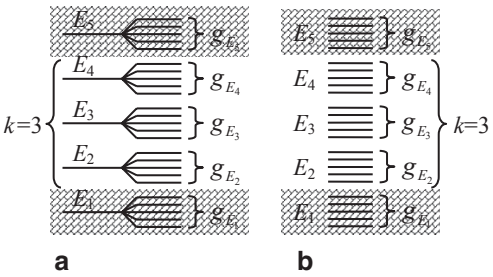

Fig. 2.5 The non strict isolation (**a**) on $k = 3$ energy levels, (**b**) in $k = 3$ groups of microstates

nonstrictly isolated and can visit k adjacent levels of energy (Fig. 2.5). Let us see how the accuracy of the isolation influences the value of the system's entropy.

Problem 2.3.2

For the Ising model without spin interactions, compare the degeneracies of k adjacent energy levels.

Solution: When we move from one energy level to the adjacent, the numbers of spins along and against the field, $N_\uparrow$ and $N_\downarrow$, are changed by unity, e.g., $N_\uparrow \Rightarrow N_\uparrow + 1$ and $N_\downarrow \Rightarrow N_\downarrow - 1$. When we move across i energy levels, we have $N_\uparrow \Rightarrow N_\uparrow + i$ and $N_\downarrow \Rightarrow N_\downarrow - i$, where $i = 0,\ldots,k-1$. Substituting these numbers into (2.14), we find

$$\frac{g_{E+\Delta E}}{g_E} = \frac{N_\uparrow! N_\downarrow!}{(N_\uparrow + i)!(N_\downarrow - i)!} = \frac{(N_\downarrow - i + 1)}{(N_\uparrow + 1)} \cdot \ldots \cdot \frac{(N_\downarrow)}{(N_\uparrow + i)}. \tag{2.29}$$

Both $N_\uparrow$ and $N_\downarrow$ are proportional to N. Therefore, ratio (2.29) is of the order of unity:

$$\frac{g_{E+\Delta E}}{g_E} \propto \underline{\underline{O}}(1) \tag{2.30}$$

which is even less than the logarithmic accuracy, $\underline{\underline{O}}(N^\alpha)$, we used in (2.16).

For an arbitrary system, we assume that similarly to Problem 2.3.2 its statistical weight changes by multiplier $\underline{\underline{O}}(1)$ when we move from one energy value to the adjacent. Substituting this assumption into (2.19) and then into (2.28), we find

$$S^{MCE} = \ln\left(k g_E \underline{\underline{O}}(1)\right) = \ln g_E + \ln k + \ln \underline{\underline{O}}(1). \tag{2.31}$$

Here g_E depends on N exponentially and, therefore, its logarithm is proportional to N while $\ln k$ and $\ln \underline{\underline{O}}(1)$ are of the order of unity. Therefore, we can neglect two

last terms to find that the entropy of the nonstrictly isolated system approximately equals the entropy of the strictly isolated system:

$$S^{MCE} \approx \ln g_E , \tag{2.32}$$

and the accuracy of the isolation does not influence the value of the entropy.

What if k depended as a power-law on N: $k \propto \underline{\underline{O}}(N^{\alpha})$? Again it would not influence the value of the entropy because logarithm of k would be of the order of $\ln N << N$. This exact situation we will encounter later in this chapter in the case of a canonical ensemble when the relative energy fluctuations are of the order of $\frac{\delta E}{E_0} \propto \frac{1}{\sqrt{N}}$ while absolute energy fluctuations are of the order of $\delta E \propto \sqrt{N}$. This corresponds to $k \propto \sqrt{N}$—the number of energy levels on which the canonical ensemble "lives." In the thermodynamic limit, k is infinite but still does not influence the value of the entropy! Of course, here as well as above we assume that the statistical weight g_E is the same (with logarithmic accuracy) for all $k \propto \sqrt{N}$ energy levels.

Now we already can answer the question when the accuracy of the system's isolation does not influence its entropy. Firstly, the number of levels (or groups of microstates), on which the system is isolated, should not exceed the power-law dependence $k \propto \underline{\underline{O}}(N^{\alpha})$ on N. Secondly, all these values of energy should be so close one to another that their statistical weights would be the same with logarithmic accuracy (with the accuracy of a multiplier with a power-law dependence $\underline{\underline{O}}(N^{\alpha})$ on N).

Also now we can answer the question how we have united microstates into groups. We do not care how many microstates we unite into a group providing that its statistical weight does not change more than by a power-law dependence $\underline{\underline{O}}(N^{\alpha})$ on N. For example, let us imagine a system strictly isolated in one group of microstates. Its entropy is $S^{MCE} = \ln g_E$. Uniting into this group 10, 100, or $\underline{\underline{O}}(N^{\alpha})$ times more microstates than it is now should influence neither the value of the system's entropy nor any further formulae of statistical physics.

Earlier we introduced the notation "$\approx_{\ln}$" of logarithmic accuracy when in the thermodynamic limit, $N \to +\infty$, we neglect all "slow" power-law multipliers in comparison with the "fast," exponential dependencies on N. Now we see that this is more than just a useful notation—this is the mechanism that "actuates" the formalism of statistical physics. Therefore, in future we will utilize the logarithmic accuracy in almost all formulae unless the opposite will be stated specifically.

And, as we will see later, almost all results of statistical physics and all concepts such as a sharp maximum of a probability distribution, the equation of state corresponding to the point of this maximum, the Gaussian distribution in the vicinity of the equilibrium state, the fact that a partition function equals its maximal term, and, finally, "magical" properties of the entropy are the results of the applicability of logarithmic accuracy. And this is also the reason why statistical physics is applicable to nonthermal, complex systems. Neglecting system-dependent power-law dependences provides the universality of the applied formalism and makes it independent on the particular details of the system considered.

Several times above we have emphasized that we consider the nonstrict isolation of a system on k levels (groups) only in the case when statistical weights g_E of these levels (groups) are identical with logarithmic accuracy. But what does happen if moving across k levels we do change the statistical weight significantly? Let us return to (2.19), only in this case we assume that all $g_{E_1},\ldots,g_{E_k}$ are significantly different (not equal one to another with logarithmic accuracy). Firstly, we find the maximal statistical weight among these values:

$$g^{\max} = \max_{i=1,\ldots,k} g_{E_i}. \tag{2.33}$$

Then we substitute this maximum value into (2.19):

$$S^{MCE} = \ln \Gamma^{MCE} = \ln\left(g_{E_1} + \ldots + g_{E_k}\right) = \ln\left(g^{\max}\left\{\beta_1 + \ldots + \beta_k\right\}\right), \tag{2.34}$$

where all parameters β_i are in the range $0 < \beta_i < 1$ and only one of them equals strictly unity. Since k is not higher than a power-law dependence on N, $k \propto \underline{\underline{O}}(N^{\alpha})$, we find

$$S^{MCE} = \ln(g^{\max}\ \underline{\underline{O}}(N^{\alpha})) \approx \ln g^{\max}. \tag{2.35}$$

This returns us to (2.32); only in this case into the logarithm function we put the maximal statistical weight among all energy levels (groups of microstates) on which the system is isolated.

So now it is not even important whether the levels (groups) on which we have isolated our system have significantly different statistical weights or not. We are just choosing the maximal among them, and it serves as the statistical weight of the MCE.

2.4 MCE: Fluctuations as Nonequilibrium Probability Distributions

Now we turn our attention to the most difficult question of the ensemble theory—the definition of a nonequilibrium fluctuation. We can define a fluctuation in many ways: by prescribing its properties, by prescribing a set of microstates belonging to this fluctuation, and so on. But the most universal way is to define a fluctuation by prescribing a nonequilibrium probability distribution.

First, let us consider a simple example, what we understand under the term "nonequilibrium distribution of probabilities." Let us imagine a kingdom whose leading scientist, Dr. Richelieu, while conducting tests in his Bastille clinic, had discovered that the most beneficial to health is to drink one glass of wine a week. Therefore, he issued an Edict of Health that everyone has to drink one glass of wine per week.

But, of course, this Edict was often violated because one week a peasant could afford a glass of wine whereas next time he could be out of money. Therefore, after severe punishments had not helped, Dr. Richelieu decided to modify the Edict.

Now it was not a deterministic prescription but a stochastic one. Everyone again should drink a glass of wine a week; however, this time not strictly but on average. With probability 1/4, a person could drink two glasses of wine during a week; with probability 1/2, one glass; and with probability 1/4, no wine at all. This way everybody would drink one glass of wine per week on average.

To follow this new law was much easier; therefore, the majority of people followed it to the letter. They could drink two glasses of wine per week or no wine at all; but, on average, they drank one glass a week. In other words, they exactly followed the prescribed probability distribution and, therefore, their own probability distribution was "in equilibrium with the law."

However, some of the people continued to violate the Edict. For example, there was a guy, called d'Artagnan, who drank two glasses of wine a week with probability 1/8, five glasses of wine with probability 1/8, and seven bottles a week with probability 3/4. On another extreme, Constance Bonacieux did not drink wine at all because she was afraid to be killed by poisoned wine. Therefore, we may say that both d'Artagnan and Mademoiselle Bonacieux were following the probability distributions nonequilibrium with the law.

Returning to the MCE, we see that according to (2.20) the ensemble dictates to a system to visit all its microstates equiprobably. If the system follows this probability distribution (2.20), its distribution of probabilities is *in equilibrium with the ensemble requirements,* or *an equilibrium distribution of probabilities*. Such distributions we mark by the symbol of the ensemble $w^{MCE}_{\{E,p\}}$ to distinguish them from other distributions.

But the system may not follow the equilibrium distribution of probabilities $w^{MCE}_{\{E,p\}}$ dictated by the MCE. Instead, it can choose to follow some other distribution of probabilities $w_{\{E,p\}}$ which in this case is called *a nonequilibrium distribution of probabilities*.

After we have discussed what is a nonequilibrium distribution of probabilities, let us return to the main question—how we can describe a fluctuation.

How do we define nonequilibrium states in thermodynamics? The most illustrative example is a gas whose density is not uniform in the volume and obeys some dependency $n(\vec{\mathbf{r}})$ on the coordinates inside the volume. For example, we can imagine a fluctuation as a state when all gas is gathered in the right half of the volume while in the left half its density is zero.

As an illustration we, however, consider not a gas, but the Ising model without spin interactions. Let the model be a one-dimensional chain of N spins. Further, for the purposes of abbreviation, we will call the spins oriented along the field h by the term "the ↑-spins" while the spins oriented against the field, "the ↓-spins."

We choose such energy E of the system's isolation that the number $N_\uparrow$ of the ↑-spins is three times higher than the number $N_\downarrow$ of the ↓-spins:

$$N_\uparrow = 3N/4 \text{ and } N_\downarrow = N/4. \tag{2.36}$$

We can do that because we are free in our choice of the value of energy with which the system is isolated. The values of $N_\uparrow$ and $N_\downarrow$ are not special and are chosen to be equal to (2.36) only to have simple fractions 3/4 and 1/4 for illustration purposes.

Since our system is isolated strictly, the statistical weight of the MCE equals the statistical weight of the given energy level:

$$\Gamma^{MCE} = g_E = \frac{N!}{\frac{3N}{4}!\frac{N}{4}!} \approx_{\ln} \left(\frac{4}{3}\right)^{3N/4} 4^{N/4}. \tag{2.37}$$

Let us discuss how we introduce a nonequilibrium fluctuation for our model. Similar to a gas with nonuniform density, we consider a nonuniform distribution of the ↓-spins along the model chain. Then the gas gathered in one half of the volume will be equivalent to the ↓-spins all gathered in one half of the chain.

Therefore, let us divide the one-dimensional chain of spins into two with $N/2$ spins in each half. We will denote by p the fraction of the ↓-spins gathered in the right half. When all $(N_\downarrow = N/4)$ ↓-spins are gathered in the left half, we have $p = 0$. When all $(N_\downarrow = N/4)$ ↓-spins are gathered in the right half, we have $p = 1$. An arbitrary value of p in the range $0 < p < 1$ corresponds to $pN/4$ ↓-spins in the right half and $(1-p)N/4$ ↓-spins in the left.

We define *a nonequilibrium fluctuation* $\{\{p\}\}$ (or *a nonequilibrium macrostate* $\{\{p\}\}$) in the MCE as a state of the system with the given fraction p of the ↓-spins in the right half of the chain. In other words, we define a fluctuation by a particular value of $\tilde{p} = p$. This value represents the criterion indicating when we observe the given fluctuation in the ensemble.

We see that the criterion "to have p ↓-spins in the right half" does not specify particular locations for these spins, and $pN/4$ ↓-spins can be distributed arbitrarily in the right half among the ↑-spins. Therefore, a lot of microstates correspond to the criterion of our fluctuation. Observing the fluctuation in the ensemble is equivalent to observing any of these microstates.

Let $\Gamma_{\{\{p\}\}}$ be the number of microstates $\{E, p\}$, corresponding to the given fluctuation $\{\{p\}\}$, among the total number Γ^{MCE} of microstates $\{E, \tilde{p}\}$ of the MCE ensemble (Fig. 2.6). We will call $\Gamma_{\{\{p\}\}}$ *the statistical weight of fluctuation* $\{\{p\}\}$.

But for the MCE we know that the distribution of probabilities for the microstates $\{E, \tilde{p}\}$ is dictated by (2.20), where Γ^{MCE} microstates $\{E, \tilde{p}\}$ serve as the fan of possible outcomes in the ensemble. The requirement to observe currently the fluctuation $\{\{p\}\}$ intervenes in the "work" of the ensemble, reducing the fan of

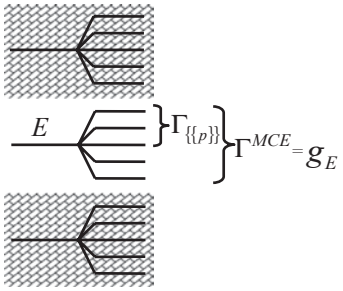

Fig. 2.6 Statistical weight $\Gamma_{\{\{p\}\}}$ of fluctuation $\{\{p\}\}$ and statistical weight $\Gamma^{MCE} = g_E$ of the MCE

possible outcomes to $\Gamma_{\{\{p\}\}}$ microstates $\{E, p\}$. In other words, if we know that the system is in the macrostate of fluctuation $\{\{p\}\}$, the distribution of probabilities for such a system is not (2.20) but reduces to

$$w_{\{\tilde{E},\tilde{p}\}} = \begin{Bmatrix} 1/\Gamma_{\{\{p\}\}} & ,\tilde{E}=E,\tilde{p}=p \\ 0 & ,otherwise \end{Bmatrix} = \frac{\delta_{\tilde{E},E}\delta_{\tilde{p},p}}{\Gamma_{\{\{p\}\}}}. \tag{2.38}$$

Distribution of probabilities (2.38) is *the nonequilibrium distribution of probabilities,* determining the given fluctuation. If our system does not obey requirement (2.20), dictated by the ensemble, but is in the macrostate $\{\{p\}\}$, the probabilities to observe particular microstates obey distribution (2.38). In contrast to (2.20), we did not use here the superscript "*MCE*" because this distribution of probabilities is not dictated by the ensemble and is not in equilibrium with the ensemble.

Instead of saying that distribution (2.38) corresponds to the fluctuation $\{\{p\}\}$, we can say that it defines the fluctuation. Therefore, any fluctuation can be described by a nonequilibrium distribution of probabilities, and, vice versa, a system obeying a nonequilibrium distribution of probabilities is in the macrostate of fluctuation determined by this distribution.

Substituting the nonequilibrium distribution of probabilities (2.38) into the definition of entropy functional (2.21), we find *the entropy of the fluctuation* $\{\{p\}\}$:

$$S_{\{\{p\}\}} = \ln \Gamma_{\{\{p\}\}}. \tag{2.39}$$

This is again Boltzmann's entropy which equals the logarithm of the number of microstates which the system visits with nonzero probabilities.

Problem 2.4.1

For the one-dimensional Ising model without spin interactions find the statistical weight $\Gamma_{\{\{p\}\}}$ and the entropy $S_{\{\{p\}\}}$ of the fluctuation $\{\{p\}\}$.

Solution: To find the statistical weight of the fluctuation, we need to find the number of microconfigurations when $pN_{\downarrow} = pN/4$ $\downarrow$-spins are distributed among the $\uparrow$-spins in the right half of the chain while $(1-p)N_{\downarrow} = (1-p)N/4$ $\downarrow$-spins are distributed in the left half:

$$\Gamma_{\{\{p\}\}} = \frac{\frac{N}{2}!}{\frac{(1-p)N}{4}!\left(\frac{N}{2}-\frac{(1-p)N}{4}\right)!} \times \frac{\frac{N}{2}!}{\frac{pN}{4}!\left(\frac{N}{2}-\frac{pN}{4}\right)!} \tag{2.40}$$

Utilizing Stirling's approximation, we find

$$\Gamma_{\{\{p\}\}} \approx_{\ln} \left(\frac{2}{1-p}\right)^{(1-p)N/4} \left(\frac{2}{1+p}\right)^{(1+p)N/4} \left(\frac{2}{p}\right)^{pN/4} \left(\frac{2}{2-p}\right)^{(2-p)N/4}. \tag{2.41}$$

Therefore, the entropy of the fluctuation is

$$S_{\{\{p\}\}} = N\ln 2 - \frac{N}{4}(1-p)\ln(1-p) - \frac{N}{4}(1+p)\ln(1+p) - \frac{N}{4}p\ln p - \frac{N}{4}(2-p)\ln(2-p). \tag{2.42}$$

Our system wants to be independent from the ensemble and to follow its own path of fluctuations. But the probabilities of these fluctuations are still dictated by the ensemble. Since all microstates of the MCE are equiprobable, the probability to observe the fluctuation $\{\{p\}\}$ in the ensemble equals the share of microstates belonging to this fluctuation:

$$W^{MCE}_{\{\{p\}\}} = \frac{\Gamma_{\{\{p\}\}}}{\Gamma^{MCE}}. \tag{2.43}$$

Here for the given boundary condition (2.36) the statistical weight of the ensemble Γ^{MCE} is constant. Therefore, the probability of a fluctuation $\{\{p\}\}$ is directly proportional to the statistical weight of this fluctuation. The smaller the statistical weight of the fluctuation, the rarer we observe this fluctuation in the ensemble. This is the reason why we never see a gas gathered in one half of the volume.

Since any microstate of the MCE must belong to one or another fluctuation $\{\{p\}\}$, the statistical weight Γ^{MCE} of the MCE is the sum of statistical weights $\Gamma_{\{\{p\}\}}$ of all possible fluctuations $\{\{p\}\}$,

$$\Gamma^{MCE} = \sum_{p=0,\Delta p=1/(N/4)}^{1} \Gamma_{\{\{p\}\}}, \tag{2.44}$$

and probability distribution (2.43) is normalized to unity,

$$\sum_{p=0,\Delta p=1/(N/4)}^{1} W^{MCE}_{\{\{p\}\}} = 1. \tag{2.45}$$

We have considered above only the simplest example (2.38) of nonequilibrium distributions when all the probabilities of microstates, not corresponding to the criterion p, were exactly zero. However, in general we can consider an arbitrary distribution of probabilities defining a particular type of fluctuations.

Problem 2.4.2

Let us consider an example of more complex fluctuations. We consider an optical device that generates red photons with the constant probability $w^{ensemble}_{\{red\}}$, green photons with the probability $w^{ensemble}_{\{green\}}$, and blue photons with

the probability $w^{ensemble}_{\{blue\}}$. Since other colors are impossible, the color of the next photon must be red, green, or blue:

$$w^{ensemble}_{\{red\}} + w^{ensemble}_{\{green\}} + w^{ensemble}_{\{blue\}} = 1. \tag{2.46}$$

Find the probability of the fluctuation $\left\{\left\{red \bigcup green\right\}\right\}$ that the next photon will be red or green but not blue. In other words, find the probability of the fluctuation defined by the following nonequilibrium distribution of probabilities:

$$w_{\{color\}} = \left\{ \begin{array}{ll} \dfrac{w^{ensemble}_{\{red\}}}{w^{ensemble}_{\{red\}} + w^{ensemble}_{\{green\}}}, & color = red \\ \dfrac{w^{ensemble}_{\{green\}}}{w^{ensemble}_{\{red\}} + w^{ensemble}_{\{green\}}}, & color = green \\ 0, & color = blue \end{array} \right\}. \tag{2.47}$$

Solution: Obviously, the probability for the next photon to be red or green is

$$W^{ensemble}_{\left\{\left\{red \bigcup green\right\}\right\}} = w^{ensemble}_{\{red\}} + w^{ensemble}_{\{green\}}. \tag{2.48}$$

In this problem, in contrast to the case of the MCE we have introduced that microstates $\{red\}$, $\{green\}$, and $\{blue\}$ are no longer equiprobable. The next problem will be even more complex.

Problem 2.4.3

For the ensemble described in Problem 2.4.2 find the probability to observe for the next photon the following nonequilibrium probability distribution:

$$w_{\{color\}} = \left\{ \begin{array}{l} w_{\{red\}}, color = red \\ w_{\{green\}}, color = green \\ w_{\{blue\}}, color = blue \end{array} \right\}. \tag{2.49}$$

Solution: The simplest way to find the probability of the fluctuation is to consider n consecutive photons. In this sample, $nw_{\{red\}}$ photons must be red, $nw_{\{green\}}$ photons green, and $nw_{\{blue\}}$ photons blue. The probability of this sample is

$$W^{ensemble}_{n\times\{\{\ \}\}} = \frac{n!}{(nw_{\{red\}})!(nw_{\{green\}})!(nw_{\{blue\}})!} \times (w^{ensemble}_{\{red\}})^{nw_{\{red\}}} (w^{ensemble}_{\{green\}})^{nw_{\{green\}}} (w^{ensemble}_{\{blue\}})^{nw_{\{blue\}}}, \quad (2.50)$$

where $(w^{ensemble}_{\{red\}})^{nw_{\{red\}}} (w^{ensemble}_{\{green\}})^{nw_{\{green\}}} (w^{ensemble}_{\{blue\}})^{nw_{\{blue\}}}$ is the probability of one such configuration while the multiplier $\frac{n!}{(nw_{\{red\}})!(nw_{\{green\}})!(nw_{\{blue\}})!}$ is the number of possible configurations given by the distribution of $nw_{\{red\}}$ red photons, $nw_{\{green\}}$ green photons, and $nw_{\{blue\}}$ blue photons among n photons.

Utilizing Stirling's approximation (2.16), we find

$$W^{ensemble}_{n\times\{\{\ \}\}} = \left(\frac{w^{ensemble}_{\{red\}}}{w_{\{red\}}}\right)^{nw_{\{red\}}} \left(\frac{w^{ensemble}_{\{green\}}}{w_{\{green\}}}\right)^{nw_{\{green\}}} \left(\frac{w^{ensemble}_{\{blue\}}}{w_{\{blue\}}}\right)^{nw_{\{blue\}}}. \quad (2.51)$$

Since the color of a photon is independent of other photons in a sequence, probability (2.51) is the product of n identical probabilities corresponding to n independent events. In other words, to find the probability of fluctuation (2.49) in the ensemble we should extract the n^{th} root of (2.51):

$$W^{ensemble}_{\{\{\ \}\}} = \left(\frac{w^{ensemble}_{\{red\}}}{w_{\{red\}}}\right)^{w_{\{red\}}} \left(\frac{w^{ensemble}_{\{green\}}}{w_{\{green\}}}\right)^{w_{\{green\}}} \left(\frac{w^{ensemble}_{\{blue\}}}{w_{\{blue\}}}\right)^{w_{\{blue\}}}. \quad (2.52)$$

Generalizing the solution of Problem 2.4.3, for the probability to observe a nonequilibrium distribution of probabilities $w_{\{\ \}}$ in the ensemble, which itself follows the probability distribution $w^{ensemble}_{\{\ \}}$, we find

$$W^{ensemble}_{\{\{\ \}\}} = \prod_{\{\ \}} \left(\frac{w^{ensemble}_{\{\ \}}}{w_{\{\ \}}}\right)^{w_{\{\ \}}}. \quad (2.53)$$

But let us return to the case of simple fluctuations (2.38) in the MCE ensemble. To find the maximum of probability (2.43), we should find when its derivative equals to zero:

$$\left.\frac{\partial W^{MCE}_{\{\{p\}\}}}{\partial p}\right|_{p_0} = 0. \quad (2.54)$$

But probability (2.43) is an exponential dependence. Therefore, it is usually more convenient to differentiate not the probability itself but its logarithm:

$$\left.\frac{\partial \ln W^{MCE}_{\{\{p\}\}}}{\partial p}\right|_{p_0} = 0. \tag{2.55}$$

Since the logarithm is the monotonically increasing function, its derivative equals zero when the derivative of the probability is zero.

Differentiating the logarithm of (2.43), into which we should substitute $\Gamma_{\{\{p\}\}}$ from (2.41), for the point of the probability maximum, we easily find $p_0 = 1/2$ when each half of the model contains exactly one half of the ↓-spins. Therefore, fluctuation $\{\{p_0 = 1/2\}\}$ is *the most probable macrostate* and corresponds to *the equilibrium state*.

The reader should clearly distinguish two equilibrium concepts: the equilibrium state as the most probable macrostate and the equilibrium distribution of probabilities. Returning to the imaginary kingdom ruled by Dr. Richelieu, we already know that most of the people followed the Edict of Health to the letter. They could drink two glasses of wine a week or no wine at all; but, on average, they drank one glass a week. In other words, they exactly followed the prescribed probability distribution and, therefore, their own probability distribution was "in equilibrium with the law," or the equilibrium distribution of probabilities. If it was so happening that during one particular week a person indeed drank literally (not on average) one glass of wine, they called it "the equilibrium week," or the most probable, equilibrium macrostate.

Similarly, in the case of the MCE, the ensemble dictates the equiprobable probability distribution (2.20). If the system follows this probability distribution, its distribution of probabilities is *in equilibrium with the ensemble requirements,* or *an equilibrium distribution of probabilities*.

But microstates visited by the system can be very different. Some of them could correspond to rare events, when, for example, all gas has been gathered in one half of the volume. But these events are rare, and on average the system stays in *equilibrium macrostate* when the gas density is uniform across the volume.

Let us now study the equilibrium macrostate. Substituting $p_0 = 1/2$ into (2.41), we find the statistical weight of the most probable fluctuation:

$$\Gamma_{\{\{p_0\}\}} \approx_{\ln} \left(\frac{4}{3}\right)^{3N/4} 4^{N/4}. \tag{2.56}$$

But this is exactly expression (2.37) for the statistical weight Γ^{MCE} of the ensemble in whole! So, the number of the microstates corresponding to the equilibrium macrostate $\{\{p_0 = 1/2\}\}$ equals the total number of the microstates in the ensemble?! How is it possible? From (2.44) we have expected that other fluctuations should also contribute to the total ensemble statistical weight. Where are then the microstates corresponding to these other fluctuations?

To answer this question we should recall that both equalities, (2.37) and (2.56), are valid with logarithmic accuracy:

$$\Gamma^{MCE} \approx_{\ln} \Gamma_{\{\{p_0\}\}}. \tag{2.57}$$

The logarithmic accuracy assumes that the left-hand side of (2.57) can be N^{α} times greater than the right-hand side. The difference is precisely the number of lost microstates corresponding to other fluctuations from sum (2.44):

$$\Gamma^{MCE} = \sum_{p=0,\Delta p=1/(N/4)}^{1} \Gamma_{\{\{p\}\}} = \Gamma_{\{\{p_0\}\}} \underline{\underline{O}}(N^{\alpha}) \approx_{\ln} \Gamma_{\{\{p_0\}\}}. \tag{2.58}$$

About equality (2.58), it is said that *the statistical weight of the ensemble equals to its largest term*. However, one should not forget that this is valid only with the logarithmic accuracy. In other words, although the statistical weight $\Gamma_{\{\{p_0\}\}}$ of the equilibrium macrostate $\{\{p_0 = 1/2\}\}$ is comparable with the total number of microstates in the ensemble, there are still a lot of other microstates to divide among other fluctuations.

In particular, all macrostates adjacent to $p_0 = 1/2$ have statistical weights comparable with $\Gamma_{\{\{p_0\}\}}$.

Problem 2.4.4

Find the statistical weight of the fluctuation adjacent to $\{\{p_0 = 1/2\}\}$.

Solution: The adjacent is the fluctuation $\left\{\left\{p = \frac{1}{2} + \frac{1}{N/4}\right\}\right\}$ when the right half of the model has two more ↓-spins than the left half. Returning to the exact expression (2.40), we find the ratio

$$\frac{\Gamma_{\left\{\left\{\frac{1}{2}+\frac{1}{N/4}\right\}\right\}}}{\Gamma_{\left\{\left\{\frac{1}{2}\right\}\right\}}} = \frac{\left(\frac{N}{8}\right)\left(\frac{N}{2}-\frac{N}{8}\right)}{\left(\frac{N}{2}-\frac{N}{8}+1\right)\left(\frac{N}{8}+1\right)} = 1 - \frac{32}{3N}. \tag{2.59}$$

We see that although the absolute difference is huge, the relative difference is negligible even from the point of view of usual, not logarithmic calculus.

Let us now find the distribution of probabilities $W^{MCE}_{\{\{p\}\}}$ of fluctuations $\{\{p\}\}$ in the vicinity of the equilibrium macrostate $\{\{p_0\}\}$. As we already know, at the point $\{\{p_0\}\}$, the first derivative of the logarithm of probability $W^{MCE}_{\{\{p\}\}}$ equals zero in accordance with (2.55). The second derivative at this point we find to be nonzero:

$$\left.\frac{\partial^2 \ln W^{MCE}_{\{\{p\}\}}}{\partial p^2}\right|_{p_0} = -\frac{4}{3}N. \tag{2.60}$$

Therefore, for the expansion of $\ln W^{MCE}_{\{\{p\}\}}$ in a power series of $(p-p_0)$, we have

$$\ln W^{MCE}_{\{\{p\}\}} = \ln W^{MCE}_{\{\{p_0\}\}} + \left.\frac{\partial \ln W^{MCE}_{\{\{p\}\}}}{\partial p}\right|_{p_0} (p-p_0) + \frac{1}{2}\left.\frac{\partial^2 \ln W^{MCE}_{\{\{p\}\}}}{\partial p^2}\right|_{p_0} (p-p_0)^2 + \ldots$$

$$= \ln W^{MCE}_{\{\{p_0\}\}} - \frac{2}{3} N (p-p_0)^2 + \ldots, \tag{2.61}$$

or, exponentiating,

$$W^{MCE}_{\{\{p\}\}} \propto e^{-\frac{2}{3}\frac{(p-p_0)^2}{1/N}}. \tag{2.62}$$

We see that in the vicinity of the equilibrium macrostate $\{\{p_0 = 1/2\}\}$ the probabilities $W^{MCE}_{\{\{p\}\}}$ of fluctuations $\{\{p\}\}$ obey the Gaussian distribution. The width of the maximum is of the order of

$$\delta(p) \propto \frac{1}{\sqrt{N}}. \tag{2.63}$$

Since beyond the "bell" of the probability maximum the fluctuations have almost zero probabilities, quantity (2.63) represents the characteristic size of fluctuations in p. And since its value is inversely proportional to the square root of N, it is very small in the thermodynamic limit, $N \to +\infty$.

Above we have considered fluctuations in p. But since statistical physics usually operates with extensive parameters (proportional to N), we can easily modify distribution (2.62) to prescribe probabilities to fluctuations $\{\{Np\}\}$ in Np:

$$W^{MCE}_{\{\{Np\}\}} \propto e^{-\frac{2}{3}\frac{(Np-Np_0)^2}{N}}. \tag{2.64}$$

Now the width of the maximum is of the order of

$$\delta(Np) \propto \sqrt{N} \tag{2.65}$$

and is called *absolute fluctuation in Np*. To find *relative fluctuation* in *Np*, we should divide (2.65) by the averaged value Np_0:

$$\frac{\delta(Np)}{Np_0} \propto \frac{1}{\sqrt{N}}. \tag{2.66}$$

The result is again very small in the thermodynamic limit, $N \to +\infty$.

Nonzero probabilities are possessed only by fluctuations located inside the probability maximum. Beyond the width of the maximum, the probabilities of fluctuations are almost zero. Let us, for example, compare the statistical weight of the

fluctuation $\{\{p=1\}\}$, when all ↓-spins are gathered in the right half of the model, with the statistical weight of the equilibrium macrostate $\{\{p_0=1/2\}\}$:

$$\frac{\Gamma_{\{\{1\}\}}}{\Gamma_{\{\{p_0\}\}}} \approx_{\ln} 4^{N/4}\left(\frac{4}{3}\right)^{-3N/4} 4^{-N/4} = \left(\frac{3}{4}\right)^{3N/4} << 1. \tag{2.67}$$

We see that probability $W^{MCE}_{\{\{1\}\}} = \dfrac{\Gamma_{\{\{1\}\}}}{\Gamma^{MCE}} \approx_{\ln} \dfrac{\Gamma_{\{\{1\}\}}}{\Gamma_{\{\{p_0\}\}}}$ to observe the fluctuation $\{\{p=1\}\}$ is infinitesimal.

Problem 2.4.5

Illustrate the dependence of the statistical weight $\Gamma_{\{\{p\}\}}$ of fluctuations $\{\{p\}\}$ on p with the example of the model consisting of $N = 400$ spins. Demonstrate the validity of formula (2.58).

Solution: Following isolation condition (2.36), there are $N_{\downarrow} = N/4 = 100$ ↓-spins in the model. The dependence of the statistical weight $\Gamma_{\{\{p\}\}}$ of fluctuations $\{\{p\}\}$ on p is presented in the following figure.

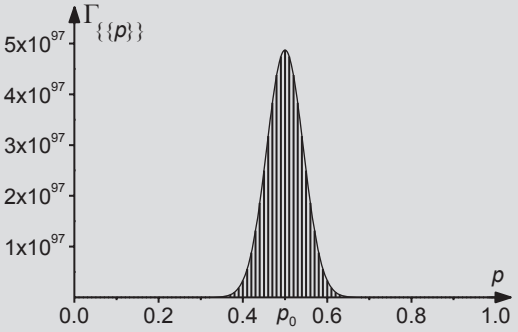

In this figure, different fluctuations $\{\{p\}\}$ are demonstrated as separate columns under the "bell" of the maximum. We see that already for the number of degrees of freedom of the order of 100 the fluctuations in the vicinity of the equilibrium macrostate have statistical weights of the order of 10^{97}. In contrast, there are only 101 separate fluctuations in the ensemble when the right half of the model contains 0,1,2,…,100 ↓-spins. Therefore, sum (2.44) contains only 101 terms, some of which are of the order of 10^{97}.

Fluctuations beyond the range $p = 0.4 - 0.6$ of the maximum have negligible statistical weights in comparison with statistical weight $\Gamma_{\{\{1/2\}\}} = 5 \cdot 10^{97}$ of the equilibrium macrostate $\{\{p_0 = 1/2\}\}$. Under the "bell" of the maximum, there are only about 20 separate fluctuations with 40, 41, 42,…,60 ↓-spins in the right half of the model $(p = 0.4 - 0.6)$. All these fluctuations

have comparable statistical weights of the order of 10^{97}. If we sum them all, we obtain the total statistical weight of the ensemble Γ^{MCE} which is only about ten times higher than the statistical weight $\Gamma_{\{\{1/2\}\}}$ of the equilibrium macrostate $\{\{p_0 = 1/2\}\}$! Therefore, comparing the logarithms of these two statistical weights,

$$\ln \Gamma^{MCE} = \ln(10 \cdot 5 \cdot 10^{97}) = 227 \tag{2.68a}$$

and

$$\ln \Gamma_{\{\{1/2\}\}} = \ln(5 \cdot 10^{97}) = 225, \tag{2.68b}$$

we can neglect their relative difference. And this happens already for the number of degrees of freedom in the model of the order of 100! But when we consider the thermodynamic limit of infinite number of degrees of freedom in the model, the relative difference between the statistical weight of the ensemble and the statistical weight of the equilibrium macrostate becomes even more negligible, and the statistical weight of the ensemble is indeed equal to its maximal term.

However, this does not mean at all that other terms are significantly smaller. There are at least 20 "near-equilibrium" fluctuations in the above figure (20 vertical columns under the "bell" of the maximum) which have statistical weights of the same order.

Equality (2.57) means that the entropy of the equilibrium macrostate equals the entropy of the ensemble:

$$S_{\{\{p_0\}\}} \approx S^{MCE}. \tag{2.69}$$

Since this equality is always valid when the rule of the logarithmic accuracy is applicable, these two different parameters are often treated as one. However, the reader should always clearly understand that one of these quantities corresponds to the equilibrium macrostate while another to the equilibrium distribution of probabilities.

2.5 Free Energy Potential of the MCE

Let us now develop the formalism of free energy potential of the MCE. Nonequilibrium processes within an isolated system lead this system to its equilibrium macrostate (Fig. 2.7).

From thermodynamics we know that for any process in an isolated system the entropy of the system always increases (or stays constant but does not decrease):

$$\Delta S \geq 0. \tag{2.70}$$

This principle is called *the entropy maximization principle*.

We define *the free energy potential* or, simply, *the free energy* to be a parameter that for any process in a system always decreases (or stays constant but does not increase):

$$\Delta \Psi \leq 0. \tag{2.71}$$

When a system reaches its equilibrium state, its free energy achieves its minimal value. Therefore, to find the equilibrium state of a system we always should look for the minimum of the system's free energy potential. This procedure is called *the free energy minimization principle*.

Comparing inequalities (2.70) and (2.71), we expect that the role of the free energy in the MCE is played by the negative entropy:

$$\Psi \equiv -S. \tag{2.72}$$

Let us return to expression (2.43) for the probability of fluctuations. Following Boltzmann's definition, the entropy of fluctuation, (2.39), is the logarithm of the fluctuation's statistical weight while the entropy of the ensemble, (2.28), is the logarithm of the ensemble statistical weight. Substituting these equations into (2.43), we find

$$W^{MCE}_{\{\{p\}\}} = \frac{\Gamma_{\{\{p\}\}}}{\Gamma^{MCE}} = e^{-(S^{MCE} - S_{\{\{p\}\}})}. \tag{2.73}$$

Since the logarithmic function is monotonic and Γ^{MCE} is constant, we see that the potential defined by (2.72) is always decreasing when the probability is increasing:

$$\Psi_{\{\{p\}\}} \equiv (-S_{\{\{p\}\}}) = -\ln(\Gamma^{MCE} W^{MCE}_{\{\{p\}\}}). \tag{2.74}$$

When the system reaches its equilibrium macrostate $\{\{p_0 = 1/2\}\}$, the probability $W^{MCE}_{\{\{p\}\}}$ is maximal and, therefore, the potential $\Psi_{\{\{p\}\}}$ achieves its minimal value $\Psi_{\{\{p_0\}\}} = -\ln \Gamma_{\{\{p_0\}\}}$. This proves that the potential $\Psi_{\{\{p\}\}}$ plays the role of the free energy in the MCE.

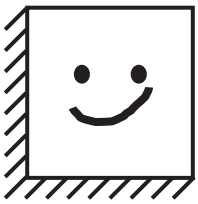

Fig. 2.7 All processes within an isolated system lead to the equilibrium macrostate

Now we see that there is nothing "magical" in the entropy growth. Since the entropy of a fluctuation is strictly correlated with the probability to observe this fluctuation in the ensemble, the entropy growth merely corresponds to the transition from less probable, nonequilibrium fluctuations to more probable, more "equilibrium" macrostates with higher statistical weights.

Each separate system, classical or quantum, is deterministic and during its evolution can pass through any microstate, even when a gas is gathered in one half of its volume. Why in reality do we not observe such fluctuations? Because they are highly improbable—their share of microstates is negligible in comparison with near-equilibrium fluctuations. But still nothing prohibits a deterministic system to be in a macrostate of such an improbable fluctuation.

But when we consider not a separate system but an ensemble of identical systems, the situation changes drastically. In the ensemble, we do not consider evolutions of separate systems. Instead, we average them stochastically.

But stochasticity claims that we are always moving in the direction of the increasing probability. Therefore, the behavior of the ensemble is governed by the rule that we have to go from less probable fluctuations to more probable, toward equilibrium. And it is not the entropy that breaks the symmetry of the time axis; it is the stochasticity forced onto the ensemble that dictates the direction of time.

Fluctuations moving the system away from its equilibrium are still possible. But they contradict the law of probability growth and, therefore, are improbable.

To illustrate these concepts, in the rest of the section we consider the aspects that lead to the growth of entropy. However, the discussion below could be confusing for the reader who just got acquainted with the MCE because we also have to discuss the equiprobability of microstates which we introduced in (2.20) as a hypothesis. Therefore, we encourage the reader to skip the rest of this section and return to it later, when the MCE would be well understood.

Let us consider an isolated quantum system whose state is described by a statistical operator (density matrix) $\hat{\rho}(t)$. The evolution of the statistical operator obeys *the Liouville–von Neumann equation* (von Neumann 1932, 1955):

$$\frac{\partial \hat{\rho}(t)}{\partial t} = \left[\frac{\hat{\mathrm{H}}}{i\hbar}, \hat{\rho}(t) \right]. \tag{2.75}$$

For the system's entropy, we utilize definition (2.22). To find how the entropy of the system changes with time, we differentiate this expression:

$$\frac{dS[\hat{\rho}]}{dt} = -\mathrm{Tr}\left(\frac{\partial \hat{\rho}}{\partial t} \ln \hat{\rho} \right) - \mathrm{Tr}\left(\frac{\partial \hat{\rho}}{\partial t} \right). \tag{2.76}$$

Since the diagonal elements of the statistical operator play the role of probabilities, its trace is always equal to unity:

$$\mathrm{Tr}(\hat{\rho}) = 1. \tag{2.77}$$

Therefore, we immediately find that the second term in (2.76) is zero:

$$\mathrm{Tr}\left(\frac{\partial\hat{\rho}}{\partial t}\right)=\frac{\partial}{\partial t}\mathrm{Tr}\left(\hat{\rho}\right)=\frac{\partial}{\partial t}1=0 \tag{2.78}$$

and the entropy growth equals

$$\frac{dS\left[\hat{\rho}\right]}{dt}=-\mathrm{Tr}\left(\frac{\partial\hat{\rho}}{\partial t}\ln\hat{\rho}\right). \tag{2.79}$$

Substituting (2.75) into this equation and rearranging the commutator's brackets, we find that the entropy growth is exactly zero:

$$\begin{aligned}\frac{dS\left[\hat{\rho}\right]}{dt}&=-\mathrm{Tr}\left(\left[\frac{\hat{\mathrm{H}}}{i\hbar},\hat{\rho}\right]\ln\hat{\rho}\right)=-\mathrm{Tr}\left(\frac{\hat{\mathrm{H}}}{i\hbar}\hat{\rho}\ln\hat{\rho}\right)+\mathrm{Tr}\left(\hat{\rho}\frac{\hat{\mathrm{H}}}{i\hbar}\ln\hat{\rho}\right)\\&=-\mathrm{Tr}\left(\frac{\hat{\mathrm{H}}}{i\hbar}\hat{\rho}\ln\hat{\rho}\right)+\mathrm{Tr}\left(\frac{\hat{\mathrm{H}}}{i\hbar}\ln\left(\hat{\rho}\right)\hat{\rho}\right)=-\mathrm{Tr}\left(\frac{\hat{\mathrm{H}}}{i\hbar}\left[\hat{\rho},\ln\hat{\rho}\right]\right)=0,\end{aligned} \tag{2.80}$$

because the statistical operator always commutates with its logarithm. Therefore, the entropy growth of a quantum system is zero even when it is not in a pure state but in a mixed state whose evolution is determined by the Liouville–von Neumann equation (2.75).

Let us, for example, consider the strictly isolated Ising model, consisting of $N=2$ spins, whose Hamiltonian is

$$\mathrm{H}_{\{\sigma_1,\sigma_2\}}=-\mu h\left(\sigma_1+\sigma_2\right)-J\sigma_1\sigma_2. \tag{2.81}$$

Here for the first time we consider an additional term in the Hamiltonian corresponding to interactions between two spins. This Hamiltonian has four eigenfunctions $\{\uparrow\uparrow\}$, $\{\uparrow\downarrow\}$, $\{\downarrow\uparrow\}$, and $\{\downarrow\downarrow\}$ with energies $E_{\{\uparrow,\uparrow\}}=-2\mu h-J$, $E_{\{\uparrow,\downarrow\}}=E_{\{\downarrow,\uparrow\}}=J$, and $E_{\{\downarrow,\downarrow\}}=2\mu h-J$. We will work in the energy representation; in other words, in the representation of microstates $\{\uparrow\uparrow\}$, $\{\uparrow\downarrow\}$, $\{\downarrow\uparrow\}$, and $\{\downarrow\downarrow\}$. Then the matrix of this Hamiltonian is

$$\left|\hat{\mathrm{H}}\right|=\sum_{\{E\}}E\left|E\right\rangle\left\langle E\right|=\begin{Vmatrix}-2\mu h-J & 0 & 0 & 0\\ 0 & J & 0 & 0\\ 0 & 0 & J & 0\\ 0 & 0 & 0 & 2\mu h-J\end{Vmatrix}. \tag{2.82}$$

Let us assume that at time $t=0$ the system is in the pure state $\{\uparrow\downarrow\}$:

$$\left|\Psi(0)\right\rangle=\left|\uparrow\downarrow\right\rangle=\begin{Vmatrix}0\\1\\0\\0\end{Vmatrix}. \tag{2.83}$$

This corresponds to the following density matrix:

$$\left|\widehat{\rho}(0)\right| = \left|\uparrow\downarrow\right\rangle\left\langle\uparrow\downarrow\right| = \begin{Vmatrix}0\\1\\0\\0\end{Vmatrix}\begin{Vmatrix}0 & 1 & 0 & 0\end{Vmatrix} = \begin{Vmatrix}0 & 0 & 0 & 0\\0 & 1 & 0 & 0\\0 & 0 & 0 & 0\\0 & 0 & 0 & 0\end{Vmatrix}. \tag{2.84}$$

The evolution of the pure quantum state is determined by *Schrödinger's equation* (Schrödinger 1926),

$$i\hbar\frac{\partial}{\partial t}\left|\Psi\right\rangle = \widehat{\mathrm{H}}\left|\Psi\right\rangle, \tag{2.85}$$

and provides the following time dependence:

$$\left|\Psi(t)\right\rangle = e^{-i\frac{J}{\hbar}t}\begin{Vmatrix}0\\1\\0\\0\end{Vmatrix}. \tag{2.86}$$

If we described the system not by the vector of state but by the density matrix, its evolution would be determined by the Liouville–von Neumann equation (2.75). But since the initial density matrix (2.84) commutes with the Hamiltonian (2.82), its derivative with respect to time is always zero

$$\frac{\partial\widehat{\rho}}{\partial t} = \frac{1}{i\hbar}\left[\widehat{\mathrm{H}},\widehat{\rho}\right] = \begin{Vmatrix}0 & 0 & 0 & 0\\0 & 0 & 0 & 0\\0 & 0 & 0 & 0\\0 & 0 & 0 & 0\end{Vmatrix} \tag{2.87}$$

and the density matrix remains unchanged:

$$\left|\widehat{\rho}(t)\right| = \left|\uparrow\downarrow\right\rangle\left\langle\uparrow\downarrow\right| = \begin{Vmatrix}0 & 0 & 0 & 0\\0 & 1 & 0 & 0\\0 & 0 & 0 & 0\\0 & 0 & 0 & 0\end{Vmatrix}. \tag{2.88}$$

But because the density matrix stays constant, the entropy (2.22) also stays constant. Substituting (2.88) into (2.22), we find the entropy of the system to be always zero (it is difficult to expect something else from the system staying in one microstate):

$$S(t) = 0. \tag{2.89}$$

We have considered clearly the most uninteresting case when the system, which is initially in the microstate $\{\uparrow\downarrow\}$, stays in this microstate forever. The system was isolated with energy $E = J$ but never visited the second microstate $\{\downarrow\uparrow\}$ which has the same value of energy (which belongs to the same energy level).

This system violates the equiprobability (2.20) hypothesis we introduced before. An analogy would be the ideal gas without particle collisions. If initially half of gas particles had velocities 10 m/s while the other half had 20 m/s, the gas would keep the velocities of its particles unchanged and we would never see the Maxwell–Boltzmann distribution. Similarly, for photons within a perfectly reflecting body we will never obtain the Planck spectrum.

To obtain the Maxwell–Boltzmann distribution for the ideal gas (to make its microstates with energies corresponding to the isolation condition all equiprobable), we should introduce rare events of particle collisions. This is equivalent to introduction of trajectory's mixing when the system can jump from one trajectory to another due to the presence of some noise.

To achieve the Planck spectrum within the perfectly reflecting body, we should introduce a small black dust particle inside the cavity. The dust particle is small and its term can be neglected in the common Hamiltonian. However, over long periods of time, it provides the equiprobability of microstates.

Similarly, for our quantum system we introduce some *noise* which leads to the system, jumping from one of microstates, $\{\uparrow\downarrow\}$ or $\{\downarrow\uparrow\}$, into another. Thereby, we consider the Hamiltonian which in the previous representation of microstates $\{\uparrow\uparrow\}$, $\{\uparrow\downarrow\}$, $\{\downarrow\uparrow\}$, and $\{\downarrow\downarrow\}$ is provided by the following matrix:

$$\left|\widehat{\mathrm{H}}\right| = \sum_{\{E\}} E\left|E\right\rangle\left\langle E\right| = \begin{Vmatrix} -2\mu h - J & 0 & 0 & 0 \\ 0 & J & i\hbar\varepsilon & 0 \\ 0 & -i\hbar\varepsilon^{*} & J & 0 \\ 0 & 0 & 0 & 2\mu h - J \end{Vmatrix}. \tag{2.90}$$

We continue to work in the representation of microstates $\{\uparrow\uparrow\}$, $\{\uparrow\downarrow\}$, $\{\downarrow\uparrow\}$, and $\{\downarrow\downarrow\}$ for the illustrative purposes, although the eigenfunctions of the new Hamiltonian may not coincide with the microstates $\{\uparrow\uparrow\}$, $\{\uparrow\downarrow\}$, $\{\downarrow\uparrow\}$, and $\{\downarrow\downarrow\}$. Thereby, we, in fact, no longer work in the energy representation of the system.

We consider the nondiagonal noise term to be small, where $\varepsilon \to 0$ is some small complex constant. For the same initial state (2.83), we integrate Schrödinger's equation (2.85) to find that system still stays in the pure state

$$\left|\Psi(t)\right\rangle = e^{-i\frac{J}{\hbar}t} \begin{Vmatrix} 0 \\ \cos(|\varepsilon|t) \\ -\dfrac{\varepsilon^{*}}{|\varepsilon|}\sin(|\varepsilon|t) \\ 0 \end{Vmatrix}. \tag{2.91}$$

Integrating the Liouville–von Neumann equation (2.75), for the density matrix we also find

$$\left|\hat{\rho}(t)\right| = \left|\Psi(t)\right\rangle\left\langle\Psi(t)\right| = \begin{Vmatrix} 0 & 0 & 0 & 0 \\ 0 & \frac{1}{2}+\frac{1}{2}\cos\left(2|\varepsilon|t\right) & -\frac{1}{2}\frac{\varepsilon}{|\varepsilon|}\sin\left(2|\varepsilon|t\right) & 0 \\ 0 & -\frac{1}{2}\frac{\varepsilon^*}{|\varepsilon|}\sin\left(2|\varepsilon|t\right) & \frac{1}{2}-\frac{1}{2}\cos\left(2|\varepsilon|t\right) & 0 \\ 0 & 0 & 0 & 0 \end{Vmatrix}. \tag{2.92}$$

From (2.91) and (2.92), we clearly see that the introduction of small noise has made the system to oscillate between microstates, $\left\{\uparrow\downarrow\right\}$ and $\left\{\downarrow\uparrow\right\}$ (has led to the mixture of these microstates). However, nothing in the formulae above has made the derivation of zero entropy growth (2.80) no longer valid. In other words, if we substitute the density matrix (2.92) into the entropy definition (2.22), the entropy will still be constant during the system's evolution. The reader can easily prove it herself/himself and find that the entropy is zero (2.89) again (the entropy will always be zero for a system in a pure state).

Even if we consider the noise, deterministically depending on time, $\varepsilon(t)$, the derivation of (2.80) will still be valid, and entropy will remain constant.

A similar situation occurs when we consider not the pure but the mixed state whose time dependence is provided by the Liouville–von Neumann equation (2.75). The entropy would probably be already nonzero, but still (2.80) would give zero growth for the entropy.

To understand what is going on let us return to the obtained solution (2.92). The density matrix is not diagonal which we expect for the equilibrium distribution (2.112). And strictly speaking, we do not see the equiprobability of microstates $\left\{\uparrow\downarrow\right\}$ and $\left\{\downarrow\uparrow\right\}$. Instead, we see oscillations between these two microstates. But we can consider the so-called *sliding (moving) time averaging* when for each time t we average any time dependence in the neighborhood of this time over the interval $t-\Delta t/2 < t < t+\Delta t/2$. Assuming that the interval of averaging is much larger than the period of oscillations, $\Delta t >> \frac{2\pi}{|\varepsilon|}$, we lose all time dependencies in (2.92) and find

$$\left\langle\hat{\rho}(t)\right\rangle_t = \begin{Vmatrix} 0 & 0 & 0 & 0 \\ 0 & 1/2 & 0 & 0 \\ 0 & 0 & 1/2 & 0 \\ 0 & 0 & 0 & 0 \end{Vmatrix}. \tag{2.93}$$

Here the density matrix becomes diagonal and microstates $\left\{\uparrow\downarrow\right\}$ and $\left\{\downarrow\uparrow\right\}$ are already undoubtedly equiprobable.

The evolution of the system has initiated from the pure state (2.84) with zero entropy (2.89). On the contrary, substituting (2.93) into (2.22), we find the nonzero entropy:

$$S\left[\left\langle\hat{\rho}(t)\right\rangle_t\right] = \ln 2 > 0. \tag{2.94}$$

This is the entropy growth, from 0 to ln 2, and we see that it has been caused by the very time averaging.

Why has it happened? Because the procedure of time averaging included averaging over classical probabilities. The averaging over the classical probabilities cannot be described by the formalism of the Liouville–von Neumann equation (2.75) which deals only with quantum uncertainties. It does not belong to quantum mechanics; and the derivation of zero entropy growth (2.80) did not consider it.

But what is time averaging? Obviously, if we consider the noise $\varepsilon(t)$ to depend on time not deterministically but stochastically, with classical probability distribution (stochastic trajectory's mixing), this will be equivalent to the time averaging and will provide the nonzero entropy growth.

We see that for the considered system the simple noise introduction leads only to the oscillations among microstates. On the contrary, introduction of averaging with classical uncertainties leads to the equiprobability of microstates and to the entropy growth.

So far we have considered time averaging of a particular system. What would happen if instead of time averaging we considered ensemble averaging over the classical probability distribution?

The evolution of our system has initiated from the pure state (2.84). Instead of a particular initial time $t = 0$, we can consider arbitrary time which is equivalent to introduction of the additional phase of oscillations:

$$\left|\hat{\rho}(t,\theta)\right| = \begin{Vmatrix} 0 & 0 & 0 & 0 \\ 0 & \frac{1}{2} + \frac{\cos\left(2|\varepsilon|t+\theta\right)}{2} & -\frac{1}{2}\frac{\varepsilon}{|\varepsilon|}\sin\left(2|\varepsilon|t+\theta\right) & 0 \\ 0 & -\frac{1}{2}\frac{\varepsilon^*}{|\varepsilon|}\sin\left(2|\varepsilon|t+\theta\right) & \frac{1}{2} - \frac{\cos\left(2|\varepsilon|t+\theta\right)}{2} & 0 \\ 0 & 0 & 0 & 0 \end{Vmatrix}. \tag{2.95}$$

We are building the ensemble by considering different initial conditions for each particular system. If we allow the role of the initial condition to be played by the phase of oscillations, averaging over the ensemble (over initial values of θ) will be given by

$$\left\langle \hat{\rho}(t) \right\rangle_{ensemble} = \int_0^{2\pi} \hat{\rho}(t,\theta)\,\mathrm{pdf}(\theta)\,d\theta, \tag{2.96}$$

where pdf is the classical probability density function:

$$\mathrm{pdf}(\theta) = \frac{1}{2\pi} \text{ while } 0 \le \theta \le 2\pi. \tag{2.97}$$

Since the statistical operator $\hat{\rho}(t,\theta)$ in the integrand represents the pure state (2.91), we are, in fact, averaging pure states with classical probabilities:

$$\left\langle \hat{\rho}(t) \right\rangle_{ensemble} = \int_0^{2\pi} \left| \Psi(t,\theta) \right\rangle \left\langle \Psi(t,\theta) \right| \text{pdf}\,(\theta)\, d\theta. \tag{2.98}$$

Although (2.98) is often considered as a quantum density matrix, it is, in fact, not in the sense that it is no longer the solution of the Liouville–von Neumann equation (2.75). The averaging over classical probability distribution is not described by the Liouville–von Neumann equation (2.75), and (2.98) no longer represents quantum statistical operator. In contrast, it is now the ensemble statistical operator.

The ensemble averaging returns us to the same density matrix (2.93) as in the case of the time averaging:

$$\left\langle \hat{\rho}(t) \right\rangle_{ensemble} = \begin{Vmatrix} 0 & 0 & 0 & 0 \\ 0 & 1/2 & 0 & 0 \\ 0 & 0 & 1/2 & 0 \\ 0 & 0 & 0 & 0 \end{Vmatrix}. \tag{2.99}$$

It would be difficult to expect something else because ensemble averaging involves the same averaging over classical probabilities.

Another important aspect here is that we have proved for our system the statement of the ergodic hypothesis that time averaging is equivalent to ensemble averaging.

2.6 MCE: Free Energy Minimization Principle (Entropy Maximization Principle)

In the previous sections, we assumed the equiprobability of all microstates in the MCE and have proved that the negative entropy is the free energy potential of the MCE. In this section, the other way around, we assume that the free energy potential of the MCE is the negative entropy and will prove the equiprobability of all ensemble microstates.

Following (2.72) and (2.21), we define the free energy in the MCE as

$$\Psi[w_{\{\}}] = \sum_{\{\}} w_{\{\}} \ln w_{\{\}}. \tag{2.100}$$

This potential is the functional defined on the function space of all possible probability distributions $w_{\{\}}$.

By definition, the equilibrium corresponds to the minimum of the free energy. Therefore, to find the equilibrium distribution of probabilities we should minimize the free energy potential (2.100) over all nonequilibrium distributions $w_{\{\}}$.

But any probability distribution is normalized to unity:

$$\sum_{\{\}} w_{\{\}} = 1 \tag{2.101}$$

and instead of all possible functional dependences $w_{\{\}}$ only normalized probability distributions $w_{\{\}}$ should be considered during minimization.

It is easy to do minimization subject to equality constraint (2.101) by utilizing the method of Lagrange multipliers,

$$\Psi[w_{\{\}}] = \sum_{\{\}} w_{\{\}} \ln w_{\{\}} + \lambda \left(\sum_{\{\}} w_{\{\}} - 1 \right), \tag{2.102}$$

where to functional (2.100) we added constraint (2.101) multiplied by the Lagrange multiplier λ.

To minimize this functional we should find when its derivatives equal zero. The derivative with respect to λ returns us to constraint (2.101),

$$0 = \frac{\partial \Psi}{\partial \lambda} = \sum_{\{\}} w_{\{\}}^{MCE} - 1, \tag{2.103}$$

where we used the superscript index "*MCE*" to emphasize that this is the equilibrium probability distribution.

The derivative with respect to the probability $w_{\{\}'}$ of microstate $\{\}'$ provides equation

$$0 = \frac{\partial \Psi}{\partial w_{\{\}'}} = \ln w_{\{\}'}^{MCE} + 1 + \lambda \text{ or } w_{\{\}'}^{MCE} = e^{-1-\lambda}. \tag{2.104}$$

We see that the equilibrium probability distribution $w_{\{\}}^{MCE}$ does not depend on the parameters of a particular microstate and, therefore, all microstates are equiprobable. Substituting $w_{\{\}}^{MCE} = const$ into (2.103), we find

$$\Gamma^{MCE} w_{\{\}}^{MCE} = 1 \tag{2.105}$$

which returns us to (2.20).

In (2.100) for the entropy functional we utilized definition (2.21) corresponding to the case of the diagonal statistical operator. But what would happen if we considered a nondiagonal statistical operator? In this case, we should substitute not (2.21), but (2.22) into (2.72) to obtain the desired functional of the free energy potential:

$$\Psi[\hat{\rho}] = \mathrm{Tr}\left(\hat{\rho} \ln \hat{\rho}\right). \tag{2.106}$$

This functional is defined on the operator space of all possible statistical operators $\hat{\rho}$. Again, the statistical operator is normalized by

$$\mathrm{Tr}\left(\hat{\rho}\right) = 1. \tag{2.107}$$

To minimize the functional subject to equality constraint (2.107), we utilize the method of Lagrange multipliers:

$$\Psi[\hat{\rho}] = \mathrm{Tr}\left(\hat{\rho}\ln\hat{\rho}\right) + \lambda\left(\mathrm{Tr}\left(\hat{\rho}\right) - 1\right). \tag{2.108}$$

To find the equilibrium statistical operator $\hat{\rho}^{MCE}$, we should minimize this functional by equaling its derivatives to zero. The derivative with respect to λ returns us to constraint (2.107). The derivative with respect to $\hat{\rho}$ provides the following equation:

$$\mathrm{Tr}\left(\delta\hat{\rho}\ln\hat{\rho}^{MCE} + \delta\hat{\rho} + \lambda\delta\hat{\rho}\right) = 0. \tag{2.109}$$

Since this equality should hold for any arbitrary variation $\delta\hat{\rho}$, we find

$$\ln\hat{\rho}^{MCE} + \hat{1} + \lambda\hat{1} = 0, \tag{2.110}$$

where $\hat{1}$ is the unity matrix. The solution of this equation is

$$\hat{\rho}^{MCE} = e^{-(1+\lambda)\hat{1}} = e^{-(1+\lambda)}\hat{1}. \tag{2.111}$$

This matrix is diagonal and all diagonal elements are equal one to another. Substituting (2.111) into constraint (2.107), we find that all diagonal elements are equal to the inverse statistical weight of the ensemble:

$$\hat{\rho}^{MCE}_{\{\},\{\}'} = \frac{\delta_{\{\},\{\}'}}{\Gamma^{MCE}}. \tag{2.112}$$

Therefore, in the operator space of all possible nonequilibrium statistical operators $\hat{\rho}$ the equilibrium operator $\hat{\rho}^{MCE}$ corresponds again to the equiprobable distribution (2.20).

2.7 Canonical Ensemble

In the previous sections, we have considered the case of the MCE corresponding to an isolated system. Now we relax the isolation constraint and allow our system to participate in heat exchange (Fig. 2.8). We still consider a system at constant volume $V = const$ ($\delta W^{\leftarrow} = 0$) and constant number of particles $N = const$ $\left(\delta\Pi^{\leftarrow} = 0\right)$. But now the system can exchange heat, $\delta Q^{\leftarrow} \neq 0$, with surrounding medium called *thermal reservoir* (or *heat reservoir*, or *heat bath*, or *thermostat*).

The thermal reservoir is assumed to be so big in comparison with our system that any energy fluctuations in our system do not influence its temperature. Besides, its heat conductance is assumed to be perfect which allows it to react immediately to

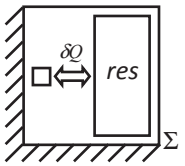

Fig. 2.8 The system in contact with the thermal reservoir

any boundary heat exchange by maintaining the temperature T^{res} always constant. Here and further by the superscript index "*res*" we denote the reservoir parameters.

The fact that the reservoir's temperature is always constant leads to two consequences. Firstly, since any fluctuations in our system are negligible for the reservoir, the last participates in heat exchange always quasistatically.

Secondly, the system is assumed to be at constant temperature condition $T^{res} = const$. An ensemble of such systems is called *a canonical ensemble* (or *CE*).

Uniting our system and the thermal reservoir into one "big" system Σ, we consider the system Σ to be isolated, $E^{\Sigma} = const$ (Fig. 2.8). Then the behavior of the system Σ is described by the MCE formalism. To avoid complications, we will always assume the strict isolation of the system Σ on one of its energy levels (in one group of microstates).

Generally speaking, heat exchange between our system and the thermal reservoir means interaction of these two subsystems when the total Hamiltonian $\widehat{\mathrm{H}}^{\Sigma}$ of the system Σ, besides the sum of the Hamiltonians of our system $\widehat{\mathrm{H}}$ and of the reservoir $\widehat{\mathrm{H}}^{res}$, contains also an interaction term $\widehat{V}$:

$$\widehat{\mathrm{H}}^{\Sigma} = \widehat{\mathrm{H}} + \widehat{\mathrm{H}}^{res} + \widehat{V}. \tag{2.113}$$

We could build energy spectra for both our system $\{E\}$ and the thermal reservoir $\left\{E^{res}\right\}^{res}$ as the eigenfunctions of the Hamiltonians $\widehat{\mathrm{H}}$ and $\widehat{\mathrm{H}}^{res}$, respectively. However, due to the presence of the interaction term $\widehat{V}$ the energy spectrum $\left\{E^{\Sigma}\right\}^{\Sigma}$ of the system Σ would not be represented by the tensor product of these spectra:

$$\left\{E^{\Sigma}\right\}^{\Sigma} \neq \{E\} \otimes \left\{E^{res}\right\}^{res}. \tag{2.114}$$

To avoid this complication, it is often assumed that the interaction term $\widehat{V}$ is small because interactions with the reservoir are provided by the parts of the system close to its surface. Since the number of degrees of freedom on the surface, $N^{\frac{d-1}{d}}$, is much smaller than the number of degrees of freedom in the system's volume, N,

$$N^{\frac{d-1}{d}} << N, \tag{2.115}$$

where d is the dimensionality of the system, we can usually neglect the surface energy in comparison with the energy in the volume of the system and thereby neglect the term $\widehat{V}$ in Hamiltonian (2.113).

However, we do not follow this approach because, firstly, heat exchange can be not limited to the surface of the model and, secondly, we consider surface energy being of extreme importance for the phase transition phenomena. Instead, we consider the *stroboscopic approximation* when we allow our system to interact with the reservoir "stroboscopically." Our system interacts with the thermal reservoir by heat exchange. After some period of time, we briefly isolate it and observe how much energy it has "consumed" or "provided." Then we allow the interactions to resume heat exchange; then again, we briefly isolate our system and observe its energy change. And so on, and so on. In other words, into the process of heat exchange we introduce very brief periods of *virtual isolation* which do not influence the system's behavior but allow us to observe the system in the absence of the interaction term $\hat{V}$.

This way, if we observe our system only during short periods of virtual isolation, we can treat it as if it were fully isolated except for the fact that its energy constantly jumps from one value to another. Therefore, we exclude the interaction term $\hat{V}$ from the total Hamiltonian,

$$\hat{\mathrm{H}}^{\Sigma} = \hat{\mathrm{H}} + \hat{\mathrm{H}}^{res}, \tag{2.116}$$

and consider microstates $\left\{E^{\Sigma}\right\}^{\Sigma}$ of the system Σ to be the tensor product of the set of microstates $\{E\}$ of our system and the set of reservoir's microstates $\left\{E^{res}\right\}^{res}$:

$$\left\{E^{\Sigma}\right\}^{\Sigma} = \{E\} \otimes \left\{E^{res}\right\}^{res}. \tag{2.117}$$

In other words, choosing a particular microstate $\{E\}$ for our system and a particular microstate $\left\{E^{res}\right\}^{res}$ for the thermal reservoir, we form a particular microstate $\left\{E^{\Sigma}\right\}^{\Sigma}$ of the system Σ. Therefore, it is often said that even in the presence of heat exchange the energy spectra of two subsystems are still identifiable separately as if for independent subsystems.

The "big" system Σ is isolated. Therefore, if the energy of our system were increasing, the energy of the thermal reservoir would be decreasing:

$$E + E^{res} = E^{\Sigma} = \mathrm{const}. \tag{2.118}$$

Let us look at Fig. 2.9 where to the left we schematically plot the energy spectrum of our system while to the right we have the energy spectrum of the thermal reservoir. Both spectra are divided into groups of microstates.

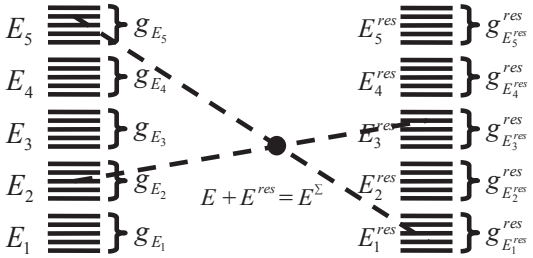

Fig. 2.9 Energy fluctuations

If our system "lives" in group E_2, the thermal reservoir must be somewhere in its group $E_3^{res} = E^{\Sigma} - E_2$. When our system takes away from the thermal reservoir some additional energy and jumps into group E_5, the thermal reservoir, following (2.118), has to move into group $E_1^{res} = E^{\Sigma} - E_5$.

As we have discussed above, a microstate $\left\{E^{\Sigma}\right\}^{\Sigma}$ can be formed by the choice of a particular microstate $\{E\}$ of our system (a horizontal line to the left in Fig. 2.9) and a particular microstate $\left\{E^{res}\right\}^{res}$ of the thermal reservoir (a horizontal line to the right), providing, of course, that equality (2.118) holds. Therefore, to find the statistical weight $\Gamma^{\Sigma,MCE}$ of the MCE ensemble of the system Σ we should go over all microstates of our system, one by one. For each microstate $\{E\}$ of our system, we should calculate in accordance with (2.118) the corresponding energy of the thermal reservoir. Then we should go over all reservoir's microstates $\left\{E^{res}\right\}^{res}$ in the group with this value of energy because the thermal reservoir could be in any of them. Finally, we obtain

$$\Gamma^{\Sigma,MCE} = \sum_{\{E\}} \sum_{\substack{\left\{E^{res}\right\}^{res}: \\ E^{res} = E^{\Sigma} - E}} 1 = \sum_{E} g_E g_{E^{\Sigma}-E}^{res}, \tag{2.119}$$

where in the last equality we went from the sum over microstates $\{E\}$ to the sum over the different values of energy for our system.

The isolated system Σ is in the MCE. Therefore, all its microstates are equiprobable:

$$w_{\left\{E^{\Sigma}\right\}^{\Sigma}}^{\Sigma,MCE} = \frac{1}{\Gamma^{\Sigma,MCE}}. \tag{2.120}$$

In this case, the probability for our system to be in a particular microstate $\{E\}$ with energy E is the sum of probabilities (2.120) over all reservoir's microstates $\left\{E^{res}\right\}^{res}$ with energy $E^{res} = E^{\Sigma} - E$:

$$w_{\{E\}}^{CE} = \frac{g_{E^{\Sigma}-E}^{res}}{\Gamma^{\Sigma,MCE}}. \tag{2.121}$$

Then the probability for our system to have energy E is just g_E times higher because in this case our system can be in any of g_E microstates of the group corresponding to this value of energy E:

$$W_E^{CE} = g_E w_{\{E\}}^{CE} = \frac{g_E g_{E^{\Sigma}-E}^{res}}{\Gamma^{\Sigma,MCE}}. \tag{2.122}$$

Problem 2.7.1

Illustrate formulae (2.119)–(2.122) with the aid of the Ising model without spin interactions when the model consists of $N = 3$ spins.

Solution: Let us assume for a moment that the system has, for example, energy $E = -\mu h$. Then it is in one of three microstates $\{\uparrow\uparrow\downarrow\}$, $\{\uparrow\downarrow\uparrow\}$, or $\{\downarrow\uparrow\uparrow\}$ while the energy of the reservoir is $E^{res} = E^{\Sigma} + \mu h$ and the reservoir is in one of its $g^{res}_{E^{\Sigma}+\mu h}$ microstates, corresponding to this value of energy. The general correspondence between two spectra is shown in the following figure.

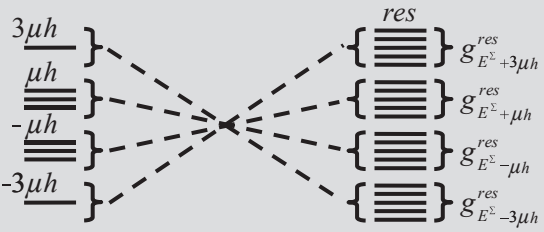

Now, when we have described how two spectra are associated one with another, we can start constructing microstates $\{E^{\Sigma}\}^{\Sigma}$ of the total system Σ. If our system is in microstate $\{\uparrow\uparrow\uparrow\}$, the thermal reservoir can be in any of its $g^{res}_{E^{\Sigma}+3\mu h}$ microstates $\{E^{res}\}^{res}$ and a combination of microstate $\{\uparrow\uparrow\uparrow\}$ and any of these reservoir's microstates form a microstate $\{E^{\Sigma}\}^{\Sigma}$ of the system Σ. When our system is in one of microstates $\{\uparrow\uparrow\downarrow\}$, $\{\uparrow\downarrow\uparrow\}$, $\{\downarrow\uparrow\uparrow\}$, a combination of any of these microstates and any of $g^{res}_{E^{\Sigma}+\mu h}$ reservoir's microstates again form a microstate $\{E^{\Sigma}\}^{\Sigma}$ of the system Σ. And so on. Summing, we find

$$\begin{aligned}\Gamma^{\Sigma,MCE} &= g_{-3\mu h}g^{res}_{E^{\Sigma}+3\mu h} + g_{-\mu h}g^{res}_{E^{\Sigma}+\mu h} + g_{\mu h}g^{res}_{E^{\Sigma}-\mu h} + g_{3\mu h}g^{res}_{E^{\Sigma}-3\mu h}\\ &= g^{res}_{E^{\Sigma}+3\mu h} + 3g^{res}_{E^{\Sigma}+\mu h} + 3g^{res}_{E^{\Sigma}-\mu h} + g^{res}_{E^{\Sigma}-3\mu h}. \qquad (2.123)\end{aligned}$$

The system Σ is isolated, and all its microstates are equiprobable:

$$w^{\Sigma,MCE}_{\{E^{\Sigma}\}^{\Sigma}} = \frac{1}{g^{res}_{E^{\Sigma}+3\mu h} + 3g^{res}_{E^{\Sigma}+\mu h} + 3g^{res}_{E^{\Sigma}-\mu h} + g^{res}_{E^{\Sigma}-3\mu h}}. \qquad (2.124)$$

How do we find the probability for our system to be, for example, in microstate $\{\uparrow\downarrow\downarrow\}$? When our system is in this microstate, its energy is $E = \mu h$ and the energy of the reservoir is $E^{res} = E^{\Sigma} - \mu h$. Therefore, the thermal reservoir can be in any of its $g^{res}_{E^{\Sigma}-\mu h}$ microstates, which, together with microstate

$\{\uparrow\downarrow\downarrow\}$, form $g^{res}_{E^{\Sigma}-\mu h}$ microstates of the system Σ. Since the probability of any of microstates of the system Σ is (2.124), to find the probability for our system to be in microstate $\{\uparrow\downarrow\downarrow\}$ we should sum probabilities (2.124) for $g^{res}_{E^{\Sigma}-\mu h}$ corresponding microstates of the system Σ:

$$w^{CE}_{\{\uparrow\downarrow\downarrow\}} = \frac{g^{res}_{E^{\Sigma}-\mu h}}{g^{res}_{E^{\Sigma}+3\mu h} + 3g^{res}_{E^{\Sigma}+\mu h} + 3g^{res}_{E^{\Sigma}-\mu h} + g^{res}_{E^{\Sigma}-3\mu h}}. \tag{2.125}$$

To find the probability for our system to have energy $E = \mu h$, we should sum the probabilities for our system to be in any of its microstates $\{\uparrow\downarrow\downarrow\}$, $\{\downarrow\uparrow\downarrow\}$, $\{\downarrow\downarrow\uparrow\}$:

$$\begin{aligned} W^{CE}_{\mu h} &= w^{CE}_{\{\uparrow\downarrow\downarrow\}} + w^{CE}_{\{\downarrow\uparrow\downarrow\}} + w^{CE}_{\{\downarrow\downarrow\uparrow\}} \\ &= \frac{3g^{res}_{E^{\Sigma}-\mu h}}{g^{res}_{E^{\Sigma}-3\mu h} + 3g^{res}_{E^{\Sigma}-\mu h} + 3g^{res}_{E^{\Sigma}+\mu h} + g^{res}_{E^{\Sigma}+3\mu h}}. \end{aligned} \tag{2.126}$$

2.8 Nonequilibrium Fluctuations of the Canonical Ensemble

In formulae (2.121) and (2.122), we have utilized the superscript "*CE*" because these probability distributions corresponded to the rules dictated by the CE and, therefore, were in equilibrium with the ensemble. In this section, we introduce nonequilibrium fluctuations as nonequilibrium probability distributions.

In the MCE, the microstates $\{E, p\}$ were distinguished by some set of fluctuating parameters p while their energy was prescribed by the isolation condition. In the CE, energy E of the system becomes a new fluctuating parameter. Then we define *the nonequilibrium fluctuation* $\{\{E, p\}\}$ $\left(\textit{macrostate } \{\{E, p\}\}\right)$ by the following nonequilibrium probability distribution:

$$w_{\{\tilde{E},\tilde{p}\}} = \begin{Bmatrix} 1/\Gamma_{\{\{E,p\}\}} & ,\tilde{E} = E \textit{ and } \tilde{p} = p \\ 0 & ,\textit{otherwise} \end{Bmatrix} = \frac{\delta_{\tilde{E},E}\delta_{\tilde{p},p}}{\Gamma_{\{\{E,p\}\}}}. \tag{2.127}$$

The simplest case, which we consider in future formulae, is when we distinguish macrostates only by the values of energy of the system. These fluctuations $\{\{E\}\}$ are defined by the distribution

$$w_{\{\tilde{E}\}} = \begin{Bmatrix} 1/\Gamma_{\{\{E\}\}} & ,\tilde{E} = E \\ 0 & ,\textit{otherwise} \end{Bmatrix} = \frac{\delta_{\tilde{E},E}}{\Gamma_{\{\{E\}\}}}. \tag{2.128}$$

In this case, the macrostate $\{\{E\}\}$ is just the fluctuation corresponding to the system with energy E; and we will call this macrostate as *the energy fluctuation* in the system.

The statistical weight $\Gamma_{\{\{E\}\}}$ of energy fluctuation $\{\{E\}\}$ is just the statistical weight of this energy level (of this group of microstates):

$$\Gamma_{\{\{E\}\}} = g_E. \tag{2.129}$$

Substituting the nonequilibrium distribution of probabilities (2.128) into the definition of entropy (2.21), we find *the entropy of the fluctuation* $\{\{E\}\}$:

$$S_{\{\{E\}\}} = -\sum_{\{\tilde{E}\}} w_{\{\tilde{E}\}} \ln w_{\{\tilde{E}\}} = \ln \Gamma_{\{\{E\}\}}, \tag{2.130}$$

again obeying Boltzmann's rule.

Problem 2.8.1

Explain what energy fluctuations are with the aid of the Ising model without spin interactions when the model consists of $N = 3$ spins.

Solution: There are four energy fluctuations in this model: $\{\{-3\mu h\}\}$, $\{\{-\mu h\}\}$, $\{\{\mu h\}\}$, and $\{\{3\mu h\}\}$.

Macrostate $\{\{-3\mu h\}\}$ corresponds to the fluctuation with energy $E = -3\mu h$. Only one microstate $\{\uparrow\uparrow\uparrow\}$ corresponds to this fluctuation; therefore, its statistical weight equals unity, $\Gamma_{\{\{-3\mu h\}\}} = 1$, and its entropy is zero, $S_{\{\{-3\mu h\}\}} = 0$.

Three microstates $\{\uparrow\uparrow\downarrow\}$, $\{\uparrow\downarrow\uparrow\}$, and $\{\downarrow\uparrow\uparrow\}$ correspond to energy fluctuation $\{\{-\mu h\}\}$ with statistical weight $\Gamma_{\{\{-\mu h\}\}} = 3$ and entropy $S_{\{\{-\mu h\}\}} = \ln 3$.

Similarly, for two remaining energy fluctuations we have $\Gamma_{\{\{\mu h\}\}} = 3$ and $S_{\{\{\mu h\}\}} = \ln 3$, $\Gamma_{\{\{3\mu h\}\}} = 1$ and $S_{\{\{3\mu h\}\}} = 0$.

What is the probability to observe fluctuation $\{\{E\}\}$ in the CE, that is, the probability to observe the system in the CE at a particular energy level (group of microstates)? Obviously, we have already found this probability as probability (2.122) for the system to have energy E:

$$W^{CE}_{\{\{E\}\}} = \Gamma_{\{\{E\}\}} w^{CE}_{\{E\}} = \frac{\Gamma_{\{\{E\}\}} \Gamma^{res}_{\{\{E^\Sigma - E\}\}^{res}}}{\Gamma^{\Sigma,MCE}}. \tag{2.131}$$

While $\Gamma^{\Sigma,MCE}$ is some constant, two other quantities, $\Gamma_{\{\{E\}\}} \equiv g_E$ and $\Gamma^{res}_{\{\{E^\Sigma - E\}\}^{res}} \equiv g^{res}_{E^\Sigma - E}$, depend on the energy E of the fluctuation $\{\{E\}\}$. Since both these quantities also depend exponentially on N, these are very fast dependencies.

When the system is taking some energy away from the thermal reservoir, its statistical weight rapidly increases while the statistical weight of the reservoir rapidly decreases. The "clash" of these two "fast" dependencies leads to the appearance of a very narrow maximum of the probability distribution (2.131). To obtain this maximum, we find when the derivative of the probability distribution (2.131) (or the derivative of the logarithm of this distribution) becomes zero at the point of the most probable, equilibrium fluctuation $\{\{E_0\}\}$:

$$\left.\frac{\partial W^{CE}_{\{\{E\}\}}}{\partial E}\right|_{E_0} = 0 \text{ and } \left.\frac{\partial \ln W^{CE}_{\{\{E\}\}}}{\partial E}\right|_{E_0} = 0. \tag{2.132}$$

Equation (2.132) is called *the equation of the equilibrium macrostate*. Differentiating (2.131), we find

$$\frac{1}{\Gamma_{\{\{E\}\}}}\frac{d\Gamma_{\{\{E\}\}}}{dE} = -\frac{1}{\Gamma^{res}_{\{\{E^{\Sigma}-E\}\}^{res}}}\frac{d\Gamma^{res}_{\{\{E^{\Sigma}-E\}\}^{res}}}{dE} = \frac{1}{\Gamma^{res}_{\{\{E^{res}\}\}^{res}}}\frac{d\Gamma^{res}_{\{\{E^{res}\}\}^{res}}}{dE^{res}}, \tag{2.133}$$

$$\text{or } \frac{d\ln\Gamma_{\{\{E\}\}}}{dE} = \frac{d\ln\Gamma^{res}_{\{\{E^{res}\}\}^{res}}}{dE^{res}}, \text{ or } \frac{dS_{\{\{E\}\}}}{dE} = \frac{dS^{res}_{\{\{E^{res}\}\}^{res}}}{dE^{res}}$$

where $S^{res}_{\{\{E^{res}\}\}^{res}}$ is the entropy of the fluctuation $\left\{\left\{E^{res}\right\}\right\}^{res}$ of the reservoir.

Following thermodynamics, for quasistatic processes we define a system's temperature as the derivative of the system's energy with respect to system's entropy:

$$T \equiv \frac{dE}{dS_{\{\{E\}\}}}. \tag{2.134}$$

Since in the vicinity of the equilibrium all fluctuations are small (near quasistatic), the equilibrium equality (2.133) transforms into the requirement for the system's temperature to be equal to the reservoir's temperature:

$$\frac{1}{T} = \frac{1}{T^{res}} \text{ or } \beta = \beta^{res}, \tag{2.135}$$

where β usually denotes the inverse temperature, $\beta \equiv 1/T$.

Let us now obtain a more suitable expression for the probability to observe our system in microstate $\{E\}$. Since $\Gamma^{\Sigma,MCE}$ is constant and does not depend on the system's energy, we transform (2.121) into

$$w^{CE}_{\{E\}} \propto e^{S^{res}_{\{\{E^{\Sigma}-E\}\}^{res}}}. \tag{2.136}$$

Our system and its fluctuations are small in comparison with the energy of the thermal reservoir. Therefore, we can expand the reservoir's entropy in powers of the energy E of our system as a small parameter:

$$w_{\{E\}}^{CE} \propto e^{S^{res}_{\{\{E^{res}\}\}^{res}}\Big|_{E^{res}=E^{\Sigma}} - E\left.\frac{dS^{res}_{\{\{E^{res}\}\}^{res}}}{dE^{res}}\right|_{E^{res}=E^{\Sigma}}} \propto e^{-E/T^{res}}. \tag{2.137}$$

Since all processes are quasistatic for the thermal reservoir, we have utilized here definition (2.134) for its temperature. Also we should note that the reservoir's temperature has been defined at the point when all the energy of the total system Σ is gathered inside the reservoir and our system has zero energy:

$$T^{res} = \left.\frac{dE^{res}}{dS^{res}_{\{\{E^{res}\}\}^{res}}}\right|_{E^{res}=E^{\Sigma}}. \tag{2.138}$$

But the thermal reservoir is so huge in comparison with the energy of fluctuations in our system that its temperature does not depend on what the energy of our system is. That is why the thermal reservoir provides the constant temperature boundary condition $T^{res} = const$ and we can refer to its temperature as to a constant regardless of what is currently the energy of our system.

The obtained probability distribution

$$w_{\{E\}}^{CE} = \frac{1}{Z^{CE}} e^{-E/T^{res}} \tag{2.139}$$

is called *Gibbs probability distribution,* where Z^{CE} is the normalization constant of this distribution,

$$Z^{CE} \equiv \sum_{\{E\}} e^{-E/T^{res}}, \tag{2.140}$$

which is called *a partition function* of the CE. Similar to the statistical weight of the MCE, this function normalizes the distribution of probabilities of separate microstates. Therefore, it is often referred to as *a statistical sum* of the CE. Later we will see that there is more to this similarity than we have mentioned here.

We have defined a partition function as a sum of terms $e^{-E/T^{res}}$ over all microstates of the system. But since terms $e^{-E/T^{res}}$ depend only on system's energy, we can transform sum (2.140) into summation over energy levels (groups of microstates):

$$Z^{CE} = \sum_{E} g_E e^{-E/T^{res}}. \tag{2.141}$$

Recalling that we have built macrostates $\{\{E\}\}$ as energy fluctuations equivalent to observe the system at a particular energy level (group of microstates) and that the statistical weight of fluctuation (2.129) is the statistical weight of this energy level

(group of microstates), we can interpret (2.141) as the summation over all possible energy fluctuations:

$$Z^{CE} = \sum_{\{\{E\}\}} \Gamma_{\{\{E\}\}} e^{-E/T^{res}}. \tag{2.142}$$

The difference between (2.141) and (2.142) is just a matter of notation; and we will utilize both expressions at our convenience.

2.9 Properties of the Probability Distribution of Energy Fluctuations

Having found in the previous section the probability (2.139) of one microstate, we substitute it into (2.131) to find the probability of energy fluctuations in the CE:

$$W^{CE}_{\{\{E\}\}} = \Gamma_{\{\{E\}\}} w^{CE}_{\{E\}} = \Gamma_{\{\{E\}\}} \frac{1}{Z^{CE}} e^{-E/T^{res}}, \tag{2.143}$$

where the normalization of this distribution follows from

$$\sum_{\{\{E\}\}} W^{CE}_{\{\{E\}\}} = \sum_{\{\{E\}\}} \Gamma_{\{\{E\}\}} w^{CE}_{\{E\}} = 1. \tag{2.144}$$

Earlier we have assumed that the probability distribution (2.143) has a very narrow maximum. Let us now prove this statement. For the first derivative of the logarithm of (2.143), we find

$$\frac{d \ln W^{CE}_{\{\{E\}\}}}{dE} = \frac{d \ln \Gamma_{\{\{E\}\}}}{dE} - \frac{1}{T^{res}} = \frac{1}{T} - \frac{1}{T^{res}}. \tag{2.145}$$

At the point E_0 of the maximum, this derivative is zero and, therefore, the equality of equilibrium (2.135) is valid.

The second derivative

$$\frac{d^2 \ln W^{CE}_{\{\{E\}\}}}{dE^2} = \frac{d}{dE}\frac{1}{T} = -\frac{1}{T^2 C_V} \tag{2.146}$$

at the point E_0 equals

$$\left.\frac{d^2 \ln W^{CE}_{\{\{E\}\}}}{dE^2}\right|_{E_0} = -\frac{1}{(T^{res})^2 C_V\big|_{E_0}}. \tag{2.147}$$

Substituting these derivatives into the expansion of $\ln W^{CE}_{\{\{E\}\}}$ in powers of small energy deviations from E_0,

$$\ln W^{CE}_{\{\{E\}\}} = \ln W^{CE}_{\{\{E_0\}\}} + \left.\frac{d \ln W^{CE}_{\{\{E\}\}}}{dE}\right|_{E_0} (E - E_0) + \frac{1}{2} \left.\frac{d^2 \ln W^{CE}_{\{\{E\}\}}}{dE^2}\right|_{E_0} (E - E_0)^2 + \ldots, \tag{2.148}$$

and exponentiating the obtained equality, we find the probability distribution of nonequilibrium energy fluctuations in the vicinity of the equilibrium macrostate $\{\{E_0\}\}$ to be Gaussian:

$$W^{CE}_{\{\{E\}\}} \propto e^{-\frac{(E-E_0)^2}{2\left(T^{res}\right)^2 C_V|_{E_0}}}. \tag{2.149}$$

Since both energy and heat capacity are extensive parameters (proportional to N), for *absolute energy fluctuation* and *relative energy fluctuation* we find

$$\delta E \propto \underline{\underline{O}}(1)\sqrt{N} \tag{2.150}$$

and

$$\frac{\delta E}{E_0} \propto \underline{\underline{O}}(1)\frac{1}{\sqrt{N}}. \tag{2.151}$$

Here $\underline{\underline{O}}(1)$ means the absence of a dependence on N, but contains constants related to energy spectrum, like μh in the case of the Ising model. Therefore, $\underline{\underline{O}}(1)$ can, in fact, be significantly less or more than unity and we have utilized here the notation $\underline{\underline{O}}(1)$ only to emphasize the absence of a dependence on N.

Only energy fluctuations under the Gaussian "bell" (2.149) of the probability maximum have nonzero probabilities and, therefore, only these fluctuations determine system's behavior. To find how many fluctuations $\{\{E\}\}$ are under the "bell," we should divide (2.150) by the energy difference ΔE between two adjacent energy levels (groups of microstates).

For the ideal gas, the adjacent energy values differ by the transition of one of gas particles into the next cell in its phase space $\Delta E = \Delta \frac{p^2}{2m} \propto \Delta p \propto \frac{2\pi\hbar}{L}$. For the Ising model, one spin flip $\Delta E \propto 2\mu h$ moves the system to the next energy level. In both cases, the difference between two adjacent energy levels (groups of microstates) of the energy spectrum is some small quantity that does not depend on N. Dividing δE by ΔE, we find that the number of energy fluctuations under the Gaussian "bell" of the probability maximum is proportional to $\sqrt{N}$:

$$\frac{\delta E}{\Delta E} \propto \underline{\underline{O}}(1)\sqrt{N}. \tag{2.152}$$

However, if ΔE depended on N as a power-law $\Delta E \propto N^{-\alpha}$, the number of energy fluctuations with nonzero probabilities would still be a power-law dependence on N but with different exponent:

$$\frac{\delta E}{\Delta E} \propto \underline{\underline{O}}(1) N^{\alpha+\frac{1}{2}}. \tag{2.153}$$

From (2.151) we see that the relative width of the probability maximum is inversely proportional to $\sqrt{N}$ and, therefore, is indeed very small. The maximum is provided by "clash" (2.143) of two dependencies, $\Gamma_{\{\{E\}\}}$ and $w^{CE}_{\{E\}}$, exponential on the energy E of fluctuation (which means exponential dependence on N because $E \propto N$). Therefore, these dependencies are very "fast" (very sensitive to energy change) and their product creates a very narrow probability maximum at the point E_0.

Since the maximum is very narrow, its point E_0 should correspond to the averaged system's energy in the CE. Let us prove this statement.

The averaged value of an arbitrary parameter f in the ensemble is provided by definition (2.24). Applying this definition to system's energy in the CE, we find

$$\langle E \rangle_{CE} \equiv \sum_{\{E\}} E w^{CE}_{\{E\}} = \sum_{\{\{E\}\}} E \Gamma_{\{\{E\}\}} w^{CE}_{\{E\}} = \sum_{\{\{E\}\}} E W^{CE}_{\{\{E\}\}}. \tag{2.154}$$

Here $\Gamma_{\{\{E\}\}}$ and $w^{CE}_{\{E\}}$ again depend exponentially on energy (on N) while the multiplier E is a power-law dependence on N (proportional to N). Therefore, both functions, $\Gamma_{\{\{E\}\}}$ and $w^{CE}_{\{E\}}$, are much more "faster" than the "slow" dependence of multiplier E; and the product $\Gamma_{\{\{E\}\}} w^{CE}_{\{E\}} = W^{CE}_{\{\{E\}\}}$, which has a very narrow maximum, seems to act like a δ-function at the point E_0: $\delta(E - E_0)$. All the more so that this δ-function is normalized to unity by (2.144). So, we expect that (2.154) can be transformed into

$$\langle E \rangle_{CE} \approx \int E \delta(E - E_0) dE = E_0 \tag{2.155}$$

which would indeed prove our statement that the point E_0 of the probability maximum equals the averaged value of energy in the CE.

To prove (2.155), we should find how the change δE of the "slow" dependence E over the width of the maximum influences the value of integral (2.155). Since the change δE of E over the width of the maximum is provided by (2.150), neglecting δE in comparison with E itself would lead to the following error in the integral:

$$\langle E \rangle_{CE} \approx \int (E + \underline{\underline{O}}(\sqrt{N})) \delta(E - E_0) dE = E_0 + \underline{\underline{O}}(\sqrt{N}). \tag{2.156}$$

We see that E_0 does not equal exactly to $\langle E \rangle_{CE}$ but the difference is of the order of $\sqrt{N}$. And since $E_0 \propto N$, we can indeed neglect $\underline{\underline{O}}(\sqrt{N})$ in comparison with E_0 which finally proves our statement.

Problem 2.9.1

Illustrate formulae (2.150)–(2.156) with the aid of the Ising model without spin interactions.

Solution: As an example, we consider the Ising model with 100 spins and for simplicity will assume that $\mu h = 1$ and $T^{res} = 1$. In the following figure, we plot the "clash" between the statistical weight of fluctuations $\Gamma_{\{\{E\}\}}$ and the probability $w^{CE}_{\{E\}}$ of microstates. Their product provides the maximum of $W^{CE}_{\{\{E\}\}}$ at the point E_0. In the figure, we apply the logarithmic scale for the ordinate axis. Therefore, all the dependencies only seem to be slow while in reality they change by many orders of magnitude.

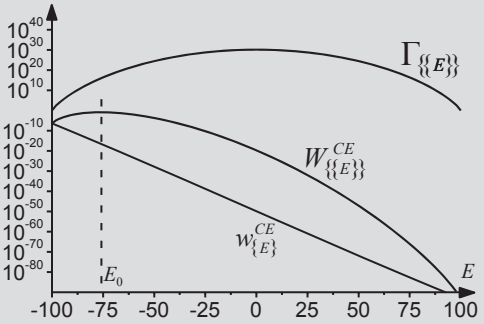

In the next figure, we plot the dependence of the probability distribution $W^{CE}_{\{\{E\}\}}$ on the energy of fluctuations in linear axes. Fluctuations are presented by separate columns under the common "bell" of the maximum; the distance between two adjacent fluctuations corresponds to one spin "flip" $\Delta E = 2$.

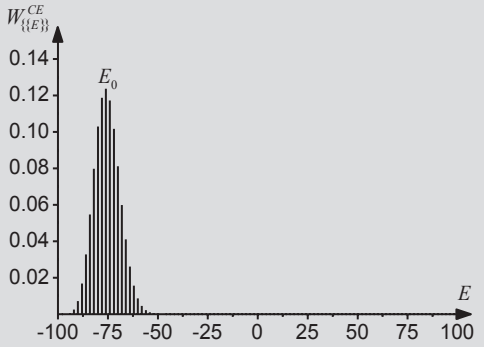

The absolute width of the maximum is of the order of $\delta E \propto \sqrt{N}\Delta E = 10\Delta E$ and there are only about $\sqrt{N} = 10$ separate fluctuations under the "bell." The

averaged energy corresponds to averaging over these fluctuations with nonzero probabilities. Therefore, $\langle E \rangle_{CE}$ lies also somewhere under the "bell" and its difference with the point E_0 of the maximum is of the order of the maximum width: $\langle E \rangle_{CE} = E_0 \pm \delta E$. Since $E_0 \propto N = 100$ and $\delta E \propto \sqrt{N} = 10$, we can neglect the difference; the more so, the higher number of degrees of freedom in the system.

The energy E_0 of the most probable macrostate $\{\{E_0\}\}$ is determined by the equation of the equilibrium macrostate (2.132). Solving this equation for a real system, we find E_0 as a function of the ensemble boundary condition T^{res}, volume, and the number of particles in the system. For example, for the ideal monatomic gas we would find $E_0 = \frac{3}{2} NT$.

But now in accordance with (2.156) we have proved that the energy E_0 of the most probable macrostate equals the averaged energy in the CE. Substituting (2.156) in the equation of equilibrium macrostate (2.132), we find *the equation of state* of the system. For the ideal monatomic gas this provides $\langle E \rangle_{CE} = \frac{3}{2} NT$.

Since (2.156) is always valid, in future we will not distinguish the equation of the equilibrium macrostate and the equation of state. So, we will refer to (2.132) as to just the equation of state.

The possibility to neglect "slow," power-law dependences in comparison with "fast," exponential dependences presents a useful method which we will often apply in future. Let us, for example, consider the condition of the probability distribution normalization (2.144). Here the sum goes, in fact, only over those fluctuations that are lying under the "bell" of the maximum because only these fluctuations have nonzero probabilities. Following (2.153), the number of these fluctuations is a power-law dependence on N $\left(\sqrt{N}\right.$ in the particular case of the Ising model considered in Problem 2.9.1). Therefore, we can approximate the sum as

$$1 = \sum_{\{\{E\}\}} \Gamma_{\{\{E\}\}} w^{CE}_{\{E\}} \approx_{\ln} \underline{\underline{O}}\left(N^{\alpha+\frac{1}{2}} \right) \Gamma_{\{\{E_0\}\}} w^{CE}_{\{E_0\}} \approx_{\ln} \Gamma_{\{\{E_0\}\}} w^{CE}_{\{E_0\}} \equiv W^{CE}_{\{\{E_0\}\}}. \quad (2.157)$$

We have obtained a very important equality. Firstly, it proves that at the point E_0 of the maximum, the probability $w^{CE}_{\{E_0\}}$ of microstates equals with logarithmic accuracy the inverse statistical weight $\Gamma_{\{\{E_0\}\}}$ of the equilibrium macrostate $\{\{E_0\}\}$:

$$w^{CE}_{\{E_0\}} \approx_{\ln} \frac{1}{\Gamma_{\{\{E_0\}\}}}. \quad (2.158)$$

Secondly, equality (2.157) means that the sum $\sum_{\{\{E\}\}} W^{CE}_{\{\{E\}\}}$, which normalizes the probability distribution $W^{CE}_{\{\{E\}\}}$, gathers (with logarithmic accuracy!) its unity value only over its maximal term. We have emphasized here that this is valid only with

the logarithmic accuracy because there are at least $N^{\alpha+\frac{1}{2}}$ other fluctuations under the "bell" of the maximum with similar probabilities $W^{CE}_{\{\{E\}\}} \approx_{\ln} W^{CE}_{\{\{E_0\}\}}$. Therefore, the maximal term $W^{CE}_{\{\{E_0\}\}}$ is $N^{\alpha+\frac{1}{2}}$ times less than unity.

It is customary to present equality (2.157) in a more intuitively clear form. Let us multiply this equality by the partition function Z^{CE} of the ensemble:

$$Z^{CE} = \sum_{\{\{E\}\}} \Gamma_{\{\{E\}\}} e^{-E/T^{res}} \approx_{\ln} \Gamma_{\{\{E_0\}\}} e^{-E_0/T^{res}}. \tag{2.159}$$

The first equality here is just definition (2.142) of the partition function while the second equality is much more important because it claims that *the partition function of the ensemble is equal (with logarithmic accuracy) to its maximal term*.

Problem 2.9.2

Illustrate formulae (2.157)–(2.159) with the aid of the Ising model from Problem 2.9.1.

Solution: From the second figure in Problem 2.9.1, we see that the sum $\sum_{\{\{E\}\}} W^{CE}_{\{\{E\}\}}$ gathers its unity value over the width of the maximum. But there are about $\sqrt{N} = 10$ fluctuations with similar probabilities under the "bell" of the maximum

$$1 = \sum_{\{\{E\}\}} W^{CE}_{\{\{E\}\}} \approx \sum_{\{\{E\}\}:-85<E<-65} W^{CE}_{\{\{E\}\}} \propto \sqrt{N} W^{CE}_{\{\{E_0\}\}}. \tag{2.160}$$

In other words, the total sum is $\sqrt{N} = 10$ times higher than its maximal term $W^{CE}_{\{\{E_0\}\}}$:

$$W^{CE}_{\{\{E_0\}\}} \equiv \Gamma_{\{\{E_0\}\}} w^{CE}_{\{E_0\}} \propto \frac{1}{\sqrt{N}}. \tag{2.161}$$

But both functions, $\Gamma_{\{\{E\}\}}$ and $w^{CE}_{\{E\}}$, depend exponentially on N. Therefore, applying logarithmic accuracy to this equation, we return to (2.158). Indeed, if we look at the first figure in Problem 2.9.1, we see that at the point E_0 both values, $\Gamma_{\{\{E_0\}\}} = 7 \cdot 10^{15}$ and $w^{CE}_{\{E_0\}} = 1.4 \cdot 10^{-17}$, are symmetric relative to unity

$$w^{CE}_{\{E_0\}} \approx \frac{1}{10\Gamma_{\{\{E_0\}\}}} = \frac{1}{\sqrt{N}\Gamma_{\{\{E_0\}\}}} \approx_{\ln} \frac{1}{\Gamma_{\{\{E_0\}\}}}. \tag{2.162}$$

In comparison with the order of 10^{15} (and it is already for only 100 spins in the model!), we always can neglect multiplier 10 with logarithmic accuracy.

Multiplying equality (2.160) by the partition function Z^{CE} of the CE, we find

$$Z^{CE} = \sum_{\{\{E\}\}} \Gamma_{\{\{E\}\}} e^{-E/T^{res}} \approx \sum_{\{\{E\}\}:-85<E<-65} \Gamma_{\{\{E\}\}} e^{-E/T^{res}}$$
$$\propto 10 \Gamma_{\{\{E_0\}\}} e^{-E_0/T^{res}} \propto \sqrt{N} \Gamma_{\{\{E_0\}\}} e^{-E_0/T^{res}}. \quad (2.163)$$

The first equality here is the definition of the partition function. The second equality tells us that the sum gathers its value over ten fluctuations under the "bell" of the maximum. Both the main term $\Gamma_{\{\{E_0\}\}} e^{-E_0/T^{res}}$ of the partition function and the partition function itself, $Z^{CE} = 7 \times 10^{49}$, depend exponentially on N. Therefore, we can neglect the power-law multiplier $\sqrt{N} = 10$ (10 in comparison with 10^{49}!) which returns us to (2.159).

In this section, we have considered the behavior of the probability distribution $W^{CE}_{\{\{E\}\}}$ and have found that it has a very narrow maximum provided by the "clash" of two "fast" dependencies: $\Gamma_{\{\{E\}\}}$ and $w^{CE}_{\{E\}}$. But does this situation always take place? Are there situations when two "fast" dependences happen to be not enough to create a narrow maximum of the probability distribution?

Unfortunately, there are indeed situations when the presented formalism does not work. Let us consider a system whose statistical weight $\Gamma_{\{\{E\}\}}$ obeys a simple exponential dependence on the energy of the system:

$$\Gamma_{\{\{E\}\}} \approx_{\ln} e^{const \cdot E}. \quad (2.164)$$

We should mention here that everywhere above we have assumed something more complex. For example, the statistical weight (2.17) of the Ising model was more complex than the simple exponential dependence. But what would happen if we indeed had (2.164)?

Substituting (2.164) into the probability distribution (2.143), we find that both "clashing" functions are exactly exponential on E,

$$W^{CE}_{\{\{E\}\}} = \Gamma_{\{\{E\}\}} w^{CE}_{\{E\}} = e^{const \cdot E} \frac{1}{Z^{CE}} e^{-\frac{1}{T^{res}} E}, \quad (2.165)$$

when one exponential dependence cancels another leaving us with just simple exponential probability decay (the maximum now is at $E = 0$):

$$W^{CE}_{\{\{E\}\}} = \frac{1}{Z^{CE}} e^{-\left(\frac{1}{T^{res}} - const\right) E}. \quad (2.166)$$

Unfortunately, a similar situation takes place in the case of percolation which we consider in Chap. 4. From our point of view, this is the reason why the complete analogy between percolation phenomena and phase transition phenomena of statistical physics has not been developed yet.

In the rest of this chapter, we consider only "good" systems whose probability distribution $W^{CE}_{\{\{E\}\}}$ for energy fluctuations in the CE has a narrow maximum at point E_0. To the opposite situation in the case of percolation, we return in Chap. 6.

2.10 Method of Steepest Descent

In Sect. 2.8, we have utilized expression (2.142) for the partition function when instead of summing over microstates $\{E\}$ we summed over energy fluctuations $\{\{E\}\}$. But energy fluctuations are represented by energy levels (groups of microstates) separated by very small interval ΔE (which, in general, could vary over the spectrum: $\Delta E(E)$). Therefore, we can approximate the sum $\sum_{\{\{E\}\}} \Gamma_{\{\{E\}\}}$ by the integral $\int \frac{\Gamma_{\{\{E\}\}} dE}{\Delta E(E)} \equiv \int g(E)dE$, where we introduced the quantity

$$g(E) \equiv \frac{\Gamma_{\{\{E\}\}}}{\Delta E(E)} = \frac{g_E}{\Delta E(E)} \tag{2.167}$$

called *the density of microstates in the spectrum* because the product $g(E)dE \equiv \frac{g_E dE}{\Delta E(E)}$ provides the number of microstates in dE. Let us illustrate this quantity with the aid of the Ising model.

Problem 2.10.1

Find the density of microstates for the Ising model without spin interactions.

Solution: In the case of the Ising model, two adjacent energy levels are divided by one spin flip

$$|\Delta E| = 2\mu h. \tag{2.168}$$

Therefore, the density of microstates equals

$$g(E) \equiv \frac{g_E}{2\mu h}, \tag{2.169}$$

where the dependence of the statistical weight g_E on system's energy E is provided by (2.7) and (2.17)

$$g_E = \frac{N!}{\left(\frac{N}{2}-\frac{E}{2\mu h}\right)!\left(\frac{N}{2}+\frac{E}{2\mu h}\right)!}$$
$$\approx_{\ln} \left(\frac{1}{2}-\frac{E}{2N\mu h}\right)^{-N\left(\frac{1}{2}-\frac{E}{2N\mu h}\right)} \left(\frac{1}{2}+\frac{E}{2N\mu h}\right)^{-N\left(\frac{1}{2}+\frac{E}{2N\mu h}\right)}. \quad (2.170)$$

Applying approximation (2.167) to (2.142), for the partition function we find

$$Z^{CE} \approx_{\ln} \int dE\ g(E) e^{-E/T^{res}}. \quad (2.171)$$

Problem 2.10.2

For the Ising model without spin interactions, approximate the sum over energy fluctuations by integral.

Solution: Utilizing the obtained density of microstates (2.169), for the partition function we find

$$Z^{CE} \approx_{\ln} \int_{-N\mu h}^{+N\mu h} dE\ g(E) e^{-E/T^{res}}. \quad (2.172)$$

However, for the purpose of convenience for the Ising model it is standard practice to integrate not over system's energy but over system's magnetization. Indeed, from (2.7) we recall that the energy of the Ising model without interactions is bijectively associated with the specific magnetization,

$$E = -N\mu h m, \quad (2.173)$$

when any energy fluctuation $\{\{E\}\}$ bijectively corresponds to a magnetization fluctuation $\{\{m\}\}$. Therefore, instead of summing over energy fluctuations, we can sum terms of the partition function over magnetization fluctuations,

$$Z^{CE} = \sum_{\{\{m\}\}} \Gamma_{\{\{m\}\}} e^{-E(m)/T^{res}}, \quad (2.174)$$

where the statistical weight $\Gamma_{\{\{m\}\}}$ of a fluctuation is provided by (2.17):

$$\Gamma_{\{\{m\}\}} \approx_{\ln} \left(\frac{1+m}{2}\right)^{-N\frac{1+m}{2}} \left(\frac{1-m}{2}\right)^{-N\frac{1-m}{2}}. \quad (2.175)$$

In equality (2.174) the sum can also be approximated by integral

$$Z^{CE} \approx_{\ln} \int_{-1}^{+1} \frac{dm}{2/N} \Gamma_{\{\{m\}\}} e^{-E(m)/T^{res}}, \tag{2.176}$$

where we again utilized that the difference between two fluctuations corresponds to one spin flip:

$$|\Delta m| = 2/N. \tag{2.177}$$

From expressions (2.171), (2.172), and (2.176), we see that the common feature of all these integrals is the exponential dependence of the integrand on N. To find such integrals, *the method of steepest descent* (*saddle-point method*) is often applied. Since this method is not always included in the textbooks on statistical physics, we develop it in the current section.

Our purpose will be to find in the complex plane $z = x + iy$ the integral

$$I \equiv \int_{z_1}^{z_2} e^{Nf(z)} F(z)\, dz, \tag{2.178}$$

where in the integrand's exponent the number N is finite but very large: $N >> 1$. We assume both functions, $f(z)$ and $F(z)$, to be analytic.

Let us separate the function $f(z)$ into its real and imaginary part,

$$f(z) = u(x, y) + iv(x, y), \tag{2.179}$$

where both functions, $u(x, y)$ and $v(x, y)$, are real and, since $f(z)$ is analytic, obey Cauchy–Riemann conditions:

$$\frac{\partial u}{\partial x} = \frac{\partial v}{\partial y} \text{ and } \frac{\partial u}{\partial y} = -\frac{\partial v}{\partial x}. \tag{2.180}$$

From (2.180) we easily find that

$$\frac{\partial^2 u}{\partial x^2} = -\frac{\partial^2 u}{\partial y^2} \text{ and } \frac{\partial^2 v}{\partial x^2} = -\frac{\partial^2 v}{\partial y^2}. \tag{2.181}$$

These equalities mean that both surfaces, $u(x, y)$ and $v(x, y)$, are the saddle surfaces when one curvature equals minus another curvature.

Let us assume that for the function $f(z)$ we have found its saddle point determined by the condition

$$f'(z_0) = 0. \tag{2.182}$$

Then we deform the contour of integration so that it passes through this point.

Next, we expand $f(z)$ in the vicinity of z_0 in powers of $z - z_0$,

$$f(z) = f(z_0) + C_2 (z - z_0)^2 + \sum_{n=3}^{+\infty} C_n (z - z_0)^n, \tag{2.183}$$

with the radius R of convergence. The coefficients of the power expansion are

$$C_n = \frac{1}{n!} f^{(n)}(z_0) = \frac{1}{2\pi i} \oint_{C_R} \frac{f(\zeta) d\zeta}{(\zeta - z_0)^{n+1}}, \tag{2.184}$$

where C_R is the contour of radius R with the center at z_0.

Since the function $f(z)$ is analytic, it is bounded at the given contour,

$$\left| f\left(z_0 + Re^{i\phi}\right) \right| \le \text{const}, \tag{2.185}$$

along with its coefficients:

$$|C_n| = \left| \frac{1}{2\pi i} \oint_{C_R} \frac{f(\zeta) d\zeta}{(\zeta - z_0)^{n+1}} \right| \le \frac{2\pi R}{2\pi} \frac{\text{const}}{R^{n+1}} = \frac{\text{const}}{R^n}. \tag{2.186}$$

In the neighborhood of z_0 we will utilize Euler's form for z,

$$z = re^{i\phi}, \tag{2.187}$$

where we always bound the considered neighborhood by the convergence radius R of series (2.183):

$$r < R. \tag{2.188}$$

Let us consider how significant is the contribution of the last sum in (2.183). Utilizing (2.186) and the expression for the sum of geometric progression, we find

$$\left| N \sum_{n=3}^{+\infty} C_n (z - z_0)^n \right| \le N \,\text{const} \sum_{n=3}^{+\infty} \left(\frac{r}{R} \right)^n = \frac{N \,\text{const}\, r^3}{R^2 (R - r)}. \tag{2.189}$$

Considering small $r << R$, we can neglect r in the denominator:

$$\left| N \sum_{n=3}^{+\infty} C_n (z - z_0)^n \right| \le N \,\text{const} \left(\frac{r}{R} \right)^3. \tag{2.190}$$

So far we have considered arbitrary r, providing it is small enough. However, now we choose r to obey the particular inequality,

$$r \le r_0 = const \cdot N^{-\alpha} << R \text{ when } \alpha > 0, \tag{2.191}$$

which is, obviously, always possible because $N >> 1$. This neighborhood of the point z_0 we will call the r_0-neighborhood.

Substituting the radius of the r_0-neighborhood into (2.190), we obtain

$$\left| N \sum_{n=3}^{+\infty} C_n \left(z - z_0 \right)^n \right| \le N^{1-3\alpha} \frac{\text{const}}{R^3}. \tag{2.192}$$

Parameter α in (2.191) is some positive real number. After choosing

$$\alpha > \frac{1}{3}, \tag{2.193}$$

sum (2.192) inside the r_0-neighborhood becomes of the order of $\underline{\underline{O}}\left(1/N^{3\alpha-1}\right)$ while its exponent is of the order of $e^{\underline{\underline{O}}\left(1/N^{3\alpha-1}\right)} = 1 + \underline{\underline{O}}\left(1/N^{3\alpha-1}\right)$. Therefore, its contribution to the integral over the r_0-neighborhood provides the integrand multiplier of the order of unity and in the r_0-neighborhood we can consider only two first terms of (2.183):

$$f(z) \approx f(z_0) + C_2 (z - z_0)^2 \text{ when } r \le r_0. \tag{2.194}$$

We want to develop the method in such a way that the main contribution to integral (2.178) would be provided by the integration over the r_0-neighborhood of the saddle point z_0 and that both terms in (2.194) would participate significantly. The estimation of the participation of the second term is

$$\left| N C_2 \left(z - z_0 \right)^2 \right| \le N^{1-2\alpha} \frac{\text{const}}{R^2}. \tag{2.195}$$

For it to be significant, we should require that

$$\alpha < \frac{1}{2}. \tag{2.196}$$

As we will see later, condition (2.196) also allows us to neglect the integration over the contour beyond the r_0-neighborhood of the saddle point z_0.

Inside the r_0-neighborhood we will utilize Euler's form for (2.194):

$$f(z) - f(z_0) \approx \left| C_2 \right| r^2 e^{i \arg C_2 + 2i\phi}. \tag{2.197}$$

Earlier we have deformed the contour of integration so that it would pass through the saddle point z_0. Now we choose the direction at which it crosses the r_0-neighborhood of this point:

$$\phi = -\frac{\arg C_2 + \pi}{2}. \tag{2.198}$$

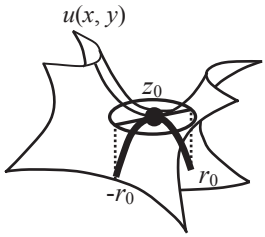

Fig. 2.10 The contour corresponds to the direction of the steepest descent of function $u(x, y)$

Substituting this angle into (2.197), we find

$$f(z) - f(z_0) \approx -|C_2| r^2. \tag{2.199}$$

In other words, along the chosen path the increment of the function is real. Recalling (2.179), we see that inside the r_0-neighborhood the imaginary part $v(x, y)$ of $f(z)$ remains approximately constant, $v(x, y) \approx v(x_0, y_0)$. And since on the complex plane the curves $v = const$ and $u = const$ are always perpendicular one to another, we conclude that our contour corresponds now to the direction of the steepest descent of the real part $u(x, y)$ as it is schematically shown in Fig. 2.10.

Further we assume that function $u(x, y)$ continues to decrease monotonically while we move away from the r_0-neighborhood along the contour. This is the main assumption of our method. If it happened to be not valid, we should be more careful with the obtained results. In particular, this assumption is not valid in the presence of several saddle points. In this case, we should take into account all of them by a similar approach.

Let us divide the contour of integration into three parts (Fig. 2.11): from z_1 up to the r_0-neighborhood of the saddle point z_0, inside this neighborhood, and from this neighborhood to z_2. We will denote two cross-points of the contour and the r_0 -neighborhood as $-r_0$ and r_0.

Since z_0 is constant, we can move the integrand's multiplier $e^{Nf(z_0)}$ ahead of the integral (2.178),

$$I = e^{Nf(z_0)} \int_{z_1}^{z_2} e^{N\{f(z) - f(z_0)\}} F(z)\, dz; \tag{2.200}$$

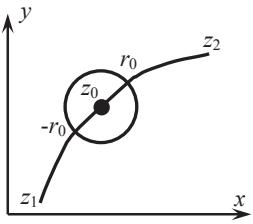

Fig. 2.11 The contour corresponds to the direction of the steepest descent of the function $u(x, y)$

and our purpose becomes to find the integral:

$$\tilde{I} \equiv \int_{z_1}^{z_2} e^{N\{f(z)-f(z_0)\}} F(z)\,dz. \tag{2.201}$$

The variable r has been, in fact, parametrizing the contour of integration inside the r_0-neighborhood in accordance with (2.187). We will continue to utilize the parametrizing definition (2.187) outside of the r_0-neighborhood as well; however, in this case the angle is no longer provided by (2.198) but is some other dependence $\phi(r)$ on the parameter r.

Let us estimate the contribution to integral (2.201) coming from the path from z_1 up to $-r_0$:

$$\left| \int_{z_1}^{-r_0 e^{i\phi}} e^{N\{f(z)-f(z_0)\}} F(z)\,dz \right| \le \int_{-|z_1-z_0|}^{-r_0} e^{N\{u(r)-u(0)\}} \left| F(z)\frac{dz}{dr} \right| dr, \tag{2.202}$$

where we have utilized that always $\left| \int_{z_a}^{z_b} f(z)dz \right| \le \int_{z_a}^{z_b} |f(z)dz|$ and that $\left| e^{Nf(z)} \right| = e^{Nu(x,y)}$. If we also recall that we have assumed the function $u(x,y)$ to be monotonically decreasing while we move away from the point z_0, we obtain

$$\left| \int_{z_1}^{-r_0 e^{i\phi}} e^{N\{f(z)-f(z_0)\}} F(z)\,dz \right| \le e^{N\{u(-r_0)-u(0)\}} \int_{z_1}^{-r_0 e^{i\phi}} |F(z)\,dz| \propto \text{const}\, e^{N\{u(-r_0)-u(0)\}}. \tag{2.203}$$

But the difference in the exponent is provided by (2.199),

$$u(-r_0) - u(0) \approx -|C_2| r_0^2, \tag{2.204}$$

where the radius r_0 of the r_0-neighborhood is defined by (2.191):

$$u(-r_0) - u(0) \approx -const \cdot |C_2| N^{-2\alpha}. \tag{2.205}$$

Substituting (2.205) into (2.203), we find

$$\left| \int_{z_1}^{-r_0 e^{i\phi}} e^{N\{f(z)-f(z_0)\}} F(z)\,dz \right| \le const \cdot e^{-const \cdot N^{1-2\alpha} |C_2|}. \tag{2.206}$$

However, earlier in (2.196) we have considered only $\alpha < 1/2$. Now we see that this particular requirement provides that in the limit $N >> 1$ we can neglect the integration along the contour from z_1 to $-r_0$. A similar statement is valid and for the integration from r_0 to z_2. Therefore, requirement (2.196) provides that the main value of integral (2.201) comes from the r_0-neighborhood of the saddle point z_0 while the integration along the rest of the contour may be neglected.

$$\tilde{I} \approx \int_{-r_0 e^{i\phi}}^{r_0 e^{i\phi}} e^{N\{f(z)-f(z_0)\}} F(z)\,dz = \int_{-r_0}^{r_0} e^{-N|C_2|r^2} F\left(z_0 + re^{i\phi}\right) e^{i\phi}\,dr. \tag{2.207}$$

Since in the general case function $F(z)$ is not singular at the point z_0, we can neglect its change inside the small r_0-neighborhood:

$$\tilde{I} \approx F(z_0)\, e^{i\phi} \int_{-r_0}^{r_0} e^{-N|C_2|r^2}\,dr. \tag{2.208}$$

Changing the variable,

$$x^2 \equiv N|C_2|r^2, \tag{2.209}$$

we obtain

$$\tilde{I} \approx \frac{F(z_0)\, e^{i\phi}}{\sqrt{N|C_2|}} \int_{-\sqrt{N|C_2|}r_0}^{\sqrt{N|C_2|}r_0} e^{-x^2}\,dx. \tag{2.210}$$

Since $N >> 1$, the upper and lower integration limits are also some large numbers and we would like to know whether it would be possible to replace both integration limits with infinity. In order to do that, we should evaluate the asymptotic behavior of the error function:

$$Err(+\infty) - Err(X >> 1) \equiv \int_{X>>1}^{+\infty} e^{-x^2}\,dx. \tag{2.211}$$

Changing the variable

$$y \equiv x^2, \tag{2.212}$$

we find that

$$\int_{X>>1}^{+\infty} e^{-x^2}\,dx = \frac{1}{2}\int_{X^2}^{+\infty} \frac{e^{-y}}{\sqrt{y}}\,dy. \tag{2.213}$$

The second variable change

$$z \equiv y - X^2 \tag{2.214}$$

allows us to set the lower limit to zero:

$$\int_{X>>1}^{+\infty} e^{-x^2}\,dx = \frac{e^{-X^2}}{2X}\int_0^{+\infty} \frac{e^{-z}}{\sqrt{1+\dfrac{z}{X^2}}}\,dz. \tag{2.215}$$

The integrand's multiplier e^{-z} provides that the integral gathers its main value while z is of the order of unity. In this limit, the value of $\frac{z}{X^2} << 1$ is negligible in comparison with unity:

$$\int\limits_{X>>1}^{+\infty} e^{-x^2} dx \approx \frac{e^{-X^2}}{2X} \int\limits_{0}^{+\infty} e^{-z} dz = \frac{e^{-X^2}}{2X}. \tag{2.216}$$

Applying this result to evaluate the following integral

$$\int\limits_{\sqrt{N|C_2|}r_0}^{+\infty} e^{-x^2} dx \approx \frac{e^{-N|C_2|r_0^2}}{2\sqrt{N|C_2|}r_0} = \frac{e^{-\text{const}\, N^{1-2\alpha}|C_2|}}{2\,\text{const}\, N^{\frac{1}{2}-\alpha}\sqrt{|C_2|}}, \tag{2.217}$$

we see that we indeed can replace both integration limits in integral (2.210) with infinity

$$\tilde{I} \approx \frac{F(z_0)\, e^{i\phi}}{\sqrt{N|C_2|}} \int\limits_{-\infty}^{+\infty} e^{-x^2} dx = \frac{F(z_0)\, e^{i\phi}}{\sqrt{N|C_2|/\pi}}. \tag{2.218}$$

Substituting this result into the initial integral (2.178), we finally obtain

$$I = e^{Nf(z_0)} \frac{F(z_0)\, e^{i\phi}}{\sqrt{N|C_2|/\pi}} = e^{Nf(z_0)} \sqrt{\frac{2\pi}{N\left|f^{(2)}(z_0)\right|}} F(z_0)\, e^{i\phi}. \tag{2.219}$$

We should note that this result is valid with the accuracy of the multiplier of the order of unity: $1 + \underline{\underline{O}}\left(\frac{1}{N^{\beta}}\right)$, where $\beta > 0$. However, in statistical physics for statistical weights and partition functions, both exponentially depending on N, we generally utilize the logarithmic accuracy. Applying logarithmic accuracy to (2.219), we should neglect all power-law multipliers to find

$$I \equiv \int\limits_{z_1}^{z_2} e^{Nf(z)} F(z)\, dz \approx_{\ln} e^{Nf(z_0)}, \tag{2.220}$$

where the saddle point z_0 of the function $f(z)$ is determined by

$$f'(z_0) = 0. \tag{2.221}$$

To apply this result to the sum of partition function we, firstly, should present this sum in the form

$$Z^{CE} = \sum_{\{\{E\}\}} \Gamma_{\{\{E\}\}} e^{-E/T^{res}} = \sum_{\{\{E\}\}} e^{S_{\{\{E\}\}} - E/T^{res}}, \tag{2.222}$$

where we have emphasized that the integrand depends exponentially on N because both entropy $S_{\{\{E\}\}}$ and energy E are extensive parameters. Transforming the sum into integral

$$Z^{CE} \approx_{\ln} \int \frac{dE}{\Delta E(E)} e^{S_{\{\{E\}\}} - E/T^{res}} \tag{2.223}$$

and applying (2.220), we find that with logarithmic accuracy the sum in (2.222) is equal to one of its terms,

$$Z^{CE} \approx_{\ln} e^{S_{\{\{E_0\}\}} - E_0/T^{res}} = \Gamma_{\{\{E_0\}\}} e^{-E_0/T^{res}}, \tag{2.224}$$

where E_0 is determined by

$$\left\{ \frac{\partial}{\partial E} \left(S_{\{\{E\}\}} - \frac{E}{T^{res}} \right) \right\} \Bigg|_{E_0} = 0. \tag{2.225}$$

Modifying the left-hand side of (2.225) as

$$\left\{ \frac{\partial}{\partial E} \ln \left(\Gamma_{\{\{E\}\}} e^{-\frac{E}{T^{res}}} \right) \right\} \Bigg|_{E_0} = \left\{ \frac{\partial}{\partial E} \ln \left(Z^{CE} W^{CE}_{\{\{E\}\}} \right) \right\} \Bigg|_{E_0} \tag{2.226}$$

and recalling that Z^{CE} does not depend on the energy of fluctuation $\{\{E\}\}$, we find that E_0 is determined by the equation of the equilibrium macrostate (2.132)

$$\left. \frac{\partial \ln W^{CE}_{\{\{E\}\}}}{\partial E} \right|_{E_0} = 0 \tag{2.227}$$

corresponding to the point of the maximum of probability distribution $W^{CE}_{\{\{E\}\}}$ and simultaneously to the point of the maximal term (2.159) of the partition function. Therefore, the method of steepest descent represents the "essence" of the main rule in the CE: *the partition function of the ensemble is equal with logarithmic accuracy to its maximal term*.

The method of steepest descent is often utilized to find partition functions of nonideal systems when the exact solution may be unknown. We consider this question in more detail in the following chapters.

2.11 Entropy of the CE. The Equivalence of the MCE and CE

So far we have considered only the entropy (2.130) of energy fluctuations $\{\{E\}\}$ but not the entropy of the ensemble itself. To find the entropy of the CE, we should substitute the equilibrium probability distribution (2.139) into definition (2.21) of the entropy functional:

$$S^{CE} \equiv -\sum_{\{E\}} w^{CE}_{\{E\}} \ln w^{CE}_{\{E\}}. \tag{2.228}$$

Transforming the sum over microstates $\{E\}$ into the sum over macrostates $\{\{E\}\}$ and utilizing (2.143), we find

$$S^{CE} = -\sum_{\{\{E\}\}} W^{CE}_{\{\{E\}\}} \ln w^{CE}_{\{E\}}. \tag{2.229}$$

Here $W^{CE}_{\{\{E\}\}}$ is again the very "exponentially fast" dependence on E which is equivalent to $\delta(E-E_0)$. On the contrary, $\ln w^{CE}_{\{E\}}$ is only proportional to E (to N) and is, therefore, a "slow" power-law dependence. So, for the entropy of the CE we expect to find

$$S^{CE} \approx -\int dE \delta(E-E_0) \ln w^{CE}_{\{E\}} = -\ln w^{CE}_{\{E_0\}}. \tag{2.230}$$

To prove this equality, we should prove that the relative change of the function $\ln w^{CE}_{\{E\}}$ over the width of the maximum of the probability distribution $W^{CE}_{\{\{E\}\}}$ is negligible. Indeed, we find that

$$\frac{\delta\left(\ln w^{CE}_{\{E\}}\right)}{\ln w^{CE}_{\{E_0\}}} = \frac{-\delta E / T^{res}}{-\ln Z^{CE} - E_0 / T^{res}} << 1 \tag{2.231}$$

because $\delta E \propto \sqrt{N}$ while $E_0 \propto N$. This proves (2.230).

Substituting (2.158) into (2.230)

$$S^{CE} \approx -\ln w^{CE}_{\{E_0\}} \approx \ln \Gamma_{\{\{E_0\}\}}, \tag{2.232}$$

we find that the entropy of the CE (with the accuracy of terms small in comparison with N) equals the entropy of the equilibrium macrostate:

$$S^{CE} \approx S_{\{\{E_0\}\}}. \tag{2.233}$$

Similar to our statement after (2.69), we should mention here that these two parameters are often treated as one because of equality (2.233). However, the reader should clearly understand the difference: the entropy S^{CE} of the ensemble is the entropy

of the equilibrium probability distribution (2.139) while the entropy $S_{\{\{E_0\}\}}$ is the logarithm of the statistical weight of the most probable fluctuation $\{\{E_0\}\}$.

Since the statistical weight (2.129) of an energy fluctuation $\{\{E\}\}$ is just the statistical weight of this energy level (of this group of microstates), for the entropy of the CE we find

$$S^{CE} \approx \ln g_{E_0}. \tag{2.234}$$

Let us now imagine the same system but strictly isolated with the energy E_0. This corresponds to the case of the MCE, and the statistical weight and entropy of this ensemble are

$$\Gamma^{MCE} = g_{E_0} \tag{2.235}$$

and

$$S^{MCE} = \ln \Gamma^{MCE} = \ln g_{E_0}. \tag{2.236}$$

Comparing (2.234) and (2.236), we see the equality between the entropies of two different ensembles (which means equality of other thermodynamic potentials besides the entropy):

$$S^{CE} \approx S^{MCE}. \tag{2.237}$$

This equality is called the *principle of equivalence between canonical and microcanonical ensembles*.

Only energy fluctuations $\{\{E\}\}$ under the "bell" of the maximum of probability distribution $W^{CE}_{\{\{E\}\}}$ have nonzero probabilities. The number of these fluctuations is provided by (2.153), and each of them contains the number of microstates $\{E\}$ of the order of $\Gamma_{\{\{E_0\}\}}$.

Let us call the total number of microstates $\{E\}$ under the "bell" of the maximum of the probability distribution $W^{CE}_{\{\{E\}\}}$ as *the statistical weight of the CE*, Γ^{CE}. It is of the order of

$$\Gamma^{CE} = \underline{\underline{O}}\left(N^{\alpha+\frac{1}{2}}\right)\Gamma_{\{\{E_0\}\}} \approx_{\ln} \Gamma_{\{\{E_0\}\}}, \tag{2.238}$$

so the entropy of the ensemble again obeys Boltzmann's rule and equals the logarithm of the number of microstates where the system "lives" with nonzero probability:

$$S^{CE} = \ln \Gamma^{CE}. \tag{2.239}$$

2.12 Free Energy Potential of the CE

From thermodynamics we know that for any system what is always valid is the inequality

$$\Delta S \geq \frac{\delta Q^{\leftarrow}}{T^{res}}, \tag{2.240}$$

where $\delta Q^{\leftarrow}$ is the amount of heat supplied to the system. This inequality is a mixture of two different phenomena. Firstly, any heat, quasistatically transferred into the system, increases the entropy of the system while any heat leaving the system decreases its entropy. This corresponds to the equality $\Delta S = \frac{\delta Q^{\leftarrow}}{T^{res}}$. However, if we consider nonequilibrium processes in an isolated system, there is already no heat exchange but the entropy of the system is increasing while the system achieves its equilibrium state: $\Delta S \geq 0$. The mixture of these two different phenomena is presented by the very inequality (2.240).

Thermodynamics defines *the Helmholtz energy* as

$$F \equiv -T^{res} S + E. \tag{2.241}$$

We will call (2.241) the "*thermodynamic*" definition.

Also, we should emphasize here that in this definition as well as in (2.240) we have utilized the temperature T^{res} of thermal reservoir but not the temperature T of the system itself. As we will see below, this is very important because only such a definition makes the Helmholtz energy free in the CE.

Finding the increment of the Helmholtz free energy, we should always remember the boundary condition $T^{res} = const$ of the CE:

$$\Delta F = -T^{res} \Delta S + \Delta E. \tag{2.242}$$

From the law of conservation of energy it follows that

$$\Delta E = \delta Q^{\leftarrow}. \tag{2.243}$$

Substituting (2.242 and 2.243) into (2.240), we find that for arbitrary processes in the system the Helmholtz energy can only decrease (or stay constant):

$$\Delta F \leq 0. \tag{2.244}$$

This suggests that the Helmholtz energy plays the role of the free energy potential in the CE.

To prove this statement we return from the thermodynamic considerations to statistical physics. First, we want to understand how inequality (2.240) is associated with inequality (2.70). Is one a consequence of the other?

To answer this question let us return to the "big" system Σ consisting of two subsystems, our system and the thermal reservoir (Fig. 2.8). The system Σ is isolated and, therefore, obeys the rules of the MCE.

To investigate its behavior, we should construct somehow nonequilibrium fluctuations $\{\{p\}\}$, where p is some set of system's fluctuating parameters. In Sects. 2.4 and 2.5, as p we utilized the fluctuations of concentration of the ↓-spins. But we are free in the choice of the type of fluctuations because fluctuations are just a tool helping us to investigate system's behavior.

Being consistent with the previous discussions of the CE, we choose p to represent the energy of our system in contact with the thermal reservoir. In other words, for the system Σ we construct MCE fluctuations as macrostates $\left\{\left\{E, E^{\Sigma} - E\right\}\right\}^{\Sigma}$ when our system has energy E while the thermal reservoir has energy $E^{res} = E^{\Sigma} - E$. We define these fluctuations with the aid of the following nonequilibrium probability distribution:

$$w^{\Sigma}_{\left\{\tilde{E}, E^{\Sigma} - \tilde{E}\right\}^{\Sigma}} = \begin{Bmatrix} 1/\Gamma^{\Sigma}_{\left\{\left\{E, E^{\Sigma} - E\right\}\right\}^{\Sigma}} & , \tilde{E} = E \\ 0 & , \tilde{E} \neq E \end{Bmatrix} = \frac{\delta_{\tilde{E}, E}}{\Gamma^{\Sigma}_{\left\{\left\{E, E^{\Sigma} - E\right\}\right\}^{\Sigma}}}. \tag{2.245}$$

The statistical weight $\Gamma^{\Sigma}_{\left\{\left\{E, E^{\Sigma} - E\right\}\right\}^{\Sigma}}$ of the fluctuation $\left\{\left\{E, E^{\Sigma} - E\right\}\right\}^{\Sigma}$ equals the number of microstates of the system Σ when our system has energy E while the reservoir has energy $E^{res} = E^{\Sigma} - E$:

$$\Gamma^{\Sigma}_{\left\{\left\{E, E^{\Sigma} - E\right\}\right\}^{\Sigma}} = g_E g^{res}_{E^{\Sigma} - E}, \tag{2.246}$$

and for the entropy $S^{\Sigma}_{\left\{\left\{E, E^{\Sigma} - E\right\}\right\}^{\Sigma}}$ of this fluctuation we find

$$S^{\Sigma}_{\left\{\left\{E, E^{\Sigma} - E\right\}\right\}^{\Sigma}} = \ln \Gamma^{\Sigma}_{\left\{\left\{E, E^{\Sigma} - E\right\}\right\}^{\Sigma}} = \ln g_E + \ln g^{res}_{E^{\Sigma} - E}. \tag{2.247}$$

We have specifically constructed fluctuations $\left\{\left\{E, E^{\Sigma} - E\right\}\right\}^{\Sigma}$ of the isolated system Σ in such a way that they correspond to fluctuations $\{\{E\}\}$ of our system in the CE. Considering now the latter, the entropy $S_{\{\{E\}\}}$ of the fluctuation $\{\{E\}\}$ is

$$S_{\{\{E\}\}} = \ln \Gamma_{\{\{E\}\}} = \ln g_E. \tag{2.248}$$

Similarly, for fluctuations $\left\{\left\{E^{res}\right\}\right\}^{res}$ of the thermal reservoir we have

$$S^{res}_{\left\{\left\{E^{\Sigma} - E\right\}\right\}^{res}} = \ln \Gamma^{res}_{\left\{\left\{E^{\Sigma} - E\right\}\right\}^{res}} = \ln g^{res}_{E^{\Sigma} - E}. \tag{2.249}$$

Substituting (2.248) and (2.249) into (2.247), we find that the entropy of the system Σ is *additive* over its subsystems:

$$S^{\Sigma}_{\left\{\left\{E,E^{\Sigma}-E\right\}\right\}^{\Sigma}} = S_{\left\{\left\{E\right\}\right\}} + S^{res}_{\left\{\left\{E^{\Sigma}-E\right\}\right\}^{res}}. \tag{2.250}$$

We have to mention that we have been able to obtain the property of additivity here only because we considered the stroboscopic approximation of virtual isolation for the heat exchange properties when during the brief periods of isolation two subsystems become, in fact, independent. Otherwise, the rule of additivity would not be applicable.

Equality similar to (2.250) should be valid and for increments of these quantities:

$$\Delta S^{\Sigma}_{\left\{\left\{E,E^{\Sigma}-E\right\}\right\}^{\Sigma}} = \Delta S_{\left\{\left\{E\right\}\right\}} + \Delta S^{res}_{\left\{\left\{E^{\Sigma}-E\right\}\right\}^{res}}. \tag{2.251}$$

But the system Σ is isolated. Therefore, following inequality (2.70), the increment of its entropy is positive (or zero):

$$\Delta S^{\Sigma}_{\left\{\left\{E,E^{\Sigma}-E\right\}\right\}^{\Sigma}} = \Delta S_{\left\{\left\{E\right\}\right\}} + \Delta S^{res}_{\left\{\left\{E^{\Sigma}-E\right\}\right\}^{res}} \geq 0. \tag{2.252}$$

Earlier, in (2.137), we have already expanded the entropy $S^{res}_{\left\{\left\{E^{\Sigma}-E\right\}\right\}^{res}}$ of the thermal reservoir:

$$S^{res}_{\left\{\left\{E^{\Sigma}-E\right\}\right\}^{res}} = S^{res}_{\left\{\left\{E^{res}\right\}\right\}^{res}}\Bigg|_{E^{res}=E^{\Sigma}} - E\left.\frac{dS^{res}_{\left\{\left\{E^{res}\right\}\right\}^{res}}}{dE^{res}}\right|_{E^{res}=E^{\Sigma}} = S^{res}_{\left\{\left\{E^{res}\right\}\right\}^{res}}\Bigg|_{E^{res}=E^{\Sigma}} - \frac{E}{T^{res}}. \tag{2.253}$$

Since the first term in the right-hand side of (2.253) is some constant which does not depend on fluctuations, for the increment of the entropy of the reservoir we obtain

$$\Delta S^{res}_{\left\{\left\{E^{\Sigma}-E\right\}\right\}^{res}} = -\frac{\Delta E}{T^{res}}. \tag{2.254}$$

Following the law of conservation of energy, we have

$$\delta Q^{res\leftarrow} = \Delta E^{res} = -\Delta E = -\delta Q^{\leftarrow}, \tag{2.255}$$

where the left-hand side is the amount of heat received by the thermal reservoir. Substituting $-\Delta E$ into (2.254), we find

$$\Delta S^{res}_{\left\{\left\{E^{\Sigma}-E\right\}\right\}^{res}} = \frac{\delta Q^{res\leftarrow}}{T^{res}}. \tag{2.256}$$

We have found that for the thermal reservoir, inequality (2.240) happens, in fact, to be always the equality. From thermodynamics we know that inequality (2.240) turns into equality only when all processes of heat exchange are quasistatic. This is indeed the case for the thermal reservoir because it difficult to expect something else from a system that has to provide the constancy of the boundary constraint $T^{res} = const$. Therefore, the heat exchange could be not quasistatic for our small system but it is always quasistatic for the reservoir.

Substituting (2.254) into (2.252), we find

$$\Delta S_{\{\{E\}\}} \geq \frac{\Delta E}{T^{res}} = \frac{\delta Q^{\leftarrow}}{T^{res}} \tag{2.257}$$

which proves that inequality (2.240) is the consequence of inequality (2.70). And we indeed see that this inequality should contain the temperature of the reservoir but not the temperature of our system.

Let us now define nonequilibrium Helmholtz energy. For energy fluctuations $\{\{E\}\}$ in the CE, we utilize thermodynamic definition (2.241) to obtain

$$F_{\{\{E\}\}} \equiv -T^{res} S_{\{\{E\}\}} + E. \tag{2.258}$$

Substituting into this expression entropy (2.130) of fluctuations $\{\{E\}\}$

$$F_{\{\{E\}\}} \equiv T^{res} \sum_{\{E\}} w_{\{E\}} \ln w_{\{E\}} + E \tag{2.259}$$

and normalization constraint $\sum_{\{E\}} w_{\{E\}} = 1$, we transform definition (2.258) into

$$F_{\{\{E\}\}} = \sum_{\{E\}} w_{\{E\}} \left\{ T^{res} \ln w_{\{E\}} + E \right\}, \tag{2.260}$$

where the probability distribution $w_{\{E\}}$ is the probability distribution (2.128), nonequilibrium with the CE.

Generalizing (2.260) to the case of an arbitrary ensemble and arbitrary probability distribution $w_{\{\ \}}$ of microstates $\{\ \}$, we obtain the "*stochastic*" definition of the Helmholtz energy:

$$F[w_{\{\}}] \equiv \sum_{\{\}} w_{\{\}} \left\{ T^{res} \ln w_{\{\}} + E_{\{\}} \right\}, \tag{2.261}$$

Of course, this definition is valid as long as there is such a quantity as temperature of the thermal reservoir in the ensemble. With the exception of this limitation, definition (2.261) is completely equivalent to Gibbs definition (2.21) of entropy and could be used instead of (2.21) as a "cornerstone" for all our formulae. It can be even further generalized to the case when the statistical operator (quantum density matrix) is not diagonal:

$$F \equiv \mathrm{Tr}\left(\hat{\rho} \left\{ T^{res} \ln \hat{\rho} + \hat{\mathrm{H}} \right\} \right), \tag{2.262}$$

which is again valid in any ensemble providing that the quantity T^{res} makes sense.

Similar to how we have found the entropy (2.228) of the CE, we can find the Helmholtz energy of the CE by substituting Gibbs probability distribution (2.139) into (2.261):

$$F^{CE} = \sum_{\{E\}} w_{\{E\}}^{CE} \left\{ T^{res} \ln w_{\{E\}}^{CE} + E \right\} = -T^{res} \ln Z^{CE}. \tag{2.263}$$

This equality is often treated as the definition of the Helmholtz energy. However, we should always remember that it defines only the equilibrium value of the Helmholtz energy corresponding to the equilibrium probability distribution (2.139). To be valid for nonequilibrium values of the Helmholtz energy as well, equality (2.263) should be modified as we will see below.

Earlier we introduced the partition function Z^{CE} of the ensemble as the normalizing constant of Gibbs probability distribution (2.139). Now we see that this distribution can also be normalized by the Helmholtz energy of the ensemble:

$$w_{\{E\}}^{CE} = e^{\frac{F^{CE} - E}{T^{res}}}. \tag{2.264}$$

We expect the Helmholtz energy to be the free energy potential of the CE. Let us now prove this statement by finding the connection of the Helmholtz energy with the probability distribution $W_{\{\{E\}\}}^{CE}$ of fluctuations $\left\{\left\{E\right\}\right\}$. Considering again the MCE of the system Σ with fluctuations $\left\{\left\{ E, E^{\Sigma} - E \right\}\right\}^{\Sigma}$, for the probability of a fluctuation in accordance with (2.73) we have

$$W^{\Sigma}_{\left\{\left\{E, E^{\Sigma} - E\right\}\right\}^{\Sigma}} \propto e^{S^{\Sigma}_{\{\{E, E^{\Sigma} - E\}\}^{\Sigma}}}. \tag{2.265}$$

Substituting (2.250) and (2.253) into this expression and also recalling that fluctuations $\left\{\left\{ E, E^{\Sigma} - E \right\}\right\}^{\Sigma}$ of the MCE of the system Σ correspond to fluctuations $\left\{\left\{E\right\}\right\}$ of the CE of our system, for the probabilities of latter we find

$$W_{\{\{E\}\}}^{CE} \propto e^{\left\{T^{res} S_{\{\{E\}\}} - E\right\}/T^{res}} = e^{-F_{\{\{E\}\}}/T^{res}}. \tag{2.266}$$

Transforming (2.258) into

$$e^{-F_{\{\{E\}\}}/T^{res}} \equiv \Gamma_{\{\{E\}\}} e^{-E/T^{res}}, \tag{2.267}$$

we can easily normalize the probability distribution (2.266):

$$W_{\{\{E\}\}}^{CE} = \frac{1}{Z^{CE}} e^{-F_{\{\{E\}\}}/T^{res}} = e^{(F^{CE} - F_{\{\{E\}\}})/T^{res}}. \tag{2.268}$$

We have utilized here the MCE of the system Σ only to illustrate how the probability of fluctuations in the CE happens to be the consequence of the probability distribution (2.73) of the MCE. However, a much simpler way to obtain formula (2.268) is just to substitute (2.258) in its form (2.267) into (2.143):

$$W^{CE}_{\{\{E\}\}} = \Gamma_{\{\{E\}\}} w^{CE}_{\{E\}} = \Gamma_{\{\{E\}\}} \frac{1}{Z^{CE}} e^{-E/T^{res}} = \frac{1}{Z^{CE}} e^{-F_{\{\{E\}\}}/T^{res}}. \qquad (2.269)$$

From equality (2.268) we see that the probabilities of energy fluctuations in the CE exponentially decrease with the increase of the Helmholtz energy of these fluctuations. To emphasize this association, we transform (2.268) into

$$F_{\{\{E\}\}} = -T^{res} \ln(Z^{CE} W^{CE}_{\{\{E\}\}}). \qquad (2.270)$$

This expression can also serve as a definition of the Helmholtz energy and we will call it the "*probabilistic*" definition.

The logarithm is the monotonically increasing function. Therefore, the increase of the probability always leads to the decrease of the Helmholtz energy in the CE. This proves that the Helmholtz energy is indeed the free energy potential of the CE and that its minimum corresponds to the equilibrium state.

Let us now obtain the last definition of the Helmholtz energy. But first we need to define *a partial partition function* as the sum of terms $e^{-E/T^{res}}$ not over all system's microstates $\{E\}$ but only over microstates corresponding to a particular energy level (to a particular group of microstates):

$$Z^{CE}_{E} \equiv \sum_{\{\tilde{E}\}:\tilde{E}=E} e^{-\tilde{E}/T^{res}} = g_E e^{-E/T^{res}}. \qquad (2.271)$$

And since each energy fluctuation $\{\{E\}\}$ corresponds to a particular energy level (group of microstates), the sum in (2.271) can be treated as if over the microstates $\{E\}$ of this fluctuation $\{\{E\}\}$ and, therefore, we can call (2.271) *the partial partition function of this fluctuation* $\{\{E\}\}$:

$$Z^{CE}_{\{\{E\}\}} \equiv \sum_{\{\tilde{E}\}:\{\tilde{E}\}\in\{\{E\}\}} e^{-\tilde{E}/T^{res}} = \Gamma_{\{\{E\}\}} e^{-E/T^{res}}. \qquad (2.272)$$

The difference between two definitions, (2.271) and (2.272), is just a matter of notation.

Substituting (2.272) into (2.143), we find that the probability of an energy fluctuation $\{\{E\}\}$ is just the ratio of the partial partition function of this fluctuation $\{\{E\}\}$ to the partition function of the ensemble:

$$W^{CE}_{\{\{E\}\}} \equiv \frac{Z^{CE}_{\{\{E\}\}}}{Z^{CE}} \qquad (2.273)$$

which clearly reminds us (2.43) of the MCE. We see that while in the MCE the probability of a fluctuation is the ratio of the statistical weight of the fluctuation to the statistical weight of the ensemble, in the CE the probability of a fluctuation is the ratio of the partial partition function of the fluctuation to the partition function of the ensemble. In other words, the statistical weight in the MCE plays the role similar to the partition function in the CE. We will return to this similarity later.

The quantity $Z^{CE}W^{CE}_{\{\{E\}\}}$ in (2.273) is just what defines the Helmholtz energy in (2.270). Therefore, we obtain the last, "*partition*" definition of the Helmholtz energy:

$$F_{\{\{E\}\}} = -T^{res} \ln Z^{CE}_{\{\{E\}\}}. \tag{2.274}$$

We see that this definition differs from (2.263) only by the fact that under the sign of the logarithm is the partial partition function of this fluctuation but not the ensemble partition function. But the partition function of the CE is the sum (2.142) of partial partition functions of energy fluctuations:

$$Z^{CE} \equiv \sum_{\{\{E\}\}} \Gamma_{\{\{E\}\}} e^{-E/T^{res}} = \sum_{\{\{E\}\}} Z^{CE}_{\{\{E\}\}}. \tag{2.275}$$

Since the partition function of the ensemble is equal with logarithmic accuracy to its maximal term

$$Z^{CE} \approx_{\ln} Z^{CE}_{\{\{E_0\}\}}, \tag{2.276}$$

the ensemble Helmholtz energy approximately equals the Helmholtz energy of the equilibrium macrostate $\{\{E_0\}\}$:

$$F^{CE} = -T^{res} \ln Z^{CE} \approx -T^{res} \ln Z^{CE}_{\{\{E_0\}\}} = F_{\{\{E_0\}\}}. \tag{2.277}$$

2.13 Free Energy Minimization Principle

For the Helmholtz energy as the free energy potential, we will utilize the stochastic definition (2.261)

$$\Psi[w_{\{E\}}] = \sum_{\{E\}} w_{\{E\}} \left\{ T^{res} \ln w_{\{E\}} + E \right\}, \tag{2.278}$$

acting as a functional on the function space of all possible probability distributions $w_{\{E\}}$. Since the probability distribution is always normalized,

$$\sum_{\{E\}} w_{\{E\}} = 1, \tag{2.279}$$

we add this constraint into our functional by the method of Lagrange multipliers:

$$\Psi[w_{\{E\}}] = \sum_{\{E\}} w_{\{E\}} \left\{ T^{res} \ln w_{\{E\}} + E \right\} + \lambda \left(\sum_{\{E\}} w_{\{E\}} - 1 \right). \tag{2.280}$$

To follow the free energy minimization principle, we should find the equilibrium distribution $w_{\{E\}}^{CE}$ corresponding to minimal value of functional (2.280). To do that, we find when the derivatives of (2.280) become zero.

Differentiation with respect to λ returns us to constraint (2.279),

$$0 = \frac{\partial \Psi}{\partial \lambda} = \sum_{\{E\}} w_{\{E\}}^{CE} - 1, \tag{2.281}$$

while the differentiation with respect to the probability $w_{\{E\}'}$ of microstate $\{E\}'$ provides

$$0 = \frac{\partial \Psi}{\partial w_{\{E\}'}} = T^{res} + T^{res} \ln w_{\{E\}'}^{CE} + E + \lambda \tag{2.282}$$

or

$$w_{\{E\}'}^{CE} = e^{-\frac{T^{res}+\lambda}{T^{res}} - \frac{E}{T^{res}}}. \tag{2.283}$$

Substituting (2.283) into (2.279), we find

$$w_{\{E\}'}^{CE} = \frac{1}{Z^{CE}} e^{-\frac{E}{T^{res}}} \tag{2.284}$$

which is equivalent to (2.139).

We have found the equilibrium distribution of probabilities for the case when the statistical operator (quantum density matrix) of the system was diagonal. In the opposite case, we should utilize the definition (2.262):

$$\Psi[\hat{\rho}] = \mathrm{Tr}\left(\hat{\rho} \left\{ T^{res} \ln \hat{\rho} + \hat{\mathrm{H}} \right\} \right) \tag{2.285}$$

subject to constraint

$$\mathrm{Tr}\left(\hat{\rho} \right) = 1 \tag{2.286}$$

which provides the functional

$$\Psi[\hat{\rho}] = \mathrm{Tr}\left(\hat{\rho} \left\{ T^{res} \ln \hat{\rho} + \hat{\mathrm{H}} \right\} \right) + \lambda \left(\mathrm{Tr}\left(\hat{\rho} \right) - 1 \right). \tag{2.287}$$

Differentiation with respect to λ returns us to (2.286) while the variation with respect to $\hat{\rho}$ provides

$$\mathrm{Tr}\left(\delta\hat{\rho}\left\{T^{res}\ln\hat{\rho}^{CE}+\hat{\mathrm{H}}\right\}+T^{res}\delta\hat{\rho}+\lambda\delta\hat{\rho}\right)=0. \tag{2.288}$$

Since (2.288) should be valid for an arbitrary variation $\delta\hat{\rho}$, we find

$$T^{res}\ln\hat{\rho}^{CE}+\hat{\mathrm{H}}+\left(T^{res}+\lambda\right)\hat{1}=0. \tag{2.289}$$

The solution of (2.289) is the operator

$$\hat{\rho}^{CE}=e^{-\left(1+\frac{\lambda}{T^{res}}\right)\hat{1}-\frac{\hat{\mathrm{H}}}{T^{res}}}=e^{-\left(1+\frac{\lambda}{T^{res}}\right)}e^{-\frac{\hat{\mathrm{H}}}{T^{res}}}, \tag{2.290}$$

where $\hat{1}$ is the unity operator. Substituting (2.290) into (2.286), we finally find the equilibrium statistical operator:

$$\hat{\rho}^{CE}=\frac{1}{Z^{CE}}e^{-\frac{\hat{\mathrm{H}}}{T^{res}}}, \tag{2.291}$$

where the partition function is now defined by

$$Z^{CE}\equiv\mathrm{Tr}\left(e^{-\frac{\hat{\mathrm{H}}}{T^{res}}}\right). \tag{2.292}$$

2.14 Other Ensembles

First let us consider as an example the case of the μ–P–T-ensemble when the system is maintained at constant chemical potential $\mu^{res}=const$, constant pressure $P^{res}=const$, and constant temperature $T^{res}=const$. Therefore, fluctuating parameters are the system's number of particles (degrees of freedom) N, volume V, and energy E.

Microstates of the system now are the eigenfunctions not only of the Hamiltonian of the system but also of the volume operator and the operator of the number of particles: $\{N,V,E\}$. Being more correct, the energy spectrum of the system depends now on the system's volume and number of particles: $\{N,V,E(V,N)\}$ but we will utilize simpler notation $\{N,V,E\}$ just for the purpose of the simplicity.

Our system interacts with the reservoir by heat exchange $\delta Q^{\leftarrow}\neq 0$, "volume exchange" $\delta W^{\leftarrow}\neq 0$, and particle exchange $\delta\Pi^{\leftarrow}\neq 0$, where $\delta Q^{\leftarrow}$ is the amount of heat supplied to our system, $\delta W^{\leftarrow}$ is the work of external forces performed on our system, and $\delta\Pi^{\leftarrow}$ is the energy gain of our system due to the particle exchange.

The total system Σ, including our system and the reservoir as subsystems, is again isolated in the MCE:

$$N+N^{res}=N^{\Sigma}=const, \tag{2.293a}$$

$$V+V^{res}=V^{\Sigma}=const, \tag{2.293b}$$

$$E+E^{res}=E^{\Sigma}=const. \tag{2.293c}$$

Applying the stroboscopic approximation of brief periods of virtual isolation, we construct microstates of the system Σ as combinations of microstates of our system and the reservoir:

$$\left\{N^{\Sigma},V^{\Sigma},E^{\Sigma}\right\}^{\Sigma}=\left\{N,V,E\right\}\otimes\left\{N^{res},V^{res},E^{res}\right\}^{res}. \tag{2.294}$$

In other words, the choice of a particular microstate $\{N,V,E\}$ of our system and a particular microstate $\left\{N^{res},V^{res},E^{res}\right\}^{res}$ of the reservoir forms the particular microstate $\left\{N^{\Sigma},V^{\Sigma},E^{\Sigma}\right\}$ of the system Σ.

We define a nonequilibrium fluctuation $\left\{\left\{N,V,E\right\}\right\}$ (a macrostate $\left\{\left\{N,V,E\right\}\right\}$) in the system as a macrostate with the energy E, volume V, and number of particles N. In other words, we define a fluctuation by the nonequilibrium probability distribution

$$w_{\{\tilde{N},\tilde{V},\tilde{E}\}}=\left\{\begin{matrix}1/\Gamma_{\{\{N,V,E\}\}},\tilde{N}=N\text{ and }\tilde{V}=V\text{ and }\tilde{E}=E\\0,otherwise\end{matrix}\right\}=\frac{\delta_{\tilde{N},N}\delta_{\tilde{V},V}\delta_{\tilde{E},E}}{\Gamma_{\{\{N,V,E\}\}}}. \tag{2.295}$$

Obviously, the statistical weight $\Gamma_{\{\{N,V,E\}\}}$ of the fluctuation $\left\{\left\{N,V,E\right\}\right\}$ is the statistical weight of this energy level (this group of microstates) when the volume and the number of particles in the system correspond to the given values:

$$\Gamma_{\{\{N,V,E\}\}}=g_{E(N,V)}. \tag{2.296}$$

Substituting (2.295) into the definition of entropy (2.21), we find that the entropy of the fluctuation $\left\{\left\{N,V,E\right\}\right\}$ follows Boltzmann's rule and equals the logarithm of the fluctuation statistical weight:

$$S_{\{\{N,V,E\}\}}=-\sum_{\{\tilde{N},\tilde{V},\tilde{E}\}}w_{\{\tilde{N},\tilde{V},\tilde{E}\}}\ln w_{\{\tilde{N},\tilde{V},\tilde{E}\}}=\ln\Gamma_{\{\{N,V,E\}\}}. \tag{2.297}$$

The behavior of any physical system is determined by two sets of factors: external influence and the structure or the properties of the system itself. In the case of a thermodynamic system, the external influence consists of the rules dictated to the system by the reservoir while the properties of the system itself are represented by the structure of its energy spectrum, $g_{E(N,V)}$. Let us, with the aid of the considered μ–P–T-ensemble, understand what part in system's behavior is dictated by the reservoir and what part is determined by the properties of the system.

Firstly, the reservoir dictates the boundary conditions $\mu^{res},P^{res},T^{res}=const$ to the system. This boundary constraint provides for the system at least three fluctuating parameters: N,V,E. The fluctuating behavior of the system is much more rich than these three parameters (for example, the density of the gas could fluctuate from one point to another within the volume which would be described by the additional set of fluctuating parameters p). However, in our study we restrict ourselves to fluctuations (2.295) only of these three fluctuating parameters N,V,E and ignore the rest of other possible fluctuating parameters p.

Secondly, the reservoir dictates the equilibrium probability distribution of system's microstates

$$w_{\{N,V,E\}}^{\mu-P-T} = \frac{\Gamma_{\left\{\left\{N^{\Sigma}-N,V^{\Sigma}-V,E^{\Sigma}-E\right\}\right\}}^{res}}{\Gamma^{\Sigma,MCE}} \propto \Gamma_{\left\{\left\{N^{\Sigma}-N,V^{\Sigma}-V,E^{\Sigma}-E\right\}\right\}}^{res} = e^{S_{\{\{N^{\Sigma}-N,V^{\Sigma}-V,E^{\Sigma}-E\}\}}^{res}} \quad (2.298)$$

without regard to which system it is dealing with (without regard to the spectrum $g_{E(N,V)}$ of the system considered).

For quasistatic processes, we define temperature, pressure, and chemical potential as

$$\frac{1}{T} \equiv \left(\frac{\partial S_{\{\{N,V,E\}\}}}{\partial E} \right)_{N,V}, \quad (2.299a)$$

$$\frac{P}{T} \equiv \left(\frac{\partial S_{\{\{N,V,E\}\}}}{\partial V} \right)_{N,E}, \quad (2.299b)$$

$$-\frac{\mu}{T} \equiv \left(\frac{\partial S_{\{\{N,V,E\}\}}}{\partial N} \right)_{V,E}. \quad (2.299c)$$

Expanding the reservoir's entropy in (2.298) and applying (2.299) (because all processes are quasistatic for the reservoir), we return to the exponential dependence similar to the case of the CE with the exception that now we have three fluctuating parameters in it,

$$w_{\{N,V,E\}}^{\mu-P-T} = \frac{1}{Z^{\mu-P-T}} e^{-\frac{N}{(-T^{res}/\mu^{res})} - \frac{V}{(T^{res}/P^{res})} - \frac{E}{T^{res}}}, \quad (2.300)$$

where $Z^{\mu-P-T}$ is the partition function of the μ–P–T-ensemble:

$$\begin{aligned} Z^{\mu-P-T} &\equiv \sum_{\{N,V,E\}} e^{-\frac{N}{(-T^{res}/\mu^{res})} - \frac{V}{(T^{res}/P^{res})} - \frac{E}{T^{res}}} \\ &= \sum_{\{\{N,V,E\}\}} \Gamma_{\{\{N,V,E\}\}} e^{-\frac{N}{(-T^{res}/\mu^{res})} - \frac{V}{(T^{res}/P^{res})} - \frac{E}{T^{res}}}. \end{aligned} \quad (2.301)$$

So far the properties of the system itself have influenced only the last expression for the partition function as a normalization constant and, therefore, we may say that the probability distribution of system's microstates was dictated almost entirely by the reservoir. However, the energy spectrum $g_{E(N,V)} \equiv \Gamma_{\{\{N,V,E\}\}}$ of the system becomes indeed important when we consider the probability distribution not of system's microstates $\{N,V,E\}$ but of system's fluctuations $\{\{N,V,E\}\}$:

$$W^{\mu-P-T}_{\{\{N,V,E\}\}} = \frac{\Gamma_{\{\{N,V,E\}\}}\Gamma^{res}_{\{\{N^\Sigma-N,V^\Sigma-V,E^\Sigma-E\}\}^{res}}}{\Gamma^{\Sigma,MCE}} = \Gamma_{\{\{N,V,E\}\}} w^{\mu-P-T}_{\{N,V,E\}}. \tag{2.302}$$

The energy spectrum works here as one of two multipliers with the exponential dependence on N,V,E whose "clash" determines the narrow probability maximum around the equilibrium macrostate $\{\{N_0,V_0,E_0\}\}$. The relative width of this maximum is again inversely proportional to $\sqrt{N_0}$ and, therefore, is very small in the thermodynamic limit:

$$\frac{\delta N}{N_0} \propto \frac{1}{\sqrt{N_0}}, \tag{2.303a}$$

$$\frac{\delta V}{V_0} \propto \frac{1}{\sqrt{N_0}}, \tag{2.303b}$$

$$\frac{\delta E}{E_0} \propto \frac{1}{\sqrt{N_0}}. \tag{2.303c}$$

At the point of the maximum, three equilibrium equalities are valid,

$$\frac{1}{T} = \frac{1}{T^{res}},\ \frac{P}{T} = \frac{P^{res}}{T^{res}},\ \text{and}\ -\frac{\mu}{T} = -\frac{\mu^{res}}{T^{res}}, \tag{2.304}$$

when temperature, pressure, and chemical potential of our system are equal to $T^{res}, P^{res}, \mu^{res}$, respectively.

Let us now discuss thermodynamic considerations about what quantity could serve as the free energy potential for our ensemble. One inequality (2.240) we already know,

$$\delta Q^{\leftarrow} \le T^{res}\Delta S \text{ or } \Delta S \ge \frac{\delta Q^{\leftarrow}}{T^{res}}, \tag{2.305}$$

which states that the entropy of the system grows not only due to the heat supplied to the system but also due to the internal processes leading the system into its equilibrium macrostate.

To find the second inequality we should consider the case when pressure P inside the system differs from the value P^{res} dictated by the reservoir. Illustrative examples are the expansion of a gas into a vacuum and a weight dropped on a piston of a volume containing gas. When the boundary of the system moves, the performed work is determined by the least of two pressure values:

$$\delta W^{\leftarrow} = -\min\left(P, P^{res}\right)\Delta V. \tag{2.306}$$

For example, for the gas expanding into a vacuum the work is zero because no force counteracts the expansion:

$$\delta W^{\leftarrow} = -P^{res}\Delta V = 0. \tag{2.307}$$

On the contrary, when a weight is dropped upon a piston, the work is determined by the nonequilibrium gas pressure while initially the weight pressure is much higher:

$$\delta W^{\leftarrow} = -P\Delta V. \tag{2.308}$$

Therefore, if the system's pressure were higher, $P > P^{res}$, the system would expand, performing work $\delta W^{\rightarrow} = P^{res}\Delta V$ on the reservoir. On the contrary, if the system's pressure were lower, $P < P^{res}$, the system would contract and the reservoir would perform work $\delta W^{\leftarrow} = P\,|\,\Delta V\,| < P^{res}\,|\,\Delta V\,|$ on the system. For both cases, the following inequality is valid:

$$\delta W^{\leftarrow} \le -P^{res}\Delta V \text{ or } -\Delta V \ge \frac{\delta W^{\leftarrow}}{P^{res}}. \tag{2.309}$$

which we consider to be fundamental, no less than inequality (2.305).

Considering heat exchange leads us to inequality (2.305), and considering "volume exchange" leads us to inequality (2.309). For particle exchange, when the chemical potential μ of the system differs from the chemical potential μ^{res} of the reservoir, similar considerations provide

$$\delta\Pi^{\leftarrow} \le \mu^{res}\Delta N \text{ or } \Delta N \ge \frac{\delta\Pi^{\leftarrow}}{\mu^{res}}. \tag{2.310}$$

But all three considered inequalities characterize the change of energy of the system. Applying the law of conservation of energy, we find

$$\Delta E = \delta Q^{\leftarrow} + \delta W^{\leftarrow} + \delta\Pi^{\leftarrow} \le T^{res}\Delta S - P^{res}\Delta V + \mu^{res}\Delta N. \tag{2.311}$$

Developing this inequality, we have utilized thermodynamic considerations. Let us now prove the last inequality from the point of view of statistical physics. We again consider the isolated system Σ. Only now as its fluctuations we employ macrostates $\left\{\left\{(N,V,E);(N^{\Sigma}-N,V^{\Sigma}-V,E^{\Sigma}-E)\right\}\right\}^{\Sigma}$ when our system has energy E, volume V, and the number of particles N while the reservoir has $E^{res} = E^{\Sigma} - E$, $V^{res} = V^{\Sigma} - V$, and $N^{res} = N^{\Sigma} - N$.

These fluctuations we define by the nonequilibrium probability distribution:

$$
\begin{aligned}
& w^{\Sigma}_{\left\{\left(\tilde{N},\tilde{V},\tilde{E}\right),\left(N^{\Sigma}-\tilde{N},V^{\Sigma}-\tilde{V},E^{\Sigma}-\tilde{E}\right)\right\}^{\Sigma}} \\
&= \begin{Bmatrix} 1/\Gamma^{\Sigma}_{\left\{\left\{(N,V,E),\left(N^{\Sigma}-N,V^{\Sigma}-V,E^{\Sigma}-E\right)\right\}\right\}^{\Sigma}} & ,\tilde{N}=N,\tilde{V}=V,\text{and }\tilde{E}=E \\ 0 & ,\text{otherwise} \end{Bmatrix} \\
&= \frac{\delta_{\tilde{N},N}\delta_{\tilde{V},V}\delta_{\tilde{E},E}}{\Gamma^{\Sigma}_{\left\{\left\{(N,V,E),\left(N^{\Sigma}-N,V^{\Sigma}-V,E^{\Sigma}-E\right)\right\}\right\}^{\Sigma}}}.
\end{aligned}
\tag{2.312}
$$

The statistical weight $\Gamma^{\Sigma}_{\left\{\left\{(N,V,E),(N^{\Sigma}-N,V^{\Sigma}-V,E^{\Sigma}-E)\right\}\right\}^{\Sigma}}$ of the fluctuation $\left\{\left\{\left(N,V,E\right);\left(N^{\Sigma}-N,V^{\Sigma}-V,E^{\Sigma}-E\right)\right\}\right\}^{\Sigma}$ is the number of microstates of the system Σ when our system has fluctuating parameters E,V,N:

$$
\Gamma^{\Sigma}_{\left\{\left\{(N,V,E);\left(N^{\Sigma}-N,V^{\Sigma}-V,E^{\Sigma}-E\right)\right\}\right\}^{\Sigma}} = g_{E(N,V)}g^{res}_{E^{\Sigma}-E(N,V)},
\tag{2.313}
$$

where $g_{E(N,V)}$ is the statistical weight of the energy level (group of microstates) E of our system when its volume is V and the number of particles is N. Respectively, $g^{res}_{E^{\Sigma}-E(N,V)}$ is the statistical weight of the energy level (group of microstates) $E^{\Sigma}-E$ of the reservoir when its volume is $V^{\Sigma}-V$ and the number of particles is $N^{\Sigma}-N$.

The entropy $S^{\Sigma}_{\left\{\left\{(N,V,E);(N^{\Sigma}-N,V^{\Sigma}-V,E^{\Sigma}-E)\right\}\right\}^{\Sigma}}$ of the fluctuation is the logarithm of the fluctuation's statistical weight:

$$
\begin{aligned}
S^{\Sigma}_{\left\{\left\{(N,V,E);\left(N^{\Sigma}-N,V^{\Sigma}-V,E^{\Sigma}-E\right)\right\}\right\}^{\Sigma}} &= \ln\Gamma^{\Sigma}_{\left\{\left\{(N,V,E);\left(N^{\Sigma}-N,V^{\Sigma}-V,E^{\Sigma}-E\right)\right\}\right\}^{\Sigma}} \\
&= \ln g_{E(N,V)} + \ln g^{res}_{E^{\Sigma}-E(N,V)}.
\end{aligned}
\tag{2.314}
$$

We have specifically constructed fluctuations $\left\{\left\{\left(N,V,E\right);\left(N^{\Sigma}-N,V^{\Sigma}-V,E^{\Sigma}-E\right)\right\}\right\}^{\Sigma}$ of the system Σ in such a way so they could represent fluctuations $\left\{\left\{N,V,E\right\}\right\}$ of our system in the *μ–P–T*-ensemble. Considering the latter now, the entropy $S_{\left\{\left\{N,V,E\right\}\right\}}$ of a fluctuation $\left\{\left\{N,V,E\right\}\right\}$ is

$$
S_{\left\{\left\{N,V,E\right\}\right\}} = \ln\Gamma_{\left\{\left\{N,V,E\right\}\right\}} = \ln g_{E(V,N)}
\tag{2.315}
$$

while for fluctuations $\left\{\left\{N^{res},V^{res},E^{res}\right\}\right\}^{res}$ of the reservoir we have

$$
S^{res}_{\left\{\left\{N^{res},V^{res},E^{res}\right\}\right\}^{res}} = \ln\Gamma^{res}_{\left\{\left\{N^{res},V^{res},E^{res}\right\}\right\}^{res}} = \ln g^{res}_{E^{\Sigma}-E(N,V)}.
\tag{2.316}
$$

Substituting (2.315) and (2.316) into (2.314), we prove the additivity of the entropy of the system Σ over its subsystems:

$$S^{\Sigma}_{\left\{\left\{(N,V,E);(N^{\Sigma}-N,V^{\Sigma}-V,E^{\Sigma}-E)\right\}\right\}^{\Sigma}} = S_{\left\{\left\{N,V,E\right\}\right\}} + S^{res}_{\left\{\left\{N^{\Sigma}-N,V^{\Sigma}-V,E^{\Sigma}-E\right\}\right\}^{res}}. \quad (2.317)$$

We have been able to prove this property of additivity only because we consider the stroboscopic approximation when during the brief periods of virtual isolation two subsystems become, in fact, independent. Otherwise, the rule of additivity would not be valid.

Differentiating (2.317), for the increments of entropies we find:

$$\Delta S^{\Sigma}_{\left\{\left\{(N,V,E);(N^{\Sigma}-N,V^{\Sigma}-V,E^{\Sigma}-E)\right\}\right\}^{\Sigma}} = \Delta S_{\left\{\left\{N,V,E\right\}\right\}} + \Delta S^{res}_{\left\{\left\{N^{\Sigma}-N,V^{\Sigma}-V,E^{\Sigma}-E\right\}\right\}^{res}}. \quad (2.318)$$

Since the system Σ is isolated, in accordance with inequality (2.70) the increment of its entropy is positive (or zero):

$$\Delta S^{\Sigma}_{\left\{\left\{(N,V,E);(N^{\Sigma}-N,V^{\Sigma}-V,E^{\Sigma}-E)\right\}\right\}^{\Sigma}} = \Delta S_{\left\{\left\{N,V,E\right\}\right\}} + \Delta S^{res}_{\left\{\left\{N^{\Sigma}-N,V^{\Sigma}-V,E^{\Sigma}-E\right\}\right\}^{res}} \geq 0. \quad (2.319)$$

Expanding the entropy $S^{res}_{\left\{\left\{N^{\Sigma}-N,V^{\Sigma}-V,E^{\Sigma}-E\right\}\right\}^{res}}$ of the reservoir in an assumption that N,V,E are infinitesimal relatively to N^{res},V^{res},E^{res}, we find

$$S^{res}_{\left\{\left\{N^{\Sigma}-N,V^{\Sigma}-V,E^{\Sigma}-E\right\}\right\}^{res}} = S^{res}_{\left\{\left\{N^{res},V^{res},E^{res}\right\}\right\}^{res}}\Bigg|_{\substack{N^{res}=N^{\Sigma},\\ V^{res}=V^{\Sigma},\\ E^{res}=E^{\Sigma}}} - \frac{N}{(-T^{res}/\mu^{res})} - \frac{V}{T^{res}/P^{res}} - \frac{E}{T^{res}}. \quad (2.320)$$

Here the first term in the right-hand side is some constant, not depending on fluctuations. Therefore, for the increment of the entropy of the reservoir we obtain

$$\Delta S^{res}_{\left\{\left\{N^{\Sigma}-N,V^{\Sigma}-V,E^{\Sigma}-E\right\}\right\}^{res}} = -\frac{\Delta N}{(-T^{res}/\mu^{res})} - \frac{\Delta V}{T^{res}/P^{res}} - \frac{\Delta E}{T^{res}}. \quad (2.321)$$

Substituting here the law of conservation of energy

$$\delta Q^{res\leftarrow} + \delta W^{res\leftarrow} + \delta\Pi^{res\leftarrow} = \Delta E^{res} = -\Delta E = -\delta Q^{\leftarrow} - \delta W^{\leftarrow} - \delta\Pi^{\leftarrow} \quad (2.322)$$

along with (2.293) into (2.321), we find

$$\Delta E^{res} = T^{res}\Delta S^{res}_{\left\{\left\{N^{\Sigma}-N,V^{\Sigma}-V,E^{\Sigma}-E\right\}\right\}^{res}} - P^{res}\Delta V^{res} + \mu^{res}\Delta N^{res}. \quad (2.323)$$

Comparing (2.323) with (2.311), we see that for the reservoir all processes are indeed quasistatic. It would be difficult to expect something else from the system which has to provide constant boundary conditions $\mu^{res}, P^{res}, T^{res} = const$. To maintain the temperature constant, no matter what are the processes within the system in contact, the reservoir has to possess the superior heat conductance. To support constant pressure, when there is an arbitrary pressure at the other side of the boundary, the reservoir has to possess the superior "pressure conductance." To provide constant chemical potential, "particle conductance" has to be superior also.

Substituting (2.321) into (2.319), we find

$$\Delta E \le T^{res}\Delta S_{\{\{N,V,E\}\}} - P^{res}\Delta V + \mu^{res}\Delta N \tag{2.324}$$

which proves that (2.311) is the consequence of inequality (2.70).

Inequality (2.311) means that under the ensemble boundary conditions $\mu^{res}, P^{res}, T^{res} = const$ the following potential would be always decreasing (or staying constant but not increasing) for arbitrary processes in the system:

$$\Delta(-T^{res}S - \mu^{res}N + P^{res}V + E) \le 0. \tag{2.325}$$

Therefore, we thermodynamically define the Y-energy of the μ–P–T-ensemble as

$$\mathrm{Y} \equiv -T^{res}S - \mu^{res}N + P^{res}V + E. \tag{2.326}$$

The important fact here is that this definition contains parameters of the reservoir $\mu^{res}, P^{res}, T^{res}$ but not parameters μ, P, T of the system.

Inequality (2.325) suggests that the Y-energy plays the role of the free energy potential in the μ–P–T- ensemble.

To prove this, we define the Y-energy of a fluctuation $\{\{N,V,E\}\}$ as

$$\mathrm{Y}_{\{\{N,V,E\}\}} \equiv -T^{res}S_{\{\{N,V,E\}\}} - \mu^{res}N + P^{res}V + E \tag{2.327}$$

which provides the stochastic definition:

$$\mathrm{Y}[w_{\{\}}] \equiv \sum_{\{\}} w_{\{\}}\left\{T^{res}\ln w_{\{\}} - \mu^{res}N_{\{\}} + P^{res}V_{\{\}} + E_{\{\}}\right\}. \tag{2.328}$$

Substituting (2.297) into (2.327), we obtain the probabilistic definition connecting the Y-energy with the probabilities of fluctuations in the system

$$\mathrm{Y}_{\{\{N,V,E\}\}} \equiv -T^{res}\ln\left(Z^{\mu-P-T}W^{\mu-P-T}_{\{\{N,V,E\}\}}\right) \tag{2.329}$$

which finally proves that Y-energy is indeed the free energy potential of the μ–P–T-ensemble.

Introducing partial partition functions of fluctuations as

$$Z^{\mu-P-T}_{\{\{N,V,E\}\}} \equiv \sum_{\{\tilde{N},\tilde{V},\tilde{E}\}:\tilde{N}=N,\,\tilde{V}=V,\,\tilde{E}=E} e^{-\frac{\tilde{N}}{(-T^{res}/\mu^{res})}-\frac{\tilde{V}}{(T^{res}/P^{res})}-\frac{\tilde{E}}{T^{res}}}$$
$$= \Gamma_{\{\{N,V,E\}\}} e^{-\frac{N}{(-T^{res}/\mu^{res})}-\frac{V}{(T^{res}/P^{res})}-\frac{E}{T^{res}}}, \tag{2.330}$$

we find the last, partition definition of the Y-energy:

$$\mathrm{Y}_{\{\{N,V,E\}\}} \equiv -T^{res} \ln Z^{\mu-P-T}_{\{\{N,V,E\}\}}. \tag{2.331}$$

Now, when we already understand how to generalize the free energy formalism for the case of an arbitrary ensemble, let us briefly summarize formulae for different ensembles. We will consider the following sets of boundary conditions:

$$E^{res}, V^{res}, N^{res} = const \text{ for the MCE,} \tag{2.332a}$$

$$T^{res}, V^{res}, N^{res} = const \text{ for the CE,} \tag{2.332b}$$

$$T^{res}, V^{res}, \mu^{res} = const \text{ for the GCE,} \tag{2.332c}$$

$$T^{res}, P^{res}, N^{res} = const \text{ for the } P\text{-}T\text{-E,} \tag{2.332d}$$

$$T^{res}, P^{res}, \mu^{res} = const \text{ for the } \mu\text{-}P\text{-}T\text{-E,} \tag{2.332e}$$

where *GCE* is *the grand canonical ensemble*, *P–T*-E is *the P–T-ensemble*, and *μ–P–T*-E is the *μ–P–T*-ensemble.

The probability distribution for system's microstates is dictated by the reservoir:

$$w^{MCE}_{\{P\}} = \frac{1}{Z^{MCE}} e^{-0}, \tag{2.333a}$$

$$w^{CE}_{\{E\}} = \frac{1}{Z^{CE}} e^{-\frac{E}{T^{res}}}, \tag{2.333b}$$

$$w^{GCE}_{\{N,E\}} = \frac{1}{Z^{GCE}} e^{-\frac{N}{(-T^{res}/\mu^{res})}-\frac{E}{T^{res}}}, \tag{2.333c}$$

$$w^{P-T}_{\{V,E\}} = \frac{1}{Z^{P-T}} e^{-\frac{V}{(T^{res}/P^{res})}-\frac{E}{T^{res}}}, \tag{2.333d}$$

$$w^{\mu-P-T}_{\{N,V,E\}} = \frac{1}{Z^{\mu-P-T}} e^{-\frac{N}{(-T^{res}/\mu^{res})}-\frac{V}{(T^{res}/P^{res})}-\frac{E}{T^{res}}}, \tag{2.333e}$$

where each ensemble has its own partition function as a normalization constant for this distribution:

$$Z^{MCE} \equiv \sum_{\{p\}} e^{-0}, \tag{2.334a}$$

$$Z^{CE} \equiv \sum_{\{E\}} e^{-\frac{E}{T^{res}}}, \tag{2.334b}$$

$$Z^{GCE} \equiv \sum_{\{N,E\}} e^{-\frac{N}{(-T^{res}/\mu^{res})}-\frac{E}{T^{res}}}, \tag{2.334c}$$

$$Z^{P-T} \equiv \sum_{\{V,E\}} e^{-\frac{V}{(T^{res}/P^{res})}-\frac{E}{T^{res}}}, \tag{2.334d}$$

$$Z^{\mu-P-T} \equiv \sum_{\{N,V,E\}} e^{-\frac{N}{(-T^{res}/\mu^{res})}-\frac{V}{(T^{res}/P^{res})}-\frac{E}{T^{res}}}. \tag{2.334e}$$

In Sect. 2.12, we have already seen the analogy between the statistical weight of the MCE and the partition function of the CE. To emphasize this symmetry, we here call the statistical weight $\Gamma^{MCE} \equiv \sum_{\{p\}} 1$ of the MCE by the term *the partition function of the MCE* $Z^{MCE} \equiv \sum_{\{p\}} e^{-0} = \Gamma^{MCE}$. The meaning of the quantity remains the same—it is the number of equiprobable microstates in the ensemble. But the change of terminology has allowed us to symmetrize the formulae above. We will utilize a similar definition and for the partial partition functions of the MCE which are just the statistical weights of fluctuations: $Z_{\{\{p\}\}} \equiv \sum_{\{\tilde{p}\}:\tilde{p}=p} e^{-0} = \Gamma_{\{\{p\}\}}$.

For the entropy of fluctuations, Boltzmann's rule is applicable

$$S_{\{\{p\}\}} = \ln \Gamma_{\{\{p\}\}}, \tag{2.335a}$$

$$S_{\{\{E\}\}} = \ln \Gamma_{\{\{E\}\}}, \tag{2.335b}$$

$$S_{\{\{N,E\}\}} = \ln \Gamma_{\{\{N,E\}\}}, \tag{2.335c}$$

$$S_{\{\{V,E\}\}} = \ln \Gamma_{\{\{V,E\}\}}, \tag{2.335d}$$

$$S_{\{\{N,V,E\}\}} = \ln \Gamma_{\{\{N,V,E\}\}} \tag{2.335e}$$

while for the probability of fluctuations we find

$$W^{MCE}_{\{\{p\}\}} = \frac{Z_{\{\{p\}\}}}{Z^{MCE}} = \frac{1}{Z^{MCE}} e^{S_{\{\{p\}\}}}, \tag{2.336a}$$

$$W^{CE}_{\{\{E\}\}} = \frac{Z_{\{\{E\}\}}}{Z^{CE}} = \frac{1}{Z^{CE}} e^{S_{\{\{E\}\}} - \frac{E}{T^{res}}}, \tag{2.336b}$$

$$W^{GCE}_{\{\{N,E\}\}} = \frac{Z_{\{\{N,E\}\}}}{Z^{GCE}} = \frac{1}{Z^{GCE}} e^{S_{\{\{N,E\}\}} - \frac{N}{(-T^{res}/\mu^{res})} - \frac{E}{T^{res}}}, \tag{2.336c}$$

$$W^{P-T}_{\{\{V,E\}\}} = \frac{Z_{\{\{V,E\}\}}}{Z^{P-T}} = \frac{1}{Z^{P-T}} e^{S_{\{\{V,E\}\}} - \frac{V}{(T^{res}/P^{res})} - \frac{E}{T^{res}}}, \tag{2.336d}$$

$$W^{\mu-P-T}_{\{\{N,V,E\}\}} = \frac{Z_{\{\{N,V,E\}\}}}{Z^{\mu-P-T}} = \frac{1}{Z^{\mu-P-T}} e^{S_{\{\{N,V,E\}\}} - \frac{N}{(-T^{res}/\mu^{res})} - \frac{V}{(T^{res}/P^{res})} - \frac{E}{T^{res}}}. \tag{2.336e}$$

Next, for each ensemble we introduce its free energy potential,

$$\Psi_{\{\{p\}\}} \equiv -S_{\{\{p\}\}}, \tag{2.337a}$$

$$\Psi_{\{\{E\}\}} \equiv -T^{res} S_{\{\{E\}\}} + E, \tag{2.337b}$$

$$\Psi_{\{\{N,E\}\}} \equiv -T^{res} S_{\{\{N,E\}\}} - \mu^{res} N + E, \tag{2.337c}$$

$$\Psi_{\{\{V,E\}\}} \equiv -T^{res} S_{\{\{V,E\}\}} + P^{res} V + E, \tag{2.337d}$$

$$\Psi_{\{\{N,V,E\}\}} \equiv -T^{res} S_{\{\{N,V,E\}\}} - \mu^{res} N + P^{res} V + E, \tag{2.337e}$$

which are called

$$\text{negative entropy (X-energy), } \mathrm{X} \equiv -S, \tag{2.338a}$$

$$\text{the Helmholtz energy, } F \equiv -T^{res} S + E, \tag{2.338b}$$

$$\Omega\text{-energy, } \Omega \equiv -T^{res} S - \mu^{res} N + E, \tag{2.338c}$$

$$\text{the Gibbs energy, } \Phi \equiv -T^{res} S + P^{res} V + E, \tag{2.338d}$$

$$\text{Y-energy, } \mathrm{Y} \equiv -T^{res} S - \mu^{res} N + P^{res} V + E. \tag{2.338e}$$

Definition (2.337) can be presented in a more universal form as

$$\mathrm{X}[w_{\{\}}] \equiv \sum_{\{\}} w_{\{\}} \ln w_{\{\}}, \tag{2.339a}$$

$$F[w_{\{\}}] \equiv \sum_{\{\}} w_{\{\}} \left(T^{res} \ln w_{\{\}} + E_{\{\}} \right), \tag{2.339b}$$

$$\Omega[w_{\{\}}] \equiv \sum_{\{\}} w_{\{\}} \left(T^{res} \ln w_{\{\}} - \mu^{res} N_{\{\}} + E_{\{\}} \right), \tag{2.339c}$$

$$\Phi[w_{\{\}}] \equiv \sum_{\{\}} w_{\{\}} \left(T^{res} \ln w_{\{\}} + P^{res} V_{\{\}} + E_{\{\}} \right), \tag{2.339d}$$

$$\mathrm{Y}[w_{\{\}}] \equiv \sum_{\{\}} w_{\{\}} \left(T^{res} \ln w_{\{\}} - \mu^{res} N_{\{\}} + P^{res} V_{\{\}} + E_{\{\}} \right). \tag{2.339e}$$

If the statistical operator (density matrix) $\hat{\rho}$ is not diagonal, (2.339) transforms into

$$\mathrm{X}[\hat{\rho}] \equiv \mathrm{Tr}\left(\hat{\rho} \ln \hat{\rho} \right), \tag{2.340a}$$

$$F[\hat{\rho}] \equiv \mathrm{Tr}\left(\hat{\rho} \left\{ T^{res} \ln \hat{\rho} + \hat{\mathrm{H}} \right\} \right), \tag{2.340b}$$

$$\Omega[w_{\{\}}] \equiv \mathrm{Tr}\left(\hat{\rho} \left\{ T^{res} \hat{\rho} - \mu^{res} \hat{N} + \hat{\mathrm{H}} \right\} \right), \tag{2.340c}$$

$$\Phi[\hat{\rho}] \equiv \mathrm{Tr}\left(\hat{\rho} \left\{ T^{res} \ln \hat{\rho} + P^{res} \hat{V} + \hat{\mathrm{H}} \right\} \right), \tag{2.340d}$$

$$\mathrm{Y}[\hat{\rho}] \equiv \mathrm{Tr}\left(\hat{\rho} \left\{ T^{res} \ln \hat{\rho} - \mu^{res} \hat{N} + P^{res} \hat{V} + \hat{\mathrm{H}} \right\} \right). \tag{2.340e}$$

To prove that (2.337) is the free energy potential, we substitute (2.337) into (2.336) and see that probabilities of fluctuations indeed depend exponentially on (2.337):

$$W^{MCE}_{\{\{p\}\}} = \frac{1}{Z^{MCE}} e^{-\Psi_{\{\{p\}\}}}, \tag{2.341a}$$

$$W^{CE}_{\{\{E\}\}} = \frac{1}{Z^{CE}} e^{-\frac{\Psi_{\{\{E\}\}}}{T^{res}}}, \tag{2.341b}$$

$$W^{GCE}_{\{\{N,E\}\}} = \frac{1}{Z^{GCE}} e^{-\frac{\Psi_{\{\{N,E\}\}}}{T^{res}}}, \tag{2.341c}$$

$$W^{P-T}_{\{\{V,E\}\}} = \frac{1}{Z^{P-T}} e^{-\frac{\Psi_{\{\{V,E\}\}}}{T^{res}}}, \tag{2.341d}$$

$$W^{\mu-P-T}_{\{\{N,V,E\}\}} = \frac{1}{Z^{\mu-P-T}} e^{-\frac{\Psi_{\{\{N,V,E\}\}}}{T^{res}}}. \tag{2.341e}$$

Inverting (2.341), we find

$$\Psi_{\{\{p\}\}} = -\ln(Z^{MCE} W^{MCE}_{\{\{p\}\}}) = -\ln Z_{\{\{p\}\}}, \tag{2.342a}$$

$$\Psi_{\{\{E\}\}} = -T^{res} \ln(Z^{CE} W^{CE}_{\{\{E\}\}}) = -T^{res} \ln Z_{\{\{E\}\}}, \tag{2.342b}$$

$$\Psi_{\{\{N,E\}\}} = -T^{res} \ln(Z^{GCE} W^{GCE}_{\{\{N,E\}\}}) = -T^{res} \ln Z_{\{\{N,E\}\}}, \tag{2.342c}$$

$$\Psi_{\{\{V,E\}\}} = -T^{res} \ln(Z^{P-T} W^{P-T}_{\{\{V,E\}\}}) = -T^{res} \ln Z_{\{\{V,E\}\}}, \tag{2.342d}$$

$$\Psi_{\{\{N,V,E\}\}} = -T^{res} \ln(Z^{\mu-P-T} W^{\mu-P-T}_{\{\{N,V,E\}\}}) = -T^{res} \ln Z_{\{\{N,V,E\}\}}. \tag{2.342e}$$

Substituting the equilibrium distribution of probabilities (2.333) into (2.339), we find the free energy potential of the ensemble:

$$\Psi^{MCE} = -\ln Z^{MCE}, \tag{2.343a}$$

$$\Psi^{CE} = -T^{res} \ln Z^{CE}, \tag{2.343b}$$

$$\Psi^{GCE} = -T^{res} \ln Z^{GCE}, \tag{2.343c}$$

$$\Psi^{P-T} = -T^{res} \ln Z^{P-T}, \tag{2.343d}$$

$$\Psi^{\mu-P-T} = -T^{res} \ln Z^{\mu-P-T}. \tag{2.343e}$$

We see that the difference between (2.342) and (2.343) is that in the former we used partial partition functions while in the latter we used ensemble partition functions. We can utilize (2.343) to normalize the probability distribution (2.341) which provides

$$W^{MCE}_{\{\{p\}\}} = e^{\Psi^{MCE} - \Psi_{\{\{p\}\}}}, \tag{2.344a}$$

$$W^{CE}_{\{\{E\}\}} = e^{\frac{\Psi^{CE} - \Psi_{\{\{E\}\}}}{T^{res}}}, \tag{2.344b}$$

$$W^{GCE}_{\{\{N,E\}\}} = e^{\frac{\Psi^{GCE} - \Psi_{\{\{N,E\}\}}}{T^{res}}}, \tag{2.344c}$$

$$W^{P-T}_{\{\{V,E\}\}} = e^{\frac{\Psi^{P-T} - \Psi_{\{\{V,E\}\}}}{T^{res}}}, \tag{2.344d}$$

$$W^{\mu-P-T}_{\{\{N,V,E\}\}} = e^{\frac{\Psi^{\mu-P-T} - \Psi_{\{\{N,V,E\}\}}}{T^{res}}}. \tag{2.344e}$$

In expressions (2.341)–(2.344), we see the asymmetry of the MCE which, in contrast to other ensembles, does not contain in its formulae the temperature of the reservoir. However, as we will see in Sect. 2.16, it is not the MCE that is asymmetrical but, on the contrary, other ensembles lack the symmetry.

Since the partition function of any ensemble equals with logarithmic accuracy its maximal term

$$Z^{MCE} \approx_{\ln} Z_{\{\{p_0\}\}}, \tag{2.345a}$$

$$Z^{CE} \approx_{\ln} Z_{\{\{E_0\}\}}, \tag{2.345b}$$

$$Z^{GCE} \approx_{\ln} Z_{\{\{N_0,E_0\}\}}, \tag{2.345c}$$

$$Z^{P-T} \approx_{\ln} Z_{\{\{V_0,E_0\}\}}, \tag{2.345d}$$

$$Z^{\mu-P-T} \approx_{\ln} Z_{\{\{N_0,V_0,E_0\}\}}, \tag{2.345e}$$

probabilities (2.344) we can normalize by the free energy of the most probable macrostate:

$$W^{MCE}_{\{\{p\}\}} \approx_{\ln} e^{\Psi_{\{\{p_0\}\}}-\Psi_{\{\{p\}\}}}, \tag{2.346a}$$

$$W^{CE}_{\{\{E\}\}} \approx_{\ln} e^{\frac{\Psi_{\{\{E_0\}\}}-\Psi_{\{\{E\}\}}}{T^{res}}}, \tag{2.346b}$$

$$W^{GCE}_{\{\{N,E\}\}} \approx_{\ln} e^{\frac{\Psi_{\{\{N_0,E_0\}\}}-\Psi_{\{\{N,E\}\}}}{T^{res}}}, \tag{2.346c}$$

$$W^{P-T}_{\{\{V,E\}\}} \approx_{\ln} e^{\frac{\Psi_{\{\{V_0,E_0\}\}}-\Psi_{\{\{V,E\}\}}}{T^{res}}}, \tag{2.346d}$$

$$W^{\mu-P-T}_{\{\{N,V,E\}\}} \approx_{\ln} e^{\frac{\Psi_{\{\{N_0,V_0,E_0\}\}}-\Psi_{\{\{N,V,E\}\}}}{T^{res}}}. \tag{2.346e}$$

2.15 Fluctuations as the Investigator's Tool

Fluctuations are a very convenient tool allowing us to investigate system's behavior. And as for any other tool, a particular choice of a particular type of fluctuations is the investigator's prerogative allowing her/him in her/his studies focusing on this or that particular type of system's behavior.

For the MCE we considered fluctuations $\{\{p\}\}$ of concentrations of the ↓-spins along the model length (fluctuations of gas density in the volume). But instead we could consider any other fluctuations. For example, as a fluctuation we could consider a vortex of gas particles, or fluctuations in the distribution of particle velocities, or energy fluctuations from one point within the volume to another, and so on.

In the CE, we have chosen fluctuations to be energy fluctuations $\{\{E\}\}$ when our system took away from the reservoir this or that amount of energy. But, in addition to energy fluctuations, we also could consider, for example, fluctuations of gas density within its volume or something else. Our choice was based on the wish to study energy exchange with the reservoir. If we wanted to study another type of behavior, we would choose a different type of fluctuations.

However, one concept has remained constant when we have moved from one type of fluctuation to another—the probabilities of all fluctuations have depended exponentially on the free energy of these fluctuations:

$$W^{ensemble}_{\{\{\ \}\}} = e^{(\Psi^{ensemble} - \Psi_{\{\{\ \}\}})/T^{res}} \approx_{\ln} e^{(\Psi_{\{\{0\}\}} - \Psi_{\{\{\ \}\}})/T^{res}}. \tag{2.347}$$

(We consider here all ensembles but the MCE which lacks the concept of temperature. Removing temperature from (2.347) would generalize this equation and for the case of the MCE. We will discuss it in more detail in the following section.)

Fluctuations always represent deviations from the equilibrium macrostate $\{\{0\}\}$. Therefore, the free energy of fluctuations is always higher than the free energy of the equilibrium macrostate: $\Psi_{\{\{\ \}\}} \geq \Psi_{\{\{0\}\}}$ (Fig. 2.12). And the probability of fluctuations decays as the exponential dependence on this difference.

To illustrate that the choice of fluctuations is merely a tool we return to the case of the CE. Earlier in the CE we constructed an energy fluctuation $\{\{E\}\}$ as a system having a particular value of energy E:

$$w_{\{\tilde{E}\}} = \left\{ \begin{matrix} 1/\Gamma_{\{\{E\}\}} & ,\tilde{E} = E \\ 0 & ,otherwise \end{matrix} \right\} = \frac{\delta_{\tilde{E},E}}{\Gamma_{\{\{E\}\}}}. \tag{2.348}$$

On the contrary, now we will construct a fluctuation as a system being in its particular microstate $\{\{\ \ \}\} \equiv \{E\}$:

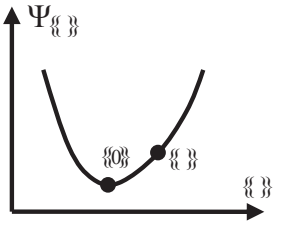

Fig. 2.12 Fluctuations always have higher free energy than the equilibrium macrostate

$$w_{\{E\}'} = \begin{Bmatrix} 1, \{E\}' = \{E\} \\ 0, \{E\}' \neq \{E\} \end{Bmatrix} = \delta_{\{E\}',\{E\}}. \tag{2.349}$$

The statistical weight of such a fluctuation is always unity,

$$\Gamma_{\{E\}} = 1, \tag{2.350}$$

and the entropy of the fluctuation is zero:

$$S_{\{E\}} = \ln \Gamma_{\{E\}} = 0. \tag{2.351}$$

The probability to observe a fluctuation $\{E\}$ in the CE,

$$W_{\{E\}}^{CE} = \Gamma_{\{E\}} w_{\{E\}}^{CE} = w_{\{E\}}^{CE} = \frac{1}{Z^{CE}} e^{-E/T^{res}}, \tag{2.352}$$

is just Gibbs probability (2.139) of a microstate $\{E\}$.

Substituting the nonequilibrium probability distribution (2.349) into the stochastic definition (2.261), we obtain the Helmholtz energy of fluctuations:

$$F_{\{E\}} = 1\{T^{res} \ln 1 + E\} = -T^{res} S_{\{E\}} + E = E. \tag{2.353}$$

Substituting (2.353) into (2.352), we see that the probability of a fluctuation decays as the exponential dependence on the free energy of this fluctuation:

$$W_{\{E\}}^{CE} \propto e^{-F_{\{E\}}/T^{res}}. \tag{2.354}$$

But simultaneously, in accordance with (2.352), it depends exponentially on the energy of the fluctuation:

$$W_{\{E\}}^{CE} = w_{\{E\}}^{CE} \propto e^{-E/T^{res}}. \tag{2.355}$$

This coincidence has happened only because we have so constructed the fluctuations that their entropy (2.351) was always zero. If it were not the case, the probability of fluctuations would be always the exponential dependence (2.347) on the free energy of fluctuations, not on the energy of them.

Simultaneously we can conclude that Gibbs probability distribution (2.139) depends exponentially on the energy of microstates only because the entropy of one microstate is zero. If it were not the case, Gibbs probability distribution would also depend on free energies, not energies.

2.16 The Action of the Free Energy

For illustrative purposes, we consider the μ–P–T-ensemble when the equilibrium equalities (2.304) for our system in contact with the reservoir are

$$\frac{1}{T}=\frac{1}{T^{res}},\ \frac{P}{T}=\frac{P^{res}}{T^{res}}\ \text{and}\ -\frac{\mu}{T}=-\frac{\mu^{res}}{T^{res}}. \tag{2.356}$$

The equilibrium probability distribution of microstates is given by (2.333e):

$$w_{\{N,V,E\}}^{\mu-P-T}=\frac{1}{Z^{\mu-P-T}}e^{-\frac{N}{(-T^{res}/\mu^{res})}-\frac{V}{(T^{res}/P^{res})}-\frac{E}{T^{res}}}, \tag{2.357}$$

where the partition function of the ensemble is

$$Z^{\mu-P-T}\equiv\sum_{\{N,V,E\}}e^{-\frac{N}{(-T^{res}/\mu^{res})}-\frac{V}{(T^{res}/P^{res})}-\frac{E}{T^{res}}}. \tag{2.358}$$

To find the entropy of the ensemble $S^{\mu-P-T}$ we substitute the equilibrium probability distribution (2.357) into the entropy functional (2.21):

$$S^{\mu-P-T}\equiv-\sum_{\{N,V,E\}}w_{\{N,V,E\}}^{\mu-P-T}\ln w_{\{N,V,E\}}^{\mu-P-T}. \tag{2.359}$$

However, this time let us explicitly substitute expression (2.357) only under the sign of the logarithm function, keeping the probabilities in front of it in their original form:

$$S^{\mu-P-T}=-\sum_{\{N,V,E\}}w_{\{N,V,E\}}^{\mu-P-T}\left\{-\ln Z^{\mu-P-T}-\frac{N}{(-T^{res}/\mu^{res})}-\frac{V}{(T^{res}/P^{res})}-\frac{E}{T^{res}}\right\} \tag{2.360}$$

The right-hand side of this equation represents ensemble averaging with the equilibrium probability distribution $w_{\{N,V,E\}}^{\mu-P-T}$:

$$S^{\mu-P-T}=\ln Z^{\mu-P-T}+\frac{\langle N\rangle_{\mu-P-T}}{(-T^{res}/\mu^{res})}+\frac{\langle V\rangle_{\mu-P-T}}{(T^{res}/P^{res})}+\frac{\langle E\rangle_{\mu-P-T}}{T^{res}}. \tag{2.361}$$

Expressing $Z^{\mu-P-T}$ from this equation and substituting it into (2.343e),

$$\Psi^{\mu-P-T}=-T^{res}\ln Z^{\mu-P-T}, \tag{2.362}$$

we find the connection of the ensemble free energy with the averaged energy, volume, and number of particles:

$$\Psi^{\mu-P-T}=-T^{res}S^{\mu-P-T}-\mu^{res}\langle N\rangle_{\mu-P-T}+P^{res}\langle V\rangle_{\mu-P-T}+\langle E\rangle_{\mu-P-T}. \tag{2.363}$$

The equality we have obtained merely represents the averaging of the free energy definition (2.337e).

Quasistatically changing the boundary conditions of the ensemble, we can change the averaged fluctuating parameters of the system. Differentiating (2.363), we obtain

$$d\Psi^{\mu-P-T} = -T^{res} dS^{\mu-P-T} - S^{\mu-P-T} dT^{res} - \mu^{res} d\left\langle N\right\rangle_{\mu-P-T} - \left\langle N\right\rangle_{\mu-P-T} d\mu^{res} + P^{res} d\left\langle V\right\rangle_{\mu-P-T} + \left\langle V\right\rangle_{\mu-P-T} dP^{res} + d\left\langle E\right\rangle_{\mu-P-T}, \quad (2.364)$$

Recalling that for quasistatic processes the change of the energy equals

$$d\left\langle E\right\rangle_{\mu-P-T} = T^{res} dS^{\mu-P-T} - P^{res} d\left\langle V\right\rangle_{\mu-P-T} + \mu^{res} d\left\langle N\right\rangle_{\mu-P-T}, \quad (2.365)$$

for the increment of the free energy we finally find

$$d\Psi^{\mu-P-T} = -S^{\mu-P-T} dT^{res} - \left\langle N\right\rangle_{\mu-P-T} d\mu^{res} + \left\langle V\right\rangle_{\mu-P-T} dP^{res}. \quad (2.366)$$

We see here three differentials of the boundary conditions. For two of them, $d\mu^{res}$ and dP^{res}, we see in front of them the corresponding fluctuating parameters, $\left\langle N\right\rangle_{\mu-P-T}$ and $\left\langle V\right\rangle_{\mu-P-T}$, respectively. But in front of the third differential dT^{res} we see not the corresponding fluctuating parameter, the energy, but the entropy. Therefore, our formulae are not completely symmetric.

Where has the asymmetry come into the above expressions? If we consider the equilibrium equalities (2.356) and the probability distribution (2.357), we see that there are, in fact, three independent "*effective*" *temperatures* in our ensemble,

$$\Theta_1 = T,\ \Theta_2 = \frac{T}{P},\ \Theta_3 = -\frac{T}{\mu}, \quad (2.367)$$

and three equilibrium equalities (2.356) transform into

$$\frac{1}{\Theta_1} = \frac{1}{\Theta_1^{res}},\ \frac{1}{\Theta_2} = \frac{1}{\Theta_2^{res}},\ \text{and}\ \frac{1}{\Theta_3} = \frac{1}{\Theta_3^{res}}. \quad (2.368)$$

Why then in (2.362), (2.342e), and (2.343e) we have made a choice in favor of the first temperature, $\Theta_1^{res} = T^{res}$, putting it ahead of the logarithm? This was the very asymmetry which we have introduced into our formulae. Let us recall, for example, the case of multifractals (1.126). There were K temperatures in that system, and none of them could be chosen as a favorite.

But it is easy to remove this asymmetry from all expressions above. We need only to divide all formulae for the free energy Ψ by the reservoir's temperature T^{res} to obtain *the action of the free energy potential* A. Thereby, (2.337e) transforms into the action of a fluctuation:

$$\mathrm{A}_{\{\{N,V,E\}\}} \equiv -S_{\{\{N,V,E\}\}} + \frac{N}{\Theta_3^{res}} + \frac{V}{\Theta_2^{res}} + \frac{E}{\Theta_1^{res}}. \tag{2.369}$$

Definitions (2.339e) and (2.340e) transform into the stochastic definition of the action:

$$\mathrm{A}[w_{\{\}}] \equiv \sum_{\{\}} w_{\{\}} \left(\ln w_{\{\}} + \frac{N_{\{\}}}{\Theta_3^{res}} + \frac{V_{\{\}}}{\Theta_2^{res}} + \frac{E_{\{\}}}{\Theta_1^{res}} \right), \tag{2.370}$$

$$\mathrm{A}[\widehat{\rho}] \equiv \mathrm{Tr}\left(\widehat{\rho} \left\{ \ln \widehat{\rho} + \frac{\widehat{N}}{\Theta_3^{res}} + \frac{\widehat{V}}{\Theta_2^{res}} + \frac{\widehat{\mathrm{H}}}{\Theta_1^{res}} \right\} \right). \tag{2.371}$$

Definitions (2.342e) and (2.343e) transform into the partition definition of the action:

$$\mathrm{A}_{\{\{N,V,E\}\}} = -\ln(Z^{\mu-P-T} W^{\mu-P-T}_{\{\{N,V,E\}\}}) = -\ln Z_{\{\{N,V,E\}\}}, \tag{2.372}$$

$$\mathrm{A}^{\mu-P-T} = -\ln Z^{\mu-P-T}. \tag{2.373}$$

Finally, (2.341e) and (2.344e) transform into the probabilities of a fluctuation:

$$W^{\mu-P-T}_{\{\{N,V,E\}\}} = \frac{1}{Z^{\mu-P-T}} e^{-\mathrm{A}_{\{\{N,V,E\}\}}}, \tag{2.374}$$

$$W^{\mu-P-T}_{\{\{N,V,E\}\}} = e^{\mathrm{A}^{\mu-P-T} - \mathrm{A}_{\{\{N,V,E\}\}}}. \tag{2.375}$$

Dividing (2.363) by the reservoir's temperature T^{res}, we find

$$\mathrm{A}^{\mu-P-T} = -S^{\mu-P-T} + \frac{\langle N \rangle_{\mu-P-T}}{\Theta_3^{res}} + \frac{\langle V \rangle_{\mu-P-T}}{\Theta_2^{res}} + \frac{\langle E \rangle_{\mu-P-T}}{\Theta_1^{res}}. \tag{2.376}$$

Since the differential of energy (2.365) transforms into

$$\frac{d\langle E \rangle_{\mu-P-T}}{\Theta_1^{res}} = dS^{\mu-P-T} - \frac{d\langle V \rangle_{\mu-P-T}}{\Theta_2^{res}} - \frac{d\langle N \rangle_{\mu-P-T}}{\Theta_3^{res}}, \tag{2.377}$$

for the differential of action (2.376), we find

$$d\mathrm{A}^{\mu-P-T} = -dS^{\mu-P-T} + \frac{d\left\langle N\right\rangle_{\mu-P-T}}{\Theta_3^{res}} + \left\langle N\right\rangle_{\mu-P-T} d\left(\frac{1}{\Theta_3^{res}}\right) +$$
$$+ \frac{d\left\langle V\right\rangle_{\mu-P-T}}{\Theta_2^{res}} + \left\langle V\right\rangle_{\mu-P-T} d\left(\frac{1}{\Theta_2^{res}}\right) + \frac{d\left\langle E\right\rangle_{\mu-P-T}}{\Theta_1^{res}} + \left\langle E\right\rangle_{\mu-P-T} d\left(\frac{1}{\Theta_1^{res}}\right)$$
$$= \left\langle N\right\rangle_{\mu-P-T} d\left(\frac{1}{\Theta_3^{res}}\right) + \left\langle V\right\rangle_{\mu-P-T} d\left(\frac{1}{\Theta_2^{res}}\right) + \left\langle E\right\rangle_{\mu-P-T} d\left(\frac{1}{\Theta_1^{res}}\right). \tag{2.378}$$

We see that differential (2.378) of the action is more symmetric than differential (2.366) because in the right-hand side of (2.378) each differential of the inverse temperature is coupled to the corresponding fluctuating parameter staying ahead of this differential.

Let us return to probabilities (2.344) of fluctuations for different ensembles:

$$W_{\{\{p\}\}}^{MCE} = e^{\Psi^{MCE} - \Psi_{\{\{p\}\}}}, \tag{2.379a}$$

$$W_{\{\{E\}\}}^{CE} = e^{\frac{\Psi^{CE} - \Psi_{\{\{E\}\}}}{T^{res}}}, \tag{2.379b}$$

$$W_{\{\{N,E\}\}}^{GCE} = e^{\frac{\Psi^{GCE} - \Psi_{\{\{N,E\}\}}}{T^{res}}}, \tag{2.379c}$$

$$W_{\{\{V,E\}\}}^{P-T} = e^{\frac{\Psi^{P-T} - \Psi_{\{\{V,E\}\}}}{T^{res}}}, \tag{2.379d}$$

$$W_{\{\{N,V,E\}\}}^{\mu-P-T} = e^{\frac{\Psi^{\mu-P-T} - \Psi_{\{\{N,V,E\}\}}}{T^{res}}}. \tag{2.379e}$$

For the MCE, we define action of the free energy potential as the free energy itself. For the rest of the ensembles, we divide the free energy by the temperature of the reservoir:

$$\mathrm{A} \equiv \Psi, \tag{2.380a}$$

$$\mathrm{A} \equiv \Psi / T^{ref}, \tag{2.380b}$$

$$\mathrm{A} \equiv \Psi / T^{ref}, \tag{2.380c}$$

$$\mathrm{A} \equiv \Psi / T^{ref}, \tag{2.380d}$$

$$\mathrm{A} \equiv \Psi / T^{ref}. \tag{2.380e}$$

Then probabilities (2.379) transform into

$$W^{MCE}_{\{\{p\}\}} = e^{\mathrm{A}^{MCE} - \mathrm{A}_{\{\{p\}\}}}, \tag{2.381a}$$

$$W^{CE}_{\{\{E\}\}} = e^{\mathrm{A}^{CE} - \mathrm{A}_{\{\{E\}\}}}, \tag{2.381b}$$

$$W^{GCE}_{\{\{N,E\}\}} = e^{\mathrm{A}^{GCE} - \mathrm{A}_{\{\{N,E\}\}}}, \tag{2.381c}$$

$$W^{P-T}_{\{\{V,E\}\}} = e^{\mathrm{A}^{P-T} - \mathrm{A}_{\{\{V,E\}\}}}, \tag{2.381d}$$

$$W^{\mu-P-T}_{\{\{N,V,E\}\}} = e^{\mathrm{A}^{\mu-P-T} - \mathrm{A}_{\{\{N,V,E\}\}}}. \tag{2.381e}$$

We see that it was not the MCE that was asymmetric but the rest of the ensembles. Removing the asymmetry of the temperature $\Theta_1 = T$ from our formulae, we have come to the symmetric expression

$$W^{ensemble}_{\{\{\ \}\}} = e^{\mathrm{A}^{ensemble} - \mathrm{A}_{\{\{\ \}\}}} \tag{2.382}$$

for the case of an arbitrary ensemble.

Looking backward from the position of our current understanding, we see that it would be reasonable to consider the concept of the action of the free energy from the very beginning instead of references to the free energy potential itself. However, this seems to be impossible because the majority of the studies in the literature consider the free energy, not its action.

We have already seen a similar situation earlier when in (2.334a) we have introduced the partition function of the MCE. It seems to be reasonable to unite both concepts of the statistical weight of the MCE and of the partition functions of other considered ensembles by introducing the common term "statistical sum." However, the current terminology is applied in so many publications that it seems almost impossible to change it. For this particular reason, in this chapter we followed the "common practice" terminology but at the end of the chapter demonstrated its possible flaws.

References

Abaimov, S.G.: Statistical Physics of Complex Systems (in Russian), 2nd edn. Synergetics: From Past to Future, vol. **57**, URSS, Moscow (2013)

Abrikosov, A.A., Gor'kov, L.P., Dzyaloshinskii, I.Y.: Quantum Field Theoretical Methods in Statistical Physics. Pergamon, Oxford (1965)

Balescu, R.: Equilibrium and Nonequilibrium Statistical Mechanics. Wiley, New York (1975)
Boltzmann, L. (ed.) McGuinness, B.F.: Theoretical Physics and Philosophical Problems: Selected Writings. Springer, Netherlands (1974)
Chrisholm, J.S.R., Borde, A.H.: An Introduction to Statistical Mechanics. Pergamon, New York (1958)
Clausius, M.R.: On the moving force of heat, and the laws regarding the nature of heat itself which are deducible therefrom. Phil. Mag. **2** (4th Series), 1–21, 102–119 (1851)
Clausius, R.: Mechanical Theory of Heat, with its Applications to the Steam-Engine and to the Physical Properties of Bodies. John van Voorst, London (1867)
Ehrenfest, P., Ehrenfest, T.: The Conceptual Foundations of the Statistical Approach in Mechanics. Cornell University Press, Ithaca (1959)
Eyring, H., Henderson, D., Stover, B.J., Eyring, E.M.: Statistical Mechanics and Dynamics. Wiley, New York (1963)
Feynman, R.P.: Statistical Mechanics: A Set of Lectures. W.A. Benjamin, Reading (1972)
Fowler, R.H.: Statistical Mechanics, 2nd edn. Cambridge University Press, Cambridge (1955)
Gibbs, J.W.: On the equilibrium of heterogeneous substances. Trans. Conn. Acad. **3**, 108–248 (1876)
Gibbs, J.W.: On the equilibrium of heterogeneous substances. Trans. Conn. Acad. **3**, 343–520 (1878)
Gibbs, J.W.: Elementary Principles in Statistical Mechanics. Scribner's, New York (1902)
Gibbs, J.W.: The Scientific Papers, vol. 1. Longman, London (1906)
Hill, T.L.: Statistical Mechanics. McGraw-Hill, New York (1956)
Huang, K.: Statistical Mechanics, 2nd edn. Wiley, New York (1987)
Ising, E.: Beitrag zur theorie des ferromagnetismus. Z. Physik. **31**, 253–258 (1925)
Kittel, C.: Elementary Statistical Physics. Wiley, New York (1958)
Kittel, C.: Thermal Physics. Wiley, New York (1969)
Kubo, R., Ichimura, H., Usui, T., Hashitsume, N.: Statistical Mechanics: An Advanced Course with Problems and Solutions, 8th edn. North Holland, Amsterdam (1988)
Landau, L.D., Lifshitz, E.M.: Statistical Physics, Part 1, 3rd edn. Course of Theoretical Physics, vol. **5**. Pergamon, Oxford (1980)
Ma, S.K.: Statistical Mechanics. World Scientific, Singapore (1985)
Mayer, J.E., Mayer, M.G.: Statistical Mechanics. Wiley, New York (1940)
Pathria, R.K.: Statistical Mechanics, 2nd edn. Butterworth-Heinemann, Oxford (1996)
Plischke, M., Bergersen, B.: Equilibrium Statistical Physics, 3rd edn. World Scientific, Singapore (2005)
Reif, F.: Fundamentals of Statistical and Thermal Physics. McGraw-Hill, New York (1965)
Reif, F.: Statistical Physics, vol. **5**. Berkeley Physics Course. McGraw-Hill, New York (1967)
Rushbrooke, G.S.: Introduction to Statistical Mechanics. Clarendon, Oxford (1955)
Schrödinger, E.: An undulatory theory of the mechanics of atoms an molecules. Phys. Rev. **28**(6), 1049–1070 (1926)
Shannon, C.E.: A mathematical theory of communication. Bell Sys. Tech. J. **27**, 379–423, 623–656 (1948)
Sommerfeld, A.: Thermodynamics and Statistical Mechanics. Academic, New York (1956)
ter Haar, D.: Elements of Statistical Mechanics. Rinehart, New York (1954)
Tolman, R.C.: The Principles of Statistical Mechanics. Oxford University Press, Oxford (1938)
von Neumann, J.: Mathematische Grundlagen der Quantenmechanik. Springer, Berlin (1932)
von Neumann, J.: Mathematical Foundations of Quantum Mechanics. Princeton University Press, Princeton (1955)

Chapter 3
The Ising Model

Abstract In the previous chapter, we have discussed the formalism of statistical physics. A big help for us was the Ising model which provided the very intuitive understanding for all the concepts considered.

However, the Ising model serves even better as an illustration of phase-transition phenomena. Therefore, in this chapter, we study the behavior of this model in detail.

3.1 Definition of the Model

There are many magnetic lattice models: the Heisenberg model (Heisenberg 1928), the O(n)-vector model, the X–Y model (Matsubara and Matsuda 1956), the Potts model (Potts 1952), the spherical model (Berlin and Kac 1952), the Ising model (Lenz 1920; Ising 1925), etc. In all these models, magnetic moments (or spins) are located at the lattice sites and interact with an external field h and with each other. Primarily, the models differ by the rule, what projections on coordinate axes a magnetic moment can have? For example, in the classical O(n)-vector model, magnetic moments are assumed to be classical and their projections are arbitrary, limited only by the module of the vector. On the contrary, the quantum Heisenberg model (Heisenberg 1928) considers spins as quantum operators whose projections are determined by the laws of quantum mechanics. In the Ising model, we consider a spin projection only on the axis of a magnetic field h, and there are, generally, only two possible values, $\sigma = +1$ and $\sigma = -1$.

Phase-transition phenomena can be illustrated with the aid of any of these models, both quantum and classical. However, the simplest approach would be to consider the Ising model. This model possesses the quantum discreteness of its energy spectrum because spin projections are discrete: $\sigma = +1$ or $\sigma = -1$; and it is much simpler to work with a discrete spectrum than with a continuous spectrum. On the other hand, spin projections, other than on the axis of the magnetic field, are not considered in this model which allows avoiding the complications of matrix calculations. Therefore, the Ising model can be considered as the most convenient example, illustrating the phenomena of phase transitions.

S. G. Abaimov, *Statistical Physics of Non-Thermal Phase Transitions,*
Springer Series in Synergetics, DOI 10.1007/978-3-319-12469-8_3

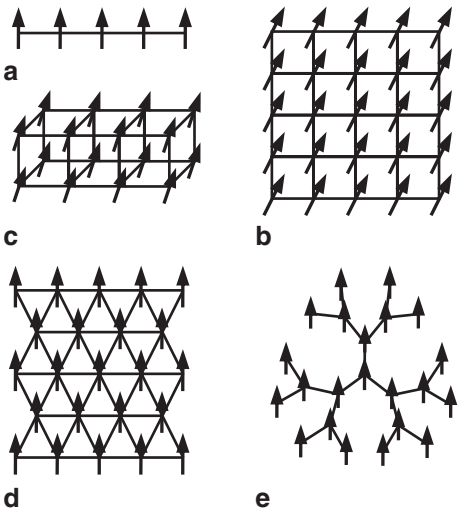

Fig. 3.1 A schematic representation of different geometrical forms of lattice: **a** one-dimensional chain of spins; **b** two-dimensional square lattice; **c** three-dimensional cubic lattice; **d** two-dimensional triangular lattice; **e** Bethe lattice

The Ising model was invented by Wilhelm Lenz (Lenz 1920) and has been named after his student Ernst Ising who in his doctoral dissertation obtained a solution and proved the absence of a phase transition for the one-dimensional case. The question whether there is a phase transition in higher dimensions, which was elusive at the beginning, was answered positively by Lars Onsager (Onsager 1944) who found the exact solution for the two-dimensional model.

Initially, the Ising model was intended to serve as a crude but efficient description of ferromagnetic phenomena. However, later the model has become popular due to the exemplariness of its phase transition. Nowadays, the latter is considered to be the main merit of the model; and similarly to the models of an ideal gas, van der Waals gas, etc., the Ising model has become canonical in the sense that its properties are worth investigating as such, without association with particular, real physical systems.

We consider N magnetic moments μ located at the sites of the lattice. The limit $N \to +\infty$ of an infinite system is called *the thermodynamic limit*. The geometrical form and dimensionality of the lattice can be arbitrary (Fig. 3.1). Boundary conditions are usually considered to be either free or periodic. In the last case, the opposite sides of the lattice are "glued" together, forming a ring in the one-dimensional case and a torus in the two-dimensional case.

Spins σ_i are enumerated by numbers i of the lattice sites. Only spin projections on the axis of the magnetic field h are considered. These projections can be equal only to +1 or −1. These two possible values represent the two possible projections, $\sigma = +1/2$ and $\sigma = -1/2$, of an electron's spin on the axis of a magnetic field. For the purpose of convenience, the multiplier 1/2 has been moved inside of the constants of interactions, leaving two spin projections $\sigma_i = +1$ and $\sigma_i = -1$.

In the case $\sigma_i = +1$, we will say that spin i is oriented along the magnetic field h, and we will denote this spin orientation as $\uparrow$. In the opposite case $\sigma_i = -1$, we will

say that spin i is oriented against the magnetic field h, and we will denote this spin orientation as $\downarrow$.

The energy of spin σ_i in the magnetic field h is $-\mu h\sigma_i$, where μ is the value of the spin's magnetic moment. If there were no other interactions, due to the interaction with the magnetic field h, each spin could have only two possible values of the energy: $-\mu h$ and $+\mu h$. In this case, the system would be *a two-level system*. However, besides the interaction with the magnetic field h, the exchange interaction $-\sum_{<i,j>} J(\vec{\mathbf{r}}_i,\vec{\mathbf{r}}_j)\sigma_i\sigma_j$ of spins in pairs is also usually considered, where the sum $\sum_{<i,j>}$ goes over all pairs $< i, j >$ of spins on the lattice.

Positive sign of J corresponds to the ferromagnetic case when two spins have lower mutual value of the energy if they are both oriented in the same direction: $E_{\uparrow\uparrow} < E_{\uparrow\downarrow}$. In other words, if $J > 0$, any spin in the ferromagnet attempts to rotate all its neighbors so that their orientations become coincident with its own and the interaction energy decreases. On the contrary, $J < 0$ corresponds to the antiferromagnetic case when the energy is lower, when two spins have opposite orientations: $E_{\uparrow\downarrow} < E_{\uparrow\uparrow}$. So, in the antiferromagnet, any spin attempts to rotate its neighbors so that they have their orientations opposite to its own.

The dependence of $J(R_{i,j})$ on the distance $R_{i,j} \equiv \left|\vec{\mathbf{r}}_i - \vec{\mathbf{r}}_j\right|$ between two spins in a pair can be arbitrary. Often a power-law or exponential decay of $J(R_{i,j})$ on $R_{i,j}$ is assumed. Also, often two extremes are considered. The first extreme (*long-range interactions*) assumes that J does not depend on the distance $R_{i,j}$ between two spins in a pair: $-J\sum_{<i,j>}\sigma_i\sigma_j$.

The second extreme (*short-range interactions*), on the contrary, considers only the interactions of *the nearest neighbors*, when $R_{i,j}$ equals the lattice constant a and neglects interactions of spins over longer distances: $-J\sum_{<i,j>_{n.n.}}\sigma_i\sigma_j$. Here, notation "n.n." means that the sum goes over only those pairs whose spins are nearest neighbors. This type of the Ising model is often called *the n.n. Ising model*.

A particular realization of spin projections on the lattice is called *a microconfiguration* $\{\sigma\}$. In other words, prescribing to each spin on the lattice its particular orientation ($\sigma_i = +1$ along the magnetic field or $\sigma_i = -1$ against the field), we form a particular microconfiguration $\{\sigma\}$. The Hamiltonian of the system is defined as

$$\mathrm{H}_{\{\sigma\}} = -\mu h\sum_{i=1}^{N}\sigma_i - \sum_{<i,j>} J(\vec{\mathbf{r}}_i,\vec{\mathbf{r}}_j)\sigma_i\sigma_j. \tag{3.1}$$

The lattice of the model is assumed to be absolutely rigid. So, neither the volume nor the number of particles can change in the system. Therefore, the system can only belong to either the microcanonical ensemble (MCE), when it is isolated, or to the canonical ensemble (CE), when a fluctuating parameter is the energy of the system.

3.2 Microstates, MCE, CE, Order Parameter

Hamiltonian (3.1) is written in terms of spin projections. But to find the microstates of the system, we should start with its predecessor, the quantum operator

$$\hat{\mathrm{H}} = -\mu h \sum_{i=1}^{N} \hat{\sigma}_i - \sum_{<i,j>} J(\vec{\mathbf{r}}_i, \vec{\mathbf{r}}_j) \hat{\sigma}_i \hat{\sigma}_j, \tag{3.2}$$

which corresponds to (3.1), only now instead of spin projections it contains the quantum operators.

Microstates $\{E, p\}$ of the system can be found as the solutions of the quantum Schrödinger equation,

$$\hat{\mathrm{H}} \{E, p\} = E \{E, p\}, \tag{3.3}$$

where E is the eigenvalue of the energy corresponding to the eigenvector $\{E, p\}$ of the operator $\hat{\mathrm{H}}$.

A quantum vector of state of the system will be the eigenvector $\{E, p\}$ of this Hamiltonian if it is the common eigenvector for all spin operators $\hat{\sigma}_i$:

$$\hat{\sigma}_i \{E, p\} = \sigma_i \{E, p\}. \tag{3.4}$$

Indeed, substituting (3.2) and (3.4) into (3.3), we immediately prove (3.3) to be valid.

This means that the system's microstates $\{E, p\}$ are just the system's microconfigurations $\{\sigma\}$, where the role of the set of parameters p, distinguishing microstates with equal energy one from another, is played by the eigenvalues σ_i of the spin projections.

In other words, to specify a particular microstate $\{E, p\}$ of the system, we should prescribe particular projections for all spins on the lattice. Flipping one of the spins, we create a new microstate, and so on. Then, Hamiltonian (3.1) becomes the eigenvalue $E_{\{\sigma\}}$ of the operator $\hat{\mathrm{H}}$

$$E_{\{\sigma\}} = -\mu h \sum_{i=1}^{N} \sigma_i - \sum_{<i,j>} J(\vec{\mathbf{r}}_i, \vec{\mathbf{r}}_j) \sigma_i \sigma_j, \tag{3.5}$$

corresponding to the given microstate $\{\sigma\}$.

As an example, we consider the Ising model with $N = 3$ spins. There are eight possible microconfigurations $\{\sigma\}$ of spin orientations on the lattice: $\{\uparrow\uparrow\uparrow\}$, $\{\uparrow\uparrow\downarrow\}$, $\{\uparrow\downarrow\uparrow\}$, $\{\downarrow\uparrow\uparrow\}$, $\{\uparrow\downarrow\downarrow\}$, $\{\downarrow\uparrow\downarrow\}$, $\{\downarrow\downarrow\uparrow\}$, and $\{\downarrow\downarrow\downarrow\}$. If there are no interactions among spins in our model, $J = 0$, the microstates, corresponding to these microconfigurations, are $\{E = -3\mu h, p = \uparrow\uparrow\uparrow\}$, $\{E = -\mu h, p = \uparrow\uparrow\downarrow\}$, $\{E = -\mu h, p = \uparrow\downarrow\uparrow\}$, $\{E = -\mu h, p = \downarrow\uparrow\uparrow\}$, $\{E = \mu h, p = \uparrow\downarrow\downarrow\}$, $\{E = \mu h, p = \downarrow\uparrow\downarrow\}$, $\{E = \mu h, p = \downarrow\downarrow\uparrow\}$, and

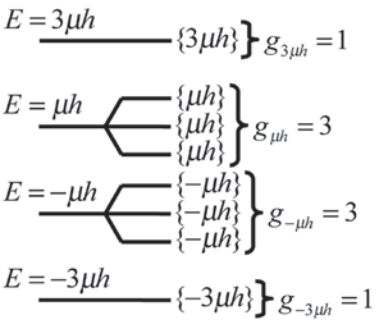

Fig. 3.2 The energy spectrum of the ideal Ising model with $N = 3$ spins

$\{E = 3\mu h, p = \downarrow\downarrow\downarrow\}$. Further, we may utilize simpler notations for these microstates: $\{-3\mu h\}$, $\{-\mu h\}$, $\{-\mu h\}$, $\{-\mu h\}$, $\{\mu h\}$, $\{\mu h\}$, $\{\mu h\}$, and $\{3\mu h\}$. The energy spectrum of such a system is presented in Fig. 3.2.

In the future, we will sometimes refer to the microstates of the system by the notation "$\{\sigma\}$" when we want to distinguish them by spin orientations on the lattice. This is the most convenient notation when we want to count the number of these microstates. However, when the energy of microstates becomes important, we will utilize another notation "$\{E, p\}$," where the energy of the microstate is shown explicitly and p represents particular spin orientations on the lattice corresponding to the given value of the energy. Finally, in the CE, only the energy of a microstate plays a significant role, and in this case, we will use the notation "$\{E\}$." All three different types of notation are equivalent and refer to the same set of microstates. In the future, we will use that type which will be the most convenient in a given situation.

In the MCE, all microstates, corresponding to the given value of the energy, are equiprobable (2.20):

$$w^{MCE}_{\{\tilde{E},p\}} = \left\{ \begin{array}{c} \dfrac{1}{\Gamma^{MCE}}, \tilde{E} = E \\ 0, \tilde{E} \neq E \end{array} \right\} = \frac{\delta_{\tilde{E},E}}{\Gamma^{MCE}}, \tag{3.6}$$

where Γ^{MCE} is the statistical weight of the ensemble. So, if the system from Fig. 3.2 is isolated with the energy $-\mu h$, the probabilities of three microstates, $\{\uparrow\uparrow\downarrow\}$, $\{\uparrow\downarrow\uparrow\}$, and $\{\downarrow\uparrow\uparrow\}$, corresponding to this value of the energy, will be 1/3 while the probabilities of other microstates are zero.

In the CE, we consider a fluctuation $\{\{E\}\}$ as the macrostate of the system when it has the energy E. While the probability (2.139) of microstates $\{E, p\}$ is

$$w^{CE}_{\{E\}} = \frac{1}{Z^{CE}} e^{-E/T}, \tag{3.7}$$

the probability (2.143) of energy fluctuations is

$$W^{CE}_{\{\{E\}\}} = \Gamma_{\{\{E\}\}} w^{CE}_{\{E\}} = \Gamma_{\{\{E\}\}} \frac{1}{Z^{CE}} e^{-E/T}, \tag{3.8}$$

where the statistical weight $\Gamma_{\{\{E\}\}}$ of the fluctuation is just the statistical weight g_E of this energy level (of this group of microstates), and the partition function Z^{CE} serves as the normalization constant of the probability distribution:

$$Z^{CE} \equiv \sum_{\{E\}} e^{-E/T} = \sum_{\{\{E\}\}} \Gamma_{\{\{E\}\}} e^{-E/T}. \tag{3.9}$$

Probability (3.8) has a very narrow maximum at the point E_0 which corresponds to the averaged value $\langle E \rangle_{CE} \equiv \sum_{\{E\}} E w^{CE}_{\{E\}}$ of the system's energy in the CE. The point E_0 of the maximum is given by the equation

$$\left. \frac{\partial W^{CE}_{\{\{E\}\}}}{\partial E} \right|_{E_0} = 0 \quad \text{or} \quad \left. \frac{\partial \ln W^{CE}_{\{\{E\}\}}}{\partial E} \right|_{E_0} = 0, \tag{3.10}$$

which is the equation of state of the system.

As we will see later, the nonideal Ising model with interactions of spins in pairs possesses a phase transition. *The magnetization* of the system,

$$M_{\{\sigma\}} \equiv \mu \sum_{i=1}^{N} \sigma_i, \tag{3.11}$$

plays the role of the order parameter, distinguishing phases. Instead of full magnetization (3.11), it is often more convenient to work with *the specific magnetization*,

$$m_{\{\sigma\}} \equiv \frac{1}{N} \sum_{i=1}^{N} \sigma_i, \tag{3.12}$$

as the full magnetization M divided by N, the total number of spins, and μ, the magnetic moment of one spin.

The specific magnetization is convenient because it always changes from –1, when all spins are against the field, to +1, when all spins are along the field. It is, in fact, the spin projection averaged over the spin orientations on the lattice for a particular microstate $\{\sigma\}$:

$$m_{\{\sigma\}} \equiv \langle \sigma_i \rangle_{\{\sigma\}}. \tag{3.13}$$

To emphasize that the averaging goes over the spin orientations of one microstate and not over the ensemble, we have used the subscript $\langle \ldots \rangle_{\{\sigma\}}$.

The magnetization is called *the long-range order parameter*, because it represents the interactions of the system as a whole with the external magnetic field or with the mean field generated by the spins themselves.

Besides the long-range order parameter, a short-range order parameter is also introduced as we will see later.

Let us assume that we have found the ensemble partition function Z^{CE} of the system. Differentiating it with respect to magnetic field h, we find

$$\frac{\partial Z^{CE}}{\partial h} \equiv \frac{\partial}{\partial h} \sum_{\{\sigma\}} e^{-\mathrm{H}_{\{\sigma\}}/T} = \sum_{\{\sigma\}} \frac{N\mu m_{\{\sigma\}}}{T} e^{-\mathrm{H}_{\{\sigma\}}/T}. \tag{3.14}$$

The equilibrium value of any quantity $f_{\{\sigma\}}$ in the CE of our model is found by averaging with Gibbs distribution of probabilities:

$$\langle f \rangle_{CE} \equiv \sum_{\{\sigma\}} f_{\{\sigma\}} w^{CE}_{\{\sigma\}} = \sum_{\{\sigma\}} f_{\{\sigma\}} \frac{1}{Z^{CE}} e^{-\mathrm{H}_{\{\sigma\}}/T}. \tag{3.15}$$

We see that (3.14) resembles (3.15), we only need to divide the exponential function by the value of the partition function. Thereby, (3.14) transforms into averaging of the magnetization:

$$\frac{\partial Z^{CE}}{\partial h} = \frac{Z^{CE} N\mu}{T} \sum_{\{\sigma\}} m_{\{\sigma\}} w^{CE}_{\{\sigma\}} = \frac{Z^{CE} N\mu \langle m \rangle_{CE}}{T}. \tag{3.16}$$

Therefore, if we have found the ensemble partition function, then the equilibrium value of the magnetization is as follows:

$$\langle m \rangle_{CE} = \frac{T}{N\mu} \frac{\partial \ln Z^{CE}}{\partial h}. \tag{3.17}$$

3.3 Two-Level System Without Pair Spins Interactions

As the first and simplest example, let us consider the Ising model without interactions of spins in pairs: $J = 0$. The Hamiltonian of such a system is

$$\mathrm{H}_{\{\sigma\}} = -\mu h \sum_{i=1}^{N} \sigma_i. \tag{3.18}$$

The system is *the two-level system* when the energy of the system is the sum of the energy of separate spins and each spin can have only two possible values of the energy: $-\mu h$ along the field and μh against the field.

Let us consider a particular microstate $\{\sigma\}$. If, in this microconfiguration, the number $N_\uparrow$ represents the number of spins along the field while $N_\downarrow$ is the number of spins against the field, then the energy of this microstate is

$$E_{\{\sigma\}} = -\mu h(N_\uparrow - N_\downarrow). \tag{3.19}$$

Recalling that the number of spins is conserved,

$$N = N_\uparrow + N_\downarrow, \tag{3.20}$$

from (3.19), we can find the numbers $N_\uparrow$ and $N_\downarrow$ for our system:

$$N_\uparrow = \frac{1}{2}\left(N - \frac{E_{\{\sigma\}}}{\mu h}\right), \quad N_\downarrow = \frac{1}{2}\left(N + \frac{E_{\{\sigma\}}}{\mu h}\right). \tag{3.21}$$

Simultaneously, for the specific magnetization (3.12) we obtain

$$m_{\{\sigma\}} = \frac{N_\uparrow - N_\downarrow}{N} = -\frac{E_{\{\sigma\}}}{N\mu h}. \tag{3.22}$$

So, if we know the energy of the microstate, we know the number of spins along the field h and the specific magnetization of the system; and vice versa, knowing the specific magnetization, we find

$$N_\uparrow = N\frac{1+m_{\{\sigma\}}}{2}, \quad N_\downarrow = N\frac{1-m_{\{\sigma\}}}{2}, \tag{3.23}$$

and

$$E_{\{\sigma\}} = -\mu h N m_{\{\sigma\}} = -hM_{\{\sigma\}}, \tag{3.24}$$

because the correspondence between the energy and magnetization is bijective.

We should emphasize here that the obtained correspondence is valid for an arbitrary microstate. If we consider an ensemble, MCE or CE, similar correspondence will, of course, appear for the averaged quantities as well. However, the reader should always distinguish equalities valid for microstates from equalities valid only on average in the ensemble—the former are more basic and cause the appearance of the latter.

In the MCE, the system is isolated with energy E. So, in accordance with (3.21) and (3.22), we immediately find the numbers $N_\uparrow$ and $N_\downarrow$. The statistical weight Γ^{MCE} of the ensemble is the number of microstates corresponding to this energy level. In other words, it is the number of microconfigurations $\{\sigma\}$, when among N spins, we should choose $N_\uparrow$ spins along the field and $N_\downarrow$ spins against the field:

$$\Gamma^{MCE} = g_E = \frac{N!}{N_\uparrow! N_\downarrow!}. \tag{3.25}$$

By applying Stirling's approximation, we find

$$g_E \approx_{\ln} \left(\frac{1+m(E)}{2}\right)^{-N\frac{1+m(E)}{2}} \left(\frac{1-m(E)}{2}\right)^{-N\frac{1-m(E)}{2}}, \tag{3.26}$$

where

$$m(E) = -\frac{E}{N\mu h}. \tag{3.27}$$

In the MCE, all microstates corresponding to the given value of the energy are equiprobable,

$$w_{\{E\}}^{MCE} = \frac{1}{g_E} \approx_{\ln} \left(\frac{1+m(E)}{2}\right)^{N\frac{1+m(E)}{2}} \left(\frac{1-m(E)}{2}\right)^{N\frac{1-m(E)}{2}}, \tag{3.28}$$

while all other microstates have zero probabilities.

In the CE, the statistical weight $\Gamma_{\{\{E\}\}}$ of the fluctuation $\{\{E\}\}$ is just the statistical weight g_E of the given energy level,

$$\Gamma_{\{\{E\}\}} = g_E = \frac{N!}{N_\uparrow! N_\downarrow!} \tag{3.29}$$

which is provided by (3.26) and (3.27). The probability of a microstate is determined by Gibbs probability distribution as follows:

$$w_{\{E\}}^{CE} = \frac{1}{Z^{CE}} e^{-E/T} = \frac{1}{Z^{CE}} e^{\mu h N m(E)/T}, \tag{3.30}$$

while to find the probability of the fluctuation $\{\{E\}\}$ we have to multiply this quantity by the statistical weight $\Gamma_{\{\{E\}\}}$ of the fluctuation as follows:

$$W_{\{\{E\}\}}^{CE} = \Gamma_{\{\{E\}\}} w_{\{E\}}^{CE}. \tag{3.31}$$

Let us find the partition function (3.9) of the CE. The sum $\sum_{\{E\}}$ over all microstates of the system's energy spectrum is just the sum $\sum_{\sigma_1=\pm1} \cdots \sum_{\sigma_N=\pm1}$ over all possible microconfigurations $\{\sigma\}$. For the partition function, this provides

$$\begin{aligned} Z^{CE} &= \sum_{\sigma_1=\pm1} \cdots \sum_{\sigma_N=\pm1} e^{-E_{\{\sigma\}}/T} = \left(\sum_{\sigma_1=\pm1} e^{\mu h \sigma_1/T}\right) \cdots \left(\sum_{\sigma_N=\pm1} e^{\mu h \sigma_N/T}\right) = \\ &= (e^{\mu h/T} + e^{-\mu h/T})^N, \end{aligned} \tag{3.32}$$

where we have *factorized* the partition function, transforming it into the product of N identical multipliers, each of which is the one-spin partition function.

The method of the factorization of the partition function works for any ideal system. Therefore, no wonder it works for our two-level system as well, which is ideal. If we are going to consider the nonideal systems in the future, we should have a method to calculate the partition function when the method of factorization is not applicable.

For this purpose, in Chap. 2, we have developed the method of steepest descent. Although applying this method to the two-level system is like crushing a fly upon a wheel, let us still do it for the illustrative purposes.

We know that the distance $2\mu h$ between two adjacent energy levels in our system corresponds to one-spin flip. Transforming sum (3.9) into the integral,

$$Z^{CE} \approx_{\ln} \int_{-N\mu h}^{+N\mu h} \frac{dE}{2\mu h} g_E e^{-E/T}, \tag{3.33}$$

we use this distance to normalize dE. Applying the method of steepest descent, we find that the integral equals its maximal term (the partition function equals its maximal partial partition function):

$$Z^{CE} \approx_{\ln} g_{E_0} e^{-E_0/T}, \tag{3.34}$$

where the point of the maximal term is determined by

$$\left.\frac{\partial(g_E e^{-E/T})}{\partial E}\right|_{E_0} = 0 \quad \text{or} \quad \left.\frac{\partial \ln(g_E e^{-E/T})}{\partial E}\right|_{E_0} = 0, \tag{3.35}$$

which, when divided by Z^{CE}, is equivalent to the equation of state (3.10).

Substituting (3.26) and (3.27) into (3.35), we find

$$E_0 = -\mu h N \tanh \frac{\mu h}{T}. \tag{3.36}$$

Substituting in turn (3.36) into (3.34), we return to (3.32).

Instead of integrating over E, it is much simpler to integrate over m which is bijectively connected with E by equality (3.27). If the distance between two adjacent energy levels is $2\mu h$, the distance between corresponding values of m is $2/N$. Integral (3.33) transforms into

$$Z^{CE} \approx_{\ln} \int_{-1}^{+1} \frac{dm}{2/N} \Gamma_{\{\{m\}\}} e^{\mu h N m/T}, \tag{3.37}$$

where

$$\Gamma_{\{\{m\}\}} \approx_{\ln} \left(\frac{1+m}{2}\right)^{-N\frac{1+m}{2}} \left(\frac{1-m}{2}\right)^{-N\frac{1-m}{2}}. \tag{3.38}$$

Again, in accordance with the method of steepest descent, the integral equals its maximal term

$$Z^{CE} \approx_{\ln} \Gamma_{\{\{m_0\}\}} e^{\mu h N m_0/T}, \tag{3.39}$$

where m_0 is provided by

$$\left.\frac{\partial(\Gamma_{\{\{m\}\}} e^{\mu h N m/T})}{\partial m}\right|_{m_0} = 0 \quad \text{or} \quad \left.\frac{\partial \ln(\Gamma_{\{\{m\}\}} e^{\mu h N m/T})}{\partial m}\right|_{m_0} = 0. \tag{3.40}$$

The solution of (3.40) is the equation of state

$$m_0 = \tanh\frac{\mu h}{T}, \tag{3.41}$$

which returns us to (3.36) and (3.32).

3.4 A One-Dimensional Nonideal System with Short-Range Pair Spin Interactions: The Exact Solution

Let us obtain an exact solution for the one-dimensional Ising model with spin interactions in n.n. pairs.

Problem 3.4.1

Consider the one-dimensional n.n. Ising model in the absence of magnetic field. For simplicity, consider the periodic boundary conditions $\sigma_{N+1} \equiv \sigma_1$ when the model is a one-dimensional chain of spins closed into a ring. Find the ensemble partition function of the system.

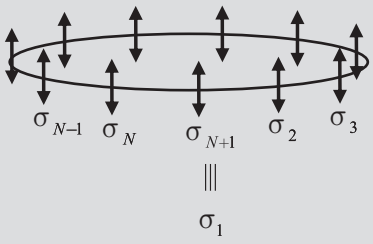

Solution: The Hamiltonian of the system is

$$\mathrm{H}_{\{\sigma\}} = -J\sum_{i=1}^{N}\sigma_i\sigma_{i+1}. \tag{3.42}$$

The partition function of the CE is determined by

$$Z^{CE} = \sum_{\sigma_1=\pm1}\sum_{\sigma_2=\pm1}\cdots\sum_{\sigma_N=\pm1} e^{\frac{J}{T}\sum_{i=1}^{N}\sigma_i\sigma_{i+1}} = \sum_{\sigma_1=\pm1}\sum_{\sigma_2=\pm1}\cdots\sum_{\sigma_N=\pm1}\prod_{i=1}^{N} e^{\frac{J}{T}\sigma_i\sigma_{i+1}}. \tag{3.43}$$

Let us define the so-called transfer matrix T (Kramers and Wannier 1941a, b) by

$$T_{\sigma_i\sigma_j} \equiv e^{\frac{J}{T}\sigma_i\sigma_j}, \tag{3.44}$$

where the matrix indices σ_i, σ_j can take the values +1 or −1. So, this is the 2×2 square matrix

$$T \equiv \begin{Vmatrix} e^{\frac{J}{T}} & e^{-\frac{J}{T}} \\ e^{-\frac{J}{T}} & e^{\frac{J}{T}} \end{Vmatrix}, \tag{3.45}$$

where the first row/column corresponds to +1 while the second row/column corresponds to −1:

$$\begin{aligned} T_{+1,+1} &= e^{\frac{J}{T}}, \quad T_{+1,-1} = e^{-\frac{J}{T}}, \\ T_{-1,+1} &= e^{-\frac{J}{T}}, \quad T_{-1,-1} = e^{\frac{J}{T}}. \end{aligned} \tag{3.46}$$

Returning to (3.43), we can substitute (3.44) into that expression:

$$Z^{CE} = \sum_{\sigma_1=\pm1}\sum_{\sigma_2=\pm1}\cdots\sum_{\sigma_N=\pm1}\prod_{i=1}^{N} T_{\sigma_i\sigma_{i+1}} = \sum_{\sigma_1=\pm1}\sum_{\sigma_2=\pm1}\cdots\sum_{\sigma_N=\pm1} T_{\sigma_1\sigma_2}T_{\sigma_2\sigma_3}\ldots T_{\sigma_N\sigma_{N+1}}. \tag{3.47}$$

Here,

$$\sum_{\sigma_2=\pm1}\cdots\sum_{\sigma_N=\pm1} T_{\sigma_1\sigma_2}T_{\sigma_2\sigma_3}\ldots T_{\sigma_N\sigma_{N+1}} = (T^N)_{\sigma_1\sigma_{N+1}} \tag{3.48}$$

is the matrix product of N transfer matrices. But we are considering the periodic boundary conditions $\sigma_{N+1} \equiv \sigma_1$. Therefore, if we add the sum $\sum_{\sigma_1=\pm1}$ in front of this expression,

$$\sum_{\sigma_1=\pm 1} (T^N)_{\sigma_1\sigma_{N+1}} = \sum_{\sigma_1=\pm 1} (T^N)_{\sigma_1\sigma_1} = \mathrm{Tr}(T^N), \tag{3.49}$$

we obtain that partition function (3.47) equals the trace of T^N:

$$Z^{CE} = \mathrm{Tr}\ (T^N). \tag{3.50}$$

We assume that T has two independent eigenvalues, λ_1 and λ_2. Let us prove this assumption. To find these eigenvalues, we should solve the characteristic equation:

$$\det \begin{Vmatrix} e^{\frac{J}{T}} - \lambda & e^{-\frac{J}{T}} \\ e^{-\frac{J}{T}} & e^{\frac{J}{T}} - \lambda \end{Vmatrix} = 0. \tag{3.51}$$

This equation, indeed, provides two independent eigenvalues:

$$\lambda_1 = e^{\frac{J}{T}} + e^{-\frac{J}{T}} = 2\cosh\frac{J}{T}, \tag{3.52}$$

$$\lambda_2 = e^{\frac{J}{T}} - e^{-\frac{J}{T}} = 2\sinh\frac{J}{T}. \tag{3.53}$$

From linear algebra, we know that the trace of the N^{th} power of a matrix with independent eigenvalues equals to the sum of the N^{th} powers of its eigenvalues:

$$Z^{CE} = {\lambda_1}^N + {\lambda_2}^N. \tag{3.54}$$

But comparing (3.52) and (3.53), we see that

$$\lambda_1 > \lambda_2. \tag{3.55}$$

Therefore, in the thermodynamic limit $N \to +\infty$, we can neglect the second eigenvalue in (3.54) to find

$$Z^{CE} \approx {\lambda_1}^N. \tag{3.56}$$

Problem 3.4.2

Consider the model of Problem 3.4.1 in the presence of magnetic field. Find the equilibrium magnetization $\langle m \rangle_{CE}$.

Solution: The Hamiltonian of the system is

$$\mathrm{H}_{\{\sigma\}} = -\mu h \sum_{i=1}^{N} \sigma_i - J \sum_{i=1}^{N} \sigma_i \sigma_{i+1}. \tag{3.57}$$

The transfer matrix in this case is

$$T_{\sigma_i \sigma_j} \equiv e^{\frac{\mu h}{T}\sigma_i + \frac{J}{T}\sigma_i \sigma_j}, \tag{3.58}$$

$$T \equiv \begin{Vmatrix} e^{\frac{\mu h}{T}+\frac{J}{T}} & e^{\frac{\mu h}{T}-\frac{J}{T}} \\ e^{-\frac{\mu h}{T}-\frac{J}{T}} & e^{-\frac{\mu h}{T}+\frac{J}{T}} \end{Vmatrix} \tag{3.59}$$

which provides again

$$Z^{CE} = \sum_{\sigma_1=\pm 1} \sum_{\sigma_2=\pm 1} \cdots \sum_{\sigma_N=\pm 1} \prod_{i=1}^{N} T_{\sigma_i \sigma_{i+1}} = \mathrm{Tr}(T^N). \tag{3.60}$$

The eigenvalues of the transfer matrix are

$$\lambda_{1,2} = e^{\frac{J}{T}} \left\{ \cosh \frac{\mu h}{T} \pm \sqrt{\sinh^2 \frac{\mu h}{T} + e^{-\frac{4J}{T}}} \right\}. \tag{3.61}$$

In the thermodynamic limit, only the greater eigenvalue participates in the partition function:

$$Z^{CE} = \lambda_1{}^N + \lambda_2{}^N \approx \lambda_1{}^N. \tag{3.62}$$

Differentiating the logarithm of the last expression with respect to the magnetic field h, we in accordance with (3.17) find the equilibrium magnetization:

$$\langle m \rangle_{CE} = \frac{\sinh \frac{\mu h}{T}}{\sqrt{\sinh^2 \frac{\mu h}{T} + e^{-\frac{4J}{T}}}}. \tag{3.63}$$

For nonzero temperature $T > 0$, in the absence of magnetic field, $h = 0$, the magnetization (3.63) is zero

$$\langle m \rangle_{CE} = 0. \tag{3.64}$$

However, when the limit of zero temperature, $T \to 0$, is taken before the limit of zero magnetic field, we find

$$\langle m \rangle_{CE} = \pm 1. \tag{3.65}$$

The appearance of nonzero magnetization in the zero field is called *the spontaneous magnetization*, which generally corresponds to the presence of a phase transition. We now see that in the one-dimensional case, the phase transition is present only at zero temperature, when *the critical point* is determined by $T_C = 0$, $h_C = 0$.

The magnetic susceptibility is defined by the response of the averaged magnetization to the change in the magnetic field:

$$\chi \equiv \left(\frac{\partial \langle m \rangle_{CE}}{\partial h} \right)_T. \tag{3.66}$$

Differentiating (3.63), we find

$$\chi = \frac{\frac{\mu}{T} e^{-\frac{4J}{T}} \cosh \frac{\mu h}{T}}{\left(\sinh^2 \frac{\mu h}{T} + e^{-\frac{4J}{T}} \right)^{3/2}}. \tag{3.67}$$

Let us approach the critical point along the isofield curve $h = h_C$. First, we take the limit $h \to 0$, and only then the limit $T \to 0$. For this case, we find

$$\chi = \frac{\mu}{T} e^{\frac{2J}{T}}. \tag{3.68}$$

We see that the susceptibility diverges exponentially.

Second, we consider the isotherm $T = T_C$. We take the limit $T \to 0$ while h remains either finite or the limit $h \to 0$ is taken after the limit $T \to 0$. For the susceptibility, we find

$$\chi = \frac{4\mu}{T} e^{-\frac{2\mu|h|}{T} - \frac{4J}{T}} \to 0. \tag{3.69}$$

We see that along the critical isotherm $T = T_C$, the susceptibility remains zero. Indeed, for any value of the magnetic field, the magnetization is either +1 or −1 in accordance with (3.65) and does not depend on the field.

We have proved that the one-dimensional Ising model with short-range interactions possesses the phase transition only at zero temperature and has at this point the exponentially diverging susceptibility. As we will see later, for longer ranges of interactions and in higher dimensions, the critical point is expected to be not at the zero temperature while the divergences are expected to be the power law, not

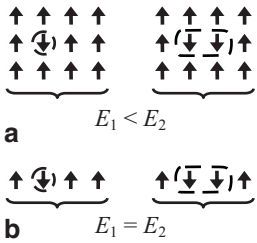

Fig. 3.3 The two-dimensional n.n. Ising model on square lattice versus the one-dimensional n.n. Ising model

exponential. Therefore, the one-dimensional case of short-range interactions can be considered as "degenerate."

But why this case is "degenerate"? To answer this question, let us compare two n.n. ferromagnets: one, on the two-dimensional square lattice, and another, on the one-dimensional lattice. We consider zero magnetic field, $h = 0$, and temperature near zero, $T \to 0$.

In the n.n. ferromagnet, all spins are attempting to reorient their nearest neighbors in their own direction. So, the ground state is achieved when all spins are oriented in the same direction, which is "up" in Fig. 3.3.

Although we consider the temperature to be low, it is still higher than zero. This means that there are thermal fluctuations which are attempting to disorder the system by disaligning the spins randomly.

On the square lattice, the orientation "up" of each spin is supported by $q = 4$ nearest neighbors; and it is problematic for thermal fluctuations to flip the spin because they need to increase the energy of four spin pairs from $-J$ to $+J$.

But let us assume that a thermal fluctuation has managed to flip one of the spins (Fig. 3.3a). This spin is now oriented "down" and is, in turn, attempting to rotate its nearest neighbors "down" also. On the contrary, these neighbors are attempting to restore the previous orientation of this spin.

So, what will happen next? Will the spin flip its nearest neighbors? Or will these neighbors flip the spin? To answer this question, we should compare the energies of the possible outcomes. From Fig. 3.3a, we see that restoring the spin orientation will reduce the energy of the system. On the contrary, orienting "down" more and more spins will require more and more energy.

Therefore, the preferable outcome is for the nearest neighbors to reorient the considered spin "up," restoring the order in the system (all spins are "up" again). That is why the n.n. systems in dimensions higher than one can possess the nonzero spontaneous magnetization at temperatures above zero.

Next for comparison, let us consider the n.n. Ising model in one dimension (Fig. 3.3b). Now only $q = 2$ nearest neighbors are keeping the spin's orientation "up." Therefore, it is easier for thermal fluctuations to flip the spin.

But this is not all. The main difference with higher dimensions is that when one spin is aligned "down," no more energy is required to rotate "down" its neighbors! When in Fig. 3.3b, the nearest neighbor to the right rotates "down" also, the energy of one pair increases but simultaneously the energy of another pair decreases. So, the total change in the energy is zero!

Then, the next neighbor to the right can flip, then the next, and so on. In the result, the whole right half of the lattice can become oriented "down."

We see that just one-spin flip can cause the succession of flips along the lattice, forming a domain, oriented "down." But in the middle of this domain, thermal fluctuations can disorient another spin, so it rotates "up." It causes a new succession of flips, this time orienting the spins "up," and the domain oriented "up" appears right in the middle of the domain oriented "down." And so on, and so on while no spontaneous magnetization is left.

In the result, even the tiny thermal fluctuations, equivalent only to one-spin flip, are capable to break the spontaneous magnetization of the one-dimensional Ising model with short-range interactions. As we will see later, the spontaneous magnetization represents the appearance of a phase transition in the system. Therefore, we can conclude that the phase transition in the one-dimensional n.n. Ising model is possible only at zero temperature.

We intend to study the "full-blown" phase transitions; and the "degenerate" case is of little interest to us. What can be done to improve the situation? One possibility we already know is to increase the dimensionality of the system so that more spins would support their mutual orientation. The case of higher dimensions is considered in the following sections.

But there is another way also. Instead of increasing dimensionality, we can make the spin interactions long-ranged. More spins would be attempting to keep the common orientation unchanged, so it would be harder for thermal fluctuations to break the order. The extreme of this scenario, when the amplitude of interactions does not depend on the distance between spins in a pair, is considered in Problem 3.7.4.

3.5 Nonideal System with Pair Spin Interactions: The Mean-Field Approach

In the model with interactions among spins, $J \neq 0$, the exact analytical solutions can be obtained only in the rare cases of some lattices. Indeed, in the previous section, we were able to find the exact solution for the one-dimensional case. It is generally true that a one-dimensional case of a system can be solved exactly. However, the one-dimensional case is "degenerate." It has a phase transition only at zero temperature and instead of common power-law dependencies in the vicinity of a critical point it generally demonstrates exponential dependencies. Therefore, the one-dimensional model can hardly be considered as a general representative of a system with a phase transition, and we have to look at higher dimensions.

But in higher dimensions, the possibility to obtain the exact solution is rare. So, while the exact solution of the two-dimensional Ising model on square lattice has been found by several ingenious methods (Kramers and Wannier 1941a, b; Onsager 1944; Kac and Ward 1952; Potts and Ward 1955; Hurst and Green 1960; Vdovichenko 1965a, b; Glasser 1970), the three-dimensional case remains a mystery even nowadays.

Thereby, for an arbitrary lattice type of an arbitrary dimensionality, it is usually necessary to apply some approximations. In Chap. 7, we will consider the approximation of the renormalization group. However, there is also another approximation—the mean-field approximation which we discuss in the following paragraphs.

The mean-field approach has appeared much earlier than the renormalization group approach. It does not work always, sometimes only for the given range of parameters. However, this approximation has become canonical due to its capability to crudely but exemplarily illustrate the phase-transition phenomena.

Why can we not find the exact solution for the case of an arbitrary lattice? The reason is that for the nonideal system the energy of microstate $\{\sigma\}$ depends already not only on the averaged spin over the lattice, $\langle \sigma_i \rangle_{\{\sigma\}}$, but also on the orientations of one spin relative to another. Therefore, the energy spectrum of the system becomes much more complex in comparison with the ideal system. The number of microstates, corresponding to the given value of magnetization, is still determined by (3.38)

$$\Gamma_{\{\{m\}\}} \approx \ln \left(\frac{1+m}{2} \right)^{-N\frac{1+m}{2}} \left(\frac{1-m}{2} \right)^{-N\frac{1-m}{2}} \tag{3.70}$$

but it is very difficult to find the number g_E of microstates, corresponding to the given value of energy.

In addition to the long-range order parameter, another parameter emerges in a nonideal system—*the short-range order parameter*, which is responsible for the local orientations of one spin relative to another. For simplicity, further, we will generally consider only the n.n. Ising model. For this model, the short-range order parameter is introduced as

$$S_{\{\sigma\}} \equiv \left\langle \sigma_i \sigma_j \right\rangle_{<i,j>_{n.n.} \in \{\sigma\}} \equiv \frac{1}{Nq/2} \sum_{<i,j>_{n.n.}} \sigma_i \sigma_j . \tag{3.71}$$

Here, we average the interactions between spins, $\sigma_i \sigma_j$, over the nearest-neighbor spin pairs, $< i, j >_{n.n.}$, of a microstate $\{\sigma\}$. The total number of the n.n. pairs on the lattice is $Nq/2$, where q is the lattice coordination number (the number of neighbors of a spin; $q = 2$ in Fig. 3.1a; $q = 4$ in Fig. 3.1b; $q = 6$ in Fig. 3.1c, d; and $q = 3$ in Fig. 3.1e.

In terms of two order parameters, we can rewrite Hamiltonian (3.1) for the n.n. case as

$$\mathrm{H}_{\{\sigma\}} = -\mu h N m_{\{\sigma\}} - J \frac{Nq}{2} S_{\{\sigma\}}. \tag{3.72}$$

The mean-field approach is introduced as an approximation which substitutes the exact behavior of the short-range order parameter by some equivalent behavior depending on the long-range order parameter. Let us assume that from some a priori

considerations for every microstate $\{\sigma\}$, we have been able to approximate the exact value of $S_{\{\sigma\}}$ by some function of $m_{\{\sigma\}}$. In this case, Hamiltonian (3.72) becomes a function only of the long-range order parameter:

$$\mathrm{H}_{\{\sigma\}} \approx \mathrm{H}(m_{\{\sigma\}}) \tag{3.73}$$

Equality (3.73), like for the case of the ideal system, provides the correspondence between the energy of a microstate and its magnetization. So, the energy level of the system again determines the numbers $N_\uparrow$ and $N_\downarrow$, and the statistical weight of this energy level is

$$g_E = \frac{N!}{N_\uparrow! N_\downarrow!} \approx_{\ln} \left(\frac{1+m(E)}{2}\right)^{-N\frac{1+m(E)}{2}} \left(\frac{1-m(E)}{2}\right)^{-N\frac{1-m(E)}{2}}. \tag{3.74}$$

To find the partition function of the CE, we can now transform the sum (3.9) into the integral

$$Z^{CE} \approx_{\ln} \int_{E_{\min}}^{E_{\max}} \frac{dE}{\Delta E}\, g_E e^{-E/T}, \tag{3.75}$$

where $E_{\min}$ and $E_{\max}$ are the minimal and maximal energies in the spectrum and ΔE is the energy shift corresponding to one-spin flip. The particular dependencies of these three quantities are not important because the integral equals again its maximal term (the partition function equals its maximal partial partition function),

$$Z^{CE} \approx_{\ln} g_{E_0} e^{-E_0/T}, \tag{3.76}$$

which is determined by

$$\left.\frac{\partial(g_E e^{-E/T})}{\partial E}\right|_{E_0} = 0 \quad \text{or} \quad \left.\frac{\partial \ln(g_E e^{-E/T})}{\partial E}\right|_{E_0} = 0. \tag{3.77}$$

If we divide (3.77) by Z^{CE}, we return to the equation of state (3.10).

However, it is again much easier to integrate not over the energy but over the magnetization:

$$Z^{CE} \approx_{\ln} \int_{-1}^{+1} \frac{dm}{2/N}\, \Gamma_{\{\{m\}\}} e^{-\mathrm{H}(m)/T} \approx_{\ln} \Gamma_{\{\{m_0\}\}} e^{-\mathrm{H}(m_0)/T}, \tag{3.78}$$

where the point m_0 of the maximal term is determined by

$$\left.\frac{\partial\left(\Gamma_{\{\{m\}\}} e^{-\mathrm{H}(m)/T}\right)}{\partial m}\right|_{m_0} = 0 \quad \text{or} \quad \left.\frac{\partial \ln\left(\Gamma_{\{\{m\}\}} e^{-\mathrm{H}(m)/T}\right)}{\partial m}\right|_{m_0} = 0. \tag{3.79}$$

Substituting (3.70) into (3.79), we find the equation of state

$$m_0 = \tanh\left(-\frac{1}{NT}\frac{\partial \mathrm{H}(m)}{\partial m}\bigg|_{m_0} \right). \tag{3.80}$$

Once we have obtained m_0 from this equation, we substitute it into (3.78) to find the value of Z^{CE} and, correspondingly, the equilibrium free energy of the system:

$$F^{CE} = -T \ln Z^{CE}. \tag{3.81}$$

Substituting (3.70), (3.73), and (3.78) into (3.81), we find

$$F^{CE} = NT\frac{1+m_0}{2}\ln\left(\frac{1+m_0}{2}\right) + NT\frac{1-m_0}{2}\ln\left(\frac{1-m_0}{2}\right) + \mathrm{H}(m_0). \tag{3.82}$$

The term "mean field" appears because dependence (3.73) is generally assumed to be the result of the approximation when the interactions of spins in pairs are substituted by the interactions of separate spins with the effective field created by all spins together:

$$\mathrm{H}_{\{\sigma\}} \approx -\mu(h + h^{eff}_{\{\sigma\}})Nm_{\{\sigma\}}, \tag{3.83}$$

where the effective field is some function $h^{eff}_{\{\sigma\}}(m_{\{\sigma\}})$ of the specific magnetization of this microstate $\{\sigma\}$. The difference between (3.73) and (3.83) is just a matter of notation. Meanwhile, (3.80) transforms into

$$m_0 = \tanh\left(\frac{\mu}{T}\left\{ h + h^{eff}(m_0) + m_0 \frac{\partial h^{eff}}{\partial m}\bigg|_{m_0} \right\} \right). \tag{3.84}$$

As an example, we consider further the mean-field approach for a ferromagnet that is applied often and often. In this approach, it is assumed that the effective field is proportional to the magnetization of a ferromagnet:

$$h^{eff}_{\{\sigma\}} = Am_{\{\sigma\}}. \tag{3.85}$$

For this simple case, the equation of state (3.84) transforms into

$$m_0 = \tanh\left(\frac{\mu}{T}\{h + 2Am_0\} \right). \tag{3.86}$$

Let us consider the model in the absence of the external magnetic field, $h = 0$:

$$m_0 = \tanh\frac{2\mu A m_0}{T}. \tag{3.87}$$

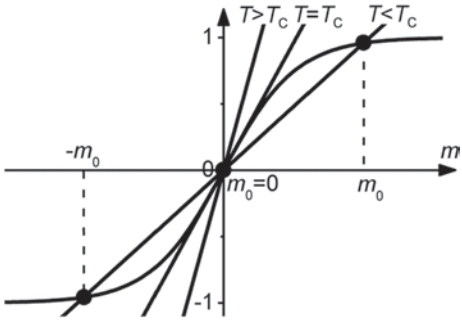

Fig. 3.4 The graphical solution for the value of the equilibrium magnetization m_0 in the absence of magnetic field

If the magnetization is present when the external magnetic field is zero, this magnetization is called *spontaneous*.

The easiest way to obtain the solution of (3.87) is to find graphically when the linear dependence intersects with the hyperbolic tangent function (Fig. 3.4).

As we see from Fig. 3.4, two different situations are possible. If in the vicinity of the point $m = 0$ the linear dependence is steeper than the hyperbolic tangent,

$$1 > \frac{2\mu A}{T} \quad \text{or} \quad T > 2\mu A, \tag{3.88}$$

there is only one solution $m_0 = 0$, corresponding to the absence of spontaneous magnetization.

On the contrary, if in the vicinity of the point $m = 0$ the linear dependence is less steep than the hyperbolic tangent,

$$1 < \frac{2\mu A}{T} \quad \text{or} \quad T < 2\mu A, \tag{3.89}$$

there are three points of intersection: $-m_0, 0, m_0$. Two of them, $-m_0$ and m_0, are nonzero which correspond to the presence of *the spontaneous magnetization*.

In the absence of magnetic field, the orientation "up" is no more or less preferable than the orientation "down." It is said that there is the symmetry in the model for these two orientations. However, we see that below the critical point, the system chooses one of the two directions to align spins along it. This is called *the spontaneous symmetry breaking*.

The third point of intersection for $T < 2\mu A$, corresponding to zero magnetization, is not, in fact, a solution. It is easy to see that if we return to (3.79). To find the maximal term of the partition function, we differentiated it and equated the derivative to zero. But a zero derivative returns all extrema, both maxima and minima. The point of zero magnetization corresponds to a minimum. Therefore, it should be discarded.

Comparing inequalities (3.88 and 3.89), we see that the temperature

$$T_C = 2\mu A, \tag{3.90}$$

plays the role of *the critical temperature* of a ferromagnet. Above the critical temperature, $T > T_C$, there is only one phase corresponding to zero magnetization. Below the critical temperature, $T < T_C$, there are two solutions, $-m_0$ and m_0, corresponding to two different phases. The point $T = T_C$, $h = h_C = 0$ is called *the critical point*.

From Fig. 3.4, we see that in the vicinity of the critical point (when the linear dependence is almost tangent to the hyperbolic tangent) the magnetization is small. This gives us an opportunity to investigate the neighborhood of the critical point in detail.

3.6 Landau Theory

3.6.1 The Equation of State

Let us return to the general case of a ferromagnet in the nonzero magnetic field h. If we consider the close proximity of the critical point, we can assume that the field h, specific magnetization m_0, and relative deviation of temperature from its critical value

$$t \equiv \frac{T - T_C}{T_C} \tag{3.91}$$

are small. Therefore, we can expand the hyperbolic tangent (3.86) in these small parameters to find the equation of state of a ferromagnet:

$$0 = -h + 2atm_0 + 4bm_0^3 + \ldots, \tag{3.92}$$

where

$$a = A \text{ and } b = \frac{A}{6} \tag{3.93}$$

Here, we have introduced two parameters, a and b, whose true purpose will become clear later. Let us now abstract away from the particular system discussed in the previous section and in the future consider an arbitrary magnetic system whose equation of state is (3.92) and whose mean-field approximation is (3.73).

The equilibrium value of spontaneous magnetization is the solution of the equation of state (3.92); and in zero magnetic field, $h = h_C = 0$, we find

$$m_0 = 0 \tag{3.94}$$

$$\text{and } m_0 = \pm\sqrt{-\frac{at}{2b}}. \tag{3.95}$$

Above the critical point ($T > T_C$), there is only zero solution (3.94) because for $t > 0$ both square roots provide only complex numbers. The nonzero spontaneous magnetization (3.95) appears only below the critical point ($t < 0$).

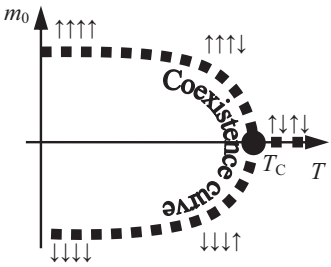

Fig. 3.5 The equation of state in zero magnetic field

In fact, the zero spontaneous magnetization $m_0 = 0$ formally remains the solution of the equation of state (3.92) and below the critical point. However, later we will prove that this solution is not genuine, leaving only the nonzero magnetization at $T < T_C$

$$m_0 = 0 \quad \text{at} \quad T > T_C, t > 0, \tag{3.96}$$

$$m_0 = \pm\sqrt{-\frac{at}{2b}} \quad \text{at} \quad T < T_C, t < 0. \tag{3.97}$$

This behavior is illustrated in Fig. 3.5 by a *dotted line*. The part of the critical isofield curve $h = h_C = 0$ for temperatures below critical is called *the coexistence curve* or *binodal curve*. The *filled dot* in Fig. 3.5 represents the critical point.

The appearance of the spontaneous magnetization in the zero magnetic field is sometimes called as *self-organization*, because of the appearance of the nonzero order parameters in the system when the field parameter is zero. In other words, there is no external magnetic field which would prescribe for spins their directions. Instead, the spins themselves choose one of two possible directions as preferable and align themselves along it.

We see that below the critical point the dependence of the spontaneous magnetization on $|t|$ along the binodal curve $h = h_C = 0$ is a power law with exponent $1/2$. If we introduce a critical index β_t^C as

$$m_0 \propto |t|^{\beta_t^C}, \tag{3.98}$$

then, we immediately find that Landau theory provides for spontaneous magnetization critical index $\beta_t^C = 1/2$. In turn, Landau theory is the consequence of the mean-field approach. So, we attribute the critical index, which is just a simple rational number (simple rational fraction), to the properties of the mean-field approximation.

Next, instead of the critical isofield curve of zero magnetic field, we consider the critical isotherm $T = T_C$. On this isotherm, the equation of state (3.92) provides the

following power-law dependence of the magnetization on the value of the magnetic field:

$$m_0 = \left(\frac{h}{4b}\right)^{1/3} \tag{3.99}$$

If we define the second critical index β_h^{C} by

$$m_0 \propto |h|^{\beta_h^{\mathrm{C}}}, \tag{3.100}$$

we see that the mean-field approach determines $\beta_h^{\mathrm{C}} = 1/3$.

3.6.2 The Minimization of Free Energy

As we already know, the equation of state (3.92) must follow from the free energy minimization. To illustrate this principle for our particular system, we should investigate closer the free energy behavior.

Since we are working in the CE, the free energy potential of this ensemble is the Helmholtz energy. From (2.274), we know that the Helmholtz energy of a fluctuation $\{\{E\}\}$ is provided by

$$F_{\{\{E\}\}} = -T \ln Z^{CE}_{\{\{E\}\}}. \tag{3.101}$$

Here, $Z^{CE}_{\{\{E\}\}}$ is the partial partition function:

$$Z^{CE}_{\{\{E\}\}} \equiv Z^{CE} W^{CE}_{\{\{E\}\}} \equiv \sum_{\{\tilde{E}\}:\{\tilde{E}\}\in\{\{E\}\}} e^{-\tilde{E}/T} = \Gamma_{\{\{E\}\}} e^{-E/T} = g_E e^{-E/T} \tag{3.102}$$

or

$$Z^{CE}_{\{\{m\}\}} = \Gamma_{\{\{m\}\}} e^{-\mathrm{H}(m)/T}, \tag{3.103}$$

where in the last equation we have again decided that it is more convenient to work with the magnetization than with the energy. Substituting (3.70) and (3.73) into (3.103), we find the dependence of the nonequilibrium free energy on the nonequilibrium value of system's magnetization m (the magnetization which does not obey the equation of state (3.92)):

$$F_{\{\{m\}\}} = NT\frac{1+m}{2}\ln\left(\frac{1+m}{2}\right) + NT\frac{1-m}{2}\ln\left(\frac{1-m}{2}\right) + \mathrm{H}(m), \tag{3.104}$$

Remarkable is that this is the same functional dependence as (3.82). Only difference is that there we were looking for the equilibrium value of the Helmholtz energy; and, correspondingly, the dependence was on the equilibrium value m_0 of the magnetization which obeys the equation of state (3.92). On the contrary, energy (3.104) is nonequilibrium, and the dependence is on the nonequilibrium value m of the magnetization.

Similar to how we have expanded the hyperbolic tangent (3.86) to obtain the equation of state (3.92), we now expand dependence (3.104) in small parameters h, t, and m for the close proximity of the critical point:

$$F_{\{\{m\}\}} = N\mu(-2A\ln 2 - hm + atm^2 + bm^4 + \ldots). \tag{3.105}$$

Here, $-2A\ln 2$ is a constant, and therefore, it can be easily removed by the shift of the free energy. Further, we will neglect this term as not influencing behavior of the system.

Functional dependence (3.105) represents Landau theory, developed for our magnetic system, while a and b, introduced earlier in (3.93), are, in fact, the coefficients of the free energy expansion.

We already know that to find the equilibrium state we should minimize the free energy over all nonequilibrium states. To do this, we differentiate dependence (3.105) with respect to m and equate the derivative to zero

$$\left.\frac{\partial F_{\{\{m\}\}}}{\partial m}\right|_{m_0} = 0. \tag{3.106}$$

This returns us to the equation of state (3.92), and we see that this equation is indeed the consequence of the free energy minimization principle.

Let us now investigate the system's behavior with the aid of expression (3.105) obtained for nonequilibrium states in the vicinity of the critical point. If we look at the definition (3.85), we see that constant A, as the constant of proportionality between the effective field and magnetization, is expected to be positive for a ferromagnet. Therefore, in accordance with (3.93), both coefficients, a and b, are also positive.

Let us consider first the system in the absence of magnetic field, $h = 0$. The sketch of the free energy dependence on nonequilibrium magnetization m is presented in Fig. 3.6. For temperatures higher than critical ($t > 0$), both the quadratic dependence and the fourth-order dependence in (3.105) have minima at the point of zero magnetization. Therefore, their sum also has a minimum at $m = 0$.

At critical temperature ($t = 0$), the quadratic dependence disappears, and the minimum becomes flatter, following the fourth-order dependence. Below the critical point ($t < 0$), the fourth-order dependence has again a minimum at zero magnetization while the quadratic dependence turns upside down and has a maximum at $m = 0$. For small values of m, the free energy dependence is dominated by the

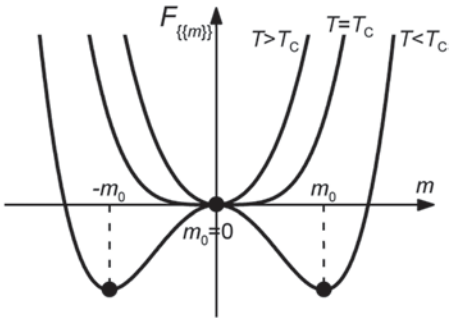

Fig. 3.6 The nonequilibrium free energy in the absence of magnetic field

quadratic term while in the infinity the fourth-order dependence becomes in turn dominant. This "wrestle" of the quadratic dependence and the fourth-order dependence causes the appearance of two minima at the nonzero values of spontaneous magnetization, $-m_0, m_0$, which correspond to solutions (3.95) we obtained earlier. Between these two minima, there is a maximum at zero magnetization.

Now, we can answer the question why in (3.97) we discarded zero solution (3.94) of the equation of state (3.92) below the critical point. To find equilibrium states, we should minimize the free energy potential. We did this by finding its derivative and equating it to zero (3.106). But this procedure returns not only minima but also maxima, and maxima do not correspond to equilibrium solutions. In accordance with Fig. 3.6, the zero magnetization below the critical point corresponds precisely to the maximum and, therefore, is not an equilibrium solution.

We see now the beauty of Landau theory. We kept only first terms in the free energy expansion (3.105), and in zero magnetic field only two of them influenced the system's behavior. But these two terms were enough to illustrate the behavior of *criticality*.

However, this is not all what Landau theory is capable of! Besides the second-order phase transitions, it can also illustrate the first-order phase transitions. To be applicable, the theory requires only that the system should still be in the vicinity of the critical point. However, both the coexistence curve and spinodal curve originate just at the critical point. Therefore, in its vicinity we are still able to consider the first-order phase transitions.

We consider the temperature below critical. In Fig. 3.7, we first draw the curve for $h = 0$ similar to Fig. 3.6. Let us now increase the value of the field h. Due to the term $-hm$ in the free energy expansion (3.105), the left minimum becomes *local* (less deep) in comparison with the right, *global minimum*.

Following the free energy minimization principle, the system would prefer to move to the global minimum. However, if it is initially in a state close to the local minimum, a *potential barrier* between two minima prevents the system to leave. Therefore, the system will stay in a quasi-equilibrium, *metastable state*, corresponding to the fluctuations in the vicinity of the local minimum.

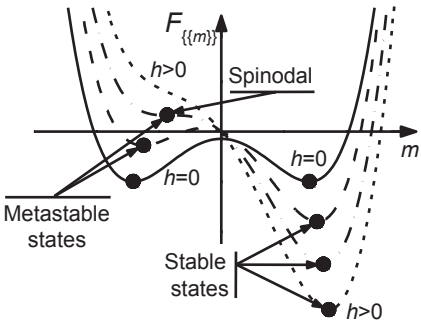

Fig. 3.7 The nonequilibrium free energy in the presence of magnetic field

Because of these fluctuations, the system performs many attempts to climb out of the local minimum. If we studied dynamic phenomena of phase transitions, for the linear response, we would find to be valid the time-dependent evolution equation (*the Ginzburg–Landau–Langevin equation* for the nonconserved order parameter): [1]

$$\frac{\partial m}{\partial(time)} = -B\frac{\partial F_{\{\{m\}\}}}{\partial m} + \zeta. \tag{3.107}$$

Here, ζ is the noise which constantly generates fluctuations in the vicinity of the system's current state. However, when due to the presence of this noise, the system "jumps" up the slope of the potential barrier, the gradient $\frac{\partial F_{\{\{m\}\}}}{\partial m}$ of the free energy at the minimum's "wall" "rolls it down." The system "jumps" again, but the free energy gradient returns it back again, and so on.

Saying that the system performs "many attempts" to climb out of the local minimum, we mean really many. The reader can imagine an ant in a sand cone. While the ant tries to climb up, the sand avalanches constantly drop it back to the bottom.

After a large number of attempts, it could so happen that a very improbable fluctuation would take place, so the system could climb up to the top of the potential barrier. After that, it slides down to the bottom of the right, global minimum, corresponding to *the stable state*, by the "explosive," nonequilibrium process.[2]

At further increase of the magnetic field, the left minimum becomes shallower and shallower and finally disappears at *the spinodal point*. The disappearance of

[1] Unfortunately, to avoid confusion with the relative deviation t of temperature from its critical value for the derivative with respect to time we have to use here the notation $\partial / \partial(time)$.

[2] Once during a lecture, when I colorfully described how it is difficult for the system to climb up to the top of the potential barrier and how many attempts it would require, a student asked a question: "What if at the top of the potential barrier the system would reel not to the "right" but to the "left," back into the local minimum?" "In this case we will call it a looser!" was the only answer I could then come up with.

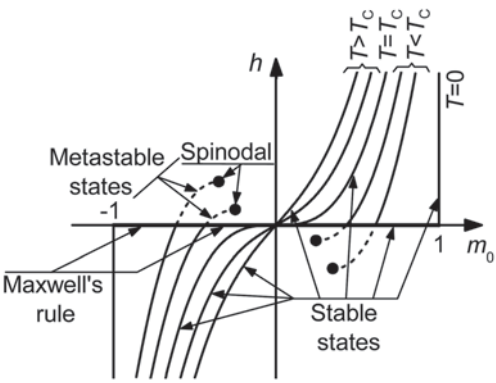

Fig. 3.8 The equation of state

the left minimum is caused by its coalescence with the maximum of the potential barrier.

"After" the spinodal point, there is no potential barrier, only one, global minimum is left, and therefore, there are no metastable states. This means that for any initial state the gradient of the free energy leads the system directly into the equilibrium state at the bottom of the single minimum left.

3.6.3 Stable, Metastable, Unstable States, and Maxwell's Rule

We already know that the equation of state (3.92) corresponds to the minimum of the free energy potential. Now, we also see that it represents not only stable states, corresponding to the global minimum of the free energy, but also metastable states of the local minimum. The stable and metastable isotherms, corresponding to the equation of state (3.92), are presented in Fig. 3.8.

Above the critical point ($T > T_C$), these isotherms are continuous curves with zero spontaneous magnetization in zero field, and they represent only stable states. There is only one phase here which is called *paramagnetic*.

The critical isotherm $T = T_C$ is tangent to the abscissa axis (recall (3.99) and (3.100)) and, therefore, has an infinite derivative, $dm_0 / dh = \infty$, at the zero magnetic field $h = 0$. This can be considered as an inheritance of the spinodal curve disappearing at the critical point. We will discuss the spinodal curve in detail later.

Below the critical temperature ($T < T_C$) the isotherms intersect with the abscissa axis at two nonzero values which represent two phases of spontaneous magnetization. These phases are called *ferromagnetic*. The isotherms are *stable* while the sign of the magnetic field coincides with the sign of the magnetization. If the field changes its sign, the isotherms are continued as *metastable* until the spinodal point.

In Fig. 3.7, the spinodal point corresponded to the field at which the local minimum disappeared. In Fig. 3.8, the spinodal can be found as a point on the isotherm

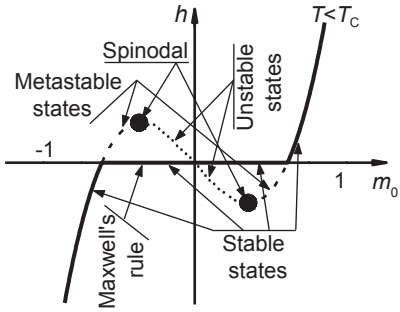

Fig. 3.9 The equation of state below the critical point

at which the derivative of the magnetization with respect to the field becomes infinite, $dm_0 / dh = \infty$. After the spinodal point (Fig. 3.9), this derivative is negative, $dm_0 / dh < 0$, which corresponds to *unstable states*. Therefore, the spinodal point $dm_0 / dh = \infty$ delimits the metastable states with positive derivative $dm_0 / dh > 0$ from the unstable states with negative derivative $dm_0 / dh < 0$. A similar situation takes place in liquid–gas systems, for example, in the case of a van der Waals gas, when spinodal corresponds to the infinite derivative of concentration with respect to pressure $dn / dP = \infty$ and delimits stable $dn / dP > 0$ and unstable $dn / dP < 0$ parts of the van der Waals equation of state.

If we continued analogy with the liquid–gas systems, we would recall that for these systems there is such an important concept as Maxwell's rule. For the pressure, that at given temperature coincides with the Clausius–Clapeyron pressure of the liquid–gas phase transition, Maxwell's rule introduces heterogeneity into the system when the volume of the system is divided into separate *domains* (*clusters*) of liquid and gas phases.

For magnetic systems, similar rule is illustrated in Figs. 3.8 and 3.9 as a horizontal line at zero magnetic field $h = 0$, which connects two stable parts of an isotherm. In the absence of magnetic field, the lattice breaks up into a set of separate domains with positive and negative magnetizations. The system's spontaneous magnetization equals the domain's magnetizations averaged over the lattice and can take any value between two homogeneous solutions (3.97)

$$-\sqrt{-\frac{at}{2b}} \le m_0 \le +\sqrt{-\frac{at}{2b}} \quad \text{at} \quad T < T_C, h = h_C = 0. \tag{3.108}$$

We have built Fig. 3.5 to correspond to the case of a homogeneous system. To include heterogeneous Maxwell's rule into this figure, we should allow the system to be in any state inside of the coexistence curve (Fig. 3.10). That is why this curve is called the coexistence curve; it delimits the one-phase region from the two-phase region of phase coexistence.

In liquid–gas systems, we know that at given temperature any deviation of the pressure from the Clausius–Clapeyron pressure immediately transforms the het-

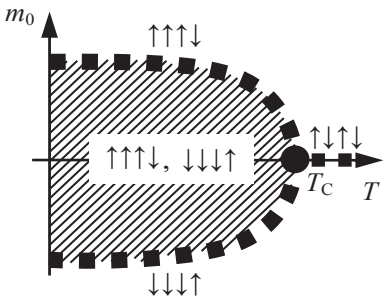

Fig. 3.10 The equation of state in zero magnetic field

erogeneous system into one of the homogeneous phases. In magnetic systems, the appearance of a nonzero field, no matter how small, immediately transforms a heterogeneous state into one of the homogeneous phases as well. In other words, the appearing field breaks the phase coexistence. It keeps domains of one phase as favorable but breaks domains of another phase, transforming them into the favorable phase.

Therefore, minor changes in the magnetic field around its zero value transfer the system from one phase to another along Maxwell's rule. Stronger changes in the field lead to the appearance of a *hysteresis loop* along the metastable parts of an isotherm (Fig. 3.11). We observe similar phenomena in liquid–gas systems when we transform one phase into another not by means of Maxwell's rule but through the region of metastable states.

In Fig. 3.8, we plotted the equation of state (3.92) by means of separate isotherms. But the equation of state is, in fact, a three-dimensional surface; and isotherms represent merely its two-dimensional cross-sections. Therefore, it would be much more illustrative to plot this equation in three-dimensional space as a three-dimensional surface (Fig. 3.12).

The behavior of the system significantly depends on whether we consider it below or above the critical point. Below the critical point, the surface of stable states consists of lateral one-phase sheets for nonzero field and a piece of the two-phase

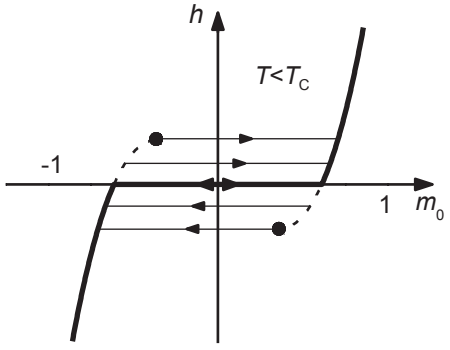

Fig. 3.11 The hysteresis loop

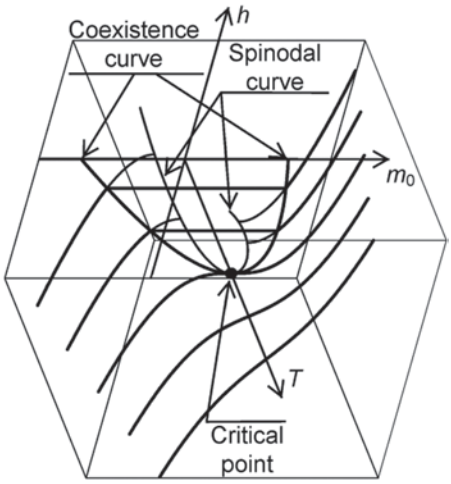

Fig. 3.12 The three-dimensional plot of the equation of state

plane inside of the coexistence curve. Two sheets of metastable states continuously extend the lateral sheets up to the spinodal curve. Above the critical point, there is only one sheet, presenting the stable paramagnetic states.

The first important curve—*the coexistence curve* (*binodal curve*)—is determined by the spontaneous magnetization (3.97) of the homogeneous system. This curve delimits the one-phase and two-phase regions for magnetic systems as well as for liquid–gas systems.

The equation of the second important curve—*the spinodal curve*—we can find by the condition that at the spinodal point in Fig. 3.7 the minimum and maximum of the free energy coalesce. In other words, we should find when the determinant of cubic equation (3.92) becomes zero. Or, differentiating this equation, we could find when the derivative of the magnetization with respect to the magnetic field becomes infinite: $\partial m_0 / \partial h = \infty$. In both cases, the solution is given by

$$m_{\mathrm{S}} = -\sqrt{\frac{-at_{\mathrm{S}}}{6b}}, \quad h_{\mathrm{S}} = 8b\left(\frac{-at_{\mathrm{S}}}{6b}\right)^{3/2}. \tag{3.109}$$

Recently, it was discovered that in the vicinity of the spinodal point physical dependences are also power-laws similar to the behavior of the system in the vicinity of the critical point. Expanding the equation of state (3.92) in small parameters $\left|m_0 - m_{\mathrm{S}}\right|$ and $\left|t - t_{\mathrm{S}}\right|$ while the magnetic field is kept equal to its spinodal value, $h = h_{\mathrm{S}}$, we find

$$\left|m_0 - m_{\mathrm{S}}\right| = \sqrt{\frac{a}{6b}\left|t - t_{\mathrm{S}}\right|}. \tag{3.110}$$

The spinodal index β_t^{S} is defined as

$$\left|m_0 - m_{\mathrm{S}}\right| \infty \left|t - t_{\mathrm{S}}\right|^{\beta_t^{\mathrm{S}}}. \tag{3.111}$$

So, the mean-field approach of Landau theory provides $\beta_t^{\mathrm{S}} = 1/2$.

On the contrary, expanding the equation of state (3.92) in small parameters $|m_0 - m_{\mathrm{S}}|$ and $|h - h_{\mathrm{S}}|$ while the temperature is kept unchanged, we find

$$|m_0 - m_{\mathrm{S}}| = \frac{|h - h_{\mathrm{S}}|^{1/2}}{(-24abt_{\mathrm{S}})^{1/4}}. \tag{3.112}$$

The spinodal index β_h^{S} is defined as

$$|m_0 - m_{\mathrm{S}}| \infty |h - h_{\mathrm{S}}|^{\beta_h^{\mathrm{S}}}, \tag{3.113}$$

and we immediately find $\beta_h^{\mathrm{S}} = 1/2$. This parabolic dependence is obvious from Fig. 3.9.

3.6.4 Susceptibility

We define *the magnetic susceptibility* as the response of the equilibrium magnetization to the change in the magnetic field:

$$\chi \equiv \left(\frac{\partial m_0}{\partial h} \right)_t. \tag{3.114}$$

In more detail, the importance of this quantity will be discussed in Chap. 6. Here, we investigate only the divergence of the susceptibility in the vicinity of the critical and spinodal points.

Differentiating the equation of state (3.92) with respect to the magnetic field h, we find

$$\chi = \frac{1}{2at + 12bm_0^{\,2}}. \tag{3.115}$$

First, we approach the critical point along the isofield curve, $h = h_{\mathrm{C}} = 0$, which below the critical temperature corresponds to the binodal curve. Substituting (3.96) and (3.97) into (3.115), we obtain

$$\chi = \frac{1}{2at} \quad \text{when} \quad t > 0, \tag{3.116}$$

$$\chi = \frac{1}{4a|t|} \quad \text{when} \quad t < 0. \tag{3.117}$$

We see that if we define the critical index γ_t^{C} by

$$\chi \propto \frac{1}{|t|^{\gamma_t^{\mathrm{C}}}}, \tag{3.118}$$

the mean-field approach provides $\gamma_t^{\mathrm{C}} = 1$.

Second, we approach the critical point along the critical isotherm $T = T_{\mathrm{C}}$. Substituting (3.99) and $t = 0$ into (3.115), we find

$$\chi = \frac{1}{3\sqrt[3]{4b}\,h^{2/3}}. \tag{3.119}$$

For the critical index γ_h^{C}, defined by

$$\chi \propto \frac{1}{|h|^{\gamma_h^{\mathrm{C}}}}, \tag{3.120}$$

we obtain $\gamma_h^{\mathrm{C}} = 2/3$.

Next, let us consider the proximity of the spinodal point. For the isofield $h = h_{\mathrm{S}}$ approach, we expand (3.115) in small parameters $|m_0 - m_{\mathrm{S}}|$ and $|t - t_{\mathrm{S}}|$ while keeping $h = h_{\mathrm{S}}$:

$$\chi = \frac{1}{2a(t - t_{\mathrm{S}}) - 24b\sqrt{-\dfrac{at_{\mathrm{S}}}{6b}}(m_0 - m_{\mathrm{S}})}. \tag{3.121}$$

Here, we should recall that along the spinodal isofield curve we have relationship (3.110) between $|m_0 - m_{\mathrm{S}}|$ and $|t - t_{\mathrm{S}}|$. Substituting it into (3.121), we find

$$\chi = \frac{1}{2a(t - t_{\mathrm{S}}) + 4a\sqrt{-t_{\mathrm{S}}}\sqrt{|t - t_{\mathrm{S}}|}} \approx \frac{1}{4a\sqrt{-t_{\mathrm{S}}}\sqrt{|t - t_{\mathrm{S}}|}}. \tag{3.122}$$

For the spinodal index, defined by

$$\chi \propto \frac{1}{|t - t_{\mathrm{S}}|^{\gamma_t^{\mathrm{S}}}}, \tag{3.123}$$

this provides $\gamma_t^{\mathrm{S}} = 1/2$.

Finally, we approach the spinodal point along the isotherm $t = t_{\mathrm{S}}$. Expanding (3.115) in small parameter $|m_0 - m_{\mathrm{S}}|$ while keeping $t = t_{\mathrm{S}}$, we find

$$\chi = \frac{1}{24b\sqrt{-\dfrac{at_{\mathrm{S}}}{6b}}\,|m_0 - m_{\mathrm{S}}|}. \tag{3.124}$$

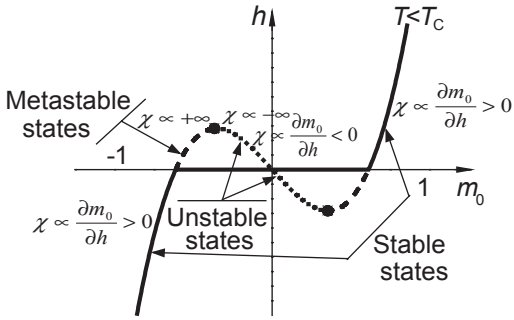

Fig. 3.13 The sign of the magnetic susceptibility distinguishes stable and metastable states from unstable states

Recalling that along the isotherm $t = t_S$ we have found earlier relationship (3.112) between $|m_0 - m_S|$ and $|h - h_S|$, we obtain

$$\chi = \frac{1}{4^{3/4}\sqrt[4]{-6abt_S}\,|h-h_S|^{1/2}}. \tag{3.125}$$

So, for the critical index

$$\chi \propto \frac{1}{|h-h_S|^{\gamma_h^S}}, \tag{3.126}$$

we find $\gamma_h^S = 1/2$.

Earlier we have discussed that the stable and metastable states are distinguished from the unstable states by the sign of the derivative $\partial m_0 / \partial h$. Now, we see that this derivative represents the susceptibility (3.114) of the system. This behavior is presented in Fig. 3.13. In more detail, we discuss the susceptibility in Chap. 6.

3.6.5 Heat Capacity

The heat capacity is defined by

$$C \equiv T\left(\frac{\partial S^{CE}}{\partial T}\right)_h = -T\left(\frac{\partial^2 F^{CE}}{\partial T^2}\right)_h, \tag{3.127}$$

where the ensemble Helmholtz free energy is given by (3.82). In the vicinity of the critical point, (3.82) can be expanded as

$$F^{CE} = N\mu(-2A\ln 2 - hm_0 + atm_0{}^2 + bm_0{}^4 + \ldots). \tag{3.128}$$

Since

$$\frac{\partial}{\partial T} \equiv \frac{1}{T_{\mathrm{C}}} \frac{\partial}{\partial t}, \tag{3.129}$$

differentiating (3.128), we find

$$C = -\frac{N\mu}{T_{\mathrm{C}}} \left\{ 4am_0 \frac{\partial m_0}{\partial t} + \left\{ 2at + 12b{m_0}^2 \right\} \left(\frac{\partial m_0}{\partial t} \right)^2 + \left\{ -h + 2atm_0 + 4b{m_0}^3 \right\} \frac{\partial^2 m_0}{\partial t^2} \right\}. \tag{3.130}$$

The last term in the right-hand side of this expression is zero due to the equation of state (3.92):

$$C = -\frac{N\mu}{T_{\mathrm{C}}} \left\{ 4am_0 \frac{\partial m_0}{\partial t} + \left\{ 2at + 12b{m_0}^2 \right\} \left(\frac{\partial m_0}{\partial t} \right)^2 \right\}. \tag{3.131}$$

Simultaneously, we differentiate the equation of state (3.92) to find the derivative of the equilibrium magnetization:

$$\frac{\partial m_0}{\partial t} = -\frac{am_0}{at + 6b{m_0}^2}, \tag{3.132}$$

which we substitute into (3.131):

$$C = \frac{N\mu}{T_{\mathrm{C}}} \frac{2a^2 {m_0}^2}{at + 6b{m_0}^2}. \tag{3.133}$$

If we approach the critical point along the isofield curve $h = h_{\mathrm{C}} = 0$, substituting (3.96) and (3.97) and $h = 0$ into (3.133), we find

$$C = 0 \quad \text{at} \quad t > 0, \tag{3.134}$$

$$C = \frac{N\mu}{T_{\mathrm{C}}} \frac{a^2}{2b} \quad \text{at} \quad t < 0. \tag{3.135}$$

Recalling from (3.90) and (3.93) that $\frac{1}{T_{\mathrm{C}}} \frac{a^2}{b} = \frac{3}{\mu}$, we find

$$C = 0 \quad \text{at} \quad t > 0, \tag{3.136}$$

$$C = \frac{3N}{2} \quad \text{at} \quad t < 0. \tag{3.137}$$

We see that the heat capacity does not have a singularity when we approach the critical point along the binodal curve. Therefore, the critical index α_t^{C}, defined by

$$C \propto \frac{1}{|t|^{\alpha_t^{\mathrm{C}}}}, \tag{3.138}$$

is zero: $\alpha_t^{\mathrm{C}} = 0$.

Next, we consider the approach of the critical point along the critical isotherm $T = T_{\mathrm{C}}$. Substituting (3.99) and $t = 0$ into (3.133), we obtain

$$C = \frac{N\mu}{T_{\mathrm{C}}}\frac{a^2}{3b} = N. \tag{3.139}$$

Again, the critical index α_h^{C}, defined by

$$C \propto \frac{1}{|h|^{\alpha_h^{\mathrm{C}}}}, \tag{3.140}$$

is zero: $\alpha_h^{\mathrm{C}} = 0$.

Above we have found that $\beta_t^{\mathrm{C}} = 1/2$ and $\gamma_t^{\mathrm{C}} = 1$. Therefore, we prove that

$$\alpha_t^{\mathrm{C}} + 2\beta_t^{\mathrm{C}} + \gamma_t^{\mathrm{C}} = 2. \tag{3.141}$$

If we considered an arbitrary magnetic system, this equality would transform into *the Rushbrooke inequality* (Essam and Fisher 1963; Rushbrooke 1963):

$$\alpha_t^{\mathrm{C}} + 2\beta_t^{\mathrm{C}} + \gamma_t^{\mathrm{C}} \geq 2. \tag{3.142}$$

We return to this relation for the critical isotherm indices in Chap. 8.

Now, let us investigate the vicinity of the spinodal point. Approaching the spinodal point along the isofield $h = h_{\mathrm{S}}$ curve, we expand (3.133) in small parameters $|m_0 - m_{\mathrm{S}}|$ and $|t - t_{\mathrm{S}}|$ while keeping $h = h_{\mathrm{S}}$:

$$C = -\frac{N\mu}{T_{\mathrm{C}}}\frac{a^3 t_{\mathrm{S}}/(3b)}{a(t - t_{\mathrm{S}}) - 12b\sqrt{-\dfrac{at_{\mathrm{S}}}{6b}}(m_0 - m_{\mathrm{S}})}. \tag{3.143}$$

Recalling (3.110), we find

$$C = \frac{N\mu}{T_{\mathrm{C}}}\frac{a^2\sqrt{-t_{\mathrm{S}}}}{6b\sqrt{|t - t_{\mathrm{S}}|}} = \frac{N}{2}\frac{\sqrt{-t_{\mathrm{S}}}}{\sqrt{|t - t_{\mathrm{S}}|}}. \tag{3.144}$$

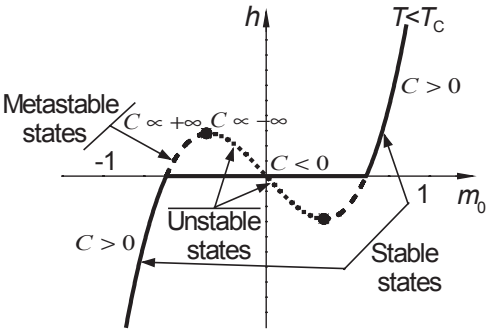

Fig. 3.14 The sign of the heat capacity distinguishes stable and metastable states from unstable states

So, for the spinodal index α_t^{S}, defined by

$$C \propto \frac{1}{|t|^{\alpha_t^{\mathrm{S}}}}, \tag{3.145}$$

we find $\alpha_t^{\mathrm{S}} = 1/2$ which provides the relation analogous to (3.141), only this time formulated for the spinodal indices:

$$\alpha_t^{\mathrm{S}} + 2\beta_t^{\mathrm{S}} + \gamma_t^{\mathrm{S}} = 2. \tag{3.146}$$

The Rushbrooke inequality arises from the general considerations of positivity of the heat capacity. Therefore, there is no reason why this inequality should not be applicable for spinodal indices as well.

Finally, we approach the spinodal point along the isotherm $t = t_{\mathrm{S}}$. Expanding (3.133) in small parameters $|m_0 - m_{\mathrm{S}}|$ and $|h - h_{\mathrm{S}}|$ while keeping $t = t_{\mathrm{S}}$, we find

$$C = \frac{N\mu}{T_{\mathrm{C}}} \frac{a^3 t_{\mathrm{S}}}{36b^2 \sqrt{-\frac{at_{\mathrm{S}}}{6b}(m_0 - m_{\mathrm{S}})}}. \tag{3.147}$$

Recalling (3.112), we find

$$C = \frac{N\mu}{T_{\mathrm{C}}} \frac{\sqrt{2}a^2(-at_{\mathrm{S}})^{3/4}}{(6b)^{5/4}|h - h_{\mathrm{S}}|^{1/2}} = \frac{N}{\sqrt{2}} \frac{(-at_{\mathrm{S}})^{3/4}}{(6b)^{1/4}} \frac{1}{|h - h_{\mathrm{S}}|^{1/2}}. \tag{3.148}$$

For the spinodal index α_h^{S}, defined by

$$C \propto \frac{1}{|h|^{\alpha_h^{\mathrm{S}}}}, \tag{3.149}$$

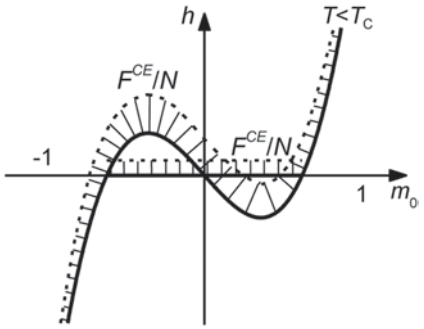

Fig. 3.15 The values of the equilibrium free energy, presented as an epure over the curve of the equation of state

we find $\alpha_h^{\mathrm{S}} = 1/2$.

We see that the heat capacity, similar to the magnetic susceptibility, diverges in the vicinity of the spinodal point and becomes negative for unstable states (Fig. 3.14). Therefore, the heat capacity, as well as the magnetic susceptibility, can be considered as an indicator determining the stability of the states. Positive values correspond to the stable or metastable states while negative values indicate the presence of instability.

3.6.6 Equilibrium Free Energy

In Figs. 3.6 and 3.7, we have considered the dependence of the free energy (3.105) on nonequilibrium values m of magnetization. Let us now turn our attention to the free energy of equilibrium states. In other words, let us return to the equilibrium free energy (3.82), which depends on the equilibrium values m_0 of magnetization as solutions of the equation of state (3.92).

In Fig. 3.15, we present the sketch of the equilibrium free energy as an epure covering the curve of the equation of state. The free energy grows in one-phase region with the decrease of the absolute value of magnetic field. In zero field, the free energy of the heterogeneous system remains constant along Maxwell's rule, and therefore, its values at the beginning and at the end of this rule are equal. In contrast, the free energy of the metastable states continues to grow in the metastable region and achieves its maximum at the spinodal point.

We already discussed above that although the equation of state (3.92) is supposed to provide only equilibrium, stable states, it, in fact, does not distinguish local and global minima and, therefore, its solutions could not only be stable but also metastable. From the free energy minimization principle, we know that metastable states must have higher values of the free energy than stable states. This can be clearly seen from Fig. 3.15, where the metastable states have higher free energy than both the heterogeneous states along Maxwell's rule and the states along the stable parts of the isotherm.

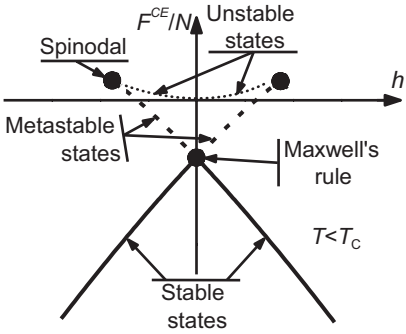

Fig. 3.16 The equilibrium free energy

In Fig. 3.16, we present the dependence of the equilibrium free energy on the magnetic field h for a given value of temperature below critical. The one-phase branches of the stable states are the lowest in the figure. The two-phase region of Maxwell's rule degenerates here into the point at the intersection of these branches. From this point, two metastable branches disperse upward which transform at the spinodal points into the unstable branch.

Again, Fig. 3.16 is only an isothermic cross-section of some three-dimensional surface. This surface itself is presented in Fig. 3.17. Above the critical point, it has only one sheet. Below the critical point, additional sheets of metastable and unstable states appear which are located higher than the stable sheet. The two-phase region of Maxwell's rule collapses into the coexistence curve. The metastable sheets are separated from the unstable sheet by two spinodal curves.

The reader should clearly distinguish Figs. 3.16 and 3.17 for the equilibrium free energy from Figs. 3.6 and 3.7 for the nonequilibrium free energy. In Figs. 3.6 and 3.7, for the given values of field and temperature, we were looking for the minimum of the free energy over all possible nonequilibrium values of m. On the contrary, in Figs. 3.16 and 3.17, magnetization is already a solution of the equation of state

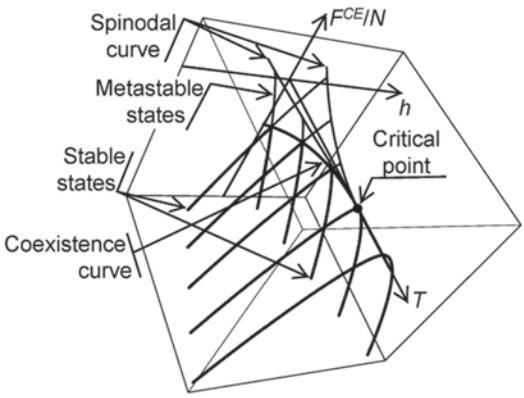

Fig. 3.17 The equilibrium free energy

(3.92), and metastable states, overlooked by it, are the only remnants of nonequilibrium states. Therefore, in Figs. 3.16 and 3.17, the free energy minimization principle degenerates into the choice between the stable and metastable branches when we choose the lower sheet.

3.6.7 Classification of Phase Transitions

The critical point is generally considered to represent a continuous (second-order) phase transition while the binodal and spinodal curves, originating at this point, are representatives of a first-order transition. Classification defines that at the point of *a continuous phase transition* the derivatives of the equilibrium free energy (or a quasi-equilibrium free energy of metastable states) with respect to field parameters of the system should be zero. On the contrary, a nonzero derivative indicates the presence of *a first-order phase transition*.

There are two field parameters in Landau theory: the magnetic field h and the relative deviation t of the temperature from critical. So, we should investigate when two derivatives, $(\partial F^{CE}/\partial h)_t$ and $(\partial F^{CE}/\partial t)_h$, are zero, where the ensemble free energy is

$$F^{CE} = N\mu(-2A\ln 2 - hm_0 + atm_0{}^2 + bm_0{}^4 + \ldots). \tag{3.150}$$

Differentiating, we find

$$\left(\frac{\partial F^{CE}}{\partial h}\right)_t = -N\mu m_0 + N\mu(-h + 2atm_0 + 4bm_0{}^3 + \ldots)\left(\frac{\partial m_0}{\partial h}\right)_t = 0 \tag{3.151}$$

and

$$\left(\frac{\partial F^{CE}}{\partial t}\right)_h = N\mu am_0{}^2 + N\mu(-h + 2atm_0 + 4bm_0{}^3 + \ldots)\left(\frac{\partial m_0}{\partial t}\right)_h = 0, \tag{3.152}$$

where the derivatives $\partial m_0/\partial h$ and $\partial m_0/\partial t$ we obtain by differentiating the equation of state (3.92):

$$\left(\frac{\partial m_0}{\partial h}\right)_t = \frac{1}{2at + 12bm_0{}^2}, \quad \left(\frac{\partial m_0}{\partial t}\right)_h = \frac{-m_0}{t + 6bm_0{}^2/a}. \tag{3.153}$$

We consider the states at the binodal curve. The binodal curve is determined by (3.97) when $h = 0, t \le 0$. Substituting these equations into (3.151) and (3.152), we find that the continuous phase transition takes place only at $t = 0$. In other words, the critical point represents the continuous phase transition in our system while the rest of the binodal curve is the first-order transition.

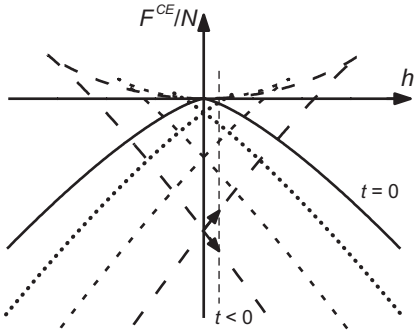

Fig. 3.18 The free energy difference between stable and metastable states

This could be easily illustrated with the aid of Fig. 3.16. For simplicity, we investigate only the behavior of the derivative $(\partial F^{CE} / \partial h)_t$. Let us suppose that we consider a point at the binodal curve below the critical point: $h = 0, t < 0$.

The meaning of the derivative $(\partial F^{CE} / \partial h)_t$ is how the equilibrium (or quasi-equilibrium) free energy would change if we introduced a nonzero magnetic field. One phase would slide downward along the stable branch while another phase would climb up the branch of metastable states (two small arrows in Fig. 3.18). We see that well below the critical point the difference is pronounced; the metastable free energy is clearly higher than the free energy of the stable phase.

However, when we approach the critical temperature, the phase branches become less and less steep (Fig. 3.18). Exactly at critical point the metastable and unstable branches disappear leaving only the single continuous stable branch with zero derivative at zero magnetic field. So, this is how in practice the first-order phase transition transforms into the continuous phase transition in the proximity of the critical point.

We see now that the first-order phase transition differs from the continuous phase transition by the presence of metastable states whose free energy is higher than the free energy of stable states. Therefore, we can add to the rule of the classification of phase transitions that the presence of metastable states clearly indicates that the phase transition is of the first order.

3.6.8 Critical and Spinodal Slowing Down

Let us study in more detail the processes of relaxation of fluctuations. First, we consider the system above the critical point ($t > 0$) in the absence of magnetic field ($h = 0$). We assume that a noise term in the Ginzburg–Landau–Langevin equation (3.107) has created a fluctuation that has "tossed" the system up along the slope of the free energy potential (Fig. 3.19). Next, we remove the noise from this equation,

$$\frac{\partial m}{\partial (time)} = -B \frac{\partial F_{\{\{m\}\}}}{\partial m}, \tag{3.154}$$

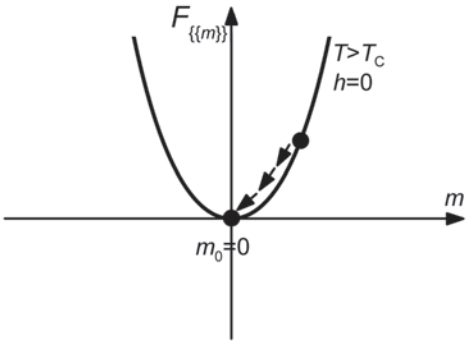

Fig. 3.19 The relaxation process attenuates the fluctuation, returning the system back to the bottom of the free energy minimum

and observe how the relaxation process returns the system back to the bottom of the free energy minimum.

The steeper the slope of the free energy "wall," the higher the derivative $|\partial F_{\{\{m\}\}} / m|$, and the faster the relaxation process (3.154) is. However, when the system approaches the bottom of the minimum, the value of the derivative $|\partial F_{\{\{m\}\}} / m|$ decreases, and so does the speed of the relaxation process.

In the vicinity of the point of the minimum $m_0 = 0$, the dependence of $F_{\{\{m\}\}}$ on m is parabolic:

$$F_{\{\{m\}\}} \propto N\mu(-2A\ln 2 + atm^2 + \ldots). \tag{3.155}$$

Substituting (3.155) into (3.154), we obtain the ordinary differential equation

$$\frac{dm}{m} = -2BN\mu at \cdot d(time) \tag{3.156}$$

whose solution is

$$|m| \propto e^{-(time)/(time)_{ref}}, \tag{3.157}$$

where $(time)_{ref}$ is

$$(time)_{ref} \equiv \frac{1}{2BN\mu at}. \tag{3.158}$$

We see that fluctuations decay exponentially with the characteristic time of the decay provided by (3.158).

We can generalize this case for the nonzero field $h > 0$ as well. This time the equilibrium value of magnetization is not zero but some value $m_0 > 0$, which is provided by the solution of the cubic equation of state (3.92). Expanding the free energy (3.105) in the vicinity of this point, we return to the parabolic dependence which is obvious from Fig. 3.20:

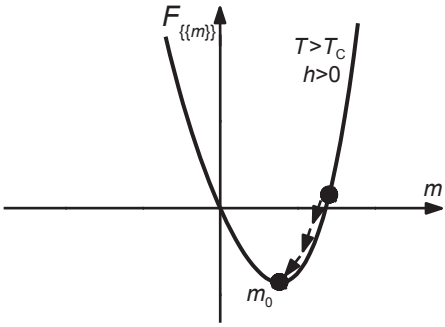

Fig. 3.20 The relaxation process for the system above the critical point in the nonzero magnetic field

$$F_{\{\{m\}\}} = F_{\{\{m_0\}\}} + N\mu(\{at + 6bm_0{}^2\}(m - m_0)^2 + \ldots). \tag{3.159}$$

But in accordance with (3.115), the susceptibility,

$$\chi = \frac{1}{2at + 12bm_0{}^2}, \tag{3.160}$$

represents the inverse coefficient we see in the expansion of the free energy (3.159):

$$F_{\{\{m\}\}} = F_{\{\{m_0\}\}} + N\mu\left(\frac{(m - m_0)^2}{2\chi} + \ldots\right). \tag{3.161}$$

Next, we again consider a fluctuation "tossing" the system up the slope of the free energy potential (Fig. 3.20). Substituting (3.161) into the Ginzburg–Landau–Langevin equation (3.154), we obtain the ordinary differential equation

$$\frac{d(m - m_0)}{(m - m_0)} = -\frac{BN\mu}{\chi} d(time) \tag{3.162}$$

whose solution is

$$| m - m_0 | \propto e^{-(time)/(time)_{ref}}, \tag{3.163}$$

where $(time)_{ref}$ is

$$(time)_{ref} \equiv \frac{\chi}{BN\mu}. \tag{3.164}$$

The decay of fluctuations is exponential with time again.

As a next example, let us consider fluctuations in the vicinity of the local minimum of the free energy when the system is below the critical point ($t < 0$) and mag-

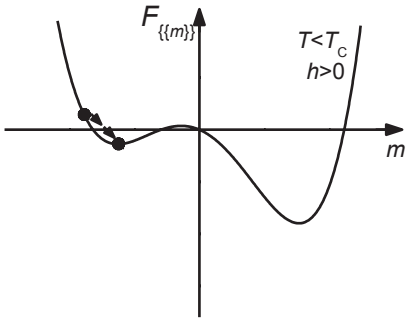

Fig. 3.21 The relaxation process below the critical point attenuates the fluctuation, returning the system back to the bottom of the local minimum

netic field is nonzero ($h > 0$). To find the point of the local minimum, we consider the solution $m_0 < 0$ of the cubic equation of state (3.92). Expanding the free energy (3.105) in the vicinity of this point, we return to the parabolic dependence (3.161), which is obvious from Fig. 3.7. Considering a relaxation process in the vicinity of the local minimum (Fig. 3.21), we obtain the solution which is identical to (3.163) and (3.164).

One more time we see that the decay of fluctuations is exponential with time. Why does this happen again and again? Is this tendency general?

Above we have considered the vicinity of the free energy minima, where the dependence of the free energy on the deviations of magnetization from the equilibrium value was parabolic. It is obvious that substituting the parabolic dependence into the Ginzburg–Landau–Langevin equation (3.154), each time we will obtain the exponential decay of fluctuations. Therefore, this tendency is quite general for the near-equilibrium fluctuations in Landau theory with the exception of some special cases we consider below.

Let us return to the relaxation process (3.163) valid both above and below the critical point. From (3.164), we see that the characteristic time of the decay of the relaxation process is proportional to the susceptibility of the system. But the susceptibility diverges in the vicinity of the critical and spinodal points. Therefore, so does the characteristic time of the decay (with the same values of critical and spinodal indices). This phenomenon is called *the (critical or spinodal) slowing down*.

However, considering the system at the critical or spinodal point, we can no longer rely on the formulae above. Indeed, at these points, the dependence of the free energy (3.105) in the vicinity of its minimum is no longer parabolic.

So, at the critical point, substituting $t = 0$ and $h = 0$ into (3.105), we should consider the fourth-power dependence:

$$F_{\{\{m\}\}} = N\mu(-2A\ln 2 + bm^4 + \ldots). \tag{3.165}$$

Considering a fluctuation (Fig. 3.22), we substitute (3.165) into the Ginzburg–Landau–Langevin equation (3.154) to obtain the ordinary differential equation:

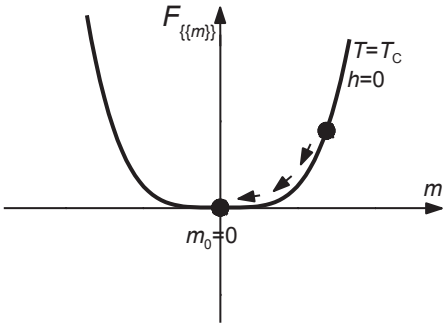

Fig. 3.22 The relaxation process at the critical point

$$\frac{dm}{m^3} = -4BN\mu b \cdot d(time). \tag{3.166}$$

The solution is

$$|\, m \,| = \frac{1}{\sqrt{8BN\mu b \cdot (time) + const}}. \tag{3.167}$$

In the limit of long relaxation time, $(time) \to +\infty$, the decay (3.167) becomes a power-law decay:

$$|\, m \,| = \frac{1}{\sqrt{8BN\mu b \cdot (time)}}. \tag{3.168}$$

If we define the critical index τ^C by

$$|\, m \,| = \frac{1}{(time)^{\tau^C}}, \tag{3.169}$$

Landau theory determines $\tau^C = 1/2$.

Finally, we consider the system at the spinodal point. Substituting (3.109) into (3.105), we find the dependence of $F_{\{\{m\}\}}$ on the nonequilibrium value of m to be cubic which is obvious in the vicinity of the point of inflection:

$$F_{\{\{m\}\}} = F_{\{\{m_S\}\}} + N\mu\left(-2\sqrt{-\frac{2}{3}abt_S}\,(m - m_S)^3 + \ldots\right). \tag{3.170}$$

Next, as usual, we consider a fluctuation. Only this time the fluctuation is not required to return the system back to the metastable state (Fig. 3.23); so the process will not attenuate fluctuation but, on the contrary, will lead the system to the bottom

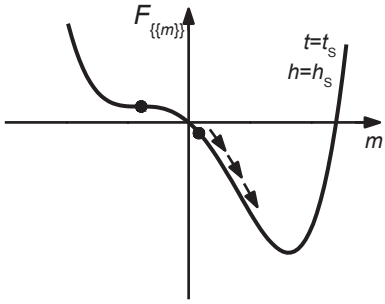

Fig. 3.23 The dynamical process at the spinodal point

of the global minimum. Nevertheless, we can discuss the speed of this process in the vicinity of the point of inflection.

Substituting (3.170) into (3.154), we find the ordinary differential equation,

$$\frac{dm}{(m-m_S)^2} = 2BN\mu\sqrt{-6abt_S}\cdot d(time), \tag{3.171}$$

whose solution is

$$(m-m_S) = -\frac{1}{const + 2BN\mu\sqrt{-6abt_S}\cdot(time)}. \tag{3.172}$$

This solution can be interpreted in two different ways. If initially $(m(0)-m_S)<0$ so that the fluctuation has "tossed" the system to the left from the inflection point in Fig. 3.23, we observe the relaxation process toward the inflection point:

$$|\,m-m_S\,| = \frac{1}{const + 2BN\mu\sqrt{-6abt_S}\cdot(time)} \tag{3.173}$$

which in the limit of long relaxation times

$$|\,m-m_S\,| = \frac{1}{2BN\mu\sqrt{-6abt_S}\cdot(time)} \tag{3.174}$$

provides the power-law decay of the fluctuation. For the spinodal index:

$$|\,m\,| = \frac{1}{(time)^{\tau^S}} \tag{3.175}$$

this returns $\tau^S = 1$.

On the contrary, if we consider $(m(0)-m_S)>0$ initially so that the fluctuation has "tossed" the system to the right in Fig. 3.23, toward the global minimum, the difference $(m-m_S)$ continue to increase as

$$(m - m_S) = \frac{1}{(m(0) - m_S)^{-1} - 2BN\mu\sqrt{-6abt_S} \cdot (time)}, \tag{3.176}$$

leading the system to the stable state at the bottom of the global minimum. The time necessary to reach this state is inversely proportional to the initial difference $(m(0) - m_S)$:

$$(time) \propto \frac{1}{(m(0) - m_S)} \tag{3.177}$$

so that the bigger the initial fluctuation is, the sooner the system will reach the stable state.

3.6.9 Heterogeneous System

So far, in all our formulae, the value of magnetization m has not depended on the coordinates within the system; and the only heterogeneous states we considered were provided by Maxwell's rule. Even when we minimized the free energy over all possible nonequilibrium states in Figs. 3.6 and 3.7, we considered, in fact, only homogeneous states with the uniform magnetization over the lattice.

But the homogeneous system is just an idealization that helps us to find the solution. Systems in nature are heterogeneous when magnetization (or density in the liquid–gas systems) is not required to be uniform over the space of a system.

What would happen if we were looking at a heterogeneous system? And first, how do we build a heterogeneous system? We should divide the lattice into magnetic *domains* (*clusters*). For simplicity, we consider that inside each domain the magnetization is uniform but it changes when we move from one domain to another. Then, the free energy will be the sum of the domain's free energies.

But how does it happen in practice? In Fig. 3.24, we consider one of the isotherms of the homogeneous system below the critical point in nonzero magnetic

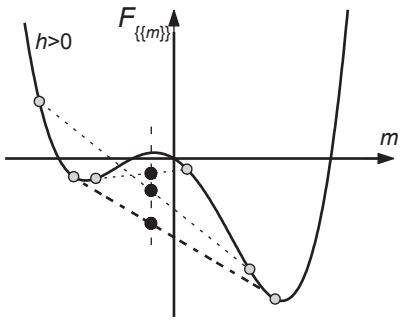

Fig. 3.24 The rule of mixture for two types of domains

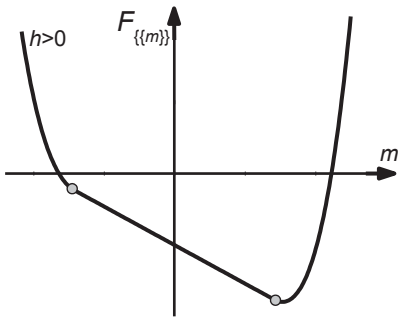

Fig. 3.25 Maxwell's rule for the case of nonzero magnetic field

field. What we want is to use this curve to build the domain's uniform magnetizations and then to mix these domains in the volume of the heterogeneous system.

Let us first build the simplest heterogeneous state when we choose a priori two different values of magnetization, and the domain's magnetizations in the heterogeneous system may be equal only to one or another of these two values. Empty circles in Fig. 3.24 represent the separate homogeneous domains, which we are mixing, while dotted lines, connecting empty circles into pairs, are the mixing itself.

The magnetization of the heterogeneous system equals the domain's magnetizations averaged over the lattice. Let a vertical dashed line represent the desired value of the averaged magnetization. Then filled circles which we build at the intersections of the dotted lines and the vertical dashed line are the results of the mixture. An ordinate of any of these filled circles equals the total free energy of the heterogeneous system provided by the domain's free energies averaged over the lattice.

Following the free energy minimization principle, we are looking for the mixture with the minimal free energy. This is the lowest filled circle when the dotted mixing line is tangent to the homogeneous isotherm at two different points. After we have built this line, we can remove the part of the isotherm above it as having higher values of the free energy and, therefore, as "less equilibrium."

The final result of our work is presented in Fig. 3.25. It represents those mixtures which have the minimal free energy for the given value of the averaged over the lattice magnetization. However, so far the free energy has not been minimized yet by the value of the averaged magnetization itself which is still nonequilibrium.

We should mention that although we have considered the simplest case when the domain's magnetizations had values only of two possible, it has lead us to the correct dependence of the free energy of the heterogeneous system. If we considered mixing domains with arbitrary magnetizations, this would not do us any better. Indeed, the reader can consider mixing not just two empty circles in Fig. 3.24 but three, four, or any number of circles lying on the homogeneous curve. In any case, the lowest value (for the given averaged magnetization) of the free energy of the mixture will still correspond to Fig. 3.25.

Let us minimize the free energy of mixture for all isotherms in Fig. 3.7. The result is presented in Fig. 3.26. In all cases, the "straightening" line has been drawn as a tangent to the curve at two points.

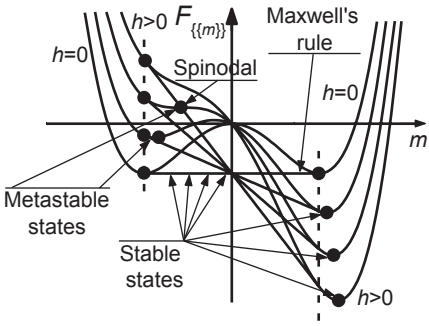

Fig. 3.26 Maxwell's rules for different values of the magnetic field

For the zero magnetic field, this line is horizontal. It starts from the bottom of one minimum and ends at the bottom of another minimum. This, in fact, is Maxwell's rule we have introduced before. It represents the line, along which the free energy potential degenerates and instead of a discrete point of global minimum provides a continuous range of minimal values. Each point on this line represents a stable heterogeneous state as a mixture of phases (3.97) with positive and negative magnetizations.

For the nonzero field, the "straightening" lines start and finish not at the points of minima. On the contrary, from Fig. 3.26, it is easy to see that they all start and finish at the same values of magnetization which are shown by vertical dashed lines. These two values of magnetization are easy to be found because we already know that in the absence of magnetic field they coincide with the equilibrium solutions (3.97).

However, here we have come to a contradiction. If we look at Fig. 3.26, we see that for all isotherms the "straightening" lines have removed the potential barriers between two minima. Now nothing prevents the system, which "follows" the "slope" of these lines, to "roll down" from any initial state into the stable state of the global minimum. In other words, the introduction of the heterogeneity has eliminated local minima and made the existence of metastable states impossible.

But although almost all systems in nature are heterogeneous (like a liquid–gas system which consists of the mixture of liquid and gas domains), this does not prevent the possibility for these systems to be metastable (like a superheated liquid or a supercooled gas).

Therefore, a system, that is described mathematically as heterogeneous, still can possess metastable states, provided by some local minima behind some potential barrier. But what causes this potential barrier, dividing metastable and stable states, to appear in a heterogeneous system?

To answer this question, we should look back at what we have overlooked in our previous analysis. We introduced the heterogeneity as the system's lattice divided into domains with different magnetizations. Then, we built the rule how to mix these domains by connecting them with dotted lines in Fig. 3.24. Simultaneously, we assumed that the total free energy of the system is the sum of the domain's free

energies, and therefore, the ordinates of our filled circles, built at dotted lines, provide correct values for the total free energy of the heterogeneous system.

This was our mistake because the theory developed above has correctly taken into account the volumetric free energy of separate domains but overlooked the interactions of domains at their boundaries. Indeed, at the boundary between two phases, adjacent spins have presumably opposite orientations. This leads to the additional free energy, necessary to create the boundary. This additional energy is the most known in liquid–gas systems as the concept of surface tension.

Let us consider the appearance of a bubble belonging to the stable phase inside a metastable medium. Inside the bubble's volume, the system gets a benefit of lower free energy because the new phase corresponds to the global minimum and, therefore, has lower volumetric free energy than the metastable medium. However, the appearance of the bubble requires some energy to create its surface. The "wrestle" of these two factors leads to the appearance of a new *potential barrier* dividing local and global minima of the free energy.

A system in a metastable state can easily produce only small nuclei of stable phase because only small fluctuations are probable. Creation of these nuclei is equivalent to that the system jumps due to a fluctuation up the slope of the barrier toward the global minimum.

But small nuclei are disadvantageous because their volumetric benefit in lower free energy of stable phase is negligible in comparison with the surface energy. Therefore, the system "rolls down" from the wall of the potential barrier back into the local minimum by dissolving all created nuclei. Then, the system experiences another fluctuation, again jumps up the slope, and returns back to the bottom. And so on, and so on.

The system would not return back to the local minimum if a created nucleus were big enough, when the loss in the volumetric energy would overcome the gain in the surface energy. But the big nucleus means a large fluctuation which is improbable.

The nucleus, when the volumetric loss equals the surface gain of the energy, corresponds to the peak of the potential barrier and is called *a critical nucleus*.

Therefore, for the long time, the system fluctuates around the local, metastable minimum until an improbable fluctuation creates a nucleus with the size larger than critical. In other words, until the improbable fluctuation tosses the system to the top of the potential barrier or even farther. Then, the quick, "explosive" process follows, transferring the system to the stable state at the bottom of the global minimum. By "rapid boiling or precipitation," the total system almost instantaneously transforms into the stable phase.

We say here "almost instantaneously" in contrast with the long lifetime of the metastable state. The difference between these two timescales may be of many orders of magnitude. As an illustration, we could imagine a bomb stored on a military base. For the long decades or centuries, the bomb remains latent although energetically it would be beneficial to split the complex chemical compound into simpler substances. But the potential barrier of self-ignition prohibits the bomb to do that. Finally, after multiple attempts, thermal fluctuations create the local heat increase

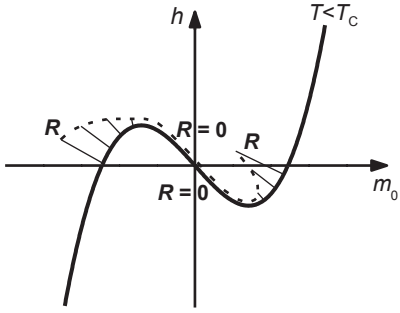

Fig. 3.27 The epure of the critical nucleus radius

equivalent to the critical nucleus. The consequence is an explosion whose duration is negligible in comparison with the previous long life in warehouse.

For the stable, one-phase parts of the isotherms below the critical point, the system always returns to the stable state, no matter how huge the fluctuations are. Therefore, the size R of the critical nucleus has no physical meaning for these states or can be considered to be infinite.

When entering the metastable region, the size of the critical nucleus continuously decreases and becomes almost zero at the spinodal point, where very small fluctuations (like a flip of one spin or a collision of a couple of molecules) can trigger the collapse of the metastable state. This behavior of the critical radius is schematically shown in Fig. 3.27 as an epure over the equation of state.

As we said, in the vicinity of the spinodal point, the radius of the critical nucleus is very small, and even small fluctuations are capable to toss the system behind the very small potential barrier. This makes the experimental investigations difficult and the spinodal itself is often unreachable in experiments. For this particular reason, the spinodal power-law scaling was discovered much later than its critical analogue.[3]

The described phenomena of nucleus birth are studied by the theory of nucleation. Generally, this theory requires functional (field) description of heterogeneous phenomena and takes into account the shape of nuclei (Gunton and Droz 1983; Kashchiev 2000). But this discussion lies beyond the scope of our book.

At the end of this chapter, we would like to say that it is wonderful how such complex and beautiful phenomena as criticality and spinodal are described only by the first three terms of the free energy expansion in Landau theory!

[3] However, there are systems (generally with long relaxation times) in which it is quite possible to observe in experiment the spinodal point and even the behavior of unstable states. The classical example is binary alloys which below the critical point split into phases of separate metals. The relaxation times in such systems can be of the order of days or months. Therefore, it is quite possible to observe these systems in the vicinity or inside of the unstable region.

3.7 Mean-Field Approach

Problem 3.7.1

For the ferromagnetic n.n. Ising model, develop the mean-field approach by replacing the interactions of spins in pairs by the effective field generated by all spins together (the Weiss theory of ferromagnetism (Weiss 1907)). Find the ensemble partition function, the ensemble Helmholtz energy, and the equation of state.

Solution: We should replace the interactions $-J\sum_{<i,j>_{n.n.}}\sigma_i\sigma_j$ of spins in pairs by some effective field. Every spin has q neighbors on the lattice, where q is the lattice coordination number. Let us replace one of spins in the product $\sigma_i\sigma_j$ by its value averaged over the lattice:

$$-J\sum_{<i,j>_{n.n.}}\sigma_i\sigma_j=-\frac{J}{2}\sum_{i=1}^{N}\sigma_i\sum_{j_{n.n.of\,i}}\sigma_j\approx-\frac{J}{2}\sum_{i=1}^{N}\sigma_i\sum_{j_{n.n.of\,i}}\left\langle\sigma_j\right\rangle_{\{\sigma\}}=$$

$$=-\frac{Jq}{2}\left\langle\sigma\right\rangle_{\{\sigma\}}\sum_{i=1}^{N}\sigma_i=-\mu h_{\{\sigma\}}^{eff}\sum_{i=1}^{N}\sigma_i, \tag{3.178}$$

where $\left\langle\ldots\right\rangle_{\{\sigma\}}$ denotes averaging over the spin orientations on the lattice of the microstate $\{\sigma\}$ and

$$h_{\{\sigma\}}^{eff}\equiv\frac{Jq}{2\mu}\left\langle\sigma\right\rangle_{\{\sigma\}}=\frac{Jq}{2\mu}m_{\{\sigma\}}. \tag{3.179}$$

Multiplier 1/2 appears due to that summing over all spins, $\sum_{i=1}^{N}\sum_{j_{n.n.of\,i}}$, we have counted each n.n. pair twice.

This provides the following approximation for the Hamiltonian:

$$H_{\{\sigma\}}\approx-\mu(h+h_{\{\sigma\}}^{eff})\sum_{i=1}^{N}\sigma_i=-\mu\left(h+\frac{Jq}{2\mu}m_{\{\sigma\}}\right)m_{\{\sigma\}}. \tag{3.180}$$

Substituting (3.180) into (3.80), we find the equation of state:

$$m_0=\tanh\left(\frac{1}{T}\{\mu h+Jqm_0\}\right). \tag{3.181}$$

For the critical temperature, this equation provides:

$$T_C=Jq. \tag{3.182}$$

Problem 3.7.2

For the ferromagnetic n.n. Ising model, develop the mean-field approach by neglecting spin correlations (the Bragg–Williams theory of ferromagnetism (Brag and Williams 1934, 1935)). Find the ensemble partition function, the ensemble Helmholtz energy, and the equation of state.

Solution: Let us consider the correlation of two n.n. spins on the lattice of a microstate $\{\sigma\}$:

$$\left\langle \left(\sigma_i - \langle \sigma_i \rangle_{\{\sigma\}}\right)\left(\sigma_{j_{n.n.of\,i}} - \left\langle \sigma_{j_{n.n.of\,i}} \right\rangle_{\{\sigma\}}\right)\right\rangle_{\{\sigma\}} = \left\langle \sigma_i \sigma_{j_{n.n.of\,i}} \right\rangle_{\{\sigma\}} - m_{\{\sigma\}}{}^2. \quad (3.183)$$

Neglecting spin correlations in (3.183),

$$\left\langle \left(\sigma_i - \langle \sigma_i \rangle_{\{\sigma\}}\right)\left(\sigma_{j_{n.n.of\,i}} - \left\langle \sigma_{j_{n.n.of\,i}} \right\rangle_{\{\sigma\}}\right)\right\rangle_{\{\sigma\}} \approx 0, \quad (3.184)$$

we find

$$\left\langle \sigma_i \sigma_{j_{n.n.of\,i}} \right\rangle_{\{\sigma\}} \approx m_{\{\sigma\}}{}^2 \quad (3.185)$$

or

$$\left\langle \sigma_i \sigma_{j_{n.n.of\,i}} \right\rangle_{\{\sigma\}} \approx \langle \sigma_i \rangle_{\{\sigma\}} \left\langle \sigma_j \right\rangle_{\{\sigma\}}. \quad (3.186)$$

Each spin has q nearest neighbors, so there are $Nq/2$ n.n. pairs on the lattice. Multiplier 1/2 appears here because summing over q nearest neighbors for each of N spins, we have countered each pair twice. The averaged over the lattice correlation of two neighboring spins is defined by

$$\left\langle \sigma_i \sigma_{j_{n.n.of\,i}} \right\rangle_{\{\sigma\}} = \frac{\sum_{<i,j>_{n.n.}} \sigma_i \sigma_j}{Nq/2} \quad (3.187)$$

while the magnetization, averaged over the lattice of a microstate $\{\sigma\}$, is defined by

$$\langle \sigma_i \rangle_{\{\sigma\}} = \frac{\sum_{i=1}^{N} \sigma_i}{N}. \quad (3.188)$$

Substituting (3.187) and (3.188) into (3.184–186), we find

$$\frac{1}{Nq/2}\sum_{<i,j>_{n.n.}}\sigma_i\sigma_j \approx \left(\frac{1}{N}\sum_{i=1}^{N}\sigma_i\right)^2. \tag{3.189}$$

So, neglecting spin correlations, we have been able to express the short-range order parameter in terms of the long-range order parameter. The rest of the solution is straightforward and follows the discussion of Sect. 3.5. As a result, we obtain the effective field and the equation of state coinciding with (3.179) and (3.181), respectively.

Problem 3.7.3

For the ferromagnetic n.n. Ising model, find the equation of state with the aid of the Gibbs–Bogolyubov–Feynman inequality. Find the ensemble partition function and the ensemble Helmholtz energy.

Solution: Let $\mathrm{H}_{\{\sigma\}}$ be the exact Hamiltonian of a model. For the case of the n.n. Ising model, the exact Hamiltonian is given by

$$\mathrm{H}_{\{\sigma\}} = -\mu h\sum_{i=1}^{N}\sigma_i - J\sum_{<i,j>_{\mathrm{n.n.}}}\sigma_i\sigma_j. \tag{3.190}$$

We approximate the exact Hamiltonian (3.190) with a model Hamiltonian $\tilde{\mathrm{H}}_{\{\sigma\}}$.

The exact partition function is defined as

$$Z^{CE} \equiv \sum_{\{\sigma\}} e^{-\mathrm{H}_{\{\sigma\}}/T}. \tag{3.191}$$

Let us perform the following transformations

$$\begin{aligned} Z^{CE} &= \left(\sum_{\{\sigma\}'} e^{-\tilde{\mathrm{H}}_{\{\sigma\}'}/T}\right)\left(\sum_{\{\sigma\}} e^{-\left(\mathrm{H}_{\{\sigma\}}-\tilde{\mathrm{H}}_{\{\sigma\}}\right)/T}\frac{e^{-\tilde{\mathrm{H}}_{\{\sigma\}}/T}}{\left(\sum_{\{\sigma\}''} e^{-\tilde{\mathrm{H}}_{\{\sigma\}''}/T}\right)}\right) = \\ &= \tilde{Z}^{CE}\left(\sum_{\{\sigma\}} e^{-\left(\mathrm{H}_{\{\sigma\}}-\tilde{\mathrm{H}}_{\{\sigma\}}\right)/T}\frac{e^{-\tilde{\mathrm{H}}_{\{\sigma\}}/T}}{\tilde{Z}^{CE}}\right), \end{aligned} \tag{3.192}$$

where $\tilde{Z}^{CE}$ is the partition function of the system with the model Hamiltonian $\tilde{\mathrm{H}}_{\{\sigma\}}$:

$$\tilde{Z}^{CE} = \sum_{\{\sigma\}} e^{-\tilde{\mathrm{H}}_{\{\sigma\}}/T}. \tag{3.193}$$

In (3.192), the sum represents the averaging of the quantity $e^{-\left(\mathrm{H}_{\{\sigma\}}-\tilde{\mathrm{H}}_{\{\sigma\}}\right)/T}$ with the probabilities $\dfrac{e^{-\tilde{\mathrm{H}}_{\{\sigma\}}/T}}{\tilde{Z}^{CE}}$, corresponding to Gibbs probabilities of the system with the model Hamiltonian $\tilde{\mathrm{H}}_{\{\sigma\}}$. In other words, it is averaging over the CE of the model Hamiltonian:

$$Z^{CE} = \tilde{Z}^{CE} \left\langle e^{-\left(\mathrm{H}_{\{\sigma\}}-\tilde{\mathrm{H}}_{\{\sigma\}}\right)/T} \right\rangle_{\tilde{\mathrm{H}}}. \tag{3.194}$$

Again, we apply some simple transformations to the last expression:

$$Z^{CE} = \tilde{Z}^{CE} e^{-\left\langle \mathrm{H}_{\{\sigma\}}-\tilde{\mathrm{H}}_{\{\sigma\}} \right\rangle_{\tilde{\mathrm{H}}}/T} \left\langle e^{-\left(\left(\mathrm{H}_{\{\sigma\}}-\tilde{\mathrm{H}}_{\{\sigma\}}\right)-\left\langle \mathrm{H}_{\{\sigma\}}-\tilde{\mathrm{H}}_{\{\sigma\}} \right\rangle_{\tilde{\mathrm{H}}}\right)/T} \right\rangle_{\tilde{\mathrm{H}}}. \tag{3.195}$$

Next, we utilize the algebraic inequality

$$e^{-x} \geq 1 - x. \tag{3.196}$$

Applying this inequality to (3.195), we find

$$\begin{aligned} Z^{CE} &\geq \tilde{Z}^{CE} e^{-\left\langle \mathrm{H}_{\{\sigma\}}-\tilde{\mathrm{H}}_{\{\sigma\}} \right\rangle_{\tilde{\mathrm{H}}}/T} \left\langle 1-\left(\left(\mathrm{H}_{\{\sigma\}}-\tilde{\mathrm{H}}_{\{\sigma\}}\right)-\left\langle \mathrm{H}_{\{\sigma\}}-\tilde{\mathrm{H}}_{\{\sigma\}} \right\rangle_{\tilde{\mathrm{H}}}\right)/T \right\rangle_{\tilde{\mathrm{H}}} \\ &= \tilde{Z}^{CE} e^{-\left\langle \mathrm{H}_{\{\sigma\}}-\tilde{\mathrm{H}}_{\{\sigma\}} \right\rangle_{\tilde{\mathrm{H}}}/T} \left(1-\left(\left\langle \mathrm{H}_{\{\sigma\}}-\tilde{\mathrm{H}}_{\{\sigma\}} \right\rangle_{\tilde{\mathrm{H}}}-\left\langle \mathrm{H}_{\{\sigma\}}-\tilde{\mathrm{H}}_{\{\sigma\}} \right\rangle_{\tilde{\mathrm{H}}}\right)/T\right) \\ &= \tilde{Z}^{CE} e^{-\left\langle \mathrm{H}_{\{\sigma\}}-\tilde{\mathrm{H}}_{\{\sigma\}} \right\rangle_{\tilde{\mathrm{H}}}/T}. \end{aligned} \tag{3.197}$$

Since the logarithm is the monotonically increasing function, we find *the Gibbs–Bogolyubov–Feynman inequality* (Gibbs 1902; Bogoliubov 1947a, b, 1962a, b; Feynman 1972) for the ensemble Helmholtz energy:

$$F^{CE} \leq \tilde{F}^{CE} + \left\langle \mathrm{H}_{\{\sigma\}} - \tilde{\mathrm{H}}_{\{\sigma\}} \right\rangle_{\tilde{\mathrm{H}}}. \tag{3.198}$$

In other words, the equilibrium value of the free energy of the real system is always less than (or equal to) the right-hand side of (3.198); and this statement is valid for an arbitrary model Hamiltonian $\tilde{\mathrm{H}}_{\{\sigma\}}$. Therefore, minimizing the functional

$$\Psi\left[\tilde{\mathrm{H}}_{\{\sigma\}}\right] = \tilde{F}^{CE} + \left\langle \mathrm{H}_{\{\sigma\}} - \tilde{\mathrm{H}}_{\{\sigma\}} \right\rangle_{\tilde{\mathrm{H}}} \tag{3.199}$$

over the functional space of all possible model Hamiltonians, we will approximate the exact value of the free energy of the real system.

To obtain the exact value F^{CE} of the free energy, we should consider all possible functional dependencies $\tilde{\mathrm{H}}_{\{\sigma\}}$. But it is very difficult. Instead, we could consider only some simple functional dependencies of model Hamiltonians and minimize functional (3.199) only over them. This would not, of course, provide the exact value F^{CE} of the free energy but it would give us at least some approximation.

The functional dependencies of model Hamiltonians, over which we will minimize functional (3.199), should be rather simple so that we could perform all calculations analytically. But the simplest dependence is the Hamiltonian (3.18) of the ideal system. Only now, to represent the nonideal system, we should add the effective field to this Hamiltonian:

$$\tilde{\mathrm{H}}_{\{\sigma\}} = -\mu\left(h + h^{eff}\right)\sum_{i=1}^{N}\sigma_i. \tag{3.200}$$

So, we are going to minimize functional (3.199) not over all possible functional dependencies of the model Hamiltonians but only over the simplest dependences presented by (3.200). These functional dependencies are parameterized by values h^{eff} of the effective field. So, our purpose is to substitute (3.200) into (3.199) and to minimize the obtained functional over the values of the effective field h^{eff} as if over the values of a fitting parameter. This will provide the approximation of the exact value of the free energy F^{CE}.

The partition function of the model Hamiltonian (3.200) has been found before in (3.32):

$$\tilde{Z}^{CE} = \left(2\cosh\frac{\mu(h + h^{eff})}{T}\right)^{N}. \tag{3.201}$$

The equilibrium magnetization is also already known from (3.41):

$$m_0 = \tanh\frac{\mu(h + h^{eff})}{T}. \tag{3.202}$$

The problem is to find the value of the real Hamiltonian averaged over the ensemble of the model Hamiltonian: $\left\langle \mathrm{H}_{\{\sigma\}}\right\rangle_{\tilde{\mathrm{H}}}$. Not of our own will, but we have to return here to the previous approximation of Problem 3.7.2 when we neglected the correlations among spins:

$$\left\langle \mathrm{H}_{\{\sigma\}}\right\rangle_{\tilde{\mathrm{H}}} = -\mu h\sum_{i=1}^{N}\left\langle\sigma_i\right\rangle_{\tilde{\mathrm{H}}} - J\sum_{<i,j>_{n.n.}}\left\langle\sigma_i\sigma_j\right\rangle_{\tilde{\mathrm{H}}} \approx -\mu hNm_0 - \frac{NqJ}{2}{m_0}^2, \tag{3.203}$$

where m_0 depends on h^{eff} in accordance with (3.202).

The averaging of the model Hamiltonian over the ensemble of the model Hamiltonian can be found in a similar way:

$$\left\langle \tilde{\mathrm{H}}_{\{\sigma\}} \right\rangle_{\tilde{\mathrm{H}}} = -\mu\left(h + h^{eff}\right)\sum_{i=1}^{N}\left\langle \sigma_i \right\rangle_{\tilde{\mathrm{H}}} \approx -\mu\left(h + h^{eff}\right)Nm_0. \tag{3.204}$$

Substituting (3.201)–(3.204) into (3.199) and minimizing the obtained functional over the values of h^{eff}, we return to (3.181).

Problem 3.7.4

Find the equation of state, the ensemble partition function, and the ensemble Helmholtz energy for the ferromagnetic Ising model with spin interactions in pairs which do not depend on the distance between spins in a pair.

Solution: So, every spin i interacts with any other spin j with the energy $-J\sigma_i\sigma_j$ which does not depend on the distance between these two spins on the lattice. The Hamiltonian of the model is determined as

$$\mathrm{H}_{\{\sigma\}} = -\mu h\sum_{i=1}^{N}\sigma_i - J\sum_{<i,j>}\sigma_i\sigma_j = -\mu h\sum_{i=1}^{N}\sigma_i - \frac{J}{2}\sum_{i,j=1:\,i\neq j}^{N}\sigma_i\sigma_j, \tag{3.205}$$

where multiplier 1/2 has appeared in front of the last sum due to the fact that the sum $\sum_{i,j=1:\ i\neq j}^{N}$ counts each spin pair twice.

Let us move the peculiarity $i \neq j$ from this sum into a separate term:

$$\mathrm{H}_{\{\sigma\}} = -\mu h\sum_{i=1}^{N}\sigma_i - \frac{J}{2}\sum_{i,j=1}^{N}\sigma_i\sigma_j + \frac{J}{2}\sum_{i=1}^{N}\sigma_i^{\,2}. \tag{3.206}$$

Since $\sigma_i^{\,2} = 1$, we find

$$\mathrm{H}_{\{\sigma\}} = -\mu h\sum_{i=1}^{N}\sigma_i - \frac{J}{2}\sum_{i,j=1}^{N}\sigma_i\sigma_j + \frac{NJ}{2}. \tag{3.207}$$

Now we can transform $\sum_{i,j=1}^{N}$ into the product of two separate sums, each over its own spins:

$$\mathrm{H}_{\{\sigma\}} = -\mu h\sum_{i=1}^{N}\sigma_i - \frac{J}{2}\left(\sum_{i=1}^{N}\sigma_i\right)\left(\sum_{j=1}^{N}\sigma_j\right) + \frac{NJ}{2}. \tag{3.208}$$

We see that spin interactions in pairs, which do not depend on the distance between spins, return us to the Hamiltonian depending only on the long-range order parameter:

$$\mathrm{H}_{\{\sigma\}} = -\mu\left(h + \frac{J}{2\mu} N m_{\{\sigma\}}\right) N m_{\{\sigma\}} + \frac{NJ}{2}. \tag{3.209}$$

However, we should emphasize that in this case this is not an approximation—Hamiltonian (3.209) is exact. And we see that the system with infinite-range interactions behaves exactly as if its behavior were determined by the mean-field approximation. Therefore, we can assume that the longer interactions in the system, the better it is described by the mean-field approach. In detail, we will return to this question in Chap. 6.

Also, we should mention here that when the amplitude of interactions does not depend on the distance between two spins in a pair, the shape or dimensionality of the lattice plays no role in the behavior of the system. Therefore, our results are applicable to all possible lattices, of all possible shapes and dimensions.

In the first half of the twentieth century, the mean-field approach was the only known approach to investigate phase transitions analytically. However, the experimental results (e.g., Ley-Ko and Green 1977; Pittman et al. 1979) suggested that the mean-field solution is far from being accurate—for some systems it is very crude (e.g., value 0.32 of the critical index versus 1/2 predicted by the mean-field). And what was even worse, there were no means to make the solution more accurate.

It suggests that there is something very wrong with the mean-field approach. Something, that in some cases, makes this approach completely inapplicable. Therefore, many attempts had been made to develop alternative approaches that would lead to different results.

However, the mean-field approach often acts as a catch-22 rule. In Problem 3.7.3, we tried to develop a different approximation, alternative to the mean-field solution. But to solve the problem analytically we had to consider only the simplest model Hamiltonians. In addition, we had to neglect the correlations again. Altogether, this returned us back to the mean-field solution.

And this problem is not attributed only to our solution in Problem 3.7.3 but is quite typical. We can develop an approximation that would be alternative to the mean-field approach. This approximation could be very complex—it could consider, for example, the heterogeneous magnetization as a field over the lattice of the model. But to find an analytical solution, we have to make some further approximations like neglecting correlations or considering only long-wave approximations. In any case, these approximations lead us back to the crude mean-field solution.

As we will see in Chap. 7, only the approach of the renormalization group is able to break this “catch-22” rule and to lead us towards a new understanding of

the problem. That is why the appearance of the renormalization group approach has caused such a boom of new discoveries in the second half of the past century.

3.8* Antiferromagnets

In the previous sections, we have studied the ferromagnetic systems, $J > 0$, in which a pair of interacting spins has lower energy if the orientations of the spins coincide. In other words, each spin in a ferromagnet attempts to make the orientations of its neighbors coinciding with its own. This behavior is the most transparent when we consider two ferromagnetic phases of the spontaneous magnetization at temperatures below critical in zero magnetic field (Fig. 3.28a).

In this section, we turn our attention to antiferromagnetic systems, $J < 0$, whose behavior is richer than the behavior of ferromagnets. In an antiferromagnet, the energy of a spin pair is lower if orientations of the spins are opposite. In other words, each spin now attempts to make orientations of its neighbors opposite to its own.

The most illustrative is the *bipartite lattices*. The lattice is called bipartite if it is possible to divide it into two sublattices, A and B, when each spin of one sublattice is surrounded only by spins of another.

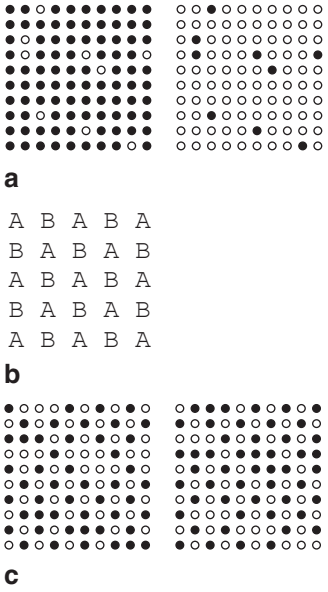

Fig. 3.28 Ferromagnets versus antiferromagnets on square lattices. **a** Two ferromagnetic phases below the critical temperature in the absence of magnetic field. *Filled* and *empty dots* represent spin orientations + 1 and − 1, respectively. Each spin is surrounded by neighbors with primarily the same orientation. **b** Sublattices of a square bipartite lattice. **c** Two antiferromagnetic phases below the critical temperature in the absence of magnetic field. *Filled* and *empty dots* represent spin orientations + 1 and − 1, respectively. Each spin is surrounded by neighbors with primarily the opposite orientation

Two examples of bipartite lattices are the two-dimensional square (Fig. 3.28b) and three-dimensional cubic lattices. At temperatures below critical in the absence of magnetic field, there are two *antiferromagnetic phases* (Fig. 3.28c). In one phase, almost all spins of sublattice A have orientations $+1$ while almost all spins of sublattice B have orientations -1. In another phase, orientations of spins of sublattice A are primarily -1 while on sublattice B spin orientations are primarily $+1$. Again, it corresponds to the *self-organization* of spins; only now the preferable spin orientations are divided between the sublattices.

Introduction of nonzero magnetic field h in the ferromagnet below the critical point breaks one of the phases, keeping only the phase with spin orientations primarily along the field. In the antiferromagnet, the situation is different. Both phases below the critical point have spins in both directions; so, a nonzero magnetic field h does not break any of them, at least while this field is small.

Problem 3.8.1

Prove that an n.n. antiferromagnet and an n.n. ferromagnet on the square lattice have equal ensemble free energies in the absence of magnetic field.

Solution: For both the n.n. antiferromagnet and n.n. ferromagnet, the Hamiltonian in the absence of magnetic field is

$$\mathrm{H}\left(J,\{\sigma_{\mathrm{A}}\},\{\sigma_{\mathrm{B}}\}\right)=-J\sum_{<i^{\mathrm{A}},j^{\mathrm{B}}>_{n.n.}}\sigma_{i^{\mathrm{A}}}\sigma_{j^{\mathrm{B}}}, \tag{3.210}$$

where index i^{A} enumerates spins of sublattice A while index i^{B}—of sublattice B. Here, we have shown explicitly that in the case of the n.n. model on the bipartite lattice the spins of one sublattice interact only with the spins of another sublattice.

From the functional dependence (3.210), it follows that

$$\mathrm{H}\left(-J,\{\sigma_{\mathrm{A}}\},\{\sigma_{\mathrm{B}}\}\right)=\mathrm{H}\left(J,\{-\sigma_{\mathrm{A}}\},\{\sigma_{\mathrm{B}}\}\right). \tag{3.211}$$

In other words, the inversion of the sign of J is equivalent to the inversion of spin orientations on one of the sublattices. The antiferromagnet corresponds to the inversion of the sign of J relative to the ferromagnet:

$$Z^{antif.,CE}=Z^{f.,CE}\left(-J\right)=\sum_{\{\sigma_{\mathrm{A}}\}}\sum_{\{\sigma_{\mathrm{B}}\}}e^{-\mathrm{H}\left(-J,\{\sigma_{\mathrm{A}}\},\{\sigma_{\mathrm{B}}\}\right)/T}=\sum_{\{\sigma_{\mathrm{A}}\}}\sum_{\{\sigma_{\mathrm{B}}\}}e^{-\mathrm{H}\left(J,\{-\sigma_{\mathrm{A}}\},\{\sigma_{\mathrm{B}}\}\right)/T}. \tag{3.212}$$

Since the first sum $\sum_{\{\sigma_A\}}$ goes over both spin orientations, +1 and −1, the partition function does not depend on the inversion of spin orientations of one of the sublattices:

$$Z^{antif.,CE} = \sum_{\{\sigma_A\}} \sum_{\{\sigma_B\}} e^{-H(J,\{\sigma_A\},\{\sigma_B\})/T} = Z^{f.,CE}(J). \tag{3.213}$$

Thereby, we have proved that the ensemble partition function of the antiferromagnet in the absence of magnetic field equals the ensemble partition function of the ferromagnet.

Problem 3.8.2

Develop the mean-field approach for the n.n. antiferromagnet on square lattice in nonzero magnetic field h.

Solution: In nonzero magnetic field, the Hamiltonian of the system is

$$H_{\{\sigma\}} = -\mu h \sum_{i^A=1}^{N/2} \sigma_{i^A} - \mu h \sum_{j^B=1}^{N/2} \sigma_{j^B} - J \sum_{<i^A, j^B>_{n.n.}} \sigma_{i^A} \sigma_{j^B}. \tag{3.214}$$

Let us carry out the following change of spin variables:

$$S_{i^A} \equiv \sigma_{i^A}, \quad S_{j^B} \equiv -\sigma_{j^B}. \tag{3.215}$$

In terms of the new spin variables, each spin again tries to reorient its neighbors so that their orientations would coincide with its own, and the Hamiltonian is

$$H_{\{S\}} = -\mu h \sum_{i^A=1}^{N/2} S_{i^A} + \mu h \sum_{j^B=1}^{N/2} S_{j^B} - |J| \sum_{<i^A, j^B>_{n.n.}} S_{i^A} S_{j^B}. \tag{3.216}$$

Now, the external field interacts with each sublattice differently, but the interactions of spins in pairs transformed into usual ferromagnet interactions.

The antiferromagnet requires two separate long-range order parameters, $m^A_{\{S^A\}}$ and $m^B_{\{S^B\}}$, one for each sublattice:

$$m^A_{\{S^A\}} \equiv \frac{1}{N/2} \sum_{i^A=1}^{N/2} S_{i^A}, \quad m^B_{\{S^B\}} \equiv \frac{1}{N/2} \sum_{j^B=1}^{N/2} S_{j^B}. \tag{3.217}$$

If we neglect the correlations among nearest neighbors, the Hamiltonian transforms into

$$\mathrm{H}_{\{S\}} = -\mu h \frac{N}{2} m^{\mathrm{A}}_{\{S^{\mathrm{A}}\}} + \mu h \frac{N}{2} m^{\mathrm{B}}_{\{S^{\mathrm{B}}\}} - |J| \frac{Nq}{2} m^{\mathrm{A}}_{\{S^{\mathrm{A}}\}} m^{\mathrm{B}}_{\{S^{\mathrm{B}}\}}. \tag{3.218}$$

Instead of fluctuations $\{\{m\}\}$ of one order parameter, the energy fluctuations $\{\{E\}\}$ in the CE are now equivalent to fluctuations $\{\{m^{\mathrm{A}}, m^{\mathrm{B}}\}\}$. The statistical weight of a fluctuation $\{\{m^{\mathrm{A}}, m^{\mathrm{B}}\}$ is

$$\begin{aligned}
\Gamma_{\{\{m^{\mathrm{A}},m^{\mathrm{B}}\}\}} &= \frac{(N/2)!}{N^{\mathrm{A}}_{\uparrow}!N^{\mathrm{A}}_{\downarrow}!}\frac{(N/2)!}{N^{\mathrm{B}}_{\uparrow}!N^{\mathrm{B}}_{\downarrow}!} = \\
&= \frac{(N/2)!}{\left(\frac{N}{2}\frac{1+m^{\mathrm{A}}}{2}\right)!\left(\frac{N}{2}\frac{1-m^{\mathrm{A}}}{2}\right)!}\frac{(N/2)!}{\left(\frac{N}{2}\frac{1+m^{\mathrm{B}}}{2}\right)!\left(\frac{N}{2}\frac{1-m^{\mathrm{B}}}{2}\right)!} \approx_{\ln} \\
&\approx_{\ln} \left(\frac{1+m^{\mathrm{A}}}{2}\right)^{-\frac{N}{2}\frac{1+m^{\mathrm{A}}}{2}} \left(\frac{1-m^{\mathrm{A}}}{2}\right)^{-\frac{N}{2}\frac{1-m^{\mathrm{A}}}{2}} \left(\frac{1+m^{\mathrm{B}}}{2}\right)^{-\frac{N}{2}\frac{1+m^{\mathrm{B}}}{2}} \left(\frac{1-m^{\mathrm{B}}}{2}\right)^{-\frac{N}{2}\frac{1-m^{\mathrm{B}}}{2}}.
\end{aligned} \tag{3.219}$$

To find the partition function, we should now integrate over two order parameters:

$$Z^{CE} = \int_{-1}^{1} \frac{dm^{\mathrm{A}}}{2/(N/2)} \int_{-1}^{1} \frac{dm^{\mathrm{B}}}{2/(N/2)} \Gamma_{\{\{m^{\mathrm{A}},m^{\mathrm{B}}\}\}} e^{-\mathrm{H}(m^{\mathrm{A}},m^{\mathrm{B}})/T}. \tag{3.220}$$

Application of the method of steepest descent proves that the integral equals its maximal term

$$Z^{CE} = \Gamma_{\{\{m^{\mathrm{A}}_0,m^{\mathrm{B}}_0\}\}} e^{-\mathrm{H}(m^{\mathrm{A}}_0,m^{\mathrm{B}}_0)/T}, \tag{3.221}$$

where the point of the maximum is determined by

$$\left.\frac{\partial\left(\Gamma_{\{\{m^{\mathrm{A}},m^{\mathrm{B}}\}\}} e^{-\mathrm{H}(m^{\mathrm{A}},m^{\mathrm{B}})/T}\right)}{\partial m^{\mathrm{A}}}\right|_{m^{\mathrm{A}}_0,m^{\mathrm{B}}_0} = 0 \quad \text{and} \quad \left.\frac{\partial\left(\Gamma_{\{\{m^{\mathrm{A}},m^{\mathrm{B}}\}\}} e^{-\mathrm{H}(m^{\mathrm{A}},m^{\mathrm{B}})/T}\right)}{\partial m^{\mathrm{B}}}\right|_{m^{\mathrm{A}}_0,m^{\mathrm{B}}_0} = 0. \tag{3.222}$$

A solution of (3.222) gives us the equations of state:

$$m^{\mathrm{A}}_0 = \tanh\left(\frac{1}{T}\left\{+\mu h + |J| q m^{\mathrm{B}}_0\right\}\right), \tag{3.223}$$

$$m_0^{\mathrm{B}} = \tanh\left(\frac{1}{T}\left\{-\mu h + |J| q m_0^{\mathrm{A}}\right\}\right) \tag{3.224}$$

or

$$m_0^{\mathrm{A}} = \tanh\left(\frac{1}{T}\left\{+\mu h + |J| q \tanh\left(\frac{1}{T}\left\{-\mu h + |J| q m_0^{\mathrm{A}}\right\}\right)\right\}\right), \tag{3.225}$$

$$m_0^{\mathrm{B}} = \tanh\left(\frac{1}{T}\left\{-\mu h + |J| q \tanh\left(\frac{1}{T}\left\{+\mu h + |J| q m_0^{\mathrm{B}}\right\}\right)\right\}\right). \tag{3.226}$$

In the absence of magnetic field, the equations of state transform into

$$\operatorname{atanh}\, m_0^{\mathrm{A}} = \frac{|J| q}{T} \tanh \frac{|J| q m_0^{\mathrm{A}}}{T}, \tag{3.227}$$

$$\operatorname{atanh}\, m_0^{\mathrm{B}} = \frac{|J| q}{T} \tanh \frac{|J| q m_0^{\mathrm{B}}}{T}. \tag{3.228}$$

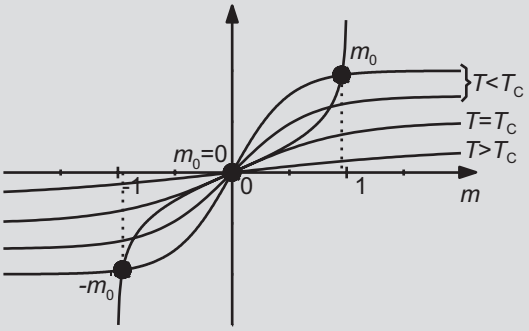

Solving these equations graphically, we find that the left- and right-hand sides of (3.227) and (3.228) always intersect at $m = 0$, which provides the solution above the critical temperature:

$$m_0^{\mathrm{A}} = 0, \quad m_0^{\mathrm{B}} = 0 \quad \text{when} \quad T > T_{\mathrm{C}}, \quad h = 0, \tag{3.229}$$

When temperature decreases, the nonzero solutions appear first when the tangents to the left- and right-hand sides of (3.227) and (3.228) coincide at $m = 0$. For the value of the critical temperature, this provides:

$$T_{\mathrm{C}} = |J| q, \tag{3.230}$$

which coincides with mean-field approximation (3.182) of the critical temperature of the ferromagnet.

Let us consider a variable x obeying the equation

$$x = \tanh(\alpha x). \tag{3.231}$$

Multiplying this equation by α and taking tanhs of both sides, we obtain

$$\tanh(\alpha x) = \tanh(\alpha \tanh(\alpha x)). \tag{3.232}$$

Substituting here $\tanh(\alpha x)$ from (3.231), we find

$$x = \tanh(\alpha \tanh(\alpha x)). \tag{3.233}$$

The obtained equation is equivalent to the equations of state (3.227 and 3.228) we are trying to solve in the absence of magnetic field. Applying the equivalent representation (3.231) to (3.227) and (3.228) and recalling the connection (3.223 and 3.224) between two order parameters, we immediately find that the solution for each of the sublattices is equivalent to the zero-field case of the ferromagnetic equation of state (3.181):

$$m_0^{\mathrm{A}} = \tanh\frac{|J|qm_0^{\mathrm{A}}}{T}, \tag{3.234}$$

$$m_0^{\mathrm{B}} = \tanh\frac{|J|qm_0^{\mathrm{B}}}{T}, \tag{3.235}$$

$$m_0^{\mathrm{B}} = m_0^{\mathrm{A}}. \tag{3.236}$$

But for the ferromagnetic case, we utilized the graphical solution of Fig. 3.4. Therefore, the equations of state can be solved in both ways, by the graphical solution in the figure above or by the graphical solution of Fig. 3.4.

Next, we return to the case of nonzero magnetic field h and the equations of state (3.223 and 3.224). Let us prescribe the direction of the field: $h > 0$. First, we consider the limit $T \to 0$ of low temperatures. In this limit, the arguments of the tanh functions are infinite which transforms the tanh functions into the sign functions

$$m_0^{\mathrm{A}} = \mathrm{sgn}\left(\frac{1}{T}\left\{+\mu h + |J|qm_0^{\mathrm{B}}\right\}\right), \tag{3.237}$$

$$m_0^{\mathrm{B}} = \mathrm{sgn}\left(\frac{1}{T}\left\{-\mu h + |J|qm_0^{\mathrm{A}}\right\}\right), \tag{3.238}$$

where

$$\operatorname{sgn}(x) \equiv \begin{cases} +1, & x > 0 \\ 0, & x = 0 \\ -1, & x < 0 \end{cases}. \tag{3.239}$$

Since $m_0^{\mathrm{A}} = \operatorname{sgn}(\ldots)$, $m_0^{\mathrm{B}} = \operatorname{sgn}(\ldots)$, the order parameters m_0^{A} and m_0^{B} can be equal only to 0 or ± 1. Zero solution below the critical temperature is unstable; therefore, we do not consider it further.

To find the solution of (3.237) and (3.238), we should consider four possible situations: $m_0^{\mathrm{A}} = +1$ and $m_0^{\mathrm{B}} = +1$, $m_0^{\mathrm{A}} = +1$ and $m_0^{\mathrm{B}} = -1$, $m_0^{\mathrm{A}} = -1$ and $m_0^{\mathrm{B}} = +1$, $m_0^{\mathrm{A}} = -1$ and $m_0^{\mathrm{B}} = -1$.

For the case $m_0^{\mathrm{A}} = +1$ and $m_0^{\mathrm{B}} = +1$ to be true, both sign functions in (3.237) and (3.238) should have positive arguments which (for the considered $h > 0$) provides the following inequality:

$$h < \frac{|J|q}{\mu}. \tag{3.240}$$

Similar inequality we obtain for $m_0^{\mathrm{A}} = -1$ and $m_0^{\mathrm{B}} = -1$.

On the contrary, for $m_0^{\mathrm{A}} = +1$ and $m_0^{\mathrm{B}} = -1$ we find

$$h > \frac{|J|q}{\mu}. \tag{3.241}$$

The last case, $m_0^{\mathrm{A}} = -1$ and $m_0^{\mathrm{B}} = +1$, requires

$$\mu h + |J|q < 0 \tag{3.242}$$

which is impossible for the considered $h > 0$.

We see that

$$h_{\mathrm{C}} = \frac{|J|q}{\mu} \tag{3.243}$$

plays the role of the critical field.

If the magnetic field h is less than its critical value, $h < h_{\mathrm{C}}$, there are two *antiferromagnetic phases* in the system: $m_0^{\mathrm{A}} = m_0^{\mathrm{B}} = +1$ and $m_0^{\mathrm{A}} = m_0^{\mathrm{B}} = -1$. Here, for both phases, one sublattice has spins along the field while another—against the field. The phases differ one from another by the choice which sublattice has spins along the field while spins of another are against the field.

On the contrary, if the magnetic field h exceeds its critical value (3.243), the strong field rotates the spins which were oriented against it, so that both

sublattices are now oriented along the strong magnetic field. Only one *paramagnetic phase* corresponds to this situation: $m_0^{\mathrm{A}} = -m_0^{\mathrm{B}} = +1$.

Finally, let us consider the case of finite temperatures. For any value of temperature T below critical, there is the corresponding value $h_{\mathrm{C}}(T)$ of the critical magnetic field which breaks the coexistence of two antiferromagnetic phases. And vice versa, for each value of the magnetic field below (3.243), there is also the corresponding value $T_{\mathrm{C}}(h)$ of the critical temperature, breaking the self-organization of spins. So, in contrast to the critical point of a ferromagnet, in the case of the antiferromagnetic system, we have not a critical point but *a critical curve*. This curve delimits two regions, one with two antiferromagnetic phases, another with one paramagnetic phase.

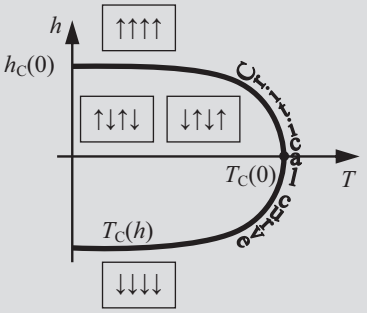

We see here the main difference between a ferromagnet and an antiferromagnet. In the ferromagnet, even a small magnetic field breaks the coexistence of ferromagnetic phases and transforms one of them into another, which is more preferable. In the antiferromagnet, the introduction of the small magnetic field does not make one of the phases more preferable than another. In Fig. 3.7, both minima of the free energy would have equal depth in the case of an antiferromagnet, even in the presence of the small nonzero magnetic field. Only the strong field breaks the antiferromagnetic phases. It does not keep one of the phases as favorable like in the ferromagnetic system. Instead, the field breaks both phases to create a new paramagnetic phase, in which both sublattices have spin orientations along the field.

Let us find the dependence $T_{\mathrm{C}}(h)$ of the critical curve on a small magnetic field in the proximity of the point $T_{\mathrm{C}}(0) = |J|q$ given by (3.230). First, we take the atanh function from both sides of the equations of state (3.223 and 3.224):

$$\operatorname{atanh} m_0^{\mathrm{A}} = \frac{1}{T}\left\{+\mu h + |J| q m_0^{\mathrm{B}}\right\}, \tag{3.244}$$

$$\operatorname{atanh} m_0^{\mathrm{B}} = \frac{1}{T}\left\{-\mu h + |J| q m_0^{\mathrm{A}}\right\}. \tag{3.245}$$

Second, we notice that in the vicinity of the point $T_C(0)$ both order parameters, m_0^A and m_0^B, are small. So, we can expand atanh functions in (3.244) and (3.245) in a power series of these small parameters:

$$m_0^A + \frac{m_0^{A^3}}{3} + \ldots = \frac{|J|q}{T} m_0^B + \frac{\mu h}{T}, \tag{3.246}$$

$$m_0^B + \frac{m_0^{B^3}}{3} + \ldots = \frac{|J|q}{T} m_0^A - \frac{\mu h}{T}. \tag{3.247}$$

Instead of considered sublattice magnetizations, $m^A_{\{S^A\}}$ and $m^B_{\{S^B\}}$, next we change the order parameters by introducing another two:

$$m_{\{S\}} = \frac{m^A_{\{S^A\}} - m^B_{\{S^B\}}}{2} = \frac{1}{N}\left(\sum_{i^A=1}^{N/2} S_{i^A} - \sum_{j^B=1}^{N/2} S_{j^B} \right) = \frac{1}{N}\sum_{i=1}^{N} \sigma_i, \tag{3.248}$$

$$\varphi_{\{S\}} = \frac{m^A_{\{S^A\}} + m^B_{\{S^B\}}}{2} = \frac{1}{N}\left(\sum_{i^A=1}^{N/2} S_{i^A} + \sum_{j^B=1}^{N/2} S_{j^B} \right) = \frac{1}{N}\sum_{i=1}^{N} S_i. \tag{3.249}$$

Here, parameter $m_{\{S\}}$ is the specific magnetization of the lattice in whole which represents interactions of the model with the external magnetic field. On the contrary, parameter $\varphi_{\{S\}}$ represents the antiferromagnetic interactions and is called *the staggered magnetization*.

Adding (3.246 and 3.247) one to another and subtracting them one from another, we find the equations of state for the new order parameters:

$$m_0 = \frac{\mu h / T}{1 + |J|q/T}, \tag{3.250}$$

$$\varphi_0 \left(1 + m_0^{\,2} - \frac{|J|q}{T} \right) + \underline{\underline{O}}(\varphi_0^{\,2}) = 0. \tag{3.251}$$

These equations are valid on both sides of the critical line. But on the one side, the staggered magnetization φ_0 is zero while on the another side, it has two nonzero values. Equation (3.251) can represent such behavior only if the coefficient $1 + m_0^{\,2} - |J|q/T$ at the term, linear in φ_0, is zero when we cross the critical line. This is similar to the ferromagnetic case when in the equation of state (3.92) the coefficient at the term, linear in m_0, was zero when we moved across the critical point.

So, the coefficient $1 + m_0^{\,2} - |J|q/T$ is zero at the critical line. Substituting here the magnetization from (3.250), we find the equation of the critical line:

$$1+\left(\frac{\mu h / T_{\mathrm{C}}(h)}{1+|J|q / T_{\mathrm{C}}(h)}\right)^{2}-\frac{|J|q}{T_{\mathrm{C}}(h)}=0. \tag{3.252}$$

Since we are working in the close neighborhood of the point $T_{\mathrm{C}}(0)=|J|q$, we can expand here $T_{\mathrm{C}}(h)$ in a power series of h:

$$T_{\mathrm{C}}(h)=T_{\mathrm{C}}(0)-\frac{(\mu h)^{2}}{4|J|q}. \tag{3.253}$$

This is the dependence we have been looking for. We see that the decrease of the critical temperature along the critical line is parabolic.

Problem 3.8.3

For the n.n. antiferromagnetic Ising model on square lattice, find the equation of state with the aid of the Gibbs-Bogolyubov-Feynman inequality. Find the ensemble partition function and the ensemble Helmholtz energy.

Solution: The exact Hamiltonian of the model is determined by (3.216). The model Hamiltonian we choose to have the following functional dependence:

$$\tilde{\mathrm{H}}_{\{S\}}=-\mu(h+h_{eff}^{\mathrm{A}})\sum_{i^{\mathrm{A}}=1}^{N/2}S_{i^{\mathrm{A}}}+\mu(h+h_{eff}^{\mathrm{B}})\sum_{j^{\mathrm{B}}=1}^{N/2}S_{j^{\mathrm{B}}}. \tag{3.254}$$

Here, h_{eff}^{A} and h_{eff}^{B} are two fitting parameters, over which we will minimize the free energy functional.

The partition function of the model Hamiltonian is

$$\tilde{Z}^{CE}=\left(2\cosh\frac{\mu(h+h_{eff}^{\mathrm{A}})}{T}\right)^{N/2}\left(2\cosh\frac{\mu(h+h_{eff}^{\mathrm{B}})}{T}\right)^{N/2}; \tag{3.255}$$

and in the ensemble of the model system the equations of state are

$$m_{0}^{\mathrm{A}}=\tanh\frac{\mu(h+h_{eff}^{\mathrm{A}})}{T},\quad m_{0}^{\mathrm{B}}=-\tanh\frac{\mu(h+h_{eff}^{\mathrm{B}})}{T}. \tag{3.256}$$

To find the averaged value of the exact Hamiltonian in the ensemble of the model Hamiltonian, we neglect correlations of n.n. spins:

$$\left\langle \mathrm{H}_{\{S\}} \right\rangle_{\tilde{\mathrm{H}}} = -\mu h \sum_{i^{\mathrm{A}}=1}^{N/2} \left\langle S_{i^{\mathrm{A}}} \right\rangle_{\tilde{\mathrm{H}}} + \mu h \sum_{j^{\mathrm{B}}=1}^{N/2} \left\langle S_{j^{\mathrm{B}}} \right\rangle_{\tilde{\mathrm{H}}} - |J| \sum_{<i^{\mathrm{A}}, j^{\mathrm{B}}>_{n.n.}} \left\langle S_{i^{\mathrm{A}}} S_{j^{\mathrm{B}}} \right\rangle_{\tilde{\mathrm{H}}}$$
$$\approx -\mu h \frac{N}{2} m_0^{\mathrm{A}} + \mu h \frac{N}{2} m_0^{\mathrm{B}} - \frac{N|J|q}{2} m_0^{\mathrm{A}} m_0^{\mathrm{B}}, \tag{3.257}$$

where $m_0^{\mathrm{A}} = \left\langle S_{i^{\mathrm{A}}} \right\rangle_{\tilde{\mathrm{H}}}$ and $m_0^{\mathrm{B}} = \left\langle S_{j^{\mathrm{B}}} \right\rangle_{\tilde{\mathrm{H}}}$ are the solutions (3.256).

Similarly, averaging the model Hamiltonian in its own ensemble, we find

$$\left\langle \tilde{\mathrm{H}}_{\{S\}} \right\rangle_{\tilde{\mathrm{H}}} = -\mu(h + h_{eff}^{\mathrm{A}}) \sum_{i^{\mathrm{A}}=1}^{N/2} \left\langle S_{i^{\mathrm{A}}} \right\rangle_{\tilde{\mathrm{H}}} + \mu(h + h_{eff}^{\mathrm{B}}) \sum_{i^{\mathrm{B}}=1}^{N/2} \left\langle S_{i^{\mathrm{B}}} \right\rangle_{\tilde{\mathrm{H}}}$$
$$\approx -\mu(h + h_{eff}^{\mathrm{A}}) \frac{N}{2} m_0^{\mathrm{A}} + \mu(h + h_{eff}^{\mathrm{B}}) \frac{N}{2} m_0^{\mathrm{B}}. \tag{3.258}$$

Substituting these expressions into functional (3.199) and minimizing this functional over the fitting parameters h_{eff}^{A} and h_{eff}^{B}, we return to the mean-field solution (3.223 and 3.224), in detail discusses in Problem 3.8.2.

3.9* Antiferromagnet on a Triangular Lattice. Frustration

Again, as the simplest example, we consider the n.n. antiferromagnetic Ising model. However, now we consider not square but triangular lattice.

The triangular lattice is not bipartite—we cannot divide this lattice into two sublattices so that each spin of one sublattice would be surrounded only by the spins of another sublattice. But we can divide the triangular lattice into three sublattices (Fig. 3.29) so that each spin of one sublattice is surrounded only by the spins of other sublattices. Such lattices are called *tripartite*.

The fact that the lattice is no longer bipartite significantly changes the behavior of the system. Let us consider, for example, the ground state of the model at zero temperature and zero field. The energy of the system is minimal in the ground state.

The ferromagnet on any lattice is able to reach the minimum energy of spin interactions for all spin pairs by just aligning all spins in one direction. This corresponds to the twofold degenerate ground state—all spins are "up," ↑↑↑↑↑, or all spins are "down," ↓↓↓↓↓.

The antiferromagnet on square lattice is also capable to minimize the energy of spin interactions for all spin pairs at once by just aligning one sublattice "up" and another "down." The ground state is again twofold degenerate; and these two ground microstates differ by which sublattice is "up" and which sublattice is "down":

$$\begin{matrix} \uparrow & \downarrow & \uparrow \\ \downarrow & \uparrow & \downarrow \\ \uparrow & \downarrow & \uparrow \end{matrix} \text{ or } \begin{matrix} \downarrow & \uparrow & \downarrow \\ \uparrow & \downarrow & \uparrow \\ \downarrow & \uparrow & \downarrow \end{matrix}.$$

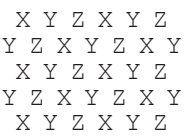

Fig. 3.29 Sublattices of a tripartite triangular lattice

However, on triangular lattice, the antiferromagnet cannot minimize the energy of all spin pairs at once. Indeed, let us consider one triangular cell with three spins at the corners: $\updownarrow$ $\updownarrow\ \updownarrow$. If one pair has been able to minimize its energy, its spins are oriented in opposite directions: $\uparrow$ $\downarrow\ \updownarrow$. Choosing now an arbitrary orientation for the third spin, $\uparrow$ $\downarrow\ \uparrow$ or $\uparrow$ $\downarrow\ \downarrow$, we see that it must have coinciding orientation with one of the previously assigned spins. Therefore, it is not possible to minimize the energy of all spin pairs at once. This is valid both for one triangular cell and for the whole triangular lattice. Therefore, the antiferromagnet on triangular lattice is called *geometrically frustrated*.

As we have seen above, both the ferromagnet on an arbitrary lattice and the antiferromagnet on square lattice have the twofold degenerate ground states. Let us now estimate the degeneracy of the ground state of the antiferromagnet on triangular lattice. We consider microstates when the spins on sublattice X are oriented "up," the spins on sublattice Y are oriented "down," and the spins on sublattice Z are oriented arbitrarily. All such microstates correspond to the ground state because two spins in any cell have minimized their pair energy, and the energy of the cell cannot become lower. But the orientations of the spins on sublattice Z are arbitrary. Therefore, the degeneracy of the ground state is at least $2^{N/3}$ and depends exponentially on N.

At zero temperature and zero magnetic field, each cell of the antiferromagnet on triangular lattice has one spin oriented "up," one spin oriented "down," and the last spin oriented arbitrarily. If this third spin were oriented "up," the cell would have positive magnetization which could be considered as a phase. If this spin were oriented "down," the magnetization of the cell would be negative, and we could consider it as another phase.

So, one homogeneous phase is when all cells on the lattice have exactly two spins oriented "up" and exactly one spin "down." Another homogeneous phase is when all cells have exactly one spin "up" and two spins "down." The introduction of a small magnetic field will break the phase coexistence and will make one of the phases preferable.

But let us return back to the case of zero magnetic field. Earlier we considered ground microstates with the spins on sublattice X oriented "up," spins on sublattice Y oriented "down," and spins on sublattice Z oriented arbitrarily. So, any typical ground microstate is the heterogeneous system consisting of domains of two phases.

Never before we saw a system that could be heterogeneous in its ground state. The reason was that the heterogeneity generally requires additional surface energy

which makes it not a ground state a priori. For example, the ferromagnet in a heterogeneous state requires additional surface energy at the boundaries among phase domains. This state cannot be ground a priori because there are states with lower energy.

But this is not true for the antiferromagnet on triangular lattice. Let us consider the homogeneous phase when the spins on sublattices X and Z are oriented "up" while the spins on sublattice Y are oriented "down." If we now divide the lattice into domains and within some of the domains invert the orientations of the spins of sublattice Z, we will form the heterogeneous system. But the energy will not change—we will still obtain one of the ground microstates! We have formed a heterogeneous microstate from a homogeneous, but it has not required additional energy.

The reason is that the surface energy on the domain boundaries is zero. Each cell on triangular lattice is frustrated and already possesses the encapsulated, irremovable energy of spin interactions. This energy can be transformed into the form of the surface energy between two domains, and any additional energy is not necessary.

First, this leads to the possibility for a heterogeneous microstate to be ground. That is why the degeneracy of the ground state is so high. Second, zero surface energy leads to the appearance of domains in all shapes and sizes—starting from the lattice size and ending by the size of a cell.

3.10* Mixed Ferromagnet-Antiferromagnet

Problem 3.10.1

Develop the mean-field approach for the mixed n.n. ferromagnet-antiferromagnet on square lattice in nonzero magnetic field h.

Solution: The Hamiltonian of the mixed n.n. ferromagnetic-antiferromagnetic Ising model is

$$\mathrm{H}_{\{\sigma\}} = -\mu h \sum_{i=1}^{N} \sigma_i - J \sum_{<i,j>_{n.n.}} \eta_i \eta_j \sigma_i \sigma_j, \tag{3.259}$$

where $J > 0$. Parameters η_i, defined a priori for each lattice site i, have fixed values +1 or –1, randomly distributed over the lattice. Since these parameters are defined a priori and do not change their values during the system's evolution, this type of disorder, introduced into a system, is called *quenched*. The presence of the disorder transforms the Ising model into the mixture of ferromagnetic and antiferromagnetic spin pairs.

The change of spin variables is introduced as:

$$S_i \equiv \eta_i \sigma_i. \tag{3.260}$$

Next, we divide the lattice into two sublattices, X and Y. Sublattice X contains only sites with $\eta_i = +1$ while sublattice Y—only sites with $\eta_i = -1$. For the sublattices, the change of spin variables (3.260) goes in accordance with

$$S_{i^{\mathrm{X}}} = \sigma_{i^{\mathrm{X}}}, \quad S_{j^{\mathrm{Y}}} = -\sigma_{j^{\mathrm{Y}}}. \tag{3.261}$$

Let us look closer at the interaction $\eta_i \eta_j \sigma_i \sigma_j$ of spins in a pair. We see that in terms of the new spin variables it transforms into simple ferromagnetic interaction:

$$\eta_i \eta_j \sigma_i \sigma_j = \left\{ \begin{array}{l} S_i S_j,\ \eta_i = +1,\ \eta_j = +1,\ i \in \mathrm{X},\ j \in \mathrm{X} \\ S_i S_j,\ \eta_i = +1,\ \eta_j = -1,\ i \in \mathrm{X},\ j \in \mathrm{Y} \\ S_i S_j,\ \eta_i = -1,\ \eta_j = +1,\ i \in \mathrm{Y},\ j \in \mathrm{X} \\ S_i S_j,\ \eta_i = -1,\ \eta_j = -1,\ i \in \mathrm{Y},\ j \in \mathrm{Y} \end{array} \right\} = S_i S_j \tag{3.262}$$

Therefore, in terms of the new spin variables, the Hamiltonian of the system is

$$\mathrm{H}_{\{S\}} = -\mu h \sum_{i^{\mathrm{X}}=1}^{N^{\mathrm{X}}} S_{i^{\mathrm{X}}} + \mu h \sum_{i^{\mathrm{Y}}=1}^{N^{\mathrm{Y}}} S_{i^{\mathrm{Y}}} - J \sum_{<i,j>_{n.n.}} S_i S_j, \tag{3.263}$$

where N^{X} and N^{Y} are the total numbers of sites in sublattices X and Y, respectively.

The following solution is similar to Problem 3.8.2 when we replace the short-range order parameter by the function of the long-range order parameters. Or to Problem 3.8.3 when we apply the Gibbs–Bogolyubov–Feynman inequality. The difference with the previous solutions is that sublattices X and Y are no longer bipartite. Therefore, the averaged product $\left\langle S_i S_{j\ \mathrm{n.n.}} \right\rangle_{\{S\}}$ of spins in a pair does not mean already that one spin belongs to sublattice X while another—to sublattice Y:

$$\left\langle S_i S_{j\ \mathrm{n.n.}} \right\rangle_{\{S\}} \neq \left\langle S_{i^{\mathrm{X}}} S_{j^{\mathrm{Y}}\ \mathrm{n.n.}} \right\rangle_{\{S\}} \approx \left\langle S_{i^{\mathrm{X}}} \right\rangle_{\{S^{\mathrm{X}}\}} \left\langle S_{j^{\mathrm{Y}}} \right\rangle_{\{S^{\mathrm{Y}}\}} \equiv m^{\mathrm{X}}_{\{S^{\mathrm{X}}\}} m^{\mathrm{Y}}_{\{S^{\mathrm{Y}}\}}. \tag{3.264}$$

In other words, both spins in a pair could belong to the same sublattice.

Instead, to solve the problem, we have to account for the randomness of the disorder. The probability for both spins in a pair to belong to sublattice X is $(N^{\mathrm{X}} / N)^2$. The probability for both spins in a pair to belong to sublattice Y is $(N^{\mathrm{Y}} / N)^2$. The probability that one spin in a pair belongs to sublattice X while another—to sublattice Y is $2N^{\mathrm{X}} N^{\mathrm{Y}} / N^2$. The sum of these probabilities is unity, as it should be.

Averaging with these probabilities, we find

$$\left\langle S_{i^{\mathrm{X}}} \right\rangle_{\{S^{\mathrm{X}}\}} \equiv m^{\mathrm{X}}_{\{S^{\mathrm{X}}\}}, \quad \left\langle S_{j^{\mathrm{Y}}} \right\rangle_{\{S^{\mathrm{Y}}\}} \equiv m^{\mathrm{Y}}_{\{S^{\mathrm{Y}}\}}, \tag{3.265}$$

$$\begin{aligned}
&\left\langle S_i S_{j\ \mathrm{n.n.}} \right\rangle_{\{S\}} \approx \left(\frac{N^{\mathrm{X}}}{N}\right)^2 \left\langle S_{i^{\mathrm{X}}} \right\rangle^2_{\{S^{\mathrm{X}}\}} + 2\frac{N^{\mathrm{X}}}{N}\frac{N^{\mathrm{Y}}}{N}\left\langle S_{i^{\mathrm{X}}} \right\rangle_{\{S^{\mathrm{X}}\}} \left\langle S_{j^{\mathrm{Y}}} \right\rangle_{\{S^{\mathrm{Y}}\}} \\
&+\left(\frac{N^{\mathrm{Y}}}{N}\right)^2 \left\langle S_{j^{\mathrm{Y}}} \right\rangle^2_{\{S^{\mathrm{Y}}\}} = \left(\frac{N^{\mathrm{X}}}{N}\left\langle S_{i^{\mathrm{X}}} \right\rangle_{\{S^{\mathrm{X}}\}} + \frac{N^{\mathrm{Y}}}{N}\left\langle S_{j^{\mathrm{Y}}} \right\rangle_{\{S^{\mathrm{Y}}\}}\right)^2 \\
&\equiv \left(\frac{N^{\mathrm{X}}}{N} m^{\mathrm{X}}_{\{S^{\mathrm{X}}\}} + \frac{N^{\mathrm{Y}}}{N} m^{\mathrm{Y}}_{\{S^{\mathrm{Y}}\}}\right)^2 .
\end{aligned} \tag{3.266}$$

We should mention here that the mixed ferromagnet-antiferromagnet is not frustrated even on the triangular lattice. Indeed, in a triangular cell for an arbitrary assignment of parameters η_i at three cell's sites all three spin pairs of the cell can minimize their energy simultaneously.

However, even the square lattice becomes frustrated if we assign parameters η_i not to lattice sites but to connections between n.n. sites, i.e., to n.n. spin pairs:

$$\mathrm{H}_{\{\sigma\}} = -\mu h \sum_{i=1}^{N} \sigma_i - J \sum_{<i,j>_{n.n.}} \eta_{<i,j>_{n.n.}} \sigma_i \sigma_j . \tag{3.267}$$

It is easy to see that the square lattice in this case is frustrated. Let us consider a square cell. If three of its "edges" (three spin pairs) were ferromagnetic while the fourth "edge" were antiferromagnetic, then this cell would be frustrated. And if one cell is frustrated—the whole lattice is frustrated.

References

Abaimov, S.G.: Statistical physics of complex systems (in Russian), 2nd ed. Synergetics: From Past to Future, vol. **57**, URSS, Moscow (2013)

Balescu, R.: Equilibrium and Nonequilibrium Statistical Mechanics. Wiley, New York (1975)

Baxter, R.J.: Exactly Solved Models in Statistical Mechanics. Academic, London (1982)

Berlin, T.H., Kac, M.: The spherical model of a ferromagnet. Phys. Rev. **86**(6), 821–835 (1952)

Bogoliubov, N.N.: On the theory of superfluidity. Bull. Russ. Acad. Sci. Phys. **11**(1), 77–90 (1947a)

Bogoliubov, N.N.: On the theory of superfluidity. J. Phys. U.S.S.R. **11**(1), 23–32 (1947b)

Bogoliubov, N.N.: Quasimittelwerte in problemen der statistischen mechanik. I. Phys. Abhandl. Sowjetunion **6**(2), 1–228 (1962a)

Bogoliubov, N.N.: Quasimittelwerte in problemen der statistischen mechanik. II. Phys. Abhandl. Sowjetunion **6**(3), 229–284 (1962b)

Bragg, W.L., Williams, E.J.: The effect of thermal agitation on atomic arrangement in alloys. Proc. Roy. Soc. A **145**, 699–730 (1934)
Bragg, W.L., Williams, E.J.: The effect of thermal agitation on atomic arrangement in alloys. II. Proc. Roy. Soc. A **151**, 540–566 (1935)
Cardy, J.: Scaling and Renormalization in Statistical Physics. Cambridge University Press, Cambridge (1996)
Domb, C., Green, M.S., and Domb, C., Lebowitz, J.L. (eds.): Phase Transitions and Critical Phenomena. Academic, London (1972–2001)
Essam, J.W., Fisher, M.E.: Padé approximant studies of the lattice gas and Ising ferromagnet below the critical point. Chem. Phys. **38**(4), 802 (1963)
Feynman, R.P.: Statistical Mechanics: A Set of Lectures. W.A. Benjamin, Reading (1972)
Gibbs, J.W.: Elementary Principles in Statistical Mechanics. Charles Scribner's Sons, New York (1902)
Glasser, M.L.: Exact partition function for the two-dimensional Ising model. Am. J. Phys. **38**(8), 1033 (1970)
Goldenfeld, N.: Lectures on Phase Transitions and the Renormalization Group. Perseus Books Publishing, L.L.C., Reading (1992)
Gunton, J.D., Droz, M.: Introduction to the Theory of Metastable and Unstable States (Lecture Notes in Physics), vol. 183. Springer-Verlag, Berlin (1983)
Heisenberg, W.: Zur theorie des ferromagnetismus. Z. Phys. **49**(9–10), 619–636 (1928)
Huang, K.: Statistical Mechanics, 2nd ed. Wiley, New York (1987)
Hurst, C.A., Green, H.S.: New solution of the Ising problem for a rectangular lattice. Chem. Phys. **33**(4), 1059 (1960)
Ising, E.: Beitrag zur theorie des ferromagnetismus. Z. Physik **31**, 253–258 (1925)
Kac, M., Ward, J.C.: A combinatorial solution of the two-dimensional Ising model. Phys. Rev. **88**(6), 1332 (1952)
Kashchiev, D.: Nucleation: Basic Theory with Applications. Butterworth Heinemann, Oxford (2000)
Kramers, H.A., Wannier, G.H.: Statistics of the two-dimensional ferromagnet. Part I. Phys. Rev. **60**(3), 252 (1941a)
Kramers, H.A., Wannier, G.H.: Statistics of the two-dimensional ferromagnet. Part II. Phys. Rev. **60**(3), 263 (1941b)
Kubo, R., Ichimura, H., Usui, T., Hashitsume, N.: Statistical Mechanics: An Advanced Course with Problems and Solutions, 8th ed. North Holland, Amsterdam (1988)
Landau, L.D., Lifshitz, E.M.: Statistical Physics, Part 1, 3rd ed. Course of Theoretical Physics, vol. 5. Pergamon Press, Oxford (1980)
Lenz, W.: Beiträge zum verständnis der magnetischen eigenschaften in festen körpern. Physik. Z. **21**, 613–615 (1920)
Ley-Koo, M., Green, M.S.: Revised and extended scaling for coexisting densities of SF_6. Phys. Rev. A **16**(6), 2483–2487 (1977)
Ma, S.K.: Modern Theory of Critical Phenomena. Benjamin, Reading (1976)
Ma, S.K.: Statistical Mechanics. World Scientific, Singapore (1985)
Matsubara, T., Matsuda, H.: A lattice model of liquid helium. Prog. Theor. Phys. **16**(4), 416–417 (1956)
Onsager, L.: Crystal statistics. I. A two-dimensional model with an order-disorder transition. Phys. Rev. **65**(3–4), 117–149 (1944)
Pathria, R.K.: Statistical Mechanics, 2nd ed. Butterworth-Heinemann, Oxford (1996)
Pittman, C., Doiron, T., Meyer, H.: Equation of state and critical exponents of ^{3}He and a ^{3}He-^{4}He mixture near their liquid-vapor critical point. Phys. Rev. B **20**(9), 3678–3689 (1979)
Potts, R.B.: Some generalized order-disorder transformation. Math. Proc. Camb. Phil. Soc. **48**(01), 106–109 (1952)
Potts, R.B., Ward, J.C.: The combinatorial method and the two-dimensional Ising model. Prog. Theor. Phys. **13**(1), 38–46 (1955)
Reif, F.: Fundamentals of Statistical and Thermal Physics. McGraw-Hill, New York (1965)

Rushbrooke, G.S.: On the thermodynamics of the critical region for the Ising problem. Chem. Phys. **39**(3), 842 (1963)
Sommerfeld, A.: Thermodynamics and Statistical Mechanics. Academic, New York (1956)
Stanley, H.E.: Introduction to Phase Transitions and Critical Phenomena. Clarendon Press, Oxford (1971)
ter Haar, D.: Elements of Statistical Mechanics. Rinehart, New York (1954)
Vdovichenko, N.V.: A calculation of the partition function for a plane dipole lattice. Sov. JETP **20**(2), 477 (1965a)
Vdovichenko, N.V.: Spontaneous magnetization of a plane dipole lattice. Sov. JETP **21**(2), 350 (1965b)
Weiss, P.M.P.: L'hypothèse du champ moléculaire et la propriété ferromagnétique. J. Phys. Théor. Appl. **6**(1), 661–690 (1907)

Chapter 4
The Theory of Percolation

Abstract In the previous chapter, we have considered the phase transition phenomenon in the Ising model. May we call this system "complex?" In the literature there is no settled definition of what we call "complex."

The theory of phase transitions is generally attributed to thermodynamic systems. However, in the second half of the last century many nonthermal systems have been discovered whose behavior resembled the theory of phase transitions in statistical physics. However, these systems belong to such diverse sciences—biology, geology, engineering, chemistry, mathematics, economics, social sciences, etc.—that their unified classification seems to be impossible. Examples include but not limited to the percolation of petroleum oil in a rock, polymerization, damage of engineering structures, earthquakes, forest fires, snow avalanches and landslides, traffic jams, chaotic systems, strange attractors, informational processes, self-organized criticality, etc.

To distinguish such systems from the classical examples of phase transition phenomena (like the Ising model), the term "*complex*" has appeared. However, beyond the fact that all these systems obey the rules of phase transitions and, therefore, can form universality classes, their common rigorous classification is deemed to be currently impossible.

We see that the term "complex" is collective and, therefore, may describe a great variety of phenomena. But what does this term mean? First, as we have said, calling a system complex, one generally assumes that this complexity is the consequence of a phase transition (or a bifurcation, catastrophe, nonanalyticity, etc.) present in the system. Second, the term "complex" is generally used to distinguish the nonthermal systems from their thermodynamic analogues.

Summarizing, we call a system *complex* if it possesses a phase transition but is nonthermal. In the sense of this definition, the Ising model is only partially complex—it possesses a phase transition but is thermal. In this chapter, as a first example of a "completely complex" system, we consider a phenomenon of percolation.

The fact that the system is supposed to be nonthermal means that fluctuating behavior is no longer described by thermodynamic fluctuations. Instead, the system must possess another source of stochastic behavior, forming nonthermal fluctuations.

S. G. Abaimov, *Statistical Physics of Non-Thermal Phase Transitions,*
Springer Series in Synergetics, DOI 10.1007/978-3-319-12469-8_4

Once the nonthermal fluctuations are generated, our main purpose is to map these fluctuations on their thermodynamic analogs so that the well-developed formalism of the theory of phase transitions in statistical physics may become available for their description.

4.1 The Model of Percolation

The name "percolation" is generally attributed to the percolation of petroleum oil through the pores in a rock. When the rock containing petroleum oil possesses a system of pores connected one to another, the oil may flow through these pores to form oil clusters. The main question of the petroleum industry is that, on drilling a well, how much oil we can pump out of this cluster.

In spite of its name, the problem was originally formulated not in the petroleum industry but in chemistry as a model describing the process of polymerization (Flory 1941a, b, c; Stockmayer 1943). During gelation, separate molecules form bonds organizing them into clusters. The question then transforms into how big these clusters are.

Besides these two examples, many other phenomena are described by the formalism of percolation theory. E.g., the formation of a conducting cluster may cause the breakdown of a dielectric, the cluster of defects may cause the failure of a structure, the formation of a big cluster of trees in a forest leads to the possibility for a significant part of the forest to be destroyed by a fire, etc.

The name "percolation" and the mathematical formulation of bond percolation appeared in 1957 (Broadbent and Hammersley 1957). The scaling of the system was first discussed by Essam and Gwilym (1971). Here we consider only the basic concepts of this theory. For further details, we refer the reader to Stauffer and Aharony (1994) and other brilliant textbooks given in the list of references.

Similar to the Ising model, a model in the theory of percolation is based on a lattice. The shape of the lattice may be arbitrary (Fig. 4.1): one-dimensional, square, triangular, cubic, or the Bethe lattice (Cayley tree). The lattice is composed of sites connected by bonds.

There are two different types of percolation models: *site percolation* and *bond percolation*. In both cases, a field parameter p is introduced. In site percolation, p is the probability for a site to be occupied (independently of the states of other sites). Correspondently, $(1-p)$ is the probability for a site to be empty. Thereby, on an average, p represents the fraction of lattice sites that are occupied. So, if N is the total number of sites on the lattice, there are Np occupied sites and $N(1-p)$ empty sites on average.

Similarly, for the case of bond percolation, the field parameter p represents the probability for a bond to be occupied while $(1-p)$ is the probability for a bond to be empty.

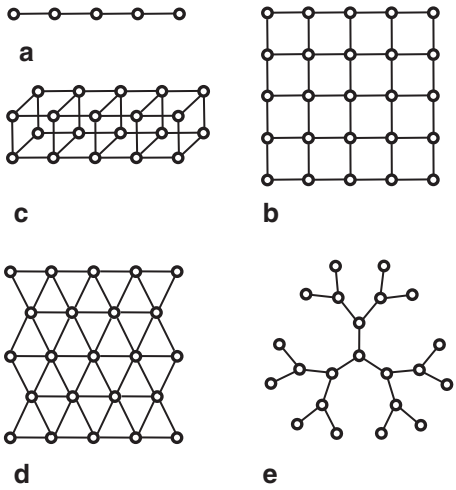

Fig. 4.1 A schematic representation of different geometrical forms of a lattice. **a** The one-dimensional chain of sites. **b** The two-dimensional square lattice. **c** The three-dimensional cubic lattice. **d** The two-dimensional triangular lattice. **e** The Bethe lattice

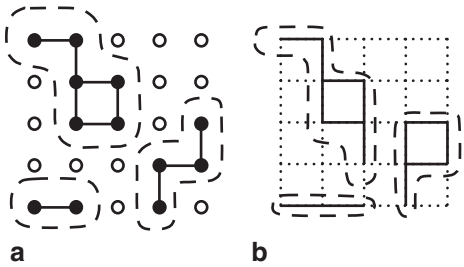

Fig. 4.2 Cluster formation for **a** site percolation, and **b** bond percolation

For both types, $0 \le p \le 1$, where $p = 0$ corresponds to a completely empty lattice while $p = 1$ corresponds to a completely occupied lattice.

The occupied sites or bonds (depending on the type of percolation considered) form clusters. Two sites are united into a common cluster if they are nearest neighbors and both are occupied. Two bonds are united into a cluster if they are connected by their ends and both are occupied.

Examples of clusters on square lattice for the case of site percolation are presented in Fig. 4.2a. Here, filled dots represent occupied sites while empty dots represent empty sites. If the distance between two occupied sites equals the lattice constant (the length of the edge of a square cell), we consider these sites to be the nearest neighbors and unite them into the common cluster (black lines represent this procedure; each cluster is surrounded by a dashed curve to separate it visually from the neighboring clusters).

We present similar examples of clusters on square lattice for the case of bond percolation in Fig. 4.2b. Here black lines represent the occupied bonds while dotted lines represent the empty bonds. Each cluster is surrounded by a dashed curve to separate it visually from other clusters.

Comparing Fig. 4.2a and b, we see that the behavior of clusters for the site percolation differs from the case of bond percolation. In Fig. 4.2b, two clusters are separated only by the lattice constant (edge of a square cell) while in Fig. 4.2a, such a situation is, obviously, impossible—the clusters must be separated at least by "the diagonal of a square cell" ($\sqrt{2}$ times the lattice constant)—otherwise these two clusters would be united into one. This comparison suggests that the behavior of the site percolation should differ from the case of bond percolation.

Although the case of bond percolation is no less interesting than the site percolation, the majority of studies are devoted to the latter. Therefore, we will primarily consider the site percolation and will return to the bond percolation only in Chap. 7, where it will present a beautiful example of the renormalization group (RG) transformation.

The size of a cluster is, obviously, measured by the number s of sites belonging to this cluster. Instead of saying "*a cluster of size s,*" we further say "*s-cluster*," which makes explanations much less cumbersome. We call separate occupied sites surrounded only by empty sites as 1-clusters.

The edges of the whole lattice play crucial role in the formulation of the percolation problem. The cluster is called *a percolating cluster* when it connects the opposite edges of the model. For example, the very percolating cluster (composed of the conducting sites) provides the breakdown of a dielectric. Since we generally consider the case of an infinite lattice, a percolating cluster generally contains an infinite number of sites.

As an example, we suggest the reader to imagine a square lattice. This lattice has left, right, top, and bottom edges. Generally, the left–right percolation is considered when a cluster should connect the left and right edges of the model (or, on the contrary, the top–bottom percolation when a cluster connects the top to bottom).

As usual, there are many modifications of the model formulation when, for example, the periodic boundary conditions are imposed, transforming, e.g., a square lattice into a torus. In this case, a percolating cluster is expected to form a ring around the torus (to go over one of the two torus dimensions and to reconnect to itself).

Many other modifications are possible. However, for simplicity we consider only the "canonic" formulation of the model with free boundary conditions when a percolating cluster should connect two opposite sides of the model.

Obviously, the possibility for a percolating cluster to exist depends on the field parameter p. When p is small ($p \to +0$), almost the whole lattice is empty and a percolating cluster is, obviously, impossible. In the opposite case, when $p \to 1-0$, almost the whole lattice is occupied and a percolating cluster certainly exists.

Between these two extremes, the field parameter p changes in the range $0 < p < 1$. If we are increasing p from zero to unity (adding more and more occupied sites to the lattice), the point p_C, when a percolating cluster appears for the first time, is called *a percolation threshold*. This point plays the role of a critical point of a continuous phase transition in the model.

A system is said to be below or above the percolation threshold if $p < p_C$ or $p > p_C$, respectively.

Also, we should mention that the case of an infinite system $N \to +\infty$ is mainly considered. The name *thermodynamic limit* for $N \to +\infty$ stays in spite of the fact that we no longer consider a thermal system. The case of a finite system will be discussed in Chap. 8,which leads to the appearance of the so called *finite-size effect*.

4.2 One-Dimensional Percolation

Problem 4.2.1

For the one-dimensional case, find the percolation threshold, the probability for a percolating cluster to exist, the cluster-size distribution, and the mean cluster size.

Solution: In the one-dimensional case, a percolating cluster is supposed to connect two opposite ends of the chain of sites. When $p < 1$, empty sites would always be present on the infinite lattice (p may be close to unity but its value is fixed while we consider the limit $N \to +\infty$), and there is no percolating cluster.

Therefore, the percolating cluster exists only when all sites of the lattice are occupied:

$$p_C = 1. \tag{4.1}$$

So, the probability for a percolating cluster to exist is

$$\Pi(p) = \begin{cases} 0, p < p_C \\ 1, p = p_C \end{cases}. \tag{4.2}$$

We see that the one-dimensional percolation resembles the one-dimensional Ising model from Problem 3.4.2. There the phase transition took place only at zero temperature because one spin oriented opposite to others could break the spontaneous magnetization. In the one-dimensional percolation, the phase transition appears only when the total lattice is occupied because one empty site breaks the percolating cluster.

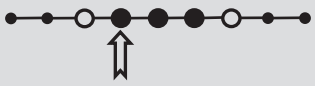

Next we consider the system below the percolation threshold: $p < p_C = 1$. We choose a particular site on the lattice and intend to find the probability $n_s(p)$ that this site happens to be the first site on the left of an s-cluster.

For example, as shown in the figure, we have built a 3-cluster. The chosen site is marked by an arrow. It is occupied (a big filled dot) as well as two more sites to the right to form a 3-cluster so that the left end of this cluster would correspond to the chosen site.

However, to finally form the cluster, we should not only prescribe the occupied sites belonging to this cluster but also surround the cluster with empty sites (so that our cluster would not spread further). For this purpose, we employ two big empty circles in the figure to denote the presence of empty sites.

Having formed the cluster of occupied sites and its *perimeter* of empty sites, we no longer care whether the rest of the lattice is occupied or not. The sites whose status is unknown are represented by small dots in the figure.

Since the probability for an arbitrary site to be occupied is p while the probability for a site to be empty is $(1-p)$, the probability of given figure (that the chosen site is the first on the left of the 3-cluster) is

$$n_3(p) = p^3(1-p)^2. \tag{4.3}$$

For an s-cluster, we similarly obtain:

$$n_s(p) = p^s(1-p)^2 = (1-p)^2 e^{-s\ln\frac{1}{p}}. \tag{4.4}$$

Talking about that the left end of an s-cluster corresponds to the chosen site, we are, in fact, talking about the probability to find an s-cluster at a particular place on the lattice. Summing probabilities (4.4) over all N sites on the lattice, we sum the probabilities to find an s-cluster at different locations. Therefore, the total averaged number of s-clusters on the lattice is expected to be $Nn_s(p)$. Here $n_s(p)$ plays the role of *the cluster-size distribution* and is often called *a normalized cluster number* because it represents the number of s-clusters on the lattice per lattice site.

Expanding (4.4) in the vicinity of the percolation threshold (4.1), $p - p_C \to -0$, we find

$$n_s(p) \propto e^{-s(1-p)} = e^{-s|p-p_C|}. \tag{4.5}$$

As we will see later, in the case of an arbitrary lattice, the good approximation is provided by the hypothesis that

$$n_s(p) \propto s^{-\tau} e^{-(c(p)s)^{\zeta}}, \tag{4.6}$$

where

$$c(p) \propto | p - p_C |^{1/\sigma} \text{ for } p \to p_C. \tag{4.7}$$

Here τ, σ, and ζ are critical indices. From (4.5), we immediately find $\tau = 0$, $\sigma = 1$, and $\zeta = 1$.

Next, let us find the probability $P_s(p)$ for an arbitrary site to belong to an *s*-cluster. It is not equal to $n_s(p)$ since this time we do not require from the given site to be located at the left end of the cluster. Instead, the site can be at any point along the length of the *s*-cluster.

Before we have found $n_s(p)$ as a probability for a site to be the first on the left of an *s*-cluster. Obviously, the probabilities for this site to be the second, the third, the s^{th} site on the left of the *s*-cluster are all the same and all equal $n_s(p)$. Summing these probabilities over different positions of the chosen site along the *s*-cluster length, we find the probability for an arbitrary site to belong to an *s*-cluster,

$$P_s(p) = sn_s(p) = sp^s(1-p)^2 \tag{4.8}$$

which is just *s* times higher than $n_s(p)$.

So far, we did not know in advance whether the chosen site is itself occupied or empty. However, if we know that this site is occupied, we should divide (4.8) by *p*:

$$P'_s(p) = sn_s(p)/p = sp^{s-1}(1-p)^2. \tag{4.9}$$

We have obtained probability (4.8) for the system below the percolation threshold, $p < p_C = 1$. At the percolation threshold $p = p_C = 1$, there are no finite *s*-clusters

$$P_s(p) = \begin{cases} sp^s(1-p)^2, p < p_C \\ 0 \qquad\quad , p = p_C \end{cases}, \tag{4.10}$$

because the whole lattice is occupied by the infinite percolating cluster. Therefore, for the probability of this cluster to exist, we find

$$P_{PC}(p) = \begin{cases} 0, p < p_C \\ 1, p = p_C \end{cases}. \tag{4.11}$$

By definition, *p* is the probability for an arbitrary site to be occupied. But if a site is occupied, it belongs either to a finite cluster or to an infinite percolating cluster. Summing the respective probabilities, we obtain *the law of conservation of probability*[1]:

[1] This equation resembles very much the law of conservation of particles in the case of the Bose–Einstein condensation. In both cases, after the critical point, one term of the discrete

$$p = \sum_s P_s(p) + P_{PC}(p). \tag{4.12}$$

This statement can be easily proved directly. Substituting (4.10 and 4.11) into (4.12), we find

$$p = \sum_s \begin{Bmatrix} sp^s(1-p)^2, p < p_C \\ 0 \qquad , p = p_C \end{Bmatrix} + \begin{Bmatrix} 0, p < p_C \\ 1, p = p_C \end{Bmatrix}. \tag{4.13}$$

For $p < p_C$, the sum over s can be transformed as

$$\sum_s sp^s = \sum_s p\frac{dp^s}{dp} = p\frac{d}{dp}\sum_s p^s = p\frac{d}{dp}\frac{p}{1-p}. \tag{4.14}$$

Substituting this result, we immediately prove (4.12).

There are several ways to determine the mean cluster size for the system. If on the lattice with N sites we counted all s-clusters, their number would be $Nn_s(p)$ on average. So, one way to define the mean cluster size is to average s with probabilities $\dfrac{Nn_s(p)}{\sum_s Nn_s(p)}$:

$$S(p) \equiv \frac{\sum_s sNn_s(p)}{\sum_s Nn_s(p)} = \frac{\sum_s sn_s(p)}{\sum_s n_s(p)}. \tag{4.15}$$

However, we may average clusters in a different way. Let us point randomly a finger at the lattice sites. If the site we have hit is occupied and belongs to an s-cluster, we register the size of the cluster s. Later, when we have repeated this procedure several times, we average the obtained cluster numbers.

The probability that a site belongs to an s-cluster is $P_s(p) = sn_s(p)$. Pointing K times at the lattice, we hit s-clusters $Ksn_s(p)$ times. So, averaging s with probabilities $\dfrac{Ksn_s(p)}{\sum_s Ksn_s(p)}$, we find

$$\tilde{S}(p) \equiv \frac{\sum_s sKsn_s(p)}{\sum_s Ksn_s(p)} = \frac{\sum_s s^2 n_s(p)}{\sum_s sn_s(p)}. \tag{4.16}$$

---

sum begins to represent the number of degrees of freedom which is comparable with N. So, in the case of the Bose–Einstein condensation, the number of particles in the condensate becomes comparable with the total number of particles in the system while in percolation the number $NP_{PC}(p)$ of sites belonging on average to a percolating cluster occupies a significant part of the lattice. In both cases, the considered term is separated from the sum to emphasize its outstanding role and not to lose it when the sum is substituted by an integral.

The difference between two methods of determining the mean cluster size is better illustrated with an example. Let us consider a lattice with one-thousand 1-clusters and one 1000-cluster. Then, following the formulae above, we find $S = \dfrac{1\cdot 1000 + 1000\cdot 1}{1000+1} \approx 2$ and $\tilde{S} = \dfrac{1^2\cdot 1000 + 1000^2\cdot 1}{1\cdot 1000 + 1000\cdot 1} \approx 500.$

It is easy to explain the difference: there are many 1-clusters on the lattice and just one 1000-cluster. Averaging all clusters by (4.15), we obtain the mean cluster size close to $s = 1$. On the contrary, the 1000-cluster is much bigger than 1-clusters and occupies a significant part of the lattice. Therefore, pointing randomly at the lattice, we hit this cluster very often; in fact, as often as all 1-clusters together. Therefore, the second method of averaging (4.16) returns the result close to $s = 1000$.

Drilling a petroleum well, we, in fact, almost randomly point at the rock and thereby follow the second method. Thus, it is probable that we hit the 1000-cluster. Thank God! because it is much better to pump out 500 barrels of oil than only 2.

For the one-dimensional case below the percolation threshold, we can find $S(p)$ and $\tilde{S}(p)$ directly:

$$S(p) = \frac{p}{\sum\limits_s p^s (1-p)^2} = \frac{1}{1-p}, \tag{4.17}$$

$$\tilde{S}(p) = \frac{\sum\limits_s s^2 p^s (1-p)^2}{p} = \frac{(1-p)^2}{p}\left(p\frac{d}{dp}\right)^2 \sum_s p^s = \frac{1+p}{1-p}. \tag{4.18}$$

As we will see in Chap. 6, $\tilde{S}(p)$ provides more interesting results than $S(p)$. In particular, in the vicinity of the percolation threshold, we define the critical index γ by

$$\tilde{S} \propto | p - p_C |^{-\gamma}. \tag{4.19}$$

A comparison with (4.18) determines $\gamma = 1$ for the one-dimensional case.

4.3 Square Lattice

Let us discuss the cluster-size distribution in the case of a square lattice. If we consider the probability to find a 1-cluster at a particular place on the lattice, first, we need to take into account that this site is itself occupied. Second, we should provide

that four neighboring sites at the cluster perimeter are empty (Fig. 4.3(a)), which would guarantee that the considered cluster is indeed a 1-cluster:

$$n_1(p) = p(1-p)^4. \tag{4.20}$$

The case of the probability to find a 2-cluster at a given place on the lattice is more difficult. This time we have to take into account that a 2-cluster may be "oriented horizontally" (Fig. 4.3(b)) as well as "vertically" (Fig. 4.3(c)). For both cases, we should provide two occupied sites of the cluster itself and six empty sites for its perimeter:

$$n_2(p) = 2p^2(1-p)^6. \tag{4.21}$$

The case of 3-cluster is even more difficult. There are two configurations with eight empty sites at the perimeter (Fig. 4.3(d–e)) and four configurations with seven empty sites at the perimeter (Fig. 4.3(f–i)). The corresponding probability is

$$n_3(p) = 2p^3(1-p)^8 + 4p^3(1-p)^7. \tag{4.22}$$

For 4-clusters, there are two configurations with ten empty sites at the perimeter (Fig. 4.3(j–k)), eight configurations with nine empty sites at the perimeter (Fig. 4.3(l–s)), and nine configurations with eight empty sites at the perimeter (Fig. 4.3(t–◊)):

$$n_4(p) = 2p^4(1-p)^{10} + 8p^4(1-p)^9 + 9p^4(1-p)^8. \tag{4.23}$$

Problem 4.3.1

Find the normalized cluster number for $s = 5$.

Different configurations of an *s*-cluster on a lattice are called *lattice animals*. The problem is that different lattice animals, in spite of the fact that they all have the same size *s,* have different perimeters. Therefore, to find the normalized cluster number $n_s(p)$ for an arbitrary *s,* we have to sum these configurations with different numbers of empty sites:

$$n_s(p) = \sum_{t_s} g_{t_s} p^s (1-p)^{t_s}. \tag{4.24}$$

Here, the sum goes over different perimeters t_s, and g_{t_s} is the degeneracy of this value of perimeter. Since the perimeter means the corresponding number of empty sites surrounding the cluster and separating it from other clusters, it represents not only the cluster's "external surface" but also the surface of "internal holes" within the cluster.

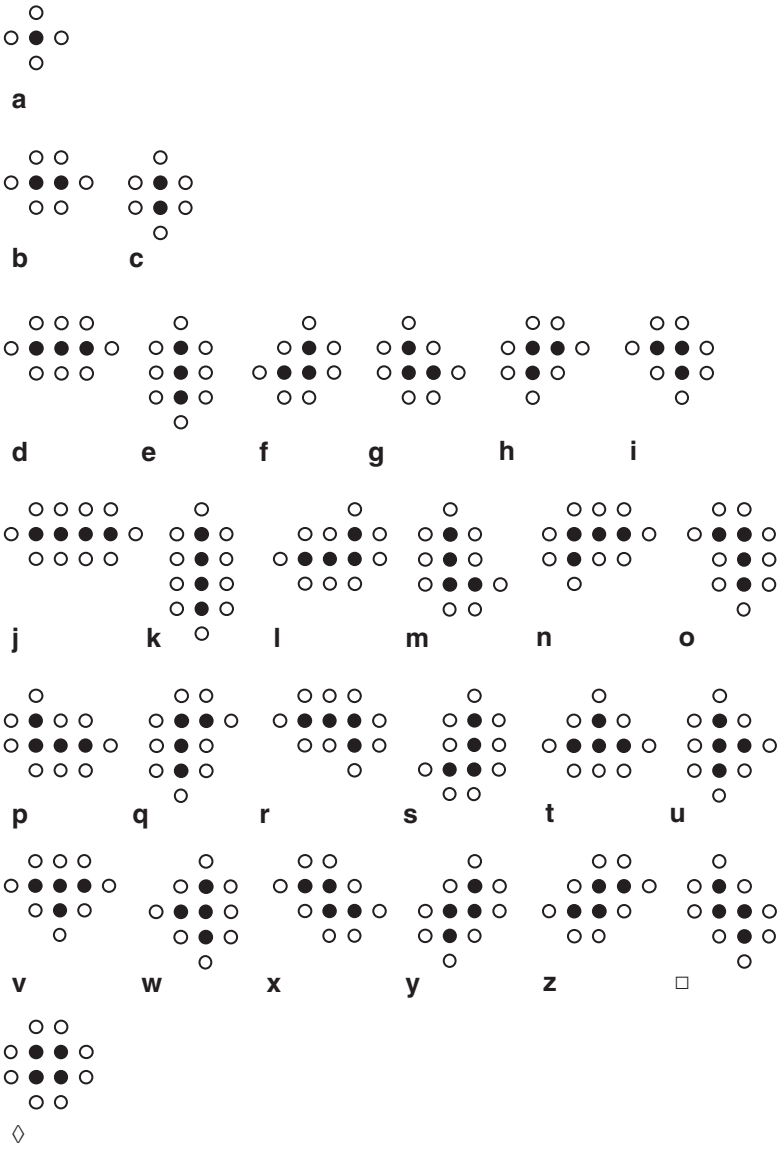

Fig. 4.3 Lattice animals on square lattice

When s increases, the corresponding number of lattice animals also increases very fast. Besides, different animals have different perimeters. All this makes exact analytical calculations of n_s impossible for high s; and the problem of percolation on square lattice has not been solved exactly yet.

The main difficulty is that the perimeter is different for different lattice animals corresponding to the same *s*. If the number of empty sites at the perimeter were fixed for fixed *s,* this would drastically simplify the problem and probably provide the possibility of an analytical solution.

But how can we achieve that? On square lattice, the animals have complex configurations due to the possibility for the clusters to form loops. A lattice which prohibited loops would significantly simplify the problem.

One way to avoid loops would be to increase the dimensionality of the system (to consider cubic or *d*-dimensional hypercubic lattices instead of the square lattice). Indeed, the higher the dimensionality of the system, the more the variety of lattice animals, which is provided by that the animals settle the multiple dimensions instead of forming loops.

For example, in Fig. 4.3(j–◊), we consider 4-clusters on square lattice. Among them there is only one loop (Fig. 4.3(◊)). Let us increase the dimensionality of the system to see that the role of the loops will be, indeed, diminishing.

If we added one more dimension to the lattice, transforming the square lattice into the cubic lattice, there would appear two more 4-loops in two appearing planes. In *d* dimensions of the hypercubic lattice to form a 4-loop, we choose one axis of *d* and then the second axis of the remaining $(d-1)$. Having chosen two axes, we form the plane for the 4-loop. However, this way we have counted all planes twice. Therefore, the total number of the 4-loops on the *d*-dimensional hypercubic lattice is $d(d-1)/2$.

But in parallel with the increase of the dimensionality of the system, the number of other lattice 4-animals would increase more significantly because now the animals may "wriggle" in the high-dimensional space.

Let us calculate, for example, the number of lattice 4-animals, "wriggling" only in the positive direction of every axis (considering only the positive direction we avoid mixture with the animals at neighboring locations). On square lattice, we choose the given location as the initial site. Then the 4-animal, to form the second site, can "wriggle" to the east or to the south only. One more step to the east or south forms the third site, and then the last step to the east or south forms the fourth, last site. The number of configurations $2\cdot 2\cdot 2=8$ includes lattice animals (j), (k), (m), (o), (p), (r), (x), and (□) from Fig. 4.3. We have counted not all "wriggling" lattice 4-animals but those that are quite enough for our proof.

In *d* dimensions, similar considerations allow us to count $d\cdot d\cdot d=d^3$ lattice 4-animals "wriggling" from the given location only in the positive directions of all axes.

In the limit $d\to+\infty$, the number of 4-loops increases as $d^2/2$ and becomes negligible in comparison with the rest of the lattice 4-animals whose number increases at least as d^3. So, one way to simplify the system is to increase its dimensionality or, better, make it infinite. But besides the infinite-dimensional lattices, are there other lattices without loops?

4.4 Bethe Lattice

A lattice without loops is *the Bethe lattice* (Fig. 4.1e). The procedure to build this lattice is the following. We create a seeding site of the 0th generation. This site emits Z bonds of the 1st generation to create Z neighboring sites of the 1st generation ($Z = 3$ in Fig. 4.1e). Each site of the 1st generation emits $Z-1$ bonds of the 2nd generation to create the sites of the 2nd generation. And so on, any site of the n^{th} generation emits $Z-1$ bonds to create the $(n+1)^{\text{th}}$ generation. In the result, we obtain the infinite lattice, spreading like the branches of a tree (called *Cayley tree*). Each site has Z neighbors, and since the bonds do not intersect, the lattice has no loops. Therefore, the Bethe lattice is often called the infinite-dimensional lattice.

Let us calculate the number of sites on the Bethe lattice located within the volume of radius R. We should sum 1 for the central site (0th generation), Z for the sites of the 1st generation, $Z(Z-1)$ for the sites of the 2nd generation, ..., $Z(Z-1)^{R-1}$ for the sites of the R^{th} generation:

$$\begin{aligned} V &= 1 + Z + Z(Z-1) + \ldots + Z(Z-1)^{R-1} \\ &= 1 + Z\frac{(Z-1)^R - 1}{(Z-1)-1} \to \frac{Z}{Z-2}(Z-1)^R \text{ for } R >> 1 \end{aligned} \tag{4.25}$$

The surface of this volume is formed by the last term in the sum:

$$S = Z(Z-1)^{R-1}; \tag{4.26}$$

hence, the ratio of the surface to the volume surrounded by it

$$\frac{S}{V} \to \frac{Z(Z-1)^{R-1}}{\frac{Z}{Z-2}(Z-1)^R} = \frac{Z-2}{Z-1} \text{ for } R >> 1, \tag{4.27}$$

does not depend on the radius R. In other words, the surface of a volume is comparable with the volume itself, which resembles the infinite-dimensional hypercubic lattice for which $\frac{S}{V} \propto \frac{V^{(d-1)/d}}{V} = \frac{1}{V^{1/d}} \to 1 \; (d \to +\infty)$.

The percolation threshold is very easy to find in the case of the Bethe lattice. Let us consider a branch of a percolating cluster. This branch is supposed to bear a stretched to infinity chain of occupied sites (further we may say that the branch leads to infinity).

Each site generates $Z-1$ daughter sites. By the definition of the field parameter p, only $(Z-1)p$ of these sites are occupied. If $(Z-1)p < 1$, each site generates less than one occupied site, and the chain of occupied sites will end sooner or later (Fig. 4.4a) so that there is no percolating cluster and our system is below its percolation threshold.

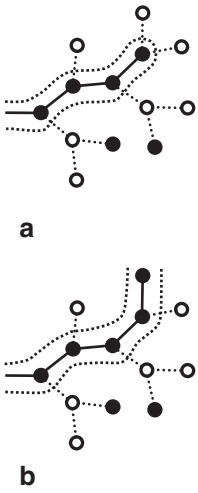

Fig. 4.4 The formation of a percolating cluster. **a** Below the percolation threshold, each site generates less than one occupied site and the chain of occupied sites ends sooner or later and does not lead to infinity. **b** Only at the percolation threshold each site generates one occupied site on average and the percolating cluster appears

If we are increasing p, the percolating cluster appears only when $(Z-1)p=1$ so that one of the generated sites would be occupied on average (Fig. 4.4b) to be able to continue the chain. This determines the percolation threshold

$$p_C = \frac{1}{Z-1}. \tag{4.28}$$

Problem 4.4.1

Each site generates $Z-1$ daughter sites of the 1st generation and $(Z-1)^2$ sites of the 2nd generation. For the given value of p, only $(Z-1)^2 p$ sites of the 2nd generation are occupied. If (similar to the previous discussion) we required that on an average only one site of the 2nd generation should be occupied, $(Z-1)^2 p=1$, this would lead to the incorrect value $p_C = 1/(Z-1)^2$ of the percolation threshold. Explain what went wrong.

Solution: One occupied site of the 2nd generation does not guarantee the presence of a percolating cluster since the corresponding site of the first generation may happen to be empty (see figure).

Instead, we should require that one of $(Z-1)^2$ chains leading from the initial site to the sites of the 2nd generation would be occupied:

$$(Z-1)^2 p_C^{\,2} = 1 \tag{4.29}$$

which would return us to the correct answer (4.28).

Therefore, on average we need not only one occupied site but $(Z-1)^2 p_C = (Z-1)$ occupied sites of the 2nd generation so that only one of them would support a stretching to infinity chain of occupied sites.

Next, for the Bethe lattice, we find the probability $P_{PC}(p)$ for a site to belong to a percolating cluster. Since the percolating cluster represents the appearance of a new phase above the percolation threshold (like the spontaneous magnetization appearing below the critical point), this probability will play the role of the order parameter.

We choose an arbitrary site on the lattice to serve as the 0th order site (site *A* in Fig. 4.5). *Z* bonds (*a, b,* and *c* in Fig. 4.5 for the case $Z = 3$) of the 1st generation emanate from this site to form *Z* branches of the lattice. Let us first find the probability *Q* that one of these branches (branch *a*) does not contain a stretching to infinity chain of occupied sites (does not lead to infinity). Thereby, this branch will not belong to a percolating cluster.

The chosen bond of the 1st generation (bond *a*) leads to one of the sites of the 1st generation (site *B*). If this site is empty with probability $1-p$, the branch *a* does not lead to infinity without regard to whether other sites along the branch are occupied or empty.

On the contrary, if site *B* is occupied with probability *p,* we consider its $Z-1$ daughter bonds (*d* and *e*) of the 2nd generation. These bonds start their own branches serving as the subbranches for the parent branch *a*. Due to the symmetry of the lattice and the symmetry of the choice of the initial site *A,* the probability for any of these daughter branches (*d* or *e*) not to lead to infinity is *Q*. The probability that they all do not lead to infinity is then Q^{Z-1}. In the result, the probability *Q* that branch *a* does not lead to infinity is provided when either site *B* is empty with probability $1-p$ or it is occupied with probability *p* and its branches do not lead to infinity:

$$Q = (1-p) + pQ^{Z-1}. \tag{4.30}$$

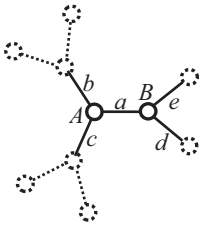

Fig. 4.5 An illustration how we find the probability for a site to belong to a percolating cluster

For the particular case $Z = 3$, this equation is quadratic and has two solutions:

$$Q = 1 \text{ and } Q = \frac{1-p}{p}. \tag{4.31}$$

In accordance with the law of conservation of probability, an occupied site belongs either to a finite cluster or to an infinite percolating cluster:

$$p = \sum_s P_s(p) + P_{PC}(p). \tag{4.32}$$

The probability that the initial site A belongs to a finite cluster equals the product of the probability p that it is occupied and the probability Q^Z that none of its Z branches (a, b, or c) lead to infinity. Substituting this result into (4.32), we find the probability for this site to belong to an infinite percolating cluster:

$$P_{PC}(p) = p(1-Q^Z), \tag{4.33}$$

where Q is provided by (4.31).

The obtained result (4.33) is obvious if we consider it from a different point of view. The probability $P_{PC}(p)$ for site A to belong to an infinite percolating cluster is the product of the probability p that it is occupied and the probability $(1-Q^Z)$ that one or more branches (a, b, or c), emanating from it lead to infinity. The last probability is unity minus the probability Q^Z that none of the branches a, b, or c lead to infinity.

For $Z = 3$, we have obtained two solutions (4.31) for Q. The first solution, $Q = 1$, substituted into (4.33) returns $P_{PC}(p) = 0$, which represents the absence of a percolating cluster below the percolation threshold. The second solution, $Q = (1-p)/p$, corresponds to the system above the percolation threshold when the probability for a site to belong to a percolating cluster is

$$P_{PC}(p) = p\left(1-\left(\frac{1-p}{p}\right)^3\right). \tag{4.34}$$

In the vicinity of the percolation threshold $p \to p_C + 0 = \frac{1}{2} + 0$, we expand (4.34) to find

$$P_{PC}(p) \propto p - p_C. \tag{4.35}$$

Since this probability represents the order parameter of the system, we define the critical index β by

$$P_{PC}(p) \propto (p - p_C)^{\beta}. \tag{4.36}$$

Comparison with (4.35) immediately provides $\beta = 1$ for the Bethe lattice.

Next, let us find the mean cluster size $\tilde{S}$ below the percolation threshold. We assume that an arbitrary branch (branch a in Fig. 4.5 for the case $Z = 3$) on average bears a bunch of T occupied, connected one-to-another sites.

If site B is empty with probability $1 - p$, then $T = 0$. If site B is occupied with probability p, then we have to consider its $(Z-1)$ daughter branches (d and e). Due to the lattice symmetry and the arbitrary choice of site A, each of the daughter branches (d and e) on average bears a bunch of T occupied, connected sites again. Therefore, the averaged number T of occupied and connected sites born by branch a equals zero with probability $1 - p$ and $1 + (Z-1)T$ with probability p:

$$T = 0 \cdot (1-p) + (1 + (Z-1)T)p. \tag{4.37}$$

The solution of this equation is

$$T = \frac{p}{1-(Z-1)p}. \tag{4.38}$$

In the result, the size of a cluster to which site A belongs is zero if site A is empty with probability $1 - p$ or $1 + ZT$ and if site A is occupied with probability p:

$$\tilde{S}(p) = 0 \cdot (1-p) + (1+ZT)p = \frac{p(1+p)}{1-(Z-1)p} \quad \text{for } p < p_C. \tag{4.39}$$

In the limit $p \to p_C - 0$, expanding (4.39), we find

$$\tilde{S} \propto \frac{1}{|\, p - p_C \,|} \tag{4.40}$$

which returns $\gamma = 1$ for the Bethe lattice.

Next, let us find the cluster-size distribution. For 1-clusters, we easily obtain

$$n_1(p) = p(1-p)^Z \tag{4.41}$$

as the probability for the site to be occupied while all its neighbors are empty (Fig. 4.6a).

For a 2-cluster, two sites are occupied while the remaining $(Z-1)$ neighbors of each of these sites are empty (Fig. 4.6b):

$$n_2(p) = g_2 p^2 (1-p)^{2(Z-1)}. \tag{4.42}$$

Here, the degeneracy g_2 represents possible configurations of a 2-cluster.

For the Bethe lattice, it is also easy to find the perimeter for a cluster of an arbitrary size. We assume that s-cluster in Fig. 4.6c has perimeter t_s. Occupying one site of this perimeter (site A), we transform our s-cluster into the $(s+1)$-cluster. Thereby

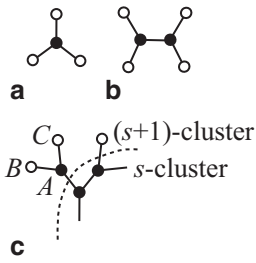

Fig. 4.6 Normalized cluster number. **a** A 1-cluster. **b** A 2-cluster. **c** When we are increasing the size of a cluster, its perimeter loses site A that becomes occupied but gains the outer neighbors B and C of this site

the perimeter loses site A that has been occupied but gains the outer $(Z-1)$ neighbors of this site (sites B and C for the case $Z=3$ of Fig. 4.6).

$$t_{s+1} = t_s - 1 + (Z-1). \tag{4.43}$$

Since

$$t_1 = Z \text{ and } t_2 = 2(Z-1), \tag{4.44}$$

by induction, we find

$$t_s = 2 + s(Z-2). \tag{4.45}$$

which determines the perimeter t_s for a cluster of an arbitrary size s. We see that in the case of the Bethe lattice, the perimeter of a cluster is the same for all clusters of the same size, which simplifies further calculations drastically.

For the cluster-size distribution in comparison with (4.24), we may omit the sum over the different perimeter values:

$$n_s(p) = g_s p^s (1-p)^{t_s} = g_s p^s (1-p)^{2+s(Z-2)}, \tag{4.46}$$

where g_s is the total number of lattice animals of size s. To avoid complications of finding g_s analytically, we normalize the cluster-size distribution (4.46) by its value at the percolation threshold:

$$\frac{n_s(p)}{n_s(p_C)} = \frac{p^s(1-p)^{2+s(Z-2)}}{{p_C}^s(1-p_C)^{2+s(Z-2)}} = \left(\frac{1-p}{1-p_C}\right)^2 e^{-c(p)s}, \tag{4.47}$$

where

$$c(p) = \ln\frac{1}{p(1-p)^{Z-2}} - \ln\frac{1}{p_C(1-p_C)^{Z-2}} = \ln\frac{p_C(1-p_C)^{Z-2}}{p(1-p)^{Z-2}}. \tag{4.48}$$

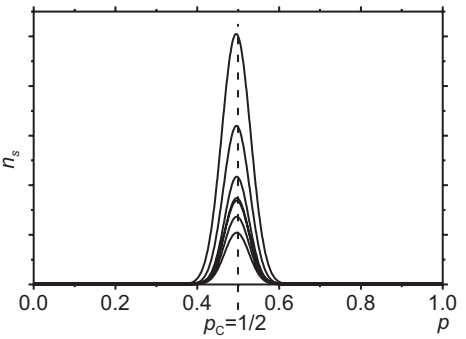

Fig. 4.7 Normalized cluster number for the case $Z = 3$

For the case $Z = 3$, we find

$$\frac{n_s(p)}{n_s(p_C)} = \left(\frac{1-p}{1-p_C}\right)^2 e^{-c(p)s}, \tag{4.49}$$

$$\text{where } c(p) = -\ln(1-4(p-p_C)^2). \tag{4.50}$$

The dependence of n_s on p for different values of s is presented in Fig. 4.7. When p is increasing from zero, the number of s-clusters on the lattice is also increasing because more and more sites become occupied. In the vicinity of the percolation threshold, n_s reaches its maximal value and then decays back to zero, due to the fact that the lattice becomes more and more consumed by a percolating cluster leaving less and less space for finite clusters.

In the vicinity of the percolation threshold $p \to p_C$, we expand (4.50) as

$$c(p) \propto (p-p_C)^2. \tag{4.51}$$

If, similar to (4.6 and 4.7), we introduce the hypothesis:

$$n_s(p) \propto s^{-\tau} e^{-(c(p)s)^{\zeta}}, \tag{4.52}$$

$$\text{where } c(p) \propto |\, p-p_C\,|^{1/\sigma} \text{ for } p \to p_C, \tag{4.53}$$

comparison with (4.49–4.51) immediately provides $\sigma = 1/2$ and $\zeta = 1$ for both cases below and above the percolation threshold.

The critical index τ cannot be determined from (4.49–4.51) because, normalizing the cluster-size distribution by its value at the percolation threshold, we have excluded this power-law decay from the dependence (4.47).

To find τ we should return to hypothesis (4.52 and 4.53). At the percolation threshold $p = p_C$, the exponential decay transforms into unity, leaving only the power-law decay:

$$n_s(p_C) \propto \frac{1}{s^\tau}. \tag{4.54}$$

From Chap. 1, we recall that power-law dependences indicate the presence of fractal scale invariance in a system. Experiments support this assumption—at the percolation threshold, clusters on a lattice become fractal.

This implies that on all scales, from the lattice constant to the size of a system as a whole, there is no characteristic length or characteristic cluster size so that the structure of clusters on the lattice becomes scale invariant. But a single possible dependence which does not possess a characteristic size is the power-law dependence (4.54). The critical index τ serves here as an exponent of the cluster-size distribution decay and is called *the Fisher exponent* (Fisher 1967a, b).

We should also mention that assumption (4.54) of scale invariance at the percolation threshold allows us to find the numbers g_s of lattice animals. Indeed, substituting (4.54) into (4.46), we obtain

$$\begin{aligned} g_s &= \frac{n_s(p_C)}{{p_C}^s (1-p_C)^{2+s(Z-2)}} = \frac{const}{s^\tau} {p_C}^{-s} (1-p_C)^{-s(Z-2)} \\ &= \frac{const}{s^\tau} e^{s \ln \frac{1}{p_C (1-p_C)^{(Z-2)}}}. \end{aligned} \tag{4.55}$$

We see that, neglecting the "slow" power-law dependence $s^{-\tau}$, the number of lattice animals grows exponentially "fast" with s increasing: $g_s \approx_{\ln} e^{const \cdot s}$.

For the Bethe lattice, it is possible to find the numbers g_s analytically. Let us return to the law of conservation of probability (4.32) below the percolation threshold:

$$p = \sum_{s=1} s n_s(p) = \sum_{s=1} s g_s p^s (1-p)^{2+s(Z-2)}. \tag{4.56}$$

Rewriting this equation as

$$(1-p)^{-Z} = \sum_{s=1} s g_s \left\{ p(1-p)^{Z-2} \right\}^{s-1}, \tag{4.57}$$

we introduce a new parameter

$$\xi \equiv p(1-p)^{Z-2} \tag{4.58}$$

in terms of which our equation transforms into a power series:

$$(1-p(\xi))^{-Z} = \sum_{s=1} s g_s \xi^{s-1}. \tag{4.59}$$

Considering ξ as a complex number, we observe that by Cauchy's theorem the coefficients of this power series are given by

$$sg_s = \frac{1}{2\pi i} \oint\limits_{C_\rho} \frac{d\xi}{(1-p(\xi))^Z \xi^s}, \tag{4.60}$$

where C_ρ is the contour of integration of radius $\rho \to +0$ encircling the point $\xi = 0$.

Substituting the variable change (4.58) into (4.60), we find

$$sg_s = \frac{1}{2\pi i} \oint\limits_{C_\rho} \frac{\{1-p(Z-1)\}\, dp}{p^s (1-p)^{(Z-2)s+3}}, \tag{4.61}$$

where C_ρ is still the contour of integration encircling the point $p = 0$; however, now it is no longer a circle.

To find the integral we need to find the residue at point $p = 0$:

$$\begin{aligned} sg_s &= \operatorname*{res}_{p=0} \frac{1-p(Z-1)}{p^s (1-p)^{(Z-2)s+3}} = \operatorname*{res}_{p=0} \left\{ \frac{1}{p^s} - \frac{Z-1}{p^{s-1}} \right\} \frac{1}{(1-p)^{(Z-2)s+3}} \\ &= \operatorname*{res}_{p=0} \left\{ \frac{1}{p^s} - \frac{Z-1}{p^{s-1}} \right\} \sum_{k=0}^{+\infty} \frac{p^k}{k!} \frac{\{(Z-2)s+3+(k-1)\}!}{\{(Z-2)s+2\}!} \\ &= \frac{\{(Z-1)s+1\}!}{(s-1)!\{(Z-2)s+2\}!} - (Z-1) \left\{ \begin{array}{c} 0,\ s=1 \\ \dfrac{\{(Z-1)s\}!}{(s-2)!\{(Z-2)s+2\}!},\ s \geq 2 \end{array} \right\} \\ &= \frac{Z\{(Z-1)s\}!}{(s-1)!\{(Z-2)s+2\}!}. \end{aligned} \tag{4.62}$$

Thereby, for the number of lattice animals we find

$$g_s = \frac{Z\{(Z-1)s\}!}{s!\{(Z-2)s+2\}!}. \tag{4.63}$$

It is easy to verify the validity of this formula for small clusters. When $s = 1$, a 1-cluster can occupy any site of the lattice, and $g_1 = N/N = 1$.

When $s = 2$, a 2-cluster can occupy any bond of the lattice. Each site has Z attached bonds; thereby, there are $NZ/2$ bonds on the lattice with N sites (where 2 comes from the fact that, counting bonds in this manner, we will count each bond twice). To find g_2 we should divide the total number $NZ/2$ of possible 2-clusters on the lattice by the total number N of sites, $g_2 = \dfrac{NZ/2}{N} = \dfrac{Z}{2}$, which coincides with the result provided by (4.63).

In the limit of big clusters $s >> 1$, applying Stirling's approximation for (4.63), we do obtain the exponential dependence on s:

$$g_s \underset{\ln}{\approx} e^{s\{(Z-1)\ln(Z-1)-(Z-2)\ln(Z-2)\}}. \tag{4.64}$$

However, keeping other multipliers as well, we find

$$g_s = \frac{Z}{(Z-2)^{5/2}}\sqrt{\frac{Z-1}{2\pi}}\frac{1}{s^{5/2}}e^{s\{(Z-1)\ln(Z-1)-(Z-2)\ln(Z-2)\}}\left(1+\overset{=}{o}(1)\right). \tag{4.65}$$

For the cluster-size distribution this provides:

$$\begin{aligned} n_s(p) &= g_s p^s (1-p)^{2+s(Z-2)} \\ &= \frac{Z}{(Z-2)^{5/2}}\sqrt{\frac{Z-1}{2\pi}}(1-p)^2 \times \\ &\quad \times \frac{1}{s^{5/2}}e^{s\{(Z-1)\ln(Z-1)-(Z-2)\ln(Z-2)+\ln p+(Z-2)\ln(1-p)\}}\left(1+\overset{=}{o}(1)\right). \end{aligned} \tag{4.66}$$

At the percolation threshold (4.28) this expression transforms into the power-law dependence representing the fractal scale invariance in the system:

$$n_s(p_c) = \frac{Z}{\sqrt{2\pi(Z-2)(Z-1)^3}}\frac{1}{s^{5/2}}\left(1+\overset{=}{o}(1)\right). \tag{4.67}$$

Comparing (4.66) with hypothesis (4.52), we see that this hypothesis is valid for the Bethe lattice. Besides, we find $\tau = 5/2$.

All critical indices we have found for the Bethe lattice are simple integers or rational fractions. As we already know, such indices are characteristic for the mean-field approach. However, many indices we have obtained exactly; and no approximation has been employed. Why then is the behavior of the Bethe lattice similar to the mean-field approach?

The reason is that the Bethe lattice is equivalent to the infinite-dimensional lattice. As we will see in Chap. 6, in high dimensions, if a dimensionality of a system exceeds the upper critical dimension, the system's exact behavior generally obeys the mean-field rules. For cluster behavior this happens because the higher the dimension of a system is, the less its behavior is influenced by clusters with loops.

Unfortunately, in nature we are surrounded by two- and three-dimensional systems whose dimensionality is below the upper critical dimension. Thereby, the mean-field approximation is crude for these systems, and their critical indices are no longer simple integers or fractions.

4.5 An Arbitrary Lattice

Now we consider the case of an arbitrary lattice. First, we should say that the law of conservation of probability was derived from the basic principles and is, therefore, lattice-independent:

$$p = \sum_s s n_s(p) + P_{PC}(p). \tag{4.68}$$

Besides, the hypothesis that at the percolation threshold the structure of clusters becomes scale invariant,

$$n_s(p_C) \propto \frac{1}{s^\tau}, \tag{4.69}$$

also follows from general considerations only and may be accepted for an arbitrary lattice as well.

For the mean cluster size $\tilde{S}$ we utilize the previous definition (4.16):

$$\tilde{S}(p) \equiv \frac{\sum_s s^2 n_s(p)}{\sum_s s n_s(p)}. \tag{4.70}$$

However, in contrast to the one-dimensional percolation when the system above the percolation threshold was impossible, now we need to discuss whether we include or do not include a percolating cluster in sums of (4.70) when $p > p_C$. If we do so, the percolating cluster will participate as an additional term with $s = +\infty$ in both sums. This may lead only to the trivial result $\tilde{S} = +\infty$ when the mean cluster size is determined by the percolating cluster.

For us such a description of the system's behavior is not interesting because above the percolation threshold we expect the mean cluster size to represent the size of finite clusters. Therefore, we do not include the percolating cluster in both sums of (4.70).

The denominator of the right-hand side of (4.70) is a number between zero and unity as a part of the law of conservation of probability (4.68). Hence, the singular behavior of the mean cluster size $\tilde{S}$ is determined only by the numerator $\sum_s s^2 n_s(p)$ of (4.70). Substituting hypothesis (4.52) into (4.70) and replacing the discrete sum by an integral, we find

$$\begin{aligned} \tilde{S}(p) &\propto \sum_s s^2 n_s(p) \propto \sum_s s^2 \frac{1}{s^\tau} e^{-(c(p)s)^\zeta} \approx \int_1^{+\infty} s^{2-\tau} e^{-(c(p)s)^\zeta} ds \\ &\propto c^{\tau-3}(p) \Gamma\left(\frac{3-\tau}{\zeta}\right), \end{aligned} \tag{4.71}$$

where $\Gamma(\nu > 0) \equiv \int_0^{+\infty} x^{\nu-1} e^{-x} dx$ is the gamma function whose argument does not depend on p.

Substituting (4.53) into (4.71), we find the divergence of the mean cluster size in the vicinity of the percolation threshold

$$\tilde{S}(p) \propto c^{\tau-3}(p) \propto \mid p - p_{\mathrm{C}} \mid^{(\tau-3)/\sigma} \tag{4.72}$$

that corresponds to the following relation among the critical indices:

$$\gamma = \frac{3-\tau}{\sigma}. \tag{4.73}$$

Recalling that for the Bethe lattice $\gamma = 1$, $\sigma = 1/2$, and $\tau = 5/2$, we immediately prove the validity of this relation for the Bethe lattice.

Let us find other relations or inequalities among the critical indices valid in the case of an arbitrary lattice. At the percolation threshold $P_{PC}(p_{\mathrm{C}}) = 0$ so that the law of conservation of probability transforms into

$$p_{\mathrm{C}} = \sum_s s n_s(p_{\mathrm{C}}). \tag{4.74}$$

Substituting here (4.69), we find

$$p_{\mathrm{C}} \approx const \sum_s s^{1-\tau} \approx const \int_1^{+\infty} s^{1-\tau} ds. \tag{4.75}$$

The left-hand side, p_{C}, is the probability and, therefore, has a value between zero and unity. The last integral in the right-hand side does not diverge only if

$$\tau > 2 \tag{4.76}$$

which is the first inequality for the Fisher exponent valid on an arbitrary lattice.

Let us now consider the system above the percolation threshold, $p > p_{\mathrm{C}}$. From (4.68), we find

$$P_{PC}(p) = p - \sum_s s n_s(p) = p - p_{\mathrm{C}} + p_{\mathrm{C}} - \sum_s s n_s(p). \tag{4.77}$$

Substituting here (4.74),

$$P_{PC}(p) = p - p_{\mathrm{C}} + \sum_s s(n_s(p_{\mathrm{C}}) - n_s(p)), \tag{4.78}$$

and then hypothesis (4.52 and 4.53), we obtain

$$\begin{aligned} P_{PC}(p) &= (p - p_{\mathrm{C}}) + const \sum_s s^{1-\tau}(1 - e^{-(c(p)s)^{\zeta}}) \\ &\approx (p - p_{\mathrm{C}}) + const \int_1^{+\infty} s^{1-\tau}\left(1 - e^{-(c(p)s)^{\zeta}}\right) ds. \end{aligned} \tag{4.79}$$

Performing a variable change $z = (c(p)s)^{\zeta}$

$$P_{PC}(p) \approx (p - p_C) + const \cdot c^{\tau-2}(p) \int\limits_{c^{\zeta}(p)\to 0}^{+\infty} z^{\frac{2-\tau-\zeta}{\zeta}} \left(1 - e^{-z}\right) dz \tag{4.80}$$

and integrating by parts, we find

$$P_{PC}(p) \approx (p - p_C) + const \cdot c^{\tau-2}(p) \left\{ -z^{\frac{2-\tau}{\zeta}} \left(1 - e^{-z}\right) \Big|_{c^{\zeta}(p)\to 0}^{+\infty} + \int\limits_{c^{\zeta}(p)\to 0}^{+\infty} z^{\frac{2-\tau}{\zeta}} e^{-z} dz \right\}$$

$$\approx (p - p_C) + const \cdot c^{\tau-2}(p) \Gamma\left(\frac{2-\tau+\zeta}{\zeta}\right) \tag{4.81}$$

In the vicinity of the percolation threshold, we may substitute $c(p)$ in (4.81) from hypothesis (4.53) that returns another relation among the critical indices of an arbitrary lattice:

$$\beta = \begin{cases} \frac{\tau-2}{\sigma}, \frac{\tau-2}{\sigma} \le 1 \\ 1, \frac{\tau-2}{\sigma} > 1 \end{cases}. \tag{4.82}$$

Obviously, this relation is true for the found above critical indices of the Bethe lattice.

In the vicinity of the percolation threshold, we expect that the order parameter tends to zero, $P_{PC}(p) \to +0$, while the mean cluster size diverges, $\tilde{S}(p) \to +\infty$. This implies that $\beta > 0$ and $\gamma > 0$. Comparing these two inequalities with (4.73 and 4.82), we see that they are possible only when

$$2 < \tau < 3. \tag{4.83}$$

These are the first and second inequalities for the Fisher exponent.

The power-law dependence $P_{PC}(p) \propto (p - p_C)^{\beta}$ has important consequences. Since $P_{PC}(p)$ is the probability for a site to belong to a percolating cluster, $NP_{PC}(p) \propto N(p - p_C)^{\beta}$ is the number of sites on the lattice belonging to the percolating cluster on average.

We see that for $p > p_C$, a finite fraction of the total number N of sites on the lattice belongs to the percolating cluster. Therefore, above the percolation threshold the percolating cluster has the dimension d of the embedding lattice and is not a fractal with a fractal dimension.

However, at the percolation threshold $p = p_C$, we obtain $P_{PC}(p) = 0$. In the meantime, the percolating cluster already exists and percolates the infinite system!

Thereby it contains an infinite number of occupied sites. However, the fraction of these sites relative to the total number N of sites on the lattice is zero. Hence, this allows us to hypothesize that at the percolation threshold the percolating cluster is fractal with a fractal dimension D which is less than the dimension d of the embedding lattice. The scaling of the number of sites belonging to the percolating cluster may be schematically represented as

$$NP_{PC}(p) \propto \begin{cases} 0, p < p_C \\ L^D, p = p_C \\ L^d, p > p_C \end{cases}, \tag{4.84}$$

where L is the linear size of the lattice: $N = L^d$. At the percolation threshold, this dependence provides

$$P_{PC}(p_C) \propto L^{D-d} \propto N^{\frac{D-d}{d}} << 1, \tag{4.85}$$

which in the thermodynamic limit $N \to +\infty$ indeed transforms into

$$P_{PC}(p_C) = 0. \tag{4.86}$$

This statement may be illustrated with the aid of the petroleum clusters in a rock. Let us assume that these clusters are formed at the percolation threshold. We drill a well and, if we are lucky, we hit not a finite cluster but the infinite percolating cluster. Then we might pump out L^D barrels of petroleum, where L is the linear size of the oil field. Meantime, the total amount of petroleum in the rock is $Np_C \propto L^d$ barrels. Since $D < d$, we have pumped out only a negligible part of the total amount of petroleum!

We have hypothesized that the normalized cluster number obeys the hypothesis (4.52):

$$n_s(p) \propto s^{-\tau} e^{-(c(p)s)^{\zeta}}. \tag{4.87}$$

For small s, the exponential function $e^{-(c(p)s)^{\zeta}}$ is of the order of unity, and the cluster-size distribution decays as a power law:

$$n_s(p) \propto s^{-\tau}, \text{ where } s << 1/c. \tag{4.88}$$

On the contrary, for large clusters $s >> 1/c$, the exponential function dominates the decay:

$$n_s(p) \approx_{\ln} e^{-(c(p)s)^{\zeta}}. \tag{4.89}$$

What values are typical for the exponent ζ?

If we consider the limit $p \to +0$, almost the whole lattice is empty. On the empty lattice there is no need to care about forming $(1-p)^{t_s}$ empty sites at the perimeter of an s-cluster because in the limit $p \to +0$, the probability $(1-p)^{t_s}$ is almost unity. Therefore, to form an s-cluster we should only form s-occupied sites:

$$n_s(p) \propto p^s = e^{-s\left\{\ln\frac{1}{p}\right\}}. \tag{4.90}$$

This returns us to the value $\zeta = 1$:

$$n_s(p) \approx_{\ln} e^{-c(p)s} \text{ for } s >> 1/c. \tag{4.91}$$

Experiments show that $\zeta = 1$ may be a crude but reasonable approximation not only in the limit $p \to +0$ but also for $p < p_C$. Similar decay we have already observed in the one-dimensional case and for the Bethe lattice. If our results were directly applicable to nucleation in liquid–gas or magnetic systems, we would say that (4.91) describes the nucleus-size distribution above the critical point.

Next, let us consider the opposite extreme $p \to 1-0$ when almost the whole lattice is occupied. This time, on the contrary, there is no need to care to form s occupied sites for an s-cluster because the probability p^s is almost unity in the limit $p \to 1-0$. Instead, we should care about the empty sites of a perimeter which "cuts" the required s-cluster from the percolating cluster.

A perimeter can be arbitrary. One cluster might be compact having a smooth surface while another could resemble a snowflake with a fractal perimeter. But the more complex the perimeter is, the more sites must be empty so that the lower is the probability $(1-p)^{t_s}$. Therefore, the most probable are the clusters with the simplest, smooth, better spherical surface which cuts from the occupied lattice a d-dimensional "chunk."[2] While such a cluster of size s has the dimension of the embedding lattice,

---

[2] While the statement is valid, the reasoning behind it is oversimplified. Further, we apply the logarithmic accuracy in the limit of big clusters, $s >> 1/c$. To find the probability for a cluster perimeter to be smooth instead of being more complex (fractal), we should compare the part of the normalized cluster number that comes from the lattice animals with smooth perimeters, $\Delta n_s = \underline{\underline{O}}(s^\alpha) p^s (1-p)^{As^{\frac{d-1}{d}}} \approx_{\ln} p^s (1-p)^{As^{\frac{d-1}{d}}}$ with the share of the normalized cluster number belonging to the complex lattice animals. $\Delta n_s \approx_{\ln} e^{Cs} p^s (1-p)^{Bs}$, where we have taken into account that the numbers g_{t_s} of lattice animals with perimeters t_s are the power-law dependences $\underline{\underline{O}}(s^\alpha)$ on s for $t_s \propto As^{\frac{d-1}{d}}$ and the exponential dependences e^{Cs} on s for $t_s \propto Bs$. In the limit $p \to 1-0$, comparing $As^{\frac{d-1}{d}} \ln(1-p)$ with $s\{C + B\ln(1-p)\} \propto Bs\ln(1-p)$, we observe that the first expression has smaller absolute value but is higher than the second expression when we take into account the negative sign, $s\{\ldots < 0\} << s^{\frac{d-1}{d}}\{\ldots < 0\}$. In other words, the number of complex lattice animals are much bigger than the number of animals with smooth perimeters, but the improbability to have larger perimeters cancels this advantage, leaving the leading role to smooth, non-fractal, compact clusters, $n_s \approx_{\ln} p^s (1-p)^{As^{\frac{d-1}{d}}}$, which proves the statement above.

its smooth surface is $(d-1)$-dimensional and contains $s^{\frac{d-1}{d}}$ empty sites. Thus, the cluster-size distribution is

$$n_s(p) \propto (1-p)^{s^{\frac{d-1}{d}}} = e^{-\ln\left(\frac{1}{1-p}\right)s^{\frac{d-1}{d}}}. \tag{4.92}$$

Comparison with (4.89) provides $\zeta = 1 - \frac{1}{d}$ and

$$n_s(p) \approx_{\ln} e^{-(c(p)s)^{1-\frac{1}{d}}} \text{ for } s >> 1/c. \tag{4.93}$$

Here for the first time we encounter an exponent ζ that is not unity.

From (4.84), we see that the percolating cluster is fractal only at the percolation threshold; however, above the percolation threshold it loses its fractal properties and gains the dimensionality of the embedding lattice. The same statement seems to be valid for big pieces of this cluster as well. Thereby we may assume the cluster-size distribution (4.92) to be valid not only in the limit $p \to 1-0$ but, crudely speaking, for $p > p_C$ as well.[3]

However, from (4.90), we recall that $\zeta = 1$ for the Bethe lattice for the cases both below and above the percolation threshold. This is due to the fact that in accordance with (4.27) on the Bethe lattice the surface of a volume is of the order of the volume itself. So, if we need to "cut" a cluster of size s, its minimal perimeter is also of the order of s. In the limit $p \to 1-0$, this provides

$$n_s(p) \propto (1-p)^s = e^{-\ln\left(\frac{1}{1-p}\right)s} \tag{4.94}$$

with $\zeta = 1$ as expected.

The Bethe lattice serves as an analogue of the infinite-dimensional hypercubic lattice. Thus, similar results are valid for a hypercubic lattice as well in the

---

[3] The argument in the footnote on the previous page is no longer valid when we consider p to be well below unity. In this case $C + B\ln(1-p)$ can become positive, transferring the leading role to complex clusters, $n_s \approx_{\ln} e^{Cs} p^s (1-p)^{Bs}$, whereas the compact clusters are neglected now. The transition occurs at $p_0 = 1 - e^{-C/B}$, where C can be estimated with the aid of the total number g_s of lattice animals with s sites. Indeed, neglecting the number of compact lattice animals in comparison with their more complex counterparts, $g_s = \underline{\underline{O}}(s^\alpha) + e^{Cs} \approx_{\ln} e^{Cs}$, we find $C = \ln g_s / s$.

Thereby, for $p_0 < p < 1$ the normalized cluster number represents the behavior of smooth perimeter clusters, $n_s \approx_{\ln} p^s (1-p)^{As^{\frac{d-1}{d}}}$. On the contrary, for $p_C < p < p_0$ the cluster-size distribution is determined by complex clusters with $t_s \propto Bs$: $n_s \approx_{\ln} e^{Cs} p^s (1-p)^{Bs}$. The constant B, here we can estimate from the requirement that n_s has a maximum in the vicinity of the percolation threshold, $0 \approx \left.\frac{d\ln n_s}{dp}\right|_{p_C} = \frac{s}{p_C} - \frac{Bs}{1-p_C}$, or $B \approx \frac{1-p_C}{p_C}$. On square lattice $e^C \approx 4.06$, $p_C \approx 0.593$ and, thereby, $B \approx 0.686$. Therefore, for p_0 our argument provides $p_0 \approx 0.870$ which is indeed greater than p_C.

limit $d \to +\infty$ when $\zeta = 1 - \frac{1}{d} \to 1$ so that the cluster-size distribution (4.94) is the limit of (4.92) for $d \to +\infty$.

4.6 The Moments of the Cluster-Size Distribution

The last in this chapter, we discuss the moments

$$M_k(p) \equiv \sum_s s^k n_s(p) \tag{4.95}$$

of the cluster-size distribution for an arbitrary lattice. We should mention at once that the sum here does not include the term of the infinite percolating cluster again for the reasons similar to the derivation of formulae (4.70–4.73).

Initially, we consider $k > \tau - 1$. Similar to how we have found $\sum_s s^2 n_s(p)$ earlier, for the general case of the k^{th}-moment we find

$$M_k(p) \propto \int_1^{+\infty} s^{k-\tau} e^{-(c(p)s)^\zeta} ds \tag{4.96}$$

$$\propto c^{\tau-k-1}(p)\Gamma\left(\frac{k+1-\tau}{\zeta}\right) \propto \mid p - p_C \mid^{\frac{\tau-k-1}{\sigma}}.$$

This formula is valid for any integer k with the exception of $k = 0$ and $k = 1$. In the special cases $k = 0$ and $k = 1$, the inequality $k > \tau - 1$ is no longer valid so that the argument of the gamma function becomes negative.

To find the first moment M_1, we differentiate (4.95) with respect to c:

$$-\frac{dM_k}{dc} \propto -\frac{d}{dc}\sum_s s^{k-\tau} e^{-(cs)^\zeta} \propto c^{\zeta-1}\sum_s s^{k-\tau+\zeta} e^{-(cs)^\zeta} \propto c^{\zeta-1} M_{k+\zeta}. \tag{4.97}$$

For $k = 1$, this equation transforms into

$$-\frac{dM_1}{dc} \propto c^{\zeta-1} M_{1+\zeta}. \tag{4.98}$$

Since for all known lattices $2 < \tau < (2+\zeta)$ and thereby $(1+\zeta) > (\tau - 1)$, to find $M_{1+\zeta}$ we may utilize (4.96):

$$-\frac{dM_1}{dc} \propto c^{\tau-3}. \tag{4.99}$$

Integrating this equation with respect to c, we obtain

$$M_1 = const_1 - const_2 c^{\tau-2} = const_1 - const_2 \mid p - p_C \mid^{\frac{\tau-2}{\sigma}} \propto const_1. \tag{4.100}$$

In other words, in the vicinity of the percolation threshold, the first moment is not singular (its critical index is zero). This result is expected because the first moment is the probability for a site to belong to a finite cluster:

$$M_1(p) \equiv \sum_s s n_s(p) = p - P_{PC}(p) \tag{4.101}$$

so that at the percolation threshold

$$M_1(p_C) = p_C. \tag{4.102}$$

The zeroth moment M_0 is also found by differentiating (4.95) with respect to c. First, we consider the case when $2\zeta \geq \tau - 1$. Differentiating (4.95) once, we find how the derivative of M_0 is associated with M_ζ:

$$-\frac{dM_0}{dc} \propto c^{\zeta - 1} M_\zeta, \tag{4.103}$$

and how the derivative of M_ζ is associated with $M_{2\zeta}$:

$$-\frac{dM_\zeta}{dc} \propto c^{\zeta - 1} M_{2\zeta}. \tag{4.104}$$

Since we consider $2\zeta \geq \tau - 1$, to find $M_{2\zeta}$, we apply (4.96):

$$M_{2\zeta} \propto c^{\tau - 2\zeta - 1}. \tag{4.105}$$

Integrating (4.104) and then (4.103), we obtain:

$$M_\zeta = const_2 + const_1 c^{\tau - \zeta - 1}, \tag{4.106}$$

$$M_0 = const_3 + const_2 c^{\zeta} + const_1 c^{\tau - 1}. \tag{4.107}$$

This result we have found for the case when $2\zeta \geq \tau - 1$. If, on the contrary, $2\zeta < \tau - 1$ but $3\zeta \geq \tau - 1$ (which might be possible on the two-dimensional lattice), we add one additional equation to (4.103 and 4.104):

$$-\frac{dM_{2\zeta}}{dc} \propto c^{\zeta - 1} M_{3\zeta}, \tag{4.108}$$

and find $M_{3\zeta}$ in accordance with (4.96):

$$M_{3\zeta} \propto c^{\tau - 3\zeta - 1}. \tag{4.109}$$

Integration returns:

$$M_{2\zeta} = const_2 + const_1 c^{\tau-2\zeta-1}, \tag{4.110}$$

$$M_{\zeta} = const_3 + const_2 c^{\zeta} + const_1 c^{\tau-\zeta-1}, \tag{4.111}$$

$$M_0 = const_4 + const_3 c^{\zeta} + const_2 c^{2\zeta} + const_1 c^{\tau-1}. \tag{4.112}$$

Both results, (4.107 and 4.112), tell us that M_0 is not singular (its critical index is zero):

$$M_0 \propto const. \tag{4.113}$$

In the vicinity of the percolation threshold, we have assumed (4.53) that c behaves as $c \propto | p - p_C |^{1/\sigma} \to 0$. Thus, the last term in (4.107 or 4.112) represents a power-law dependence:

$$c^{\tau-1} \propto | p - p_C |^{(\tau-1)/\sigma}. \tag{4.114}$$

Defining a critical index α by

$$| p - p_C |^{(\tau-1)/\sigma} \propto | p - p_C |^{2-\alpha}, \tag{4.115}$$

we see that the new critical index obeys the following inequality:

$$\alpha + 2\beta + \gamma = 2 + 2\left\{ \begin{array}{c} 0, \dfrac{\tau-2}{\sigma} \le 1 \\ 1 - \dfrac{\tau-2}{\sigma}, \dfrac{\tau-2}{\sigma} > 1 \end{array} \right\} \le 2. \tag{4.116}$$

We will discuss in more detail the index α in Chap. 6.

Earlier we considered two methods to determine the mean cluster size, (4.15 and 4.16):

$$S(p) = \frac{\sum_s s n_s(p)}{\sum_s n_s(p)} = \frac{M_1}{M_0}, \tag{4.117}$$

$$\tilde{S}(p) = \frac{\sum_s s^2 n_s(p)}{\sum_s s n_s(p)} = \frac{M_2}{M_1}, \tag{4.118}$$

but later we have studied only $\tilde{S}$. Now we can answer the question why the behavior of $\tilde{S}$ is more interesting than the behavior of S—because (with the exception of the one-dimensional case (4.17) S does not diverge generally at the percolation threshold. Indeed, from (4.117) we see that S is the ratio of the first moment to the zeroth moment. Both these moments are not singular at the percolation threshold (with the exception of the one-dimensional case).

On the contrary, while the denominator of $\tilde{S}$ is not singular, its numerator diverges as (4.71). Therefore, the behavior of $\tilde{S}$ is more interesting; the more so since the very $\tilde{S}$ represents on average the size of a cluster which we discovered while drilling a petroleum well. As we will see in Chap. 6, $\tilde{S}$ plays the role of the susceptibility in the theory of percolation.

In this chapter, we have become acquainted with the percolation model and have considered several quantities that obey power-law dependencies in the vicinity of the percolation threshold. We may consider this threshold to be a critical point of the model while with the mentioned quantities we may associate their analogues from the Ising model (this association may be traced by the fact that the critical indices of two corresponding quantities are denoted by the same Greek letter).

However, the analogy with statistical physics developed so far is incomplete—indeed, besides the mentioned power-law dependencies we have not discussed other similarities. We return to this question in details in Chap. 6 and further chapters.

But before discussing analogies with statistical physics, in the next chapter we should consider one more complex system that will participate in future comparisons also.

References

Abaimov, S.G.: Statistical Physics of Complex Systems, 2nd ed. Synergetics: From Past to Future, vol. **57**, URSS, Moscow (2013) (in Russian)

Bollobás, B., Riordan, O.: Percolation. Cambridge University Press, Cambridge (2006)

Broadbent, S.R., Hammersley, J.M.: Percolation processes. I. Crystals and mazes. Math. Proc. Camb. Phil. Soc. **53**(3), 629–641 (1957)

Bunde, A., Havlin, S. (eds.): Fractals and Disordered Systems, 2nd ed. Springer, New York (1996)

Deutscher, G., Zallen, R., Adler, J. (eds.): Percolation Structures and Processes. Adam Hilger: Bristol (1983)

Essam, J.W., Gwilym, K.M.: The scaling laws for percolation processes. J. Phys. C **4**(10), L228–L231 (1971)

Feder, J.: Fractals. Physics of Solids and Liquids. Springer, New York (1988)

Fisher, M.E.: The theory of condensation and the critical point. Physics (Long Island City, NY) **3**, 255–283 (1967a)

Fisher, M.E.: The theory of equilibrium critical phenomena. Rep. Prog. Phys. **30**(2), 615 (1967b)

Fisher, M.E., Essam, J.W.: Some cluster size and percolation problems. J. Math. Phys. 2(4), 609–619 (1961)

Flory, P.J.: Molecular size distribution in three dimensional polymers. I. Gelation. J. Am. Chem. Soc. **63**(11), 3083–3090 (1941a)

Flory, P.J.: Molecular size distribution in three dimensional polymers. II. Trifunctional branching units. J. Am. Chem. Soc. **63**(11), 3091–3096 (1941b)

Flory, P.J.: Molecular size distribution in three dimensional polymers. III. Tetrafunctional branching units. J. Am. Chem. Soc. **63**(11), 3096–3100 (1941c)
Grimmett, G.R.: Percolation. Grundlehren der Mathematischen Wissenschaften, 2nd ed, vol. **321**. Springer, Berlin (1999)
Kesten, H.: Percolation Theory for Mathematicians. Progress in Probability and Statistics, vol. **2**. Birkhäuser, Boston (1982)
Sahimi, M.: Applications of Percolation Theory. Taylor & Francis, London (1994)
Stauffer, D., Aharony, A.: Introduction to Percolation Theory, 2nd ed. Taylor & Francis, London (1994)
Stockmayer, W.H.: Theory of molecular size distribution and gel formation in branched-chain polymers. J. Chem. Phys. **11**(2), 45–55 (1943)

Chapter 5
Damage Phenomena

Abstract The problem of percolation, studied in the previous chapter, might be called complex. The system was not thermal; and the concept of thermodynamic temperature was absent. The structure of the model allowed the possibility of non-thermal fluctuations which, in turn, lead to the presence of a continuous phase transition and a critical point in the system. We saw many similarities with the thermal systems of statistical physics; however, the completely developed analogy was absent. So, we introduced a set of parameters, such as the order parameter, the field parameter, and the averaged cluster size $\tilde{S}$; but so far we have not found the counterparts of these quantities in statistical physics. In more detail, we return to this question in Chap. 6, where these analogies will be found. However, at first we need to consider one more complex, nonthermal system whose mapping on the phenomena of statistical physics will be more transparent.

The model considered represents damage phenomena. The thermodynamic temperature is absent in the system; however, the stochastic distribution, as an "input" of the model, generates fluctuations, perfectly described by the laws of statistical physics.

In fact, the analogy with statistical physics will be so complete and the model will be so illustrative that the discussion of the concepts of statistical physics itself in Chap. 2 could be illustrated with the aid of this system instead of the thermodynamic systems.

5.1 The Parameter of Damage

The classical mechanics is formed by two separate sciences: theoretical mechanics and statistical mechanics. Similarly, there are two separate sciences, describing the destruction of solids: fracture mechanics and damage mechanics. Fracture mechanics is a deterministic discipline studying the behavior of separate (a few) flaws or defects much like when theoretical mechanics studies the deterministic behavior of separate (a few) degrees of freedom. On the contrary, damage mechanics describes the behavior of very many microdefects stochastically and resembles, therefore, statistical physics, studying stochastically the behavior of many degrees of freedom.

S. G. Abaimov, *Statistical Physics of Non-Thermal Phase Transitions,*
Springer Series in Synergetics, DOI 10.1007/978-3-319-12469-8_5

Since our intention is to build analogies between complex systems and statistical physics, we will concentrate our study on the phenomena of damage mechanics in particular.

Damage mechanics is a very young science which emerged after Lazar' Kachanov had published his book (Kachanov 1986). Also, we refer the reader to another two brilliant textbooks: (Lemaitre 1996) and (Krajcinovic 1996). Besides, the equations containing the parameter of damage as an additional variable are included in many textbooks on continuum mechanics (e.g., a brilliant textbook (Narasimhan 1993)).

During the last decade of the twentieth century a new promising idea appeared in the literature: to consider the process of damage development as a phase transition phenomenon (Rundle and Klein 1989; Sornette and Sornette 1990; Blumberg Selinger et al. 1991; Sornette and Sammis 1995; Buchel and Sethna 1996; Andersen et al. 1997; Buchel and Sethna 1997; Zapperi et al. 1997; Sornette and Andersen 1998; Zapperi et al. 1999a, b). However, although the similarity of phase diagrams was impressive, the mechanism connecting damage mechanics with statistical physics has not been built completely. While the behavior of thermal fluctuations is well described by statistical mechanics, the nonthermal stochasticity requires developing separate approaches. Only recent studies began to overcome this difficulty by mapping nonthermal fluctuations on their thermal analogs (Abaimov 2008, 2009). In the following sections, we reproduce the results of these studies.

The main parameter in damage mechanics is *the parameter of damage D*. In the literature, its definition is not settled completely. However, since we will consider only a one-dimensional case, the simplest and the most illustrative definition will be sufficient for our needs.

Let us consider a solid containing many microdefects which may be microcracks, microflaws, microvoids, etc. If we passed a section perpendicular to the direction of the applied force, in the cross-section, we would see multiple holes representing these defects (Fig. 5.1).

We define damage D as the ratio of the cross-sectional area of the defects to the total cross-sectional area of the solid:

$$D \equiv \frac{S_{defects}}{S_{total}}. \tag{5.1}$$

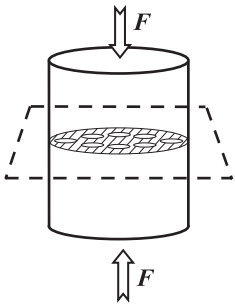

Fig. 5.1 The cross-section of a solid revealing the presence of microdefects

In the absence of defects (undamaged solid), when the total cross-section carries the load, the damage is zero: $D = 0$. When the defects coalesce and occupy the total cross-sectional area, the solid is broken and no longer supports the load. In this case, we have $D = 1$. Between these two extremes the solid is damaged partially, and only some fraction of its cross-sectional area carries the load, and $0 < D < 1$.

5.2 The Fiber-Bundle Model with Quenched Disorder

For simplicity, we will study not the three-dimensional continuum medium but a set of one-dimensional fibers (springs) connecting two absolutely rigid plates which transfer the load (Fig. 5.2). Some fibers (like the second from the left in Fig. 5.2) may be broken and do not carry the load while the intact fibers support the load transferred by the rigid plates. This model is called *the fiber-bundle model* (further, *FBM*) (Pierce 1926; Daniels 1945). Although in the following sections, we consider in detail only the original version of the FBM, there are many modifications of the model which we have briefly discussed in Sect. 5.7.

The number N of fibers in the FBM is considered to be infinite in the thermodynamic limit $N \to +\infty$ (our system is not thermal, but the limit of infinite system size is often called the thermodynamic limit by analogy with statistical physics). We assume each fiber to be elastic while its Hooke's law is linear

$$\sigma_i = E\varepsilon_i \tag{5.2}$$

right up to the point of the fiber's failure (brittle type of failure). Here σ_i is the stress of the fiber, ε_i—the strain of the fiber, and E—Young's modulus which does not depend on the strain and is the same for all fibers.

Since all fibers are loaded by means of the absolutely rigid plates, they all have the same strain coinciding with the strain of the model as a whole:

$$\varepsilon_i \equiv \varepsilon. \tag{5.3}$$

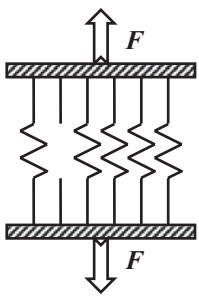

Fig. 5.2 The fiber-bundle model

A fiber breaks when its stress exceeds the strength threshold of this fiber: $\sigma_i \geq s_i$. We assume that the strength s_i of each fiber i is chosen a priori and does not change during the model evolution. This type of *noise* introduced into a system is called *quenched disorder* because once defined, deterministically or stochastically, it stays further unchanged.

Quenched disorder is generally introduced as the variability of fiber strengths, not Young's moduli, since to find elastic constants of a fiber, we average local elastic properties while fiber's strength is represented by the weakest point along the fiber and has, therefore, much higher variability.

We assume that the strengths of fibers are assigned in accordance with a stochastic probability density function $p(s)$ (further, strength PDF): $\int_0^{+\infty} p(s)\mathrm{d}s = 1$. Here, we implicitly involve the concept of an ensemble. For each particular system in the ensemble, we prescribe to each fiber its strength in accordance with the PDF $p(s)$. We load this system, observe how many fibers are broken, and move on to a new system.

So, each particular system behaves deterministically under the loading in accordance with the particular realization of strengths of its fibers, inherited at the beginning of its evolution from the PDF $p(s)$. However, the ensemble in whole behaves stochastically, exhibiting fluctuations of broken fibers. And these fluctuations are the very subject of our investigation.

Instead of the PDF $p(s)$, we will generally refer to the cumulative distribution function (further, CDF),

$$P(\sigma) = \int_0^{\sigma} p(s)ds, \tag{5.4}$$

because, while the PDF determines whether a fiber would break now, the CDF determines whether a fiber has been broken. So, if a fiber i is required to carry stress σ now, $P(\sigma)$ is the probability for this fiber to have been broken. On the contrary, $1 - P(\sigma)$ is the probability for a fiber to stay intact if its stress is σ.

After a fiber has been broken, it can no longer support the load and, therefore, redistributes its loading to other fibers. Similar to the Ising model, there are short-range and long-range types of the FBM which are different by how far the loading spreads. For example, in the nearest-neighbor version of the model, only the nearest neighbors of the broken fiber obtain from it an additional loading. On the contrary, in the mean-field type of the FBM (called *the democratic FBM* or *DFBM*) a broken fiber distributes its loading evenly among all still-intact fibers. We further consider only the last, mean-field version of the model.

The definition of the parameter of damage D is, obviously, straightforward in our model—it is a share of broken fibers. Then the numbers of broken and intact fibers are determined by

$$N_{\text{intact}} = N(1-D),\ N_{\text{broken}} = ND. \tag{5.5}$$

Microstates $\{D\}$ in our model are the particular microconfigurations of intact and broken fibers over the model. In other words, prescribing for each fiber to be intact or broken, we form one particular microstate $\{D\}$ of the system. So, if, for example, the model consists only of $N = 3$ fibers, its possible microstates are $\{|||\}$, $\{||¦\}$, $\{|¦|\}$, $\{|¦¦\}$, $\{¦||\}$, $\{¦|¦\}$, $\{¦¦|\}$, and $\{¦¦¦\}$, where the symbol '|' represents an intact fiber while the symbol '¦'—a broken fiber.

Fluctuation $\{\{D\}\}$ is then a macrostate of the system when its damage is D. For example, for the system with $N = 3$ fibers three microstates, $\{|||\}$, $\{|¦|\}$, and $\{¦||\}$, represent fluctuation $\{\{D = 1/3\}\}$. So, the statistical weight of this fluctuation is $\Gamma_{\{\{D=1/3\}\}} = 3$. For general case of an arbitrary number N of fibers, the statistical weight of a fluctuation $\{\{D\}\}$ is determined as the number of microconfigurations when there are $N_{\text{intact}} = N(1-D)$ intact fibers and $N_{\text{broken}} = ND$ broken fibers:

$$\Gamma_{\{\{D\}\}} = \frac{N!}{N_{\text{broken}}!N_{\text{intact}}!} = \frac{N!}{(ND)!(N(1-D))!} \approx_{\ln} D^{-ND}(1-D)^{-N(1-D)}. \quad (5.6)$$

5.3 The Ensemble of Constant Strain

First, we consider the ensemble of the constant strain of the system when the boundary condition of the ensemble is $\varepsilon = \text{const}$ (further, *ε-ensemble* or "ε–E"). Since the strain ε_i of each fiber i equals in accordance with (5.3) the strain of the total model, the stress (5.2) is constant for all intact fibers:

$$\sigma_i = E\varepsilon. \quad (5.7)$$

The probability for a fiber to have been broken in the ε-ensemble is $P(E\varepsilon)$. On the contrary, the probability for a fiber to stay intact in the ε-ensemble is $1 - P(E\varepsilon)$. Therefore, the probability to observe a microstate $\{D\}$ in the ε-ensemble is

$$w_{\{D\}}^{\varepsilon-\text{E}} = (P(E\varepsilon))^{ND}(1-P(E\varepsilon))^{N(1-D)}, \quad (5.8)$$

where we have raised $P(E\varepsilon)$ to the power of $N_{\text{broken}} = ND$ and $1 - P(E\varepsilon)$ —to the power of $N_{\text{intact}} = N(1-D)$.

Since the probability (5.8) depends only on the value of D and does not depend on a particular microconfiguration of broken and intact fibers, all microstates $\{D\}$, corresponding to the given value of D, have equal probabilities. The probability to observe the fluctuation $\{\{D\}\}$ in the ε-ensemble (to observe damage D) equals then the sum of these probabilities of corresponding microstates:

$$W_{\{\{D\}\}}^{\varepsilon-\text{E}} = \Gamma_{\{\{D\}\}} w_{\{D\}}^{\varepsilon-\text{E}}. \quad (5.9)$$

Substituting (5.6) into (5.9), we see that this is the binomial distribution

$$W^{\varepsilon-\mathrm{E}}_{\{\{D\}\}} = \frac{N!}{(ND)!(N(1-D))!}(P(E\varepsilon))^{ND}(1-P(E\varepsilon))^{N(1-D)}. \tag{5.10}$$

Similar to statistical physics, the probability of a fluctuation is the product of two "fast" dependencies, $\Gamma_{\{\{D\}\}}$ and $w^{\varepsilon-\mathrm{E}}_{\{D\}}$. These dependencies are "fast" because they can be presented in a form

$$\Gamma_{\{\{D\}\}} \approx_{\ln} e^{-N\{D\ln D+(1-D)\ln(1-D)\}}, \tag{5.11}$$

$$w^{\varepsilon-\mathrm{E}}_{\{D\}} = e^{N\{D\ln(P(E\varepsilon))+(1-D)\ln(1-P(E\varepsilon))\}}, \tag{5.12}$$

when the dependence on D in the exponent is multiplied by $N \to +\infty$. This provides a very narrow maximum of the probability distribution (5.9).

To find the point D_0 of this maximum, we should find when the derivative of the probability distribution is zero (or, since the logarithm is a monotonically increasing function, when the derivative of the logarithm of this distribution is zero):

$$\left.\frac{\partial W^{\varepsilon-\mathrm{E}}_{\{\{D\}\}}}{\partial D}\right|_{D_0} = 0 \text{ or } \left.\frac{\partial \ln W^{\varepsilon-\mathrm{E}}_{\{\{D\}\}}}{\partial D}\right|_{D_0} = 0. \tag{5.13}$$

Solving this equation, we find the equation of state

$$D_0 = P(E\varepsilon). \tag{5.14}$$

As it could be expected, the share D_0 of the broken fibers equals the probability $P(E\varepsilon)$ for a fiber to be broken.

Similar to Chap. 2, we can demonstrate that the most probable macrostate $\{\{D_0\}\}$ corresponds to the value of damage $\langle D\rangle_{\varepsilon-\mathrm{E}}$ averaged in the ensemble. Indeed, in the definition

$$\langle ND\rangle_{\varepsilon-\mathrm{E}} \equiv \sum_{\{D\}} ND w^{\varepsilon-\mathrm{E}}_{\{D\}} = \sum_{\{\{D\}\}} ND\Gamma_{\{\{D\}\}} w^{\varepsilon-\mathrm{E}}_{\{D\}} \tag{5.15}$$

two functions, $\Gamma_{\{\{D\}\}}$ and $w^{\varepsilon-\mathrm{E}}_{\{D\}}$, are "fast" since they depend exponentially on N. On the contrary, the function ND is "slow" since it depends on N only as a power-law. Therefore, the product $W^{\varepsilon-\mathrm{E}}_{\{\{D\}\}} = \Gamma_{\{\{D\}\}} w^{\varepsilon-\mathrm{E}}_{\{D\}}$, whose integral is normalized by unity:

$$\sum_{\{\{D\}\}} W^{\varepsilon-\mathrm{E}}_{\{D\}} = 1, \tag{5.16}$$

forms a δ-function for the "slow" function ND:

$$\langle ND \rangle_{\varepsilon-\mathrm{E}} \approx \int_0^1 ND\delta(D-D_0)dD \approx ND_0. \tag{5.17}$$

For more details of the proof of this equality, we refer the reader to Chap. 2.

Let us now return to the probability distribution (5.8) of microstates $\{D\}$. We rewrite this expression as

$$w_{\{D\}}^{\varepsilon-\mathrm{E}} = (1-P(E\varepsilon))^N e^{ND\ln\frac{P(E\varepsilon)}{1-P(E\varepsilon)}}. \tag{5.18}$$

What does this formula remind us of? We encourage the reader not to look further but first to answer this question herself/himself.

First, the boundary condition of the ε-ensemble is $\varepsilon = \text{const}$. Therefore, $P(E\varepsilon)$ is also some parameter kept constant. Let us introduce two new parameters defined by

$$T^{eff} \equiv \ln^{-1}\frac{1-P(E\varepsilon)}{P(E\varepsilon)} \tag{5.19}$$

and

$$Z^{\varepsilon-\mathrm{E}} = (1-P(E\varepsilon))^{-N}. \tag{5.20}$$

Then probability (5.18) can be presented in the form

$$w_{\{D\}}^{\varepsilon-\mathrm{E}} = \frac{1}{Z^{\varepsilon-E}} e^{-ND/T^{eff}}. \tag{5.21}$$

This expression is analogous to Gibbs probability of the canonical ensemble, where the new order parameter, instead of energy, is ND.

The parameter T^{eff} is the effective temperature and represents a new field parameter, replacing ε. Indeed, if $\varepsilon = \text{const}$, then T^{eff}, given by (5.19), is also maintained constant in the ensemble to represent the new boundary condition $T^{eff} = \text{const}$. This new boundary condition replaces the original $\varepsilon = \text{const}$; so, instead of calling our ensemble the ε-ensemble, we could call it *the effective-canonical ensemble*.

The parameter $Z^{\varepsilon-\mathrm{E}}$, given by (5.20), is the partition function of the ensemble. We can prove this statement directly by considering the definition of the partition function:

$$Z^{\varepsilon-\mathrm{E}} \equiv \sum_{\{D\}} e^{-ND/T^{eff}} = \sum_{\{\{D\}\}} \Gamma_{\{\{D\}\}} e^{-ND/T^{eff}}. \tag{5.22}$$

How many different fluctuations $\{\{D\}\}$ are there? When a fiber breaks, the damage increases by $\Delta D = 1/N$. In other words, in sum (5.22), the damage changes from 0 to 1 with the step $\Delta D = 1/N$ corresponding to the failure of a fiber:

$$Z^{\varepsilon-\mathrm{E}} = \sum_{(ND)=0}^{N} \frac{N!}{(ND)!(N(1-D))!} (e^{-1/T^{eff}})^{ND}. \tag{5.23}$$

This is the binomial sum which returns us to (5.20):

$$Z^{\varepsilon-\mathrm{E}} = \left(\mathrm{e}^{-1/T^{eff}} + 1\right)^{N} = \left(1 - P\left(E\varepsilon\right)\right)^{-N}. \tag{5.24}$$

Obviously, we could obtain nothing else, since, the partition function is the normalization constant of the probability distribution.

Summarizing, the introduction of the quenched disorder in the form of the fiber strength distribution P allowed us to build fluctuations $\{\{D\}\}$ in the ε-ensemble. These fluctuations were not thermal but generated by the stochasticity of the distribution P itself. However, considering a nonthermal system, we have obtained a complete analogy with the canonical ensemble of a thermodynamic system.

This has happened because we have been able to map the nonthermal fluctuations $\{\{D\}\}$ on their thermal analogs. Thereby, Chap. 2 as a whole has become applicable to our system. We only need to substitute energy E by damage ND in all formulas and to talk about "damage spectrum" instead of the energy spectrum. Then the statistical weight (5.6) becomes the statistical weight of the "damage level." Two adjacent "damage levels" in the spectrum are separated by $\Delta D = 1/N$. The relative width of the probability maximum is $\dfrac{\delta(ND)}{ND_0} = \dfrac{\delta(D)}{D_0} \propto \dfrac{1}{\sqrt{N}}$, and so on.

For example, transforming sum (5.22) into the integral,

$$Z^{\varepsilon-\mathrm{E}} = \int_0^1 \frac{dD}{1/N} \Gamma_{\{\{D\}\}} e^{-ND/T^{eff}}, \tag{5.25}$$

and applying the method of steepest descent, we prove that the partition function of the ensemble is equal, with logarithmic accuracy, to its maximal term,

$$Z^{\varepsilon-\mathrm{E}} \approx_{\ln} \Gamma_{\{\{D_0\}\}} e^{-ND_0/T^{eff}}, \tag{5.26}$$

where the most probable macrostate $\{\{D_0\}\}$ is determined by

$$\left.\frac{\partial\left(\Gamma_{\{\{D\}\}} w_{\{D\}}^{\varepsilon-\mathrm{E}}\right)}{\partial D}\right|_{D_0} = 0 \text{ or } \left.\frac{\partial \ln\left(\Gamma_{\{\{D\}\}} w_{\{D\}}^{\varepsilon-\mathrm{E}}\right)}{\partial D}\right|_{D_0} = 0 \tag{5.27}$$

which, when divided by $Z^{\varepsilon-\mathrm{E}}$, is equivalent to (5.13).

Let us develop the analogy of the free energy for our system. While the equilibrium free energy of the ε-ensemble is determined by the logarithm of the ensemble partition function,

$$F^{\varepsilon-\mathrm{E}} \equiv -T^{eff} \ln Z^{\varepsilon-\mathrm{E}}, \tag{5.28}$$

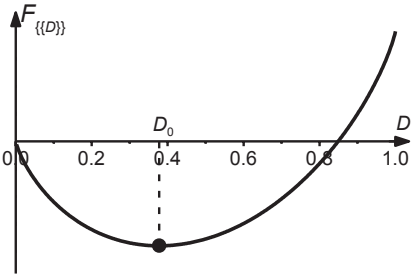

Fig. 5.3 The dependence of the nonequilibrium free energy on the nonequilibrium value of damage

the nonequilibrium free energy of a fluctuation $\{\{D\}\}$ is determined by the logarithm of the partial partition function of this fluctuation:

$$F_{\{\{D\}\}} \equiv -T^{eff} \ln Z^{\varepsilon-\mathrm{E}}_{\{\{D\}\}}, \tag{5.29}$$

where

$$Z^{\varepsilon-\mathrm{E}}_{\{\{D\}\}} \equiv Z^{\varepsilon-\mathrm{E}} W^{\varepsilon-\mathrm{E}}_{\{\{D\}\}} \equiv \sum_{\{\tilde{D}\}:\{\tilde{D}\}\in\{\{D\}\}} e^{-\tilde{D}/T^{eff}} = \Gamma_{\{\{D\}\}} e^{-D/T^{eff}}. \tag{5.30}$$

The behavior of the nonequilibrium free energy is presented in Fig. 5.3. The free energy potential has one minimum corresponding to the obtained earlier equation of state (5.14).

Why is it so important to build an analogy (5.21) with statistical physics instead of describing the system by law (5.8) of damage mechanics? What does this analogy provide us with? There are two possible answers to this question. First, the well-developed formalism of statistical physics becomes suddenly applicable to damage phenomena providing us with alternative descriptions and solutions. Second, this gives us a completely different point of view on the problem. As we will see later, this new point of view, appearing by means of comparison, can highlight what has been overlooked in damage mechanics itself. In particular, statistical physics allows us to look at a damage phenomenon as at a phase transition, as we will see in the following sections.

5.4 Stresses of Fibers

In the previous section, we have considered the ensemble when the strain of the model is maintained constant: $\varepsilon = \mathrm{const}$. However, while all systems in the ε-ensemble have the same strain, the external force F, acting on the rigid plates, obviously, varies from system to system in the ensemble due to the fluctuations of fiber strengths.

Dividing the external force F, acting on a plate, by the area of the plate, we obtain the stress σ in the plate. Considering for simplicity the model packed tightly with

fibers, we will assume further that the area of the plate coincides with the sum of the cross-sectional areas of fibers. Then, the stress σ would be the stress in the fibers if they all were still intact. This particular stress σ is assumed to be acting within the model by an external observer, who perceives the system as a "black box" and do not see that some fibers are broken.

However, within the model, some fibers may break and redistribute their load to still intact fibers. Thereby only $N(1-D)$ intact fibers carry the applied load, so their stresses σ_i are higher than σ:

$$\sigma = \sigma_i(1-D) = E\varepsilon(1-D). \tag{5.31}$$

Further for simplicity, we will assume that the area of the rigid plate is unity, so we will not distinguish the external force F and the stress σ, e.g., we will refer to σ as to the external force.

Equation (5.31) demonstrates us that for the given value of the strain ε in the ε-ensemble, the external force σ varies from system to system, depending on the fluctuating share D of broken fibers. On average, we have

$$\langle\sigma\rangle_{\varepsilon-\mathrm{E}} = E\varepsilon(1-D_0). \tag{5.32}$$

As an example, we consider a particular probability distribution of fiber strengths,

$$p(s) = \begin{cases} 0, s < s_1 \\ 1/(s_2 - s_1), s_1 < s < s_2 \\ 0, s_2 < s \end{cases}, \tag{5.33}$$

$$P(s) = \begin{cases} 0, s < s_1 \\ (s - s_1)/(s_2 - s_1), s_1 < s < s_2 \\ 1, s_2 < s \end{cases}, \tag{5.34}$$

when the strengths of fibers are distributed uniformly from s_1 to s_2 (Fig. 5.4).

We are still considering the ε-ensemble when the strain of the model is maintained constant. However, now we quasi-statically change this boundary condition, increasing strain ε from zero until the whole model fails.

When $E\varepsilon < s_1$, all fibers are intact, and the external force increases linearly with the increase of the strain. When $E\varepsilon \geq s_1$, the weakest fibers begin to break, so the dependence of $\langle\sigma\rangle_{\varepsilon-\mathrm{E}}$ on ε becomes nonlinear. When $E\varepsilon > s_2$, all fibers are broken, so the external force is zero. Substituting (5.14) into (5.32) and utilizing (5.34), for the described above tendencies we find an analytic expression:

$$\langle\sigma\rangle_{\varepsilon-\mathrm{E}} = \begin{cases} E\varepsilon, E\varepsilon < s_1 \\ E\varepsilon(s_2 - E\varepsilon)/(s_2 - s_1), s_1 < E\varepsilon < s_2 \\ 0, s_2 < E\varepsilon \end{cases}. \tag{5.35}$$

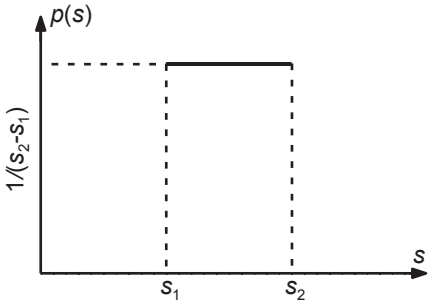

Fig. 5.4 The uniform distribution of fiber strengths from s_1 to s_2

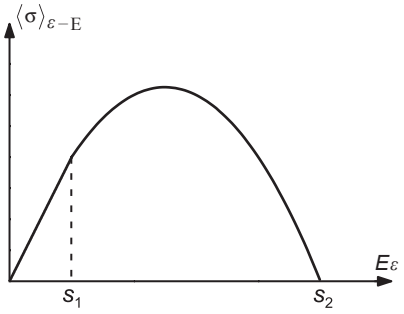

Fig. 5.5 The dependence of the averaged external force on the strain of the model

This dependence is presented in Fig. 5.5. We consider here only the nondegenerate case $s_2 > 2s_1$ when after the failure of the weakest fibers, the external force still increases with the increase of the strain.

From Fig. 5.5, we see that when the strain is increasing, the averaged external force $\langle\sigma\rangle_{\varepsilon-\mathrm{E}}$ indeed increases first linearly, then—nonlinearly. Later, it reaches its maximal value after which it decreases to zero.

Substituting CDF (5.34) into the equation of state (5.14), we find the dependence of the strain ε on the equilibrium value of damage D_0:

$$E\varepsilon = s_1 + D_0(s_2 - s_1) \text{ when } 0 < D_0 < 1. \tag{5.36}$$

Substituting (5.36) into (5.35), we find the dependence of $\langle\sigma\rangle_{\varepsilon-\mathrm{E}}$ on D_0:

$$\langle\sigma\rangle_{\varepsilon-\mathrm{E}} = (1 - D_0)(s_1 + D_0(s_2 - s_1)) \text{ when } 0 < D_0 < 1. \tag{5.37}$$

This dependence is presented in Fig. 5.6. When D_0 is increasing, the external force initially leaps to the value s_1, corresponding to the first fiber failures. Then it increases, has a maximum, and finally decreases to zero at the point $D_0 = 1$ when the whole model fails.

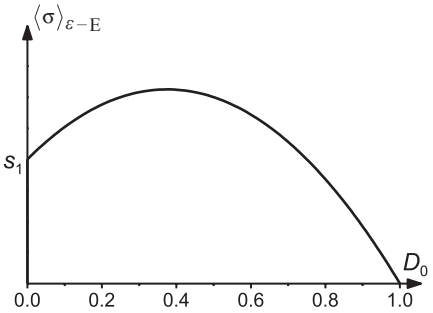

Fig. 5.6 The dependence of the averaged external force on the equilibrium value of damage

5.5 The Ensemble of Constant Stress

So far, we have considered only the ensemble of constant strain: $\varepsilon = \text{const}$. In the ε-ensemble for the given value of ε, there is only one solution of the equation of state (5.14) which is always stable and can easily be achieved experimentally (Fig. 5.7).

However, the behavior of the system changes drastically when instead of the constant strain we require the boundary condition of the constant external force: $\sigma = \text{const}$ (further, *σ-ensemble* or σ-E).

While the external force is the same for all systems of the σ-ensemble, the strain now varies from system to system in accordance with (5.31). On average, we expect to find

$$\sigma = E\left\langle \varepsilon \right\rangle_{\sigma-\mathrm{E}} (1 - D_0). \tag{5.38}$$

The probability of a microstate $\{D\}$,

$$w_{\{D\}}^{\sigma-\mathrm{E}} = \left(P\left(\frac{\sigma}{1-D} \right) \right)^{ND} \left(1 - P\left(\frac{\sigma}{1-D} \right) \right)^{N(1-D)}, \tag{5.39}$$

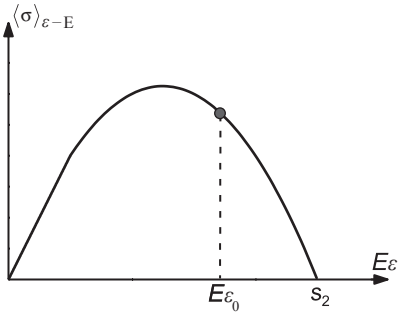

Fig. 5.7 One solution of the equation of state in the ε-ensemble

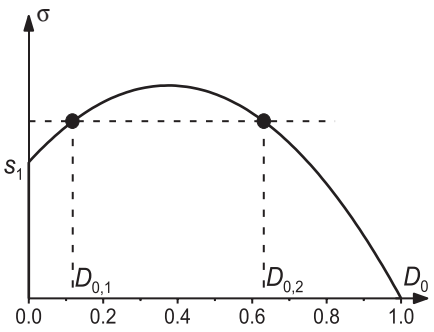

Fig. 5.8 Two solutions of the equation of state in the σ-ensemble

can no longer be transformed into the form of Gibbs probability. While the probability of a fluctuation $\{\{D\}\}$ is still provided by the product of the statistical weight and probability of a microstate,

$$W^{\sigma-\mathrm{E}}_{\{\{D\}\}} = \Gamma_{\{\{D\}\}} w^{\sigma-\mathrm{E}}_{\{D\}}, \tag{5.40}$$

its maximum generates the new equation of state:

$$D_0 = P\left(\frac{\sigma}{1-D_0}\right). \tag{5.41}$$

Since we have built our model as a mean-field system when a broken fiber redistributes its stress uniformly among all intact fibers, the behavior of the equation of state (5.41) should resemble the mean-field solution of the Ising model or the van der Waals equation. Below indeed, we will see many similarities.

In contrast to the previous ensemble, for the given value σ of the boundary condition, the equation of state (5.41) has not one but two solutions presented in Fig. 5.8. One of them, $D_{0,1}$, corresponds to positive derivative $\frac{dD_0}{d\sigma} > 0$ while another, $D_{0,2}$—to negative derivative $\frac{dD_0}{d\sigma} < 0$. When σ quasi-statically increases, two solutions approach one another while the derivatives $\frac{dD_0}{d\sigma}$ of these solutions keep their signs but diverge (Fig. 5.9).

To understand what the derivative $\frac{dD_0}{d\sigma}$ represents, we should differentiate (5.38) with respect to σ to find the derivative of the averaged strain with respect to the stress:

$$\frac{dE\langle\varepsilon\rangle_{\sigma-\mathrm{E}}}{d\sigma} = \frac{1}{1-D_0}\left\{1 + E\langle\varepsilon\rangle_{\sigma-\mathrm{E}}\frac{dD_0}{d\sigma}\right\}. \tag{5.42}$$

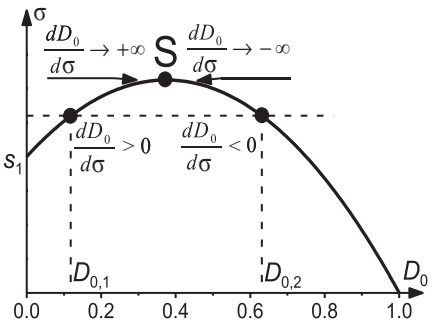

Fig. 5.9 When σ increases, two solutions approach one another while their derivatives keep signs but diverge

From this equality, it is obvious that when the derivative $\frac{dD_0}{d\sigma}$ tends to plus or minus infinity at point S in Fig. 5.9, the derivative $\frac{dE\langle\varepsilon\rangle_{\sigma-\mathrm{E}}}{d\sigma}$ has the same sign and also diverges.

But what does it mean that $\frac{dD_0}{d\sigma} > 0$ and $\frac{dE\langle\varepsilon\rangle_{\sigma-\mathrm{E}}}{d\sigma} > 0$ simultaneously? The first inequality, $\frac{dD_0}{d\sigma} > 0$, says us that when the external force increases, some fibers break so that the damage also increases. Simultaneously, $\frac{dE\langle\varepsilon\rangle_{\sigma-\mathrm{E}}}{d\sigma} > 0$ means that the increase of the load causes the strain to also increase.

These two derivatives resemble the conditions of stability (metastability) for a gas–liquid system, $\frac{\partial\rho_0}{\partial P} > 0$, and for a magnetic system, $\frac{\partial m_0}{\partial h} > 0$. Therefore, the negative values of these derivatives, $\frac{dD_0}{d\sigma} < 0$ and $\frac{dE\langle\varepsilon\rangle_{\sigma-\mathrm{E}}}{d\sigma} < 0$, correspond to the branch of unstable solutions.

So, we may conclude that point S in Fig. 5.9 separates two branches of the equation of state, one of which (to the left) is stable or metastable while another (to the right) is unstable. For example, the macrostate $\{\{D_{0,2}\}\}$ is unstable; so, if the system happens to be in this macrostate, the fibers continue to break until the whole model fails.

The presence of the unstable branch of the equation of state indicates here the presence of a phase transition in the system. But if we are talking about a phase transition, what are the phases? One of them we know—it should be the stable or metastable part of the equation of state to the left from point S. Another phase should be separated from the first by the unstable branch; so, the second phase is supposed to represent the completely broken model.

The first phase—the intact model—is transparent and easy to imagine. However, this cannot be said about the second phase, the broken model. We do not see here any dependencies on the boundary conditions—only a discrete point $D_0 = 1, \sigma = 0$. This "degeneracy" of the second phase in damage phenomena for many years concealed from scientists the fact that these phenomena can be considered as a phase transition from the intact to the broken solid.

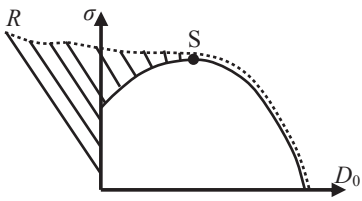

Fig. 5.10 The size of the critical nucleus schematically presented as the epure over the equation of state

Let us now consider the first phase represented by the branch of the equation of state to the left from point S. What would happen if in this system we, by means of some external forces, break very many fibers at once? Common sense suggests that the fibers, remaining still intact, may not be able to support the applied load which causes new fiber's failures and the failure of the whole model.

But broken fibers represent the second phase. So, by breaking with the aid of external forces very many fibers at once, we, in fact, include a nucleus of the broken phase within the intact phase. If the size of this nucleus (the number of broken fibers) exceeds the critical size, the nucleation process transfers the system across the potential barrier into the stable state of the broken phase.

Obviously, to the right of point S, the critical size is zero, since, the states there are all unstable and transform into the second phase on their own (Fig. 5.10). The zero critical size is always typical for the unstable branch without regard to what particular system we consider.

Also, we now know that the critical size may exist to the left of point S although here it is not zero—we need to break many fibers so that the model would fail. Does the critical size exist all along the equation of state to the left of point S? Does it exist even along the vertical part where $D_0 = 0$ and the external force is small?

To answer this question, let us imagine a model when σ is small and even the weakest fibers are all still intact. In the thermodynamic limit $N \to +\infty$, we may (by means of external forces) break all fibers but one which, left alone, would not be able to support the applied force σ, no matter how small this force is (σ is small but constant while we consider the limit $N \to +\infty$). Therefore, the critical size exists all along the equation of state, even along its vertical part (Fig. 5.10), although it may become big here—proportional to N.

But the very possibility of existence of a critical nucleus clearly indicates that the states we consider are not stable but metastable. Indeed, in a stable state the critical nucleus does not exist at all, and any possible fluctuation, no matter how big it is, cannot lead to a transition into a different phase.

So, we may conclude that the equation of state to the left of point S represents not stable but metastable states. Point S as a point where the metastable branch transforms into the unstable branch must, therefore, be the spinodal point.

In Fig. 5.11, we compare the phase diagrams for three systems: (a) a damage phenomenon, (b) a liquid–gas system, and (c) a magnetic system. The similarity of these diagrams has prompted the hypothesis that a damage phenomenon can be described as a phase transition.

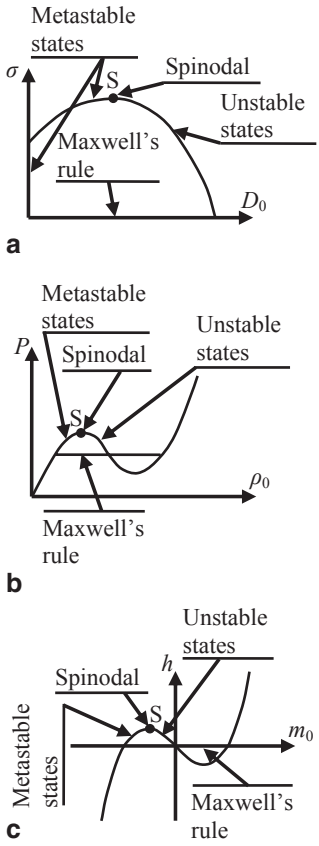

Fig. 5.11 The analogy of phase diagrams for three systems: (**a**) a damage phenomenon, (**b**) a liquid–gas system, and (**c**) a magnetic system

Liquid–gas and magnetic systems possess a hysteresis loop when a transition into the second phase takes place not along Maxwell's rule but originates from a metastable branch. For the damage phenomenon, we present the beginning of the hysteresis loop in Fig. 5.12.

However, contrary to other systems, damage is an irreversible phenomenon: once broken, the model cannot become intact again. This makes some aspects of the damage phase transition special, specific only to this type of phenomena. The simplest example—the hysteresis loop in Fig. 5.12 cannot be closed. Also, recent studies demonstrated that the irreversibility significantly modifies the lifetime of a metastable state, drastically changing the statistical distribution of nucleation times (Abaimov and Cusumano 2014).

From Fig. 5.9, we see that at the spinodal point the dependence of the external force σ on D_0 is parabolic. More rigorously, we should consider the expansion

$$\sigma = \sigma_S + \left.\frac{d\sigma}{dD_0}\right|_S (D_0 - D_S) + \frac{1}{2}\left.\frac{d^2\sigma}{dD_0^2}\right|_S (D_0 - D_S)^2 + \ldots \tag{5.43}$$

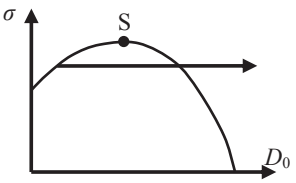

Fig. 5.12 The beginning of the hysteresis loop

By definition of the spinodal point the first derivative is zero:

$$\left.\frac{d\sigma}{dD_0}\right|_{\mathrm{S}} = 0. \tag{5.44}$$

To find the second derivative, we differentiate the equation of state (5.41):

$$dD_0 = \left(\frac{d\sigma}{1-D_0} + \frac{\sigma\, dD_0}{(1-D_0)^2}\right) P'. \tag{5.45}$$

Expressing from this equation the derivative P',

$$P' = \left(\frac{1}{1-D_0}\frac{d\sigma}{dD_0} + \frac{\sigma}{(1-D_0)^2}\right)^{-1}, \tag{5.46}$$

with the aid of (5.44) for the spinodal point we find

$$P'\,|_{\mathrm{S}} = \frac{(1-D_{\mathrm{S}})^2}{\sigma_{\mathrm{S}}}. \tag{5.47}$$

Next, we rewrite (5.45) as

$$1 = \left(\frac{1}{1-D_0}\frac{d\sigma}{dD_0} + \frac{\sigma}{(1-D_0)^2}\right) P' \tag{5.48}$$

and differentiate it with respect to D_0:

$$0 = \left(\frac{1}{1-D_0}\frac{d\sigma}{dD_0} + \frac{\sigma}{(1-D_0)^2}\right)^2 P'' + \left(\frac{1}{1-D_0}\frac{d^2\sigma}{{dD_0}^2} + \frac{2}{(1-D_0)^2}\frac{d\sigma}{dD_0} + \frac{2\sigma}{(1-D_0)^3}\right) P'. \tag{5.49}$$

At the spinodal point, this equality transforms into

$$0 = \left(\frac{\sigma_{\mathrm{S}}}{(1-D_{\mathrm{S}})^2}\right)^2 P''\,|_{\mathrm{s}} + \frac{(1-D_{\mathrm{S}})^2}{\sigma_{\mathrm{S}}}\left(\frac{1}{1-D_{\mathrm{S}}}\left.\frac{d^2\sigma}{{dD_0}^2}\right|_{\mathrm{S}} + \frac{2\sigma_{\mathrm{S}}}{(1-D_{\mathrm{S}})^3}\right) \tag{5.50}$$

or

$$\left.\frac{d^2\sigma}{dD_0{}^2}\right|_{\mathrm{S}} = -\frac{\sigma_{\mathrm{S}}{}^3}{\left(1-D_{\mathrm{S}}\right)^5} P''|_{\mathrm{s}} - \frac{2\sigma_{\mathrm{S}}}{\left(1-D_{\mathrm{S}}\right)^2}. \tag{5.51}$$

Since P is some arbitrary cumulative distribution functional dependence, its second derivative P'' is not expected to have some particular value at the spinodal point. Therefore, the right-hand side of (5.51) is expected to be nonzero so that the second order term in expansion (5.43) is also nonzero. In the result, in the close proximity of the spinodal point we find

$$| D_0 - D_{\mathrm{S}} | \propto \sqrt{| \sigma - \sigma_{\mathrm{S}} |}. \tag{5.52}$$

Considering D_0 to be the order parameter while the role of the field parameter seems to be played by σ, we may define the spinodal index $\beta_\sigma^{\mathrm{S}}$ by

$$| D - D_{\mathrm{S}} | \propto | \sigma - \sigma_{\mathrm{S}} |^{\beta_\sigma^{\mathrm{S}}}. \tag{5.53}$$

From (5.52), we immediately see that $\beta_\sigma^{\mathrm{S}} = 1/2$. However, as we will find in Chap. 6, this choice of the order parameter and field parameter is not correct. Therefore, the obtained spinodal index is also incorrect.

Concluding this section, we should say that the main purpose of fracture or damage mechanics is to predict the failure of a structure: a geological fault, a building, an aircraft, etc. The mapping of the formalism of statistical physics on damage phenomena provides us with wide prospects for these investigations.

From the theory of the first order transitions, we know that the transition happens when a nucleus with a size higher than critical becomes available in a metastable state. The damage phenomenon is especially dangerous in this sense because its nuclei grow irreversibly. So, to avoid the catastrophic consequences of a structure failure, fracture mechanics suggests detecting possible nuclei well ahead of the time when they would become dangerous. This purpose is fulfilled generally by periodic inspections, whether it is the ultrasound diagnostic of rails or visual inspection of the skin of an aircraft. A found defect is repaired, thereby suppressing fluctuations to the level below critical.

The approach of the spinodal point is especially dangerous in this sense because then the critical size tends to zero. In this case, any inspections are useless since even tiny defects may cause the cascade of total failure. Therefore, the peak loads are generally restricted to be much lower than the spinodal values.

The most complex problem arises when the experimental control of nucleus sizes in a structure becomes impossible. This happens not only when the direct inspections are impossible (like in the case of the bowels of the Earth). Another important case is when the accumulation of small nuclei fulfills the role of the presence of one big defect with the size higher than critical. The help comes here from statistical physics and nucleation theory which are capable to predict this situation by the anomalous behavior of a structure in the vicinity of the failure point. However, the detailed discussion of these approaches lies beyond the scope of this book.

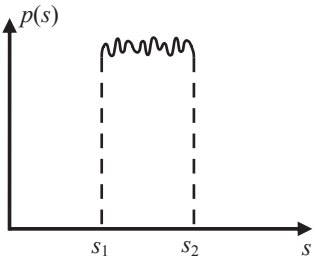

Fig. 5.13 The PDF of fiber strengths in the presence of noise

5.6 Spinodal Slowing Down

The phenomenon of critical slowing down, when the relaxation times of nonequilibrium processes diverge in the vicinity of the critical point, is well known in the literature. On the contrary, *the spinodal slowing down* has been discovered only recently and is much less understood. The damage phenomenon helps us here again—it illustrates this phenomenon (Pradhan et al. 2002, 2008, 2010; Bhattacharyya et al. 2003; Abaimov 2009) as easy as it has recreated the formalism of statistical physics in Sect. 5.3.

Earlier in Fig. 5.4, we have considered an example of the PDF for fiber strengths which was uniform in the specified range of values. However, such perfectly uniform distribution is a mathematical idealization which never exists in nature. In real systems, there is always *noise* which can be considered as a divergence from the perfect mathematical idealization. The amplitude of this noise may be small; however, taking it into account allows us to consider such important phenomenon as avalanches of broken fibers.

In Fig. 5.13 we consider the same uniform PDF, only now it is disturbed by the noise. The noise, together with the PDF itself, serves as a model input for all systems in the ensemble and, therefore, represents the quenched disorder (which varies from system to system as a particular realization of this PDF).

The presence of the noise influences the equation of state also. We present this disturbance schematically in Fig. 5.14 as the "waviness" of the curve. Important here is that due to this "waviness," the derivative $\frac{dD_0}{d\sigma}$ fluctuates locally and can even become negative. As we recall from Sect. 5.5, this causes the small interval of the curve, where $\frac{dD_0}{d\sigma} < 0$, to become unstable, leading to the appearance of a local cascade of fiber failures (horizontal arrows in Fig. 5.14).

Thereby, when we quasi-statically increase the external force σ, the system no longer responds by the quasi-static increase of damage. Instead, it may reach its new equilibrium state in the result of a nonequilibrium process as a cascade of fiber failures called *an avalanche*. Since the noise is supposed to be small, the avalanches are also small except the last one, beginning at the spinodal point and leading to the total model failure.

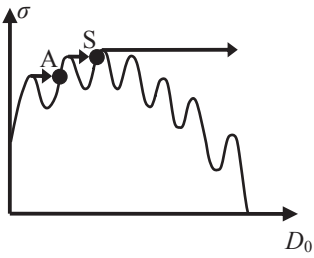

Fig. 5.14 The equation of state in the presence of noise. The horizontal arrows present avalanches of fiber failures

Let us consider what happens during a cascade of fiber failures. If at time t damage is $D_{0,t}$, how many fibers will break at the next stage of the cascade? For the given σ and $D_{0,t}$ the probability for a fiber to have been broken is $P\left(\frac{\sigma}{1-D_{0,t}}\right)$. This probability determines the damage parameter at the next step of the cascade:

$$D_{0,t+1} = P\left(\frac{\sigma}{1-D_{0,t}}\right). \tag{5.54}$$

In other words, we utilize the equation of state (5.41) as an iteration equation to form the consecutive stages of the cascade of fiber failures.

Initially, we consider an avalanche which is located far from the spinodal point (point A in Fig. 5.14 serves as a point of the cascade destination). Since we consider the avalanche to be small, as a small parameter we will consider the difference of the current value $D_{0,t}$ of damage from its value $D_{0,\mathrm{A}}$ at the point of the cascade destination: $\Delta D_{0,t} \equiv (D_{0,t} - D_{0,\mathrm{A}})$. Linearizing (5.54), we obtain

$$D_{0,t+1} = D_{0,\mathrm{A}} + P'\big|_{\mathrm{A}} \frac{\sigma_{\mathrm{A}}}{(1-D_{0,\mathrm{A}})^2} \Delta D_{0,t}. \tag{5.55}$$

Substituting (5.46), we find

$$\Delta D_{0,t+1} = \left(1 + \frac{1-D_{0,\mathrm{A}}}{\sigma_{\mathrm{A}}} \frac{d\sigma}{dD_0}\bigg|_{\mathrm{A}}\right)^{-1} \Delta D_{0,t} \tag{5.56}$$

or

$$\Delta D_{0,t+1} - \Delta D_{0,t} = -\frac{1}{1 + \frac{\sigma_{\mathrm{A}}}{1-D_{0,\mathrm{A}}} \frac{dD_0}{d\sigma}\Big|_{\mathrm{A}}} \Delta D_{0,t}. \tag{5.57}$$

Approximating the discrete time variable by a continuous time variable, we transform (5.57) into the ordinary differential equation:

$$\frac{d\Delta D_{0,t+1}}{\Delta D_{0,t}} = -\frac{dt}{1+\dfrac{\sigma_{\mathrm{A}}}{1-D_{0,\mathrm{A}}}\left.\dfrac{dD_0}{d\sigma}\right|_{\mathrm{A}}}. \tag{5.58}$$

The solution of this equation is the cascade of fiber failures decaying exponentially:

$$|\,\Delta D_{0,t}\,| \propto \mathrm{e}^{-t/t_{ref}} \tag{5.59}$$

with the characteristic decay time

$$t_{ref} = 1+\frac{\sigma_{\mathrm{A}}}{1-D_{0,\mathrm{A}}}\left.\frac{dD_0}{d\sigma}\right|_{\mathrm{A}}. \tag{5.60}$$

We have considered point A to be located far from the spinodal point. On the contrary, if point A approaches the spinodal point, the behavior of avalanches changes drastically. Indeed, from (5.60), we see that in accordance with (5.44) the characteristic time of the cascade decay diverges:

$$t_{ref} \to +\infty \text{ when } \mathrm{A} \to \mathrm{S}. \tag{5.61}$$

This phenomenon is called *the spinodal slowing down*.

Let us first crudely estimate the divergence of the characteristic time t_{ref}. Thereby, we should estimate the divergence of the derivative $\left.\dfrac{dD_0}{d\sigma}\right|_{\mathrm{A}}$ in the close proximity of the spinodal point:

$$\left.\frac{d\sigma}{dD_0}\right|_{\mathrm{A}\to\mathrm{S}} \approx \left.\frac{d\sigma}{dD_0}\right|_{\mathrm{S}} + \left.\left(\frac{d}{dD_0}\frac{d\sigma}{dD_0}\right)\right|_{\mathrm{S}} (D_{0,\mathrm{A}} - D_{0,\mathrm{S}}) = \left.\frac{d^2\sigma}{dD_0{}^2}\right|_{\mathrm{S}} (D_{0,\mathrm{A}} - D_{0,\mathrm{S}}). \tag{5.62}$$

As we have proved in (5.51), the second derivative $\dfrac{d^2\sigma}{dD_0{}^2}$ is not expected to be singular at the spinodal point. Substituting (5.62) into (5.60), we find the divergence of the characteristic decay time:

$$t_{ref} \propto \frac{1}{|\,D_{0,\mathrm{A}} - D_{0,\mathrm{S}}\,|} \propto \frac{1}{\sqrt{|\,\sigma_{\mathrm{A}} - \sigma_{\mathrm{S}}\,|}}. \tag{5.63}$$

Defining the spinodal index $\theta_\sigma^{\mathrm{S}}$ by

$$t_{ref} \propto \frac{1}{|\,\sigma_{\mathrm{A}} - \sigma_{\mathrm{S}}\,|^{\theta_\sigma^{\mathrm{S}}}}, \tag{5.64}$$

for the case of the mean-field stress redistribution, we obtain $\theta_\sigma^{\mathrm{S}} = 1/2$.

Let us consider the vicinity of the spinodal point more rigorously. From the previous discussion, we see that the linear approximation (5.55) of the iteration equation (5.54) is no longer sufficient in the vicinity of the spinodal. Instead, we should keep terms at least of the second order:

$$D_{0,t+1} = D_{0,\mathrm{S}} + P'\big|_{\mathrm{S}} \frac{\sigma_{\mathrm{S}}}{(1-D_{0,\mathrm{S}})^2}\Delta D_{0,t} + \frac{1}{2}\left\{ P''\big|_{\mathrm{S}} \frac{{\sigma_{\mathrm{S}}}^2}{(1-D_{0,\mathrm{S}})^4} + P'\big|_{\mathrm{S}} \frac{2\sigma_{\mathrm{S}}}{(1-D_{0,\mathrm{S}})^3} \right\} {\Delta D_{0,t}}^2. \tag{5.65}$$

Substituting here (5.47) and (5.50), we obtain

$$\Delta D_{0,t+1} = \Delta D_{0,t} - \frac{1-D_{0,\mathrm{S}}}{2\sigma_{\mathrm{S}}} \left.\frac{d^2\sigma}{d{D_0}^2}\right|_{\mathrm{S}} {\Delta D_{0,t}}^2 \tag{5.66}$$

or

$$\frac{d\Delta D_{0,t}}{{\Delta D_{0,t}}^2} = -\frac{1-D_{0,\mathrm{S}}}{2\sigma_{\mathrm{S}}} \left.\frac{d^2\sigma}{d{D_0}^2}\right|_{\mathrm{S}} dt. \tag{5.67}$$

The solution of this ordinary differential equation,

$$|\,\Delta D_{0,t}\,| = \left(\frac{1-D_{0,\mathrm{S}}}{2\sigma_{\mathrm{S}}} \left|\frac{d^2\sigma}{d{D_0}^2}\right|_{\mathrm{S}} \right)^{-1} \frac{1}{t+const}, \tag{5.68}$$

is well known *Omori's law* (Omori 1894; Kagan and Knopoff 1978; Utsu et al. 1995; Sornette and Ouillon 2005; Sornette 2006, and ref. therein) representing the decay of the cascade of aftershock earthquakes after the occurrence of a mainshock. Associating mainshocks with avalanches while aftershocks—with separate fiber failures, we may conclude (as far as our simple model is applicable to the real earthquake occurrence in the Earth crust) that the mainshocks happen to be generated in the vicinity of the spinodal point when the external tectonic force reaches its maximal value.

In the limit of long relaxation times, we can neglect the constant in (5.68) to obtain

$$|\,\Delta D_{0,t}\,| \propto \frac{1}{t^{\tau_\sigma^{\mathrm{S}}}}, \tag{5.69}$$

where the mean-field value of the spinodal index is $\tau_\sigma^{\mathrm{S}} = 1$.

Comparing (5.59) and (5.69), we see that in the proximity of the spinodal point not just only the characteristic time t_{ref} diverges, but the whole functional dependence of the decay changes—the exponential decay (5.59) is substituted by the power-law decay (5.69).

5.7* FBM with Annealed Disorder

In the previous sections of this chapter, we have considered the FBM in its original form formulated by (Pierce 1926; Daniels 1945) when the noise was introduced by means of quenched disorder representing the variability of fiber strengths (Coleman 1958a; Suh et al. 1970; Phoenix and Taylor 1973; Sen 1973a, b; Krajcinovic and Silva 1982; Daniels and Skyrme 1985; Daniels 1989; Sornette 1989, 1992, 1994; Hemmer and Hansen 1992; Krajcinovic et al. 1993; Hansen and Hemmer 1994a, b; Lee 1994; Andersen et al. 1997; Kloster et al. 1997; da Silveira 1998, 1999; Moreno et al. 1999, 2000; Pride and Toussaint 2002; Bhattacharyya and Chakrabarti 2006). After a fiber breaks, the distribution of its load among intact fibers was assumed to be mean-field. Besides, the plates transferring the external load to the fibers were supposed to be absolutely rigid.

Many other modifications of the FBM have been considered. Instead of mean-field load distribution, other load-sharing rules can be introduced (Gómez et al. 1993; Duxbury and Leath 1994; Hansen and Hemmer 1994a, b; Leath and Duxbury 1994; Zhang and Ding 1994, 1996; Kloster et al. 1997; Wu and Leath 1999; Moreno et al. 2001b; Hidalgo et al. 2002). Instead of rigid plates, the load to fibers can be transferred by a coupling to an elastic block (Delaplace et al. 1999; Roux et al. 1999; Batrouni et al. 2002). Plastic behavior can be simulated in the so called *continuous FBM* by fibers that are healed after their failure (Curtin and Takeda 1998; Kun et al. 2000; Hidalgo et al. 2001). More complex structures, like a chain of bundles (Harlow and Phoenix 1978; Phoenix 1979b; Smith 1980; Harlow and Phoenix 1981a, b, 1982, 1991; Smith and Phoenix 1981; Smith 1982; Phoenix and Smith 1983; Harlow 1985; Sornette and Redner 1989; Phoenix and Raj 1992), can be formed.

In the case of quenched disorder, the nonthermal fluctuations are represented by the variability of the sample distribution of fiber strengths in the ensemble. However, after we have assigned fiber strengths for a particular system in the ensemble, the behavior of this system is deterministic—for the given value of load, we can always foresee which fibers will be broken. Once the load has been applied, having caused the predicted fiber failures, nothing changes in the system further—the intact fibers will remain intact forever (unless, of course, we would decide to increase the applied load). Therefore, quenched disorder is called "*frozen*" since it occurs in space and does not depend on time.

Another type of disorder often considered is *annealed disorder*. It differs from quenched disorder very much. First of all, the strengths of all fibers of all systems in the ensemble are assumed to be the same, generally equal to unity, which completely excludes the previous type of nonthermal fluctuations from the model. Instead, to generate the fluctuating behavior we consider thermal fluctuations of statistical physics.

Contrary to the case of quenched disorder which occurs in space, annealed fluctuations occur in time—they are not "frozen" but represent a time-dependent *noise* introduced into the model. General approach to consider these fluctuations is to assume that the stress carried by a fiber also fluctuates with time. When it exceeds the unit value of the fiber's strength, the fiber breaks leading to load redistribution.

Originally (Coleman 1956, 1957a, b, 1958b, c, d; Birnbaum and Saunders 1958; Phoenix 1978a, b, 1979a; Phoenix and Tierney 1983; Gómez et al. 1998; Vázquez-Prada et al. 1999; Zhang 1999; Moral et al. 2001a, b; Moreno et al. 2001a; Newman and Phoenix 2001; Turcotte et al. 2003; Yewande et al. 2003; Turcotte and Glasscoe 2004; Nanjo and Turcotte 2005; Sornette and Andersen 2006; Phoenix and Newman 2009) annealed disorder was introduced by considering the phenomenological expressions for the rate of fiber failures. So, if all fibers have the same stress σ_f (equal to $E\varepsilon$ in the ε-ensemble or $\frac{\sigma}{1-D}$ in the σ-ensemble with the mean-field load redistribution), the relative rate $\rho \equiv \frac{1}{N}\frac{|dN|}{dt} = \frac{|d\ln N|}{dt}$ of fiber failures is assumed to be the function of fiber stress:

$$-dN = N(t)\rho\left(\sigma_f(t)\right)dt. \tag{5.70}$$

Two phenomenological dependencies are generally considered: the power-law dependence $\rho(\sigma_f) \propto \sigma_f{}^{\kappa}$ leading to the Weibull distribution and the exponential dependence $\rho(\sigma_f) \propto e^{\sigma_f/\sigma_0}$ representing Gibbs probability of thermal fluctuations (Phoenix and Tierney 1983).

In later modifications of the model (Guarino et al. 1999b; Roux 2000; Ciliberto et al. 2001; Scorretti et al. 2001; Politi et al. 2002; Saichev and Sornette 2005; closely related model Sornette and Vanneste 1992; Sornette et al. 1992; Vanneste and Sornette 1992), to avoid introduction of phenomenological dependences, *thermal noise* ξ was added directly to fiber stress:

$$\sigma_f \Rightarrow \sigma_f + \xi. \tag{5.71}$$

Due to the presence of noise, the stress of a fiber fluctuates around its mean value, and a big enough fluctuation can exceed the threshold of the unit strength causing the failure of the fiber. In this model modification, we obtain the rate of fiber failures as the characteristic of the ensemble considered.

However, experimental studies (Pauchard and Meunier 1993; Bonn et al. 1998; Sollich 1998; Guarino et al. 1999a, 2002) discovered that thermal noise is not nearly enough to cause the observed rupture of materials under constant loading. To provide the desired level of fluctuations, the temperature within solids would have to be of the order of several thousands kelvin. Therefore, the annealed disorder alone cannot describe the phenomena observed experimentally.

To explain the difference between experimental and theoretical results, it was assumed (Guarino et al. 1999a, 1999b; Roux 2000; Arndt and Nattermann 2001; Ciliberto et al. 2001; Scorretti et al. 2001; Politi et al. 2002; Saichev and Sornette 2005; Sornette and Ouillon 2005) that it is not thermal noise that causes damage growth but the interaction of this noise with the quenched disorder also present in the system (i.e., the presence of defects can amplify thermal fluctuations). For example,

one possibility is to associate this phenomenon with the influence of thermal fluctuations on the unstable, frustrated parts of defects (e.g., crack tips) at the microscopic level (Abaimov and Cusumano 2014). Although these fluctuations are spatially and quantitatively microscopic, and influence only microscopic parts of cracks, their presence causes damage growth on the mesoscopic level. Thus, a "sensitive" crack tip works in this case as an amplifier, causing the microscopic thermally induced fluctuations to influence the mesoscopic growth of damage nuclei.

In the FBM, we cannot model the behavior of crack tips. However, we can discuss how the presence of defects interacts with thermal noise in general. Now, we should consider both annealed and quenched disorders present in the FBM. Thermal noise we introduce by (5.71), where ξ is white noise whose variance is determined by the temperature of the system:

$$p^{annealed}(\xi) = \frac{1}{\sqrt{2\pi T}} e^{-\frac{\xi^2}{2T}}. \tag{5.72}$$

Quenched disorder is still introduced as the variability of fiber strengths. For simplicity, the distribution we assume also to be Gaussian with variance Θ:

$$p^{quenched}(s) = \frac{1}{\sqrt{2\pi\Theta}} e^{-\frac{(s-s_0)^2}{2\Theta}}. \tag{5.73}$$

It was demonstrated (Roux 2000; Scorretti et al. 2001) that when both annealed and quenched disorders are small, the effective temperature of fluctuations in the system is the sum of the thermodynamic temperature T and the variance Θ of quenched disorder:

$$T^{eff} = T + \Theta; \tag{5.74}$$

however, other studies (Ciliberto et al. 2001; Politi et al. 2002; Saichev and Sornette 2005) proposed for the amplification of thermal fluctuations to obey a more complex dependence.

Therefore, the presence of defects does amplify thermal fluctuations significantly increasing their temperature. So, Guarino et al. (Guarino et al. 1999a, 2002) estimated experimentally that instead of 300 K, the effective temperature is about 3000 K. Nowadays, it still remains a mystery which part of this temperature increase can be attributed to the variability of strength distribution and which to the interactions of thermal fluctuations with frustrated parts of defects (crack tips).

References

Abaimov, S.G.: Applicability and non-applicability of equilibrium statistical mechanics to non-thermal damage phenomena. J. Stat. Mech. **9**, P09005 (2008). doi:10.1088/1742–5468/2008/09/P09005

Abaimov, S.G.: Applicability and non-applicability of equilibrium statistical mechanics to non-thermal damage phenomena: II. Spinodal behavior. J. Stat. Mech. **3**, P03039 (2009)
Abaimov, S.G.: Statistical physics of complex systems (in Russian), 2nd ed. Synergetics: From Past to Future, vol. **57**, URSS, Moscow (2013)
Abaimov, S.G., Cusumano, J.P.: Nucleation phenomena in an annealed damage model: Statistics of times to failure. Phys. Rev. E **90**(6), 062401 (2014)
Andersen, J.V., Sornette, D., Leung, K.-T.: Tricritical behavior in rupture induced by disorder. Phys. Rev. Lett. **78**(11), 2140–2143 (1997)
Arndt, P.F., Nattermann, T.: Criterion for crack formation in disordered materials. Phys. Rev. B. **63**(13), 134–204 (2001)
Batrouni, G.G., Hansen, A., Schmittbuhl, J.: Heterogeneous interfacial failure between two elastic blocks. Phys. Rev. E **65**(3), 036126 (2002)
Bhattacharyya, P., Chakrabarti, B.K. (eds.): Modelling Critical and Catastrophic Phenomena in Geoscience. Springer, Berlin (2006)
Bhattacharyya, P., Pradhan, S., Chakrabarti, B.K.: Phase transition in fiber bundle models with recursive dynamics. Phys. Rev. E **67**(4), 046122 (2003)
Birnbaum, Z.W., Saunders, S.C.: A statistical model for life-length of materials. J. Am. Stat. Assoc. **53**(281), 151–159 (1958)
Blumberg Selinger, R.L., Wang, Z.-G., Gelbart, W.M., Ben-Shaul, A.: Statistical-thermodynamic approach to fracture. Phys. Rev. A **43**(8), 4396–4400 (1991)
Bonn, D., Kellay, H., Prochnow, M., Ben-Djemiaa, K., Meunier, J.: Delayed fracture of an inhomogeneous soft solid. Science **280**(5361), 265–267 (1998)
Buchel, A., Sethna, J.P.: Elastic theory has zero radius of convergence. Phys. Rev. Lett. **77**(8), 1520–1523 (1996)
Buchel, A., Sethna, J.P.: Statistical mechanics of cracks: fluctuations, breakdown, and asymptotics of elastic theory. Phys. Rev. E **55**(6), 7669–7690 (1997)
Chakrabarti, B.K., Benguigui, L.G.: Statistical Physics of Fracture and Breakdown in Disordered Systems. Monographs on the Physics and Chemistry of Materials. Clarendon Press, Oxford (1997)
Ciliberto, S., Guarino, A., Scorretti, R.: The effect of disorder on the fracture nucleation process. Physica. D **158**(1–4), 83–104 (2001)
Coleman, B.D.: Time dependence of mechanical breakdown phenomena. J. Appl. Phys. **27**(8), 862–866 (1956)
Coleman, B.D.: Time dependence of mechanical breakdown in bundles of fibers. I. Constant total load. J. Appl. Phys. **28**(9), 1058–1064 (1957a)
Coleman, B.D.: Time dependence of mechanical breakdown in bundles of fibers. II. The infinite ideal bundle under linearly increasing loads. J. Appl. Phys. **28**(9), 1065–1067 (1957b)
Coleman, B.D.: On the strength of classical fibres and fibre bundles. J. Mech. Phys. Solids **7**(1), 60–70 (1958a)
Coleman, B.D.: Statistics and time dependence of mechanical breakdown in fibers. J. Appl. Phys. **29**(6), 968–983 (1958b)
Coleman, B.D.: Time dependence of mechanical breakdown in bundles of fibers. III. The power law breakdown rule. Trans. Soc. Rheology **2**(1), 195–218 (1958c)
Coleman, B.D.: Time dependence of mechanical breakdown in bundles of fibers. IV. Infinite ideal bundle under oscillating loads. J. Appl. Phys. **29**(7), 1091–1099 (1958d)
Curtin, W.A., Takeda, N.: Tensile strength of fiber-reinforced composites: I. Model and effects of local fiber geometry. J. Comp. Mat. **32**(22), 2042–2059 (1998)
da Silveira, R.: Comment on 'Tricritical behavior in rupture induced by disorder'. Phys. Rev. Lett. **80**(14), 3157 (1998)
da Silveira, R.: An introduction to breakdown phenomena in disordered systems. Am. J. Phys. **67**(12), 1177–1188 (1999)
Daniels, H.E.: The statistical theory of the strength of bundles of threads. I. Proc. Roy. Soc. A **183**(995), 405–435 (1945)

Daniels, H.E.: The maximum of a Gaussian process whose mean path has a maximum, with an application to the strength of bundles of fibres. Adv. Appl. Probab. **21**(2), 315–333 (1989)
Daniels, H.E., Skyrme, T.H.R.: The maximum of a random walk whose mean path has a maximum. Adv. Appl. Probab. **17**(1), 85–99 (1985)
Delaplace, A., Roux, S., Pijaudier-Cabot, G.: Damage cascade in a softening interface. Int. J. Solids Struct. **36**(10), 1403–1426 (1999)
Duxbury, P.M., Leath, P.L.: Exactly solvable models of material breakdown. Phys. Rev. B **49**(18), 12676–12687 (1994)
Gómez, J.B., Iñiguez, D., Pacheco, A.F.: Solvable fracture model with local load transfer. Phys. Rev. Lett. **71**(3), 380–383 (1993)
Gómez, J.B., Moreno, Y., Pacheco, A.F.: Probabilistic approach to time-dependent load-transfer models of fracture. Phys. Rev. E **58**(2), 1528–1532 (1998)
Guarino, A., Ciliberto, S., Garcimartín, A.: Failure time and microcrack nucleation. Europhys. Lett. **47**(4), 456–461 (1999a)
Guarino, A., Scorretti, R., Ciliberto, S.: Material failure time and the fiber bundle model with thermal noise. arXiv cond-mat/9908329v1, 1–11 (1999b)
Guarino, A., Ciliberto, S., Garcimartín, A., Zei, M., Scorretti, R.: Failure time and critical behaviour of fracture precursors in heterogeneous materials. Eur. Phys. J. B **26**(2), 141–151 (2002)
Hansen, A., Hemmer, P.C.: Burst avalanches in bundles of fibers: Local versus global load-sharing. Phys. Lett. A **184**(6), 394–396 (1994a)
Hansen, A., Hemmer, P.C.: Criticality in fracture: the burst distribution. Trends Stat. Phys. **1**, 213–224 (1994b)
Harlow, D.G.: The pure flaw model for chopped fibre composites. Proc. Roy. Soc. A **397**, 211–232 (1985)
Harlow, D.G., Phoenix, S.L.: The chain-of-bundles probability model for the strength of fibrous materials I: analysis and conjectures. J. Comp. Mat. **12**(2), 195–214 (1978)
Harlow, D.G., Phoenix, S.L.: Probability distributions for the strength of composite materials I: two-level bounds. Int. J. Fract. **17**(4), 347–372 (1981a)
Harlow, D.G., Phoenix, S.L.: Probability distributions for the strength of composite materials II: a convergent sequence of tight bounds. Int. J. Fract. **17**(6), 601–630 (1981b)
Harlow, D.G., Phoenix, S.L.: Probability distributions for the strength of fibrous materials under local load sharing. I. Two-level failure and edge effects. Adv. Appl. Probab. **14**(1), 68–94 (1982)
Harlow, D.G., Phoenix, S.L.: Approximations for the strength distribution and size effect in an idealized lattice model of material breakdown. J. Mech. Phys. Solids **39**(2), 173–200 (1991)
Hemmer, P.C., Hansen, A.: The distribution of simultaneous fiber failures in fiber bundles. J. Appl. Mech. **59**(4), 909–914 (1992)
Herrmann, H.J., Roux, S. (eds.): Statistical Models for the Fracture of Disordered Media. North-Holland, Amsterdam (1990)
Hidalgo, R.C., Kun, F., Herrmann, H.J.: Bursts in a fiber bundle model with continuous damage. Phys. Rev. E **64**(6), 066122 (2001)
Hidalgo, R.C., Moreno, Y., Kun, F., Herrmann, H.J.: Fracture model with variable range of interaction. Phys. Rev. E **65**(4), 046148 (2002)
Kachanov, L.M.: Introduction to Continuum Damage Mechanics. Kluwer Academic Publishers, Dordrecht (1986)
Kagan, Y., Knopoff, L.: Statistical study of the occurrence of shallow earthquakes. Geophys. J. Int. **55**(1), 67–86 (1978)
Kloster, M., Hansen, A., Hemmer, P.C.: Burst avalanches in solvable models of fibrous materials. Phys. Rev. E **56**(3), 2615–2625 (1997)
Krajcinovic, D.: Damage Mechanics. North-Holland Series in Applied Mathematics and Mechanics, vol. 41. Elsevier, Amsterdam (1996)
Krajcinovic, D., Silva, M.A.G.: Statistical aspects of the continuous damage theory. Int. J. Solids Struct. **18**(7), 551–562 (1982)

Krajcinovic, D., van Mier, J. (eds.): Damage and Fracture of Disordered Materials. Springer, Wien (2000)
Krajcinovic, D., Lubarda, V., Sumarac, D.: Fundamental aspects of brittle cooperative phenomena—effective continua models. Mech. Mater. **15**(2), 99–115 (1993)
Kun, F., Zapperi, S., Herrmann, H.J.: Damage in fiber bundle models. Eur. Phys. J. B **17**(2), 269–279 (2000)
Leath, P.L., Duxbury, P.M.: Fracture of heterogeneous materials with continuous distributions of local breaking strengths. Phys. Rev. B **49**(21), 14905 (1994)
Lee, W.: Burst process of stretched fiber bundles. Phys. Rev. E **50**(5), 3797 (1994)
Lemaitre, J.: A Course on Damage Mechanics, 2nd ed. Springer, Berlin (1996)
Lemaitre, J., Desmorat, R.: Engineering Damage Mechanics. Springer, Berlin (2005)
Moral, L., Gómez, J.B., Moreno, Y., Pacheco, A.F.: Exact numerical solution for a time-dependent fibre-bundle model with continuous damage. J. Phys. A **34**(47), 9983–9991 (2001a)
Moral, L., Moreno, Y., Gómez, J.B., Pacheco, A.F.: Time dependence of breakdown in a global fiber-bundle model with continuous damage. Phys. Rev. E **63**(6), 066106 (2001b)
Moreno, Y., Gómez, J.B., Pacheco, A.F.: Self-organized criticality in a fibre-bundle-type model. Physica A **274**(3–4), 400–409 (1999)
Moreno, Y., Gómez, J.B., Pacheco, A.F.: Fracture and second-order phase transitions. Phys. Rev. Lett. **85**(14), 2865–2868 (2000)
Moreno, Y., Correig, A.M., Gómez, J.B., Pacheco, A.F.: A model for complex aftershock sequences. J. Geophys. Res. **106**(B4), 6609–6619 (2001a)
Moreno, Y., Gómez, J.B., Pacheco, A.F.: Phase transitions in load transfer models of fracture. Physica A **296**(1–2), 9–23 (2001b)
Nanjo, K.Z., Turcotte, D.L.: Damage and rheology in a fibre-bundle model. Geophys. J. Int. **162**(3), 859–866 (2005)
Narasimhan, M.N.L.: Principles of Continuum Mechanics. Wiley, New York (1993)
Newman, W.I., Phoenix, S.L.: Time-dependent fiber bundles with local load sharing. Phys. Rev. E **63**(2), 021507 (2001)
Omori, F.: On after-shocks of earthquakes. J. Coll. Sci. Imp. U. Tokyo **7**, 111–200 (1894)
Pauchard, L., Meunier, J.: Instantaneous and time-lag breaking of a two-dimensional solid rod under a bending stress. Phys. Rev. Lett. **70**(23), 3565–3568 (1993)
Phoenix, S.L.: The asymptotic time to failure of a mechanical system of parallel members. SIAM J. Appl. Math. **34**(2), 227–246 (1978a)
Phoenix, S.L.: Stochastic strength and fatigue of fiber bundles. Int. J. Fract. **14**(3), 327–344 (1978b)
Phoenix, S.L.: The asymptotic distribution for the time to failure of a fiber bundle. Adv. Appl. Probab. **11**(1), 153–187 (1979a)
Phoenix, S.L.: Statistical aspects of failure of fibrous materials. In: Tsai, S.W. (ed.) Composite Materials: Testing and Design, vol. STP674, pp. 455–483. ASTM, Philadelphia (1979b)
Phoenix, S.L., Newman, W.I.: Time-dependent fiber bundles with local load sharing. II. General Weibull fibers. Phys. Rev. E **80**(6), 066115 (2009)
Phoenix, S.L., Raj, R.: Scalings in fracture probabilities for a brittle matrix fiber composite. Acta Metall. Mater. **40**(11), 2813–2828 (1992)
Phoenix, S.L., Smith, R.L.: A comparison of probabilistic techniques for the strength of fibrous materials under local load-sharing among fibers. Int. J. Solids Struct. **19**(6), 479–496 (1983)
Phoenix, S.L., Taylor, H.M.: The asymptotic strength distribution of a general fiber bundle. Adv. Appl. Probab. **5**, 200–216 (1973)
Phoenix, S.L., Tierney, L.-J.: A statistical model for the time dependent failure of unidirectional composite materials under local elastic load-sharing among fibers. Eng. Fract. Mech. **18**(1), 193–215 (1983)
Pierce, F.T.: Tensile tests for cotton yarns: V. The “weakest link” theorems on the strength of long and of composite specimens. J. Textile Inst. Trans. **17**(7), T355–T368 (1926)
Politi, A., Ciliberto, S., Scorretti, R.: Failure time in the fiber-bundle model with thermal noise and disorder. Phys. Rev. E **66**(2), 026107 (2002)

Pradhan, S., Bhattacharyya, P., Chakrabarti, B.K.: Dynamic critical behavior of failure and plastic deformation in the random fiber bundle model. Phys. Rev. E **66**(1), 016116 (2002)
Pradhan, S., Hansen, A., Chakrabarti, B.K.: Failure processes in elastic fiber bundles. arXiv 0808.1375 (2008)
Pradhan, S., Hansen, A., Chakrabarti, B.K.: Failure processes in elastic fiber bundles. Rev. Mod. Phys. **82**(1), 499 (2010)
Pride, S.R., Toussaint, R.: Thermodynamics of fiber bundles. Physica A **312**(1–2), 159–171 (2002)
Roux, S.: Thermally activated breakdown in the fiber-bundle model. Phys. Rev. E **62**(5), 6164–6169 (2000)
Roux, S., Delaplace, A., Pijaudier-Cabot, G.: Damage at heterogeneous interfaces. Physica A **270**(1–2), 35–41 (1999)
Rundle, J.B., Klein, W.: Nonclassical nucleation and growth of cohesive tensile cracks. Phys. Rev. Lett. **63**(2), 171–174 (1989)
Saanouni, K. (ed.): Numerical Modeling in Damage Mechanics. Hermes Science Publications, Paris (2001)
Saichev, A., Sornette, D.: Andrade, Omori, and time-to-failure laws from thermal noise in material rupture. Phys. Rev. E **71**(1), 016608 (2005)
Scorretti, R., Ciliberto, S., Guarino, A.: Disorder enhances the effects of thermal noise in the fiber bundle model. Europhys. Lett. **55**(5), 626–632 (2001)
Sen, P.K.: An asymptotically efficient test for the bundle strength of filaments. J. Appl. Probab. **10**(3), 586–596 (1973a)
Sen, P.K.: On fixed size confidence bands for the bundle strength of filaments. Ann. Stat. **1**(3), 526–537 (1973b)
Smith, R.L.: A probability model for fibrous composites with local load sharing. Proc. Roy. Soc. A **372**(1751), 539–553 (1980)
Smith, R.L.: The asymptotic distribution of the strength of a series-parallel system with equal load-sharing. Ann. Prob. **10**(1), 137–171 (1982)
Smith, R.L., Phoenix, S.L.: Asymptotic distributions for the failure of fibrous materials under series-parallel structure and equal load-sharing. J. Appl. Mech. **48**(1), 75–82 (1981)
Sollich, P.: Rheological constitutive equation for a model of soft glassy materials. Phys. Rev. E **58**(1), 738–759 (1998)
Sornette, A., Sornette, D.: Earthquake rupture as a critical-point: Consequences for telluric precursors. Tectonophysics. **179**(3–4), 327–334 (1990)
Sornette, D.: Elasticity and failure of a set of elements loaded in parallel. J. Phys. A **22**(6), L243–L250 (1989)
Sornette, D.: Mean-field solution of a block-spring model of earthquakes. J. Phys. I **2**(11), 2089–2096 (1992)
Sornette, D.: Sweeping of an instability: an alternative to self-organized criticality to get power-laws without parameter tuning. J. Phys. I **4**(2), 209–221 (1994)
Sornette, D.: Critical Phenomena in Natural Sciences, 2nd ed. Springer, Berlin (2006)
Sornette, D., Andersen, J.V.: Scaling with respect to disorder in time-to-failure. Eur. Phys. J. B **1**(3), 353–357 (1998)
Sornette, D., Andersen, J.V.: Optimal prediction of time-to-failure from information revealed by damage. Europhys. Lett. **74**(5), 778–784 (2006)
Sornette, D., Ouillon, G.: Multifractal scaling of thermally activated rupture processes. Phys. Rev. Lett. **94**(3), 038501 (2005)
Sornette, D., Redner, S.: Rupture in the bubble model. J. Phys. A **22**(13), L619–L625 (1989)
Sornette, D., Sammis, C.G.: Complex critical exponents from renormalization-group theory of earthquakes: implications for earthquake predictions. J. Phys. I **5**(5), 607–619 (1995)
Sornette, D., Vanneste, C.: Dynamics and memory effects in rupture of thermal fuse networks. Phys. Rev. Lett. **68**(5), 612–615 (1992)
Sornette, D., Vanneste, C., Knopoff, L.: Statistical model of earthquake foreshocks. Phys. Rev. A **45**(12), 8351–8357 (1992)

Suh, M.W., Bhattacharyya, B.B., Grandage, A.: On the distribution and moments of the strength of a bundle of filaments. J. Appl. Probab. **7**(3), 712–720 (1970)
Turcotte, D.L., Glasscoe, M.T.: A damage model for the continuum rheology of the upper continental crust. Tectonophysics. **383**(1–2), 71–80 (2004)
Turcotte, D.L., Newman, W.I., Shcherbakov, R.: Micro and macroscopic models of rock fracture. Geophys. J. Int. **152**(3), 718–728 (2003)
Utsu, T., Ogata, Y., Matsu'ura, R.S.: The centenary of the Omori formula for a decay law of aftershock activity. J. Phys. Earth **43**(1), 1–33 (1995)
Vanneste, C., Sornette, D.: The dynamical thermal fuse model. J. Phys. I **2**(8), 1621–1644 (1992)
Vázquez-Prada, M., Gómez, J.B., Moreno, Y., Pacheco, A.F.: Time to failure of hierarchical load-transfer models of fracture. Phys. Rev. E **60**(3), 2581–2594 (1999)
Wu, B.Q., Leath, P.L.: Failure probabilities and tough-brittle crossover of heterogeneous materials with continuous disorder. Phys. Rev. B **59**(6), 4002 (1999)
Yewande, O.E., Moreno, Y., Kun, F., Hidalgo, R.C., Herrmann, H.J.: Time evolution of damage under variable ranges of load transfer. Phys. Rev. E **68**(2), 026116 (2003)
Zapperi, S., Ray, P., Stanley, H.E., Vespignani, A.: First-order transition in the breakdown of disordered media. Phys. Rev. Lett. **78**(8), 1408–1411 (1997)
Zapperi, S., Ray, P., Stanley, H.E., Vespignani, A.: Analysis of damage clusters in fracture processes. Physica A **270**(1–2), 57–62 (1999a)
Zapperi, S., Ray, P., Stanley, H.E., Vespignani, A.: Avalanches in breakdown and fracture processes. Phys. Rev. E **59**(5), 5049–5057 (1999b)
Zhang, S.-D.: Scaling in the time-dependent failure of a fiber bundle with local load sharing. Phys. Rev. E **59**(2), 1589–1592 (1999)
Zhang, S.-D., Ding, E.-J.: Burst-size distribution in fiber-bundles with local load-sharing. Phys. Lett. A **193**(5–6), 425–430 (1994)
Zhang, S.-D., Ding, E.-J.: Failure of fiber bundles with local load sharing. Phys. Rev. B **53**(2), 646–654 (1996)

Chapter 6
Correlations, Susceptibility, and the Fluctuation–Dissipation Theorem

Abstract In the previous chapters, we were acquainted with three complex systems. For each system, our primary interest was to find its equation of state. This is quite reasonable because the equation of state provides us with the averaged system's response to the change of external field parameters. For example, if we know the dependence of the equilibrium magnetization on temperature and magnetic field for the Ising model, this knowledge is generally sufficient for practical applications. The equation of state, which represents the equilibrium state averaged over the ensemble, does not take into account the possibility of system's fluctuations in the vicinity of this equilibrium state. But generally, we can neglect fluctuations because large fluctuations are improbable.

However, the situation changes drastically in the proximity of the critical point. The fluctuations become so large that they begin to dominate the system's behavior, disguising the details of microscopic interactions of the system's degrees of freedom. The laws of the system's behavior no longer depend on what particular system we consider and become similar (universal) for very different systems. It no longer matters whether we consider the Ising model, percolation, or damage—any of these systems in the vicinity of its critical point forgets its own (specific for this particular system) laws of behavior and begins to obey the universal power-law dependencies.

It happens because the fluctuations become fractal in the vicinity of the critical point. Fractality means that fluctuations consume all possible scales of behavior—from the lattice constant to the size of a system in whole. The fluctuations become macroscopic.

Far from the critical point, large fluctuations are improbable. So, generally we observe nothing more than just a collision of several particles or several spin flips. But at the critical point, very large fluctuations become probable, so large that we can observe them even with the naked eye. For example, the phenomenon, which is called *the critical opalescence,* corresponds to the opalescence of a liquid–gas system when it is transferred through its critical point. Inasmuch as the volume of the system is divided into phase clusters whose size becomes comparable with the size of the whole system, the light refracts at cluster boundaries creating the opalescence effect.

As we saw in Chap. 1, fractality disregards the structure of the initial set and generates the universal power-law dependencies (compare, for example, fractals from figures (a) and (d) of Problem 1.2.1. So do the fractal thermal fluctuations as well

S. G. Abaimov, *Statistical Physics of Non-thermal Phase Transitions,*
Springer Series in Synergetics, DOI 10.1007/978-3-319-12469-8_6

disregarding the microscopic laws of the system's behavior and substituting them by power-law dependencies containing critical indices.

However, as we saw in Chap. 1, the fractality does not mean that everything of the initial generations is lost; the final power-law behavior of a fractal is determined by the rules of how we generate iteration $n = 1$ on the base of iteration $n = 0$. In other words, what influences the behavior of the system is the structure not of a parent branch but of the generator that transforms this branch, i.e., the laws of scaling.

Similarly, thermal fluctuations do disguise some microscopic features of a system, making it universal; however, they do not discard all of them; the scaling laws are preserved by means of fractal scale invariance and are transferred from the microscale to the meso- and macroscale by the succession of generations. Much like family relics, transferred from one generation to another and thereby kept intact for hundreds of years.

In Chap. 7, we will learn about the influence of scale invariance on the properties of a system. In this chapter, we study the first part of the phenomena discussed above when fluctuations lead to universal power-law behavior.

First, we consider correlations. Then, we introduce the susceptibility as the system's response and prove the fluctuation–dissipation theorem. Comparing these concepts for all three systems considered, the Ising model, percolation, and damage, we find the similarities behind the "curtain" of the behavior of fluctuations. Finally, we discuss a special role played by the susceptibility in the theory of phase transitions.

6.1 Correlations: The One-Dimensional Ising Model with Short-Range Interactions

We start by considering correlations. Let a function $X(\mathbf{R})$ be defined on a d-dimensional space $\mathbf{R}$. Further, we assume that the mean $\langle X \rangle$ and variance $\left\langle \left(X - \langle X \rangle \right)^2 \right\rangle = \left\langle X^2 \right\rangle - \langle X \rangle^2$ do not depend on $\mathbf{R}$.

The autocovariance function is defined as

$$g(\mathbf{R}, \mathbf{R}') \equiv \left\langle \left(X(\mathbf{R}) - \langle X \rangle \right) \left(X(\mathbf{R}') - \langle X \rangle \right) \right\rangle = \left\langle X(\mathbf{R}) X(\mathbf{R}') \right\rangle - \langle X \rangle^2 . \quad (6.1)$$

To find *the autocorrelation function*, we should normalize the autocovariance function by the value of variance:

$$G(\mathbf{R}, \mathbf{R}') = \frac{\left\langle \left(X(\mathbf{R}) - \langle X \rangle \right) \left(X(\mathbf{R}') - \langle X \rangle \right) \right\rangle}{\left\langle \left(X(\mathbf{R}) - \langle X \rangle \right)^2 \right\rangle} = \frac{\left\langle X(\mathbf{R}) X(\mathbf{R}') \right\rangle - \langle X \rangle^2}{\left\langle X^2 \right\rangle - \langle X \rangle^2} . \quad (6.2)$$

Physicists, as it sometimes happens, do not follow the rigorous mathematical definitions. Usually, the autocovariance function is called *the correlation function*.

For example, in the case of the Ising model, the spin correlation function is defined as

$$g(\mathbf{R}_{i,j}) \equiv \left\langle \left(\sigma_i - \langle\sigma\rangle\right)\left(\sigma_j - \langle\sigma\rangle\right)\right\rangle = \left\langle \sigma_i \sigma_j \right\rangle - \langle\sigma\rangle^2 . \tag{6.3}$$

Problem 6.1.1

Consider the one-dimensional ferromagnetic nearest-neighbor (n.n.) Ising model with pair (bi-spin) interactions. For simplicity, consider the periodic boundary conditions $\sigma_{N+1} \equiv \sigma_1$ when the model is the one-dimensional chain of spins closed into a ring. Find the correlation function of the system.

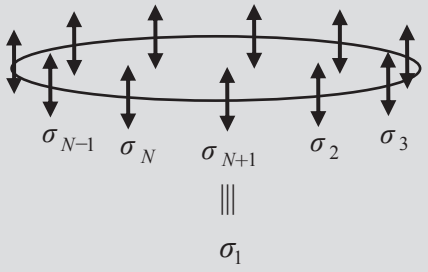

Solution: We apply here the solution similar to Problem 3.4.2 of Chap. 3. For details, we refer the reader to that problem.

First, let us find the averaged spin orientation in the canonical ensemble (CE). By definition

$$\left\langle \sigma_j \right\rangle_{CE} \equiv \sum_{\{\sigma\}} \sigma_j w^{CE}_{\{\sigma\}} = \frac{1}{Z^{CE}} \sum_{\sigma_1=\pm1} \sum_{\sigma_2=\pm1} \cdots \sum_{\sigma_N=\pm1} \sigma_j e^{\frac{\mu h}{T}\sum_{i=1}^{N}\sigma_i + \frac{J}{T}\sum_{i=1}^{N}\sigma_i\sigma_{i+1}} . \tag{6.4}$$

Here, we see again the product of transfer matrices (3.58–3.59), but now one of the indices is present as a multiplier:

$$\left\langle \sigma_j \right\rangle_{CE} = \frac{1}{Z^{CE}} \sum_{\sigma_1=\pm1} \sum_{\sigma_2=\pm1} \cdots \sum_{\sigma_N=\pm1} \sigma_j \prod_{i=1}^{N} T_{\sigma_i\sigma_{i+1}} . \tag{6.5}$$

To transform this expression into the matrix product, we should introduce the Pauli matrix

$$S^z \equiv \begin{Vmatrix} 1 & 0 \\ 0 & -1 \end{Vmatrix} . \tag{6.6}$$

It is easy to see that the following equality is valid:

$$\sum_{\sigma_j=\pm 1} T_{\sigma_{j-1}\sigma_j}\sigma_j T_{\sigma_j\sigma_{j+1}} = \sum_{\sigma_j=\pm 1}\sum_{\tilde{\sigma}_j=\pm 1} T_{\sigma_{j-1}\sigma_j} S^z_{\sigma_j\tilde{\sigma}_j} T_{\tilde{\sigma}_j\sigma_{j+1}}. \tag{6.7}$$

Substituting this equality into (6.5), we find

$$\left\langle \sigma_j \right\rangle_{CE} = \frac{1}{Z^{CE}} \mathrm{Tr}\left(T^{j-1} S^z T^{N-(j-1)} \right). \tag{6.8}$$

Since the trace is invariant under cyclic permutations (cyclic property of the trace operation), we can move the Pauli matrix ahead of the transfer matrices:

$$\left\langle \sigma_j \right\rangle_{CE} = \frac{1}{Z^{CE}} \mathrm{Tr}\left(S^z T^N \right). \tag{6.9}$$

Let us now assume that transformation $F^{-1}TF$ diagonalizes the transfer matrix (3.58) and (3.59):

$$F^{-1}TF = D \equiv \begin{Vmatrix} \lambda_1 & 0 \\ 0 & \lambda_2 \end{Vmatrix}, \tag{6.10}$$

where the eigenvalues λ_1 and λ_2 are provided by (3.61). From (6.10), it is easy to see that the matrix F is composed of the eigenvectors of the transfer matrix:

$$T\,\vec{\mathbf{x}}_{1,2} = \lambda_{1,2}\vec{\mathbf{x}}_{1,2}, \tag{6.11}$$

$$F = \left\| \vec{\mathbf{x}}_1 \vec{\mathbf{x}}_2 \right\|. \tag{6.12}$$

Next, we apply the diagonalization procedure to all transfer matrices in (6.9). This is easy to accomplish because we can substitute the unit matrix $FF^{-1} = \begin{Vmatrix} 1 & 0 \\ 0 & 1 \end{Vmatrix}$ as many times as we need:

$$\begin{aligned} \left\langle \sigma_j \right\rangle_{CE} &= \frac{1}{Z^{CE}} \mathrm{Tr}\left(S^z FF^{-1}TFF^{-1}T \ldots FF^{-1}TFF^{-1} \right) \\ &= \frac{1}{Z^{CE}} \mathrm{Tr}\left(S^z FD^N F^{-1} \right) = \frac{1}{Z^{CE}}\ \mathrm{Tr}\left(F^{-1} S^z FD^N \right). \end{aligned} \tag{6.13}$$

It is easy to find that

$$D^N = \begin{Vmatrix} {\lambda_1}^N & 0 \\ 0 & {\lambda_2}^N \end{Vmatrix}, \tag{6.14}$$

$$F^{-1}S^zF = \begin{Vmatrix} \dfrac{\sinh\dfrac{\mu h}{T}}{\sqrt{\sinh^2\dfrac{\mu h}{T}+e^{-\frac{4J}{T}}}} & K+\dfrac{K\sinh\dfrac{\mu h}{T}}{\sqrt{\sinh^2\dfrac{\mu h}{T}+e^{-\frac{4J}{T}}}} \\ \dfrac{1}{K}-\dfrac{\sinh\dfrac{\mu h}{T}}{K\sqrt{\sinh^2\dfrac{\mu h}{T}+e^{-\frac{4J}{T}}}} & -\dfrac{\sinh\dfrac{\mu h}{T}}{\sqrt{\sinh^2\dfrac{\mu h}{T}+e^{-\frac{4J}{T}}}} \end{Vmatrix}, \tag{6.15}$$

where K is some lengthy expression whose exact form is not important. Multiplying matrices, we find

$$\left\langle \sigma_j \right\rangle_{CE} = \frac{\sinh\dfrac{\mu h}{T}}{\sqrt{\sinh^2\dfrac{\mu h}{T}+e^{-\frac{4J}{T}}}} \frac{{\lambda_1}^N-{\lambda_2}^N}{{\lambda_1}^N+{\lambda_2}^N}, \tag{6.16}$$

where we have also utilized (3.62). In the thermodynamic limit $N \to +\infty$, we can discard one of the eigenvalues which returns us to (3.63):

$$\left\langle \sigma_j \right\rangle_{CE} \to \frac{\sinh\dfrac{\mu h}{T}}{\sqrt{\sinh^2\dfrac{\mu h}{T}+e^{-\frac{4J}{T}}}}. \tag{6.17}$$

Second, to find the correlation function, we have to find the averaged product of spins separated by some distance along the chain:

$$\left\langle \sigma_j\sigma_{j+k} \right\rangle_{CE} \equiv \sum_{\{\sigma\}} \sigma_j\sigma_{j+k} w^{CE}_{\{\sigma\}},\ k \geq 0. \tag{6.18}$$

In this case, the product of transfer matrices is "sandwiched" already not by one but by two Pauli matrices:

$$\left\langle \sigma_j\sigma_{j+k} \right\rangle_{CE} = \frac{1}{Z^{CE}} \mathrm{Tr}\left(T^{j-1}S^zT^kS^zT^{N-(j+k-1)}\right). \tag{6.19}$$

By consideration, similar to the previous case, we find

$$\begin{aligned}\left\langle \sigma_j \sigma_{j+k} \right\rangle_{CE} &= \frac{1}{Z^{CE}} \mathrm{Tr}\left(S^z F D^k F^{-1} S^z F D^{N-k} F^{-1} \right) \\ &= \frac{1}{Z^{CE}} \mathrm{Tr}\left(F^{-1} S^z F D^k F^{-1} S^z F D^{N-k} \right).\end{aligned} \tag{6.20}$$

Substituting and multiplying matrices, and also recalling (3.62), we obtain

$$\left\langle \sigma_j \sigma_{j+k} \right\rangle_{CE} = \frac{\sinh^2 \dfrac{\mu h}{T} + e^{-\frac{4J}{T}} \left(\dfrac{\lambda_1^{N-k} \lambda_2^{k} + \lambda_1^{k} \lambda_2^{N-k}}{\lambda_1^{N} + \lambda_2^{N}} \right)}{\sinh^2 \dfrac{\mu h}{T} + e^{-\frac{4J}{T}}}. \tag{6.21}$$

In the thermodynamic limit $N \to +\infty$, we find

$$\left\langle \sigma_j \sigma_{j+k} \right\rangle_{CE} \to \left\langle \sigma_j \right\rangle_{CE}^2 + \frac{\left(\dfrac{\lambda_2}{\lambda_1} \right)^k + \left(\dfrac{\lambda_2}{\lambda_1} \right)^{N-k}}{e^{\frac{4J}{T}} \sinh^2 \dfrac{\mu h}{T} + 1}. \tag{6.22}$$

Here, k is finite while $N-k$ is infinite. So, we can neglect the second term:

$$g\left(\mathbf{R}_{j,j+k} \right) = \left\langle \sigma_j \sigma_{j+k} \right\rangle_{CE} - \left\langle \sigma_j \right\rangle_{CE}^2 \to \frac{1}{e^{\frac{4J}{T}} \sinh^2 \dfrac{\mu h}{T} + 1} \left(\frac{\lambda_2}{\lambda_1} \right)^k. \tag{6.23}$$

This is the correlation function of two spins at distance ka, where a is the lattice constant. Therefore, we finally find

$$g(\mathbf{R}) \to \frac{(\lambda_2 / \lambda_1)^{|\mathbf{R}|/a}}{e^{\frac{4J}{T}} \sinh^2 \dfrac{\mu h}{T} + 1} = \frac{1}{e^{\frac{4J}{T}} \sinh^2 \dfrac{\mu h}{T} + 1} e^{-\frac{R}{a} \ln \frac{\lambda_1}{\lambda_2}}. \tag{6.24}$$

The correlation length ξ is defined as a characteristic distance at which the correlation function decays to zero. In our case, it is just the distance of the exponential decay:

$$\xi = \frac{a}{\ln \dfrac{\lambda_1}{\lambda_2}}. \tag{6.25}$$

In the absence of magnetic field, $h = 0$, we find

$$\xi = \frac{a}{\ln \coth \dfrac{J}{T}}. \tag{6.26}$$

The critical point of the one-dimensional model is $T_C = 0$, $h_C = 0$. If we approach this point by decreasing the temperature, $T \to 0$, along the isofield curve $h = 0$, then (6.26) diverges exponentially:

$$\xi \to \frac{a}{2} e^{\frac{2J}{T}}. \tag{6.27}$$

As we see later, the exponential divergence of the correlation length generally corresponds only to the "degenerate" one-dimensional case with short-range interactions and is substituted by a power-law divergence in higher dimensions.

However, if we consider the limit $T \to 0$ first and only then the limit $h \to 0$, we will approach the critical point along the critical isotherm $T_C = 0$. In this case, we find:

$$\xi = \frac{a}{\ln \dfrac{1 + \left|\tanh \dfrac{\mu h}{T}\right|}{1 - \left|\tanh \dfrac{\mu h}{T}\right|}} \to \frac{aT}{2\mu |h|}. \tag{6.28}$$

For the divergence of the correlation length along the critical isotherm, the special critical index is introduced:

$$\xi \propto \frac{1}{|h|^{\nu_h^C}} \text{ when, } T = T_C, h \to h_C. \tag{6.29}$$

We see that the mean-field approach provides $\nu_h^C = 1$.

Let us integrate the correlation function (6.23) along the length of the model:

$$\sum_{k=-\infty}^{+\infty} g(\mathbf{R}_{j,j+k}) = \sum_{k=-\infty}^{+\infty} \frac{1}{e^{\frac{4J}{T}} \sinh^2 \dfrac{\mu h}{T} + 1} \left(\frac{\lambda_2}{\lambda_1}\right)^{|k|} = \frac{1}{e^{\frac{4J}{T}} \sinh^2 \dfrac{\mu h}{T} + 1} \left(1 + 2\sum_{k=1}^{+\infty} \left(\frac{\lambda_2}{\lambda_1}\right)^k\right)$$

$$= \frac{1}{e^{\frac{4J}{T}} \sinh^2 \dfrac{\mu h}{T} + 1} \frac{\lambda_1 + \lambda_2}{\lambda_1 - \lambda_2} = \frac{e^{-\frac{4J}{T}} \cosh \dfrac{\mu h}{T}}{\left(\sinh^2 \dfrac{\mu h}{T} + e^{-\frac{4J}{T}}\right)^{3/2}}, \tag{6.30}$$

where we have taken into account that due to symmetry, the correlations for negative k are equal to the correlations for positive k. The sum we have found as the sum of the geometric progression.

Comparing (6.30) with (3.67), we see that the magnetic susceptibility is proportional to the integral of the correlation function:

$$\chi = \frac{\mu}{T} \sum_{k=-\infty}^{+\infty} g\left(\mathbf{R}_{j,j+k}\right). \tag{6.31}$$

This result is called *the fluctuation–dissipation theorem*.

6.2 Correlations: The Mean-Field Approach for the Ising Model in Higher Dimensions

As we have seen in Chap. 3, the mean-field approach

$$\left\langle \sigma_i \sigma_j \right\rangle_{\{\sigma\}} \approx \left\langle \sigma \right\rangle_{\{\sigma\}}^2 \tag{6.32}$$

means that we neglect spin correlations

$$\left\langle \left(\sigma_i - \left\langle \sigma \right\rangle_{\{\sigma\}}\right)\left(\sigma_j - \left\langle \sigma \right\rangle_{\{\sigma\}}\right) \right\rangle_{\{\sigma\}} \approx 0. \tag{6.33}$$

However, the very mean-field approach can be used to find the correlation function. Further, we consider the ferromagnetic Ising model with pair (bi-spin) interactions whose amplitude depends on the distance between two spins in a pair, $J(\mathbf{R}_{i,j}) \equiv J(|\,\mathbf{R}_{i,j}\,|)$, and somehow decays when this distance increases. The Hamiltonian of the model is

$$\mathrm{H}_{\{\sigma\}} = -\mu h \sum_{i=1}^{N} \sigma_i - \sum_{<i,j>} J\left(\mathbf{R}_{i,j}\right) \sigma_i \sigma_j. \tag{6.34}$$

For simplicity, we consider the system in the absence of magnetic field, $h = 0$. The mean-field approximation for the Hamiltonian (6.34) of the homogeneous system is

$$\mathrm{H}_{\{\sigma\}} = -\mu \sum_{\mathbf{R}} h_{\{\sigma\}}^{eff} \sigma_{\mathbf{R}}, \tag{6.35}$$

where the effective field $h^{eff}_{\{\sigma\}}$ is determined by

$$h^{eff}_{\{\sigma\}} \equiv \frac{m_{\{\sigma\}}}{2\mu} \sum_{\mathbf{R}\neq 0} J(\mathbf{R}). \tag{6.36}$$

The equation of state is

$$m_0 = \tanh\left(\beta m_0 \sum_{\mathbf{R}\neq 0} J(\mathbf{R}) \right). \tag{6.37}$$

The critical point corresponds to the temperature when the spontaneous magnetization appears

$$T_C = \sum_{\mathbf{R}\neq 0} J(\mathbf{R}). \tag{6.38}$$

If we returned to the case of the n.n. Ising model, the obtained expressions would transform into the formulae of Problem 3.7.1 considered in Chap. 3.

Above the critical point, there is no spontaneous magnetization. For this case, the correlation function (6.3) in the CE of the Ising model is

$$g\left(\mathbf{R}_{i,j}\right) = \left\langle \sigma_i \sigma_j \right\rangle_{CE} \equiv \frac{\sum\limits_{\{\sigma\}} \sigma_i \sigma_j e^{-\beta \mathrm{H}_{\{\sigma\}}}}{\sum\limits_{\{\sigma\}} e^{-\beta \mathrm{H}_{\{\sigma\}}}} = \frac{\sum\limits_{\sigma_1=\pm 1} \ldots \sum\limits_{\sigma_N=\pm 1} \sigma_i \sigma_j e^{-\beta \mathrm{H}_{\{\sigma\}}}}{\sum\limits_{\sigma_1=\pm 1} \ldots \sum\limits_{\sigma_N=\pm 1} e^{-\beta \mathrm{H}_{\{\sigma\}}}}, \tag{6.39}$$

Next, we separate the sum over spin σ_i and expand this sum explicitly:

$$\begin{aligned} g\left(\mathbf{R}_{i,j}\right) &= \frac{\sum\limits_{\sigma_i=\pm 1} \sum\limits_{\{\sigma\}\setminus\sigma_i} \sigma_i \sigma_j e^{-\beta \mathrm{H}_{\{\sigma\}}}}{\sum\limits_{\sigma_i=\pm 1} \sum\limits_{\{\sigma\}\setminus\sigma_i} e^{-\beta \mathrm{H}_{\{\sigma\}}}} \\ &= \frac{\sum\limits_{\{\sigma\}\setminus\sigma_i} (+1)\sigma_j e^{-\beta \mathrm{H}_{\{\sigma\}:\sigma_i=+1}} + \sum\limits_{\{\sigma\}\setminus\sigma_i} (-1)\sigma_j e^{-\beta \mathrm{H}_{\{\sigma\}:\sigma_i=-1}}}{\sum\limits_{\{\sigma\}\setminus\sigma_i} e^{-\beta \mathrm{H}_{\{\sigma\}:\sigma_i=+1}} + \sum\limits_{\{\sigma\}\setminus\sigma_i} e^{-\beta \mathrm{H}_{\{\sigma\}:\sigma_i=-1}}}. \end{aligned} \tag{6.40}$$

If for a microconfiguration $\{\sigma\}:\sigma_i = +1$, we invert the orientations of all spins, including σ_i, we obtain one of microconfigurations $\{\sigma\}:\sigma_i = -1$. It is easy to see that this transformation is bijective—one and only one microconfiguration $\{\sigma\}:\sigma_i = -1$ corresponds to each microconfiguration $\{\sigma\}:\sigma_i = +1$.

Let us utilize this bijective correspondence of microconfigurations to build the correspondence of the terms of the sums in (6.40). In the numerator, the term $(+1)\sigma_j e^{-\beta \mathrm{H}_{\{\sigma\}:\sigma_i=+1}}$ of the first sum corresponds to the term $(-1)(-\sigma_j)e^{-\beta \mathrm{H}_{\{-\sigma\}:\sigma_i=-1}}$

of the second sum. In the denominator, the term $e^{-\beta \mathrm{H}_{\{\sigma\}:\sigma_i=+1}}$ of the first sum corresponds to the term $e^{-\beta \mathrm{H}_{\{-\sigma\}:\sigma_i=-1}}$ of the second sum.

In the absence of the magnetic field, $h = 0$, Hamiltonian (6.34) does not depend on the inversion of all spins:

$$\mathrm{H}_{\{-\sigma\}:\sigma_i=-1} \equiv \mathrm{H}_{\{\sigma\}:\sigma_i=+1}. \tag{6.41}$$

Thereby all terms, for which we have built the bijective correspondence, become equal to one another, and for the correlation function we find:

$$g(\mathbf{R}_{i,j}) = \frac{2\sum\limits_{\{\sigma\}\setminus\sigma_i} \sigma_j e^{-\beta \mathrm{H}_{\{\sigma\}:\sigma_i=+1}}}{2\sum\limits_{\{\sigma\}\setminus\sigma_i} e^{-\beta \mathrm{H}_{\{\sigma\}:\sigma_i=+1}}} = \frac{\sum\limits_{\{\sigma\}\setminus\sigma_i} \sigma_j e^{-\beta \mathrm{H}_{\{\sigma\}:\sigma_i=+1}}}{\sum\limits_{\{\sigma\}\setminus\sigma_i} e^{-\beta \mathrm{H}_{\{\sigma\}:\sigma_i=+1}}} = \left\langle \sigma_j \right\rangle_{CE,\sigma_i=+1}. \tag{6.42}$$

Here, in the last expression, instead of averaging just over the CE, $\langle \ldots \rangle_{CE}$, we average over the probabilities of the ensemble $\langle \ldots \rangle_{CE,\sigma_i=+1}$. It is the same CE but with an additional boundary condition; the orientation of spin σ_i is maintained permanently "up" by external forces.

But what is the meaning of the quantity $\left\langle \sigma_j \right\rangle_{CE,\sigma_i=+1}$? We consider the CE when the orientation $\sigma_i = +1$ of spin σ_i is "frozen." This can be considered as a disturbance of the usual CE; we introduce a fixed magnetic moment into the system and observe how the system would respond to its presence.

In the ferromagnet, spin σ_i attempts to reorient its neighbors also "up." Spin σ_j is located at some distance $|\mathbf{R}_{i,j}|$ from spin σ_i. Averaging σ_j in the ensemble, we find the averaged magnetization $\left\langle \sigma_j \right\rangle_{CE,\sigma_i=+1}$ induced by the presence of the fixed magnetic moment $\sigma_i = +1$. The farther spin σ_j is located from spin σ_i, the lower, probably, is the influence. Therefore, we expect the induced magnetization $\left\langle \sigma_j \right\rangle_{CE,\sigma_i=+1}$ to decay with the distance from σ_i.

We see that equality (6.42) presents an important result: the spin correlation function above the critical point equals the decay of the system's response to the presence of the external magnetic moment. Equality (6.42), when correlations are determined by the system's response and vice versa, is, in fact, the representative of *the fluctuation–dissipation theorem* studied in detail later.

To find the quantity $\left\langle \sigma\left(\mathbf{R}_{i,j}\right) \right\rangle_{CE,\sigma_i=+1}$ we apply the mean-field approach. Now we consider the ensemble when external forces support $\sigma_i = +1$. Let this spin be located at $\mathbf{R} = 0$. The mean-field approximation of the Hamiltonian is

$$\mathrm{H}_{\{\sigma\}} = -\mu \sum_{\mathbf{R}} h^{eff}_{\{\sigma\}}(\mathbf{R}) \sigma_{\mathbf{R}}, \tag{6.43}$$

where $h^{eff}_{\{\sigma\}}(\mathbf{R})$ is determined by

$$h^{eff}_{\{\sigma\}}(\mathbf{R}) \equiv \frac{1}{2\mu} \sum_{\mathbf{R}':\mathbf{R}'\neq\mathbf{R}} J(\mathbf{R}-\mathbf{R}')\sigma_{\mathbf{R}'}, \tag{6.44}$$

and the equation of state is

$$\langle \sigma_{\mathbf{R}} \rangle_{CE,+1} = \tanh\left(\beta \sum_{\mathbf{R}':\mathbf{R}'\neq\mathbf{R}} J(\mathbf{R}-\mathbf{R}') \langle \sigma_{\mathbf{R}'} \rangle_{CE,+1} \right) \text{ for } \mathbf{R} \neq 0. \tag{6.45}$$

For $\mathbf{R} = 0$, by definition, we have

$$\langle \sigma_{\mathbf{R}=0} \rangle_{CE,+1} = +1. \tag{6.46}$$

The induced magnetization is small, so we expand the tanh function:

$$\langle \sigma_{\mathbf{R}} \rangle_{CE,+1} \approx \beta \sum_{\mathbf{R}':\mathbf{R}'\neq\mathbf{R}} J(\mathbf{R}-\mathbf{R}') \langle \sigma_{\mathbf{R}'} \rangle_{CE,+1}. \tag{6.47}$$

This equation of state is valid far from $\mathbf{R} = 0$. At the point $\mathbf{R} = 0$, spin σ_i acts as the source of disturbance:

$$\langle \sigma_{\mathbf{R}} \rangle_{CE,+1} = \beta \sum_{\mathbf{R}':\mathbf{R}'\neq\mathbf{R}} J(\mathbf{R}-\mathbf{R}') \langle \sigma_{\mathbf{R}'} \rangle_{CE,+1} + \delta(\mathbf{R}). \tag{6.48}$$

With the aid of the δ function, we have allowed here for the solution singularity, which is present due to constraint (6.46).

We assume the interactions of spins in pairs to be long-range. Then, we can substitute the discrete sum $\sum_{\mathbf{R}':\mathbf{R}'\neq\mathbf{R}}$ by the integral:

$$\langle \sigma_{\mathbf{R}} \rangle_{CE,+1} = \beta \int_{-\infty}^{+\infty} J(\mathbf{R}-\mathbf{R}') \langle \sigma_{\mathbf{R}'} \rangle_{CE,+1} \frac{d^d\mathbf{R}'}{a^d} + \delta(\mathbf{R}), \tag{6.49}$$

where we have normalized $d^d\mathbf{R}$ by the volume a^d of the lattice cell (with a being the lattice constant).

We define the Fourier spectrums of the induced magnetization and of the amplitude of pair (bi-spin) interactions by

$$\breve{m}(\mathbf{k}) \equiv \int_{-\infty}^{+\infty} e^{i\mathbf{k}\mathbf{R}} \langle \sigma_{\mathbf{R}} \rangle_{CE,+1} d^d\mathbf{R}, \tag{6.50}$$

$$\langle \sigma_{\mathbf{R}} \rangle_{CE,+1} \equiv \frac{1}{(2\pi)^d} \int_{-\infty}^{+\infty} e^{-i\mathbf{k}\mathbf{R}} \breve{m}(\mathbf{k}) d^d\mathbf{k}, \tag{6.51}$$

$$\breve{J}(\mathbf{k}) \equiv \int_{-\infty}^{+\infty} e^{i\mathbf{kR}} J(\mathbf{R}) d^d \mathbf{R}, \tag{6.52}$$

$$J(\mathbf{R}) \equiv \frac{1}{(2\pi)^d} \int_{-\infty}^{+\infty} e^{-i\mathbf{kR}} \breve{J}(\mathbf{k}) d^d \mathbf{k}. \tag{6.53}$$

For the so-defined Fourier transform, the spectrum of the δ function equals 1:

$$\breve{\delta}(\mathbf{k}) \equiv \int_{-\infty}^{+\infty} e^{i\mathbf{kR}} \delta(\mathbf{R}) d^d \mathbf{R} = 1. \tag{6.54}$$

Applying the Fourier transform to (6.49), we find

$$\breve{m}(\mathbf{k}) = \frac{\beta}{a^d} \int_{-\infty}^{+\infty} e^{i\mathbf{kR}} d^d \mathbf{R} \int_{-\infty}^{+\infty} J\left(\mathbf{R}-\mathbf{R}'\right) \left\langle \sigma_{\mathbf{R}'} \right\rangle_{CE,+1} d^d \mathbf{R}' + 1. \tag{6.55}$$

Splitting the exponential function under the sign of the integral, we obtain two independent Fourier transforms:

$$\begin{aligned} \breve{m}(\mathbf{k}) &= \frac{\beta}{a^d} \left(\int_{-\infty}^{+\infty} e^{i\mathbf{k}(\mathbf{R}-\mathbf{R}')} J\left(\mathbf{R}-\mathbf{R}'\right) d^d \left(\mathbf{R}-\mathbf{R}'\right) \right) \left(\int_{-\infty}^{+\infty} e^{i\mathbf{kR}'} \left\langle \sigma_{\mathbf{R}'} \right\rangle_{T,+1} d^d \mathbf{R}' \right) + 1 \\ &= \frac{\beta}{a^d} \breve{J}(\mathbf{k}) \breve{m}(\mathbf{k}) + 1. \end{aligned} \tag{6.56}$$

For the spectrum of the induced magnetization, this provides

$$\breve{m}(\mathbf{k}) = \frac{1}{1 - \frac{\beta}{a^d} \breve{J}(\mathbf{k})}. \tag{6.57}$$

Now, we have to recall some features of the spectrum analysis. The Fourier transform of the δ function provides unity (a constant, equation (6.54), Fig. 6.1a). The Fourier transform of a constant is the δ function (Fig. 6.1b). The constant and the δ function are two extremes of a "bell"-shaped dependence. The Fourier transform of a "bell" of width ΔR returns also the "bell"-shaped dependence of width $\Delta k \propto 1/\Delta R$ (Fig. 6.1c). The brightest examples of this principle are the wave packet theory in acoustics/radiophysics and the Heisenberg uncertainty principle in quantum mechanics.

The amplitude $J(\mathbf{R})$ of pair (bi-spin) interactions decays with the distance $\mathbf{R}$ between spins. Assuming the characteristic length of decay to be ΔR, for the

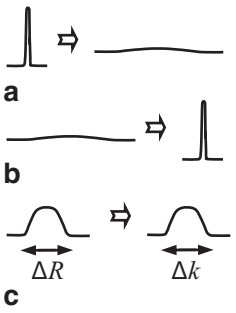

Fig. 6.1 General features of the Fourier transform. **(a)** The spectrum of the δ function is unity. **(b)** The spectrum of unity is the δ function. **(c)** The "bell" of width ΔR transforms into the "bell" of width $\Delta k \propto 1/\Delta R$

characteristic length of the spectrum's decay, we find $\Delta k \propto 1/\Delta R$. The crude approximation of the spectrum's "bell" can be represented by the parabolic decay:

$$\breve{J}(\mathbf{k}) \approx \breve{J}(\mathbf{k}=0)\left\{1 - const \cdot \Delta R^2 \mathbf{k}^2\right\}. \tag{6.58}$$

We have obtained this equation from intuitive considerations. Let us now develop it in a more rigorous way. The Fourier spectrum of the interaction amplitude is provided by (6.52). For small $\mathbf{k}$ (*the long-wave approximation*), we expand the exponential function under the sign of this integral and consider only three terms in this expansion:

$$e^{i\mathbf{kR}} = 1 + i\mathbf{kR} + \frac{1}{2}(i\mathbf{kR})^2 + \ldots \tag{6.59}$$

Substituting this expansion into (6.52), we obtain

$$\breve{J}(\mathbf{k}) \equiv \int_{-\infty}^{+\infty}\left(1 + i\mathbf{kR} - \frac{1}{2}(\mathbf{kR})^2 + \ldots\right)J(\mathbf{R})d^d\mathbf{R}. \tag{6.60}$$

The first term of the expansion provides $\breve{J}(\mathbf{k}=0)$:

$$\int_{-\infty}^{+\infty} J(\mathbf{R})d^d\mathbf{R} \equiv \breve{J}(\mathbf{k}=0). \tag{6.61}$$

The second term returns zero due to the spherical symmetry of the interaction amplitude, $J(\mathbf{R}) \equiv J(|\,\mathbf{R}\,|)$:

$$\int_{-\infty}^{+\infty} i\mathbf{kR}J(\mathbf{R})d^d\mathbf{R} = 0. \tag{6.62}$$

For the third term, again due to the spherical symmetry, we choose $\mathbf{k}$ to be oriented along the n^{th}-component of $\mathbf{R}$:

$$-\int_{-\infty}^{+\infty}\frac{1}{2}(\mathbf{kR})^2 J(\mathbf{R})d^d\mathbf{R} = -\int_{-\infty}^{+\infty}\frac{1}{2}k^2 {R_n}^2 J(\mathbf{R})d^d\mathbf{R}, \tag{6.63}$$

where R_n is the mentioned n^{th}-component of $\mathbf{R}$. Since for any n, the right-hand side of (6.63) returns the same value of the left-hand side, not depending on n, we find

$$-\int_{-\infty}^{+\infty}\frac{1}{2}(\mathbf{kR})^2 J(\mathbf{R})d^d\mathbf{R} = -\frac{1}{d}\sum_{n=1}^{d}\int_{-\infty}^{+\infty}\frac{1}{2}k^2 {R_n}^2 J(\mathbf{R})d^d\mathbf{R} \tag{6.64}$$
$$= -\frac{1}{d}\int_{-\infty}^{+\infty}\frac{1}{2}k^2 R^2 J(\mathbf{R})d^d\mathbf{R}.$$

We define the root-mean-square radius of pair (bi-spin) interactions by

$$\Delta \equiv \sqrt{\sum_{R\neq 0} R^2 J(\mathbf{R})} \approx \sqrt{\int_{-\infty}^{+\infty} R^2 J(\mathbf{R})\frac{d^d\mathbf{R}}{a^d}}. \tag{6.65}$$

Substituting it into expansion (6.60), we, indeed, return to (6.58):

$$\breve{J}(\mathbf{k}) \approx \breve{J}(\mathbf{k}=0) - \frac{k^2 a^d}{2d}\Delta^2 = \breve{J}(\mathbf{k}=0)\left(1 - \frac{k^2 a^d}{2d}\frac{\Delta^2}{\breve{J}(\mathbf{k}=0)}\right). \tag{6.66}$$

Recalling (6.38), we can express $\breve{J}(\mathbf{k}=0)$ in terms of the critical temperature:

$$\breve{J}(\mathbf{k}=0) \equiv \int_{-\infty}^{+\infty} J(\mathbf{R})d^d\mathbf{R} = a^d T_{\text{C}}. \tag{6.67}$$

Substituting it into (6.66), and then (6.66) into (6.57), for the spectrum of the induced magnetization, we find

$$\breve{m}(\mathbf{k}) = \frac{1}{1 - \frac{T_{\text{C}}}{T}\left(1 - \frac{k^2}{2d}\frac{\Delta^2}{T_{\text{C}}}\right)} = \frac{2dT_{\text{C}}/\Delta^2}{k^2 + \frac{1}{\xi^2}}, \tag{6.68}$$

where in the last equality for small relative deviations of temperature from critical

$$t = \frac{T - T_{\text{C}}}{T_{\text{C}}} \to 0, \tag{6.69}$$

we have introduced a new parameter

$$\xi \equiv \frac{\Delta}{\sqrt{2dT_{\text{C}}}}\frac{1}{\sqrt{t}}. \tag{6.70}$$

Later, we prove that this parameter is *a correlation length*. For a correlation length of an arbitrary system, its own critical index ν_t^{C} is defined as

$$\xi \propto \frac{1}{|t|^{\nu_t^{\mathrm{C}}}}. \tag{6.71}$$

From (6.70), we see that the mean-field approximation of the correlation function provides for the correlation length the simplest rational fraction, $\nu_t^{\mathrm{C}} = 1/2$, as the critical index.

In accordance with (6.42), the spectrum $\breve{m}(\mathbf{k})$ of the induced magnetization in the "CE, +1" ensemble is the spectrum $\breve{g}(\mathbf{k})$ of the correlation function in the usual CE:

$$\breve{g}(\mathbf{k}) = \frac{2dT_{\mathrm{C}}/\Delta^2}{k^2 + \dfrac{1}{\xi^2}}. \tag{6.72}$$

To find the correlation function itself, we have to apply the inverse Fourier transform:

$$g(\mathbf{R}) \equiv \frac{1}{(2\pi)^d} \int_{-\infty}^{+\infty} e^{-i\mathbf{kR}} \breve{g}(\mathbf{k}) d^d\mathbf{k} = \frac{2dT_{\mathrm{C}}/\Delta^2}{(2\pi)^d} \int_{-\infty}^{+\infty} e^{-i\mathbf{kR}} \frac{1}{k^2 + \dfrac{1}{\xi^2}} d^d\mathbf{k}. \tag{6.73}$$

This integral is tabulated by the modified Bessel function $\mathrm{K}_\alpha(x)$:

$$g(|\mathbf{R}|) \propto \frac{1}{(\xi R)^{\frac{d-2}{2}}} \mathrm{K}_{\frac{d-2}{2}}\left(\frac{R}{\xi}\right). \tag{6.74}$$

The modified Bessel function has the following asymptotes:

$$\mathrm{K}_\alpha(x) \propto \frac{e^{-x}}{\sqrt{x}} \text{ for } x >> 1, \tag{6.75}$$

$$\mathrm{K}_\alpha(x) \propto \frac{1}{x^\alpha} \text{ for } x << 1, \alpha > 0. \tag{6.76}$$

Substituting them into (6.74), we find the asymptotes of the correlation function:

$$g(R) \propto \frac{e^{-R/\xi}}{\xi^{\frac{d-3}{2}} R^{\frac{d-1}{2}}} \text{ for } R >> \xi, \tag{6.77}$$

$$g(R) \propto \frac{1}{R^{d-2}} \text{ for } R << \xi, d > 2. \tag{6.78}$$

We have obtained another important result—on scales larger than ξ, the correlations decay exponentially. The exponential decay is a very "fast" decay. Therefore, as a crude approximation, it is often assumed that on scales larger than ξ there are no correlations at all. The characteristic length ξ delimiting scales with and without correlations is called *the correlation length*.

On scales smaller than the correlation length ξ, the correlations decay as the "slow" power-law (6.78). From Chap. 1, we know that power-law dependencies often indicate the presence of fractal mathematics. This is also the case for the considered Ising model. On scales smaller than the correlation length, the phase clusters become fractal. Fractality means the absence of both characteristic length and characteristic cluster size. On these scales, the clusters are present in all shapes and sizes, limited only by the lattice constant on one side and by the correlation length on another.

Far from the critical point, the correlation length is small. However, when a system approaches its critical point, the correlation length (6.71) diverges. This means that above the critical point, the fractality is in its embryonic state, and only small clusters are present. The closer the system to its critical point, the larger the sizes of these clusters, and the larger scales are dominated by the fractality.

When the correlation length reaches the size of the system, the whole system becomes fractal. The fractality has now occupied all possible scales from the lattice constant to the size of the system. The clusters are now present in all possible shapes and sizes, including macroscopic.

Asymptote (6.78) is not valid when $d = 2$. For this case, the asymptote is

$$g(R) \propto \ln \frac{\xi}{R} \text{ for } R << \xi, d = 2. \tag{6.79}$$

The decay here is logarithmic which is even "slower" than the power-law decay.

For our three-dimensional space, $d = 3$, the modified Bessel function is found in quadratures:

$$\mathrm{K}_{\frac{1}{2}}(x) = \sqrt{\frac{\pi}{2x}} e^{-x} \quad \forall x. \tag{6.80}$$

For the correlation function, this provides

$$g(R) \propto \frac{e^{-R/\xi}}{R} \quad \forall R. \tag{6.81}$$

The asymptotes of this expression are the same as (6.77) and (6.78). On larger scales, the correlations decay exponentially. On scales smaller than the correlation length ξ, the correlations decay as a power-law:

$$g(R) \propto \frac{1}{R} \text{ for } R << \xi, d = 3. \tag{6.82}$$

The critical index of the correlation function is defined by

$$g(R) \propto \frac{1}{R^{d-2+\eta^{\mathrm{C}}}} \text{ for } R << \xi. \tag{6.83}$$

From (6.78), we see that the mean-field approach provides $\eta^{\mathrm{C}} = 0$.

Problem 6.2.1

Find the correlation function of the ferromagnetic n.n. Ising model above the critical point in the absence of magnetic field by *the method of sources* (Green 1828; Kadanoff 1976, 2000).

Solution: The Hamiltonian of the n.n. Ising model is defined as

$$\mathrm{H}_{\{\sigma\}} = -\mu h \sum_{i=1}^{N} \sigma_i - J \sum_{<i,j>_{n.n.}} \sigma_i \sigma_j. \tag{6.84}$$

Following the method of sources, we introduce the model Hamiltonian when the magnetic field is nonuniform over the model space:

$$\mathrm{H}_{\{\sigma\}} = -\mu \sum_{i=1}^{N} h_i \sigma_i - J \sum_{<i,j>_{n.n.}} \sigma_i \sigma_j. \tag{6.85}$$

Later, we return to the real Hamiltonian (6.84) by just assuming the field of being uniform again.

The mean-field approximation of the model Hamiltonian is

$$\mathrm{H}_{\{\sigma\}} = -\mu \sum_{\mathbf{R}} \left(h_{\mathbf{R}} + h^{eff}_{\{\sigma\}}(\mathbf{R}) \right) \sigma_{\mathbf{R}}, \tag{6.86}$$

where the mean-field $h^{eff}_{\{\sigma\}}(\mathbf{R})$ is defined as

$$h^{eff}_{\{\sigma\}}(\mathbf{R}) \equiv \frac{J}{2\mu} \sum_{\mathbf{R}':n.n.\mathbf{R}} \sigma_{\mathbf{R}'}. \tag{6.87}$$

Then the equation of state is

$$\langle \sigma_{\mathbf{R}} \rangle_{CE} = \tanh\left(\beta \left\{ \mu h_{\mathbf{R}} + J \sum_{\mathbf{R}':n.n.\mathbf{R}} \langle \sigma_{\mathbf{R}'} \rangle_{CE} \right\} \right). \tag{6.88}$$

Let us expand $\langle \sigma_{\mathbf{R}'} \rangle_{CE}$ in the neighborhood of $\mathbf{R}$:

$$\langle \sigma_{\mathbf{R}'} \rangle_{CE} = \langle \sigma_{\mathbf{R}} \rangle_{CE} + \left((\mathbf{R}' - \mathbf{R}) \frac{d}{d\mathbf{R}}\bigg|_{\mathbf{R}} \right) \langle \sigma_{\mathbf{R}} \rangle_{CE} + \frac{1}{2} \left((\mathbf{R}' - \mathbf{R}) \frac{d}{d\mathbf{R}}\bigg|_{\mathbf{R}} \right)^2 \langle \sigma_{\mathbf{R}} \rangle_{CE} + \cdots \tag{6.89}$$

This expansion is valid when $\langle \sigma_{\mathbf{R}'} \rangle_{CE}$ is a "slow" function of $\mathbf{R}'$. In other words, we consider *the long-wave approximation*. Here, we keep only the first three terms which is equivalent to (6.59) and (6.60).

Next, we substitute this expansion into (6.88). The second term returns zero due to the symmetry of the lattice:

$$\sum_{\mathbf{R}':n.n.\mathbf{R}} \left((\mathbf{R}' - \mathbf{R}) \frac{d}{d\mathbf{R}}\bigg|_{\mathbf{R}} \right) \langle \sigma_{\mathbf{R}} \rangle_{CE} = \left(\frac{d \langle \sigma_{\mathbf{R}} \rangle_{CE}}{d\mathbf{R}}\bigg|_{\mathbf{R}} \sum_{\mathbf{R}':n.n.\mathbf{R}} (\mathbf{R}' - \mathbf{R}) \right) = 0. \quad (6.90)$$

For the third term, we write its definition explicitly:

$$\frac{1}{2} \sum_{\mathbf{R}':n.n.\mathbf{R}} \left((\mathbf{R}' - \mathbf{R}) \frac{d}{d\mathbf{R}}\bigg|_{\mathbf{R}} \right)^2 \langle \sigma_{\mathbf{R}} \rangle_{CE}$$

$$\equiv \frac{1}{2} \sum_{n=1}^{d} \sum_{k=1}^{d} \frac{\partial^2 \langle \sigma_{\mathbf{R}} \rangle_{CE}}{\partial R_n \partial R_k}\bigg|_{\mathbf{R}} \sum_{\mathbf{R}':n.n.\mathbf{R}} (R'_n - R_n)(R'_k - R_k). \quad (6.91)$$

Due to the lattice symmetry, the expression under the sign of the sum is non-zero only if $n = k$:

$$\frac{1}{2} \sum_{\mathbf{R}':n.n.\mathbf{R}} \left((\mathbf{R}' - \mathbf{R}) \frac{d}{d\mathbf{R}}\bigg|_{\mathbf{R}} \right)^2 \langle \sigma_{\mathbf{R}} \rangle_{CE}$$

$$= \frac{1}{2} \sum_{n=1}^{d} \frac{\partial^2 \langle \sigma_{\mathbf{R}} \rangle_{CE}}{\partial R_n^{\,2}}\bigg|_{\mathbf{R}} \sum_{\mathbf{R}':n.n.\mathbf{R}} (R'_n - R_n)^2. \quad (6.92)$$

For the isotropic lattice, the sum $\sum_{\mathbf{R}':n.n.\mathbf{R}} (R'_n - R_n)^2$ does not depend on n and equals

$$\sum_{\mathbf{R}':n.n.\mathbf{R}} (R'_n - R_n)^2 = Ca^2, \quad (6.93)$$

where C is some constant depending on the lattice considered.

Finally, for the third term of the expansion, we find

$$\frac{1}{2} \sum_{\mathbf{R}':n.n.\mathbf{R}} \left((\mathbf{R}' - \mathbf{R}) \frac{d}{d\mathbf{R}}\bigg|_{\mathbf{R}} \right)^2 \langle \sigma_{\mathbf{R}} \rangle_{CE} = \frac{Ca^2}{2} \sum_{n=1}^{d} \frac{\partial^2 \langle \sigma_{\mathbf{R}} \rangle_{CE}}{\partial R_n^{\,2}}\bigg|_{\mathbf{R}} = \frac{Ca^2}{2} \Delta \langle \sigma_{\mathbf{R}} \rangle_{CE}. \quad (6.94)$$

Here, $\Delta \equiv (\nabla\nabla)$ is the Laplace operator. Substituting this expression into (6.89), we find the approximation of the equation of state:

$$\langle \sigma_{\mathbf{R}} \rangle_{CE} = \tanh\left(\beta \left\{ \mu h_{\mathbf{R}} + Jq \langle \sigma_{\mathbf{R}} \rangle_{CE} + J \frac{Ca^2}{2} \Delta \langle \sigma_{\mathbf{R}} \rangle_{CE} \right\} \right), \qquad (6.95)$$

where q is the lattice coordination number.

In the proximity of the critical point, we expand the tanh function:

$$\langle \sigma_{\mathbf{R}} \rangle_{CE} = \beta \mu h_{\mathbf{R}} \left(1 - \left\{ \beta Jq \langle \sigma_{\mathbf{R}} \rangle_{CE} + \beta J \frac{Ca^2}{2} \Delta \langle \sigma_{\mathbf{R}} \rangle_{CE} \right\}^2 \right)$$
$$+ \beta Jq \langle \sigma_{\mathbf{R}} \rangle_{CE} + \beta J \frac{Ca^2}{2} \Delta \langle \sigma_{\mathbf{R}} \rangle_{CE} - \frac{1}{3} (\beta Jq \langle \sigma_{\mathbf{R}} \rangle_{CE})^3 + \ldots \qquad (6.96)$$

Here, in the expansion we have kept only the terms, linear in the magnetic field, and have neglected the terms with higher powers of the magnetic field. Also in *the long-wave approximation,* we neglected the terms containing the products of magnetization and its derivatives.

Introducing the relative deviation (6.69) of temperature from its critical value $T_C = Jq$, we obtain

$$h_{\mathbf{R}} \approx \frac{Jq}{\mu} \left(-\frac{Ca^2}{2q} \Delta \langle \sigma_{\mathbf{R}} \rangle_{CE} + t \langle \sigma_{\mathbf{R}} \rangle_{CE} + \frac{1}{3} \langle \sigma_{\mathbf{R}} \rangle_{CE}^3 \right). \qquad (6.97)$$

This is the equation of state which almost corresponds to the equation of state (3.92) of Landau theory considered in Chap. 3. Only now, we consider a heterogeneous system instead of a homogeneous system. Therefore, the additional term $-\frac{J}{\mu}\frac{Ca^2}{2}\Delta \langle \sigma_{\mathbf{R}} \rangle_{CE}$ has appeared which takes into account how the magnetization changes from one lattice site to another. While other terms are responsible for the representation of the volumetric free energy, the term $-\frac{J}{\mu}\frac{Ca^2}{2}\Delta \langle \sigma_{\mathbf{R}} \rangle_{CE}$ represents, in fact, the surface energy of the boundaries of phase clusters.

Let us find the response of the equation of state (6.97) to the change of the external magnetic field at site $\mathbf{R}'$:

$$\delta_{\mathbf{R},\mathbf{R}'} = \frac{\partial h_{\mathbf{R}}}{\partial h_{\mathbf{R}'}} \approx \frac{Jq}{\mu} \left(-\frac{Ca^2}{2q} \Delta + t + \langle \sigma_{\mathbf{R}} \rangle_{CE}^2 \right) \frac{\partial \langle \sigma_{\mathbf{R}} \rangle_{CE}}{\partial h_{\mathbf{R}'}}. \qquad (6.98)$$

The quantity $\frac{\partial \langle \sigma_{\mathbf{R}} \rangle_{CE}}{\partial h_{\mathbf{R}'}}$ represents here the appearance of the magnetization at point $\mathbf{R}$ due to the appearance of the field at point $\mathbf{R}'$, i.e., the correlation function:

$$g(\mathbf{R}' - \mathbf{R}) \propto \frac{\partial \langle \sigma_{\mathbf{R}} \rangle_{CE}}{\partial h_{\mathbf{R}'}}. \tag{6.99}$$

Choosing $\mathbf{R}' = 0$ in (6.98), we obtain

$$\delta_{\mathbf{R}} \approx \frac{Jq}{\mu}\left(-\frac{Ca^2}{2q}\Delta + t + \langle \sigma_{\mathbf{R}} \rangle_{CE}^{\,2} \right) g(\mathbf{R}). \tag{6.100}$$

Now, we can return from the model Hamiltonian (6.85) to the external magnetic field, which is uniform over the lattice. Meanwhile, (6.100) remains valid for this particular case as well. Above the critical point, the magnetization of the system is zero, $\langle \sigma_{\mathbf{R}} \rangle_{CE} = 0$, in the zero magnetic field:

$$\delta_{\mathbf{R}} \approx \frac{Jq}{\mu}\left(-\frac{Ca^2}{2q}\Delta + t \right) g(\mathbf{R}). \tag{6.101}$$

Next, we multiply (6.101) by $e^{i\mathbf{kR}}$ and carry out summation over all sites:

$$\begin{aligned} 1 &\approx \frac{Jq}{\mu}\sum_{\mathbf{R}} e^{i\mathbf{kR}}\left(-\frac{Ca^2}{2q}\Delta + t \right) g(\mathbf{R}) \\ &\approx \frac{Jq}{\mu}\int_{-\infty}^{+\infty} e^{i\mathbf{kR}}\left(-\frac{Ca^2}{2q}\Delta + t \right) g(\mathbf{R})\frac{d^d\mathbf{R}}{a^d} \\ &\approx \frac{Jq}{\mu}\int_{-\infty}^{+\infty} e^{i\mathbf{kR}}\left(-\frac{Ca^2}{2q}\Delta \right) g(\mathbf{R})\frac{d^d\mathbf{R}}{a^d} + \frac{Jq}{\mu}t\frac{\breve{g}(\mathbf{k})}{a^d}. \end{aligned} \tag{6.102}$$

Integrating by parts twice and taking into account that the correlation function and its derivatives are zero in the infinity, we find:

$$\begin{aligned} 1 &\approx (i\mathbf{k})^2 \frac{Jq}{\mu}\int_{-\infty}^{+\infty} e^{i\mathbf{kR}}\left(-\frac{Ca^2}{2q} \right) g(\mathbf{R})\frac{d^d\mathbf{R}}{a^d} + \frac{Jq}{\mu}t\frac{\breve{g}(\mathbf{k})}{a^d} \text{ or} \\ 1 &\approx \left(\frac{J}{\mu}\frac{C}{2a^{d-2}}k^2 + \frac{Jq}{\mu}\frac{t}{a^d} \right)\breve{g}(\mathbf{k}) \text{ or } \breve{g}(\mathbf{k}) = \frac{const}{k^2 + \frac{2qt}{Ca^2}}. \end{aligned} \tag{6.103}$$

This returns us to (6.72).

Let us return to the differential equation (6.100) for the correlation function. Since in Problem 6.2.1 we considered the system above the critical point in the absence of magnetic field, we substituted the zero solution for the spontaneous magnetization, $\langle \sigma_{\mathbf{R}} \rangle_{CE} = 0$, into (6.100) to obtain (6.101), whose very solution we found later.

Let us now discuss a more general case, when we may consider the system either below or above the critical point, either in the absence or in the presence of the uniform magnetic field h. In this case we can no longer discard the value of the magnetization $\langle \sigma_{\mathbf{R}} \rangle_{CE}$ in (6.100). However, this does not complicate further analysis because in the case of the uniform field the equilibrium magnetization $\langle \sigma_{\mathbf{R}} \rangle_{CE}$ does not depend on **R** and, thereby, we obtain the solution by substituting $t + \langle \sigma \rangle_{CE}^2$ instead of t in all formulae:

$$\breve{g}(\mathbf{k}) = \frac{const}{k^2 + \frac{2q}{Ca^2}\left\{t + \langle \sigma \rangle_{CE}^2\right\}} \text{ or } \breve{g}(\mathbf{k}) = \frac{const}{k^2 + \frac{1}{\xi^2}}, \tag{6.104}$$

where the correlation length is now defined as

$$\xi = \sqrt{\frac{Ca^2}{2q}} \frac{1}{\sqrt{t + \langle \sigma \rangle_{CE}^2}}. \tag{6.105}$$

Solution (6.105) allows us to investigate the scaling behavior of the correlation length. Let us consider first the proximity of the critical point which we approach along the critical isofield curve $h = h_C = 0$. Above the critical point, the spontaneous magnetization is zero, and we return to an analogue of expression (6.70):

$$\xi = \sqrt{\frac{Ca^2}{2q}} \frac{1}{\sqrt{t}}. \tag{6.106}$$

Below the critical point, we should substitute the spontaneous magnetization (3.97) together with particular values of coefficients (3.93),

$$\langle \sigma \rangle_{CE} = \pm\sqrt{-3t}, \tag{6.107}$$

into (6.105) to find:

$$\xi = \sqrt{\frac{Ca^2}{4q}} \frac{1}{\sqrt{-t}}. \tag{6.108}$$

Defining the critical index ν_t^C by

$$\xi \propto \frac{1}{|t|^{\nu_t^C}}, \tag{6.109}$$

we see that above and below the critical point the mean-field approach provides for this critical index the value $\nu_t^{\mathrm{C}} = 1/2$.

Next, we approach the critical point along the critical isotherm $t = 0$. Here, the magnetization is determined by (3.99), and we obtain:

$$\xi \propto \frac{1}{|h|^{1/3}}. \tag{6.110}$$

Defining another critical index ν_h^{C} by

$$\xi \propto \frac{1}{|h|^{\nu_h^C}}, \tag{6.111}$$

we immediately find $\nu_h^{\mathrm{C}} = 1/3$.

Now, let us consider the proximity of the spinodal point. For the isofield approach $h = h_{\mathrm{S}}$, utilizing (3.109) and (3.93), we obtain

$$\xi \propto \frac{1}{\sqrt{(t - t_{\mathrm{S}}) + 2m_{\mathrm{S}}(m - m_{\mathrm{S}})}}. \tag{6.112}$$

Recalling (3.110), we find:

$$\xi \propto \frac{1}{|t - t_{\mathrm{S}}|^{1/4}}. \tag{6.113}$$

Thereby, for the spinodal index ν_t^{S}, defined by,

$$\xi \propto \frac{1}{|t|^{\nu_t^S}}, \tag{6.114}$$

the considered mean-field approach provides $\nu_t^{\mathrm{S}} = 1/4$.

At last, we approach the spinodal point along the isotherm $t = t_{\mathrm{S}}$. With the aid of (3.109) and (3.93), we find:

$$\xi \propto \frac{1}{\sqrt{2m_{\mathrm{S}}(m - m_{\mathrm{S}})}}. \tag{6.115}$$

Substituting (3.112) into this expression, we obtain the sought scaling:

$$\xi \propto \frac{1}{|h - h_{\mathrm{S}}|^{1/4}}. \tag{6.116}$$

Defining the spinodal index ν_h^{S} by

$$\xi \propto \frac{1}{|h|^{\nu_h^{\mathrm{S}}}}, \tag{6.117}$$

for the value of this index we find $\nu_h^{\mathrm{S}} = 1/4$.

Summarizing the obtained results of scaling, provided by the considered mean-field approach, we may say that the correlation length diverges in the vicinity of the critical point as well as spinodal point.

6.3 Magnetic Systems: The Fluctuation–Dissipation Theorem

In the previous section, we considered the behavior of correlations of the Ising model in the vicinity of its critical point. However, correlations are just one side of phenomena described by the fluctuation–dissipation theorem. Another side is the susceptibility of the system whose behavior we investigate in this section.

In Problem 6.2.1, we have assumed that quantity (6.99) serves as a correlation function. The derivative $\frac{\partial \langle \sigma_{\mathbf{R}} \rangle_{CE}}{\partial h_{\mathbf{R}'}}$ is, in fact, the response of the system to the change of the external field parameter.

Let us return to the case of the ferromagnetic Ising model with the magnetic field h which is nonuniform over the lattice. The equilibrium magnetization is defined as

$$m_0 \equiv \frac{1}{N}\sum_{i=1}^{N} \langle \sigma_i \rangle_{CE}. \tag{6.118}$$

Varying this magnetization with respect to the magnetic field, we find

$$\delta m_0 = \frac{1}{N}\sum_{i=1}^{N} \delta \langle \sigma_i \rangle_{CE} = \frac{1}{N}\sum_{i=1}^{N}\sum_{j=1}^{N} \frac{\partial \langle \sigma_i \rangle_{CE}}{\partial h_j} \delta h_j. \tag{6.119}$$

For the uniform magnetic field, all variations δh_j equal the change of the uniform field, $\delta h_j = \delta h$:

$$\delta m_0 = \frac{\delta h}{N}\sum_{i=1}^{N}\sum_{j=1}^{N} \frac{\partial \langle \sigma_i \rangle_{CE}}{\partial h_j}. \tag{6.120}$$

The magnetic susceptibility of a magnetic system is defined by

$$\chi \equiv \frac{\partial m_0}{\partial h}. \tag{6.121}$$

In other words, it is the response of the equilibrium order parameter m_0 to the change of the field parameter h. From (6.120), we see that the susceptibility of the Ising model is determined as the quantity $\frac{\partial \langle \sigma_{\mathbf{R}} \rangle_{CE}}{\partial h_{\mathbf{R}'}}$ averaged over the lattice:

$$\chi = \frac{1}{N} \sum_{i=1}^{N} \sum_{j=1}^{N} \frac{\partial \langle \sigma_i \rangle_{CE}}{\partial h_j}. \tag{6.122}$$

Recalling that in (6.99), we assumed that the derivative $\frac{\partial \langle \sigma_{\mathbf{R}} \rangle_{CE}}{\partial h_{\mathbf{R}'}}$ serves as a correlation function, we find the relationship between the correlations in the system and the system's response to the external disturbance:

$$\chi \propto \frac{1}{N} \sum_{i=1}^{N} \sum_{j=1}^{N} g(\mathbf{R}_{i,j}). \tag{6.123}$$

Since we now consider a uniform field, due to the symmetry on the lattice, the correlation function $g(\mathbf{R}_{i,j})$ depends only on the distance between two sites but not on the explicit locations of these sites. Therefore, one of the sums and the multiplier $1/N$ cancel each other out:

$$\chi \propto \sum_{j=1}^{N} g(\mathbf{R}_{0,j}) = \sum_{\mathbf{R}} g(\mathbf{R}) = \frac{\breve{g}(\mathbf{k}=0)}{a^d}. \tag{6.124}$$

We have found that the susceptibility is proportional to the integral of the correlation function over the lattice. This statement is called *the fluctuation–dissipation theorem* serving as a connection between the system's correlations and system's responses.

The quantity $\frac{\partial \langle \sigma_{\mathbf{R}} \rangle_{CE}}{\partial h_{\mathbf{R}'}}$ is often called not the correlation function but the local susceptibility as the system's response at site $\mathbf{R}$ to the external disturbance at site $\mathbf{R}'$. In this case, the fluctuation–dissipation theorem transforms from the integral form (6.124) into the local form

$$\chi_{\mathbf{R},\mathbf{R}'} = g(\mathbf{R}' - \mathbf{R}), \tag{6.125}$$

while the integral over the lattice connects now the local and the integral susceptibilities:

$$\chi \propto \sum_{j=1}^{N} \chi_{\mathbf{R}_0,\mathbf{R}_j} = \sum_{\mathbf{R}} \chi_{\mathbf{R}_0,\mathbf{R}}. \tag{6.126}$$

Earlier, we obtained an analogue of (6.125) when the correlation function (6.42) was equal to the response of the system to the external disturbance.

Since in (6.99) we only assumed that the quantity $\frac{\partial \langle \sigma_{\mathbf{R}} \rangle_{CE}}{\partial h_{\mathbf{R}'}}$ plays the role of the correlation function but did not prove this statement rigorously, we now verify directly the applicability of the fluctuation–dissipation theorem to the Ising model. We consider arbitrary pair (bi-spin) interactions (6.34). The partition function of the CE is

$$Z^{CE} \equiv \sum_{\{\sigma\}} e^{-\beta \mathrm{H}_{\{\sigma\}}} \equiv \sum_{\sigma_1=\pm 1} \dots \sum_{\sigma_N=\pm 1} e^{-\beta \mathrm{H}_{\{\sigma\}}}, \tag{6.127}$$

where we go through all microstates by considering all possible microconfigurations $\{\sigma\}$ of spin orientations on the lattice.

Let us differentiate the partition function with respect to the magnetic field:

$$\frac{\partial Z^{CE}}{\partial h} = \sum_{\{\sigma\}} \beta \mu N m_{\{\sigma\}} e^{-\beta \mathrm{H}_{\{\sigma\}}}. \tag{6.128}$$

Here, we have the sum of quantities $m_{\{\sigma\}} e^{-\beta \mathrm{H}_{\{\sigma\}}}$ over all microstates $\{\sigma\}$. If we transformed the exponential functions $e^{-\beta \mathrm{H}_{\{\sigma\}}}$ into Gibbs probabilities $w_{\{\sigma\}}^{CE} = \frac{1}{Z^{CE}} e^{-\beta \mathrm{H}_{\{\sigma\}}}$ of microstates, the sum over microstates would transform into the averaging of $m_{\{\sigma\}}$ in the CE:

$$\frac{\partial Z^{CE}}{\partial h} = Z^{CE} \beta \mu \sum_{\{\sigma\}} N m_{\{\sigma\}} w_{\{\sigma\}}^{CE} \equiv Z^{CE} \beta \mu \langle Nm \rangle_{CE} \quad \text{or} \tag{6.129}$$

$$\langle Nm \rangle_{CE} = \frac{1}{\beta \mu} \frac{\partial \ln Z^{CE}}{\partial h}. \tag{6.130}$$

Differentiating for the second time, we find

$$\frac{\partial^2 Z^{CE}}{\partial h^2} = \sum_{\{\sigma\}} \left(\beta \mu N m_{\{\sigma\}} \right)^2 e^{-\beta \mathrm{H}_{\{\sigma\}}} = Z^{CE} (\beta \mu)^2 \left\langle (Nm)^2 \right\rangle_{CE} \quad \text{or} \tag{6.131}$$

$$\left\langle (Nm)^2 \right\rangle_{CE} = \frac{1}{Z^{CE} (\beta \mu)^2} \frac{\partial^2 Z^{CE}}{\partial h^2}. \tag{6.132}$$

The susceptibility is defined as the response of the averaged order parameter (6.130) to the change of the external field:

$$\chi \equiv \frac{1}{N} \frac{\partial \langle Nm \rangle_{CE}}{\partial h} = \frac{1}{N \beta \mu} \frac{\partial^2 \ln Z^{CE}}{\partial h^2}. \tag{6.133}$$

"Moving" the logarithm in (6.133) to the left through two derivatives and utilizing (6.129–6.132), we find that the susceptibility is proportional to the variance of the order parameter in the CE:

$$\chi = \frac{1}{N\beta\mu}\left(\frac{1}{Z^{CE}}\frac{\partial^2 Z^{CE}}{\partial h^2} - \left(\frac{1}{Z^{CE}}\frac{\partial Z^{CE}}{\partial h}\right)^2\right) = \frac{\beta\mu}{N}\left(\left\langle (Nm)^2\right\rangle_{CE} - \left\langle Nm\right\rangle_{CE}{}^2\right) \quad (6.134)$$

$$= \frac{\beta\mu}{N}\left\langle \left(Nm - \left\langle Nm\right\rangle_{CE}\right)^2\right\rangle_{CE}.$$

The coefficient of proportionality $\beta\mu / N$ is not singular at the region of the phase transition at nonzero temperature and, therefore, does not influence the singular behavior of the right-hand side.

Next, we substitute the definition of the magnetization:

$$m_{\{\sigma\}} \equiv \frac{1}{N}\sum_{i=1}^{N}\sigma_i, \quad (6.135)$$

into the right-hand side of (6.134):

$$\chi = \frac{\beta\mu}{N}\left(\left\langle\left(\sum_{i=1}^{N}\sigma_i\right)\left(\sum_{j=1}^{N}\sigma_j\right)\right\rangle_{CE} - \left\langle\sum_{i=1}^{N}\sigma_i\right\rangle_{CE}\left\langle\sum_{j=1}^{N}\sigma_j\right\rangle_{CE}\right)$$

$$= \frac{\beta\mu}{N}\sum_{i=1}^{N}\sum_{j=1}^{N}\left(\left\langle\sigma_i\sigma_j\right\rangle_{CE} - \left\langle\sigma_i\right\rangle_{CE}\left\langle\sigma_j\right\rangle_{CE}\right). \quad (6.136)$$

Under the signs of the sums, we see here the definition (6.3) of the correlation function:

$$\chi = \frac{\beta\mu}{N}\sum_{i=1}^{N}\sum_{j=1}^{N} g(\mathbf{R}_{i,j}). \quad (6.137)$$

Again, due to the fact that the correlation function for the uniform magnetic field depends only on the distance between two sites but not on the numbers of the sites themselves, we substitute one of the sums by N to prove the fluctuation–dissipation theorem:

$$\chi = \beta\mu\sum_{\mathbf{R}} g(\mathbf{R}) = \beta\mu\,\frac{\breve{g}(\mathbf{k}=0)}{a^d}. \quad (6.138)$$

In comparison with (6.124), we see here the additional multiplier $\beta\mu$ which is again not singular in the region of phase transitions at nonzero temperature. Therefore, our assumption (6.99) was valid with the accuracy of unimportant coefficient of proportionality.

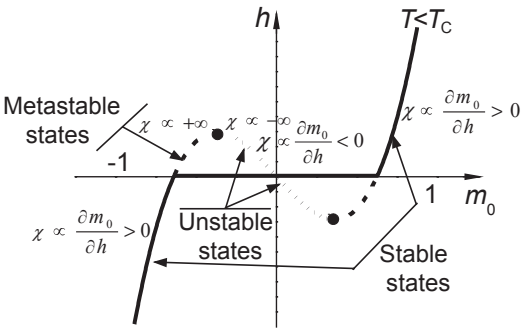

Fig. 6.2 The sign of the magnetic susceptibility distinguishes stable and metastable states from unstable states

We see now that the susceptibility (6.133) is a very interesting quantity. Firstly, by definition, it is the response of the averaged order parameter to the change in the field parameter. Secondly, it represents the variance of the order parameter in the ensemble. Thirdly, it equals the integral of the correlation function.

More importantly, since the susceptibility is proportional to variance (6.134) of the order parameter in the ensemble, it is always positive (or zero):

$$\chi \propto \left\langle \left(Nm - \langle Nm \rangle_{CE} \right)^2 \right\rangle_{CE} \geq 0. \tag{6.139}$$

As we have seen in Chap. 3, at the spinodal point, the susceptibility becomes infinite. More rigorously, the susceptibility changes from $+\infty$ to $-\infty$ when we pass across the spinodal point (Fig. 6.2). Therefore, negative values of the susceptibility correspond to the branch of unstable states.

Comparing (6.133) and (6.139), we see that the positivity of the susceptibility in the stable or metastable state requires that the second derivative of the logarithm of the ensemble partition function with respect to the magnetic field also remains positive:

$$\frac{\partial^2 \ln Z^{CE}}{\partial h^2} > 0. \tag{6.140}$$

From Chap. 2, we recall that the negative logarithm of the ensemble partition function is the ensemble action of the free energy:

$$\mathrm{A}^{CE} \equiv -\ln Z^{CE}. \tag{6.141}$$

Hence, inequality (6.140) transforms into the requirement that the second derivative of the action of the free energy with respect to the magnetic field is always negative along the stable and metastable parts of the equation of state:

$$\frac{\partial^2 \mathrm{A}^{CE}}{\partial h^2} < 0. \tag{6.142}$$

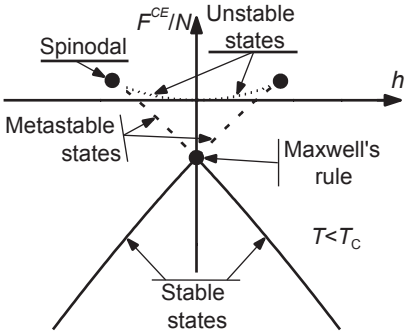

Fig. 6.3 The equilibrium free energy

Since the free energy potential differs from its action only by the temperature as a multiplier:

$$F^{CE} \equiv T\mathrm{A}^{CE} \equiv -T \ln Z^{CE}, \tag{6.143}$$

and since this multiplier is not singular at the critical or spinodal point, inequality (6.142) is valid for the free energy itself as well:

$$\frac{\partial^2 F^{CE}}{\partial h^2} < 0. \tag{6.144}$$

This clearly can be seen from the dependence of the equilibrium free energy on the magnetic field (Fig. 6.3) when the second derivative of this dependence is positive in stable and metastable states and is negative in unstable states.

Earlier, we assumed that in the vicinity of the critical point, the correlation function decays as

$$g(R) \propto \frac{1}{R^{d-2+\eta^{\mathrm{C}}}} \text{ for } R << \xi \tag{6.145}$$

while for $R >> \xi$ the decay is exponential. Since exponential decay is very "fast," we can assume that the integral of the correlation function in the fluctuation–dissipation theorem (6.138) can be approximated by the integration only over the distances of the order of the correlation length:

$$\chi \propto \sum_{|\mathbf{R}|<\xi} g(\mathbf{R}) \propto \int_{-\xi}^{+\xi} g(\mathbf{R}) d^d \mathbf{R} \propto \int_0^{\xi} g(R) R^{d-1} dR. \tag{6.146}$$

Substituting (6.145) into (6.146) and integrating, we find

$$\chi \propto \xi^{2-\eta^{\mathrm{C}}} + \ldots \tag{6.147}$$

But in the vicinity of the critical point, both the susceptibility and correlation length diverge. Along the isofield curve $h = 0$, these divergences are

$$\chi \propto \frac{1}{|t|^{\gamma_t^{\mathrm{C}}}}, \tag{6.148}$$

$$\xi \propto \frac{1}{|t|^{\nu_t^{\mathrm{C}}}}, \tag{6.149}$$

while along the critical isotherm

$$\chi \propto \frac{1}{|h|^{\gamma_h^{\mathrm{C}}}}, \tag{6.150}$$

$$\xi \propto \frac{1}{|h|^{\nu_h^{\mathrm{C}}}} \tag{6.151}$$

Substituting these divergences into (6.147), we find the relations among the critical indices:

$$\gamma_t^{\mathrm{C}} = (2-\eta^{\mathrm{C}})\nu_t^{\mathrm{C}}, \tag{6.152}$$

$$\gamma_h^{\mathrm{C}} = (2-\eta^{\mathrm{C}})\nu_h^{\mathrm{C}} \tag{6.153}$$

Earlier, we have obtained that the mean-field approach provides $\gamma_t^{\mathrm{C}} = 1$, $\gamma_h^{\mathrm{C}} = 2/3$, $\eta^{\mathrm{C}} = 0$, $\nu_t^{\mathrm{C}} = 1/2$, and $\nu_h^{\mathrm{C}} = 1/3$. Obviously, these values satisfy (6.152–6.153).

Relations (6.152 and 6.153), which for our particular system happen to be equalities, are a particular case of *the Fisher inequality* (Fisher 1969):

$$\gamma \le (2-\eta)\nu, \tag{6.154}$$

which is expected to be valid for an arbitrary magnetic system in the vicinity of its critical point.

In (6.145), we have defined the critical index η^{C} of the correlation function for the vicinity of the critical point. In a similar manner, for the proximity of the spinodal point, we define the spinodal index η^{S} of the correlation function by:

$$g(R) \propto \frac{1}{R^{d-2+\eta^S}} \text{ for } R << \xi. \tag{6.155}$$

Analysis, identical to the considered above, provides similar relations for the spinodal indices as well:

$$\gamma_t^{\mathrm{S}} = (2-\eta^{\mathrm{S}})\nu_t^{\mathrm{S}}, \tag{6.156}$$

$$\gamma_h^{\mathrm{S}} = (2-\eta^{\mathrm{S}})\nu_h^{\mathrm{S}}. \tag{6.157}$$

Therefore, the Fisher inequality again transforms into the equality for the spinodal indices.

For the Ising model, the mean-field approach provided zero values for both critical and spinodal indices of the correlation function: $\eta^{\mathrm{C}} = 0$ and $\eta^{\mathrm{S}} = 0$. Thereby, the indices of the susceptibility are just twice the indices of the correlation length. The reader can notice that the solution (3.115) we obtained for the susceptibility is proportional to the squared expression (6.105) of the correlation length:

$$\chi \propto \xi^2 \text{ if } \eta = 0. \tag{6.158}$$

Therefore, in Sect. 6.2 we could avoid investigating the scaling behavior of the correlation length saying that it is just the square root of the susceptibility. However, we did not do that for the sake of systems whose indices of the correlation function were not zero.

6.4 Magnetic Systems: The Ginzburg Criterion

In Chap. 3, we applied the mean-field approach to find the approximate solution of the Ising model. But, we have not yet developed a criterion when this approximation is applicable because this criterion would require the knowledge of the behavior of correlations in the system. Now, we turn our attention to this question.

We consider the ferromagnetic Ising model in the proximity of its critical point when we approach the critical point from below ($t < 0$) along the binodal curve ($h = h_{\mathrm{C}} = 0$). In Chap. 3, we demonstrated that the mean-field approach is equivalent to the case when we can neglect correlations (3.183–3.185) in comparison with the order parameter:

$$\left\langle \left(\sigma_{\mathbf{R}} - \langle \sigma_{\mathbf{R}} \rangle_{CE}\right)\left(\sigma_{\mathbf{R}'} - \langle \sigma_{\mathbf{R}'} \rangle_{CE}\right) \right\rangle_{CE} << \langle \sigma_{\mathbf{R}} \rangle_{CE}^2 . \tag{6.159}$$

This inequality is called *the Ginzburg criterion* (Ginzburg 1960).

To estimate the left-hand side of this inequality, we should estimate the value of the correlation function g. Since the correlation length is the characteristic length of the decay of correlations, we can estimate the correlation function as being of the order of g within the volume ξ^d and zero outside of this volume. For the susceptibility, this estimation provides

$$\chi \propto \int_{-\infty}^{+\infty} g(\mathbf{R}) d^d \mathbf{R} \propto g\xi^d. \tag{6.160}$$

Expressing g from this equation, we obtain

$$\left\langle \left(\sigma_{\mathbf{R}} - \langle \sigma_{\mathbf{R}} \rangle_{CE}\right)\left(\sigma_{\mathbf{R}'} - \langle \sigma_{\mathbf{R}'} \rangle_{CE}\right)\right\rangle_{CE} \propto g \propto \frac{\chi}{\xi^d}. \tag{6.161}$$

Both the susceptibility and the correlation length diverge when we approach the critical point along the binodal curve. Substituting the critical indices of these divergences into (6.161), we find

$$\left\langle \left(\sigma_{\mathbf{R}} - \langle \sigma_{\mathbf{R}} \rangle_{CE}\right)\left(\sigma_{\mathbf{R}'} - \langle \sigma_{\mathbf{R}'} \rangle_{CE}\right)\right\rangle_{CE} \propto |t|^{d\nu_t^{\mathrm{C}} - \gamma_t^{\mathrm{C}}}. \tag{6.162}$$

Next, we should estimate the right-hand side of criterion (6.159). This is also easy since along the binodal curve the spontaneous magnetization has its own critical index:

$$\langle \sigma_{\mathbf{R}} \rangle_{CE} \propto |t|^{\beta_t^{\mathrm{C}}}. \tag{6.163}$$

Substituting (6.162) and (6.163) into (6.159), we see that the Ginzburg criterion transforms into

$$|t|^{d\nu_t^{\mathrm{C}} - 2\beta_t^{\mathrm{C}} - \gamma_t^{\mathrm{C}}} << 1. \tag{6.164}$$

Applying a similar logic for the case when we approach the critical point not along the binodal curve but along the critical isotherm $t = 0$, we find

$$\left\langle \left(\sigma_{\mathbf{R}} - \langle \sigma_{\mathbf{R}} \rangle_{CE}\right)\left(\sigma_{\mathbf{R}'} - \langle \sigma_{\mathbf{R}'} \rangle_{CE}\right)\right\rangle_{CE} \propto |h|^{d\nu_h^{\mathrm{C}} - \gamma_h^{\mathrm{C}}}, \tag{6.165}$$

$$\langle \sigma_{\mathbf{R}} \rangle_{CE} \propto |h|^{\beta_h^{\mathrm{C}}}, \text{ and} \tag{6.166}$$

$$|h|^{d\nu_h^{\mathrm{C}} - 2\beta_h^{\mathrm{C}} - \gamma_h^{\mathrm{C}}} << 1. \tag{6.167}$$

For the mean-field approach, we have $\gamma_t^{\mathrm{C}} = 1$, $\gamma_h^{\mathrm{C}} = 2/3$, $\nu_t^{\mathrm{C}} = 1/2$, $\nu_h^{\mathrm{C}} = 1/3$, $\beta_t^{\mathrm{C}} = 1/2$, and $\beta_h^{\mathrm{C}} = 1/3$. Substituting these values into (6.164) and (6.167), we obtain

$$|t|^{\frac{d-4}{2}} << 1, \tag{6.168}$$

$$|h|^{\frac{d-4}{3}} << 1. \tag{6.169}$$

When $t \to 0$ and $h \to 0$, these inequalities require that $d > 4$. Therefore, if the dimensionality of our system is higher than four, the mean-field approach is valid in the close proximity of the critical point, providing the exact values of the critical indices (but only the approximation of the critical temperature).

However, we are living in the three-dimensional space; and dimensions $d < 4$ are of more interest to us. But for $d < 4$, inequalities (6.168 and 6.169) show that the mean-field approach is no longer valid in the very proximity of the critical point.

What does this mean? Our purpose is to study the critical indices of a system. But far from the critical point, the behavior of the system is determined by the laws specific for this particular system. The universal power-law dependencies appear only in the close proximity of the critical point. But the close proximity of the critical point is the very region where the mean-field approach does not work for $d < 4$! Therefore, although the mean-field approximation is always very illustrative, it is of little help to us in the most interesting three-dimensional or two-dimensional cases. To study models in these dimensions, we should invent new approaches.

Dimension $d^{\mathrm{UC}} = 4$ is called *the upper critical dimension* of the ferromagnetic Ising model. In dimensions higher than $d^{\mathrm{UC}} = 4$, the mean-field approach works in the vicinity of the critical point and provides the exact values of the critical indices. In dimensions lower than $d^{\mathrm{UC}} = 4$, the mean-field approach is no longer valid in the close proximity of the critical point. Therefore, the critical indices, predicted by this approach, do not correspond (and are not even close!) to the real values measured experimentally or found analytically (for example, mean-field $\beta_t^{\mathrm{C}} = 1/2$ versus exact $\beta_t^{\mathrm{C}} = 1/8$ for the two-dimensional n.n. Ising model and numerical $\beta_t^{\mathrm{C}} = 0.325$ for the three-dimensional n.n. Ising model).

Let us now consider the case $d < 4$. Criterion (6.159) is no longer valid. Instead, the correlations become comparable with the order parameter:

$$\left\langle \left(\sigma_{\mathbf{R}} - \langle \sigma_{\mathbf{R}} \rangle_{CE}\right)\left(\sigma_{\mathbf{R}'} - \langle \sigma_{\mathbf{R}'} \rangle_{CE}\right)\right\rangle_{CE} \propto \langle \sigma_{\mathbf{R}} \rangle_{CE}^2 . \tag{6.170}$$

This leads to the following relations for the critical indices:

$$d\nu_t^{\mathrm{C}} = 2\beta_t^{\mathrm{C}} + \gamma_t^{\mathrm{C}}, \tag{6.171}$$

$$d\nu_h^{\mathrm{C}} = 2\beta_h^{\mathrm{C}} + \gamma_h^{\mathrm{C}}. \tag{6.172}$$

These relations are called *the hyperscaling relations* because they "glue" together two different scales. At scales less than the correlation length, the behavior of the system is determined by correlations (6.162, 6.165)—fractal behavior of small-phase clusters. At larger scales, we see the scaling (6.163, 6.166) of the order parameter, determined for the whole system—large-phase cluster of the size of the

system. Joining these two different types of behavior at the scale of the correlation length provides the hyperscaling relations.

For $d > 4$, inequality (6.159) is valid no matter how close the critical point is. Therefore, in these dimensions, the correlations never become comparable with the order parameter, and the hyperscaling (6.171 and 6.172) is not valid.

This can be explained from another point of view. The mean-field approach is dimensionless; so far, we have never seen the mean-field approach being directly influenced by the dimensionality of the system. Therefore, while the mean-field approach determines the critical indices for $d > 4$, the dimensionality of the system cannot be part of the relations among the critical indices. Only when the mean-field approach stops to work for $d < 4$, the hyperscaling relations become valid, and the dimensionality of the system begins to influence the critical indices.

Earlier, when in Sect. 3.4, we discussed the absence of phase transitions at non-zero temperatures in the one-dimensional system with short-range interactions, we saw two ways to improve the situation: To increase the dimensionality of the system or to increase the range of interactions. So far, we have investigated only the influence of the dimensionality of the system on the applicability of the mean-field approach. Let us next turn our attention to the second aspect—the range of pair interactions.

The range of interactions is represented by the root-mean-square radius (6.65) of pair (bi-spin) interactions. When we substituted (6.161) into criterion (6.159), we did not take into account that the correlation function (6.73) is proportional to $1/\Delta^2$. Modifying (6.164) and (6.167), we find

$$|t|^{d\nu_t^{\mathrm{C}} - 2\beta_t^{\mathrm{C}} - \gamma_t^{\mathrm{C}}} << \Delta^2, \tag{6.173}$$

$$|h|^{d\nu_h^{\mathrm{C}} - 2\beta_h^{\mathrm{C}} - \gamma_h^{\mathrm{C}}} << \Delta^2. \tag{6.174}$$

The higher Δ, the stronger these inequalities. In other words, the longer the interactions in the system, the better the system is described by the mean-field approach.

For simplicity, let us consider again the ferromagnetic Ising model of dimension $d < 4$. Substituting the mean-field exponents $\gamma_t^{\mathrm{C}} = 1$, $\gamma_h^{\mathrm{C}} = 2/3$, $\nu_t^{\mathrm{C}} = 1/2$, $\nu_h^{\mathrm{C}} = 1/3$, $\beta_t^{\mathrm{C}} = 1/2$, and $\beta_h^{\mathrm{C}} = 1/3$ into (6.173) and (6.174), we find that the mean-field approach is still valid even for $d < 4$ when

$$|t|^{\frac{d-4}{2}} << \Delta^2, \tag{6.175}$$

$$|h|^{\frac{d-4}{3}} << \Delta^2. \tag{6.176}$$

Since we consider $d < 4$, it is more convenient to rewrite these inequalities as

$$|t| >> \frac{1}{\Delta^{\frac{4}{4-d}}}, \tag{6.177}$$

$$| h |>> \frac{1}{\Delta^{\frac{6}{4-d}}}. \tag{6.178}$$

The nearest vicinity of the critical point

$$| t |\leq \frac{1}{\Delta^{\frac{4}{4-d}}}, \tag{6.179}$$

$$| h |\leq \frac{1}{\Delta^{\frac{6}{4-d}}} \tag{6.180}$$

is called *the critical region*. So, we have proved that the mean-field approach is applicable even for $d < 4$ outside of the critical region. However, within the critical region, it is replaced by the hyperscaling relations (6.171 and 6.172).

There are systems (like the three-dimensional weak-coupling superconductors) when the critical region is very narrow (of the order of $|t| \leq 10^{-16}$) and is not observable experimentally. In these cases, even in low dimensions, the observed behavior is described by the mean-field critical indices.

For the particular case $d = 3$, the size of the critical region depends strongly on the range of interactions:

$$| t |\leq \frac{1}{\Delta^4}, \tag{6.181}$$

$$| h |\leq \frac{1}{\Delta^6}. \tag{6.182}$$

So, when the interactions are long-ranged, the critical region can be very narrow leaving almost all proximity of the critical point to the zone of the mean-field description. As we already know from Chap. 3, Problem 3.7.4, in the limit of infinite interaction range, the mean-field solution is exact for an arbitrary dimensionality of the system.

Another important result to observe from (6.179) and (6.180) is that the lower the dimensionality of the system, the weaker the dependence of the size of the critical region on the range of interactions. So, by lowering the dimensionality, we increase the size of the critical region, pushing the zone of the mean-field validity away from the critical point.

The reasoning (6.159–6.169) we discussed for the critical point will not work in the proximity of the spinodal point. Indeed, while the divergencies of the susceptibility and correlation length are with respect to the deviations of the field parameters from their spinodal values, $|t\text{-}t_S|$ and $|h\text{-}h_S|$, the appearance of the order parameter (6.163) should still be attributed to the critical point.

6.5 Magnetic Systems: Heat Capacity as Susceptibility

The heat capacity is somewhat similar to the magnetic susceptibility. Firstly, it is the response of the energy of the system, which is a fluctuating parameter, to the change of the temperature as a field parameter:

$$C \equiv \left(\frac{\partial E}{\partial T} \right)_h . \tag{6.183}$$

Secondly, the heat capacity is directly connected with the energy fluctuations in the system. To see that we consider the partition function of an arbitrary thermal system:

$$Z^{CE} \equiv \sum_{\{E\}} e^{-\beta \mathrm{H}_{\{E\}}} . \tag{6.184}$$

Differentiating the partition function with respect to $(-\beta) \equiv -\frac{1}{T}$, we find

$$\frac{\partial Z^{CE}}{\partial(-\beta)} = \sum_{\{E\}} \mathrm{H}_{\{E\}} e^{-\beta \mathrm{H}_{\{E\}}} = Z^{CE} \sum_{\{E\}} \mathrm{H}_{\{E\}} w_{\{E\}}^{CE} = Z^{CE} \left\langle E \right\rangle_{CE} \text{ or} \tag{6.185}$$

$$\left\langle E \right\rangle_{CE} = \frac{\partial \ln Z^{CE}}{\partial(-\beta)} . \tag{6.186}$$

Differentiation for the second time with respect to $(-\beta)$ provides

$$\frac{\partial^2 Z^{CE}}{\partial(-\beta)^2} = \sum_{\{E\}} (\mathrm{H}_{\{E\}})^2 e^{-\beta \mathrm{H}_{\{E\}}} = Z^{CE} \sum_{\{E\}} (\mathrm{H}_{\{E\}})^2 w_{\{E\}}^{CE} = Z^{CE} \left\langle E^2 \right\rangle_{CE} \text{ or} \tag{6.187}$$

$$\left\langle E^2 \right\rangle_{CE} = \frac{1}{Z^{CE}} \frac{\partial^2 Z^{CE}}{\partial(-\beta)^2} . \tag{6.188}$$

The formulae here are very similar to (6.128–6.132). To obtain the variance of the energy, we should be looking for the second derivative of the logarithm of the partition function:

$$\frac{\partial^2 \ln Z^{CE}}{\partial(-\beta)^2} = \frac{1}{Z^{CE}} \frac{\partial^2 Z^{CE}}{\partial(-\beta)^2} - \left(\frac{1}{Z^{CE}} \frac{\partial Z^{CE}}{\partial(-\beta)} \right)^2 = \left\langle E^2 \right\rangle_{CE} - \left\langle E \right\rangle_{CE}^{\ 2} = \left\langle \left(E - \left\langle E \right\rangle_{CE} \right)^2 \right\rangle_{CE} . \tag{6.189}$$

Now, when we have the variance of the energy at the right-hand side, we should transform the left-hand side into the response of some fluctuating parameter to the change of the field parameter $(-\beta)$:

$$\frac{\partial^2 \ln Z^{CE}}{\partial(-\beta)^2} = \frac{\partial}{\partial(-\beta)} \frac{\partial \ln Z^{CE}}{\partial(-\beta)} = \frac{\partial \langle E \rangle_{CE}}{\partial(-\beta)}, \tag{6.190}$$

where in the last equality we have utilized (6.186). We see that the fluctuating parameter, which we have been looking for, is the energy of the system.

What is the physical meaning of quantity (6.190)? Substituting $\beta \equiv 1/T$ explicitly, we find

$$\frac{\partial^2 \ln Z^{CE}}{\partial(-\beta)^2} = T^2 \frac{\partial}{\partial T} T^2 \frac{\partial}{\partial T} \ln Z^{CE} = T^2 \left(T \frac{\partial^2 T \ln Z^{CE}}{\partial T^2} \right) = -T^2 \left(T \frac{\partial^2 F^{CE}}{\partial T^2} \right) = T^2 C. \tag{6.191}$$

So, the parameter, we have been looking for, is proportional to the heat capacity C with the coefficient of proportionality T^2 which is not singular at the critical point. Therefore, this is the heat capacity that plays the role of the response function (6.190) and variance (6.189).

We should add here that since variance (6.189) is expected to be always positive (or zero), we expect the heat capacity to be positive (or zero) also:

$$C \propto \left\langle \left(E - \langle E \rangle_{CE} \right)^2 \right\rangle_{CE} \geq 0. \tag{6.192}$$

When this inequality is not valid, the considered state of a system cannot be stable or metastable. Therefore, as we saw in Chap. 3, the positivity of the heat capacity can serve as a criterion distinguishing stable and metastable states from unstable states (Fig. 6.4).

Comparing (6.192) with (6.191), we see that when we consider stable or metastable states, the positivity of the heat capacity determines the sign of the following second derivatives:

$$\frac{\partial^2 \ln Z^{CE}}{\partial(-\beta)^2} \geq 0, \tag{6.193}$$

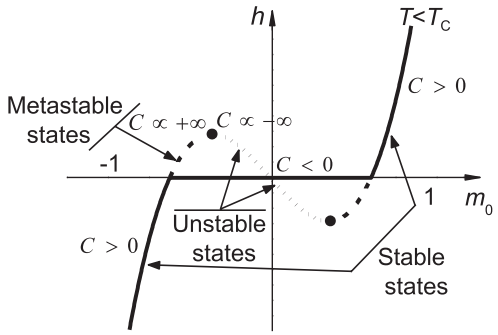

Fig. 6.4 The sign of the heat capacity distinguishes stable and metastable states from unstable states

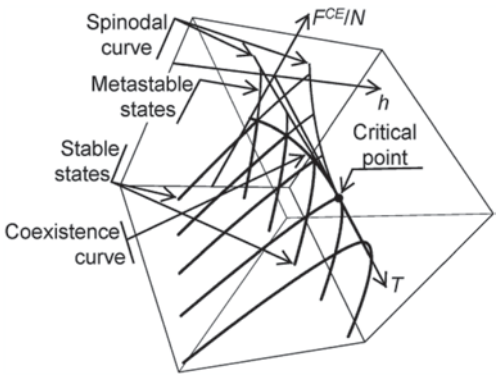

Fig. 6.5 The equilibrium free energy

$$\frac{\partial^2 \mathrm{A}^{CE}}{\partial(-\beta)^2} \leq 0, \tag{6.194}$$

$$\frac{\partial^2 F^{CE}}{\partial(-\beta)^2} \leq 0. \tag{6.195}$$

This can easily be observed from the dependence presented in Fig. 6.5.

Summarizing, we have proved that heat capacity is the response of the energy of the system (as a fluctuating parameter) to the change of the field parameter $(-\beta)$. Also, it is the variance of energy fluctuations. What we have not proved is that the heat capacity obeys some kind of a fluctuation–dissipation theorem.

If we proved that, we would be able to refer to the heat capacity as to *the heat susceptibility*. But can we expect that the heat capacity will also obey the fluctuation–dissipation theorem?

So far, we have considered the heat capacity of an arbitrary thermal system. There is a huge variety of different systems, with strong correlations and without correlations. Therefore, from an arbitrary system it is difficult to expect that the integral of its correlations would correspond to the heat capacity.

Correlations can be absent in a system at all. The reader should recall here the two-level Ising model from Sect. 3.3 when all spins were independent one from another, meaning that there are no correlations in the system. However, the heat capacity of such a system was nonzero. Therefore, considering an arbitrary thermal system, we cannot expect the fluctuation–dissipation theorem to be valid for the heat capacity of this system.

Does this mean that the heat capacity cannot be considered as a susceptibility of the system?

To answer this question, let us summarize the criteria by which we define the quantity to be a susceptibility:

1. The susceptibility must be the response of some fluctuating parameter ϕ to the change in some field parameter π:

$$\chi_{\phi,\pi} = \frac{\partial \langle \phi \rangle_{CE}}{\partial \pi}. \tag{6.196}$$

There are two field parameters in the CE of a magnetic system: the magnetic field h and the temperature T (or the inverse temperature β). For the magnetic susceptibility, the fluctuating parameter was the magnetization while for the heat capacity, the fluctuating parameter was the energy of the system. Therefore, both quantities correspond to this requirement.

2. The susceptibility must be equal to the variance of the fluctuating parameter ϕ:

$$\chi_{\phi,\pi} = \left\langle \left(\phi - \langle \phi \rangle_{CE} \right)^2 \right\rangle_{CE}. \tag{6.197}$$

At first glance, this requirement makes it more difficult to choose the appropriate quantity. However, this is not generally true. For both the magnetic susceptibility and heat capacity above, we were looking at the second derivative of the logarithm of the partition function with respect to the field parameter:

$$\chi_{\phi,\pi} = \frac{\partial^2 \ln Z^{CE}}{\partial \pi^2}. \tag{6.198}$$

We did that because the exponential functions in the partition function contained the product of the field parameter and the fluctuating parameter:

$$Z^{CE} = \sum_{\{\}} e^{const \cdot \pi\phi + f(\phi)}. \tag{6.199}$$

Therefore, if we see that the exponential function in the partition function contains linear product of a field parameter π and some expression, we choose this expression to be the fluctuating parameter:

$$Z^{CE} = \sum_{\{\}} e^{\pi f_1 + f_2} \Rightarrow \phi \equiv f_1. \tag{6.200}$$

This guarantees that the susceptibility, defined as (6.196), equals the variance of the so-chosen fluctuating parameter.

So, for the Ising model the Hamiltonian contains the term μhNm which is linear in the magnetic field h. Therefore, we have chosen μNm to be the fluctuating parameter.

In the case of the CE of an arbitrary thermal system, the partition function is defined as the sum of the exponential functions of $-\beta E$. We see that this expression is linearly proportional to the field parameter $(-\beta)$. So, we have chosen the energy of

the system to represent the fluctuating parameter. This automatically provided that the heat capacity equaled the variance of energy fluctuations.

3. The last requirement is that the susceptibility must obey the fluctuation–dissipation theorem.

We have proved this statement for the magnetic susceptibility, but we were not able to prove it for the heat capacity in the case of an arbitrary thermal system. Does this mean that the heat capacity cannot be considered as a susceptibility?

In fact, we were just one step away from a possible answer. Let us recall how we have managed to prove the fluctuation–dissipation theorem for the magnetic susceptibility. We substituted magnetization (6.135) as the sum over the spins into the variance (6.134) of the magnetization and immediately obtained the required result!

Why cannot we do the same for the heat capacity? Because in the case of an arbitrary thermal system with arbitrary interactions among the system's degrees of freedom, the Hamiltonian is no longer additive. And, we cannot split the energy into the sum over the degrees of freedom.

However, what is not possible in the general case can be quite possible for a particular system. Let us consider, for example, the ferromagnetic n.n. Ising model in the zero magnetic field. The Hamiltonian of the system is

$$\mathrm{H}_{\{\sigma\}} = -J \sum_{<i,j>_{n.n.}} \sigma_i \sigma_j . \tag{6.201}$$

We still cannot split this Hamiltonian into the sum of the energies of separate spins because of the pair (bi-spin) interactions. However, we can introduce new variables $\varepsilon_{<i,j>_{n.n.}} = -J\sigma_i\sigma_j$, one for each n.n. pair of spins, corresponding to the energy of interactions. In terms of these new variables, the Hamiltonian becomes additive

$$\mathrm{H}_{\{\sigma\}} = \sum_{<i,j>_{n.n.}} \varepsilon_{<i,j>_{n.n.}} . \tag{6.202}$$

Substituting Hamiltonian (6.202) into (6.189), we find

$$\begin{aligned} C \propto \left\langle E^2 \right\rangle_{CE} - \left\langle E \right\rangle_{CE}^{\ 2} &= \left\langle \left(\sum_{<i,j>_{n.n.}} \varepsilon_{<i,j>_{n.n.}} \right) \left(\sum_{<i',j'>_{n.n.}} \varepsilon_{<i',j'>_{n.n.}} \right) \right\rangle_{CE} \\ &\quad - \left\langle \sum_{<i,j>_{n.n.}} \varepsilon_{<i,j>_{n.n.}} \right\rangle_{CE} \left\langle \sum_{<i',j'>_{n.n.}} \varepsilon_{<i',j'>_{n.n.}} \right\rangle_{CE} \\ &= \sum_{<i,j>_{n.n.}} \sum_{<i',j'>_{n.n.}} \left(\left\langle \varepsilon_{<i,j>_{n.n.}} \varepsilon_{<i',j'>_{n.n.}} \right\rangle_{CE} - \left\langle \varepsilon_{<i,j>_{n.n.}} \right\rangle_{CE} \left\langle \varepsilon_{<i',j'>_{n.n.}} \right\rangle_{CE} \right). \end{aligned} \tag{6.203}$$

Due to the lattice symmetry over the choice of the interacting pairs, we can remove one sum, replacing it with the total number of the n.n. pairs $Nq/2$ on the lattice

$$C \propto \frac{Nq}{2} \sum_{<i',j'>_{n.n.}} \left(\left\langle \varepsilon_{<i_0,j_0>_{n.n.}} \varepsilon_{<i',j'>_{n.n.}} \right\rangle_{CE} - \left\langle \varepsilon_{<i_0,j_0>_{n.n.}} \right\rangle_{CE} \left\langle \varepsilon_{<i',j'>_{n.n.}} \right\rangle_{CE} \right), \quad (6.204)$$

where q is the lattice coordination number.

This is the result we have been looking for—the fluctuation–dissipation theorem is valid for the heat capacity of the n.n. Ising model. And, we can now refer to the heat capacity of this particular system as *the heat susceptibility*.

Looking back, we see that all that was required to prove the heat capacity to be the susceptibility was to find some quantities, making the Hamiltonian additive. However, we should always remember that the correlations in that case were correlations among the new variables $\varepsilon_{<i,j>_{n.n.}} = -J\sigma_i\sigma_j$ but not among the initial degrees of freedom of the system. So, for our particular system, the heat capacity was associated with the correlations not among the spins but among the energies of the spin pairs.

In other words, for many systems, the heat capacity can be proved to be the heat susceptibility. However, it no longer equals the integral of correlations among the degrees of freedom of the system. Instead, we should look for some new quantities, in terms of which the Hamiltonian can be made additive. Thereby the heat susceptibility will correspond to the correlations among these new quantities.

6.6 Percolation: The Correlation Length

Next, we consider the fluctuation–dissipation theorem for percolation.

We define *the correlation function* $G(\vec{\mathbf{R}})$ (also known as *a pair connectedness*) as a probability that if it is known that the initial site is occupied (and, thus, belongs to a cluster), then a site at distance $\vec{\mathbf{R}}$ is also occupied and belongs to the same cluster. Since for $\vec{\mathbf{R}} = 0$ the correlation function is always unity, $G(0) = 1$, in contrast to the Ising model the correlation function in the theory of percolation is always normalized and is, therefore, the autocorrelation function (6.2).

The correlation length is defined as a characteristic length of the decay of the correlation function. The percolation problem is unique in the sense that it provides a very illustrative representation of the behavior of clusters in the system.

What does correlation length represent? By definition, it is the characteristic length of the decay of the correlation function. But the correlation function is itself a probability that a site at distance $\vec{\mathbf{R}}$ belongs to the same cluster. Thus, the correlation length represents, crudely speaking, the linear size of clusters.

More rigorously, the correlation length is defined as the root-mean-square distance between two sites belonging to the common cluster:

$$\xi \equiv \sqrt{\frac{\sum_{\mathbf{R}} R^2 G(\mathbf{R})}{\sum_{\mathbf{R}} G(\mathbf{R})}}, \quad (6.205)$$

where the correlation function plays the role of the probability distribution. In fact, averaging (6.205) represents the ensemble averaging of squared distances between sites belonging to the common cluster:

$$\xi(p) \equiv \sqrt{\frac{\left\langle \sum\limits_{<i,j>_{connected}} R_{i,j}^2 \right\rangle_{p-\mathrm{E}}}{\left\langle \sum\limits_{<i,j>_{connected}} 1 \right\rangle_{p-\mathrm{E}}}}. \tag{6.206}$$

Here, $\sum\limits_{<i,j>_{connected}}$ denotes the sum over all pairs of occupied sites on a lattice which are connected by the common cluster. Averaging $\langle\ \rangle_{p-\mathrm{E}}$ is the averaging over all possible realizations of clusters on a lattice for the given value of the field parameter p.

In other words, we consider the ensemble of identical systems with the boundary condition $p = const$ (p-ensemble, p-E). For each system in the ensemble, we go over its sites, one by one, and for each site we decide whether it will be occupied (with probability p) or empty. So, each system will represent a particular realization of the cluster distribution. Then, we go over all pairs of connected occupied sites in the ensemble and average the distance in accordance with (6.206).

But in expression (6.206) for the correlation length, the averaging of distances over all pairs of connected occupied sites may be separated into groups where in a particular group we average only those pairs that belong to s-clusters:

$$\xi(p) = \sqrt{\frac{\sum\limits_s n_s \left\langle \sum\limits_{<i,j>\in s-cluster} R_{i,j}^2 \right\rangle_{p-\mathrm{E}}}{\sum\limits_s n_s \left\langle \sum\limits_{<i,j>\in s-cluster} 1 \right\rangle_{p-\mathrm{E}}}}. \tag{6.207}$$

The radius of gyration for a given s-cluster is introduced as the root-mean-square distance between the sites of this cluster:

$$R_{s-cluster} \equiv \sqrt{\frac{\sum\limits_{<i,j>\in s-cluster} R_{i,j}^2}{\sum\limits_{<i,j>\in s-cluster} 1}} = \sqrt{\frac{\sum\limits_{<i,j>\in s-cluster} R_{i,j}^2}{\frac{1}{2}s(s-1)}}. \tag{6.208}$$

What does this radius represent? If the center of mass of the cluster is located at point $\vec{\mathbf{R}}_0$:

$$\vec{\mathbf{R}}_0 \equiv \frac{1}{s}\sum_{i=1}^{s}\vec{\mathbf{R}}_i, \tag{6.209}$$

where the sum goes over the sites of the cluster, then for the radius of gyration we find

$$\begin{aligned} R_{s-cluster} &= \sqrt{\frac{\sum\limits_{<i,j>\in s-cluster}(\vec{\mathbf{R}}_i-\vec{\mathbf{R}}_j)^2}{\sum\limits_{<i,j>\in s-cluster}1}} \\ &= \sqrt{\frac{\frac{1}{2}\sum\limits_{i,j=1:i\neq j}^{s}\left((\vec{\mathbf{R}}_i-\vec{\mathbf{R}}_0)-(\vec{\mathbf{R}}_j-\vec{\mathbf{R}}_0)\right)^2}{\frac{1}{2}\sum\limits_{i,j=1:i\neq j}^{s}1}} \\ &= \sqrt{\frac{\frac{1}{2}\sum\limits_{i,j=1}^{s}\left\{(\vec{\mathbf{R}}_i-\vec{\mathbf{R}}_0)^2-2(\vec{\mathbf{R}}_i-\vec{\mathbf{R}}_0)(\vec{\mathbf{R}}_j-\vec{\mathbf{R}}_0)+(\vec{\mathbf{R}}_j-\vec{\mathbf{R}}_0)^2\right\}}{\frac{1}{2}s(s-1)}} \\ &= \sqrt{2}\sqrt{\frac{1}{s-1}\sum_{i=1}^{s}(\vec{\mathbf{R}}_i-\vec{\mathbf{R}}_0)^2}. \end{aligned} \tag{6.210}$$

We see that the radius of gyration of the cluster is the root-mean-square radius $\sqrt{\frac{1}{s}\sum_{i=1}^{s}(\vec{\mathbf{R}}_i-\vec{\mathbf{R}}_0)^2}$ of the cluster times the unimportant multiplier $\sqrt{2\frac{s}{s-1}}$.

Instead of considering the radius of gyration for a particular s-cluster, we may average it (root-mean-square averaging) over all s-clusters on a lattice:

$$R_s(p) \equiv \sqrt{\left\langle R_{s-cluster}^{\,2}\right\rangle_{p-\mathrm{E}}} = \sqrt{\frac{\left\langle\sum\limits_{<i,j>\in s-cluster}R_{i,j}^2\right\rangle_{p-\mathrm{E}}}{\frac{1}{2}s(s-1)}}. \tag{6.211}$$

But the expression in the numerator is exactly what we see in the numerator of the correlation length (6.207). Substituting, we find

$$\xi(p) = \sqrt{\frac{\sum\limits_{s} n_s \frac{1}{2}s(s-1)R_s^2(p)}{\sum\limits_{s} n_s \frac{1}{2}s(s-1)}}. \tag{6.212}$$

In the limit of big clusters, $s >> 1$, this expression is simplified as

$$\xi(p) = \sqrt{\frac{\sum_s n_s s^2 R_s^2(p)}{\sum_s n_s s^2}}. \tag{6.213}$$

This result is easily interpreted. Let us return to (6.205) when it is known that the site at $\vec{\mathbf{R}} = 0$ is occupied. The probability that this occupied site belongs to an s-cluster is $sn_s(p)/p$. Thus, with this probability, this site will form $(s-1)$ pairs with other sites of this cluster. Meanwhile, the square length of these pairs, averaged in the ensemble, is $R_s^2(p)$ so that our expectation for the correlation length (6.205) is:

$$\xi(p) = \sqrt{\frac{\sum_s \frac{sn_s}{p}(s-1)R_s^2(p)}{\sum_s \frac{sn_s}{p}(s-1)}}. \tag{6.214}$$

which returns us to (6.212).

That is why we have said that the percolation problem is unique; observing the structure of clusters, we immediately find the correlation length as equivalent to the (root-mean-square) linear size of the clusters which is very illustrative. Let us now see what conclusions this may lead to.

Below the percolation threshold, everything is straightforward: The correlation length is the averaged linear size of finite clusters. The higher p (which still remains below p_C), the larger correlation length and clusters. When the system tends to the percolation threshold from below, the correlation length diverges in accordance with

$$\xi \propto | p - p_C |^{-\nu}. \tag{6.215}$$

So does the size of the clusters since they are supposed to give rise to an infinite percolating cluster.

But above the percolation threshold a new length appears—the length of a percolating cluster—which coincides with the size of the whole system. So the question arises—does probability $G(\vec{\mathbf{R}})$ also predict the size of the percolating cluster? When in accordance with (6.213), we sum all the sizes of clusters, should we average the percolating cluster as well?

The situation resembles the case of magnetic systems. Above the critical point, the correlation length also represents the linear size of clusters (magnetic domains). Below the critical point, two phases arise. A homogeneous system, represented by one of the phases, may be considered as one big cluster, occupying the whole system.

But for magnetic systems, the question whether the correlation length represents the linear size of magnetic domains below the critical point does not arise. The reason is that in the correlation function (6.3), we subtract the averaged magnetization

so that the correlation function represents the heterogeneous response to an external disturbance instead of representing a homogeneous phase.

For example, let us consider the ferromagnetic Ising model below the critical point. Besides, we consider the system in the presence of magnetic field $h > 0$ so that the majority of spins in the system are oriented "up."

The external disturbance is then represented by a spin which is oriented "down" and this orientation is fixed by some external forces. The correlation function is then the response of the surrounding spins to this disturbance; and the correlation length is the characteristic length of the decay of this response. The correlation length does diverge at the critical point, but far from this point it is small and definitely not of the size of the magnetic domain which for $h > 0$ occupies the whole system.

Returning back to percolation, if we included the percolating cluster in the probability $G(\vec{\mathbf{R}})$, the correlation length would be always infinite above the percolation threshold. We would definitely not want that. Instead, we prefer that power-law (6.215) would represent the divergence of the correlation length for both sides of the percolation threshold so that above the percolation threshold the correlation length would be finite and would represent the linear size of only finite clusters. We will be able to achieve all this if $G(\vec{\mathbf{R}})$ represented only the finite clusters and the percolating cluster did not participate in averaging (6.213).

As we have already discussed, the correlation length plays the role of the characteristic length, dividing the scales. First, we consider the system below the percolation threshold. On scales smaller than the correlation length, the behavior is dominated by scale-invariant fluctuations. If we were looking at the lattice through a "window" with the linear size smaller than the correlation length, we would observe that clusters are fractal and that there is no characteristic length on all these scales, beginning from the lattice constant and ending by the size of the window.

So, in Fig. 6.6, the two smallest squares (A and B) represent the scales smaller than the correlation length. Each of these windows contains small clusters whole and parts of big clusters which may percolate the window. Obviously, the bigger window may contain bigger clusters. But the structure of clusters is scale invariant—if we shrank window B together with its clusters to match the size of window A, the structure of clusters of window B would transform into the clusters of window A (on average).

On the contrary, if we are looking at the system through the window of the size larger than the correlation length, we see the appearance of the characteristic length—the correlation length. The fractality breaks on these scales, and the structure of clusters is no longer scale invariant.

So, in Fig. 6.6, the correlation length, representing the averaged linear size of clusters, is of the order of the size of window B. Looking at the system through bigger windows, C, D, or F, we no longer see the fractal, scale-invariant structure of clusters. Instead, we see the presence of a characteristic length—indeed, we visually observe that sizes of clusters are limited from above and there no longer present parts of big clusters that are able to percolate the window.

Above the percolation threshold, almost the whole lattice is occupied by the percolating cluster (the area filled by pattern in Fig. 6.7). The finite clusters exist only within the holes of this cluster. Since the correlation length represents here the

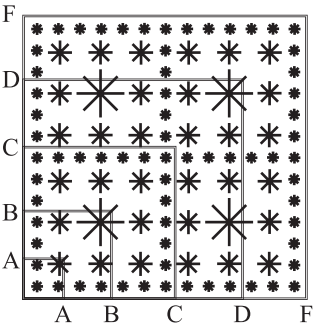

Fig. 6.6 Schematic representation of clusters below the percolation threshold

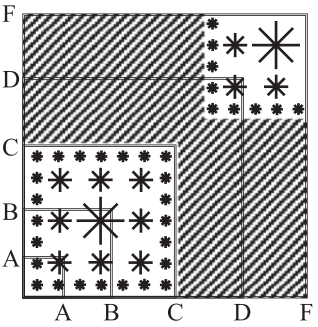

Fig. 6.7 Schematic representation of clusters above the percolation threshold. The pattern, occupying almost the whole lattice, represents the percolating cluster. Finite clusters exist only within the holes of the percolating cluster

averaged linear size of the finite clusters only, it should be of the order of the size of window B.

If we are looking at the system through a window with size less than the correlation length (windows A and B), we again see the fractal, scale-invariant structure of finite clusters and parts of percolating cluster. For bigger windows (C, D, and F) the fractality, obviously, no longer exists. The main part of the window (D and F) is occupied now by the nonfractal, *d*-dimensional mass of the percolating cluster.

6.7 Percolation: Fluctuation–Dissipation Theorem

The role of the susceptibility in percolation is played by the mean cluster size:

$$\tilde{S}(p) \equiv \frac{\sum_s s^2 n_s(p)}{\sum_s s n_s(p)}. \tag{6.216}$$

We will prove this to be true later in this section. For now, we may rely on the intuitive understanding that the numerator $\sum_s s^2 n_s(p)$ (the very quantity that is diverging

at the critical point and determines the scaling of the mean cluster size) represents the averaged square of a fluctuating parameter s. As we have seen above, the susceptibility of a system should correspond to the variance of a fluctuating parameter.

Problem 6.7.1

Find the correlation function, correlation length, and the critical index ν for the case of the one-dimensional percolation. Prove the validity of the fluctuation–dissipation theorem.

Solution: We consider the system to be below the percolation threshold, $p < p_C = 1$. When we determine the correlation function, we know about the initial site $\vec{\mathbf{R}} = 0$ that it is occupied. The probability $G(1)$ that the neighboring site to the right belongs to the same cluster is just the probability p that this site is occupied also: $G(1) = p$.

Similarly, the probability $G(R)$ that the site at distance R to the right belongs to the same cluster is the probability p^R that this site and all the intermediate sites at distances 1, 2, …, $R-1$ are occupied:

$$G(R) = p^R = e^{-R/\xi(p)}, \text{ where} \tag{6.217}$$

$$\xi(p) = -1/\ln p. \tag{6.218}$$

At the percolation threshold $p = p_C = 1$, we, obviously, have

$$G(R) \equiv 1 \text{ and } \xi(1) = +\infty. \tag{6.219}$$

In the vicinity of the percolation threshold, $p \to p_C - 0$, we expand (6.218),

$$\xi(p) \propto \frac{1}{1-p}, \tag{6.220}$$

to find $\nu = 1$.

In Chap. 4, we considered two methods to find the mean cluster size. In the vicinity of the percolation threshold, both quantities are of the order of the correlation length:

$$S(p) = \frac{1}{1-p}, \tag{6.221}$$

$$\tilde{S}(p) = \frac{1+p}{1-p}. \tag{6.222}$$

This is expected because in the one-dimensional case, the size s of a cluster equals the length of this cluster.

To obtain the analogue of the fluctuation–dissipation theorem, we integrate the correlation function:

$$\sum_{R=-\infty}^{+\infty} G(R) = G(0) + 2\sum_{R=1}^{+\infty} G(R) = 1 + 2\sum_{R=1}^{+\infty} p^R = \frac{1+p}{1-p} = \tilde{S}. \qquad (6.223)$$

Thereby we prove that the integral of the correlation function equals the mean cluster size $\tilde{S}$. So, $\tilde{S}$ does indeed play the role of the susceptibility in the one-dimensional case.

For an arbitrary lattice, the correlation function $G(\vec{\mathbf{R}})$ is defined as the probability that if the site at $\vec{\mathbf{R}} = 0$ is occupied, the site at distance $\vec{\mathbf{R}}$ is also occupied and belongs to the same cluster. If we know that the site at $\vec{\mathbf{R}} = 0$ is occupied, the probability for this site to belong to an s-cluster is $sn_s(p)/p$.

But if this site belongs to an s-cluster, it is connected with other $(s-1)$ sites of this cluster. Thereby, on average this site is connected to $\sum_{s=1}^{+\infty}(s-1)\frac{sn_s(p)}{p}$ sites.

In comparison, by the definition of the correlation function, this site is connected to $\sum_{\vec{\mathbf{R}}\neq 0} G(\vec{\mathbf{R}}) = \sum_{\vec{\mathbf{R}}} G(\vec{\mathbf{R}}) - G(0) = \sum_{\vec{\mathbf{R}}} G(\vec{\mathbf{R}}) - 1$ sites. Equating these two results, we prove the fluctuation–dissipation theorem for an arbitrary lattice:

$$\sum_{\vec{\mathbf{R}}} G(\vec{\mathbf{R}}) - 1 = \sum_{s=1}^{+\infty}(s-1)\frac{sn_s(p)}{p} = \frac{\sum_{s=1}^{+\infty} s^2 n_s(p)}{\sum_{s=1}^{+\infty} sn_s(p)} - 1 \equiv \tilde{S} - 1 \text{ or} \qquad (6.224)$$

$$\sum_{\vec{\mathbf{R}}} G(\vec{\mathbf{R}}) = \tilde{S}. \qquad (6.225)$$

Thereby, $\tilde{S}$ is indeed the susceptibility of the system.

We expect the fluctuation–dissipation theorem to be valid both below and above the critical threshold since in both cases it represents only the properties of finite clusters. Above the percolation threshold, we include the percolating cluster $s = +\infty$ neither in the correlation function nor in the sums of the susceptibility (6.216).

6.8 Percolation: The Hyperscaling Relation and the Scaling of the Order Parameter

The correlation length serves as a characteristic length, dividing the scales. On scales smaller than the correlation length clusters are scale-invariant with the fractal dimension D whilst on larger scales the fractality is broken by the appearance of the correlation length as a characteristic length.

So, for the s-clusters whose linear size $R_s(p)$ is less than the correlation length, $R_s < \xi$, by the definition of the fractal dimension D we have

$$s \propto {R_s}^D \text{ or } R_s \propto s^{1/D} \tag{6.226}$$

as a connection between the measure s and the linear size $R_s(p)$ of the fractal set.

Meanwhile, the condition $R_s < \xi$ transforms into

$$s < s_\xi(p) \equiv \xi^D(p), \tag{6.227}$$

where s_ξ-cluster is a cluster whose averaged linear size corresponds to the correlation length.

Let us return to the correlation length (6.213). When the system tends to the percolation threshold, the correlation length diverges in accordance with (6.215) so that the fractality occupies larger and larger scales. Thus, more and more clusters obey (6.226) with the exception only for the biggest clusters.

As an approximation, we consider that (6.226) is valid for all clusters, even the biggest. Substituting (6.226) into (6.213), we find

$$\xi(p) = \sqrt{\frac{\sum_s n_s s^{2(1+1/D)}}{\sum_s n_s s^2}}. \tag{6.228}$$

The singular behavior of the correlation length is accumulated in (6.215). The singular behavior of the sum $\sum_s n_s s^2$ determines the divergence of $\tilde{S}$. The sum $\sum_s n_s s^{2(1+1/D)}$ represents the moment M_k with $k = 2(1+1/D)$ whose singular behavior we find with the aid of (4.96):

$$M_{2+\frac{2}{D}}(p) \propto |p - p_C|^{\frac{\tau-3-2/D}{\sigma}}. \tag{6.229}$$

Substituting all these results into (6.228), we find the relation among the critical indices and the fractal dimension D of small clusters:

$$-2\nu = \gamma + \frac{\tau - 3 - 2/D}{\sigma} \text{ or} \tag{6.230}$$

$$\sigma\nu D = 1. \tag{6.231}$$

What does this relation mean physically? Let us return to hypothesis (4.52 and 4.53):

$$n_s(p) \propto s^{-\tau} e^{-(c(p)s)^{\zeta}}, \text{ where} \tag{6.232}$$

$$c(p) \propto | p - p_C |^{1/\sigma} \quad \text{for } p \to p_C. \tag{6.233}$$

Substituting σ from (6.231) into (6.233), in the vicinity of the percolation threshold we find

$$c(p) \propto \frac{1}{\xi^D} \equiv \frac{1}{s_\xi}. \tag{6.234}$$

This transforms hypothesis (6.232) into

$$n_s(p) \propto s^{-\tau} e^{-(s/s_\xi)^{\zeta}}. \tag{6.235}$$

We see that for clusters whose linear size $R_s(p)$ is less than the correlation length ($s < s_\xi$) the exponential function is of the order of unity, and the cluster-size distribution decays as a power-law:

$$n_s(p) \propto s^{-\tau}. \tag{6.236}$$

This is expected since all clusters on scales smaller than the correlation length are fractal.

On the contrary, for big nonfractal clusters ($s > s_\xi$), the decay is dominated by the exponential function. Although big clusters are not fractal, their parts, cut by a window with the size smaller than the correlation length, are still fractal with the same dimension D along with all small clusters. So, the big clusters are not fractal as a whole but their internal structure is fractal.

Below the percolation threshold, $p < p_C$, there is no percolating cluster while the correlation length is much smaller than the size of the system: $\xi << L = N^{1/d}$. When the system tends to the percolation threshold, the correlation length diverges, and the fractality occupies larger and larger scales. The percolating cluster appears when the correlation length becomes comparable with the linear size of the system, $\xi \propto L$ (or a bit earlier since the correlation length represents the averaged linear size of all clusters on a lattice while extremes of this statistics are larger).

If we continue to increase p, the correlation length exceeds the linear size of the system, $\xi > L$, and becomes infinite at the percolation threshold. The fractality, in the meantime, occupies all possible scales. In particular, the appearing percolating cluster, cut by the size of the system as if by Procrustes' bed, is also fractal: $s_{PC} \propto L^D$.

By definition, the order parameter NP_{PC} is the number of sites belonging to the percolating cluster. Equating it to $s_{PC} \propto L^D$, we find

$$P_{PC} \propto L^{D-d}. \tag{6.237}$$

If we continue to increase p already above the percolation threshold, $p > p_C$, the correlation length decreases. While it is still larger than the system size, $\xi > L$, the percolating cluster remains fractal as a whole whilst (6.237) remains valid.

But if, while we are increasing p, the correlation length becomes smaller than the system size, $\xi < L$, only the internal structure of the percolating cluster remains fractal on scales smaller than the correlation length. However, the percolating cluster as a whole is no longer fractal but gives rise to the scaling of the appeared order parameter:

$$P_{PC}(p) \propto | p - p_C |^{\beta}. \tag{6.238}$$

The transformation of (6.237) into (6.238) must happen when the correlation length passes the size of the system: $L \propto \xi \propto | p - p_C |^{-\nu}$. Equating (6.237) to (6.238) and substituting $L \propto | p - p_C |^{-\nu}$, we obtain *the hyperscaling relation*, which associates the critical indices with the dimensionality of the system:

$$d - D = \frac{\beta}{\nu} \text{ or } d = (1 + \beta\sigma)D. \tag{6.239}$$

The origin of this relation is that we "glue" together two types of behavior when one of them is transformed into another.

In fact, we "glue" together different scales. Due to the importance of this discussion, let us again consider the system slightly above the percolation threshold $p \to p_C + 0$. Since p is close to the percolation threshold but does not equal it, the correlation length is large but finite.

Above the percolation threshold, the percolating cluster exists and percolates the infinite system. Let us consider its structure through the windows of different size L.

When $L < \xi$, the window cuts a piece of the percolating cluster which is fractal: $s_{part\ of\ PC} \propto L^D$. However, such small scale $L < \xi$ does not represent the behavior of the infinite percolating cluster. Since the scaling dependence $P_{PC}(p) \propto | p - p_{\mathbf{C}} |^{\beta}$ is defined for the infinite cluster, we do not expect that the small piece of this cluster would represent this scaling.

When $L > \xi$, the piece of the percolating cluster, cut by the window, is no longer fractal but is already big enough to represent the scaling behavior of the order parameter: $s_{part\ of\ PC} \propto L^d \mid p - p_C \mid^{\beta}$. "Gluing" these two scales, as two sides of one coin, together at $L = \xi$, we obtain the hyperscaling relation (6.239).

In Chap. 4, we hypothesized that the number of sites in the percolating cluster scales as

$$NP_{PC}(p, L = +\infty) \propto \begin{cases} 0, p < p_{\mathrm{C}} \\ L^{D}, p = p_{\mathrm{C}}, \\ L^{d}, p > p_{\mathrm{C}} \end{cases} \tag{6.240}$$

when there is no percolating cluster below the percolation threshold, it is fractal at the percolation threshold, and inherits the dimensionality of the embedding lattice above the percolation threshold. However, we should always remember that this hypothesis was introduced for the case of the infinite system.

So, if we consider an infinite system above the percolation threshold, the whole percolating cluster is not fractal and has the dimension *d*, but its structure on scales smaller than the correlation length is fractal with the dimension *D*. But how is it possible? How can a union of sets with the dimension *D* form a set with the dimension *d*?

To illustrate this transition of the dimensionality, let us consider a system of size L above the percolation threshold. If $L < \xi$, the percolating cluster is fractal and contains $s_{PC} \propto L^{D}$ sites.

If, on the contrary, $L > \xi$, we divide the system of linear size L into cells of size ξ. The part of the percolating cluster within each cell is fractal and consists of ξ^{D} sites. Since there are $(L/\xi)^{d}$ cells, the total number of sites in the percolating cluster is $\xi^{D}(L/\xi)^{d}$.

Summarizing these tendencies, we obtain

$$NP_{PC}(p, L) \propto \begin{cases} L^{D}, L < \xi \\ \xi^{D}\left(\dfrac{L}{\xi}\right)^{d}, L > \xi \end{cases} \text{for } p > p_{\mathrm{C}} \text{ or} \tag{6.241}$$

$$NP_{PC}(p, L) \propto \begin{cases} L^{D}, L < \xi \\ L^{d}\xi^{D-d}, L > \xi \end{cases} \text{for } p > p_{\mathrm{C}}. \tag{6.242}$$

We see that on different scales, the order parameter has, indeed, different dimensionalities. The transformation of one dimensionality into another happens similar to fractals considered in Chap. 1 when the dimension of a fractal did not depend on the dimension of the initial branch but, instead, was determined by the properties of the fractal generator.

Considering the infinite lattice, $\xi < L = +\infty$, from (6.242) we find

$$P_{PC}(p, L = +\infty) \propto \frac{1}{L^{d}} L^{d}\xi^{D-d} = \xi^{D-d} \text{ for } p > p_{\mathrm{C}}. \tag{6.243}$$

But the scaling of the order parameter in the case of the infinite lattice is defined as $P_{PC}(p, L = +\infty) \propto |\, p - p_{\mathrm{C}} \,|^{\beta}$ while the scaling of the correlation length

is $\xi \propto | p - p_C |^{-\nu}$. Substituting these power-law dependencies into (6.243), we return to the hyperscaling relation (6.239).

Functional dependence (6.241 and 6.242) may be written as

$$NP_{PC}(p) \propto L^D \begin{cases} 1, L < \xi \\ \left(\frac{L}{\xi}\right)^{d-D}, L > \xi \end{cases} \text{ for } p > p_C, \tag{6.244}$$

representing the finite-size effect in the system. The role of the scaling parameter is played by the ratio L / ξ whose value chooses one of two possible scaling asymptotes of the system's behavior. We will return to the finite-size effect in Chap. 8 in more detail.

In the case of magnetic systems, the hyperscaling relation (6.171 and 6.172) was valid only below the upper critical dimension. A similar situation is observed in percolation, only now the upper critical dimension is $d = 6$. In higher dimensions, the dimensionality d of the system does not influence the values of critical indices because in these dimensions they are determined by the mean-field approach and are equal to the critical indices of the infinite-dimensional system (the Bethe lattice).

For magnetic systems, we saw situations when the hyperscaling relation was not valid even below the upper critical dimension. These cases corresponded to systems with long-range interactions. Similar behavior can be observed in percolation as well when we introduce long-range interactions by connecting into a common cluster not only the occupied nearest neighbors but also occupied sites separated by larger distances.

When $\frac{\tau - 2}{\sigma} \le 1$ and $d \le 6$, with the aid of the hyperscaling relation (6.239) we obtain

$$\frac{\tau - k - 1}{\sigma} = \beta + \frac{1 - k}{\sigma} = \beta + \nu D(1 - k) = \nu d - k\nu D. \tag{6.245}$$

This transforms the divergence (4.96) of the moment M_k, found in Chap. 4, into

$$M_k(p) \propto | p - p_C |^{\frac{\tau - k - 1}{\sigma}} \propto \frac{\xi^{kD}}{\xi^d} \propto \frac{s_\xi{}^k}{\xi^d}. \tag{6.246}$$

This expression illustrates that the logarithm of the moment is proportional to *k:*

$$\ln M_k(p) \propto k \ln s_\xi - d \ln \xi \propto (kD - d) \ln \xi. \tag{6.247}$$

6.9 Why Percolation Differs from Magnetic Systems

Considering percolation, we have built several quantities, n_s, P_{PC}, $\tilde{S}$, $G(\vec{\mathbf{R}})$, ξ, which resemble the quantities of magnetic systems but have no direct relations with them. For example, the correlation function and the susceptibility required specific definitions and were not built on the base of the formalism of statistical physics.

Why is the problem of percolation special? To answer this question, let us compare the principles lying behind correlation functions in percolation and in magnetic systems.

Problem 6.9.1

Consider percolation on an arbitrary lattice. Introduce spin variables σ_i when $\sigma_i = +1$ for an occupied site and $\sigma_i = 0$ for an empty site. Find the correlation function (6.3):

$$g(R_{ij}) \equiv \left\langle \left(\sigma_i - \left\langle \sigma_i \right\rangle_{p-\mathrm{E}}\right)\left(\sigma_j - \left\langle \sigma_j \right\rangle_{p-\mathrm{E}}\right)\right\rangle_{p-\mathrm{E}}$$
$$= <\sigma_i\sigma_j>_{p-\mathrm{E}} - <\sigma_j>^2_{p-\mathrm{E}}. \qquad (6.248)$$

Solution: By definition, $\sigma_i = +1$ with probability p for an occupied site and $\sigma_i = 0$ with probability $(1-p)$ for an empty site. Since the probability for a site to be occupied or empty does not depend on whether other sites are occupied or empty, each spin is independent of the state of other spins:

$$<\sigma_i\sigma_j>_{p-\mathrm{E}} = <\sigma_i>_{p-\mathrm{E}} <\sigma_j>_{p-\mathrm{E}}. \qquad (6.249)$$

This immediately provides that the correlation function defined in accordance with (6.248) is always zero when $R_{ij} \neq 0$.

Problem 6.9.1 demonstrates that if we decided to define the correlation function in percolation similar to magnetic systems, it would make no sense since whether a site is occupied or not does not depend in percolation on whether other sites are occupied or not.

That is why we have employed a different definition of the correlation function $G(\vec{\mathbf{R}})$ for percolation—as the probability that if the initial site is occupied, the site at distance $\vec{\mathbf{R}}$ is also occupied and belongs to the same cluster.

The key phrase here is *belongs to the same cluster*. For magnetic systems, we did not care whether two spins at distance $\vec{\mathbf{R}}$ were or were not connected by a chain of spins with the same orientation. For spins what was important is how many spins are "up" or "down."

On the contrary, in percolation first we care about how occupied sites are connected to one another. The origin of this specific request arises from the criterion we employ to represent a phase transition. In particular, we associate the percolation threshold with the appearance of a chain of occupied, connected to one another sites which connect the opposite edges of a lattice.

While statistical physics cares about the states of sites so that the ensemble assigns probabilities for a site to be in this or other state, percolation studies the connectivity among sites when the ensemble deals with probabilities for sites to form clusters.

The simplest example is when we try to build a microcanonical or canonical ensembles for percolation. Let us imagine a lattice which contains exactly $N_\bullet$ occupied sites (which is isolated with $N_\bullet$ occupied sites). As a microstate, we may consider a particular configuration of occupied sites on the lattice. For example, for the lattice with $N = 3$ sites, two of which are occupied ($N_\bullet = 2$), the possible microstates are $\{\bullet\bullet\circ\}$, $\{\bullet\circ\bullet\}$, and $\{\circ\bullet\bullet\}$.

The diversity of all microstates represents the microcanonical ensemble with the boundary condition $N_\bullet = const$. The statistical weight of the ensemble corresponds to the number of ways to distribute $N_\bullet$ occupied sites among N sites:

$$\Gamma^{MCE} = \frac{N!}{N_\bullet!(N-N_\bullet)!}. \tag{6.250}$$

Here, we even comply with the requirement of statistical physics for all microstates to be equiprobable:

$$w^{MCE}_{\{\}} = \frac{1}{\Gamma^{MCE}}. \tag{6.251}$$

To build the canonical ensemble, we should substitute the boundary condition $N_\bullet = const$ by the boundary condition $p = const$. We imagine a small system to be in contact with a big reservoir of occupied sites. Our system may consume as many occupied sites from the reservoir as it wishes so that we may consider fluctuations $\{\{N_\bullet\}\}$ of the number $N_\bullet$ of occupied sites in our system.

In the canonical ensemble, the reservoir dictates the equilibrium probability distribution for microstates $\{N_\bullet\}$:

$$w^{CE}_{\{N_\bullet\}} = p^{N_\bullet}(1-p)^{N-N_\bullet} = (1-p)^N e^{-N_\bullet \ln\frac{1-p}{p}}, \tag{6.252}$$

which resembles Gibbs probability in statistical physics with the effective temperature $T^{eff} = ln^{-1}\dfrac{1-p}{p} = const$ as a new boundary condition and ensemble partition function $Z^{CE} = (1-p)^{-N}$.

Nothing is wrong in the presented approach of statistical physics to the phenomena of percolation with the exception that this approach neither can predict the appearance of a percolating cluster nor knows anything about clusters in the system. The problem is that ensembles of statistical physics do not master the connectivity of occupied sites within clusters.

6.10 Percolation: The Ensemble of Clusters

Since we cannot describe the connectivity of clusters with the traditional means of statistical physics, the direct analogy between percolation and statistical physics is not possible. Instead, we should seek an approach in which the ensemble would be based not on the probabilities of states of sites but on the probabilities of connectivity among the sites. In other words, the partition function of the ensemble should sum not the probabilities of states but the probabilities of clusters:

$$Z^E(p) \equiv \sum_s n_s(p). \tag{6.253}$$

Since the partition function is supposed to be the normalization constant of the distribution of probabilities, these probabilities are

$$W_s^E \equiv \frac{1}{Z^E} n_s \tag{6.254}$$

so that an averaged value of quantity f_s in the ensemble we define by

$$\langle f \rangle_E \equiv \sum_s f_s W_s^E = \frac{1}{Z^E} \sum_s f_s n_s. \tag{6.255}$$

For simplicity, as an example we consider further the Bethe lattice below the percolation threshold when into hypothesis (4.52 and 4.53) we should substitute $\zeta = 1$:

$$n_s(p) \propto s^{-\tau} e^{-c(p)s}, \text{ where} \tag{6.256}$$

$$c(p) \propto | p - p_C |^{1/\sigma} \text{ for } p \to p_C. \tag{6.257}$$

Differentiating the partition function with respect to the field parameter $(-c)$:

$$\frac{dZ^E}{d(-c)} = \sum_s s n_s(p) = Z^E \langle s \rangle_E, \tag{6.258}$$

we find that the ensemble averaging of the cluster size is equivalent to the mean cluster size S defined in Chap. 4 by (4.117):

$$\langle s \rangle_E = \frac{d \ln Z^E}{d(-c)} = \frac{1}{Z^E} \sum_s s n_s(p) \equiv S. \tag{6.259}$$

Differentiating the partition function for the second time with respect to the field parameter $(-c)$:

$$\frac{d^2 Z^E}{d(-c)^2} = \sum_s s^2 n_s(p) = Z^E \left\langle s^2 \right\rangle_E, \tag{6.260}$$

for the averaged squared cluster size we find

$$\left\langle s^2 \right\rangle_E = \frac{1}{Z^E} \frac{d^2 Z^E}{d(-c)^2} = \frac{1}{Z^E} \sum_s s^2 n_s(p) \equiv S \cdot \tilde{S}. \tag{6.261}$$

Thereby the second derivative of the logarithm of the partition function equals the variance of the cluster sizes in the ensemble:

$$\frac{d^2 \ln Z^E}{d(-c)^2} = \left\langle s^2 \right\rangle_E - \langle s \rangle_E{}^2 = \left\langle \left(s - \langle s \rangle_E \right)^2 \right\rangle_E. \tag{6.262}$$

From another point of view, this derivative represents the response of the averaged cluster size $\langle s \rangle_E$ to the change in the field parameter $(-c)$:

$$\frac{d^2 \ln Z^E}{d(-c)^2} = \frac{d \langle s \rangle_E}{d(-c)}. \tag{6.263}$$

Thus, it seems to be reasonable to define the susceptibility by

$$\chi \equiv \frac{d \langle s \rangle_E}{d(-c)} = \left\langle s^2 \right\rangle_E - \langle s \rangle_E{}^2 = S \cdot \tilde{S} - S^2. \tag{6.264}$$

In the vicinity of the percolation threshold, the mean cluster size S is not singular whilst the mean cluster size $\tilde{S}$ diverges to determine the divergence of the susceptibility:

$$\chi \propto \tilde{S} \propto \frac{1}{| p - p_C |^{\gamma}}. \tag{6.265}$$

We define the equilibrium action of the free energy as the minus logarithm of the partition function:

$$\mathrm{A}^E = -\ln Z^E. \tag{6.266}$$

By definition (6.253), the partition function is the 0th moment M_0 whose value (4.107) for the case $\zeta = 1$ we have found in Chap. 4 in the vicinity of the percolation threshold:

$$M_0 = const_3 + const_2 c + const_1 c^{\tau-1} \text{ or} \tag{6.267}$$

$$M_0 = const_3 + const_2 \mid p - p_C \mid^{1/\sigma} + const_1 \mid p - p_C \mid^{2-\alpha}. \tag{6.268}$$

Expanding (6.266) in the vicinity of the percolation threshold, we find

$$\mathrm{A}^E = const_1 + const_2 \mid p - p_C \mid^{1/\sigma} + const_3 \mid p - p_C \mid^{2-\alpha}. \tag{6.269}$$

Differentiating this expression twice with respect to p and assuming that for the Bethe lattice $\sigma = 1/2$, we obtain an analogue of the heat capacity:

$$C \propto \frac{d^2 \mathrm{A}^E}{dp^2} \propto \mid p - p_C \mid^{-\alpha}. \tag{6.270}$$

Let us now discuss the developed approach. In (6.254), we have assumed that the cluster-size distribution n_s plays the role of the probability $W^E_{\{\{s\}\}}$ of fluctuations $\{\{s\}\}$. In other words, we consider each lattice s-animal as a microstate $\{s\}$ with the probability

$$w^E_{\{s\}} \propto p^s (1-p)^{t_s} = p^s (1-p)^{2+s(Z-2)} = (1-p)^2 e^{-s \ln \frac{1}{p(1-p)^{Z-2}}}. \tag{6.271}$$

This probability resembles Gibbs probability with *the effective temperature*

$$T^{eff} \equiv \ln^{-1} \frac{1}{p(1-p)^{Z-2}}. \tag{6.272}$$

Since we consider $p = const$ to be the condition of the model, the requirement $T^{eff} = const$ may be considered as the boundary condition of the ensemble so that we may call our ensemble *the effective canonical*.

The number g_s of lattice s-animals plays the role of the statistical weight of the fluctuation $\{\{s\}\}$. Thereby, the probability of this fluctuation is

$$W^E_{\{\{s\}\}} = g_s w^E_{\{s\}} \propto n_s, \tag{6.273}$$

which we have hypothesized by (6.254).

Since g_s does not depend on p, in hypothesis (6.256) dependence $c(p)$ on p may come only from the effective temperature in (6.271). Indeed, by comparison with (4.48) we find

$$c(p) = \frac{1}{T^{eff}(p)} - \frac{1}{T^{eff}(p_C)}. \tag{6.274}$$

Therefore, if we neglect the multiplier $(1-p)^2$ in (6.271), derivatives (6.258) and (6.260) with respect to $(-c)$ can be considered as the derivatives with respect to the field parameter $\left(-1/T^{eff}(p)\right)$ similar to our previous formulae (6.185 and 6.187) for magnetic systems.

Taking into account the multiplier $(1-p)^2$ in (6.271) makes the derivatives more complex since, differentiating with respect to $\left(-1/T^{eff}(p)\right)$, we, in fact, are differentiating with respect to p and should differentiate $(1-p)^2$ as well.

But this is not the main difficulty. Considering (below the percolation threshold) an arbitrary lattice instead of the Bethe lattice, we can no longer use hypothesis (6.256 and 6.257) with $\zeta = 1$.

Indeed, let us consider the formulae above as if they were applicable in the case of an arbitrary lattice as well. The mean cluster size

$$\tilde{S}(p) \equiv \frac{\sum_s s^2 n_s(p)}{\sum_s s n_s(p)} \tag{6.275}$$

can be presented in the form

$$\tilde{S} = \frac{d}{d(-c)} \ln \sum_s s n_s(p). \tag{6.276}$$

But in accordance with the law of conservation of probabilities below the percolation threshold, the sum $\sum_s s n_s(p)$ equals p:

$$\tilde{S} = \frac{d \ln p}{d(-c)}. \tag{6.277}$$

Since p is not singular at the percolation threshold, the divergence $\tilde{S} \propto | p - p_C |^{-\gamma}$ of the mean cluster size must come from the denominator of (6.277) as the differential of the singular dependence (6.257):

$$\frac{d \ln p}{d(-c)} \propto \frac{dp}{d \mid p - p_C \mid^{1/\sigma}} \propto | p - p_C |^{-1/\sigma+1}. \tag{6.278}$$

Comparing the exponents, we find the relation between the critical indices

$$\gamma = \frac{1}{\sigma} - 1. \tag{6.279}$$

Although this relation is valid for the mean-field critical indices of the Bethe lattice, the exact or experimental values of critical indices below the upper critical dimension do not obey this relation. This clearly indicates that hypothesis (6.256 and 6.257) cannot be applied for lattices below the upper critical dimension.

To avoid this difficulty, other approaches have been developed. So, we may, for example, instead of (4.24) consider the cluster-size distribution in the form (Fisher and Essam 1961):

$$n_s(p,q) = p^s \sum_{t_s} g_{t_s} q^{t_s}, \tag{6.280}$$

where q is a parameter, we initially consider it to be independent of p.

Utilizing the definition (6.253) of the partition function again, for its derivatives with respect to p we find

$$\frac{dZ^E}{dp} = \sum_s s n_s(p,q), \tag{6.281}$$

$$\frac{d^2 Z^E}{dp^2} = \sum_s s^2 n_s(p,q), \tag{6.282}$$

which would return us to the previous formalism if we substituted $q = 1 - p$ in all formulae later.

Another approach is called *an approach of a ghost field* (Griffiths 1967; Kasteleyn and Fortuin 1969; Coniglio 1976; Reynolds et al. 1977). Similar to magnetic systems, the cluster-size distribution is assumed to contain interactions of each cluster site with the external magnetic field *h:*

$$n_s(p,h) = e^{hs} \sum_{t_s} g_{t_s} p^s (1-p)^{t_s}. \tag{6.283}$$

Defining the partition function by (6.253) and differentiating it with respect to the field, we find

$$\frac{dZ^E}{dh} = \sum_s s n_s(p,h), \tag{6.284}$$

$$\frac{d^2 Z^E}{dh^2} = \sum_s s^2 n_s(p,h). \tag{6.285}$$

Substituting then $h = 0$, we return to the previous formulae.

These approaches seem to be self-consistent. Why should we not accept the developed formalism as an analogy with statistical physics? Unfortunately, there are

reasons for criticism. To illustrate it, let us return to the simple example of the Bethe lattice below the percolation threshold.

Firstly, in statistical physics we get used to the situation when the probability of fluctuations is determined by the "clash" of two "fast" multipliers, depending exponentially on N in the thermodynamic limit $N \to +\infty$. The product of two "fast" dependences generates a very narrow maximum of probability, corresponding to the most probable macrostate of a system.

Probability (6.273) imitates this type of behavior. Here, the number g_s of lattice s-animals, provided by the Bethe lattice result (4.55) from Chap. 4, is the function increasing very "fast" with the increase of s in the limit $s \to +\infty$:

$$g_s = \frac{const}{s^\tau} e^{s \ln \frac{1}{p_C (1-p_C)^{(Z-2)}}} = \frac{const}{s^\tau} e^{s/T^{eff}(p_C)}. \tag{6.286}$$

On the contrary, the probability $w^E_{\{s\}}$ of microstates, given by (6.271) for the Bethe lattice, decreases very "fast" with the increase of s in the limit $s \to +\infty$.

However, as we have said, probability (6.273) only imitates the expected behavior. Indeed, there is no narrow maximum of this probability. Instead, the dependence $W^E_{\{\{s\}\}} \propto n_s$ monotonically decreases with the increase of s (the point of maximum is $s = 0$)!

Why has this happened? Such a situation is possible only if one exponential dependence on s completely cancels out another. In other words,

$$\begin{aligned} W^E_{\{\{s\}\}} &= g_s w^E_{\{s\}} \propto \frac{1}{s^\tau} e^{s/T^{eff}(p_C)} e^{-s/T^{eff}(p)} = \frac{1}{s^\tau} e^{-s\left\{\frac{1}{T^{eff}(p)} - \frac{1}{T^{eff}(p_C)}\right\}} \\ &= \frac{1}{s^\tau} e^{-c(p)s} = n_s, \end{aligned} \tag{6.287}$$

leaving no narrow maximum but only the decaying dependence on s. Thereby, maximum of the obtained probability distribution $W^E_{\{\{s\}\}}$ corresponds to $s = 0$ and returns no interesting results.

Therefore, the product of two "fast" dependences is not enough to guarantee the applicability of the formalism of statistical physics. In addition, one of these dependencies (generally, the statistical weight) must be complex enough not to be cancelled immediately by the second dependence.

The statistical physics would also no longer work if the statistical weight of a thermodynamic system were determined by a simple exponential dependence $g_E \propto \underline{\underline{O}}(E^\alpha) e^{const \cdot E}$ on the energy of a system. If $const < 1/T$, the statistical weight would be canceled by Gibbs probability, leading to the maximum of probability at near zero energy. The point of this maximum would no longer be determined by the "clash" of two exponential dependencies on E but by the product of one exponential dependence $e^{-\left(\frac{1}{T} - const\right)E}$ and one power-law dependence $\underline{\underline{O}}(E^\alpha)$. But, as we saw in Chap. 2, the formalism of statistical physics works well only with the logarithmic

accuracy. Therefore, it would fail to describe such a "degenerate" case, and we would have to start to develop the new formalism from the beginning.

Secondly, returning to the question why we do not consider the developed approach (6.253–273) to be a complete analogy with statistical physics, we see that for susceptibility (6.264) the fluctuation–dissipation theorem is valid only in the vicinity of the percolation threshold when $\chi \propto \tilde{S}$. Beyond this neighborhood, the true susceptibility is $\tilde{S}$, not χ.

But $\tilde{S}$ is not the second derivative of the logarithm of the partition function, defined by (6.253). Instead, it is determined by

$$\tilde{S} \equiv \frac{\sum_s s^2 n_s(p)}{\sum_s s n_s(p)} = \frac{d}{d(-c)} \ln \sum_s s n_s(p) = \frac{d}{d(-c)} \ln \frac{d}{d(-c)} Z^E. \qquad (6.288)$$

In other words, instead of putting the logarithm under the sign of the second derivative, we should put it between the differentiating operators. This indicates that the averaged order parameter is not the derivative of the logarithm of the partition function but the logarithm of the derivative of the partition function: not $\frac{d \ln Z^E}{d(-c)}$, but $\ln \frac{dZ^E}{d(-c)} = \ln p$.

Although we have developed some analogy with statistical physics, the complete solution of the problem remains a mystery. We leave the solution of this problem to the reader as an exercise.

6.11 The FBM: The Fluctuation–Dissipation Theorem

Next in this chapter, we consider the fluctuation–dissipation behavior of the fiber-bundle model (FBM) representing damage phenomena (Abaimov 2009). In the ε-ensemble, it is easy to define the susceptibility of the system. Let us recall expression (5.22) for the ensemble partition function,

$$Z^{\varepsilon-\mathrm{E}} \equiv \sum_{\{D\}} e^{-\beta^{eff} ND} = \sum_{\{\{D\}\}} \Gamma_{\{\{D\}\}} e^{-\beta^{eff} ND}, \text{ where} \qquad (6.289)$$

$$\beta^{eff} \equiv \frac{1}{T^{eff}} \equiv \ln \frac{1 - P(E\varepsilon)}{P(E\varepsilon)}. \qquad (6.290)$$

Following the discussion of the magnetic systems, it is reasonable to choose $\left(-\beta^{eff}\right)$ as a field parameter and ND as an order parameter. The specific susceptibility is

then defined as the response of the specific averaged order parameter to the change in the field parameter:

$$\chi \equiv \frac{\partial \langle D \rangle_{\varepsilon-\mathrm{E}}}{\partial(-\beta^{eff})}. \tag{6.291}$$

Differentiating the partition function (6.289) twice with respect to the field parameter, we find

$$\frac{\partial Z^{\varepsilon-\mathrm{E}}}{\partial(-\beta^{eff})} = \sum_{\{D\}} ND e^{-\beta^{eff} ND} = Z^{\varepsilon-\mathrm{E}} \langle ND \rangle_{\varepsilon-\mathrm{E}}, \tag{6.292}$$

$$\frac{\partial^2 Z^{\varepsilon-\mathrm{E}}}{\partial(-\beta^{eff})^2} = \sum_{\{D\}} (ND)^2 e^{-\beta^{eff} ND} = Z^{\varepsilon-\mathrm{E}} \left\langle (ND)^2 \right\rangle_{\varepsilon-\mathrm{E}}. \tag{6.293}$$

Comparing (6.291) and (6.292), we see that the susceptibility is the second derivative of the logarithm of the partition function:

$$N\chi = \frac{\partial^2 \ln Z^{\varepsilon-\mathrm{E}}}{\partial(-\beta^{eff})^2}. \tag{6.294}$$

Substituting the partition function here, we find the susceptibility of the system:

$$\chi = D_0(1 - D_0). \tag{6.295}$$

However, we are more interested not in finding the susceptibility but in proving the fluctuation–dissipation theorem. Differentiating the logarithm twice, we find the connection of the susceptibility with the fluctuations of the order parameter:

$$\begin{aligned} N\chi &= \frac{1}{Z^{\varepsilon-\mathrm{E}}} \frac{\partial^2 Z^{\varepsilon-\mathrm{E}}}{\partial(-\beta^{eff})^2} - \left(\frac{1}{Z^{\varepsilon-\mathrm{E}}} \frac{\partial Z^{\varepsilon-\mathrm{E}}}{\partial(-\beta^{eff})} \right)^2 \\ &= \left\langle (ND)^2 \right\rangle_{\varepsilon-\mathrm{E}} - \langle ND \rangle_{\varepsilon-\mathrm{E}}^{\ 2} = \left\langle \left(ND - \langle ND \rangle_{\varepsilon-\mathrm{E}} \right)^2 \right\rangle_{\varepsilon-\mathrm{E}}. \end{aligned} \tag{6.296}$$

We have proved the first part of the fluctuation–dissipation theorem: The susceptibility, as the response of the order parameter to the change in the field parameter, equals the variance of the order parameter. To prove the second part of the theorem, we should build the correlation function whose integral would be equal to the susceptibility.

It is also easy to accomplish—we need only to define the effective spin variables σ_i. We substitute each fiber i by a spin σ_i which equals +1 if the fiber is intact and 0

if the fiber is broken. Then, in terms of the new spin variables the damage parameter D is defined by

$$D = 1 - \frac{1}{N}\sum_{i=1}^{N}\sigma_i. \tag{6.297}$$

Substituting this parameter into variance (6.296), we find

$$\begin{aligned} N\chi &= \left\langle (ND)^2 \right\rangle_{\varepsilon-\mathrm{E}} - \left\langle ND \right\rangle_{\varepsilon-\mathrm{E}}^{2} \\ &= \left\langle \left(\sum_{i=1}^{N}\sigma_i \right)\left(\sum_{j=1}^{N}\sigma_j \right) \right\rangle_{\varepsilon-\mathrm{E}} - \left\langle \sum_{i=1}^{N}\sigma_i \right\rangle_{\varepsilon-\mathbf{E}} \left\langle \sum_{j=1}^{N}\sigma_j \right\rangle_{\varepsilon-\mathrm{E}} \\ &= \sum_{i=1}^{N}\sum_{j=1}^{N}\left(\left\langle \sigma_i\sigma_j \right\rangle_{\varepsilon-\mathrm{E}} - \left\langle \sigma_i \right\rangle_{\varepsilon-\mathrm{E}} \left\langle \sigma_j \right\rangle_{\varepsilon-\mathrm{E}} \right). \end{aligned} \tag{6.298}$$

Due to the symmetry of choice of site i on the lattice, we substitute one of the sums by N:

$$N\chi = N\sum_{j=1}^{N}\left(\left\langle \sigma_{i_0}\sigma_j \right\rangle_{\varepsilon-\mathrm{E}} - \left\langle \sigma_{i_0} \right\rangle_{\varepsilon-\mathrm{E}} \left\langle \sigma_j \right\rangle_{\varepsilon-\mathrm{E}} \right), \tag{6.299}$$

which provides the sought relation between the susceptibility and the integral of the correlation function:

$$\chi = \sum_{j=1}^{N}\left(\left\langle \sigma_{i_0}\sigma_j \right\rangle_{\varepsilon-\mathrm{E}} - \left\langle \sigma_{i_0} \right\rangle_{\varepsilon-\mathrm{E}} \left\langle \sigma_j \right\rangle_{\varepsilon-\mathrm{E}} \right). \tag{6.300}$$

In the σ-ensemble, the probability (5.39) of a microstate $\{D\}$ no longer obeys the functional dependence of Gibbs probability (the distribution of probabilities is not Gibbsian). Thereby we can define neither the partition function of the ensemble nor the susceptibility as the second derivative of the logarithm of this partition function.

How then can we define the susceptibility? Damage D_0 seems to be a good candidate to play the role of the order parameter while the reasonable choice of the field parameter is the external force σ as the boundary condition of the ensemble. The susceptibility is then naturally defined as the response of the order parameter to the change in the field parameter:

$$\chi \propto \frac{\partial D_0}{\partial \sigma}. \tag{6.301}$$

This hypothesis seems to be supported by our results from Chap. 5, where the characteristic time (5.60) of relaxation processes was proportional to $\chi \propto \dfrac{\partial D_0}{\partial \sigma}$ in analogy with (3.164).

Recalling the parabolic dependence (5.52) of the stress σ on D_0 in the vicinity of the spinodal point, we immediately find

$$\chi \propto \frac{1}{|\sigma - \sigma_S|^{\gamma_\sigma^S}}, \tag{6.302}$$

where the spinodal index $\gamma_\sigma^S = 1/2$ coincides with the spinodal index (3.126) of the magnetic system, $\gamma_h^S = 1/2$, and with the spinodal index $\theta_\sigma^S = 1/2$ of (5.63).

However, in spite of the fact that hypothesis (6.301) is beautiful and returns the reasonable value of the mean-field spinodal index, it is, in fact, wrong! The reason of such a harsh conclusion is that hypothesis (6.301) does not obey the fluctuation–dissipation theorem.

How can we prove that? Defining the susceptibility in this chapter, we have discussed its role in the fluctuation–dissipation theorem. However, what we have not discussed yet is a special role played by the susceptibility in the theory of phase transitions. We overcome this drawback in the following sections. Simultaneously, it will help us to answer the question about the susceptibility definition in the σ-ensemble.

6.12 The Ising Model

First, we consider the mean-field approach (3.85) of the ferromagnetic n.n. Ising model:

$$\mathrm{H}_{\{\sigma\}} = -\mu h N m_{\{\sigma\}} - \mu A N m_{\{\sigma\}}{}^2. \tag{6.303}$$

The probability of a fluctuation $\{\{m\}\}$ is

$$W_{\{\{m\}\}}^{CE} = \Gamma_{\{\{m\}\}} w_{\{m\}}^{CE}, \text{ where} \tag{6.304}$$

$$\Gamma_{\{\{m\}\}} \approx_{\ln} \left(\frac{1+m}{2}\right)^{-N\frac{1+m}{2}} \left(\frac{1-m}{2}\right)^{-N\frac{1-m}{2}}, \tag{6.305}$$

$$w_{\{m\}}^{CE} = \frac{1}{Z^{CE}} e^{-\mathrm{H}_{\{m\}}/T}. \tag{6.306}$$

The maximum of $W_{\{\{m\}\}}^{CE}$,

$$\left.\frac{\partial \ln W_{\{\{m\}\}}^{CE}}{\partial m}\right|_{m_0} = 0, \tag{6.307}$$

corresponds to the equilibrium magnetization m_0 determined by the equation of state (3.86):

$$m_0 = \tanh(\beta\mu(h + 2Am_0)). \tag{6.308}$$

In the vicinity of the critical point $T_C = 2A\mu$, we expand this equation as

$$0 = -h + 2atm_0 + 4b{m_0}^3, \tag{6.309}$$

$$\text{where } a = A \text{ and } b = \frac{A}{6}. \tag{6.310}$$

Let us expand the logarithm of (6.304) in powers of fluctuating m in the vicinity of m_0:

$$\ln W^{CE}_{\{\{m\}\}} = \ln W^{CE}_{\{\{m_0\}\}} + \frac{1}{2}\frac{\partial^2 \ln W^{CE}_{\{\{m\}\}}}{\partial m^2}\bigg|_{m_0}(m-m_0)^2 + \frac{1}{6}\frac{\partial^3 \ln W^{CE}_{\{\{m\}\}}}{\partial m^3}\bigg|_{m_0}(m-m_0)^3 + \frac{1}{24}\frac{\partial^4 \ln W^{CE}_{\{\{m\}\}}}{\partial m^4}\bigg|_{m_0}(m-m_0)^4. \tag{6.311}$$

For the second derivative, expanding in small t, h, and m, we find

$$\frac{1}{N}\frac{\partial^2 \ln W^{CE}_{\{\{m\}\}}}{\partial m^2}\bigg|_{m_0} = -\frac{1}{2}\frac{1}{1+m_0} - \frac{1}{2}\frac{1}{1-m_0} + 2\beta\mu A \approx -t - {m_0}^2 = -\frac{1}{2A\chi}, \tag{6.312}$$

where we have utilized (3.115) for the magnetic susceptibility.

In a similar manner, we find the third and fourth derivatives:

$$\frac{1}{N}\frac{\partial^3 \ln W^{CE}_{\{\{m\}\}}}{\partial m^3}\bigg|_{m_0} = -2m_0, \tag{6.313}$$

$$\frac{1}{N}\frac{\partial^4 \ln W^{CE}_{\{\{m\}\}}}{\partial m^4}\bigg|_{m_0} = -2. \tag{6.314}$$

Substituting (6.312) into (6.311) and exponentiating the obtained expansion, we find the Gaussian probability distribution of fluctuations in the vicinity of the point m_0:

$$W^{CE}_{\{\{m\}\}} \propto e^{-\frac{(Nm-Nm_0)^2}{4A(N\chi)}}, \tag{6.315}$$

where, as we already know, the susceptibility plays the role of the variance of the distribution and determines the amplitude of the relative fluctuations of the magnetization:

$$\frac{\delta Nm}{Nm} \propto \sqrt{\frac{\chi}{N}}. \tag{6.316}$$

We have seen similar expression (2.151) before, in Chap. 2. In addition to that result, now we find that the numerator of this expression is not just unity but the square root of the susceptibility.

As we know from Chap. 3, the magnetic susceptibility diverges in the vicinity of both the critical and spinodal points. Thereby the second derivative (6.312) becomes zero. This means the divergence of fluctuations (6.316) which become infinite at the critical or spinodal points.

Let us firstly approach the critical point $m_C = 0$, $h_C = 0$. The third derivative (6.313) is also zero at the critical point while the fourth derivative remains nonzero. The probability distribution $W^{CE}_{\{\{m\}\}}$ stops being Gaussian. Instead, there emerges the probability distribution determined by the 4th-order term in expansion (6.311):

$$W^{CE}_{\{\{m\}\}} \propto e^{-\frac{(Nm-Nm_0)^4}{12N^3}}. \tag{6.317}$$

For the relative fluctuations of the magnetization this provides:

$$\frac{\delta Nm}{Nm} \propto \frac{1}{\sqrt[4]{N}}. \tag{6.318}$$

On the contrary, if we approach the spinodal point, $m_S = \mp\sqrt{-\frac{at_S}{6b}}$, $h_S = \pm 8b\left(-\frac{at_S}{6b}\right)^{3/2}$, the third derivative (6.313) is not zero. This means that the local Gaussian maximum of the probability distribution is broken leaving the point of inflection leading to the global maximum of probability. Therefore, it is meaningless to discuss small fluctuations at the spinodal point.

Finally, we should recall that in accordance with (2.269) and (2.270), the definition of the free energy potential is to be equivalent to the minus logarithm of the probability distribution. Therefore, instead of maximizing probability for the Ising model, we could minimize the Helmholtz free energy. In this case, we would

again invoke Figs. 3.6 and 3.7 of Chap. 3. So, we would discuss, for example, the inflection point not of the probability distribution but the inflection point of the free energy in Fig. 3.7. However, we have preferred to consider in this chapter the probability distribution and not the free energy with the purpose to compare the results later with the FBM under the constant force boundary condition which possesses neither a partition function nor a free energy potential.

6.13 The FBM: The ε-Ensemble

For the FBM, we consider the ε-ensemble first. The probability of a fluctuation $\{\{D\}\}$ is provided by (5.9) and (5.10). The point of a maximum of this probability distribution is determined by

$$\left.\frac{\partial \ln W^{\varepsilon-\mathrm{E}}_{\{\{D\}\}}}{\partial D}\right|_{D_0} = 0, \tag{6.319}$$

generating the equation of state (5.14):

$$D_0 = P(E\varepsilon). \tag{6.320}$$

Similar to the previous section, we expand the logarithm of the probability distribution $W^{\varepsilon-\mathrm{E}}_{\{\{D\}\}}$ in a series of small fluctuations of D in the vicinity of the equilibrium value D_0:

$$\ln W^{\varepsilon-\mathrm{E}}_{\{\{D\}\}} = \ln W^{\varepsilon-\mathrm{E}}_{\{\{D_0\}\}} + \frac{1}{2}\left.\frac{\partial^2 \ln W^{\varepsilon-\mathrm{E}}_{\{\{D\}\}}}{\partial D^2}\right|_{D_0} (D-D_0)^2 + \ldots \tag{6.321}$$

For the second derivative we find again the connection with the susceptibility, given by (6.295):

$$\frac{1}{N}\left.\frac{\partial^2 \ln W^{\varepsilon-\mathrm{E}}_{\{\{D\}\}}}{\partial D^2}\right|_{D_0} = -\frac{1}{D_0(1-D_0)} = -\frac{1}{\chi}. \tag{6.322}$$

With the exception of trivial points $D_0 = 0$ and $D_0 = 1$, susceptibility (6.295) is always nonsingular. Therefore, the distribution of probabilities $W^{\varepsilon-\mathrm{E}}_{\{\{D\}\}}$ is always Gaussian:

$$W^{\varepsilon-\mathrm{E}}_{\{\{D\}\}} \propto e^{-\frac{(ND-ND_0)^2}{2(N\chi)}}. \tag{6.323}$$

Again, the susceptibility plays in this distribution the role of the squared standard deviation due to its association with the variance of ND. For the relative fluctuation of ND we, therefore, find

$$\frac{\delta ND}{ND} \propto \sqrt{\frac{\chi}{N}}. \tag{6.324}$$

6.14 The FBM: The σ-Ensemble

In the σ-ensemble, the distribution of probabilities is not Gibbsian, the partition function is not defined, and therefore, we cannot find the susceptibility as the second derivative of its logarithm.

However, there is no need to define the susceptibility by means of the derivatives of the partition function. Instead, we can utilize the fluctuation–dissipation theorem and define the susceptibility by its connection with the variance of the order parameter:

$$N\chi = \left\langle \left(ND - \langle ND \rangle_{\sigma-\mathrm{E}} \right)^2 \right\rangle_{\sigma-\mathrm{E}}. \tag{6.325}$$

We can find directly this variance by averaging D and D^2 in the σ-ensemble. However, it is much easier to look again at the squared standard deviation of the probability distribution $W^{\sigma-\mathrm{E}}_{\{\{D\}\}}$ itself.

The distribution of probabilities $W^{\sigma-\mathrm{E}}_{\{\{D\}\}}$ in the σ-ensemble is given by (5.40). The point of maximum

$$\left. \frac{\partial \ln W^{\sigma-\mathrm{E}}_{\{\{D\}\}}}{\partial D} \right|_{D_0} = 0 \tag{6.326}$$

determines the equation of state (5.41):

$$D_0 = P\left(\frac{\sigma}{1-D_0} \right). \tag{6.327}$$

Next, we again expand the logarithm of the probability $W^{\sigma-\mathrm{E}}_{\{\{D\}\}}$ in a series of small fluctuations of D in the vicinity of the equilibrium value D_0:

$$\ln W^{\sigma-\mathrm{E}}_{\{\{D\}\}} = \ln W^{\sigma-\mathrm{E}}_{\{\{D_0\}\}} + \frac{1}{2} \left. \frac{\partial^2 \ln W^{\sigma-\mathrm{E}}_{\{\{D\}\}}}{\partial D^2} \right|_{D_0} (D-D_0)^2 + \frac{1}{6} \left. \frac{\partial^3 \ln W^{\sigma-\mathrm{E}}_{\{\{D\}\}}}{\partial D^3} \right|_{D_0} (D-D_0)^3$$
$$+ \frac{1}{24} \left. \frac{\partial^4 \ln W^{\sigma-\mathrm{E}}_{\{\{D\}\}}}{\partial D^4} \right|_{D_0} (D-D_0)^4. \tag{6.328}$$

For the second derivative, we find

$$\frac{1}{N}\frac{\partial^2 \ln W^{\sigma-\mathrm{E}}_{\{\{D\}\}}}{\partial D^2}\bigg|_{D_0} = -\frac{1}{D_0(1-D_0)}\left(1-\frac{\sigma}{(1-D_0)^2}P'\big|_{D_0}\right)^2 \tag{6.329}$$

or, applying (5.46):

$$\frac{1}{N}\frac{\partial^2 \ln W^{\sigma-\mathrm{E}}_{\{\{D\}\}}}{\partial D^2}\bigg|_{D_0} = -\frac{1}{D_0(1-D_0)}\left(1+\frac{\sigma}{1-D_0}\frac{dD_0}{d\sigma}\right)^{-2}. \tag{6.330}$$

Being consistent with the previous discussions, we define the susceptibility as the squared standard deviation of the probability distribution which represents the variance of *D:*

$$\frac{1}{N}\frac{\partial^2 \ln W^{\sigma-\mathrm{E}}_{\{\{D\}\}}}{\partial D^2}\bigg|_{D_0} \equiv -\frac{1}{\chi} \text{ or} \tag{6.331}$$

$$\chi \equiv D_0(1-D_0)\left(1-\frac{\sigma}{(1-D_0)^2}P'\big|_{D_0}\right)^{-2} = D_0(1-D_0)\left(1+\frac{\sigma}{1-D_0}\frac{dD_0}{d\sigma}\right)^2. \tag{6.332}$$

When the susceptibility is not divergent, exponentiating (6.328), we return to the case of the Gaussian distribution:

$$W^{\sigma-\mathrm{E}}_{\{\{D\}\}} \propto e^{-\frac{(ND-ND_0)^2}{2(N\chi)}}. \tag{6.333}$$

The relative fluctuations of *D* are determined by the previous dependence:

$$\frac{\delta ND}{ND} \propto \sqrt{\frac{\chi}{N}}. \tag{6.334}$$

In the vicinity of the spinodal point susceptibility (6.332) diverges as

$$\chi \propto \left(\frac{dD_0}{d\sigma}\right)^2 \tag{6.335}$$

in contrast to our previous hypothesis (6.301).

Recalling (5.52), for the spinodal index $\gamma^{\mathrm{S}}_{\sigma}$, defined by

$$\chi \propto \frac{1}{|\sigma - \sigma_{\mathrm{S}}|^{\gamma_\sigma^{\mathrm{S}}}}, \tag{6.336}$$

we find the mean-field value $\gamma_\sigma^{\mathrm{S}} = 1$ which is quite different from the wrong value $\gamma_\sigma^{\mathrm{S}} = 1/2$ predicted by hypothesis (6.301).

Susceptibility (6.332) corresponds to the variance (6.325) of D just by definition. To prove that it also equals the integral of the correlation function, we introduce the effective variables σ_i and substitute (6.297) into (6.325). The rest of the proof follows formulae (6.297–6.300).

The last relation we have to build for the susceptibility is to prove that it is a response of some order parameter to the change in some field parameter. The sought order parameter has been, in fact, already chosen implicitly to be ND by our decision that the distribution of probabilities $W_{\{\{D\}\}}^{\sigma-\mathrm{E}}$ should depend on D (and not, e.g., on some function of D). Hence, we built fluctuations $\left\{\left\{D\right\}\right\}$ and expanded $W_{\{\{D\}\}}^{\sigma-\mathrm{E}}$ in a series of these small fluctuations. This led to the definition (6.332) of the susceptibility (as the squared standard deviation of $W_{\{\{D\}\}}^{\sigma-\mathrm{E}}$) to represent the variance of the already chosen order parameter ND.

Therefore, the order parameter is proposed to be D by all our formulae above. On the contrary, the choice of the field parameter π is much more ambiguous. Writing the susceptibility as the response of D_0 to the change in π,

$$\chi = \frac{\partial D_0}{\partial \pi}, \tag{6.337}$$

we find the last by integration

$$\begin{aligned}
\pi &= \int_0^{D_0} \frac{d\tilde{D}_0}{\tilde{D}_0(1-\tilde{D}_0)} \left(1 - \frac{1}{1-\tilde{D}_0} \frac{P^{-1}(\tilde{D}_0)}{\dfrac{dP^{-1}(\tilde{D}_0)}{d\tilde{D}_0}} \right)^2 \\
&= \int_0^{D_0} \frac{d\tilde{D}_0}{\tilde{D}_0(1-\tilde{D}_0)} \left(1 - \frac{1}{1-\tilde{D}_0} \frac{1}{\dfrac{d\ln P^{-1}(\tilde{D}_0)}{d\tilde{D}_0}} \right)^2,
\end{aligned} \tag{6.338}$$

where we have substituted σ from the inversion of the equation of state (5.41):

$$\sigma = (1 - D_0) P^{-1}(D_0). \tag{6.339}$$

After integrating (6.338), we should find the dependence $D_0(\sigma)$ from the equation of state and substitute it into the result of integration, leaving the dependence of the field parameter π only on the value of σ.

Unfortunately, it is impossible to perform integration (6.338) analytically for an arbitrary strength CDF P.

Problem 6.14.1

Find the field parameter π for the particular case of the strength distribution (5.33 and 34).

Solution: Substituting (5.34) into (5.41), we find the equation of state:

$$\sigma = (1-D_0)(D_0(s_2-s_1)+s_1) \text{ or} \tag{6.340}$$

$$D_0 = \frac{s_2 - 2s_1 \pm \sqrt{s_2{}^2 - 4\sigma(s_2-s_1)}}{2(s_2-s_1)}. \tag{6.341}$$

Differentiating (6.340) with respect to D_0, we find the derivative

$$\frac{d\sigma}{dD_0} = s_2 - 2(D_0(s_2-s_1)+s_1). \tag{6.342}$$

Substituting this derivative and (6.340) into the definition of susceptibility (6.332), we obtain:

$$\chi = D_0(1-D_0)\left(\frac{(1-D_0)(s_2-s_1)}{s_2-2(D_0(s_2-s_1)+s_1)}\right)^2. \tag{6.343}$$

To find the field parameter π, we should integrate this dependence

$$\pi = \int_0^{D_0} \frac{d\tilde{D}_0}{\chi(\tilde{D}_0)} \text{ or} \tag{6.344}$$

$$\pi = \int_0^{D_0} \frac{dx}{x(1-x)}\left(2 - \frac{s_2/(s_2-s_1)}{1-x}\right)^2. \tag{6.345}$$

Integrating, we find the functional dependence $\pi = \pi(D_0)$. Substituting here D_0 from (6.341), we obtain the connection of the field parameter π with the external force, $\pi = \pi(\sigma)$, which is cumbersome and, therefore, not presented here.

Why does quantity (6.332), which we have proved to be the susceptibility of the system, differ from our earlier hypothesis (6.301)? The one reason that we already know is that hypothesis (6.301) does not correspond to the variance (6.325) of the order parameter.

But hypothesis (6.301) was indirectly supported by our expectations that the characteristic time (5.60) of the decay of relaxation processes should be proportional to the susceptibility of the system and, thereby, in the vicinity of the spinodal point should diverge with the same exponent. In Chap. 5, we found $\theta_\sigma^{\mathrm{S}} = 1/2$ which coincides with $\gamma_\sigma^{\mathrm{S}} = 1/2$ but not with $\gamma_\sigma^{\mathrm{S}} = 1$. This supports hypothesis (6.301) but not the true susceptibility (6.332). Why?

To answer this question, we should understand that susceptibility (6.332) represents the probability distribution $W_{\{\{D\}\}}^{\sigma-\mathrm{E}}$ in the ensemble. This probability distribution is responsible for differences of the quenched strength disorder among the systems of the ensemble; however, it cannot represent the evolution of fiber failures during a relaxation process for one particular system.

For magnetic systems, this question did not arise because in Chap. 3 the probability distribution $W_{\{\{m\}\}}^{CE}$ represented the statistical properties of reversible fluctuations $\{\{m\}\}$ and was responsible for both the differences among the systems in the ensemble and evolution (3.107) of one particular system $\left(\text{since } -\dfrac{\partial F_{\{\{m\}\}}}{\partial m} \propto \dfrac{\partial \ln W_{\{\{m\}\}}^{CE}}{\partial m} \right)$. Thereby, the susceptibility determined both the variance of fluctuations and characteristic time of relaxation processes.

In the case of damage phenomena, this logic is no longer applicable since we no longer consider reversible phenomena. Damage is irreversible.

Unfortunately, in our model the probability $W_{\{\{D\}\}}^{\sigma-\mathrm{E}}$ does not take into account the irreversibility. Thereby, the probability distribution $W_{\{\{D\}\}}^{\sigma-\mathrm{E}}$ does represent the fluctuations of the quenched disorder in the ensemble; but we cannot rely on it to describe the dynamical evolution of avalanches in one particular system.

Instead of applying the Ginzburg–Landau–Langevin equation, in Chap. 5 we considered the irreversible iteration equation (5.54). This equation directly employed the probabilities to fail for each fiber separately if this fiber was supposed to carry the prescribed load. Since the iteration equation is not associated with susceptibility (6.332), we can no longer expect the critical indices to be equal to one another.

Why is the Ginzburg–Landau–Langevin equation (3.107) not valid for the irreversible processes? Because this equation employs the probability $W_{\{\{D\}\}}^{\sigma-\mathrm{E}}$, describing the ensemble, not the evolution of a particular system. Imagine, for example, that the current microstate of the system is $\{\overset{|||}{|||}||\}$ when the first three fibers are broken. Let us suppose that at the next state of the system the Ginzburg–Landau–Langevin equation recommends us to break one more fiber. But this equation employs the

probability $W^{\sigma-\mathrm{E}}_{\{\{D\}\}}$ which is the product $W^{\sigma-\mathrm{E}}_{\{\{D\}\}} = \Gamma_{\{\{D\}\}} w^{\sigma-\mathrm{E}}_{\{D\}}$. Here, the statistical weight $\Gamma_{\{\{D\}\}}$ considers all possible microstates, including those when some of the first three fibers are still intact. Therefore, generating its recommendation, the Ginzburg–Landau–Langevin equation considered microstates with arbitrary distribution of broken fibers as possible outcomes. For example, one of the considered outcomes, when we break one more fiber, was not necessarily $\{|||||\} \Rightarrow \{|||||\}$ or $\{|||||\} \Rightarrow \{|||||\}$, but may be $\{|||||\} \Rightarrow \{|||||\}$.

But damage is irreversible. Therefore, our system cannot heal the broken fibers, and the majority of microstates, contained in the statistical weight $\Gamma_{\{\{D\}\}}$, are not suitable for its further evolution. For the Ising model, we did not have such a problem since nothing prevents for all spins to flip at once. However, we may encounter similar difficulties for heterogeneous gas–liquid systems when, for example, a void within the volume of the liquid cannot disappear or appear immediately but only through a chain of intermediate states. In other words, the system becomes partially irreversible and, applying the Ginzburg–Landau–Langevin equation here, we should consider not the total set of microstates as possible outcomes, but only some subset of them.

As we have mentioned above, for the general case of an arbitrary distribution P, we cannot find the field parameter π analytically. However, we can find its scaling in the vicinity of the spinodal point. Indeed, considering definition (6.337) applied in the close proximity of the point S,

$$\chi = \frac{D_0 - D_\mathrm{S}}{\pi_0 - \pi_\mathrm{S}}, \tag{6.346}$$

and recalling (5.52), we obtain

$$\chi \propto \frac{\sqrt{|\sigma_0 - \sigma_\mathrm{S}|}}{|\pi_0 - \pi_\mathrm{S}|}. \tag{6.347}$$

But for the susceptibility, we have found divergence (6.336) with $\gamma^{\mathrm{S}}_{\sigma} = 1$. Substituting it into (6.347), we find the scaling of the field parameter π in the vicinity of the spinodal point:

$$|\pi_0 - \pi_\mathrm{S}| \propto |\sigma_0 - \sigma_\mathrm{S}|^{3/2}. \tag{6.348}$$

The new field parameter π is a "true" field parameter, coupled to the order parameter D_0 by the standard deviation of the probability distribution; and we should reconsider all scaling dependencies, recreating them with respect to this parameter instead of the previous field parameter σ. With the aid of (5.52) and (6.336), we find the scaling of the order parameter,

$$\left|D_0 - D_{\mathrm{S}}\right| \propto \left|\pi_0 - \pi_{\mathrm{S}}\right|^{\beta_\pi^{\mathrm{S}}}, \tag{6.349}$$

and of the susceptibility,

$$\chi \propto \frac{1}{\left|\pi_0 - \pi_{\mathrm{S}}\right|^{\gamma_\pi^{\mathrm{S}}}}, \tag{6.350}$$

with two new spinodal indices: $\beta_\pi^{\mathrm{S}} = 1/3$ and $\gamma_\pi^{\mathrm{S}} = 2/3$.

But let us return to the fluctuations in the ensemble. The divergence of susceptibility (6.332) at the spinodal point leads to the divergence of fluctuations (6.334). Thereby the second derivative (6.331) becomes zero, transferring the leading role in expansion (6.328) to higher-order corrections.

The third derivative at the spinodal point is zero also

$$\frac{1}{N}\frac{\partial^3 \ln W_{\{\{D\}\}}^{\sigma-\mathrm{E}}}{\partial D^3}\bigg|_{D_{\mathrm{S}}} = 0; \tag{6.351}$$

but the fourth derivative happens to be nonzero:

$$\frac{1}{N}\frac{\partial^4 \ln W_{\{\{D\}\}}^{\sigma-\mathrm{E}}}{\partial D^4}\bigg|_{D_{\mathrm{S}}} = -3\frac{1}{D_{\mathrm{S}}(1-D_{\mathrm{S}})}\left(\frac{1-D_{\mathrm{S}}}{\sigma_{\mathrm{S}}}\frac{d^2\sigma}{dD^2}\bigg|_{\mathrm{S}}\right)^2. \tag{6.352}$$

Substituting these derivatives into expansion (6.328), we obtain the distribution of probabilities in the vicinity of the spinodal point:

$$W_{\{\{D\}\}}^{\sigma-\mathrm{E}} \propto e^{-\frac{(ND-ND_0)^4}{8N^3 D_{\mathrm{S}}(1-D_{\mathrm{S}})\left(\frac{1-D_{\mathrm{S}}}{\sigma_{\mathrm{S}}}\frac{d^2\sigma}{dD^2}\Big|_{\mathrm{S}}\right)^{-2}}} \tag{6.353}$$

The fact that the third derivative is zero at the spinodal point indicates that our model (as well as, e.g., the van der Waals equation) does not contain a mechanism to operate with the unstable states $\frac{\partial D_0}{\partial \sigma} < 0$. In particular, the model provides maxima of probability $W_{\{\{D\}\}}^{\sigma-\mathrm{E}}$ for both the unstable state $D_{0,2}$ and stable state $D_{0,1}$ from Fig. 5.9, not taking into account the fact that in the unstable state $D_{0,2}$ the fibers continue to fail leading to lower values of the supported force σ. The correct model should possess the nonzero third derivative to generate the point of inflection.

Instead, in our model we see two maxima of the probability distribution $W^{\sigma-\mathrm{E}}_{\{\{D\}\}}$, one at $D_{0,1}$, another at $D_{0,2}$, which coalesce when the external force σ approaches its spinodal value. This is very similar to the critical behavior and has led several studies to the conclusion that this is not the first-order phase transition but a continuous phase transition.

The question whether point S in Fig. 5.9 is a spinodal point or a critical point still remains open in the literature (Rundle and Klein 1989; Sornette and Sornette 1990; Blumberg Selinger et al. 1991; Sornette and Sammis 1995; Buchel and Sethna 1996; Andersen et al. 1997; Buchel and Sethna 1997; Zapperi et al. 1997; Sornette and Andersen 1998; Zapperi et al. 1999a, b; Kun et al. 2000; Moreno et al. 2000, 2001; Pradhan et al. 2002; Bhattacharyya et al. 2003; Sornette 2006; Abaimov 2008; 2009; and ref. therein) and requires further investigation.

References

Abaimov, S.G.: Applicability and non-applicability of equilibrium statistical mechanics to non-thermal damage phenomena. J. Stat. Mech., **9**, P09005 (2008). doi:10.1088/1742–5468/2008/09/P09005

Abaimov, S.G.: Applicability and non-applicability of equilibrium statistical mechanics to non-thermal damage phenomena: II. Spinodal behavior. J. Stat. Mech., **3**, P03039 (2009)

Abaimov, S.G.: Statistical Physics of Complex Systems (in Russian), 2nd ed. Synergetics: From Past to Future, Vol. **57**, URSS, Moscow (2013)

Andersen, J.V., Sornette, D., Leung, K.-T.: Tricritical behavior in rupture induced by disorder. Phys. Rev. Lett. **78**(11), 2140–2143 (1997)

Balescu, R.: Equilibrium and Nonequilibrium Statistical Mechanics. John Wiley, New York (1975)

Baxter, R.J.: Exactly Solved Models in Statistical Mechanics. Academic, London (1982)

Bhattacharyya, P., Pradhan, S., Chakrabarti, B.K.: Phase transition in fiber bundel models with recursive dynamics. Phys. Rev. E **67**(4), 046122 (2003)

Blumberg Selinger, R.L., Wang, Z.-G., Gelbart, W.M., Ben-Shaul, A.: Statistical-thermodynamic approach to fracture. Phys. Rev. A **43**(8), 4396–4400 (1991)

Buchel, A., Sethna, J.P.: Elastic theory has zero radius of convergence. Phys. Rev. Lett. **77**(8), 1520–1523 (1996)

Buchel, A., Sethna, J.P.: Statistical mechanics of cracks: Fluctuations, breakdown, and asymptotics of elastic theory. Phys. Rev. E **55**(6), 7669–7690 (1997)

Cardy, J.: Scaling and Renormalization in Statistical Physics. Cambridge University Press, Cambridge (1996)

Coniglio, A.: Some cluster-size and percolation problems for interacting spins. Phys. Rev. B **13**(5), 2194–2207 (1976)

Domb, C., Green, M.S., Lebowitz, J.L. (eds.): Phase Transitions and Critical Phenomena. Academic, London (1972–2001)

Essam, J.W.: Percolation theory. Rep. Prog. Phys. **43**(7), 833–912 (1980)

Fisher, M.E.: Rigorous inequalities for critical-point correlation exponents. Phys. Rev. **180**(2), 594 (1969)

Fisher, M.E., Essam, J.W.: Some cluster size and percolation problems. J. Math. Phys. **2**(4), 609–619 (1961)

Ginzburg, V.L.: Some remarks on phase transitions of the second kind and the microscopic theory of the ferroelectric materials. Soviet Phys. Solid State **2**, 1824–1834 (1960)

Goldenfeld, N.: Lectures on Phase Transitions and the Renormalization Group. Perseus Books Publishing, L.L.C., Reading (1992)
Green, G.: An Essay on the Application of Mathematical Analysis to the Theories of Electricity ang Magnetism. T. Wheelhouse, Nottingham (1828)
Griffiths, R.B.: Correlations in Ising ferromagnets: II. External magnetic fields. J. Math. Phys. **8**(3), 484–489 (1967)
Huang, K.: Statistical Mechanics, 2nd ed. John Wiley & Sons, New York (1987)
Kadanoff, L.P.: Scaling, universality and operator algebras. In: Domb, C., Green, M.S. (eds.) Phase Transitions and Critical Phenomena, Vol. **5a**, pp. 1–34. Academic, London (1976)
Kadanoff, L.P.: Statistical Physics: Statistics, Dymanics and Renormalization. World Scientific, Singapore (2000)
Kasteleyn, P.W., Fortuin, C.M.: Phase Transitions in Lattice Systems with Random Local Properties. J. Phys. Soc.**26**(suppl.), 11–14 (1969)
Kun, F., Zapperi, S., Herrmann, H.J.: Damage in fiber bundle models. Eur. Phys. J. B **17**(2), 269–279 (2000)
Landau, L.D., Lifshitz, E.M.: Statistical Physics, Part 1, 3rd ed. Course of Theoretical Physics, Vol. **5**. Pergamon, Oxford (1980)
Ma, S.K.: Modern Theory of Critical Phenomena. Benjamin, Reading (1976)
Moreno, Y., Gómez, J.B., Pacheco, A.F.: Fracture and second-order phase transitions. Phys. Rev. Lett. **85**(14), 2865–2868 (2000)
Moreno, Y., Gómez, J.B., Pacheco, A.F.: Phase transitions in load transfer models of fracture. Physica A **296**(1–2), 9–23 (2001)
Pathria, R.K.: Statistical Mechanics, 2nd ed. Butterworth-Heinemann, Oxford (1996)
Pradhan, S., Bhattacharyya, P., Chakrabarti, B.K.: Dynamic critical behavior of failure and plastic deformation in the random fiber bundle model. Phys. Rev. E **66**(1), 016116 (2002)
Reif, F.: Fundamentals of Statistical and Thermal Physics. McGraw-Hill, New York (1965)
Reynolds, P.J., Stanley, H.E., Klein, W.: Ghost fields, pair connectedness, and scaling: Exact results in one-dimensional percolation. J. Phys. A **10**(11), L203–L209 (1977)
Rundle, J.B., Klein, W.: Nonclassical nucleation and growth of cohesive tensile cracks. Phys. Rev. Lett. **63**(2), 171–174 (1989)
Sornette, A., Sornette, D.: Earthquake rupture as a critical-point: Consequences for telluric precursors. Tectonophysics **179**(3–4), 327–334 (1990)
Sornette, D.: Critical Phenomena in Natural Sciences, 2nd ed. Springer, Berlin (2006)
Sornette, D., Andersen, J.V.: Scaling with respect to disorder in time-to-failure. Eur. Phys. J. B **1**(3), 353–357 (1998)
Sornette, D., Sammis, C.G.: Complex critical exponents from renormalization-group theory of earthquakes: Implications for earthquake predictions. J. Phys. I **5**(5), 607–619 (1995)
Stanley, H.E.: Introduction to Phase Transitions and Critical Phenomena. Clarendon, Oxford (1971)
Stauffer, D., Aharony, A.: Introduction to Percolation Theory, 2nd ed. Taylor & Francis, London (1994)
Zapperi, S., Ray, P., Stanley, H.E., Vespignani, A.: First-order transition in the breakdown of disordered media. Phys. Rev. Lett. **78**(8), 1408–1411 (1997)
Zapperi, S., Ray, P., Stanley, H.E., Vespignani, A.: Analysis of damage clusters in fracture processes. Physica A **270**(1–2), 57–62 (1999a)
Zapperi, S., Ray, P., Stanley, H.E., Vespignani, A.: Avalanches in breakdown and fracture processes. Phys. Rev. E **59**(5), 5049–5057 (1999b)

Chapter 7
The Renormalization Group

Abstract In the previous chapters, we saw that the mean-field approach always determines the critical or spinodal indices as simple integers or rational fractions, like 1 or 5/2. Even more, such indices are considered to be an indicator that the behavior of a system is dominated by the mean-field approach. If the exact solution of a problem provided such simple numbers, the dimensionality of the considered system would probably be above the upper critical dimension, when the mean-field approach represents the exact critical indices, or interactions in the system would be long-range which would lead to the same result.

However, as we know from Chap. 6, the Ginzburg criterion states that if the dimensionality of a system with short-range interactions is lower than the upper critical dimension (which generally corresponds to our three-dimensional space), the mean-field approach is too crude to describe the behavior of the system within the critical region. The mean-field approach may still be considered as a good illustration of a phase transition, but the predicted values of the critical indices are far from being accurate.

Besides, as we discussed in Chap. 6, the mean-field approach is not at all capable to explain the influence of the dimensionality of a system on its behavior—there would be much poorer diversity of the critical indices if all systems obeyed the mean-field approach exactly.

And what is even worse, it is not possible to improve the accuracy of the mean-field approach within the method itself. Only the introduction of newer approaches, within the mean-field approach as well as independent, can improve the situation.

In this chapter, we consider the renormalization group (RG) of coarse graining as an alternative approach to the mean-field approximation. The critical indices determined by this technique are no longer simple integers or fractions. And what is more important is that the RG approach contains, within its formalism, the recipes of how to make calculations more accurate so that the predicted results would be closer to the experimental values.

That is why the RG has been met with such general approval in the literature. Even for the critical indices themselves, to distinguish them from the "habitual" mean-field

S. G. Abaimov, *Statistical Physics of Non-Thermal Phase Transitions,*
Springer Series in Synergetics, DOI 10.1007/978-3-319-12469-8_7

values, a special term *anomalous dimension* has been introduced which represents the difference between the real index and its value provided by Landau theory[1].

7.1 Scaling

As we saw in Chap. 6, the topological behavior of clusters depends significantly on the scale considered. The characteristic length dividing two types of behavior is the correlation length ξ which diverges at the critical point.

On scales less than the correlation length, the fluctuations are probable so that they dominate the behavior of a system. These scales could be called *the scales of fluctuation foam* (similar to the term "quantum foam" with very close meaning). There is no own characteristic length on these scales, so the clusters are fractal (scale invariant) and come in all shapes and sizes, from the lattice constant to the correlation length.

Scale invariant is not only the distribution of clusters but also the inner structure of these clusters. An example is shown in Fig. 7.1 where we plot a cluster near the percolation threshold.

In Fig. 7.1a, we consider the finest scale of linear size $L = 31$. Increasing the size of the window through which we are looking at the system, we see in Fig. 7.1b that although for $L = 62$ the piece of the cluster is four times bigger, the fractal structure of the cluster remains the same—if we distinguished only the cluster perimeter and were not able to distinguish separate sites, we would not see any difference between Figs. 7.1a and b.

In Fig. 7.1c, we again increase the scale twice—now the linear size of the window is $L = 125$. And again, nothing changes in the fractal structure of the piece cut from the cluster by the frame of the window.

We observe the first changes when the scale becomes $L = 250$ (Fig. 7.1d). The gaps in the cluster are now wider, while the "external" boundary of the cluster is less fractal and starts to resemble a perimeter of a nonfractal compact set. What has happened? Probably, we have crossed the scale of the correlation length.

[1] Here, we have oversimplified the definition of the term "anomalous dimension." It can be demonstrated by dimensional analysis that the mean-field critical indices are the consequence of the presence of a characteristic length in the system—the correlation length. However, the *anomalous* "additions" on top of the mean-field values can be explained only by the presence of another characteristic length in the system beside the correlation length. This new characteristic length is generally associated with the lattice constant. However, as we see in this chapter, the lattice constant does not survive the coarse graining. Therefore, we support the point of view that this new characteristic length of the system is associated not with the lattice constant but with the properties of scale invariance. So in Chap. 1, we saw that the dimensionality of a fractal depended not on the properties of the initial branch but on the properties of the fractal generator. Something similar happens during the coarse graining as well when critical indices depend not on the lattice constant but on the correspondence we build between the initial and new models during the RG transformation. We return to this question, in more detail, in the next chapter where we will find that the RG transformation can explain the scaling appearing in a system in the vicinity of its critical point.

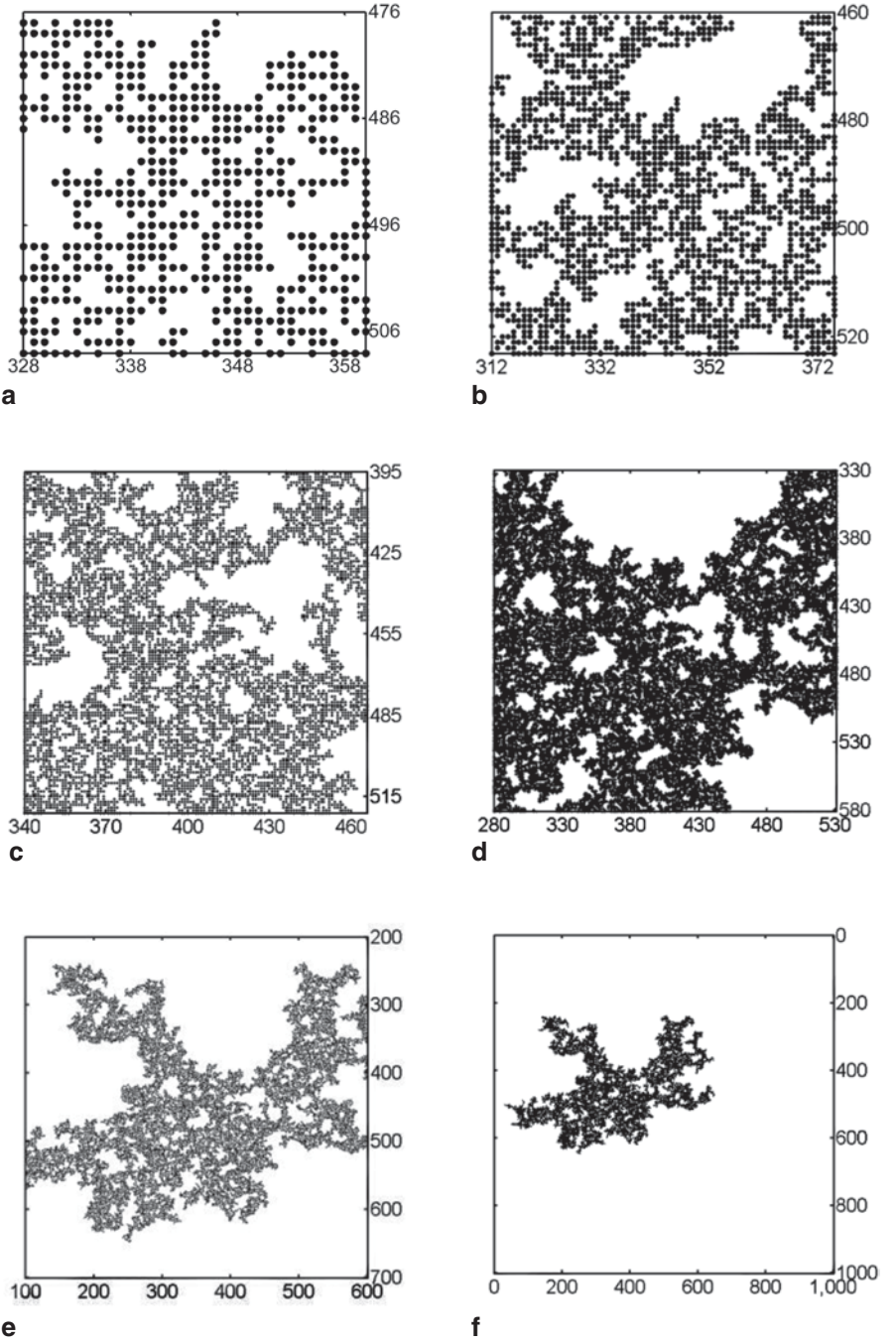

Fig. 7.1 The structure of a cluster near the percolation threshold

These changes become even more apparent for $L = 500$ and $L = 1000$ in Figs. 7.1e and f. On scales larger than the correlation length, the structure of the cluster is no longer fractal.

The fractality (scale invariance) of the system's fluctuations on scales smaller than the correlation length is the physical property itself. And since it is a physical property, it should be described by some physical laws. It would be very important to find these laws because they presented something new in the description of our system; something that we have not studied in the previous chapters.

The scale invariance means that if we know the behavior of the system in Fig. 7.1a, we should be able to derive the system's behavior in Fig. 7.1b just by simple analogy. Would it be possible to develop the laws of the system's behavior just from the concept that the system is scale invariant?

Such a technique does exist and is called *coarse graining*. The mathematical formalism of this technique is based on *the renormalization group* (RG). Initially, the RG was developed in quantum field theory but nobody suspected then that it is also applicable in statistical physics. The first ideas of coarse graining were postulated by Leo Kadanoff (Kadanoff 1966). Later, the mathematical formalism of the RG in application to critical phenomena in statistical physics was developed by Kenneth Wilson (Wilson 1971a, b; Wilson and Kogut 1974) who, in 1982, was awarded the Nobel Prize for this discovery.

The appearance of the RG caused a boom of new discoveries in the literature. The RG has happened to be applicable not only to thermal systems but also to systems which have never been considered by statistical physics. This has led to the hope that the formalism of statistical physics is able to describe not only thermal but also complex phenomena.

The RG transformation can be formulated in both momentum and real (coordinate) space. In our book, we consider only the real-space RG because this approach has been applied to a wide variety of complex systems. Besides, the real-space renormalization seems, to us, to be the most illustrative.

We start our discussion with the approach that we consider to be the most rigorous.

7.2 RG Approach of a Single Survivor: One-Dimensional Magnetic Systems

To study RG, we start from the simplest example—the canonical ensemble (CE) of the one-dimensional ferromagnetic nearest-neighbor (n.n.) Ising model with the periodic boundary conditions (a chain of spins forms a ring). The Hamiltonian of the model is

$$\mathrm{H}_{\{\sigma\}} = -h\mu \sum_{i=1}^{N} \sigma_i - J \sum_{i=1}^{N} \sigma_i \sigma_{i+1}. \tag{7.1}$$

Here, $\sigma_{N+1} \equiv \sigma_1$ due to the periodicity of the boundary conditions.

For convenience, we rewrite Hamiltonian (7.1) as

$$\mathrm{H}_{\{\sigma\}} = -h\mu\sum_{i=1}^{N}\frac{\sigma_i+\sigma_{i+1}}{2} - J\sum_{i=1}^{N}\sigma_i\sigma_{i+1}. \tag{7.2}$$

The partition function of the CE is

$$Z^{CE} = \sum_{\{\sigma\}}\exp\left(\beta h\mu\sum_{i=1}^{N}\frac{\sigma_i+\sigma_{i+1}}{2} + \beta J\sum_{i=1}^{N}\sigma_i\sigma_{i+1}\right), \tag{7.3}$$

while Gibbs probability distribution of microstates $\{\sigma\}$ is

$$w_{\{\sigma\}}^{CE} = \frac{1}{Z^{CE}}\exp\left(\beta h\mu\sum_{i=1}^{N}\frac{\sigma_i+\sigma_{i+1}}{2} + \beta J\sum_{i=1}^{N}\sigma_i\sigma_{i+1}\right). \tag{7.4}$$

We see that neither temperature nor interaction constants are included in the probability distribution (7.4) separately but form two combinations:

$$K_1 = \frac{\beta h\mu}{2},\ K_2 = \beta J, \tag{7.5}$$

which are called *the coupling constants*. In terms of these coupling constants, Gibbs probability distribution is

$$w_{\{\sigma\}}^{CE} = \frac{1}{Z^{CE}}\exp\left(\sum_{i=1}^{N}\left\{K_1(\sigma_i+\sigma_{i+1}) + K_2\sigma_i\sigma_{i+1}\right\}\right). \tag{7.6}$$

Coarse graining means that, investigating the system's behavior, we do not want to see all the microdetails of how one spin interacts with another. Indeed, why should we, when at rougher scales the behavior is the same?

Therefore, we are going to coarse grain our model by half. In other words, we are going to halve the number of degrees of freedom in the system so that the remaining half would represent the same behavior. Therefore, we consider the number N of spins in the chain to be even.

To perform the coarse graining, we divide the chain of spins into cells with $b = 2$ spins in each cell (Fig. 7.2, top). Then, we build a new model when each cell of the initial model generates only one spin in the new model (Fig. 7.2).

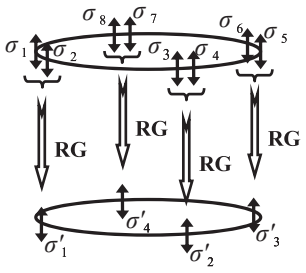

Fig. 7.2 The RG in action: Each cell of the initial model (*top*) generates one spin in the new model (*bottom*)

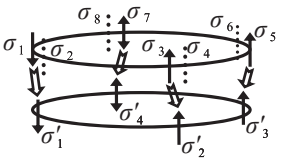

Fig. 7.3 The single-survivor approach

The new model contains twice less spins: $N' = N/2$. The lattice constant of the new model is twice larger. However, we intend the new lattice to look exactly like the initial one with the same lattice constant. Therefore, we rescale the length of the new model twice so that the RG does not change the lattice constant but the length of the model shrinks twice. To put it in a different way, we always measure the length of the model in units of the lattice constant. Our RG transformation has the parameter $b = 2$. We see now that $r = 1/b$ is *the scale factor* which determines how the size of the lattice shrinks.

Each cell of the initial model contains two spins. Possible microconfigurations of spin orientations for a cell are $\{\uparrow\uparrow\}$, $\{\uparrow\downarrow\}$, $\{\downarrow\uparrow\}$, and $\{\downarrow\downarrow\}$. To form a microstate $\{\sigma\}$ of the initial system, we should prescribe to each cell of it one of these four microconfigurations.

The new model has its own microstates $\{\sigma'\}$. Somehow, we should build the correspondence between the initial microstates $\{\sigma\}$ and the final microstates $\{\sigma'\}$.

There are no explicit rules how we do that. This is the subjectivity introduced into the formalism by an investigator (very much like a hypothesis in Bayesian analysis). Even more, as we will see later, this is the measure of the skillfulness of the investigator. The more ingenuous the investigator was inventing the rule of correspondence, the more accurate results the RG would return.

Another side of this concept is that since the investigator introduces some subjectivity into the formalism, the RG cannot provide exact results. We should understand that the RG is merely a tool helping us to investigate the system's behavior; and it returns not exact but approximate results.

Our purpose is to keep the behavior of the system unchanged during the coarse graining. What if, for microstates $\{\sigma'\}$ to represent microstates $\{\sigma\}$, we would keep the orientations of some spins untouched, while not paying attention to the orientations of the rest of the spins?

In other words, we look at the orientation of the first spin in a cell and make the orientation of the spin on the new lattice the same. Simultaneously, we completely disregard the orientation of the second spin in the cell (Fig. 7.3). We call it *the single-survivor approach* since only the first spin in the cell "survives" the RG transformation and is transferred onto the new lattice with its orientation intact. The second spin "disappears." Therefore, this procedure is also called *decimation*.

As a result, two cell microconfigurations, $\{\uparrow\uparrow\}$ and $\{\uparrow\downarrow\}$, provide the new spin oriented "up," while another two cell microconfigurations, $\{\downarrow\uparrow\}$ and $\{\downarrow\downarrow\}$, provide the new spin oriented "down." Thereby, we have built the rule of the correspondence between the initial microstates $\{\sigma\}$ and the new microstates $\{\sigma'\}$. Also, we see that there are many initial microstates $\{\sigma\}$ corresponding to the same final microstate $\{\sigma'\}$—these initial microstates $\{\sigma\}$ differ from each other by the orientations of the second spins in the cells.

To keep the behavior of the system unchanged, we should require that the probability to observe a microstate $\{\sigma'\}$ on the new lattice would equal the probability to observe the corresponding microstates $\{\sigma\}$ on the initial lattice. In other words, for each particular $\{\sigma'\}$, we should sum Gibbs probabilities (7.6) of the corresponding $\{\sigma\}$—this provides the very probability of $\{\sigma'\}$:

$$= \sum_{\sigma_2,\sigma_4,\ldots,\sigma_{2i},\ldots,\sigma_N=\pm 1} w^{CE}_{\{\sigma_1=\sigma'_1,\sigma_2,\sigma_3=\sigma'_2,\sigma_4,\ldots,\sigma_{2i-1}=\sigma'_i,\sigma_{2i},\ldots,\sigma_{N-1}=\sigma'_{N/2},\sigma_N\}}. \quad (7.7)$$

Here, we keep the "surviving" spins unchanged, $\sigma_{2i-1} = \sigma'_i$, while summing over the orientations of the "disappearing" spins σ_{2i}. Equality (7.7) is *the rule of invariant probabilities* of our RG transformation.

Our purpose is that the new system would resemble the initial one in all respects. Under the term "resemble," we understand that the lattice shape and the functional form of the Hamiltonian (spins interact with the external field and in pairs) should be exactly the same for the initial and final systems. The systems similar in this sense are said to belong to the same *universality class*.

Therefore, the new Hamiltonian $\mathrm{H}'_{\{\sigma'\}}$ and Gibbs probability $w'^{CE'}_{\{\sigma'\}}$ should have the same functional dependences, (7.1) and (7.6), on spin orientations:

$$\mathrm{H}'_{\{\sigma'\}} = -h'\mu' \sum_{i=1}^{N/2} \sigma'_i - J' \sum_{i=1}^{N/2} \sigma'_i \sigma'_{i+1}, \quad (7.8)$$

$$w'^{CE'}_{\{\sigma'\}} = \frac{1}{Z'^{CE'}} \exp\left(\sum_{i=1}^{N/2} \left\{ K'_1 (\sigma'_i + \sigma'_{i+1}) + K'_2 \sigma'_i \sigma'_{i+1} \right\} \right). \quad (7.9)$$

However, both coupling constants, K'_1 and K'_2, can change. In other words, coarse graining of our system may change its field parameters, T and h, or interaction constants, μ and J, for the sake of keeping unchanged both the lattice shape and the functional form of the Hamiltonian. This was the purpose of introduction of the coupling constants as quantities that "absorb" all parameters which may change.

Substituting (7.6) and (7.9) into (7.7), we find

$$\begin{aligned}
&\frac{1}{Z'^{CE'}} \prod_{i=1}^{N/2} \exp\left(K'_1 (\sigma'_i + \sigma'_{i+1}) + K'_2 \sigma'_i \sigma'_{i+1} \right) \\
&= \sum_{\sigma_2,\sigma_4,\ldots,\sigma_N=\pm 1} \frac{1}{Z^{CE}} \prod_{i=1}^{N/2} \exp\left(\begin{array}{l} K_1 (\sigma_{2i-1}|_{\sigma'_i} + \sigma_{2i}) + K_2\, \sigma_{2i-1}|_{\sigma'_i}\, \sigma_{2i} \\ + K_1 (\sigma_{2i} + \sigma_{2i+1}|_{\sigma'_{i+1}}) + K_2 \sigma_{2i}\, \sigma_{2i+1}|_{\sigma'_{i+1}} \end{array} \right) \\
&= \frac{1}{Z^{CE}} \prod_{i=1}^{N/2} \sum_{\sigma_{2i}=\pm 1} \exp\left(K_1 (\sigma'_i + 2\sigma_{2i} + \sigma'_{i+1}) + K_2 \sigma_{2i} (\sigma'_i + \sigma'_{i+1}) \right) \\
&= \frac{1}{Z^{CE}} \prod_{i=1}^{N/2} 2 \exp\left(K_1 (\sigma'_i + \sigma'_{i+1}) \right) \cosh\left(2K_1 + K_2 (\sigma'_i + \sigma'_{i+1}) \right). \quad (7.10)
\end{aligned}$$

This equality should be valid for arbitrary orientations of spins σ'_i and σ'_{i+1}:

$$\sigma'_i = +1, \sigma'_{i+1} = +1 \Rightarrow \frac{1}{\sqrt[N/2]{Z'^{CE'}}} e^{2K'_1 + K'_2} = \frac{2}{\sqrt[N/2]{Z^{CE}}} e^{2K_1} \cosh(2K_1 + 2K_2),$$

$$\sigma'_i = +1, \sigma'_{i+1} = -1 \Rightarrow \frac{1}{\sqrt[N/2]{Z'^{CE'}}} e^{-K'_2} = \frac{2}{\sqrt[N/2]{Z^{CE}}} \cosh(2K_1),$$

$$\sigma'_i = -1, \sigma'_{i+1} = +1 \Rightarrow \frac{1}{\sqrt[N/2]{Z'^{CE'}}} e^{-K'_2} = \frac{2}{\sqrt[N/2]{Z^{CE}}} \cosh(2K_1),$$

$$\sigma'_i = -1, \sigma'_{i+1} = -1 \Rightarrow \frac{1}{\sqrt[N/2]{Z'^{CE'}}} e^{-2K'_1 + K'_2} = \frac{2}{\sqrt[N/2]{Z^{CE}}} e^{-2K_1} \cosh(2K_1 - 2K_2). \quad (7.11)$$

There are three independent equations here and three independent variables: K'_1, K'_2, and $Z'^{CE'}$. The solution is

$$\frac{\beta' h' \mu'}{2} = K'_1 = K_1 + \frac{1}{4} \ln \frac{\cosh(2K_1 + 2K_2)}{\cosh(2K_1 - 2K_2)}, \quad (7.12)$$

$$\beta' J' = K'_2 = \frac{1}{4} \ln \cosh(2K_1 + 2K_2) + \frac{1}{4} \ln \cosh(2K_1 - 2K_2) - \frac{1}{2} \ln \cosh(2K_1), \quad (7.13)$$

$$\ln Z'^{CE'} = \ln Z^{CE} - N \ln \left\{ \begin{matrix} \sqrt{2} \cosh^{1/8}(2K_1 + 2K_2) \\ \times \cosh^{1/8}(2K_1 - 2K_2) \cosh^{1/4}(2K_1) \end{matrix} \right\}. \quad (7.14)$$

These equations associate the new coupling constants with the initial coupling constants. We see that the RG transformation has created a system identical to the initial one, but supported at different values of the field parameters and interaction constants. The initial and final systems, connected by the RG transformation, are said to belong to the same *universality class*.

From the third equation, we see that for any values of the coupling constants, the logarithm of the partition function always decreases, at least by the quantity $N \ln \sqrt{2}$ (when all cosh functions equal unity). This happens because the coarse graining reduces the degrees of freedom so that the partition function must decrease. The minimal decrease,

$$Z'^{CE'} = \frac{Z^{CE}}{2^{N/2}}, \quad (7.15)$$

corresponds to the case when both coupling constants are zero (when temperature is infinite). This result could be foreseen. When the temperature is very high, the exponential functions $e^{-\beta \mathrm{H}_{\{\sigma\}}}$ in the partition function all equal unity without regard to the energies of particular microstates. The partition function, as the sum of these exponential functions over the energy spectrum, transforms into the total number

2^N of microstates in the Ising model. Therefore, by reducing the number of degrees of freedom twofold, we should divide the partition function by $2^{N/2}$.

The RG transformation is not always built in a manner similar to the approach presented above. Often, an additional coupling constant K_0 is introduced in Gibbs probability (7.6):

$$w_{\{\sigma\}}^{CE} = \frac{1}{Z^{CE}} \exp\left(\sum_{i=1}^{N} \{K_0 + K_1(\sigma_i + \sigma_{i+1}) + K_2\sigma_i\sigma_{i+1}\} \right). \tag{7.16}$$

The purpose of this coupling constant is to keep the partition function unchanged:

$$K'_0 = 2K_0 + 2\ln\left\{ \begin{array}{l} \sqrt{2}\cosh^{1/8}(2K_1 + 2K_2) \\ \times \cosh^{1/8}(2K_1 - 2K_2)\cosh^{1/4}(2K_1) \end{array} \right\}, \tag{7.17}$$

while

$$Z'^{CE'} = Z^{CE}. \tag{7.18}$$

For thermal systems, the difference between the two approaches is just a matter of notation or convenience. However, we do not consider the introduction of K_0 to be expedient for several reasons. First, the coarse graining must reduce the number of degrees of freedom which requires the decrease of the partition function. Introducing K_0, we replace intuitively understandable decrease of the partition function by the change of the new coupling constant K_0.

Second, in the future, we will pay attention to the fixed points, $K'_i = K_i \ \forall\, i$, of the RG transformation on the space of coupling constants. In other words, we will be looking for the values of coupling constants which the RG transformation does not change. Obviously, the partition function cannot have a fixed value and always decreases. Thereby, the new coupling constant K_0 must always increase during the RG transformation and cannot have a fixed value either. And after the introduction of K_0, the RG cannot have a fixed point on the space of coupling constants! So, we would have to say constantly that K_0 is not a true coupling constant, that it is a "white crow" among other coupling constants, and that we are looking for the fixed points of the RG on the reduced space of coupling constants when K_0 is not included in this space. So, finally, we will have to exclude K_0 from consideration.

What was the reason of introduction of K_0 in the literature? This coupling constant appears inevitably when instead of considering *rule* (7.7) *of invariant probabilities,* we build our RG transformation on *rule* (7.18) *of invariant partition function*. In other words, instead of equating probabilities (7.7) of corresponding states, we equate the partition functions (7.18) to guarantee that the behavior of the new model represents the behavior of the spins on the initial lattice. This means that to keep the behavior of the system unchanged, as unchanged we transfer from the initial system to the final system not the probabilities but the partition function!

For thermal systems, both approaches appear to be valid and return exactly the same results due to the fact that they differ only by the variable change. So, for thermal systems, this is just a matter of notation.

However, if we study complex systems like percolation or damage, these systems often do not possess the partition function as such. To find the susceptibility of the fiber-bundle model (FBM) under the constant load condition, we had to return in the previous chapter from the partition function formalism to the probability distribution itself.

Similarly, the RG transformations cannot be built on the base of rule (7.18) for these systems. Instead, we have to return to the probability distribution itself and to consider rule (7.7) when we keep invariant the probabilities of the corresponding states. Therefore, the rule (7.7) of invariant probabilities is more fundamental than the rule (7.18) of invariant partition function.

Here, we encounter that particular case when the application of the formalism of statistical physics to complex systems demonstrates in the result of the comparison analysis what is imperfect in statistical physics itself! Obviously, equating the probabilities appears much more reasonable and understandable intuitively than equating partition functions. Therefore, in future, as the rule of the RG transformation, we will always utilize (7.7).

Problem 7.2.1

In the absence of magnetic field, build the RG transformation for the one-dimensional ferromagnetic n.n. Ising model with the periodic boundary conditions when the cell of the RG transformation contains an arbitrary number b of spins.

Solution: The Hamiltonian of the system is

$$\mathrm{H}_{\{\sigma\}} = -J\sum_{i=1}^{N}\sigma_i\sigma_{i+1}, \tag{7.19}$$

the partition function of the CE is

$$Z^{CE} = \sum_{\{\sigma\}}\exp\left(\beta J\sum_{i=1}^{N}\sigma_i\sigma_{i+1}\right), \tag{7.20}$$

and Gibbs probability is

$$w_{\{\sigma\}}^{CE} = \frac{1}{Z^{CE}}\exp\left(\beta J\sum_{i=1}^{N}\sigma_i\sigma_{i+1}\right). \tag{7.21}$$

There is only one coupling constant in this case:

$$K = \beta J, \tag{7.22}$$

so Gibbs probability transforms into

$$w_{\{\sigma\}}^{CE} = \frac{1}{Z^{CE}}\exp\left(\sum_{i=1}^{N}K\sigma_i\sigma_{i+1}\right). \tag{7.23}$$

We divide the chain of spins into blocks of size b (assuming that N is a multiple of b). The first spin of each cell "survives" the RG transformation keeping its orientation in the new model (*the approach of a single survivor*). The rest of the spins in the cell "disappears" (*decimation*). For example, for $b = 3$, the initial cell microconfigurations $\{\uparrow\uparrow\uparrow\}$, $\{\uparrow\uparrow\downarrow\}$, $\{\uparrow\downarrow\uparrow\}$, and $\{\uparrow\downarrow\downarrow\}$ result in the spin oriented "up" on the new lattice. The rest of the cell microconfigurations transform into the spin oriented "down."

This is our subjective rule of microstate correspondence. After we have hypothesized it, the next step is straightforward—applying the rule (7.7) of the RG, we guarantee that the probabilities of the corresponding states are unchanged by the transformation:

$$w'^{CE'}_{\{\sigma'_1,\ldots\}} = \sum_{\sigma_2,\sigma_3,\ldots,\sigma_b,\ldots} w^{CE}_{\{\sigma_1=\sigma'_1,\sigma_2,\sigma_3,\ldots,\sigma_b,\ldots\}}. \tag{7.24}$$

In other words, for the given orientation of the "surviving" spin $\sigma_{ib-(b-1)} = \sigma'_i$, we sum the orientations of the "disappearing" spins $\sigma_{ib-(b-2)},\ldots,\sigma_{ib}$:

$$\begin{aligned}
&\frac{1}{Z'^{CE'}}\prod_{i=1}^{N/b}\exp\left(K'\sigma'_i\sigma'_{i+1}\right)\\
&\quad=\sum_{\ldots,\sigma_{ib-(b-2)},\sigma_{ib-(b-3)},\ldots,\sigma_{ib-1},\sigma_{ib},\ldots=\pm1}\frac{1}{Z^{CE}}\prod_{i=1}^{N/b}\exp\left(\begin{array}{l}K\sigma_{ib-(b-1)}\big|_{\sigma'_i}\sigma_{ib-(b-2)}\\ +K\sigma_{ib-(b-2)}\sigma_{ib-(b-3)}+\ldots\\ +K\sigma_{ib-1}\sigma_{ib}+K\sigma_{ib}\sigma_{ib+1}\big|_{\sigma'_{i+1}}\end{array}\right).
\end{aligned} \tag{7.25}$$

Noticing that equality

$$\cosh K(1+\sigma_i\sigma_j\tanh K) = e^{K\sigma_i\sigma_j} \tag{7.26}$$

is valid for arbitrary spin orientations $\sigma_i = \pm1, \sigma_j = \pm1$, we transform (7.25) into

$$\begin{aligned}
&\frac{1}{Z'^{CE'}}\prod_{i=1}^{N/b}\cosh K'\left(1+\sigma'_i\sigma'_{i+1}\tanh K'\right)\\
&\quad=\frac{1}{Z^{CE}}\prod_{i=1}^{N/b}\sum_{\substack{\sigma_{ib-(b-2)},\sigma_{ib-(b-3)},\ldots,\\ \sigma_{ib-1},\sigma_{ib}=\pm1}}\left(\begin{array}{l}\cosh^b K\times\left(1+\sigma_{ib-(b-1)}\big|_{\sigma'_i}\sigma_{ib-(b-2)}\tanh K\right)\\ \times\left(1+\sigma_{ib-(b-2)}\sigma_{ib-(b-3)}\tanh K\right)\times\ldots\\ \times\left(1+\sigma_{ib-1}\sigma_{ib}\tanh K\right)\times\left(1+\sigma_{ib}\sigma_{ib+1}\big|_{\sigma'_{i+1}}\tanh K\right)\end{array}\right).
\end{aligned} \tag{7.27}$$

Removing the brackets in the right-hand side, we obtain terms, containing the "disappearing" spins in the 0th, 1st, and 2nd powers. Since the sums go over two projections $\sigma_i = \pm 1$, all terms, linear in the "disappearing" spins, cancel themselves out.

So, in the right-hand side, only the terms with the 0th or 2nd powers of the "disappearing" spins remain. If a "disappearing" spin σ_i is in the 2nd power in a particular term, this term must have been formed as the product of $\sigma_{i-1}\sigma_i \tanh K$ and $\sigma_i\sigma_{i+1} \tanh K$. Therefore, this term contains σ_{i-1} and σ_{i+1} also. For this term not to be cancelled out, σ_{i-1} and σ_{i+1} must be in the 2nd powers. But then this term must also contain $\sigma_{i-2}{}^2$ and $\sigma_{i+2}{}^2$. And so on by induction.

As a result, we conclude that when the brackets in the right-hand side of (7.27) are removed, almost all terms are cancelled out leaving only two terms: the first is formed only by unities from all brackets, the second is formed only by $\sigma_i\sigma_{i+1} \tanh K$ from all brackets:

$$\begin{aligned}
&\frac{1}{Z'^{CE'}}\prod_{i=1}^{N/b}\cosh K'\left(1+\sigma'_i\sigma'_{i+1}\tanh K'\right) = \\
&= \frac{1}{Z^{CE}}\prod_{i=1}^{N/b}\sum_{\sigma_{ib-(b-2)},\sigma_{ib-(b-3)},\ldots,\,\sigma_{ib-1},\sigma_{ib}=\pm 1}\cosh^b K\left\{1\times\ldots\times 1+\right. \\
&\left.+\sigma_{ib-(b-1)}\Big|_{\sigma'_i}\sigma_{ib-(b-2)}{}^2\sigma_{ib-(b-3)}{}^2\ldots\sigma_{ib-1}{}^2\sigma_{ib}{}^2\sigma_{ib+1}\Big|_{\sigma'_{i+1}}\tanh^b K\right\} = \\
&= \frac{1}{Z^{CE}}\prod_{i=1}^{N/b}\cosh^b(K)\left\{1+\sigma'_i\sigma'_{i+1}\tanh^b K\right\}\sum_{\sigma_{ib-(b-2)},\sigma_{ib-(b-3)},\ldots,\,\sigma_{ib-1},\sigma_{ib}=\pm 1}1 = \\
&= \frac{1}{Z^{CE}}\prod_{i=1}^{N/b}\cosh^b(K)\left\{1+\sigma'_i\sigma'_{i+1}\tanh^b K\right\}2^{b-1}
\end{aligned} \tag{7.28}$$

The solution of this equation is

$$\tanh K' = \tanh^b K, \tag{7.29}$$

$$\ln Z'^{CE'} = \ln Z^{CE} - N\ln\frac{2^{\frac{b-1}{b}}\cosh K}{\cosh^{1/b} K'}. \tag{7.30}$$

Problem 7.2.2:

In the absence of magnetic field, build the RG transformation for the one-dimensional ferromagnetic n.n. Ising model with the periodic boundary conditions when the spins can have three possible values of projections: $\sigma_i = -1, 0, +1$ (*the spin*-1 *model* also known as *the Blume–Capel model,* (Blume 1966; Capel 1966)).

Solution: The Hamiltonian of the system is (7.19), the partition function of the CE is (7.20), and Gibbs probability is (7.21). Introducing the coupling constant (7.22), we transform Gibbs probability into (7.23).

For simplicity, in this problem, we consider the cell consisting of $b = 2$ spins (N is assumed to be even). For the rule of correspondence, we again utilize the approach of a single survivor: The first spin of each cell "survives" keeping its orientation, and the second spin"disappears." Equating probabilities in accordance with (7.7), we find

$$w'^{CE'}_{\{\sigma'_1,\sigma'_2,\ldots,\sigma'_i,\ldots\}} = \sum_{\sigma_2,\sigma_4,\ldots,\sigma_{2i},\ldots=-1,0,1} w^{CE}_{\{\sigma_1=\sigma'_1,\sigma_2,\sigma_3=\sigma'_2,\sigma_4,\ldots,\sigma_{2i-1}=\sigma'_i,\sigma_{2i},\ldots\}}. \tag{7.31}$$

In other words, for the given value $\sigma_{2i-1} = \sigma'_i$ of the "surviving" spin, we sum orientations of the "disappearing" spin σ_{2i}:

$$\begin{aligned}\frac{1}{Z'^{CE'}}\prod_{i=1}^{N/2}\exp(K'\sigma'_i\sigma'_{i+1}) &= \sum_{\sigma_2,\sigma_4,\ldots,\sigma_{2i},\ldots=-1,0,1}\frac{1}{Z^{CE}}\prod_{i=1}^{N/2}\exp\left(\begin{matrix}K\sigma_{2i-1}\big|_{\sigma'_i}\sigma_{2i}\\ +K\sigma_{2i}\sigma_{2i+1}\big|_{\sigma'_{i+1}}\end{matrix}\right)\\ &= \frac{1}{Z^{CE}}\prod_{i=1}^{N/2}\sum_{\sigma_{2i}=-1,0,1}\exp\left(K\sigma_{2i}\left(\sigma'_i+\sigma'_{i+1}\right)\right)\\ &= \frac{1}{Z^{CE}}\prod_{i=1}^{N/2}\left\{2\cosh\left(K\left(\sigma'_i+\sigma'_{i+1}\right)\right)+1\right\}.\end{aligned} \tag{7.32}$$

This equality should be valid for arbitrary orientations of spins σ'_i and σ'_{i+1}:

$$\begin{aligned}&\left.\begin{matrix}\sigma'_i=+1,\sigma'_{i+1}=+1\\ \sigma'_i=-1,\sigma'_{i+1}=-1\end{matrix}\right\}\Rightarrow\frac{1}{\sqrt[N/2]{Z'^{CE'}}}e^{K'}=\frac{1}{\sqrt[N/2]{Z^{CE}}}\left\{2\cosh(2K)+1\right\},\\ &\left.\begin{matrix}\sigma'_i=+1,\sigma'_{i+1}=-1\\ \sigma'_i=-1,\sigma'_{i+1}=+1\end{matrix}\right\}\Rightarrow\frac{1}{\sqrt[N/2]{Z'^{CE'}}}e^{-K'}=\frac{3}{\sqrt[N/2]{Z^{CE}}},\\ &\left.\begin{matrix}\sigma'_i=0,\sigma'_{i+1}=\pm1\\ \sigma'_i=\pm1,\sigma'_{i+1}=0\end{matrix}\right\}\Rightarrow\frac{1}{\sqrt[N/2]{Z'^{CE'}}}=\frac{1}{\sqrt[N/2]{Z^{CE}}}\left\{2\cosh(K)+1\right\},\\ &\sigma'_i=0,\sigma'_{i+1}=0\Rightarrow\frac{1}{\sqrt[N/2]{Z'^{CE'}}}=\frac{3}{\sqrt[N/2]{Z^{CE}}}.\end{aligned} \tag{7.33}$$

There are four independent equations here but only two unknown variables, K' and $Z'^{CE'}$. There is no possible solution of this system of equations.

For the first time, we have encountered the case when the RG seems to be inapplicable. However, such difficulties are usually easily overcome. What is the reason of the absence of a solution? That the number of the coupling constants is less than the number of the RG equations. If we introduced new coupling constants, the transformation would become possible.

What is the role of the coupling constants? We see that each coupling constant is responsible for its own type of spin interactions: one for interactions of spins with the external magnetic field, and another for the pair bi-spin interactions among spins.

Therefore, we may conclude that in the considered model, some interactions are overlooked. That is why we were not able to find another system belonging to the same universality class.

Next, we consider three coupling constants instead of one:

$$K_1 = \beta J,\ K_2 = 0, \text{ and } K_3 = 0. \tag{7.34}$$

The first coupling constant K_1, as before, is responsible for the pair spin interactions, the second coupling constant K_2 is responsible for the interactions of the second powers of spin projections with some effective field, and the third coupling constant K_3 is responsible for the second power of pair spin interactions:

$$Z^{CE} = \sum_{\{\sigma\}} \exp\left(\sum_{i=1}^{N} \left\{ K_1 \sigma_i \sigma_{i+1} + K_2 (\sigma_i{}^2 + \sigma_{i+1}{}^2) + K_3 (\sigma_i \sigma_{i+1})^2 \right\} \right), \tag{7.35}$$

$$w_{\{\sigma\}}^{CE} = \frac{1}{Z^{CE}} \exp\left(\sum_{i=1}^{N} \left\{ K_1 \sigma_i \sigma_{i+1} + K_2 (\sigma_i{}^2 + \sigma_{i+1}{}^2) + K_3 (\sigma_i \sigma_{i+1})^2 \right\} \right). \tag{7.36}$$

Why have we chosen these particular forms of interaction? Why not consider, for example, triple-spin interactions, quadro-spin interactions, or some other kind of interactions?

The most honest answer is: “Why not?”! We are trying to build the universality class for our particular system, but we do not know what this universality class is. If we were able to build the RG for some particular type of interactions, we would prove that our system belongs to the universality class of these interactions. Choosing other interactions, we may prove that it also belongs to a different universality class.

We again divide the lattice into cells of size $b = 2$ and again apply the approach of a single survivor. Substituting (7.36) into (7.31), we find

$$\frac{1}{Z'^{CE'}}\prod_{i=1}^{N/2}\exp\left(K_1'\sigma_i'\sigma_{i+1}'+K_2'(\sigma_i'^{\,2}+\sigma_{i+1}'^{\,2})+K_3'(\sigma_i'\sigma_{i+1}')^2\right)=$$

$$=\sum_{\sigma_2,\sigma_4,\ldots,\sigma_{2i},\ldots=-1,0,1}\frac{1}{Z^{CE}}\prod_{i=1}^{N/2}\exp\left\{K_1\,\sigma_{2i-1}\big|_{\sigma_i'}\sigma_{2i}+\right.$$

$$+K_2\left(\left(\sigma_{2i-1}\big|_{\sigma_i'}\right)^2+\sigma_{2i}^{\,2}\right)+K_3\left(\sigma_{2i-1}\big|_{\sigma_i'}\sigma_{2i}\right)^2+K_1\sigma_{2i}\,\sigma_{2i+1}\big|_{\sigma_{i+1}'}+$$

$$\left.+K_2\left(\sigma_{2i}^{\,2}+\left(\sigma_{2i+1}\big|_{\sigma_{i+1}'}\right)^2\right)+K_3\left(\sigma_{2i}\,\sigma_{2i+1}\big|_{\sigma_{i+1}'}\right)^2\right\}=$$

$$=\frac{1}{Z^{CE}}\prod_{i=1}^{N/2}\sum_{\sigma_{2i}=-1,0,1}\exp\left\{K_1\,\sigma_{2i}(\sigma_i'+\sigma_{i+1}')+\right.$$

$$\left.+K_2(\sigma_i'^{\,2}+2\sigma_{2i}^{\,2}+\sigma_{i+1}'^{\,2})+K_3\sigma_{2i}^{\,2}(\sigma_i'^{\,2}+\sigma_{i+1}'^{\,2})\right\}=$$

$$=\frac{1}{Z^{CE}}\prod_{i=1}^{N/2}\exp\left(K_2(\sigma_i'^{\,2}+\sigma_{i+1}'^{\,2})\right)\left\{2\cosh\left(K_1(\sigma_i'+\sigma_{i+1}')\right)\times\right.$$

$$\left.\times\exp\left(2K_2+K_3(\sigma_i'^{\,2}+\sigma_{i+1}'^{\,2})\right)+1\right\}. \tag{7.37}$$

This equality should be valid for any values of spin projections σ'_i and σ'_{i+1}:

$$\left.\begin{aligned}\sigma_i'=+1,\sigma_{i+1}'=+1\\ \sigma_i'=-1,\sigma_{i+1}'=-1\end{aligned}\right\}\Rightarrow\frac{1}{\sqrt[N/2]{Z'^{CE'}}}e^{K_1'+2K_2'+K_3'}$$

$$=\frac{1}{\sqrt[N/2]{Z^{CE}}}e^{2K_2}\left\{2\cosh\left(2K_1\right)e^{2K_2+2K_3}+1\right\},$$

$$\left.\begin{aligned}\sigma_i'=+1,\sigma_{i+1}'=-1\\ \sigma_i'=-1,\sigma_{i+1}'=+1\end{aligned}\right\}\Rightarrow\frac{1}{\sqrt[N/2]{Z'^{CE'}}}e^{-K_1'+2K_2'+K_3'}$$

$$=\frac{1}{\sqrt[N/2]{Z^{CE}}}e^{2K_2}\left\{2e^{2K_2+2K_3}+1\right\},$$

$$\left.\begin{aligned}\sigma_i'=0,\sigma_{i+1}'=\pm1\\ \sigma_i'=\pm1,\sigma_{i+1}'=0\end{aligned}\right\}\Rightarrow\frac{1}{\sqrt[N/2]{Z'^{CE'}}}e^{K_2'}$$

$$=\frac{1}{\sqrt[N/2]{Z^{CE}}}e^{K_2}\left\{2\cosh\left(K_1\right)e^{2K_2+K_3}+1\right\}, \tag{7.38}$$

$$\sigma_i'=0,\sigma_{i+1}'=0\Rightarrow\frac{1}{\sqrt[N/2]{Z'^{CE'}}}=\frac{1}{\sqrt[N/2]{Z^{CE}}}\left\{2e^{2K_2}+1\right\}.$$

There are four independent equations and four independent variables: K'_1, K'_2, K'_3, and $Z'^{CE'}$. The solution of this system of equations exists; but we do not adduce it here because it is cumbersome.

So, we have proved that the initial system and the final system belong to the same universality class with interactions (7.35 and 7.36). For the initial system, these interactions were not obvious because they were disguised by zero values of the coupling constants.

In the examples considered above, we have built the RG transformation which has transformed the initial system into the new system, belonging to the same universality class (with the same lattice shape and the same interactions, but having different values of coupling constants). But for the new system, we could again perform the RG transformation with the aid of the same equations, connecting the second generation of the coupling constants with their values at the end of the first RG transformation. This new system would again belong to the same universality class. And so on, we can perform the RG transformation very many times, creating succession of systems, inheriting properties from one another.

In the result, we obtain a chain of systems with the same interactions (with the same functional form of the Hamiltonian, with the same lattice shape, with the same behavior). These systems differ only by the values of their coupling constants representing field parameters and interaction constants.

If on the space of coupling constants we draw the succession of RG jumps as a curve, this curve is called *the RG flow curve* (Fig. 7.4). We obtain a new flow curve by slightly changing the coupling constants of the initial system. Since the lattice and the spin interactions are still the same, the new flow curve belongs to the same universality class.

How long can we continue the succession of the RG transformations? Can we do it infinite number of times? Obviously not, because the initial system is scale invariant only on scales less than the correlation length ξ, but on larger scales there is no scale invariance.

Performing coarse graining with $r = 1/b$ being the linear-scale factor, we move from a detailed system to the less detailed system, reducing the "excessive" degrees of freedom. To keep the lattice invariant, we measure all distances in units of the lattice constant. Obviously, the new lattice constant is b times larger than the old one. Therefore, all distances in the model shrink b-fold. So does the correlation length:

$$\xi' = r\xi = \xi / b. \tag{7.39}$$

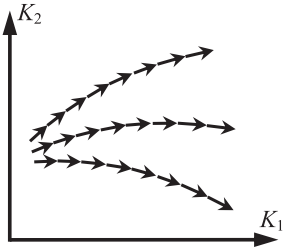

Fig. 7.4 The RG flow curves form a universality class

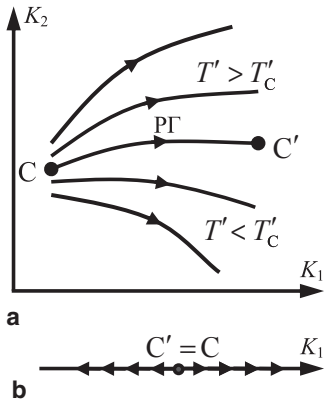

Fig. 7.5 The RG transformation moves the system away from the vicinity of a critical point. Only a critical point can transform into a critical point

Performing the RG transformation many times, we sometime reach the state when the linear size of the RG cell becomes comparable with the correlation length: $b \propto \xi'$. Obviously, further transformations are impossible since there is no more scale invariance in the system. We have reached the limit of maximal coarse graining when we have reduced all "excessive" degrees of freedom. The number of the remaining degrees of freedom is the minimal number required to represent the system's behavior correctly; and any further reductions will no longer reproduce the same behavior.

The coarse graining is the physical process; and (7.39) is the law representing this process without regard to a particular system under consideration.

Since the RG transformation always decreases the correlation length, this law has two important consequences. First, because shorter correlation length means larger distance from the critical point, we may conclude that the RG transformation always moves the system away from the critical point.

Second, the correlation length diverges at the critical point. Therefore, if the final system of the RG transformation is at its critical point, it corresponds to the infinite correlation length, $\xi' = +\infty$. In accordance with (7.39), this means that the correlation length of the initial system was also infinite, $\xi = +\infty$, and the initial system was also at its critical point. So, only the critical point can transform into the critical point.

The opposite statement is generally not true—the critical point can transform into a noncritical point. However, in accordance with (7.39), we see that each time the correlation length decreases only b-fold. Therefore, to obtain the finite value of the correlation length from the initial infinite value may require an infinite number of transformations.

These tendencies of the RG transformation are presented in Fig. 7.5a—the flow curve originating at the critical point goes through a succession of critical points. This curve is called *the critical flow curve* or *the critical manifold* (or a part of this manifold if it has dimensionality higher than one). Adjacent flow curves with near-critical coupling constants diverge away from the critical flow curve.

However, in advance, we should say that the critical flow curve does not always exist. Very often, this curve shrinks into a point to represent *a critical fixed point* of the RG transformation. In particular, this is true when there is only one coupling constant (Fig. 7.5b). Since the RG transformation tends to move systems away from the critical point, this fixed point must be *a repeller*.

Figure 7.5b illustrates that the flow curve, emerging from the critical point, not necessarily generates critical points also—there is only one critical point in Fig. 7.5b, and two-flow curves, spreading from it to the left and to the right, take the system farther and farther away from the critical state.

7.3 RG Approach of a Single Survivor: Two-Dimensional Magnetic Systems

As we have seen in Chap. 3, the one-dimensional n.n. Ising model cannot have a phase transition at nonzero temperature. Therefore, we move to the two-dimensional systems and consider first the ferromagnetic n.n. Ising model on square lattice in the absence of magnetic field. The Hamiltonian of the system is

$$\mathrm{H}_{\{\sigma\}} = -J \sum_{<i,j>_{n.n.}} \sigma_i \sigma_j, \tag{7.40}$$

the partition function of the system is

$$Z^{CE} = \sum_{\{\sigma\}} \exp\left(\beta J \sum_{<i,j>_{n.n.}} \sigma_i \sigma_j \right), \tag{7.41}$$

and Gibbs probability of microstates $\{\sigma\}$ is

$$w^{CE}_{\{\sigma\}} = \frac{1}{Z^{CE}} \exp\left(\beta J \sum_{<i,j>_{n.n.}} \sigma_i \sigma_j \right). \tag{7.42}$$

If we introduced the single-coupling constant $K_1 = \beta J$, similar to Problem 7.2.2, the number of equations would be higher than one, and we would not be able to build the RG again. This suggests that the universality class of our system has more complex spin interactions that are disguised in the particular case of our initial system by zero values of coupling constants.

In particular, we consider bi-spin n.n.n. interactions and quadro-spin interactions of cells:

$$\mathrm{H}_{\{\sigma\}} = -TK_1 \sum_{<i,j>_{n.n.}} \sigma_i \sigma_j - TK_2 \sum_{<i,j>_{n.n.n.}} \sigma_i \sigma_j - TK_3 \sum_{cells} \sigma_i \sigma_j \sigma_k \sigma_l, \tag{7.43}$$

$$w^{CE}_{\{\sigma\}} = \frac{1}{Z^{CE}} \exp\left(\begin{array}{l} K_1 \sum\limits_{<i,j>_{n.n.}} \sigma_i \sigma_j + K_2 \sum\limits_{<i,j>_{n.n.n.}} \sigma_i \sigma_j \\ + K_3 \sum\limits_{cells} \sigma_i \sigma_j \sigma_k \sigma_l \end{array} \right). \tag{7.44}$$

Here, $\sum_{<i,j>_{n.n.}}$ is again the sum of bi-spin interactions over the n.n. spin pairs. For site 5 in Fig. 7.6, this sum goes over the n.n. spin pairs $\sigma_5\sigma_2$, $\sigma_5\sigma_6$, $\sigma_5\sigma_8$, and $\sigma_5\sigma_4$. The sum $\sum_{<i,j>_{n.n.n.}}$ represents also bi-spin interactions and goes over the next-nearest-neighbor (n.n.n.) spin pairs. For site 5 in Fig. 7.6, this sum goes

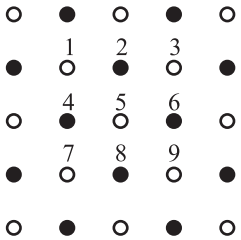

Fig. 7.6 The RG on square lattice

over the n.n.n. spin pairs $\sigma_5\sigma_1$, $\sigma_5\sigma_3$, $\sigma_5\sigma_9$, and $\sigma_5\sigma_7$. The sum $\sum_{cells}$ represents the quadro-spin interactions inside separate cells. For cell 1–2–5–4, this sum contains the term $\sigma_1\sigma_2\sigma_5\sigma_4$.

Our initial system is the "degenerate" case of this universality class when two of three coupling constants become zero:

$$K_1 = \beta J,\ K_2 = 0,\ K_3 = 0. \tag{7.45}$$

Again, there has been no reason to consider these particular types of interactions. We just assume that our system may belong to this particular universality class. And if we will be lucky to build the RG transformation for these types of interactions, we will prove this statement. However, nothing prevents our system to belong to another universality class also as a "degenerate" case when some other coupling constants of that class are zero.

Let us look at the lattice of the initial model in Fig. 7.6. We will apply the same rule of a single survivor. "Surviving" spins σ_2, σ_4, σ_6, and σ_8 are presented as filled circles while "disappearing" spins σ_1, σ_3, σ_5, σ_7, and σ_9 are represented by empty circles.

From Fig. 7.6, we see that the linear-scale factor of the RG transformation is $r = 1/b = 1/\sqrt{2}$ since the lattice constant (the length of the cell's edge) increases by multiplier $\sqrt{2}$ (Fig. 7.7).

Applying the rule of invariant probabilities, we find

$$\begin{aligned}
&\frac{1}{Z'^{CE'}} e^{\ldots + K_1'\{\sigma_2'\sigma_6' + \sigma_6'\sigma_8' + \sigma_8'\sigma_4' + \sigma_4'\sigma_2'\} + K_2'\{\sigma_2'\sigma_8' + \sigma_4'\sigma_6'\} + K_3'\sigma_2'\sigma_6'\sigma_8'\sigma_4'} = \\
&= \sum_{\ldots,\sigma_1,\sigma_3,\sigma_5,\sigma_7,\sigma_9,\ldots=\pm 1} \frac{1}{Z^{CE}} e^{\ldots + K_1(\sigma_1\sigma_2' + \sigma_2'\sigma_3 + \sigma_4'\sigma_5 + \sigma_5\sigma_6' + \sigma_7\sigma_8' + \sigma_8'\sigma_9)} \times \\
&\quad \times e^{K_1(\sigma_1\sigma_4' + \sigma_4'\sigma_7 + \sigma_2'\sigma_5 + \sigma_5\sigma_8' + \sigma_3\sigma_6' + \sigma_6'\sigma_9)} \times \\
&\quad \times e^{K_2\{\sigma_2'\sigma_6' + \sigma_1\sigma_5 + \sigma_5\sigma_9 + \sigma_4'\sigma_8' + \sigma_2'\sigma_4' + \sigma_3\sigma_5 + \sigma_5\sigma_7 + \sigma_6'\sigma_8'\}} \times \\
&\quad \times e^{K_3\{\sigma_1\sigma_2'\sigma_5\sigma_4' + \sigma_2'\sigma_3\sigma_6'\sigma_5 + \sigma_4'\sigma_5\sigma_8'\sigma_7 + \sigma_5\sigma_6'\sigma_9\sigma_8'\}}.
\end{aligned} \tag{7.46}$$

Here, we have shown explicitly only spins enumerated in Fig. 7.6. Contrary to the previous examples, we have kept the site numbers unchanged so that "surviving" spins have the same numbers on the initial and final lattices: $\sigma'_2 = \sigma_2$, $\sigma'_4 = \sigma_4$, $\sigma'_6 = \sigma_6$, $\sigma'_8 = \sigma_8$.

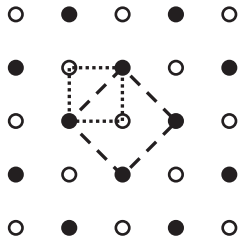

Fig. 7.7 A cell of the initial lattice versus a cell of the final lattice

The sum goes over the projections of all "disappearing" spins σ_1, σ_3, σ_5, σ_7, σ_9 ,… Let us, in this expression, keep only multipliers significant for the sum over the projections of the central spin σ_5:

$$\frac{1}{Z'^{CE'}} e^{\ldots+K_1'\{\sigma_2'\sigma_6'+\sigma_6'\sigma_8'+\sigma_8'\sigma_4'+\sigma_4'\sigma_2'\}+K_2'\{\sigma_2'\sigma_8'+\sigma_4'\sigma_6'\}+K_3'\sigma_2'\sigma_6'\sigma_8'\sigma_4'}$$
$$= \frac{1}{Z^{CE}} e^{\ldots+K_2\{\sigma_2'\sigma_6'+\sigma_4'\sigma_8'+\sigma_2'\sigma_4'+\sigma_6'\sigma_8'\}} \times \sum_{\ldots,\sigma_1,\sigma_3,\sigma_7,\sigma_9,\ldots=\pm1} \sum_{\sigma_5=\pm1} e^{\ldots+K_1\{\sigma_4'\sigma_5+\sigma_5\sigma_6'+\sigma_2'\sigma_5+\sigma_5\sigma_8'\}} \times$$
$$\times e^{K_2\{\sigma_1\sigma_5+\sigma_5\sigma_9+\sigma_3\sigma_5+\sigma_5\sigma_7\}} e^{K_3\{\sigma_1\sigma_2'\sigma_5\sigma_4'+\sigma_2'\sigma_3\sigma_6'\sigma_5+\sigma_4'\sigma_5\sigma_8'\sigma_7+\sigma_5\sigma_6'\sigma_9\sigma_8'\}}. \qquad (7.47)$$

We see that in comparison with the one-dimensional systems, we can no longer separate the sum $\sum_{\sigma_5=\pm1}$ so that it would contain only σ_5 and the surviving spins. Indeed, the bi-spin n.n.n. interactions, like $\sigma_1\sigma_5$, or the quadro-spin interactions, like $\sigma_1\sigma'_2\sigma_5\sigma'_4$, would not allow that. Therefore, it is not possible to perform the summation analytically for the general case.

However, our initial system contained neither the bi-spin n.n.n. interactions nor the quadro-spin interactions: (7.45). Therefore, if we return to the particular case of our initial system, this will significantly simplify the summation. However, we should remember that in this case, we will build only one step of the RG transformation, from the initial system to the next system in the universality class. The obtained solution will not describe the following RG steps because these steps will start from systems with nonzero K_2 and K_3. So, having only one step of the RG, we would only guess what the whole flow curve is.

Substituting (7.45) into (7.47), we find

$$\frac{1}{Z'^{CE'}} e^{\ldots+K_1'\{\sigma_2'\sigma_6'+\sigma_6'\sigma_8'+\sigma_8'\sigma_4'+\sigma_4'\sigma_2'\}+K_2'\{\sigma_2'\sigma_8'+\sigma_4'\sigma_6'\}+K_3'\sigma_2'\sigma_6'\sigma_8'\sigma_4'}$$
$$= \frac{1}{Z^{CE}} \sum_{\ldots,\sigma_1,\sigma_3,\sigma_7,\sigma_9,\ldots=\pm1} \sum_{\sigma_5=\pm1} e^{\ldots+K_1\{\sigma_4'\sigma_5+\sigma_5\sigma_6'+\sigma_2'\sigma_5+\sigma_5\sigma_8'\}}$$
$$= \frac{1}{Z^{CE}} \sum_{\ldots,\sigma_1,\sigma_3,\sigma_7,\sigma_9,\ldots=\pm1} 2e^{\ldots} \cosh\left(K_1\{\sigma_4'+\sigma_6'+\sigma_2'+\sigma_8'\}\right). \qquad (7.48)$$

Summation over the projections of other "disappearing" spins leads to the appearance of similar multipliers $2\cosh(K_1\{\ldots\})$ on the right-hand side of (7.48):

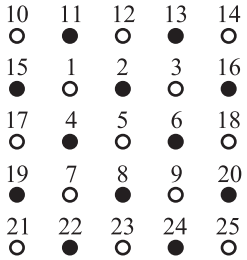

Fig. 7.8 Numbers of sites

$$\frac{1}{Z'^{CE'}}e^{...+K'_1\{\sigma'_2\sigma'_6+\sigma'_6\sigma'_8+\sigma'_8\sigma'_4+\sigma'_4\sigma'_2\}+K'_2\{\sigma'_2\sigma'_8+\sigma'_4\sigma'_6\}+K'_3\sigma'_2\sigma'_6\sigma'_8\sigma'_4}$$
$$=\frac{1}{Z^{CE}}\times...\times 2\cosh\left(K_1\{\sigma'_4+\sigma'_6+\sigma'_2+\sigma'_8\}\right)$$
$$\times 2\cosh\left(K_1\{\sigma'_{15}+\sigma'_2+\sigma'_{11}+\sigma'_4\}\right)\times 2\cosh\left(K_1\{\sigma'_2+\sigma'_{16}+\sigma'_{13}+\sigma'_6\}\right)$$
$$\times 2\cosh\left(K_1\{\sigma'_{19}+\sigma'_8+\sigma'_4+\sigma'_{22}\}\right)\times 2\cosh\left(K_1\{\sigma'_8+\sigma'_{20}+\sigma'_6+\sigma'_{24}\}\right), \tag{7.49}$$

where the numbers of sites are presented in Fig. 7.8.

Equality (7.49) is formulated for the whole lattice. Instead, we can formulate an analogue of this equality but now only for just one cell. To move to the case of a separate cell, we notice that multipliers, associated with K_1, K'_2, and K'_3 in (7.49), belong to a particular cell of the new model. However, multipliers, associated with K'_1 in (7.49), belong each to an edge between two adjacent cells of the new lattice. To reformulate (7.49) for the case of a separate cell, we, therefore, should take the square root of the last multipliers:

$$\frac{1}{\sqrt[N/2]{Z'^{CE'}}}e^{\frac{K'_1}{2}\{\sigma'_2\sigma'_6+\sigma'_6\sigma'_8+\sigma'_8\sigma'_4+\sigma'_4\sigma'_2\}+K'_2\{\sigma'_2\sigma'_8+\sigma'_4\sigma'_6\}+K'_3\sigma'_2\sigma'_6\sigma'_8\sigma'_4}$$
$$=\frac{1}{\sqrt[N/2]{Z^{CE}}}2\cosh\left(K_1\left\{\sigma'_4+\sigma'_6+\sigma'_2+\sigma'_8\right\}\right). \tag{7.50}$$

Here, we have used the fact that the number of new cells equals the number of new spins: $N' = N/b^2 = N/2$.

Equality (7.50) should be valid for arbitrary spin projections σ'_2, σ'_4, σ'_6, σ'_8. If all spins have the same orientation, (7.50) transforms into

$$\frac{1}{\sqrt[N/2]{Z'^{CE'}}}e^{2K'_1+2K'_2+K'_3}=\frac{2}{\sqrt[N/2]{Z^{CE}}}\cosh(4K_1). \tag{7.51}$$

If one spin is oriented opposite to three others:

$$\frac{1}{\sqrt[N/2]{Z'^{CE'}}} e^{-K'_3} = \frac{2}{\sqrt[N/2]{Z^{CE}}} \cosh(2K_1). \tag{7.52}$$

If one cell's edge has spins oriented "up," while the second edge is "down":

$$\frac{1}{\sqrt[N/2]{Z'^{CE'}}} e^{-2K'_2+K'_3} = \frac{2}{\sqrt[N/2]{Z^{CE}}}. \tag{7.53}$$

If one cell's diagonal is "up," while the second diagonal is "down":

$$\frac{1}{\sqrt[N/2]{Z'^{CE'}}} e^{-2K'_1+2K'_2+K'_3} = \frac{2}{\sqrt[N/2]{Z^{CE}}}. \tag{7.54}$$

There are four independent equations and four independent variables, K'_1, K'_2, K'_3, and $Z'^{CE'}$. Therefore, the solution exists but is valid only for the first RG step when in the initial system we have $K_2 = 0$ and $K_3 = 0$.

7.4 RG Approach of Representation: Two-Dimensional Magnetic Systems in the Absence of Magnetic Field

Considering the RG approach above of a single survivor for the n.n. Ising model on square lattice, we were able to build only the first step of the RG transformation.

Due to the introduction of a subjective rule of microstate correspondence, the RG does not represent a physical process exactly. Strictly speaking, the subjectivity does not make it an approximation either[2]. Instead, we consider an investigator's hypothesis as a subjective rule of microstate correspondence. Similar to the Bayesian analysis, this hypothesis is just our "lucky guess" that may be right or wrong. Therefore, the RG is just a tool that helps us to investigate particular systems.

As any tool, it is not unique. There are many possible approaches, each useful for a specific system. The validity of these approaches is determined by how accurately they can predict the exact or experimental results.

So far, we have built the "subjective" rule of microstate correspondence only with the aid of the single-survivor approach. Let us consider now a different approach (Niemeijer and van Leeuwen 1974, 1976) which we call *the approach of representation*.

We consider the two-dimensional ferromagnetic n.n. Ising model on a triangular lattice in the absence of magnetic field. The Hamiltonian, partition function, and Gibbs probability of the system are identical to (7.40–7.42) of the square lattice. There is a single-coupling constant, $K = \beta J$.

[2] We are talking right now about the RG in real space when we consider the subjective rule of correspondence among initial and final microstates. In momentum space, the RG is generally built by truncating the spectrum from above since, truncating high frequencies, we are discarding fine details. In this case, the RG can be considered to be the approximation.

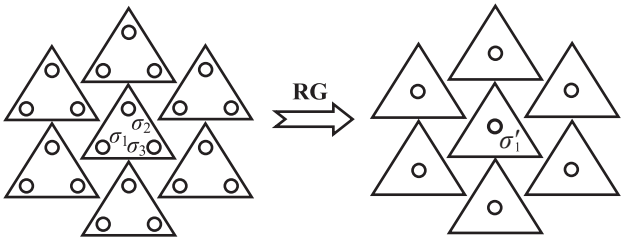

Fig. 7.9 The RG transformation on triangular lattice

We divide the lattice into triangular cells with three spins in each cell (Fig. 7.9). The linear-scale factor is $r = 1/b = 1/\sqrt{3}$.

In the single-survivor approach, we chose the spins which would "survive" with their orientations intact and then summed initial probabilities over the orientations of the rest of the spins.

In *the approach of representation,* we consider all spins as "disappearing," and we sum the microstate probabilities over all spins without exclusions. We consider the new spins to be appearing in the centers of the RG cells. So, spins σ_1, σ_2, and σ_3 in Fig. 7.9 "disappear," giving birth to spin σ'_1 in the middle of the cell.

Now, we have to state the subjective rule of microstate correspondence. In other words, knowing orientations of spins σ_1, σ_2, σ_3, we should prescribe a particular orientation to the new spin σ'_1. We do not have "surviving" spins now; all spins are "disappearing."

The order parameter of magnetic systems with spin interactions is the spontaneous magnetization. So, to keep the behavior of phase transitions invariant, we may require the orientation of the new spin to *represent* the magnetization of the initial cell. In other words, if three or two spins at the corners of the cell are oriented "up" $\left(\text{i.e., } \left\{\begin{matrix}\uparrow & \\ \uparrow & \uparrow\end{matrix}\right\}, \left\{\begin{matrix}\downarrow & \\ \uparrow & \uparrow\end{matrix}\right\}, \left\{\begin{matrix}\uparrow & \\ \uparrow & \downarrow\end{matrix}\right\}, \left\{\begin{matrix}\uparrow & \\ \downarrow & \uparrow\end{matrix}\right\}\right)$, the new spin will also be oriented "up." Otherwise, if only one or none of the spins is "up," the new spin is "down."

Having built the rule of correspondence, we require the invariance of the corresponding probabilities:

$$\frac{1}{Z'^{CE'}} \exp\left(K' \sum_{<i',j'>_{n.n.}} \sigma'_{i'} \sigma'_{j'} \right) = \frac{1}{Z^{CE}} \sum_{\{\sigma\}:\{\sigma'\}} \exp\left(K \sum_{<i,j>_{n.n.}} \sigma_i \sigma_j \right), \tag{7.55}$$

where, $\sum_{\{\sigma\}:\{\sigma'\}}$ is the sum over the initial microstates $\{\sigma\}$ corresponding to the final microstate $\{\sigma'\}$ considered by the left-hand side of (7.55).

Let us consider further the orientations of all new spins $\sigma'_1, \ldots, \sigma'_{N/3}$ to be fixed. When the new microstate $\{\sigma'\}$ is given, the set of the possible original microstates $\{\sigma\}$ is limited by the correspondence to the final microstate: $\{\sigma\}:\{\sigma'\}$. In other words, if a spin on the new lattice is "up," we should consider only those microstates $\{\sigma\}$ of the initial lattice when the corresponding cell is

$\left\{\begin{matrix}\uparrow & \\ \uparrow & \uparrow\end{matrix}\right\}$, or $\left\{\begin{matrix}\downarrow & \\ \uparrow & \uparrow\end{matrix}\right\}$, or $\left\{\begin{matrix}\uparrow & \\ \uparrow & \downarrow\end{matrix}\right\}$, or $\left\{\begin{matrix}\uparrow & \\ \downarrow & \uparrow\end{matrix}\right\}$.

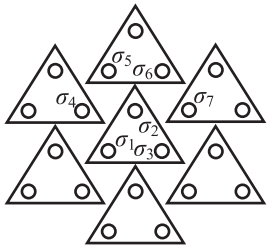

Fig. 7.10 Spin interactions

For the initial model, let us consider a CE with an additional boundary condition that our system can only be in one of the microstates $\{\sigma\}:\{\sigma'\}$ while other original microstates $\{\sigma\}$ are prohibited either by the external forces or by the model formulation. Then the properties of this ensemble should *represent* the properties of the given microstate $\{\sigma'\}$.

Similar to the n.n. Ising ferromagnet on square lattice, we see that we cannot separate the sum over the orientations of one cell from the spins of other cells. Indeed, each spin of a cell interacts with two spins of its own cell and with four spins of three adjacent cells.

To overcome this difficulty, we divide the Hamiltonian into two parts:

$$\mathrm{H} = \widetilde{\mathrm{H}} + V, \tag{7.56}$$

where, the first term $\widetilde{\mathrm{H}}$ is responsible for spin interactions within the cells. For the spins enumerated in Fig. 7.10, $\widetilde{\mathrm{H}}$ contains

$$\widetilde{\mathrm{H}}_{\{\sigma\}} = \ldots - J(\sigma_1\sigma_2 + \sigma_2\sigma_3 + \sigma_3\sigma_1) - J(\sigma_5\sigma_6 + \ldots). \tag{7.57}$$

The second term V in (7.56) represents spin interactions across the boundaries of the cells:

$$V_{\{\sigma\}} = \ldots - J(\sigma_1\sigma_4 + \sigma_2\sigma_4 + \sigma_2\sigma_5 + \sigma_2\sigma_6 + \sigma_2\sigma_7 + \sigma_3\sigma_7 + \ldots). \tag{7.58}$$

We consider an approximation of small interactions among the cells when V can be considered small so that we can apply the perturbation theory.

Further, we consider the CE of the unperturbed Hamiltonian $\widetilde{\mathrm{H}}$ with the additional boundary condition $\{\sigma\}:\{\sigma'\}$, when the system can visit only those original microstates $\{\sigma\}$ which correspond to the given $\{\sigma'\}$. Let us denote this ensemble as "*CE of* $\widetilde{\mathrm{H}}$ *over* $\{\sigma\}:\{\sigma'\}$" or, simpler, as "$\widetilde{\mathrm{H}}:\{\sigma'\}$." Then the averaging of an arbitrary quantity $A_{\{\sigma\}}$ over this ensemble we define as

$$\left\langle A_{\{\sigma\}} \right\rangle_{\widetilde{\mathrm{H}}:\{\sigma'\}} \equiv \sum_{\{\sigma\}:\{\sigma'\}} A_{\{\sigma\}} w_{\{\sigma\}}^{\widetilde{\mathrm{H}}:\{\sigma'\}} = \frac{\sum\limits_{\{\sigma\}:\{\sigma'\}} A_{\{\sigma\}} \exp\left(-\dfrac{\widetilde{\mathrm{H}}_{\{\sigma\}}}{T}\right)}{\sum\limits_{\{\sigma\}:\{\sigma'\}} \exp\left(-\dfrac{\widetilde{\mathrm{H}}_{\{\sigma\}}}{T}\right)}. \tag{7.59}$$

Choosing $A_{\{\sigma\}} = \exp(-V_{\{\sigma\}} / T)$, we transform (7.55) into

$$\begin{aligned}
&\frac{1}{Z'^{CE'}} \exp\left(K' \sum_{<i',j'>_{n.n.}} \sigma'_{i'} \sigma'_{j'} \right) \\
&= \frac{1}{Z^{CE}} \sum_{\{\sigma\}:\{\sigma'\}} \exp\left(-\frac{V_{\{\sigma\}}}{T} \right) \exp\left(-\frac{\widetilde{\mathrm{H}}_{\{\sigma\}}}{T} \right) \\
&= \frac{1}{Z^{CE}} \left\langle \exp\left(-\frac{V_{\{\sigma\}}}{T} \right) \right\rangle_{\widetilde{\mathrm{H}}:\{\sigma'\}} \sum_{\{\sigma\}:\{\sigma'\}} \exp\left(-\frac{\widetilde{\mathrm{H}}_{\{\sigma\}}}{T} \right).
\end{aligned} \tag{7.60}$$

The sum,

$$Z^{\widetilde{\mathrm{H}}:\{\sigma'\}} \equiv \sum_{\{\sigma\}:\{\sigma'\}} \exp\left(-\frac{\widetilde{\mathrm{H}}_{\{\sigma\}}}{T} \right), \tag{7.61}$$

is the partition function of the unperturbed Hamiltonian. Exponential functions under the sign of the sum contain spin interactions only within the cells. So, the spins, enumerated in Fig. 7.10, provide $\exp(\ldots)\exp(K(\sigma_1\sigma_2 + \sigma_2\sigma_3 + \sigma_3\sigma_1))\exp(K(\sigma_5\sigma_6 + \ldots))$.

If $\sigma'_1 = \uparrow$, then the sum $\sum_{\{\sigma\}:\{\sigma'\}}$ goes over the following orientations of spins σ_1, σ_2, σ_3 of the considered cell: $\left\{ \begin{matrix} \uparrow & \uparrow \\ \uparrow & \end{matrix} \right\}, \left\{ \begin{matrix} \downarrow & \uparrow \\ \uparrow & \end{matrix} \right\}, \left\{ \begin{matrix} \uparrow & \uparrow \\ \uparrow & \downarrow \end{matrix} \right\}, \left\{ \begin{matrix} \uparrow & \uparrow \\ \downarrow & \end{matrix} \right\}$. For the partition function (7.61) this provides

$$\begin{aligned}
Z^{\widetilde{\mathrm{H}}:\{\sigma'\}} &= \sum_{\{\sigma\setminus\sigma_1,\sigma_2,\sigma_3\}:\{\sigma'\}} e^{\cdots} \sum_{\left\{ \begin{matrix} \sigma_2 & \\ \sigma_1 & \sigma_3 \end{matrix} \right\} = \left\{ \begin{matrix} \uparrow & \uparrow \\ \uparrow & \end{matrix} \right\}, \left\{ \begin{matrix} \downarrow & \uparrow \\ \uparrow & \end{matrix} \right\}, \left\{ \begin{matrix} \uparrow & \uparrow \\ \uparrow & \downarrow \end{matrix} \right\}, \left\{ \begin{matrix} \uparrow & \uparrow \\ \downarrow & \end{matrix} \right\}} e^{K(\sigma_1\sigma_2 + \sigma_2\sigma_3 + \sigma_3\sigma_1)} \\
&= \left(e^{3K} + 3e^{-K} \right) \sum_{\{\sigma\setminus\sigma_1,\sigma_2,\sigma_3\}:\{\sigma'\}} e^{\cdots}.
\end{aligned} \tag{7.62}$$

If $\sigma'_1 = \downarrow$, analogous considerations lead to exactly the same result, so expression (7.62) is valid for an arbitrary orientation of σ'_1. Performing the summation for all other cells, we find

$$Z^{\widetilde{\mathrm{H}}:\{\sigma'\}} = \left(e^{3K} + 3e^{-K} \right)^{N/3}. \tag{7.63}$$

This transforms (7.60) into

$$\frac{1}{Z'^{CE'}} \exp\left(K' \sum_{<i',j'>_{n.n.}} \sigma'_{i'} \sigma'_{j'} \right) = \frac{1}{Z^{CE}} \left\langle \exp\left(-V_{\{\sigma\}} / T \right) \right\rangle_{\widetilde{\mathrm{H}}:\{\sigma'\}} \left(e^{3K} + 3e^{-K} \right)^{N/3}. \tag{7.64}$$

The last quantity to be found is $\left\langle \exp\left(-V_{\{\sigma\}} / T \right) \right\rangle_{\widetilde{\mathrm{H}}:\{\sigma'\}}$. Assuming the perturbation V being small, we expand the exponential function in its powers:

$$\left\langle \exp\left(-\frac{V_{\{\sigma\}}}{T} \right) \right\rangle_{\widetilde{\mathrm{H}}:\{\sigma'\}} = 1 - \frac{\left\langle V_{\{\sigma\}} \right\rangle_{\widetilde{\mathrm{H}}:\{\sigma'\}}}{T} + \frac{\left\langle V_{\{\sigma\}}^{\,2} \right\rangle_{\widetilde{\mathrm{H}}:\{\sigma'\}}}{2T^2} + \ldots \tag{7.65}$$

Taking logarithm on both sides of this equation, expanding the logarithm of the right-hand side,

$$\ln\left\langle \exp\left(-\frac{V_{\{\sigma\}}}{T}\right)\right\rangle_{\widetilde{\mathrm{H}}:\{\sigma'\}} = -\frac{\left\langle V_{\{\sigma\}}\right\rangle_{\widetilde{\mathrm{H}}:\{\sigma'\}}}{T} + \frac{\left\langle V_{\{\sigma\}}{}^2\right\rangle_{\widetilde{\mathrm{H}}:\{\sigma'\}}}{2T^2} - \frac{\left\langle V_{\{\sigma\}}\right\rangle^2_{\widetilde{\mathrm{H}}:\{\sigma'\}}}{2T^2} + ..., \tag{7.66}$$

and exponentiating, we find[3]

$$\left\langle \exp\left(-\frac{V_{\{\sigma\}}}{T}\right)\right\rangle_{\widetilde{\mathrm{H}}:\{\sigma'\}} = \exp\left(-\frac{\left\langle V_{\{\sigma\}}\right\rangle_{\widetilde{\mathrm{H}}:\{\sigma'\}}}{T} + \frac{\left\langle V_{\{\sigma\}}{}^2\right\rangle_{\widetilde{\mathrm{H}}:\{\sigma'\}} - \left\langle V_{\{\sigma\}}\right\rangle^2_{\widetilde{\mathrm{H}}:\{\sigma'\}}}{2T^2} + ...\right). \tag{7.67}$$

Since perturbation V is small, we keep only the first term in the right-hand side of this equation:

$$\left\langle \exp\left(-\frac{V_{\{\sigma\}}}{T}\right)\right\rangle_{\widetilde{\mathrm{H}}:\{\sigma'\}} \approx \exp\left(-\frac{\left\langle V_{\{\sigma\}}\right\rangle_{\widetilde{\mathrm{H}}:\{\sigma'\}}}{T}\right). \tag{7.68}$$

The perturbation V contains interactions, (7.58), of adjacent cells. Averaging perturbation in the ensemble $\widetilde{\mathrm{H}}:\{\sigma'\}$ of the unperturbed Hamiltonian $\widetilde{\mathrm{H}}$, we find

$$\left\langle V_{\{\sigma\}}\right\rangle_{\widetilde{\mathrm{H}}:\{\sigma'\}} = ... - J\begin{pmatrix}\left\langle \sigma_1\sigma_4\right\rangle_{\widetilde{\mathrm{H}}:\{\sigma'\}} + \left\langle \sigma_2\sigma_4\right\rangle_{\widetilde{\mathrm{H}}:\{\sigma'\}} + \left\langle \sigma_2\sigma_5\right\rangle_{\widetilde{\mathrm{H}}:\{\sigma'\}} \\ + \left\langle \sigma_2\sigma_6\right\rangle_{\widetilde{\mathrm{H}}:\{\sigma'\}} + \left\langle \sigma_2\sigma_7\right\rangle_{\widetilde{\mathrm{H}}:\{\sigma'\}} + \left\langle \sigma_3\sigma_7\right\rangle_{\widetilde{\mathrm{H}}:\{\sigma'\}} + ...\end{pmatrix}. \tag{7.69}$$

But the unperturbed Hamiltonian $\widetilde{\mathrm{H}}$ is responsible for spin interactions within the cells. In the ensemble of this Hamiltonian two spins, belonging to different cells, are independent, so the averaging of their product is the product of independent averaged values:

$$\left\langle \sigma_1\sigma_4\right\rangle_{\widetilde{\mathrm{H}}:\{\sigma'\}} = \left\langle \sigma_1\right\rangle_{\widetilde{\mathrm{H}}:\{\sigma'\}}\left\langle \sigma_4\right\rangle_{\widetilde{\mathrm{H}}:\{\sigma'\}}, \left\langle \sigma_2\sigma_4\right\rangle_{\widetilde{\mathrm{H}}:\{\sigma'\}} = \left\langle \sigma_2\right\rangle_{\widetilde{\mathrm{H}}:\{\sigma'\}}\left\langle \sigma_4\right\rangle_{\widetilde{\mathrm{H}}:\{\sigma'\}}, ... \tag{7.70}$$

To find the averaged spin value, e.g., $\left\langle \sigma_2\right\rangle_{\widetilde{\mathrm{H}}:\{\sigma'\}}$, we utilize averaging (7.59):

$$\left\langle \sigma_2\right\rangle_{\widetilde{\mathrm{H}}:\{\sigma'\}} \equiv \frac{\sum\limits_{\{\sigma\}:\{\sigma'\}} \sigma_2 \exp\left(-\dfrac{\widetilde{\mathrm{H}}_{\{\sigma\}}}{T}\right)}{\sum\limits_{\{\sigma\}:\{\sigma'\}} \exp\left(-\dfrac{\widetilde{\mathrm{H}}_{\{\sigma\}}}{T}\right)} = \frac{\sum\limits_{\sigma_1,\sigma_2,\sigma_3:\sigma_1'} \sigma_2 \exp\left(K(\sigma_1\sigma_2 + \sigma_2\sigma_3 + \sigma_3\sigma_1)\right)}{\sum\limits_{\sigma_1,\sigma_2,\sigma_3:\sigma_1'} \exp\left(K(\sigma_1\sigma_2 + \sigma_2\sigma_3 + \sigma_3\sigma_1)\right)}. \tag{7.71}$$

[3] Generally two operations, taking the logarithm and exponentiation, performed consecutively, make students smile. This is quite unmerited since it has helped us to transfer averaging from outside of the exponential function under the sign of this function.

For $\sigma'_1 = \uparrow$, we find

$$\langle \sigma_2 \rangle_{\tilde{\mathrm{H}}:\{\sigma'\}} = \frac{(+1)e^{3K} + 2(+1)e^{-K} + (-1)e^{-K}}{e^{3K} + 3e^{-K}} = \frac{e^{3K} + e^{-K}}{e^{3K} + 3e^{-K}}, \tag{7.72}$$

while for $\sigma'_1 = \downarrow$,

$$\langle \sigma_2 \rangle_{\tilde{\mathrm{H}}:\{\sigma'\}} = \frac{(-1)e^{3K} + 2(-1)e^{-K} + (+1)e^{-K}}{e^{3K} + 3e^{-K}} = \frac{-e^{3K} - e^{-K}}{e^{3K} + 3e^{-K}}. \tag{7.73}$$

These two expressions differ only by the sign of σ'_1, so for the general case of the orientation of spin σ'_1, we have

$$\langle \sigma_2 \rangle_{\tilde{\mathrm{H}}:\{\sigma'\}} = \sigma'_1 \frac{e^{3K} + e^{-K}}{e^{3K} + 3e^{-K}}. \tag{7.74}$$

To find

$$\left\langle V_{\{\sigma\}} \right\rangle_{\tilde{\mathrm{H}}:\{\sigma'\}} = \ldots - J \begin{pmatrix} \langle \sigma_1 \rangle_{\tilde{\mathrm{H}}:\{\sigma'\}} \langle \sigma_4 \rangle_{\tilde{\mathrm{H}}:\{\sigma'\}} + \langle \sigma_2 \rangle_{\tilde{\mathrm{H}}:\{\sigma'\}} \langle \sigma_4 \rangle_{\tilde{\mathrm{H}}:\{\sigma'\}} \\ + \langle \sigma_2 \rangle_{\tilde{\mathrm{H}}:\{\sigma'\}} \langle \sigma_5 \rangle_{\tilde{\mathrm{H}}:\{\sigma'\}} + \langle \sigma_2 \rangle_{\tilde{\mathrm{H}}:\{\sigma'\}} \langle \sigma_6 \rangle_{\tilde{\mathrm{H}}:\{\sigma'\}} \\ + \langle \sigma_2 \rangle_{\tilde{\mathrm{H}}:\{\sigma'\}} \langle \sigma_7 \rangle_{\tilde{\mathrm{H}}:\{\sigma'\}} + \langle \sigma_3 \rangle_{\tilde{\mathrm{H}}:\{\sigma'\}} \langle \sigma_7 \rangle_{\tilde{\mathrm{H}}:\{\sigma'\}} + \ldots \end{pmatrix}, \tag{7.75}$$

we should take into account that each pair of adjacent cells has always two pairs of interacting spins (Fig. 7.11):

$$\left\langle V_{\{\sigma\}} \right\rangle_{\tilde{\mathrm{H}}:\{\sigma'\}} = -2J \left(\frac{e^{3K} + e^{-K}}{e^{3K} + 3e^{-K}} \right)^2 \sum_{<i',j'>_{n.n.}} \sigma'_{i'} \sigma'_{j'}. \tag{7.76}$$

Here, we are counting all pairs of adjacent cells by counting the n.n. pairs of the new spins. For each pair of cells, we are taking into account two pairs of interacting spins by introducing multiplier 2.

Fig. 7.11 Spin interactions

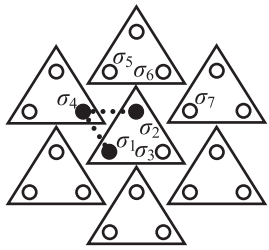

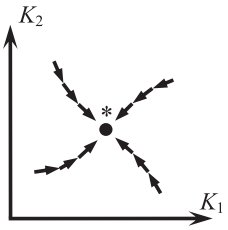

Fig. 7.12 A trivial fixed point—attractor

Substituting this result into (7.68) and (7.64), we finally find

$$\frac{1}{Z'^{CE'}}\exp\left(K'\sum_{<i',j'>_{n.n.}}\sigma'_{i'}\sigma'_{j'}\right)=\frac{1}{Z^{CE}}(e^{3K}+3e^{-K})^{N/3}\times\exp\left(2K\left(\frac{e^{3K}+e^{-K}}{e^{3K}+3e^{-K}}\right)^2\sum_{<i',j'>_{n.n.}}\sigma'_{i'}\sigma'_{j'}\right). \tag{7.77}$$

This equation provides the connection between the coupling constants and partition functions of the initial and final lattices:

$$K'=2K\left(\frac{e^{3K}+e^{-K}}{e^{3K}+3e^{-K}}\right)^2, \tag{7.78}$$

$$Z'^{CE'}=Z^{CE}(e^{3K}+3e^{-K})^{-N/3}. \tag{7.79}$$

The set of coupling constants K_i is often represented by a vector $\vec{\mathbf{K}}$. In future, we will choose the notation that will be the most convenient for the particular case considered.

A point on the space of coupling constants, transforming into itself, $\vec{\mathbf{K}}'=\vec{\mathbf{K}}$, is called *the fixed point* $\vec{\mathbf{K}}^*$ of the RG transformation. Since each RG transformation changes the correlation length in accordance with (7.39), fixed points correspond to either $\xi=0$ or $\xi=+\infty$.

The first type of fixed points, $\xi=0$, generally corresponds to a singularity of boundary conditions or interaction constants (zero or infinite values of field parameters or interaction constants). These fixed points are called *trivial*. Since the RG transformation decreases the correlation length in accordance with (7.39), a trivial fixed point always possesses some incoming manifold of flow curves, attracted by this point. If this manifold occupies all neighborhood of the fixed point, the trivial fixed point attracts all flow curves in its vicinity (Fig. 7.12) and becomes an *attractor* (*a sink*).

However, this is not necessarily the case. There are systems when flow curves emerge from one trivial fixed point to be consumed by another trivial fixed point. In this case, the first trivial fixed point is *the hyperbolic* (*saddle*) *fixed point* (or an even more complex formation) and has an outgoing manifold which plays the role of the incoming manifold for the second trivial fixed point (Fig. 7.13). Since along the manifold, connecting two trivial fixed points, the correlation length can only decrease

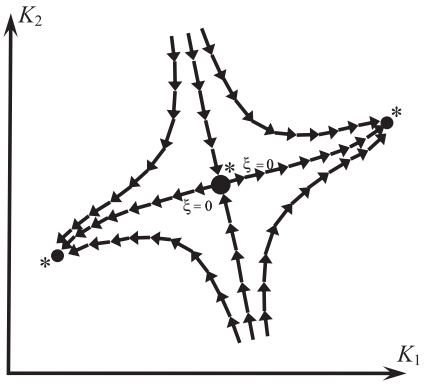

Fig. 7.13 Hyperbolic trivial fixed point

while it has been already zero at the first fixed point considered, we may conclude that the correlation length is zero everywhere along this manifold (Fig. 7.13).

The reader should understand that Figs. 7.12 and 7.13 are schematic at best because we drew them only to illustrate the most general considerations. In reality, the trivial fixed points correspond to a singularity of boundary conditions or interaction constants. This means that the values of coupling constants are zero or infinite also. Therefore, the trivial fixed points are often located at the boundaries of the considered space of coupling constants and do not possess both sides of the incoming manifold. So, we treat Figs. 7.12 and 7.13 only as schematic illustrations and will see what is going on in reality with the aid of particular examples discussed later.

The second type of fixed points with $\xi = +\infty$ represents critical phenomena, and these points are called *critical*. From (7.39), we know that the RG transformation always decreases the correlation length. This leads to important consequences. When there is only one coupling constant (Fig. 7.5b) and the critical manifold degenerates into the fixed point of the RG transformation, this critical fixed point is expected to be *a repeller*.

However, in the case of higher dimensionality of the space of coupling constants, the situation may become more complex. The critical manifold ends up at the critical fixed point which in this case becomes *the hyperbolic* (*saddle*) *fixed point* or an even more complex formation.

We are looking for the fixed points in the space of the coupling constants. Obviously, the RG transformation (7.79) of the partition function cannot have fixed points because the RG transformation is intended to decrease the number of degrees of freedom in the system.

Let us find fixed points of (7.78):

$$K^* = 2K^* \left(\frac{e^{3K^*} + e^{-K^*}}{e^{3K^*} + 3e^{-K^*}} \right)^2 . \tag{7.80}$$

We immediately see that the trivial fixed points are $K^* = 0$ and $K^* = +\infty$. In accordance with the definition of the coupling constant $K = \beta J$, the first trivial fixed point $K^* = 0$ corresponds to an infinite temperature or the absence of the pair spin

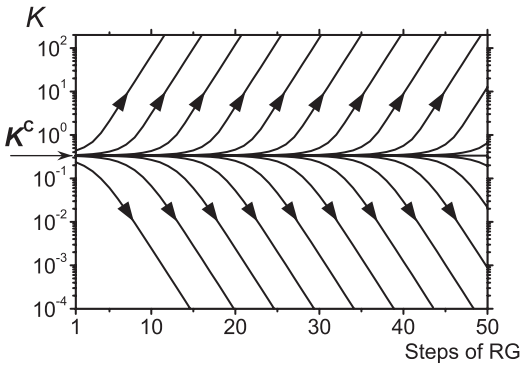

Fig. 7.14 Evolution of the coupling constant K

interactions. The second trivial fixed point $K^* = +\infty$ corresponds, on the contrary, to zero temperature or the infinite amplitude of the pair spin interactions.

However, the RG transformation in (7.80) possesses also a critical fixed point:

$$K^{\mathrm{C}} = \frac{1}{4}\ln(2\sqrt{2}+1) \approx 0.34. \tag{7.81}$$

In comparison, the exact solution provides (Onsager 1944; Houtappel 1950):

$$K^{\mathrm{C}} = \frac{1}{4}\ln 3 \approx 0.27. \tag{7.82}$$

We see that the RG transformation returns not the exact but only the approximate value. However, the approximation is accurate enough to rely on it as on an illustration of the system's behavior.

The evolution of the coupling constant K is presented as the dependence on the number of RG transformations in Fig. 7.14. We see that the system moves away from the critical fixed point K^{C} (repeller) towards one or another trivial fixed point (attractors). Since the correlation length is infinite at the critical fixed point, an infinite number of steps of the RG transformation is required for the system to leave this point because at each step the correlation length decreases only by the linear-scale factor $r = 1/b = 1/\sqrt{3}$.

The flow curves of the system are presented in Fig. 7.15, where, for illustrative purposes, we have put ahead of the axis the trivial fixed point $K^* = +\infty$ also.

When there is only one coupling constant, its evolution is often illustrated by a map (mapping transformation). In Fig. 7.16, we plot the dependence $K'(K)$ as well as the diagonal line $K' = K$ of the square area of the plot. To build the RG transformation, we choose a particular value of K and draw a vertical arrow up to

Fig. 7.15 The flow curves of the RG transformation

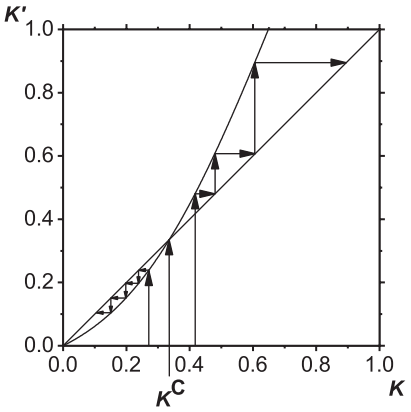

Fig. 7.16 A map of the RG transformation

the dependence $K'(K)$ to find K'. For the second RG step, we need to project K' on the abscissa axis (horizontal arrow up to the diagonal); and then for the found value of K', we need to find $(K')'$ by drawing the vertical arrow again. And so on. In the result, the succession of the RG steps is presented by the succession of horizontal and vertical arrows.

If initial K is less than K^{C}, the succession of arrows moves the system to the left, to the region of lower Ks, away from K^{C}. If initial K is higher than K^{C}, the system moves again away from K^{C}, in this case to the right, to the region of higher Ks. From Fig. 7.16, it is easy to see that the critical fixed point K^{C} is the repeller, while both trivial fixed points are attractors.

In the vicinity of the critical fixed point K^{C}, the RG transformation can be linearized:

$$RG(K) = K^{\mathrm{C}} + \lambda_K (K - K^{\mathrm{C}}) \tag{7.83}$$

where

$$\lambda_K \equiv \left.\frac{\partial K'}{\partial K}\right|_{K^{\mathrm{C}}} = 1 + \frac{1}{2}(8 - 5\sqrt{2})\ln(2\sqrt{2} + 1) \approx 1.62 \tag{7.84}$$

is the eigenvalue of the linearized RG transformation. Subscript "K" here emphasizes that this eigenvector corresponds to the coupling constant K. The exact solution provides the close value $\lambda_K = \sqrt{3} \approx 1.73$.

Let us return to the most general statement (7.39), determining the transformation of the correlation length:

$$\xi' = r\xi = \xi / b. \tag{7.85}$$

We consider one step of the RG transformation in the vicinity of the critical point (in our system with just one coupling constant, the critical state is represented by

the critical fixed point K^{C}). The correlation lengths of the initial and final models are diverging in accordance with

$$\xi \propto \frac{1}{|t|^{\nu_t^{\mathrm{C}}}} \equiv \left|\frac{T-T_{\mathrm{C}}}{T_{\mathrm{C}}}\right|^{-\nu_t^{\mathrm{C}}} \quad \text{and} \quad \xi' \propto \frac{1}{|t'|^{\nu_{t'}^{\mathrm{C}}}} \equiv \left|\frac{T'-T'_{\mathrm{C}}}{T'_{\mathrm{C}}}\right|^{-\nu_{t'}^{\mathrm{C}}}. \tag{7.86}$$

First, the scaling of the system is determined by the coupling constant $K = \beta J \equiv J/T$. Therefore, let us express these divergences as

$$\xi \propto \left|\frac{\frac{T}{J}-\frac{T_{\mathrm{C}}}{J}}{\frac{T_{\mathrm{C}}}{J}}\right|^{-\nu_t^{\mathrm{C}}} \quad \text{and} \quad \xi' \propto \left|\frac{\frac{T'}{J'}-\frac{T'_{\mathrm{C}}}{J'}}{\frac{T'_{\mathrm{C}}}{J'}}\right|^{-\nu_{t'}^{\mathrm{C}}}. \tag{7.87}$$

Second, the critical points of the initial and final models are represented by the same critical fixed point of the RG transformation:

$$K^{\mathrm{C}} = \frac{J}{T_{\mathrm{C}}} = \frac{J'}{T'_{\mathrm{C}}}, \tag{7.88}$$

and we transform (7.87) into

and

$$\xi \propto \left|\frac{\frac{1}{K}-\frac{1}{K^{\mathrm{C}}}}{\frac{1}{K^{\mathrm{C}}}}\right|^{-\nu_t^{\mathrm{C}}} = \left|\frac{K-K^{\mathrm{C}}}{K}\right|^{-\nu_t^{\mathrm{C}}} \approx \left|\frac{K-K^{\mathrm{C}}}{K^{\mathrm{C}}}\right|^{-\nu_t^{\mathrm{C}}}$$

$$\xi' \propto \left|\frac{\frac{1}{K'}-\frac{1}{K^{\mathrm{C}}}}{\frac{1}{K^{\mathrm{C}}}}\right|^{-\nu_{t'}^{\mathrm{C}}} = \left|\frac{K'-K^{\mathrm{C}}}{K'}\right|^{-\nu_{t'}^{\mathrm{C}}} \approx \left|\frac{K'-K^{\mathrm{C}}}{K^{\mathrm{C}}}\right|^{-\nu_{t'}^{\mathrm{C}}}. \tag{7.89}$$

So, the divergences are the divergences with respect to the relative deviations of the coupling constant from its critical value. Therefore, instead of the subscript "t" in the critical index ν_t^{C}, we could use the subscript "K" of the coupling constant, corresponding to the field parameter t: ν_K^{C}. However, the change of notation would introduce confusion, so we will keep the original notation ν_t^{C}.

The RG transformation keeps the lattice shape and the functional dependence of the Hamiltonian invariant. Therefore, critical indices of the initial and final systems must coincide, so we can omit apostrophes at the notation of the critical index:

$$\xi \propto \left|\frac{K-K^{\mathrm{C}}}{K^{\mathrm{C}}}\right|^{-\nu_t^{\mathrm{C}}} \quad \text{and} \quad \xi' \propto \left|\frac{K'-K^{\mathrm{C}}}{K^{\mathrm{C}}}\right|^{-\nu_t^{\mathrm{C}}}. \tag{7.90}$$

Substituting these divergences into (7.85), we find

$$\left|\frac{K'-K^{\mathrm{C}}}{K-K^{\mathrm{C}}}\right| = \frac{1}{r^{1/\nu_t^{\mathrm{C}}}} = b^{1/\nu_t^{\mathrm{C}}}. \tag{7.91}$$

But the left-hand side of this equation is the eigenvalue, (7.84), of the RG transformation:

$$|\lambda_K| = \frac{1}{r^{1/\nu_t^{\mathrm{C}}}} = b^{1/\nu_t^{\mathrm{C}}}. \tag{7.92}$$

So, for the critical index ν_t^{C}, we find

$$\nu_t^{\mathrm{C}} = \frac{\ln\frac{1}{r}}{\ln|\lambda_K|} = \frac{\ln b}{\ln|\lambda_K|} = \frac{\ln\sqrt{3}}{\ln\left\{1+\frac{1}{2}(8-5\sqrt{2})\ln(2\sqrt{2}+1)\right\}} \approx 1.13. \tag{7.93}$$

The exact value is $\nu_t^{\mathrm{C}} = 1$. So, we see that the RG transformation we have built provides the approximate value of the critical index which is close to the exact value.

Problem 7.4.1

Build the RG approach of representation for the ferromagnetic n.n. Ising model on the square lattice in the absence of magnetic field.

Solution: The solution of the problem is similar to the considered above case of the triangular lattice. The main difference is in the subjective rule of the microstate correspondence. For the triangular lattice, the sign of a new spin was determined by the majority of spin orientations in the cell. However, for the square lattice, this rule cannot be applied directly because in a square cell half of the spins can be oriented "up," while another half—"down," like $\begin{bmatrix}\uparrow & \downarrow\\ \uparrow & \downarrow\end{bmatrix}$. In this case there is no majority that would suggest us the orientation of the final spin.

What should we do in such a case? The answer is very simple: We should divide the "undetermined" configurations in two, prescribing for the first half to generate the spin oriented "up," $\begin{bmatrix}\uparrow & \downarrow\\ \uparrow & \downarrow\end{bmatrix}, \begin{bmatrix}\uparrow & \uparrow\\ \downarrow & \downarrow\end{bmatrix} \Rightarrow \uparrow$, while for the second half, the spin is oriented "down" $\begin{bmatrix}\downarrow & \uparrow\\ \downarrow & \uparrow\end{bmatrix}, \begin{bmatrix}\downarrow & \downarrow\\ \uparrow & \uparrow\end{bmatrix} \Rightarrow \downarrow$.

7.5 RG Approach of Representation: Two-Dimensional Magnetic Systems in the Presence of Magnetic Field

In the previous section, we have discussed the ferromagnetic n.n. Ising model on the triangular lattice in the absence of magnetic field. In this section, we consider a more complex case when the magnetic field is nonzero.

Gibbs probability

$$w_{\{\sigma\}}^{CE} = \frac{1}{Z^{CE}} \exp\left(K_1 \sum_{i=1}^{N} \sigma_i + K_2 \sum_{<i,j>_{n.n.}} \sigma_i \sigma_j \right), \tag{7.94}$$

contains now two coupling constants:

$$K_1 \equiv \beta\mu h \quad \text{and} \quad K_2 \equiv \beta J. \tag{7.95}$$

So, the rule of invariant probabilities transforms into

$$\begin{aligned} &\frac{1}{Z'^{CE'}} \exp\left(K'_1 \sum_{i'=1}^{N/3} \sigma'_{i'} + K'_2 \sum_{<i',j'>_{n.n.}} \sigma'_{i'} \sigma'_{j'} \right) \\ &= \frac{1}{Z^{CE}} \sum_{\{\sigma\}:\{\sigma'\}} \exp\left(K_1 \sum_{i=1}^{N} \sigma_i + K_2 \sum_{<i,j>_{n.n.}} \sigma_i \sigma_j \right). \end{aligned} \tag{7.96}$$

We include the interactions of spins with the magnetic field in the unperturbed Hamiltonian $\widetilde{\mathrm{H}}$, while the perturbation is exactly the same as in the previous section. For the partition function of the unperturbed Hamiltonian,

$$Z^{\widetilde{\mathrm{H}}:\{\sigma'\}} \equiv \sum_{\{\sigma\}:\{\sigma'\}} \exp\left(-\frac{\widetilde{\mathrm{H}}_{\{\sigma\}}}{T} \right), \tag{7.97}$$

whose exponential functions contain $\exp(...)\exp\left(K_1(\sigma_1+\sigma_2+\sigma_3)+K_2(\sigma_1\sigma_2+\sigma_2\sigma_3+\sigma_3\sigma_1)\right)$, we should consider again two possibilities: $\sigma'_1 = \uparrow$ and $\sigma'_1 = \downarrow$. If $\sigma'_1 = \uparrow$, we have

$$\begin{aligned} Z^{\tilde{\mathrm{H}}:\{\sigma'\}} &= \sum_{\{\sigma\setminus\sigma_1,\sigma_2,\sigma_3\}:\{\sigma'\}} e^{\cdots} \sum_{\begin{Bmatrix} \sigma_2 & \sigma_3 \\ \sigma_1 & \end{Bmatrix} = \left\{ \begin{matrix} \uparrow & \uparrow \\ \uparrow & \end{matrix} \right\}, \left\{ \begin{matrix} \downarrow & \uparrow \\ \uparrow & \end{matrix} \right\}, \left\{ \begin{matrix} \uparrow & \downarrow \\ \uparrow & \end{matrix} \right\}, \left\{ \begin{matrix} \uparrow & \uparrow \\ \downarrow & \end{matrix} \right\}} e^{K_1(\sigma_1+\sigma_2+\sigma_3)+K_2(\sigma_1\sigma_2+\sigma_2\sigma_3+\sigma_3\sigma_1)} \\ &= \left(e^{3K_1+3K_2} + 3e^{K_1-K_2} \right) \sum_{\{\sigma\setminus\sigma_1,\sigma_2,\sigma_3\}:\{\sigma'\}} e^{\cdots}. \end{aligned} \tag{7.98}$$

If $\sigma'_1 = \downarrow$, we obtain

$$Z^{\widetilde{\mathrm{H}}:\{\sigma'\}} = \sum_{\{\sigma\setminus\sigma_1,\sigma_2,\sigma_3\}:\{\sigma'\}} e^{\cdots} \sum_{\substack{\begin{Bmatrix}\sigma_2\\ \sigma_1\ \ \sigma_3\end{Bmatrix}=\begin{Bmatrix}\downarrow\\ \downarrow\ \ \downarrow\end{Bmatrix},\begin{Bmatrix}\uparrow\\ \downarrow\ \ \downarrow\end{Bmatrix},\\ \begin{Bmatrix}\downarrow\\ \downarrow\ \ \uparrow\end{Bmatrix},\begin{Bmatrix}\downarrow\\ \uparrow\ \ \downarrow\end{Bmatrix}}} e^{K_1(\sigma_1+\sigma_2+\sigma_3)+K_2(\sigma_1\sigma_2+\sigma_2\sigma_3+\sigma_3\sigma_1)}$$
$$= \left(e^{-3K_1+3K_2} + 3e^{-K_1-K_2}\right) \sum_{\{\sigma\setminus\sigma_1,\sigma_2,\sigma_3\}:\{\sigma'\}} e^{\cdots}. \tag{7.99}$$

In the result for the partition function of the unperturbed Hamiltonian, we find

$$Z^{\widetilde{\mathrm{H}}:\{\sigma'\}} = \prod_{i'=1}^{N/3}\left(e^{3\sigma'_{i'}K_1+3K_2} + 3e^{\sigma'_{i'}K_1-K_2}\right). \tag{7.100}$$

The average

$$\left\langle\sigma_2\right\rangle_{\widetilde{\mathrm{H}}:\{\sigma'\}} \equiv \frac{\sum\limits_{\{\sigma\}:\{\sigma'\}} \sigma_2 \exp\left(-\dfrac{\widetilde{\mathrm{H}}_{\{\sigma\}}}{T}\right)}{\sum\limits_{\{\sigma\}:\{\sigma'\}} \exp\left(-\dfrac{\widetilde{\mathrm{H}}_{\{\sigma\}}}{T}\right)}$$
$$= \frac{\sum\limits_{\sigma_1,\sigma_2,\sigma_3:\sigma'_1} \sigma_2 \exp\left(\begin{matrix}K_1(\sigma_1+\sigma_2+\sigma_3)\\ +K_2(\sigma_1\sigma_2+\sigma_2\sigma_3+\sigma_3\sigma_1)\end{matrix}\right)}{\sum\limits_{\sigma_1,\sigma_2,\sigma_3:\sigma'_1} \exp\left(\begin{matrix}K_1(\sigma_1+\sigma_2+\sigma_3)\\ +K_2(\sigma_1\sigma_2+\sigma_2\sigma_3+\sigma_3\sigma_1)\end{matrix}\right)} \tag{7.101}$$

we find in a similar way. If $\sigma'_1 = \uparrow$,

$$\left\langle\sigma_2\right\rangle_{\widetilde{\mathrm{H}}:\{\sigma'\}} = \frac{(+1)e^{3K_1+3K_2} + 2(+1)e^{K_1-K_2} + (-1)e^{K_1-K_2}}{e^{3K_1+3K_2} + 3e^{K_1-K_2}}$$
$$= \frac{e^{3K_1+3K_2} + e^{K_1-K_2}}{e^{3K_1+3K_2} + 3e^{K_1-K_2}}, \tag{7.102}$$

while for $\sigma'_1 = \downarrow$,

$$\left\langle\sigma_2\right\rangle_{\widetilde{\mathrm{H}}:\{\sigma'\}} = \frac{(-1)e^{-3K_1+3K_2} + 2(-1)e^{-K_1-K_2} + (+1)e^{-K_1-K_2}}{e^{-3K_1+3K_2} + 3e^{-K_1-K_2}}$$
$$= \frac{-e^{-3K_1+3K_2} - e^{-K_1-K_2}}{e^{-3K_1+3K_2} + 3e^{-K_1-K_2}}. \tag{7.103}$$

Finally, for $\langle\sigma_2\rangle_{\widetilde{\mathrm{H}}:\{\sigma'\}}$, we obtain

$$\langle\sigma_2\rangle_{\widetilde{\mathrm{H}}:\{\sigma'\}} = \sigma'_1 \frac{e^{3\sigma'_1K_1+3K_2} + e^{\sigma'_1K_1-K_2}}{e^{3\sigma'_1K_1+3K_2} + 3e^{\sigma'_1K_1-K_2}}, \tag{7.104}$$

which provides for $\left\langle V_{\{\sigma\}}\right\rangle_{\widetilde{\mathrm{H}}:\{\sigma'\}}$ the following expression

$$\left\langle V_{\{\sigma\}}\right\rangle_{\widetilde{\mathrm{H}}:\{\sigma'\}} = -2J \sum_{<i',j'>_{n.n.}} \sigma'_{i'} \frac{e^{3\sigma'_{i'}K_1+3K_2} + e^{\sigma'_{i'}K_1-K_2}}{e^{3\sigma'_{i'}K_1+3K_2} + 3e^{\sigma'_{i'}K_1-K_2}} \sigma'_{j'} \frac{e^{3\sigma'_{j'}K_1+3K_2} + e^{\sigma'_{j'}K_1-K_2}}{e^{3\sigma'_{j'}K_1+3K_2} + 3e^{\sigma'_{j'}K_1-K_2}}. \tag{7.105}$$

Substituting (7.100 and 7.105) into (7.96), we find

$$\frac{1}{Z'^{CE'}} \exp\left(K'_1 \sum_{i'=1}^{N/3} \sigma'_{i'} + K'_2 \sum_{<i',j'>_{n.n.}} \sigma'_{i'}\sigma'_{j'} \right) = \frac{1}{Z^{CE}} \prod_{i'=1}^{N/3} \left(e^{3\sigma'_{i'}K_1+3K_2} + 3e^{\sigma'_{i'}K_1-K_2} \right)$$
$$\times \exp\left(2K_2 \sum_{<i',j'>_{n.n.}} \sigma'_{i'} \frac{e^{3\sigma'_{i'}K_1+3K_2} + e^{\sigma'_{i'}K_1-K_2}}{e^{3\sigma'_{i'}K_1+3K_2} + 3e^{\sigma'_{i'}K_1-K_2}} \sigma'_{j'} \frac{e^{3\sigma'_{j'}K_1+3K_2} + e^{\sigma'_{j'}K_1-K_2}}{e^{3\sigma'_{j'}K_1+3K_2} + 3e^{\sigma'_{j'}K_1-K_2}} \right). \tag{7.106}$$

This relationship is formulated for the spins of the whole new lattice with $\frac{N'q}{2} = \frac{(N/3)6}{2} = N$ spin pairs. To transform it into the relationship, formulated for a separate spin pair, we notice that each separate spin participates in six spin pairs. Therefore, each multiplier of a separate spin in (7.106) belongs simultaneously to six pairs, while for each of them it provides only $\sqrt[6]{\ }$ of its total value:

$$\frac{1}{\sqrt[N]{Z'^{CE'}}} \exp\left(\frac{K'_1}{6}\sigma'_{i'} + \frac{K'_1}{6}\sigma'_{j'} + K'_2\sigma'_{i'}\sigma'_{j'} \right)$$
$$= \frac{1}{\sqrt[N]{Z^{CE}}} \sqrt[6]{e^{3\sigma'_{i'}K_1+3K_2} + 3e^{\sigma'_{i'}K_1-K_2}} \sqrt[6]{e^{3\sigma'_{j'}K_1+3K_2} + 3e^{\sigma'_{j'}K_1-K_2}} \times \exp\left(\begin{array}{l} 2K_2\sigma'_{i'} \dfrac{e^{3\sigma'_{i'}K_1+3K_2} + e^{\sigma'_{i'}K_1-K_2}}{e^{3\sigma'_{i'}K_1+3K_2} + 3e^{\sigma'_{i'}K_1-K_2}} \\ \times \sigma'_{j'} \dfrac{e^{3\sigma'_{j'}K_1+3K_2} + e^{\sigma'_{j'}K_1-K_2}}{e^{3\sigma'_{j'}K_1+3K_2} + 3e^{\sigma'_{j'}K_1-K_2}} \end{array} \right). \tag{7.107}$$

This equality should be valid for arbitrary projections of $\sigma'_{i'}$ and $\sigma'_{j'}$:

$$\sigma'_{i'} = +1, \sigma'_{j'} = +1 \Rightarrow \frac{1}{\sqrt[N]{Z'^{CE'}}} e^{\frac{K'_1}{3}+K'_2}$$
$$= \frac{1}{\sqrt[N]{Z^{CE}}} \left(e^{3K_1+3K_2} + 3e^{K_1-K_2} \right)^{1/3} \exp\left(2K_2 \left(\frac{e^{3K_1+3K_2} + e^{K_1-K_2}}{e^{3K_1+3K_2} + 3e^{K_1-K_2}} \right)^2 \right), \tag{7.108}$$

$$\left.\begin{matrix}\sigma'_{i'}=+1,\sigma'_{j'}=-1\\ \sigma'_{i'}=-1,\sigma'_{j'}=+1\end{matrix}\right\}\Rightarrow \frac{1}{\sqrt[N]{Z'^{CE'}}}e^{-K'_2}$$
$$=\frac{1}{\sqrt[N]{Z^{CE}}}\begin{pmatrix}e^{3K_1+3K_2}\\ +3e^{K_1-K_2}\end{pmatrix}^{1/6}\begin{pmatrix}e^{-3K_1+3K_2}\\ +3e^{-K_1-K_2}\end{pmatrix}^{1/6}$$
$$\times\exp\left(-2K_2\frac{e^{3K_1+3K_2}+e^{K_1-K_2}}{e^{3K_1+3K_2}+3e^{K_1-K_2}}\frac{e^{-3K_1+3K_2}+e^{-K_1-K_2}}{e^{-3K_1+3K_2}+3e^{-K_1-K_2}}\right), \tag{7.109}$$

$$\sigma'_{i'}=-1,\sigma'_{j'}=-1\Rightarrow\frac{1}{\sqrt[N]{Z'^{CE'}}}e^{-\frac{K'_1}{3}+K'_2}$$
$$=\frac{1}{\sqrt[N]{Z^{CE}}}(e^{-3K_1+3K_2}+3e^{-K_1-K_2})^{1/3}\exp\left(2K_2\left(\frac{e^{-3K_1+3K_2}+e^{-K_1-K_2}}{e^{-3K_1+3K_2}+3e^{-K_1-K_2}}\right)^2\right). \tag{7.110}$$

Dividing (7.108) by (7.110) and dividing (7.108) by (7.109), we find:

$$K'_1=\frac{1}{2}\ln\left(\frac{e^{3K_1+3K_2}+3e^{K_1-K_2}}{e^{-3K_1+3K_2}+3e^{-K_1-K_2}}\right)+3K_2\left(\frac{e^{3K_1+3K_2}+e^{K_1-K_2}}{e^{3K_1+3K_2}+3e^{K_1-K_2}}\right)^2$$
$$-3K_2\left(\frac{e^{-3K_1+3K_2}+e^{-K_1-K_2}}{e^{-3K_1+3K_2}+3e^{-K_1-K_2}}\right)^2, \tag{7.111}$$

$$K'_2=\frac{1}{2}K_2\left(\frac{e^{3K_1+3K_2}+e^{K_1-K_2}}{e^{3K_1+3K_2}+3e^{K_1-K_2}}+\frac{e^{-3K_1+3K_2}+e^{-K_1-K_2}}{e^{-3K_1+3K_2}+3e^{-K_1-K_2}}\right)^2. \tag{7.112}$$

The trivial fixed points of this RG transformation are $\vec{\mathbf{K}}^*=\begin{Vmatrix}0\\0\end{Vmatrix}$ (zero field, infinite temperature), $\vec{\mathbf{K}}^*=\begin{Vmatrix}0\\+\infty\end{Vmatrix}$ (zero field, zero temperature), and $\vec{\mathbf{K}}^*=\begin{Vmatrix}\pm\infty\\0\end{Vmatrix}$ (infinite field, infinite temperature). The critical fixed point is the critical fixed point of the system in the absence of magnetic field:

$$\vec{\mathbf{K}}^{\mathrm{C}}=\begin{Vmatrix}0\\\frac{1}{4}\ln(2\sqrt{2}+1)\end{Vmatrix}\approx\begin{Vmatrix}0\\0.34\end{Vmatrix} \tag{7.113}$$

The behavior of flow curves is presented in Fig. 7.17. When the magnetic field is zero, $K_1=0$, the space of the coupling constants degenerates into the abscissa

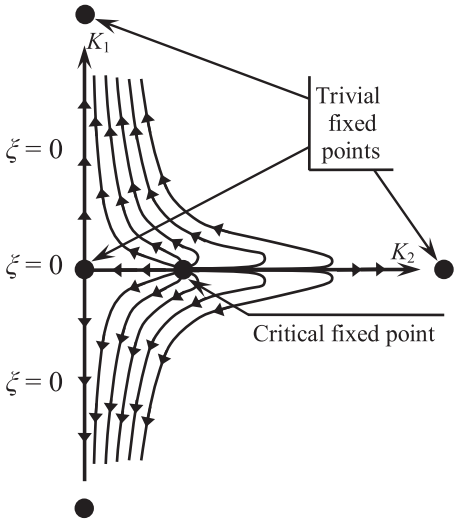

Fig. 7.17 Flow curves of the ferromagnetic n.n. Ising model in nonzero magnetic field

axis whose flow curves we have studied in Fig. 7.15. When the magnetic field is nonzero, two additional trivial fixed points appear, $\vec{\mathbf{K}}^* = \begin{Vmatrix} \pm\infty \\ 0 \end{Vmatrix}$, which correspond to the case of infinite field and are working like attractors.

The appearance of the new trivial fixed points transforms two previous trivial fixed points, $\vec{\mathbf{K}}^* = \begin{Vmatrix} 0 \\ 0 \end{Vmatrix}$ and $\vec{\mathbf{K}}^* = \begin{Vmatrix} 0 \\ +\infty \end{Vmatrix}$, into saddle points. The manifold, leaving $\vec{\mathbf{K}}^* = \begin{Vmatrix} 0 \\ 0 \end{Vmatrix}$ and arriving at $\vec{\mathbf{K}}^* = \begin{Vmatrix} \pm\infty \\ 0 \end{Vmatrix}$, corresponds to zero correlation length. Similar manifold connects $\vec{\mathbf{K}}^* = \begin{Vmatrix} 0 \\ +\infty \end{Vmatrix}$ with $\vec{\mathbf{K}}^* = \begin{Vmatrix} \pm\infty \\ 0 \end{Vmatrix}$. To see that the reader may consider an alternative space of coupling constants when K_2 is substituted by $1/K_2$.

Linearizing the RG transformation in the vicinity of the critical fixed point, we find

$$K'_1 - K_1^{\mathrm{C}} = \left\{ \frac{3}{\sqrt{2}} + \frac{3}{4}(8 - 5\sqrt{2}) \ln(2\sqrt{2} + 1) \right\} \left(K_1 - K_1^{\mathrm{C}} \right), \tag{7.114}$$

$$K'_2 - K_2^{\mathrm{C}} = \left\{ 1 + \frac{1}{2}(8 - 5\sqrt{2}) \ln(2\sqrt{2} + 1) \right\} \left(K_2 - K_2^{\mathrm{C}} \right). \tag{7.115}$$

We see that the increments of two coupling constants are independent from one another. This means that the linearized matrix of the RG transformation is diagonal in the axes of coupling constants,

$$\left. \frac{\partial \vec{\mathbf{K}}'}{\partial \vec{\mathbf{K}}} \right|_{\vec{\mathbf{K}}^{\mathrm{C}}} = \begin{Vmatrix} \lambda_{K_1} & 0 \\ 0 & \lambda_{K_2} \end{Vmatrix}, \tag{7.116}$$

with two eigenvalues,

$$\lambda_{K_1} = \frac{3}{\sqrt{2}} + \frac{3}{4}(8-5\sqrt{2})\ln(2\sqrt{2}+1) \approx 3.06, \tag{7.117}$$

$$\lambda_{K_2} = 1 + \frac{1}{2}(8-5\sqrt{2})\ln(2\sqrt{2}+1) \approx 1.62, \tag{7.118}$$

and two corresponding eigenvectors,

$$\kappa_{K_1} = \left\| \begin{matrix} 1 \\ 0 \end{matrix} \right\|, \kappa_{K_2} = \left\| \begin{matrix} 0 \\ 1 \end{matrix} \right\| \tag{7.119}$$

Considering the critical isofield curve similarly to Sect. 7.4, we find

$$\nu_t^{\mathrm{C}} = \frac{\ln \dfrac{1}{r}}{\ln \left| \lambda_{K_2} \right|} = \frac{\ln b}{\ln \left| \lambda_{K_2} \right|}. \tag{7.120}$$

Substituting into this expression λ_{K_2} from (7.118), we find

$$\nu_t^{\mathrm{C}} = \frac{\ln \sqrt{3}}{\ln \left\{ 1 + \dfrac{1}{2}(8-5\sqrt{2})\ln(2\sqrt{2}+1) \right\}} \approx 1.13. \tag{7.121}$$

If, instead of the approximate value of λ_{K_2}, given by (7.118), we substituted the exact eigenvalue $\lambda_{K_2} = \sqrt{3}$, we would obtain the exact value of the critical index ν_t^{C}:

$$\nu_t^{\mathrm{C}} = \frac{\ln \sqrt{3}}{\ln \sqrt{3}} = 1. \tag{7.122}$$

To find the second critical index ν_h^{C} of the correlation length, we consider the critical isotherm $t = 0$. By definition

$$\xi \propto \frac{1}{\left| h \right|^{\nu_h^{\mathrm{C}}}}. \tag{7.123}$$

Since after the RG transformation, the system has the same value of the critical index ν_h^{C} and the same value of the critical field $h_{\mathrm{C}} = 0$, for the new system we have

$$\xi' \propto \frac{1}{\left| h' \right|^{\nu_h^{\mathrm{C}}}}. \tag{7.124}$$

For the critical isotherm

$$K_1 = \frac{\mu h}{T_C},\ K'_1 = \frac{\mu h'}{T_C} \text{ and } K'_2 = K_2 = K_2^C = \frac{J}{T_C}. \tag{7.125}$$

From these equalities, we obtain

$$h = \frac{T_C K_1}{\mu},\ h' = \frac{T_C K'_1}{\mu}, \quad \text{where} \quad T_C = \frac{J}{\frac{1}{4}\ln(2\sqrt{2}+1)}. \tag{7.126}$$

Substituting (7.126) into (7.123) and (7.124), we find

$$\xi \propto \frac{1}{|K_1|^{\nu_h^C}} \quad \text{and} \quad \xi' \propto \frac{1}{|K'_1|^{\nu_h^C}}. \tag{7.127}$$

So, the divergences are the divergences with respect to the deviations of K_1 from its critical value $K_1^C = 0$. Therefore, instead of the subscript "h" in the critical index ν_h^C, we could use the subscript "K_1" of the coupling constant, corresponding to the field parameter h: $\nu_{K_1}^C$. However, we will keep the original notation ν_h^C to avoid confusion.

Substituting (7.127) into (7.85), we obtain

$$\left|\frac{K'_1}{K_1}\right| = \frac{1}{r^{1/\nu_h^C}} = b^{1/\nu_h^C}. \tag{7.128}$$

The left-hand side of this equation is the eigenvalue (7.117) of the RG transformation:

$$\left|\lambda_{K_1}\right| = \frac{1}{r^{1/\nu_h^C}} = b^{1/\nu_h^C}. \tag{7.129}$$

For the critical index ν_h^C, this provides

$$\nu_h^C = \frac{\ln\frac{1}{r}}{\ln\left|\lambda_{K_1}\right|} = \frac{\ln b}{\ln\left|\lambda_{K_1}\right|}. \tag{7.130}$$

Substituting the RG approximation (7.117), we find the approximation of the critical index ν_h^C:

$$\nu_h^C = \frac{\ln\sqrt{3}}{\ln\left\{\frac{3}{\sqrt{2}} + \frac{3}{4}(8-5\sqrt{2})\ln(2\sqrt{2}+1)\right\}} \approx 0.491. \tag{7.131}$$

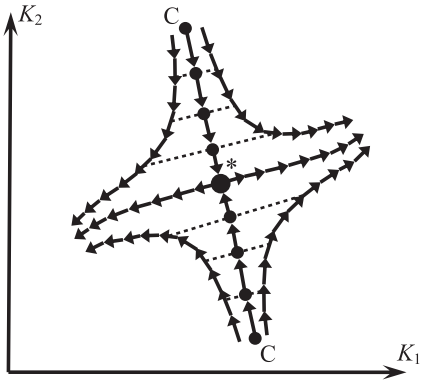

Fig. 7.18 Flow curves of the RG transformation in high dimensions of the space of coupling constants

We see that indeed the eigenvalues of the RG transformation, linearized in the vicinity of the critical fixed point, provide the critical indices of the system. We will discuss this question in Chap. 8 in more detail.

Since the RG transformation is merely an approximation, it is always reasonable to compare its results with exact or experimental values. The exact solution provides $\lambda_{K_1} = 3^{15/16}$. Substituting this eigenvalue into (7.130), we find the exact value of the critical index ν_h^{C},

$$\nu_h^{\mathrm{C}} = \frac{\ln\sqrt{3}}{\frac{15}{8}\ln\sqrt{3}} = \frac{8}{15} \approx 0.533, \tag{7.132}$$

to which the RG value (7.131) serves as a good approximation.

In higher dimensions of the space of coupling constants, the criticality of the system may no longer be described by a single critical fixed point of Figs. 7.15 and 7.17. There could exist the critical manifold, ending up at the critical fixed point. In Fig. 7.18, the critical manifold is plotted schematically by the succession of filled dots which ends up at the critical fixed point "*." The manifold, emerging from the critical fixed point, is not necessarily critical; however, it would require an infinite number of the RG steps to make the correlation length finite.

The near-critical system in Fig. 7.18 is moved away from its critical point by the RG transformation. This is demonstrated by the dotted lines, schematically representing the distance from the critical point (how far the coupling constants are from their critical values).

As an example of such behavior, we present in Fig. 7.19 the flow curves on the space of coupling constants for the case of zero magnetic field of the ferromagnetic Ising model with spin interactions in n.n. and n.n.n. pairs. There are two coupling constants, $K_1 = \beta J_{n.n.}$ and $K_2 = \beta J_{n.n.n.}$, where the first coupling constant is responsible for the n.n. interactions, while the second is for the n.n.n. interactions.

If we consider $K_2 = 0$ in the model, we return to the n.n. Ising model. On its space of coupling constants (which is the abscissa axis of Fig. 7.19), we see the

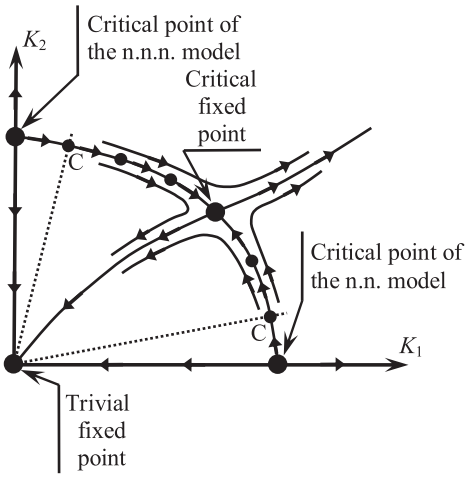

Fig. 7.19 Flow curves of the ferromagnetic n.n.–n.n.n. Ising model in zero magnetic field

flow curves of Fig. 7.15. We see a similar behavior for the n.n.n. Ising model with $K_1 = 0$ which is represented in Fig. 7.19 by the ordinate axis.

For the n.n.–n.n.n. mixture model, we should consider particular values of the interaction constants $J_{n.n.}$ and $J_{n.n.n.}$. This corresponds to the particular value of the ratio K_2 / K_1 of the coupling constants. Then the model is represented by one of the dotted lines in Fig. 7.19; and its critical point is formed by the intersection of this dotted line with the critical manifold.

Why are we so interested in the critical fixed points of the RG transformation? Because they perform the role of the "capacitors" of criticality. The RG transformation keeps invariant the functional form of the Hamiltonian and the lattice shape. Therefore, all systems of the universality class possess the same critical indices which are invariant also.

So, critical indices are the same in the initial system and in the system at the critical fixed point. But it is much easier to find critical indices in the vicinity of the critical fixed point by linearizing the RG transformation there. We have already seen two examples, (7.120) and (7.130): In the vicinity of the critical fixed point, we were able to find the critical indices ν_t^C and ν_h^C from the general considerations and from the eigenvalues (7.117) and (7.118) of the linearized RG transformation. A similar procedure can be performed for other critical indices as well, as we will study in Chap. 8.

Of course, if for a one-dimensional space of coupling constants a critical manifold degenerates into the critical fixed point—repeller (Fig. 7.15), the critical point of the initial system is just the fixed point of the RG transformation; and the invariance of critical indices becomes trivial in this case.

7.6 Percolation

Let us now consider how the RG transformation is built for the percolation phenomena.

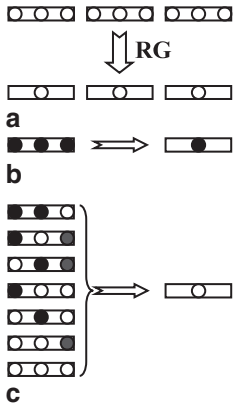

Fig. 7.20 The approach of representation for the one-dimensional percolation. (**a)** The RG transformation with $b = 3$. **(b–c)** The rule of correspondence of microstates. Only a completely occupied cell transforms into the occupied site. The rest of microstates transform into an empty site

As the first example, we consider the one-dimensional site percolation. We divide the one-dimensional chain of sites into cells of size b ($b = 3$ in Fig. 7.20a). Each cell of the initial system generates a site of the new system.

How should we build the rule of correspondence of microstates? In Chap. 6, we saw that direct, thoughtless application of statistical physics to percolation phenomena does not provide the desired results.

Indeed, the primary concern in percolation is the connectivity of sites within clusters. The percolation threshold itself represents a situation when the opposite edges of the lattice become connected. Therefore, the subjective rule of correspondence of microstates should be built keeping invariant the connectivity within clusters.

To keep the percolating properties of the cluster structure unchanged, the initial cell which is percolated should transform into the percolating (occupied) site on the new lattice. On the contrary, if the initial cell is not percolated, it should be transformed into non-percolating (empty) site.

The one-dimensional cell is percolated only when all its b sites are occupied (Fig. 7.20b). Therefore, applying the approach of representation, we say that only a completely occupied cell is transformed into an occupied site, while the rest of the microstates generate an empty site (Fig. 7.20c).

After we have built the rule of correspondence of microstates, it is easy to create the rule of invariant probabilities:

$$p' = p^b, \tag{7.133}$$

where the probability p' for the new site to be occupied is generated only by the completely occupied cell. If we decided to sum instead the probabilities for the new site to be empty (to sum the probabilities of microstates from Fig. 7.20c), we would, obviously, obtain the complementary equality $1 - p' = 1 - p^b$.

We see that in percolation, the role of a coupling constant is fulfilled by the field parameter p which "absorbs" all that changes during the RG transformation.

Since the lattice and model are invariant, the point of the percolation threshold stays unchanged, $p'_C = p_C = 1$, and plays the role of the critical fixed point of the RG transformation. The trivial fixed point is $p = 0$.

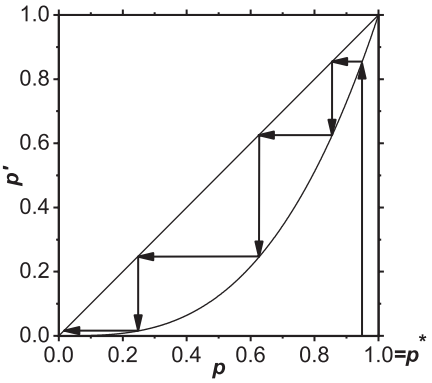

Fig. 7.21 The map representing flows of the one-dimensional RG transformation

Again, since, in percolation, there is always only one coupling constant, the most illustrative way to study the flows of the RG transformation is to represent the solution (7.133) graphically as a map (Fig. 7.21). The map clearly demonstrates that the critical fixed point is a repeller, and the system moves away from it towards the trivial fixed point.

As we have already discussed in (7.39), the RG transformation decreases the correlation length b times:

$$\xi' = r\xi = \xi / b. \tag{7.134}$$

Since the critical index ν stays unchanged, for the divergences of the initial and new correlation lengths in the vicinity of the percolation threshold we have:

$$\xi \propto \frac{1}{|\, p - p_C \,|^{\nu}} \quad \text{and} \quad \xi' \propto \frac{1}{|\, p' - p_C \,|^{\nu}}. \tag{7.135}$$

Substituting them into (7.134), we find:

$$\nu = \frac{\ln b}{\ln \dfrac{|\, p' - p_C \,|}{|\, p - p_C \,|}} = \frac{\ln b}{\ln \left.\dfrac{dp'}{dp}\right|_{p_C}}. \tag{7.136}$$

Substituting (7.133) into this equation, for the one-dimensional percolation we find:

$$\nu = \frac{\ln b}{\ln \dfrac{1 - p^b}{1 - p}} \to 1 \; (p \to p_C = 1), \tag{7.137}$$

which complies with the exact result (6.220).

Above, we have discussed that the rule of correspondence of microstates should take into account the connectivity of sites within clusters. Let us, with the aid of the

following problem, demonstrate what happens when we applied the techniques of statistical physics thoughtlessly.

Problem 7.6.1

Apply the approach of a single survivor to the one-dimensional percolation.

Solution: To employ the approach of a single survivor, we should divide the chain of sites into cells of size b and require that the first site of each cell survives the RG transformation to keep its state (occupied or empty) on the new lattice. The rest of the sites in the cell disappear:

$$p' = p\sum_{k=0}^{b-1}\frac{(b-1)!}{k!(b-1-k)!}p^k(1-p)^{b-1-k} = p(p+1-p)^{b-1} = p, \qquad (7.138)$$

where the probability for the new site to be occupied equals p times the sum of the probabilities for other sites within the cell to have arbitrary states. Obviously, this sum equals unity so that $p' = p$. The situation resembles the RG transformation (7.12–7.14) for the magnetic system when in the absence of interactions among spins, $K_2 = 0$, the RG transformation becomes trivial: $K'_1 = K_1$, $K'_2 = K_2 = 0$.

From one point of view, the model transforms into itself exactly, keeping even the value of the field parameter unchanged. Therefore, the correlation length must stay unchanged also. But from another point of view, the RG transformation must decrease the correlation length b times.

This contradiction clearly shows that the built RG transformation is incorrect. In particular, what is wrong is the rule of correspondence of microstates which we introduced subjectively. This example clearly demonstrates that, coarse graining our system, we must take into account the primary concern in percolation—the connectivity within clusters. The correlation length in percolation is the direct representative of the connectivity; and paying no attention to the latter, we have lost the correct behavior of the former.

Let us now consider the RG transformation for two-dimensional site percolation; first, on triangular lattice. We divide the lattice into triangular cells. Each cell generates a site on the new lattice. The geometry of transformation is analogous to the geometry of magnetic system in Fig. 7.9.

Next, we should formulate the rule of correspondence of microstates. Following the general rule to transform a percolated cell into an occupied site and not percolated cell into an empty site, we need only to formulate the criterion for a triangular cell to be percolated. We will consider a triangular cell as percolated when at least two of its three sites are occupied (Fig. 7.22a) so that at least one edge of the cell percolates. Otherwise, we consider the cell not to be percolated (Fig. 7.22b).

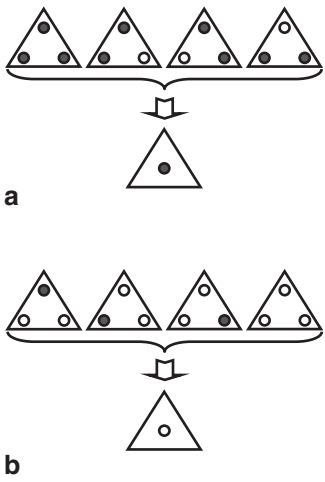

Fig. 7.22 The rule of correspondence of microstates on triangular lattice

The rule of invariant probabilities sums the probabilities of microstates from Fig. 7.22a:

$$p' = p^3 + 3p^2(1-p), \tag{7.139}$$

where p^3 is the probability for all three sites to be occupied and $3p^2(1-p)$ represents three microstates, each bringing the probability $p^2(1-p)$ for two sites to be occupied, while one site is empty.

Similarly, we can sum the probabilities from Fig. 7.22b to obtain the probability for the new site to be empty:

$$1-p' = 3p(1-p)^2 + (1-p)^3. \tag{7.140}$$

However, this equation does not contain any new information and returns us to (7.139).

Again, the behavior of the RG flows is better illustrated by a map presented in Fig. 7.23. The critical fixed point $p_C = 1/2$ serves as a repeller so that the RG

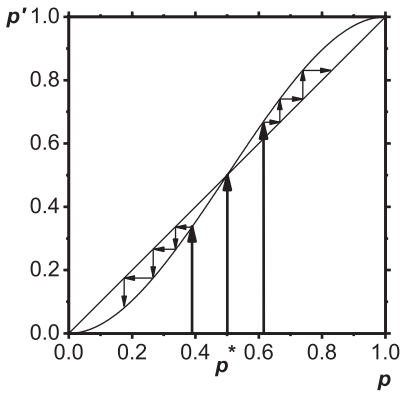

Fig. 7.23 A map of the flows of the RG transformation for the percolation on triangular lattice

transformation moves the system away from it towards one of the two trivial fixed points: $p = 0$ or $p = 1$.

The predicted value $p_C = 1/2$ of the percolation threshold coincides with the exact solution of the system. This is one of those cases when the RG transformation returns not an approximate but the exact result which proves us to be "lucky" (or "skilful" if one prefers) in the formulation of the subjective criterion for the rule of correspondence of microstates.

In the vicinity of the percolation threshold, we substitute (7.139) and $b = \sqrt{3}$ into (7.136) to find the critical index

$$\nu \to \frac{\ln \sqrt{3}}{\ln \frac{3}{2}} \approx 1.355. \tag{7.141}$$

It is close to the exact value $\nu = 4/3 = 1.333$.

Problem 7.6.2:

Build the RG transformation for site percolation on square lattice.

Solution: We divide the square lattice into cells of linear size $b = 2$ when each cell generates a site of the new lattice (part a of the figure).

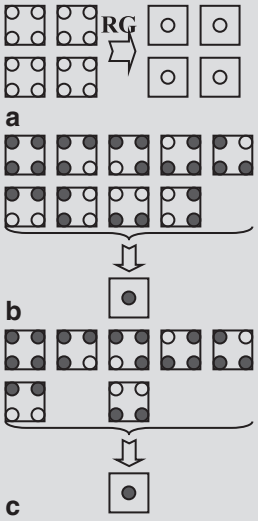

To formulate the rule of correspondence of microstates, we, similar to the case of the triangular lattice, as a percolated cell, consider a cell, at least one edge of which is occupied. This cell transforms into the occupied site (part b of the figure). Such a choice seems to be reasonable—one occupied edge of the cell means that this cell can percolate along this edge to form a percolating cluster.

Thereby, for the rule of invariant probabilities we find:

$$p' = p^4 + 4p^3(1-p) + 4p^2(1-p)^2, \tag{7.142}$$

where the first term represents the completely occupied cell, the second—four microstates with three occupied sites, and the third—four microstates with two occupied sites. However, the critical fixed point of this RG transformation:

$$p_C = \frac{1}{2}(3-\sqrt{5}) \approx 0.38, \tag{7.143}$$

does not approximate the experimental value $p_C \approx 0.59$.

Why the predicted value of the percolation threshold was so crude? As we will see below, there is a technique to improve the accuracy of the RG transformation. However, in our case, the prediction is so crude that it indicates we have not been "skilful" enough (or "lucky" if one prefers) in our formulation of the subjective criterion for the rule of correspondence of microstates.

Returning to the second row of microstates (part b of the figure), we see that as percolated we have considered all four microstates when one edge of the cell is occupied, while another is empty. But filling the lattice randomly with these four microstates, we would never obtain a percolating cluster, connecting, for example, the left and the right sides of the model—one cell would percolate horizontally, another vertically, and a chain of occupied sites would end sooner or later.

For a percolating cluster to connect the left side of the model to the right side, we expect all cells to percolate horizontally on average. Instead, we have considered cells, percolating vertically, as also helping this cluster to be formed. Thereby, we significantly weakened the criterion of percolation and obtained the percolation threshold much lower than the real value.

To improve the situation, we keep only two of the discussed four microstates, corresponding to the cell percolated horizontally (part c of the figure). Now, all microstates, forming the occupied site on the new lattice, contain at least one occupied *horizontal* edge to form the percolating cluster from the left to the right of the model.

The corrected rule of invariant probabilities,

$$p' = p^4 + 4p^3(1-p) + 2p^2(1-p)^2, \tag{7.144}$$

possesses a critical fixed point

$$p_C = \frac{1}{2}(\sqrt{5}-1) \approx 0.62, \tag{7.145}$$

which approximates the experimental value $p_C \approx 0.59$ much better. This problem illustrates that the RG transformation in real space is merely a tool whose accuracy depends on the skillfulness of the investigator who formulates the subjective criterion for the rule of correspondence of microstates.

Problem 7.6.3:

Build the RG transformation for bond percolation on the square lattice.

Solution: In this problem, we, for the first time, consider not the site but bond percolation. Again, we divide square lattice into cells of linear size $b = 2$ when each cell generates two bonds of the new lattice (part a of the figure).

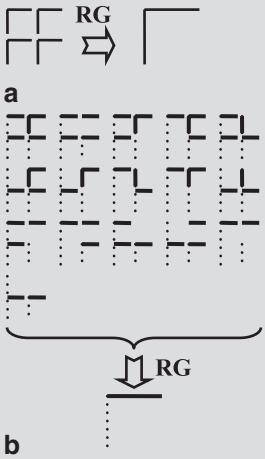

We intend to study percolation from the left to the right of the model. The rule of correspondence of microstates is presented in part b of the figure, where the occupied horizontal bond on the new lattice is generated only by cells percolating from the left to the right. Solid lines represent the occupied bonds, absent lines represent empty bonds, and dotted lines are bonds whose state (occupied or empty) is undetermined since it does not influence the left–right percolation.

The rule of invariant probabilities is

$$p' = p^5 + 5p^4(1-p) + 8p^3(1-p)^2 + 2p^2(1-p)^3. \tag{7.146}$$

The predicted value of the critical fixed point,

$$p_C = \frac{1}{2}, \tag{7.147}$$

coincides with the exact value.

For the critical index ν from (7.136), we find:

$$\nu \to \frac{\ln 2}{\ln \frac{13}{8}} \approx 1.43, \tag{7.148}$$

while the exact solution provides a close value $\nu = 4/3 = 1.333$.

7.7 Damage Phenomena

In previous sections, we considered coarse graining in the vicinity of a critical point, where the divergence of the correlation length provided the possibility to consider flow curves of the RG transformation. However, in Chap. 6 we found that the correlation length diverges in the proximity of the spinodal point as well. The divergence of the correlation length leads to scale invariance which allows us to build an RG transformation in the vicinity of the spinodal as well. As an example, we consider the fiber-bundle model (FBM) again (Allegre et al. 1982; Smalley et al. 1985; Sornette 1989a, b; Narkunskaya and Shnirman 1990; Newman and Gabrielov 1991; Newman et al. 1994; Sornette and Sammis 1995; Shnirman and Blanter 1998, 2003; Sornette 2006). However, this time, the model will not be formulated as a mean-field system—a broken fiber will not redistribute its loading uniformly among all intact fibers. Instead, we will consider the nearest-neighbor stress redistribution.

In contrast to the FBMs considered earlier, this time we arrange the ends of all fibers along an imaginary line, so the model becomes plane like a ply of a composite material (Fig. 7.24). This makes our model a one-dimensional chain of fibers which will further simplify the organization of fibers into the RG cells.

The load is transferred to fibers in such a way that when all fibers are intact, the stress of each of them is σ. We again consider the strength CDF $P(\sigma)$ as a probability for a fiber to have been broken when it is supposed to carry the stress σ.

To form the RG cells, we divide the chain of fibers into cells with $b = 2$ fibers in each. The RG transforms each cell of the initial model into a fiber of the final model.

The primary concern in damage phenomena is the behavior of the damage parameter. Therefore, to keep the behavior of the system unchanged, the state of the

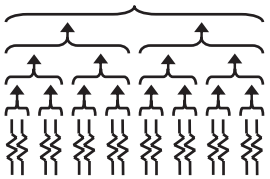

Fig. 7.24 All fibers are arranged in pairs forming the RG cells

new fiber (broken or intact) should represent the initial cell. If both fibers or at least one fiber are still intact in the initial cell, $\{\|\}$, $\{|\,|\}$, or $\{\,|\,\}$, we consider this cell as still able to carry the load, and the new fiber should also be intact: $\{|\}$. On the contrary, if both fibers are broken, $\{\,\,\}$, the new fiber also has to be broken: $\{\,\}$.

Let us consider all these cases and situations leading to them separately:

- If both initial fibers are intact, $\{\|\}$, when the stress in both fibers is σ, the probability of such a case is $(1-P(\sigma))^2$. The new fiber is also intact.
- One fiber is broken while another remains intact. Then the first fiber breaks when its stress is σ so that the probability of this is $P(\sigma)$. Considering the nearest-neighbor stress redistribution, we assume that the broken fiber transfers its stress σ to the second fiber in the cell so that the stress in the second fiber becomes 2σ. Therefore, the probability for the second fiber to still remain intact is $(1-P(2\sigma))$. Since two microconfigurations, $\{|\,|\}$ and $\{\,|\,\}$, correspond to this case, the total probability of such a situation is $2P(\sigma)(1-P(2\sigma))$. The initial cell transforms into an intact fiber.
- Both fibers of the initial cell break at once when their stresses are equal to σ: $\{\|\} \Rightarrow \{\,\,\}$. The probability of this case is $P^2(\sigma)$; and the new fiber is also broken.
- One fiber breaks at once, when its stress is σ, with probability $P(\sigma)$. The second fiber, when its stress was σ also, stayed intact but breaks when the first fiber transfers its stress so that the stress in the second fiber becomes 2σ: $\{\|\} \Rightarrow \{|\,\} \Rightarrow \{\,\,\}$. The corresponding probability for the second fiber is $(P(2\sigma)-P(\sigma))$. Again, due to the presence of an alternative scenario, $\{\|\} \Rightarrow \{|\,|\} \Rightarrow \{\,\,\}$, leading to the same outcome, in the total probability $2P(\sigma)(P(2\sigma)-P(\sigma))$ of such a situation, we should use the multiplier 2 again. The new fiber is broken.

Summarizing these possible outcomes, for the probability of the new fiber to be broken, we find:

$$P'(\sigma') = P^2(\sigma) + 2P(\sigma)[P(2\sigma)-P(\sigma)] = P(\sigma)[2P(2\sigma)-P(\sigma)]. \quad (7.149)$$

Here, the role of a coupling constant is fulfilled by the stress σ which is transformed by the RG into σ'. Since we build the RG transformation so that the behavior of the system would remain invariant, the functional dependence of $P'(\sigma')$ on σ' should be the same as the functional dependence $P(\sigma)$ on σ. However, the strength CDF P contains some parameters that can change. For example, the two-parameter Weibull distribution

$$P(s) = 1 - e^{-\left(\frac{s}{s_0}\right)^{\beta}}, \quad (7.150)$$

contains two parameters, s_0 and β. These parameters may, in principle, also serve as coupling constants. Therefore, we rewrite (7.149) as

$$P(\sigma', a', b', \ldots) = P(\sigma, a, b, \ldots)[2P(2\sigma, a, b, \ldots) - P(\sigma, a, b, \ldots)]. \quad (7.151)$$

However, since we have only one equation, connecting the previous and the new values of the coupling constants, we expect that there is only a single-coupling constant in this equation. Therefore, the parameters of the strength CDF P are usually kept invariant, leaving only σ to change:

$$P(\sigma') = P(\sigma)[2P(2\sigma) - P(\sigma)]. \tag{7.152}$$

Problem 7.7.1:

Build the RG transformation for the model considering the Weibull distribution to be the strength CDF.

Solution: Substituting the Weibull distribution (7.150) into (7.152), we find:

$$\sigma' = s_0 \left(2\left(\frac{\sigma}{s_0}\right)^{\beta} - \ln\left\{ 1 - 2e^{-(2^{\beta}-1)\left(\frac{\sigma}{s_0}\right)^{\beta}} + 2e^{-(2^{\beta}-2)\left(\frac{\sigma}{s_0}\right)^{\beta}} \right\} \right)^{1/\beta}. \tag{7.153}$$

7.8 Why does the RG Transformation Return only Approximate Results?

For almost every model, we saw that the RG transformation returns not exact but approximate results. Often the culprit is our misjudgment within the subjective criterion which does not represent the real behavior of the system. But what if it were absolutely correct? Are there other factors influencing the accuracy of the results of the RG transformation?

The most illustrative is to discuss this question with the aid of clusters in the theory of percolation. In Fig. 7.25 we apply the RG transformation to the triangular lattice in accordance with the rule of correspondence of microstates from Fig. 7.22. Small filled and empty circles represent initial occupied and empty sites, respectively. Big circles are the new sites. Dashed lines connect the initial occupied sites from one to another to form clusters.

In Fig. 7.25a, we see that the RG transformation unites two clusters, which have been separate as yet, into one common cluster. On the contrary, in Fig. 7.25b, the RG transformation breaks a cluster in two.

Therefore, even if the subjective criterion keeps the behavior of the system unchanged within cells, on the cells' boundaries the RG transformation does not manage to keep the connectivity invariant.

Thereby, the standard technique to improve the accuracy of the RG predictions is to make the cells bigger. The larger the volume b^d of a cell, the less is the influence of its surface $b^{\frac{d-1}{d}}$. However, increasing the size of the cell, we drastically increase

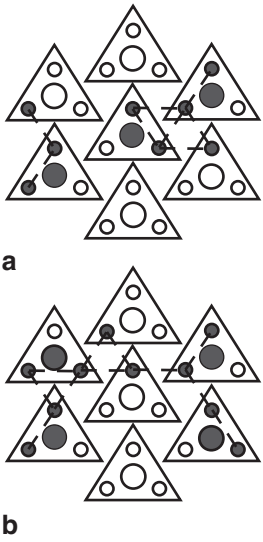

Fig. 7.25 The RG transformation does not represent the real behavior of a system at the cells' boundaries. **(a)** The RG transformation unites two clusters which have been separate as yet. **(b)** The RG transformation breaks a cluster in two

the complexity of analytical calculations since we should take into account more and more microstates. Thus, the obtained values generally represent a compromise between the complexity of calculations and the accuracy of the results.

For example, in percolation, we consider a new site to be occupied if the initial cell is percolated. Similar to Chap. 4, we can write this condition with the aid of the probability $\Pi(p, L)$ for a system of size $L = b$ to be percolated at the given value of p:

$$p' = \Pi(p, b). \tag{7.154}$$

All previous rules of invariant probabilities represented, in fact, this equation.

Since the percolation threshold is the critical fixed point of the RG transformation, it obeys the equation:

$$p_{\mathrm{C}} = \Pi(p_{\mathrm{C}}, b). \tag{7.155}$$

The larger the size of the cell is, the more accurate results this equation returns. As we will find in the following chapter, the percolation threshold of a finite system differs from the percolation threshold of an infinite system by the value of the order of $L^{-1/\nu}$. Thus, $b^{-1/\nu}$ is the accuracy of the RG transformation.

Increasing the size of the cell step-by-step, we would obtain more and more accurate results of, e.g., the percolation threshold p_{C}. Often, we do not even need to consider very big cells. Instead, knowing the dependence $p_{\mathrm{C}}(b)$ of the approximate result on the cell's size, we could forecast this dependence for larger b or even find the exact solution.

It is the knowledge of scaling,

$$p_{\mathrm{C}}(b) - p_{\mathrm{C}}^{exact} \propto b^{-1/\nu} \quad \text{for} \quad b \to +\infty, \tag{7.156}$$

that helps us. Substituting a linear-scale factor of the RG transformation, $r \equiv 1/b$, into (7.156), we obtain

$$p_{\mathrm{C}}(1/r) - p_{\mathrm{C}}^{exact} \propto r^{1/\nu} \quad \text{for} \quad r \to +0. \tag{7.157}$$

Taking the logarithm of both sides of this equation

$$\ln(p_{\mathrm{C}}(1/r) - p_{\mathrm{C}}^{exact}) \propto \frac{\ln r}{\nu} \quad \text{for} \quad r \to +0, \tag{7.158}$$

we find that $\ln(p_{\mathrm{C}}(1/r) - p_{\mathrm{C}}^{exact})$ should be proportional to $\ln r$.

If we correctly guessed the value p_{C}^{exact}, the dependence of $\ln(p_{\mathrm{C}}(1/r) - p_{\mathrm{C}}^{exact})$ on $\ln r$ should become a straight line. Thereby, the sought p_{C}^{exact} is provided as the value straightening dependence (7.158).

References

Abaimov, S.G.: Statistical Physics of Complex Systems, 2nd ed. Synergetics: From Past to Future, vol. **57**, URSS, Moscow (2013) (in Russian)

Allegre, C.J., Le Mouel, J.L., Provost, A.: Scaling rules in rock fracture and possible implications for earthquake prediction. Nature **297**, 47–49 (1982)

Balescu, R.: Equilibrium and Nonequilibrium Statistical Mechanics. Wiley, New York (1975)

Blume, M.: Theory of the first-order magnetic phase change in UO2. Phys. Rev. **141**(2), 517 (1966)

Capel, H.W.: On the possibility of first-order phase transitions in Ising systems of triplet ions with zero-field splitting. Physica **32**(5), 966–988 (1966)

Cardy, J.: Scaling and Renormalization in Statistical Physics. Cambridge University Press, Cambridge (1996)

Domb, C., Green, M.S., Domb, C., Lebowitz, J.L. (eds.): Phase Transitions and Critical Phenomena. Academic Press, London (1972–2001)

Goldenfeld, N.: Lectures on Phase Transitions and the Renormalization Group. Perseus Books Publishing, Reading (1992)

Grimmett, G.R.: Percolation, 2nd ed. Grundlehren der Mathematischen Wissenschaften, vol. 321. Springer, Berlin (1999)

Houtappel, R.M.F.: Order-disorder in hexagonal lattices. Physica **16**(5), 425–455 (1950)

Huang, K.: Statistical Mechanics, 2nd ed. Wiley, New York (1987)

Kadanoff, L.P.: Scaling laws for Ising models near T_C. Phys. (Long Island City, NY) **2**, 263 (1966)

Kramers, H.A., Wannier, G.H.: Statistics of the two-dimensional ferromagnet. Part I. Phys. Rev. **60**(3), 252 (1941a)

Kramers, H.A., Wannier, G.H.: Statistics of the two-dimensional ferromagnet. Part II. Phys. Rev. **60**(3), 263 (1941b)

Landau, L.D., Lifshitz, E.M.: Statistical Physics, Part 1, 3rd ed. Course of Theoretical Physics, vol. 5. Pergamon Press, Oxford (1980)

Ma, S.K.: Modern Theory of Critical Phenomena. Benjamin, Reading (1976)

Narkunskaya, G.S., Shnirman, M.G.: Hierarchical model of defect development and seismicity. Phys. Earth Planet Inter. **61**(1–2), 29–35 (1990)
Newman, W.I., Gabrielov, A.M.: Failure of hierarchical distributions of fiber-bundles. I. Int. J. Fract. **50**(1), 1–14 (1991)
Newman, W.I., Gabrielov, A.M., Durand, T.A., Phoenix, S.L., Turcotte, D.L.: An exact renormalization model for earthquakes and material failure. Statics and dynamics. Physica D **77**(1–3), 200–216 (1994)
Niemeijer, T., van Leeuwen, J.M.J.: Wilson theory for 2-dimensional Ising spin systems. Physica **71**(1), 17–40 (1974)
Niemeijer, T., van Leeuwen, J.M.J.: Renormalization theory for Ising-like spin systems. In: Domb, C., Green, M.S. (eds.) Phase Transitions and Critical Phenomena, vol. 6, pp. 425–505. Academic Press, London (1976)
Onsager, L.: Crystal statistics. I. A two-dimensional model with an order-disorder transition. Phys. Rev. **65**(3–4), 117–149 (1944)
Pathria, R.K.: Statistical Mechanics, 2nd ed. Butterworth-Heinemann, Oxford (1996)
Shnirman, M.G., Blanter, E.M.: Self-organized criticality in a mixed hierarchical system. Phys. Rev. Lett. **81**(24), 5445–5448 (1998)
Shnirman, M., Blanter, E.: Hierarchical models of seismicity. In: Keilis-Borok, V.I., Soloviev, A.A. (eds.) Nonlinear Dynamics of the Lithosphere and Earthquake Prediction, pp. 37–69. Springer, Berlin (2003)
Smalley, R.F., Turcotte, D.L., Solla, S.A.: A renormalization group approach to the stick-slip behavior of faults. J. Geophys. Res. **90**(B2), 1894–1900 (1985)
Sornette, D.: Elasticity and failure of a set of elements loaded in parallel. J. Phys. A. **22**(6), L243–L250 (1989a)
Sornette, D.: Failure thresholds in hierarchical and euclidian space by real space renormalization group. J. Phys. France **50**(7), 745–755 (1989b)
Sornette, D.: Critical Phenomena in Natural Sciences, 2nd ed. Springer, Berlin (2006)
Sornette, D., Sammis, C.G.: Complex critical exponents from renormalization-group theory of earthquakes: Implications for earthquake predictions. J. Phys. I **5**(5), 607–619 (1995)
Stanley, H.E.: Introduction to Phase Transitions and Critical Phenomena. Clarendon Press, Oxford (1971)
Stauffer, D., Aharony, A.: Introduction to Percolation Theory, 2nd ed. Taylor & Francis, London (1994)
Wilson, K.G.: Renormalization group and critical phenomena. I. Renormalization group and the Kadanoff scaling picture. Phys. Rev. B. **4**(9), 3174 (1971a)
Wilson, K.G.: Renormalization group and critical phenomena. II. Phase-space cell analysis of critical behavior. Phys. Rev. B. **4**(9), 3184 (1971b)
Wilson, K.G., Kogut, J.: The renormalization group and the ε expansion. Phys. Rep. **12**(2), 75–199 (1974)

Chapter 8
Scaling: The Finite-Size Effect and Crossover Effects

Abstract In the previous chapter, we have considered different approaches to build the renormalization group (RG) transformation. The behavior of a system in the vicinity of its critical point is scale invariant. This allows us to build relationships among different systems of the universality class.

However, in the previous chapter, our primary concern was to study how we can build the RG transformation, and we did not spend much time investigating the emerging scaling.

We overcome this drawback in the current chapter. Initially, we consider the basic principles of scaling (Widom 1965a; Widom 1965b; Domb and Hunter 1965; Patashinski and Pokrovskii 1966; Kadanoff 1966). Then we see that scaling leads to such important concepts as a finite-size effect and crossover effects. Finally, we study the origins of scaling and find that it is described by the formalism of general homogeneous functions. In turn, we demonstrate that the last formalism originates from the scaling hypothesis of the RG transformation.

8.1 Percolation: Why Is the Cluster-Size Distribution Hypothesis Wrong?

Let us first consider percolation. In Chap. 4, we have obtained the critical index (4.82) of the order parameter. Assuming the presence of a nonzero order parameter, it was understood that we were considering the system above the percolation threshold: $p > p_C$.

However, if we take a look at formulae (4.74–4.82) again, we would find nothing that would prevent us to apply them also for the system below the percolation threshold: $p < p_C$. But this would mean the presence of a nonzero order parameter (a percolating cluster) for $p < p_C$, which makes no sense just by the definition of the percolation threshold itself.

What went wrong? Our single assumption was the hypothesis (4.52 and 4.53) for the cluster-size distribution:

$$n_s(p) \propto s^{-\tau} e^{-(c(p)s)^{\zeta}}, \tag{8.1}$$

S. G. Abaimov, *Statistical Physics of Non-Thermal Phase Transitions,*
Springer Series in Synergetics, DOI 10.1007/978-3-319-12469-8_8

where

$$c(p) \propto \left| p - p_{\mathrm{C}} \right|^{1/\sigma} \text{ for } p \to p_{\mathrm{C}}. \tag{8.2}$$

Therefore, this hypothesis is the first to be suspected.

Let us look closer at the hypothesis (8.1 and 8.2). We know that the real cluster-size distribution $n_s(p)$ is determined by the sum of probabilities of all lattice animals corresponding to the given s:

$$n_s(p) = \sum_{t_s} g_{t_s} p^s (1-p)^{t_s}, \tag{8.3}$$

where the sum goes over the possible values t_s of perimeters of s-clusters. Here g_{t_s} is the number of lattice s-animals corresponding to the given value of the perimeter.

Let us choose some particular value of s that is large, $s >> 1$, but finite. Then the sum (8.3) contains large but finite number of lattice animals. Thereby, this sum is the finite-order polynomial of p, all derivatives $\left(\frac{\partial^k n_s}{\partial p^k} \right)_s$ of which are also finite.

On the contrary, the k^{th} derivative $\left(\frac{\partial^k n_s}{\partial p^k} \right)_s$ of hypothesis (8.1 and 8.2) contains the k^{th} derivative of c, $\left(\frac{\partial^k c}{\partial p^k} \right)_s \propto \left| p - p_{\mathrm{C}} \right|^{\frac{1}{\sigma} - k}$, which in the limit $p \to p_{\mathrm{C}}$ diverges for high values of k when $1/\sigma$ is not an integer. For lattices below the upper critical dimension, $1/\sigma$ is generally not an integer so that hypothesis (8.1 and 8.2) turns out to be, indeed, too crude.

But what is wrong with hypothesis (8.1 and 8.2)? What should be corrected? Let us consider the case when $\frac{\tau - 2}{\sigma} < 1$ so that we can neglect the term $(p - p_{\mathrm{C}})$ in (4.78):

$$P_{PC}(p) \approx \sum_s s \left(n_s(p_{\mathrm{C}}) - n_s(p) \right). \tag{8.4}$$

Due to the symmetry of the function $c(p) \propto \left| p - p_{\mathrm{C}} \right|^{1/\sigma}$ in the vicinity of the percolation threshold, the dependence of our hypothesis (8.1 and 8.2) on p (for fixed s) is symmetric (returns the same value for $p_{\mathrm{C}} \pm \Delta p$) and has a maximum exactly at $p = p_{\mathrm{C}}$. Therefore, the difference $n_s(p_{\mathrm{C}}) - n_s(p)$ is positive both above and below the percolation threshold which leads to the nonzero value of $P_{PC}(p)$ for $p < p_{\mathrm{C}}$ as well.

Let us transform statistics (8.1 and 8.2) as

$$n_s(p) \propto \frac{1}{s^{\tau}} \exp\left\{ -const \left(\left| p - p_{\mathrm{C}} \right|^{1/\sigma} s \right)^{\zeta} \right\} \text{ for } p \to p_{\mathrm{C}}, s >> 1. \tag{8.5}$$

Replacing the particular dependence $\exp\left\{ -const \left| z \right|^{\zeta} \right\}$ on parameter

$$z = \text{sign}(p - p_C)\left|p - p_C\right|^{1/\sigma} s \tag{8.6}$$

by more general functional dependence $f(z)$, we obtain

$$n_s(p) \propto \frac{1}{s^\tau} f(z) \text{ or} \tag{8.7}$$

$$n_s(p) = n_s(p_C) f(z). \tag{8.8}$$

Parameter z is called *the scaling parameter* while $f(z)$ is called *the scaling function* of one variable. This name comes from the fact that if we drew curves (8.5) for a particular lattice in the vicinity of its percolation threshold, for example, as dependences on s for fixed p, for each value of p, we obtain its own curve. However, if we plot quantities $s^\tau n_s(p)$ as dependences on z, all curves collapse onto one common functional dependence $f(z)$. This very technique is generally utilized to discover the presence of a scaling dependence for experimental results while the quality of the "collapse" characterizes the applicability of the scaling hypothesis in the model.

Of course, each particular lattice may have its own functional dependence $f(z)$. However, there are some features of behavior that characterize all lattices in common, and even the dependence $f(z)$ can become universal.

So, there are two asymptotes of the functional dependence $f(z)$ when we know in advance what to expect from a system. As we will see later, relation (6.231),

$$\sigma \nu D = 1, \tag{8.9}$$

can be proved for the case of an arbitrary scaling dependence $f(z)$ as well. This relation suggests that the limit $\left|z\right| << 1$ corresponds to the case $s << s_\xi(p) \equiv \xi^D(p)$ when we consider clusters whose average linear size is smaller than the correlation length. In this limit from statistics (8.7 and 8.8), we expect that the function $f(z)$ depends weakly on z to provide the power-law decay $n_s(p_C) \propto s^{-\tau}$ of the cluster-size distribution:

$$f(z) \propto \underline{\underline{O}}(1) \text{ for } |z| << 1. \tag{8.10}$$

This is one asymptote of the scaling.

On the contrary, in the limit $\left|z\right| >> 1$, when we consider big clusters with the linear size larger than the correlation length, $s >> s_\xi \equiv \xi^D$, we expect the exponentially "fast" decay of statistics (8.7 and 8.8) which is provided by the exponentially "fast" decay of the function $f(z)$ to form another asymptote of the scaling.

Problem 8.1.1

Find the scaling function of the cluster-size distribution for the one-dimensional percolation.

Solution: The cluster-size distribution (4.4) for the one-dimensional percolation has been found in Chap. 4:

$$n_s(p) = p^s(1-p)^2 = (1-p)^2 e^{-s\ln\frac{1}{p}}. \tag{8.11}$$

In the vicinity of the percolation threshold $p \to p_C - 0$, we transform this dependence into the scaling form:

$$n_s(p) \to (p - p_C)^2 e^{(p-p_C)s}. \tag{8.12}$$

Introducing *the scaling parameter z* by

$$z = (p - p_C)s \text{ with } \sigma = 1, \tag{8.13}$$

for the cluster-size distribution, we obtain the scaling

$$n_s(p) = \frac{1}{s^\tau} f(z), \tag{8.14}$$

where $\tau = 2$, and the scaling function is defined by

$$f(z) \equiv z^2 e^{-|z|}. \tag{8.15}$$

For $|z| >> 1$, this function decays exponentially "fast" with the increase of $|z|$. However, for $|z| << 1$, contrary to the previous discussion, it is not of the order of unity and tends to zero as z^2. This is the special case of the presence of the so-called *dangerous coupling constant* which we discuss in Sect. 8.11.

How does the introduction of scaling change our results from Chap. 4 obtained for an arbitrary lattice? Repeating almost to the letter formulae (4.71–4.73) for the mean cluster size, we find

$$\tilde{S}(p) \propto \sum_s s^2 n_s(p) \propto \int_1^{+\infty} s^{2-\tau} f(z) ds$$
$$= \text{sign}(p - p_C) \cdot |p - p_C|^{\frac{\tau-3}{\sigma}} \int_0^{+\infty \cdot \text{sign}(p-p_C)} |z|^{2-\tau} f(z) dz. \tag{8.16}$$

The integral in the right-hand side is some nonsingular constant. Thereby, the introduction of scaling does not change the relation among the critical indices:

$$\gamma = \frac{3-\tau}{\sigma}. \tag{8.17}$$

Next, we repeat formulae (6.228–6.231). The difference is that now, to find the divergence of the moment $M_{2+\frac{2}{D}}(p)$, we can no longer use hypothesis (8.1 and 8.2). Instead, we should employ scaling (8.7 and 8.8):

$$M_{2+\frac{2}{D}}(p) \equiv \sum_s s^{2+\frac{2}{D}} n_s(p) \sim \int_1^{+\infty} s^{2+\frac{2}{D}-\tau} f(z)ds$$

$$\sim \operatorname{sign}(p-p_C)\cdot |\, p-p_C\,|^{\frac{\tau-3-\frac{2}{D}}{\sigma}} \int_0^{+\infty\cdot\operatorname{sign}(p-p_C)} |\, z\,|^{2+\frac{2}{D}-\tau} f(z)dz. \tag{8.18}$$

Substituting this result into (6.228), we prove the validity of relation (8.9).

At last, let us consider the scaling of the order parameter. Almost repeating (4.77–4.82), we find

$$\begin{aligned} P_{PC}(p) &= (p-p_C) + const \sum_{s=1}^{+\infty} s^{1-\tau}\left(f(0)-f(z)\right) \\ &\approx (p-p_C) + const \int_1^{+\infty} s^{1-\tau}\left(f(0)-f(z)\right)ds \\ &= (p-p_C) + const\cdot \operatorname{sign}(p-p_C) \\ &\quad \times |\, p-p_C\,|^{\frac{\tau-2}{\sigma}} \int_0^{+\infty\cdot\operatorname{sign}(p-p_C)} |\, z\,|^{1-\tau}\left(f(0)-f(z)\right)dz. \end{aligned} \tag{8.19}$$

Again, the integral in the right-hand side does not influence the scaling so that we return to the second relation among the critical indices:

$$\beta = \begin{cases} \dfrac{\tau-2}{\sigma}, & \dfrac{\tau-2}{\sigma} \le 1 \\ 1, & \dfrac{\tau-2}{\sigma} > 1 \end{cases}. \tag{8.20}$$

For simplicity, let us consider the case $\dfrac{\tau-2}{\sigma} < 1$. Then we can neglect the term $(p-p_C)$ in the right-hand side of (8.19):

$$P_{PC}(p) \propto \operatorname{sign}(p-p_C)\cdot |\, p-p_C\,|^{\beta} \int_0^{+\infty\cdot\operatorname{sign}(p-p_C)} |\, z\,|^{1-\tau}\left(f(0)-f(z)\right)dz. \tag{8.21}$$

This equation is supposed to be valid both above and below the percolation threshold. However, for $p < p_C$, the order parameter $P_{PC}(p)$ by definition is expected to be zero. It is possible only when the integral in (8.21) is zero:

$$\int_{-\infty}^{0} |\, z\,|^{-(\beta\sigma+1)}\left(f(z)-f(0)\right)dz \equiv 0. \tag{8.22}$$

We know that the above function $f(z)$ for $|\,z\,| << 1$ is of the order of unity but decays exponentially for $|\,z\,| >> 1$ so that it is zero in the infinity: $f(\pm\infty) = 0$.

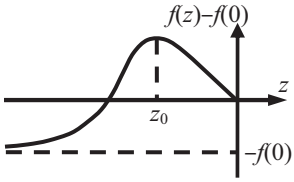

Fig. 8.1 The maximum of the scaling function provides the absence of a percolating cluster below the percolation threshold

Thereby, the difference $(f(z)-f(0))$ is zero when $z=0$ and equals $-f(0)$ when $z=\pm\infty$ (Fig. 8.1).

But the integral in (8.22) can be zero only if the difference $(f(z)-f(0))$ is positive somewhere for negative z and, thereby, has a maximum at some point $z_0<0$ (Fig. 8.1).

This means that for a fixed value of s, the cluster-size distribution $n_s(p)$, as a dependence on p, has a maximum at point

$$p_0 = p_C - |z_0|^{\sigma} s^{-\sigma} < p_C. \tag{8.23}$$

The point p_0 of the maximum depends on s and tends to p_C when $s\to+\infty$. But the very fact that it only tends to p_C but does not equal p_C exactly provides the absence of a percolating cluster below the percolation threshold!

If we return to the exact result, (4.49) and (4.50) for the Bethe lattice with $Z=3$,

$$\frac{n_s(p)}{n_s(p_C)} = \left(\frac{1-p}{1-p_C}\right)^2 e^{-c(p)s}, \tag{8.24}$$

where

$$c(p) = -\ln\left(1-4(p-p_C)^2\right), \tag{8.25}$$

we see that the point of the maximum has been moved away from p_C toward lower values of p only by the presence of the multiplier $(1-p)^2$. This multiplier does not participate in scaling, only in corrections to scaling:

$$n_s(p) \propto \frac{1}{s^{\tau}}\left(1-\frac{\sqrt{(p-p_C)^2 s}}{(1-p_C)\sqrt{s}}\right)^2 e^{-4(p-p_C)^2 s} = \frac{1}{s^{\tau}}\left(1-\frac{\sqrt{|z|}}{(1-p_C)\sqrt{s}}\right)^2 e^{-4|z|}$$

$$= \frac{1}{s^{\tau}} e^{-4|z|} - \frac{1}{s^{\tau+1/2}} \frac{2\sqrt{|z|}}{(1-p_C)} e^{-4|z|}. \tag{8.26}$$

Therefore, the situation may be more complex than we considered in Fig. 8.1: The dependence that moves the maximum of the cluster-size distribution away from the percolation threshold toward lower values of p may be not in scaling function $f(z)$ itself but in corrections to scaling.

Let us now return to the definition (8.6) of the scaling parameter z. Where has the critical index σ come into this dependence from? Initially, it appeared in (8.2)

as a parameter of the exponential decay (8.1). But later, we have substituted this decay with more general functional dependence $f(z)$. Thus, the origins of the index σ have disappeared from the formalism, while the index is still present in the definition of the scaling parameter.

Thereby, defining the scaling parameter (8.6), we define in parallel the index σ. Does it mean that its value is arbitrary? No, it does not, because the value of the index σ is determined by relations (8.9, 8.17, and 8.20). In other words, we hypothesize the presence of this index within the scaling parameter and are attempting to develop the scaling of the cluster-size distribution. In the result, we do obtain the desired scaling, but it requires from us that the so-defined index σ should obey relations (8.9, 8.17, and 8.20).

The presence of an index within the scaling parameter is, in fact, quite general, although, as we will see later, for magnetic systems, Greek letter Δ is usually utilized while the index is called *the critical crossover index*. But why do we need an index?

We have to generate two asymptotes of the scaling function. To this purpose, we need to compare a large integer s with a small quantity $|p - p_C|$ (which are both present in definition (8.6)) to say, for example, that s is so large that it overpowers the small multiplier $|p - p_C|$.

But we cannot compare s with $|p - p_C|$ directly because they represent different physical quantities. Instead, we introduce index σ to compare s with $|p - p_C|^{-1/\sigma} = |p - p_C|^{-\nu D} = \xi^D \equiv s_\xi$ which is the characteristic cluster size. Thereby, the scaling parameter (8.6) transforms into ratio

$$|z| = \frac{s}{s_\xi}. \tag{8.27}$$

The reader should not think that only the cluster-size distribution possesses the scaling behavior. Generally, it is quite the opposite—whichever quantity we choose, it is expected to generate the scaling behavior.

For example, let us consider the radius of gyration $R_s(p)$ above the percolation threshold. Small clusters, $s << s_\xi$, are fractal so that their radius of gyration depends on the cluster size s as $R_s(p) \propto s^{1/D}$. On the contrary, big clusters, $s >> s_\xi$, lose their fractality and, similarly to the percolating cluster, acquire the dimension d of the embedding lattice: $R_s(p) \propto s^{1/d}$.

These are two asymptotes of one scaling dependence,

$$R_s(p) \propto s^{1/D} \Xi_R(s / s_\xi), \tag{8.28}$$

generated by the asymptotes of the scaling function $\Xi_R(z)$:

$$\Xi_R(z) \propto \underline{\underline{O}}(1) \text{ for } |z| << 1, \tag{8.29}$$

$$\Xi_R(z) \propto z^{\frac{1}{d} - \frac{1}{D}} \text{ for } |z| >> 1. \tag{8.30}$$

We have seen one more example of scaling behavior in Chap. 6 when the correlation function was considered. The correlation function $G(\vec{\mathbf{R}})$ is itself the

scaling dependence when the role of the scaling parameter is played by the ratio of the distance R to the correlation length ξ:

$$G(\vec{\mathbf{R}}) = \frac{1}{R^{d-2+\eta}} \Xi_G(\vec{\mathbf{R}}/\xi), \tag{8.31}$$

where $\Xi_G(z) \propto \underline{\underline{O}}(1)$ for $|z| << 1$ and exponentially decays for $|z| >> 1$.

8.2 Percolation: The Finite-Size Effect

So far, we have generally discussed only infinite systems in the thermodynamic limit $N \to +\infty$. What would happen if we considered a finite system of size $L = N^{1/d}$?

In this case, *the finite-size effect* takes place which drastically changes the behavior of the system. To distinguish results we have obtained for the infinite lattice, we will further use for them the superscript "∞."

On the infinite lattice for $p < p_c^{\infty}$, there are clusters of all sizes, as big as we are looking for; however, their fraction on the lattice is exponentially small in comparison with smaller clusters.

For the finite lattice, in turn, this statement is already not true. By definition of the cluster-size distribution n_s, the product Nn_s represents the number of s-clusters on the finite lattice of size $N = L^d$. If we increase s, the number Nn_s decreases until it reaches unity,

$$Nn_{s_0} = 1, \tag{8.32}$$

when there is only one such cluster on the lattice. Thus, s_0 represents the size of the biggest cluster present on average on the finite lattice. For even bigger clusters, $s > s_0$, we have $Nn_s < 1$ so that, although such s-clusters are possible as extremes of the statistics, there are no such clusters on average.

For simplicity, we again consider hypothesis (8.1 and 8.2) as an approximation of the real cluster-size distribution:

$$s_0^{-\tau} e^{-c(p)s_0} \propto \frac{1}{L^d}. \tag{8.33}$$

We are considering the system below the percolation threshold when the linear size L of the system is finite but is still much larger than the correlation length: $L >> \xi^{\infty}$ (where ξ^{∞} is the correlation length in the infinite system). Since we are considering big clusters with the linear size much larger than the average size represented by the correlation length, the exponential decay dominates the statistics, and we can neglect the power-law multiplier:

$$e^{-c(p)s_0} \propto \frac{1}{L^d} \text{ or } s_0 \propto \frac{\ln L^d}{c(p)}. \tag{8.34}$$

Problem 8.2.1

Consider a d-dimensional hypercubic lattice with $d > 1$. One possible microstate is when pL^d occupied sites on the lattice form a straight chain which is a cluster of size $s = pL^d$ and length pL^d. Since $L >> \ln L$, the size of the considered cluster is much larger than (8.34). Besides, the considered cluster starts to percolate the lattice at the value of p

$$pL^d = L \text{ or } p = L^{1-d} \to +0 \text{ for } L \to +\infty \tag{8.35}$$

which is much less than the percolation threshold. Explain the contradiction.

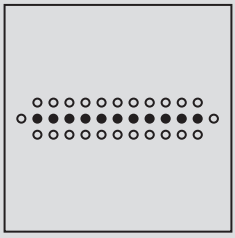

Solution: The considered cluster represents an extreme event of the cluster-size distribution. The normalized cluster number of this animal is the probability p^{pL^d} for pL^d sites to be occupied times the probability $(1-p)^{2(d-1)pL^d+2}$ for the required perimeter:

$$n_{pL^d}(p) = p^{pL^d}(1-p)^{2(d-1)pL^d+2}. \tag{8.36}$$

By definition of the normalized cluster number, there are

$$Nn_{pL^d}(p) = L^d p^{pL^d}(1-p)^{2(d-1)pL^d+2} \tag{8.37}$$

such clusters on average on the lattice.

Applying the logarithmic accuracy, we find that the possibility to encounter such a cluster in the ensemble is very improbable:

$$Nn_{pL^d}(p) \approx_{\ln} p^{pL^d}(1-p)^{2(d-1)pL^d} << 1. \tag{8.38}$$

However, we are generally interested not in extremes of the statistics but in the behavior on average. Expression (8.34) represents the size of the biggest *on average* cluster on the finite lattice.

Let us now consider the vicinity of the percolation threshold when the power-law divergences of the correlation length and quantity c become applicable:

$$\xi^{\infty} \propto \mid p - p_C^{\infty} \mid^{-\nu} \text{ and } c \propto \mid p - p_C^{\infty} \mid^{1/\sigma}. \tag{8.39}$$

But still we consider the case when the correlation length has not reached yet the size of the system: $L > \xi^{\infty}$. Substituting (8.39) into (8.34), we find

$$s_0 \propto \left| p - p_C^{\infty} \right|^{-1/\sigma} \ln L^d \propto s_{\xi} \ln L^d. \tag{8.40}$$

If p tends to $p_C^{\infty} - 0$, the correlation length diverges together with $s_{\xi} \equiv (\xi^{\infty})^D$. Thereby, s_0 diverges also. Since s_0 represents the size of the biggest on average cluster, this cluster is first on average to reach the system size and to form a percolating cluster, but in accordance with (8.40) $s_0 >> s_{\xi}$ because $\ln L^d >> 1$. Thereby, when the percolating cluster appears, the correlation length is still smaller than the system size: $L > \xi^{\infty}$. Therefore, the percolating cluster in the finite system appears earlier than in the infinite system (when $\xi^{\infty} = +\infty$) and even earlier than when the correlation length reaches the size of the system $\left(\xi^{\infty} \propto L\right)$.

Since the correlation length is still less than the system's size when the percolating cluster appears first on average, the whole s_0-cluster is not fractal with dimension D. But still we may say that its logarithm should be proportional to the logarithm of L (times some constant representing the averaged dimensionality):

$$\ln s_0 \propto \ln L. \tag{8.41}$$

Taking logarithm of both sides of (8.40), we find

$$\ln s_0 \propto \ln \left\{ (\xi^{\infty})^D \ln L^d \right\} = D \ln \xi^{\infty} + \ln \ln L + \ln d. \tag{8.42}$$

Substituting (8.41) into (8.42),

$$\ln L \propto D \ln \xi^{\infty} + \ln \ln L + \ln d, \tag{8.43}$$

we see that in the right-hand side of (8.43), we may neglect not only $\ln d << \ln L$ but also $\ln \ln L << \ln L$:

$$\ln \xi^{\infty} \propto \ln L \text{ or } \xi^{\infty} \propto L. \tag{8.44}$$

Thereby, when we are increasing p and the biggest cluster for the first time percolates the finite system, the correlation length is, indeed, smaller than the system size but differs from it only by the corrections that we can neglect with logarithmic accuracy:

$$\ln \xi^{\infty} \propto \ln L - const_1 \ln \ln L - const_2 \ln d \approx \ln L. \tag{8.45}$$

Another display of the finite-size effect is the hyperscaling relation (6.239) found in Chap. 6. To obtain this relation, we glued together two scales. Above the

percolation threshold, $p > p_C^{\infty}$, on scales smaller than the correlation length, $L < \xi^{\infty}$, the piece of the percolating cluster is fractal, $s_{part\ of\ PC} \propto L^D$. On scales larger than the correlation length, $L > \xi^{\infty}$, it, on the contrary, represents the appearing scaling of the order parameter: $s_{part\ of\ PC} \propto P_{PC}^{\infty}(p)L^d$. By gluing these two types of behavior at the scale of the correlation length, $L \propto \xi^{\infty}$, we obtain the hyperscaling relation (6.239).

With the aid of this relation, the scaling of a piece of the percolating cluster, cut by different scales, can be presented in the form:

$$s_{part\ of\ PC}(p,L) \propto \begin{cases} L^D, L < \xi^{\infty} \\ \left|p - p_C^{\infty}\right|^{\beta} L^d, L > \xi^{\infty} \end{cases} = L^D \begin{cases} 1, L < \xi^{\infty} \\ \left(\dfrac{L}{\xi^{\infty}}\right)^{d-D}, L > \xi^{\infty} \end{cases} \tag{8.46}$$

to be represented by a scaling function

$$s_{part\ of\ PC}(p,L) \propto L^D \Xi_s\left(L/\xi^{\infty}\right) \tag{8.47}$$

which has two asymptotes,

$$\Xi_s(z) \propto \underline{\underline{O}}(1) \text{ for } 0 < z << 1, \tag{8.48}$$

$$\Xi_s(z) \propto z^{d-D} \text{ for } z >> 1. \tag{8.49}$$

So far, we have discussed only the order parameter $P_{PC}^{\infty}(p)$ on the infinite lattice as the probability for a site to belong to an infinite percolating cluster. On the finite lattice, we define the order parameter $P_{PC}(p,L)$ as the probability for a site to belong to a cluster percolating the finite lattice.

Multiplying $P_{PC}(p,L)$ by the number L^d of sites on the finite lattice, we obtain the number $L^d P_{PC}(p,L)$ of sites which belong to the cluster percolating the finite lattice.

But we can consider our finite lattice as a window through which we are looking at the infinite lattice with its infinite percolating cluster. Does $L^d P_{PC}(p,L)$ represent the volume $s_{part\ of\ PC}$ of the infinite percolating cluster cut by the finite lattice as if by Procrustes' bed and determined by scaling (8.46–8.49)?

The answer is, obviously, negative because the finite lattice may be percolated not only by the infinite cluster of the infinite lattice but also by finite clusters of the infinite lattice with the linear size larger than our finite lattice (Fig. 8.2). In other words, decreasing the size of the window, we see that it is still percolated by the infinite cluster. But, besides the infinite cluster, it is also percolated now by other clusters that were earlier enclosed entirely by the larger window (Fig. 8.2).

Thereby, the order parameter $P_{PC}(p,L)$ of the finite lattice is higher than its infinite analogue $P_{PC}^{\infty}(p)$. This can also be illustrated from a different point of view: if we see a cluster that percolates our finite system, we do not know whether it is infinite (Fig. 8.2) or finite (Fig. 8.3) beyond the window of our system.

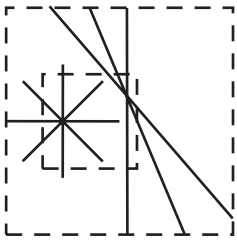

Fig. 8.2 The finite system (as a window through which we are looking at the infinite system) can be percolated not only by the infinite percolating cluster but also by finite clusters on the infinite lattice

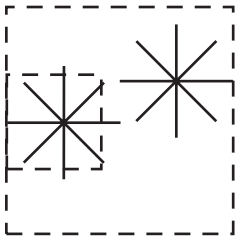

Fig. 8.3 If a finite lattice (as a window through which we are looking at the infinite system) is percolated by a cluster, we do not know whether this cluster is finite or infinite on the infinite lattice

Problem 8.2.2

Consider the one-dimensional finite lattice with free boundary conditions (part a of the figure below) below the percolation threshold $p_C^{\infty} = 1$ of the infinite lattice: $p < 1$. Find the exact expression for the scaling function of the mean cluster size $\tilde{S}$.

Solution: Let us first find the cluster-size distribution. Far from the boundary, the probability to find s-cluster at the given place on the lattice is still the probability $p^s(1-p)^2$ to have s occupied sites and two empty perimeter sites.

Here, by "far from the boundary," we mean that the cluster touches neither left nor right boundaries (part b of the figure). There are $(L-s-1)$ different locations for such s-clusters on the finite lattice with L sites.

Two more locations appear when the cluster touches the left or the right boundary (part c of the figure). The corresponding probability is $p^s(1-p)$ because we have to require for only one perimeter site to be empty.

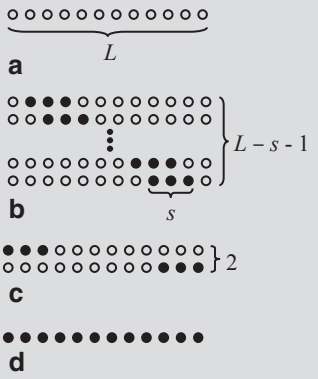

The last lattice animal we should count is the percolating cluster $s = L$. The probability of this cluster is the probability p^L for the lattice to be occupied completely (part d of the figure).

This probability p^L is nonzero for $p < 1$, and therefore, the finite lattice is percolated at values of p lower than the percolation threshold $p_C^\infty = 1$ of the infinite lattice. In other words, for the finite lattice, the percolation threshold p_C is lower than the percolation threshold $p_C^\infty = 1$ of the infinite lattice:

$$p_C < p_C^\infty. \tag{8.50}$$

Summarizing the probabilities we discussed above, we find the cluster-size distribution (as the number of s-clusters per one lattice site):

$$n_s(p) = \frac{1}{L}\begin{cases} (L-s-1)p^s(1-p)^2 + 2p^s(1-p), s < L \\ p^L, s = L \\ 0, s > L \end{cases}. \tag{8.51}$$

On the infinite lattice, we have defined the mean cluster size $\tilde{S}^\infty$ by (4.118). For the finite lattice, we utilize a similar expression

$$\tilde{S}(p,L) \equiv \frac{\sum_s s^2 n_s(p)}{\sum_s s n_s(p)}. \tag{8.52}$$

As it was discussed in details in Chap. 6, we must not include the term $s = L$, corresponding to the percolating cluster, into both sums of (8.52):

$$\tilde{S}(p,L) \equiv \frac{\sum_{s=1}^{L-1} s^2 n_s(p)}{\sum_{s=1}^{L-1} s n_s(p)}. \tag{8.53}$$

We find the sum in the denominator by utilizing the trick already known to us when we replace s with the derivative $\partial/\partial p$:

$$\begin{aligned} \sum_{s=1}^{L-1} s n_s(p) &= \sum_{s=1}^{L-1} \frac{s}{L}\left\{(L-s-1)p^s(1-p)^2 + 2p^s(1-p)\right\} \\ &= \frac{(1-p)}{L}\left(\left\{(1-p)(L-1)+2\right\}\left(p\frac{\partial}{\partial p}\right) - (1-p)\left(p\frac{\partial}{\partial p}\right)^2\right)\sum_{s=1}^{L-1} p^s \\ &= p - p^L. \end{aligned} \tag{8.54}$$

The obtained equation is already known to us as the law of conservation of probability, especially if we rewrite it as

$$\sum_{s=1}^{L-1} s n_s(p) + p^L = p. \tag{8.55}$$

The right-hand side is the probability for a site to be occupied. The first term of the left-hand side is the probability for the site to belong to a finite cluster while the second term represents the percolating cluster.

For the sum in the numerator of (8.53), we similarly find

$$\begin{aligned}\sum_{s=1}^{L-1} s^2 n_s(p) = \frac{(1-p)}{L}\Bigg(& \left\{(1-p)(L-1)+2\right\}\left(p\frac{\partial}{\partial p}\right)^2 \\ & -(1-p)\left(p\frac{\partial}{\partial p}\right)^3\Bigg)\sum_{s=1}^{L-1} p^s \\ = \frac{p}{1-p}\left\{1+p-\frac{2p}{L}\frac{1-p^L}{1-p}\right\} & - Lp^L. \end{aligned} \tag{8.56}$$

Substituting (8.54) and (8.56) into (8.53), we obtain the exact expression for the mean cluster size:

$$\tilde{S}(p,L) = \frac{\dfrac{1}{1-p}\left\{1+p-\dfrac{2p}{L}\dfrac{1-p^L}{1-p}\right\} - Lp^{L-1}}{1-p^{L-1}}. \tag{8.57}$$

Far from the percolation threshold $p_C^\infty = 1$, this expression does not obey scaling. However, when the system tends to $p_C^\infty - 0$, expression (8.57) transforms into

$$\tilde{S}(p,L) \to \frac{2}{1-p}\,\frac{1-\dfrac{1}{L(1-p)}\left(1-e^{-L(1-p)}\right)-\dfrac{1}{2}L(1-p)e^{-L(1-p)}}{1-e^{-L(1-p)}}, \tag{8.58}$$

where we have expanded (8.57) in small parameter $(1-p)$ but so far have not assumed anything about the order of the product $L(1-p)$.

Let us recall from Chap. 6 that in the vicinity of the percolation threshold, the correlation length diverges as (6.220):

$$\xi^\infty \propto \frac{1}{|\,p - p_C^\infty\,|}, \tag{8.59}$$

so that the product $L(1-p)$ plays the role of the scaling parameter $z = L/\xi^{\infty}$. Thereby we can transform (8.58) into a scaling function

$$\tilde{S}(p,L) \to \frac{2}{\mid p - p_{\mathrm{C}}^{\infty} \mid^{\gamma}} \Xi_S(L/\xi^{\infty}), \text{ where } \gamma = 1 \text{ and} \tag{8.60}$$

$$\Xi_S(z) \equiv \frac{1 - \frac{1}{z}(1 - e^{-z}) - \frac{z}{2}e^{-z}}{1 - e^{-z}}. \tag{8.61}$$

When $L >> \xi^{\infty}$ (and, correspondingly, $\mid z \mid >> 1$), the scaling function (8.61) is of the order of unity, $\Xi_S(z) \propto 1$, to recreate the divergence $\tilde{S}^{\infty} \propto \left| p - p_{\mathrm{C}}^{\infty} \right|^{-\gamma}$ of the susceptibility on the infinite lattice:

$$\tilde{S}(p,L) \propto \frac{1}{\mid p - p_{\mathrm{C}}^{\infty} \mid^{\gamma}}, \ \gamma = 1 \text{ when } L >> \xi^{\infty}. \tag{8.62}$$

This is the first asymptote of the mean cluster size.

The second asymptote appears when $L << \xi^{\infty}$ (and, correspondingly, $\mid z \mid << 1$). The expansion of (8.61) in the small parameter $\mid z \mid$ demonstrates that in this limit the scaling function behaves as

$$\Xi_S(z) \propto z/3, \tag{8.63}$$

which cancels the divergence (8.62) to provide constant asymptote:

$$\tilde{S}(p,L) \propto \frac{2L}{3} \text{ when } L << \xi^{\infty}. \tag{8.64}$$

Let us now discuss the obtained results. We assume that a scientist investigates percolation on a lattice of large but finite size L. The scientist is interested in the critical indices; therefore, she/he, step by step, tends p to p_{C}^{∞} from below.

First, when the system is far from the percolation threshold, the scientist observes complex behavior (8.57) which is specific for this particular system.

But the closer the percolation threshold is, the larger the correlation length becomes, and therefore, the previous complex behavior (8.57) transforms into the power-law divergence (8.62).

The best way to measure the critical index γ is to approach the percolation threshold closer and closer, following the power-law divergence (8.62) for several orders of $\tilde{S}$. Thereby the scientist could plot $\ln \tilde{S}$ versus $\ln \left| p - p_{\mathrm{C}}^{\infty} \right|$; the slope of this line will provide the unknown critical index γ.

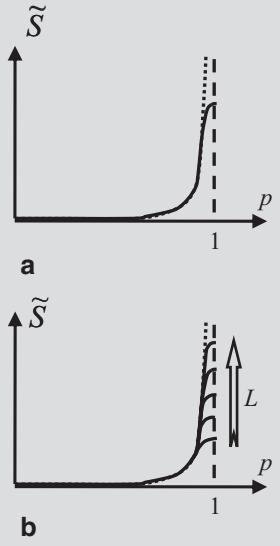

But due to the logarithmic dependences, one step of $\ln\left|p - p_C^{\infty}\right|$ requires, roughly speaking, one order of magnitude of $\left|p - p_C^{\infty}\right|$. Therefore, the equipment the scientist is utilizing has to provide very precise measurements in the very close proximity of the percolation threshold.

As the system approaches the percolation threshold, the correlation length diverges according to (8.59) and sometime achieves the size of the system L. The scaling switches from asymptote (8.62) to asymptote (8.64). Thus, as the scientist tries to approach the percolation threshold closer and closer, instead of the expected power-law divergence, she/he observes the tendency to a constant with respect to p value (part a of the figure above). The value of this constant is proportional to the system size L in accordance with (8.64).

The experiment was designed to provide high-accuracy measurements at low values of $\left|p - p_C^{\infty}\right|$ and probably required a lot of funding and efforts. But all efforts were in vain because scaling (8.64) limited the range of the power-law validity, and the finite-size effect camouflaged the expected divergence.

The way to suppress the finite-size effect is to increase the system's size. This idea is presented in the figure (part b) as a sketch. The larger the size of the system is, the farther the last will follow the power-law dependence, and later the mean cluster size will approach the constant value.

But for numerical calculations, the increase in system size requires much higher computer resources and calculation time. Unfortunately, there is no escape.

Nowadays, the number of degrees of freedom in computer models of complex systems is often higher than 10^6–10^9 which is already difficult to call small. In the near future, this number will be probably equal to or exceed the Avogadro constant 10^{23} which is generally associated with the infinite number of particles in the thermodynamic limit.

Problem 8.2.3

Similar to Problem 8.2.2, find the scaling function of the mean cluster size $\tilde{S}$ if the boundary conditions are periodic.

Solution: For the one-dimensional lattice, the periodic boundary conditions mean that the chain of sites is closed in a ring (part a of the figure below).

The probability for a small s-cluster to be at a given place on the lattice still equals $p^s(1-p)^2$, and the number of possible locations is L (part b of the figure).

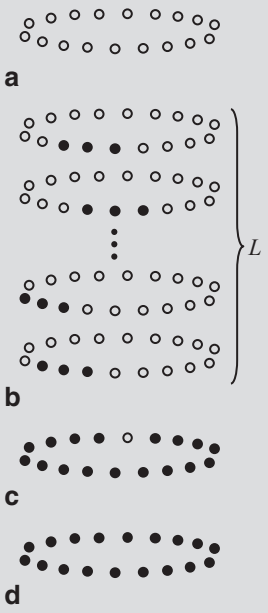

But for $(L-1)$-clusters (part c of the figure), whose number of possible locations is still L, only one empty perimeter site is required, and therefore, the probability equals $p^{L-1}(1-p)$.

For the percolating cluster, which again occupies all sites on the lattice (part d of the figure), the probability is p^L.

Summarizing these probabilities, we find the cluster-size distribution:

$$n_s(p)=\frac{1}{L}\begin{cases} Lp^s(1-p)^2, s<L-1 \\ Lp^{L-1}(1-p), s=L-1 \\ p^L, s=L \\ 0, s>L \end{cases}. \tag{8.65}$$

Calculating the mean cluster size, we should again exclude the percolating cluster from the sums of (8.53). The denominator sum we find as follows:

$$\sum_{s=1}^{L-1} s n_s(p) = \sum_{s=1}^{L-2} s p^s (1-p)^2 + (L-1)p^{L-1}(1-p)$$
$$= (1-p)^2 \left(p\frac{\partial}{\partial p} \right) \sum_{s=1}^{L-2} p^s + (L-1)p^{L-1}(1-p) = p - p^L \tag{8.66}$$

while the numerator sum equals

$$\sum_{s=1}^{L-1} s^2 n_s(p) = (1-p)^2 \left(p\frac{\partial}{\partial p} \right)^2 \sum_{s=1}^{L-2} p^s + (L-1)^2 p^{L-1}(1-p)$$
$$= \frac{p}{1-p}\left\{1 + p + p^{L-1}(1-2L) + p^L(2L-3)\right\}. \tag{8.67}$$

Therefore, the mean cluster size we obtain as follows:

$$\tilde{S}(p,L) = \frac{\frac{1}{1-p}\left\{1 + p + p^{L-1}(1-3p-2L(1-p))\right\}}{1-p^{L-1}}. \tag{8.68}$$

Far from the percolation threshold, this expression does not possess any scaling properties. In the vicinity of p_C^∞, we expand (8.68) in a small parameter $(1-p)$, while we do not assume anything about the order of the product $L(1-p)$, keeping it as it is:

$$\tilde{S}(p,L) \to \frac{2}{1-p}\frac{\left\{1 - e^{-L(1-p)}(1+L(1-p))\right\}}{1-e^{-L(1-p)}}. \tag{8.69}$$

Thereby, we have found the scaling function

$$\tilde{S}(p,L) \to \frac{2}{|\, p - p_C^\infty \,|^\gamma}\Xi_S(L/\xi^\infty) \quad \text{where} \quad \gamma = 1 \text{ and} \tag{8.70}$$

$$\Xi_S(z) \equiv \frac{1 - e^{-z}(1+z)}{1-e^{-z}}. \tag{8.71}$$

In the limit $|\, z \,| >> 1$, this scaling function is of the order of unity, $\Xi_S(z) \propto 1$, while in the limit $|\, z \,| << 1$, it becomes a power-law dependence $\Xi_S(z) \propto z/2$. For the mean cluster size (8.70), this provides two scaling asymptotes:

$$\tilde{S}(p,L) \propto \frac{2}{|\, p - p_C^\infty \,|^\gamma} \quad \text{when} \quad L >> \xi^\infty \text{ and} \tag{8.72a}$$

$$\tilde{S}(p,L) \propto L \quad \text{when} \quad L << \xi^\infty. \tag{8.72b}$$

We see that, similarly to Problem 8.2.2, when approaching the percolation threshold, the power-law divergence is replaced with the constant asymptote of the order of the lattice size L.

As we saw in Problems 8.2.2 and 8.2.3, the finite-size effect cancels singular divergences by replacing them with a finite value depending on the size of the system. For the mean cluster size, this result is obvious and could be foreseen in advance: The closer the percolation threshold is, the larger scales are occupied by the fractality, and the bigger the clusters on the infinite lattice are; however, the finite size of the finite system, like Procrustes' bed, limits the size of the clusters, not allowing them to grow to the size they would have on the infinite lattice.

For the one-dimensional case, the size of a cluster equals its length; therefore, $\tilde{S}(p,L)$ was limited by L. For the d-dimensional lattice, we expect that $\tilde{S}(p,L)$ would be limited by L raised to some power. Let us assume the following scaling dependence:

$$\tilde{S}(p,L) \propto \frac{1}{|\, p - p_{\mathrm{C}}^{\infty} \,|^{\gamma}} \Xi_S\left(\mathrm{sign}(p - p_{\mathrm{C}}^{\infty}) L / \xi^{\infty}\right), \tag{8.73}$$

where the first asymptote of the scaling function is

$$\Xi_S(z) \propto \underline{\underline{\mathrm{O}}}(1) \text{ for } |\, z \,| >> 1 \tag{8.74}$$

to provide the power-law divergence of the mean cluster size on the infinite lattice.

From the second asymptote, we, on the contrary, expect to cancel the singular behavior $\tilde{S} \sim |\, p - p_{\mathrm{C}}^{\infty} \,|^{-\gamma}$. This is possible only when this asymptote is the power law:

$$\Xi_S(z) \propto |\, z \,|^{\gamma/\nu} \quad \text{for} \quad |\, z \,| << 1. \tag{8.75}$$

Indeed, substituting (8.75) into (8.73), we find

$$\tilde{S}(p,L) \propto \frac{1}{|\, p - p_{\mathrm{C}}^{\infty} \,|^{\gamma}} \left(\frac{L}{\xi^{\infty}}\right)^{\gamma/\nu} \propto L^{\gamma/\nu} \text{ for } L << \xi^{\infty}. \tag{8.76}$$

We see that the scaling itself suggests us that L should be raised to the power γ/ν to represent the finite value replacing the divergence. By utilizing all relations we have obtained before (including the hyperscaling relation which is valid below the upper critical dimension), we find

$$\gamma / \nu = D(3 - \tau) = D - (d - D). \tag{8.77}$$

Similar behavior is observed for other quantities, including the correlation length itself. So far, we have referred only to the value ξ^{∞} of the correlation length on the infinite lattice. However, we may apply expression (6.206) as a definition for the

correlation length $\xi(p,L)$ on a finite lattice. The first asymptote of the so-defined correlation length determines the divergence of the correlation length ξ^{∞} on the infinite lattice:

$$\xi(p,L) \propto \frac{1}{\mid p - p_C^{\infty} \mid^{\nu}} \text{ for } L >> \xi^{\infty}. \tag{8.78}$$

Assuming the scaling

$$\xi(p,L) \propto \frac{1}{\mid p - p_C^{\infty} \mid^{\nu}} \Xi_{\xi}\left(\text{sign}(p - p_C^{\infty})L / \xi^{\infty}\right), \tag{8.79}$$

where (8.78) is provided by the first asymptote of the scaling function,

$$\Xi_{\xi}(z) \propto \underline{\underline{O}}(1) \text{ for } \mid z \mid >> 1, \tag{8.80}$$

we see that the second asymptote of the scaling function must be

$$\Xi_{\xi}(z) \propto \mid z \mid \text{ for } \mid z \mid << 1, \tag{8.81}$$

to cancel the power-law divergence on $\mid p - p_C^{\infty} \mid$ and generate the finite value:

$$\xi(p,L) \propto L \text{ for } L << \xi^{\infty}. \tag{8.82}$$

We have obtained one more result that could be predicted from the beginning: While $L > \xi^{\infty}$, the correlation length $\xi(p,L)$ of the finite system repeats the behavior of its counterpart ξ^{∞} on the infinite lattice. However, the correlation length, defined by (6.206) as the averaged root-mean-square distance between sites within clusters, cannot, obviously, exceed the size of the system. Therefore, when $\xi(p,L)$ reaches L, it stays at this limit, not able to grow farther.

So far, we have considered only how the finite-size effect can cancel the power-law divergences. But the power-law divergences are just one type of possible singular behavior. Another type is represented by the singular power-law dependences, tending to zero at the percolation threshold. An example is the order parameter:

$$P_{PC}^{\infty}(p) \propto \mid p - p_C^{\infty} \mid^{\beta}. \tag{8.83}$$

How does the finite-size effect influence this type of behavior?

Problem 8.2.4

For the one-dimensional percolation on the finite lattice, find the scaling of the order parameter.

Solution: The order parameter $P_{PC}(p,L)$ on the finite lattice is defined as the probability for a site to belong to a cluster percolating the finite lattice. For the one-dimensional chain of sites, we immediately find

$$P_{PC}(p,L)=\begin{cases} p^L = e^{-L/\xi^\infty}, p<1 \\ 1, p=1 \end{cases}, \tag{8.84}$$

where for ξ^∞, we utilized (6.220).

We see that the order parameter is not zero for $p < p_C^\infty$. Instead, it obeys the scaling

$$P_{PC}(p,L)=\Xi_P(L/\xi^\infty) \text{ where } \Xi_P(z)=e^{-z}. \tag{8.85}$$

For an arbitrary lattice, the finite-size effect cancels the singularity of $P(p,L)$ by "smoothing" the tendency to zero at the percolation threshold p_C^∞ (Fig. 8.4). Thereby, the probability to observe the percolating cluster becomes nonzero for $p < p_C^\infty$. For the scaling of $P(p,L)$, we may assume

$$P(p,L) = \mid p - p_C^\infty \mid^\beta \Xi_P\left(\text{sign}(p-p_C^\infty)L/\xi^\infty\right), \tag{8.86}$$

where the asymptotes of the scaling function are

$$\Xi_P(-\infty)=0, \tag{8.87}$$

$$\Xi_P(z) \propto \underline{\underline{O}}(1) \text{ for } z >> 1, \text{ and} \tag{8.88}$$

$$\Xi_P(z) \propto \mid z \mid^{-\beta/\nu} \text{ for } \mid z \mid << 1. \tag{8.89}$$

At last, we consider the probability Π for the system to be percolated. On the infinite lattice, since the percolation threshold p_C^∞ is defined as the point of appear-

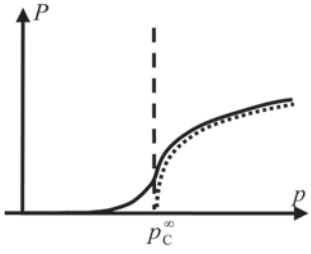

Fig. 8.4 The finite-size effect for the order parameter

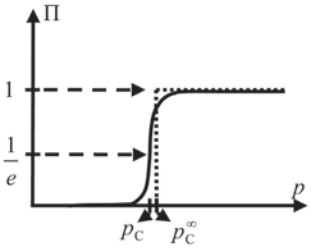

Fig. 8.5 The finite-size effect for the probability for a system to be percolated

ance of a percolating cluster, this probability is, obviously, zero below p_C^∞ and unity above p_C^∞ (Fig. 8.5, the *dotted line*):

$$\Pi^\infty(p) = \begin{cases} 0, p < p_C^\infty \\ 1, p \geq p_C^\infty \end{cases}. \tag{8.90}$$

On a finite lattice, the dependence $\Pi(p, L)$ "smoothes" the singularity at p_C^∞ (Fig. 8.5, the *solid line*).

There was no question how to determine the percolation threshold on the infinite lattice—it is the point of the singular step of Π^∞ from zero to unity. On the contrary, on a finite lattice, the dependence $\Pi(p, L)$ changes from zero to one continuously so that there is no particular point that can be associated with the percolation threshold. To choose the value p_C of the percolation threshold on a finite lattice, we initially should specify what value of $\Pi(p, L)$ we attribute to the appearance of a percolating cluster. Choosing $\Pi(p_C, L) = 1/e$ in Fig. 8.5, we see that p_C may be not equal to p_C^∞.

Problem 8.2.5

Find the percolation threshold p_C for the one-dimensional percolation on the finite lattice.

Solution: The probability for the one-dimensional lattice of size L to be percolated is

$$\Pi(p, L) = \begin{cases} p^L = e^{-L/\xi^\infty}, p < p_C^\infty = 1 \\ 1, p = p_C^\infty = 1 \end{cases}, \tag{8.91}$$

where for ξ^∞, we utilized (6.220).

Choosing $\Pi(p_C, L) = 1/e$ to represent the percolation threshold, we find

$$L = \xi^\infty\Big|_{p_C} = \frac{1}{p_C^\infty - p_C} \text{ or } p_C = p_C^\infty - \frac{1}{L}. \tag{8.92}$$

We see that on the finite lattice, the percolation threshold is lower than on the infinite lattice.

The general expectation is that $p_C < p_C^\infty$, i.e., when we are increasing p, the finite system is percolated earlier than the infinite system. We expect this statement to be true because to percolate the infinite system, we need an infinite percolating cluster $\left(\xi^\infty = +\infty\right)$, while the finite system is percolated by a finite cluster with linear size of the order of the system size $\left(\xi \propto L\right)$ which happens at lower values of p.

For an arbitrary lattice, we may assume the presence of scaling:

$$\Pi(p, L) = \Xi_\Pi\left(\text{sign}(p - p_C^\infty)L / \xi^\infty\right) \tag{8.93}$$

with two asymptotes:

$$\Xi_\Pi(-\infty) = 0 \text{ and } \Xi_\Pi(+\infty) = 1. \tag{8.94}$$

The scaling function $\Xi_\Pi(z)$ and its scaling parameter z are dimensionless. Therefore, we expect $\Xi_\Pi(z)$ to change from zero to unity when its argument z also changes by the order of unity:

$$\Delta z = \Delta\left(\frac{L}{\xi^\infty}\right) \propto 1. \tag{8.95}$$

Substituting here the divergence of ξ^∞, we find that the probability $\Pi(p, L)$ changes from zero to one when p changes by

$$\Delta\left(L \mid p - p_C^\infty \mid^\nu\right) \propto 1. \tag{8.96}$$

For the percolation threshold p_C on the finite lattice, this provides

$$\mid p_C - p_C^\infty \mid \propto L^{-1/\nu}. \tag{8.97}$$

8.3 Magnetic Systems: The Scaling of Landau Theory

We now turn our attention to magnetic systems, in particular to Landau theory of the Ising ferromagnet, which was considered in Chap. 3. The minimization of the specific Helmholtz free energy (3.105)

$$\frac{F_{\{\{m\}\}}}{N\mu} = -2A\ln 2 - hm + atm^2 + bm^4 + \ldots \tag{8.98}$$

provides the equation of state (3.92):

$$h = 2atm_0 + 4bm_0^{\,3} + \ldots \tag{8.99}$$

and the equilibrium Helmholtz energy

$$\frac{F^{CE}}{N\mu} = -2A\ln 2 - hm_0 + atm_0{}^2 + bm_0{}^4 + \ldots \tag{8.100}$$

By rearranging multipliers, we present the equation of state in the form:

$$h = |t|^{3/2}\left\{2a\left(\frac{m_0}{\sqrt{|t|}}\right)\text{sign } t + 4b\left(\frac{m_0}{\sqrt{|t|}}\right)^3 + \ldots\right\}. \tag{8.101}$$

Considering the isofield approach $h = 0$ of the critical point,

$$0 = 2a\left(\frac{m_0}{\sqrt{|t|}}\right)\text{sign } t + 4b\left(\frac{m_0}{\sqrt{|t|}}\right)^3, \tag{8.102}$$

we expect that (8.102) should provide the equilibrium value of the homogeneous spontaneous magnetization (3.98):

$$m_0 \propto |t|^{\beta_t^C}. \tag{8.103}$$

In Chap. 3, we had $\beta_t^C = 1/2$ in particular. That is why the magnetization participates in (8.102) in the form of the ratio $m_0/\sqrt{|t|}$. For more general case, we expect in (8.102) the presence of the ratio $m_0/|t|^{\beta_t^C}$:

$$0 = 2a\left(\frac{m_0}{|t|^{\beta_t^C}}\right)\text{sign } t + 4b\left(\frac{m_0}{|t|^{\beta_t^C}}\right)^3. \tag{8.104}$$

For the magnetic field (8.101), this provides

$$h = |t|^{3\beta_t^C}\left\{2a\left(\frac{m_0}{|t|^{\beta_t^C}}\right)\text{sign } t + 4b\left(\frac{m_0}{|t|^{\beta_t^C}}\right)^3 + \ldots\right\} \text{ or} \tag{8.105a}$$

$$h = 2at^{2\beta_t^C} m_0 + 4bm_0{}^3 + \ldots \tag{8.105b}$$

Differentiating (8.105b) with respect to m_0, we find the susceptibility of the system:

$$\chi \propto \frac{\partial m_0}{\partial h} = \frac{1}{2at^{2\beta_t^C} + 12bm_0{}^2 + \ldots}. \tag{8.106}$$

But in Chap. 3 for the susceptibility, we have introduced the critical index γ_t^C defined by

$$\chi \propto \frac{1}{|t|^{\gamma_t^{\mathrm{C}}}} \tag{8.107}$$

when we approach the critical point along the isofield curve $h = 0$. Comparing (8.106) and (8.107), we see that

$$\gamma_t^{\mathrm{C}} = 2\beta_t^{\mathrm{C}}, \tag{8.108}$$

which is, indeed, correct for the mean-field indices $\gamma_t^{\mathrm{C}} = 1$ and $\beta_t^{\mathrm{C}} = 1/2$. However, this relation between the critical indices is not complete yet, so we will discuss it in more detail later.

For more general case, we can improve (8.105) as

$$h = |t|^{\gamma_t^{\mathrm{C}} + \beta_t^{\mathrm{C}}} \left\{ 2a \left(\frac{m_0}{|t|^{\beta_t^{\mathrm{C}}}} \right) \mathrm{sign}\ t + 4b \left(\frac{m_0}{|t|^{\beta_t^{\mathrm{C}}}} \right)^3 + \ldots \right\} \text{ or} \tag{8.109a}$$

$$h = 2at^{\gamma_t^{\mathrm{C}}} m_0 + 4b{m_0}^3 + \ldots \tag{8.109b}$$

Comparing (8.109b) with (8.99), we see that for the general case, we should modify the initial expression of the Helmholtz energy (8.98) as

$$\frac{F_{\{\{m\}\}}}{N\mu} = -2A \ln 2 - hm + at^{\gamma_t^{\mathrm{C}}} m^2 + bm^4 + \ldots, \tag{8.110a}$$

$$\frac{F^{\mathrm{CE}}}{N\mu} = -2A \ln 2 - hm_0 + at^{\gamma_t^{\mathrm{C}}} {m_0}^2 + b{m_0}^4 + \ldots \tag{8.110b}$$

Substituting scaling (8.109a) of the magnetic field into (8.110b), we find

$$\frac{F^{CE}}{N\mu} + 2A \ln 2 = |t|^{\gamma_t^{\mathrm{C}} + 2\beta_t^{\mathrm{C}}} \times \left\{ - \left(2a \left(\frac{m_0}{|t|^{\beta_t^{\mathrm{C}}}} \right) \mathrm{sign}\, t + 4b \left(\frac{m_0}{|t|^{\beta_t^{\mathrm{C}}}} \right)^3 + \ldots \right) \left(\frac{m_0}{|t|^{\beta_t^{\mathrm{C}}}} \right) \right.$$
$$\left. + a\,\mathrm{sign}(t) \left(\frac{m_0}{|t|^{\beta_t^{\mathrm{C}}}} \right)^2 + b \left(\frac{m_0}{|t|^{\beta_t^{\mathrm{C}}}} \right)^4 + \ldots \right\}. \tag{8.111}$$

From Chap. 3, we know that along the isofield curve $h = 0$, the critical index of the heat capacity is defined by

$$C \propto \frac{1}{|t|^{\alpha_t^{\mathrm{C}}}}, \tag{8.112}$$

which means that the singular part of the specific Helmholtz energy scales as

$$\frac{F^{CE}}{N\mu} + 2A\ln 2 \propto |t|^{2-\alpha_t^C}. \tag{8.113}$$

Comparing (8.112) with (8.111), we find the relation among the critical indices:

$$\alpha_t^C + 2\beta_t^C + \gamma_t^C = 2, \tag{8.114}$$

which is, obviously, valid for the mean-field exponents $\alpha_t^C = 0$, $\beta_t^C = 1/2$, and $\gamma_t^C = 1$. The generalization of this equality is the so-called *Rushbrooke inequality* (Essam and Fisher 1963; Rushbrooke 1963):

$$\alpha_t^C + 2\beta_t^C + \gamma_t^C \geq 2. \tag{8.115}$$

So far, we have dealt only with the divergences along the critical isofield curve. Next, we consider the critical isotherm $t = 0$ when $h \neq 0$:

$$0 = -h + 4bm_0^{\,3} + \ldots \text{ or} \tag{8.116}$$

$$1 = 4b\left(\frac{m_0}{\sqrt[3]{h}}\right)^3 + \ldots \tag{8.117}$$

For the magnetization on the critical isotherm, we introduced in Chap. 3 its own critical index,

$$m_0 \propto h^{\beta_h^C}, \tag{8.118}$$

which happened to be equal to $\beta_h^C = 1/3$. Again, substituting the ratio $m_0/\sqrt[3]{h}$ in (8.117) by the more general expression $m_0/h^{\beta_h^C}$, we find

$$1 = 4b\left(\frac{m_0}{h^{\beta_h^C}}\right)^3 + \ldots \tag{8.119}$$

Returning to (8.109), we need to decide how we should modify this equation. We cannot modify the exponent of the h like

$$h^{3\beta_h^C} \neq |t|^{\gamma_t^C + \beta_t^C}\left\{2a\left(\frac{m_0}{|t|^{\beta_t^C}}\right)\text{sign } t + 4b\left(\frac{m_0}{|t|^{\beta_t^C}}\right)^3 + \ldots\right\} \tag{8.120}$$

because well above the critical temperature $|t| >> 1$ for small values of the field h, we expect the magnetization to be linearly proportional to the field. Therefore, there is only one way to modify (8.109)—to tune the exponent of the second term in the right-hand side:

$$h = |t|^{\gamma_t^{\mathrm{C}} + \beta_t^{\mathrm{C}}} \left\{ 2a \left(\frac{m_0}{|t|^{\beta_t^{\mathrm{C}}}} \right) \operatorname{sign} t + \left(\frac{1}{\beta_h^{\mathrm{C}}} + 1 \right) b \left(\frac{m_0}{|t|^{\beta_t^{\mathrm{C}}}} \right)^{1/\beta_h^{\mathrm{C}}} + \ldots \right\} \text{ or } \quad (8.121a)$$

$$h = 2at^{\gamma_t^{\mathrm{C}}} m_0 + \left(\frac{1}{\beta_h^{\mathrm{C}}} + 1 \right) b {m_0}^{1/\beta_h^{\mathrm{C}}} + \ldots \quad (8.121b)$$

Simultaneously, we have modified the coefficient at this term because this equation of state is supposed to be generated by differentiating the Helmholtz free energy:

$$\frac{F_{\{\{m\}\}}}{N\mu} = -2A \ln 2 - hm + at^{\gamma_t^{\mathrm{C}}} m^2 + b m^{1/\beta_h^{\mathrm{C}} + 1} + \ldots, \quad (8.122a)$$

$$\frac{F^{CE}}{N\mu} = -2A \ln 2 - hm_0 + at^{\gamma_t^{\mathrm{C}}} {m_0}^2 + b {m_0}^{1/\beta_h^{\mathrm{C}} + 1} + \ldots \quad (8.122b)$$

But, by comparing (8.121) with (8.99), we find that the absence of the temperature dependence at the second term of the right-hand side is possible only when

$$\gamma_t^{\mathrm{C}} = \beta_t^{\mathrm{C}} \left(\frac{1}{\beta_h^{\mathrm{C}}} - 1 \right). \quad (8.123)$$

This relation among the critical indices (consuming (8.108) as a particular case) is, in turn, a particular case of the more general inequality:

$$\gamma_t^{\mathrm{C}} \geq \beta_t^{\mathrm{C}} \left(\frac{1}{\beta_h^{\mathrm{C}}} - 1 \right), \quad (8.124)$$

called the *Griffiths inequality* (Griffiths 1965, 1972).

Differentiating (8.121b),

$$\chi \propto \frac{\partial m_0}{\partial h} = \left\{ 2at^{\gamma_t^{\mathrm{C}}} + \left(\frac{1}{\beta_h^{\mathrm{C}}} + 1 \right) \frac{1}{\beta_h^{\mathrm{C}}} b {m_0}^{1/\beta_h^{\mathrm{C}} - 1} + \ldots \right\}^{-1}, \quad (8.125)$$

we find that for the susceptibility at the critical isotherm $t = 0$, the explicit temperature dependence disappears in the limit $t \to 0$:

$$\chi \propto \left\{ \left(\frac{1}{\beta_h^{\mathrm{C}}} + 1 \right) \frac{1}{\beta_h^{\mathrm{C}}} b m_0^{\,1/\beta_h^{\mathrm{C}} - 1} + \ldots \right\}^{-1} \propto \frac{1}{h^{1-\beta_h^{\mathrm{C}}}}, \tag{8.126}$$

leaving only the scaling with respect to the magnetic field. Comparing this scaling with the definition of the critical index γ_h^{C},

$$\chi \propto \frac{1}{|h|^{\gamma_h^{\mathrm{C}}}}, \tag{8.127}$$

we find the relation

$$\gamma_h^{\mathrm{C}} = 1 - \beta_h^{\mathrm{C}}, \tag{8.128}$$

which is obvious due to the fact that the susceptibility is just the derivative (8.125) of the magnetization with respect to the field. However, with the aid of (8.128), equality (8.123) can be generalized as

$$\frac{\gamma_t^{\mathrm{C}}}{\gamma_h^{\mathrm{C}}} = \frac{\beta_t^{\mathrm{C}}}{\beta_h^{\mathrm{C}}}, \tag{8.129}$$

which, in turn, generalizes the Griffiths inequality:

$$\gamma_t^{\mathrm{C}} \geq \beta_t^{\mathrm{C}} \frac{\gamma_h^{\mathrm{C}}}{\beta_h^{\mathrm{C}}}. \tag{8.130}$$

Finally, we investigate the scaling behavior of the equilibrium Helmholtz energy (8.122b) on the critical isotherm. In the limit $t \to 0$, we see that the explicit temperature dependence disappears from (8.122b),

$$\frac{F^{CE}}{N\mu} + 2A\ln 2 = -hm_0 + b m_0^{\,1/\beta_h^{\mathrm{C}} + 1} + \ldots, \tag{8.131}$$

leaving only the scaling with respect to the field:

$$\frac{F^{CE}}{N\mu} + 2A\ln 2 \sim h^{1+\beta_h^{\mathrm{C}}} \tag{8.132}$$

This scaling is, again, obvious because the negative derivative of the Helmholtz energy with respect to h should return us to the scaling of the magnetization:

$$m_0 = -\frac{1}{N\mu} \frac{\partial F^{CE}}{\partial h} \propto h^{\beta_h^{\mathrm{C}}}. \tag{8.133}$$

However, it seems that Landau theory allows us to generalize the critical indices not for every quantity. Let us discuss, for example, the scaling of the heat capacity along the critical isotherm. Differentiating twice the Helmholtz energy (8.122) with respect to *T,* one of the terms we obtain is

$$C = -T\frac{\partial^2 F^{CE}}{\partial T^2} = -\frac{N\mu}{T_C}\left(a\gamma_t^C\left(\gamma_t^C - 1\right)t^{\gamma_t^C - 2}m_0{}^2 + \ldots\right) \tag{8.134}$$

whose temperature divergence $\left(\gamma_t^C - 1\right)t^{\gamma_t^C - 2}$ cannot be canceled or neglected in the limit $t \to 0$ unless we consider only the mean-field value of the critical index $\gamma_t^C = 1$. Therefore, it seems that in accordance with Landau theory, the scaling of the heat capacity is possible only when the critical indices are determined by the mean-field approach. In more detail, we will return to this question in Sect. 8.5.

After we have generalized the equation of state (8.99) by associating its exponents with critical indices, let us study the behavior of the obtained equation of state (8.121). Far from the critical point, expansion (8.122) is not valid and the magnetic field h depends on T and m_0 in accordance with some laws, specific for the given system. However, when we approach the critical point, we see that (8.121) generates *a scaling function* for the magnetic field (Widom 1965a):

$$h = |t|^{\gamma_t^C + \beta_t^C}\ \Xi_h^{\pm}\left(\frac{m_0}{|t|^{\beta_t^C}}\right), \tag{8.135}$$

where the superscript "±" means that there are two separate scaling functions: ("+") above the critical point and ("–") below the critical point. *The scaling parameter* here is

$$z \equiv \frac{m_0}{|t|^{\beta_t^C}}. \tag{8.136}$$

Comparing (8.121) and (8.135), we find that the scaling function is

$$\Xi_h^{\pm}(z) = \pm 2az + \left(\frac{1}{\beta_h^C} + 1\right)bz^{1/\beta_h^C} + \ldots \tag{8.137}$$

It is not convenient to work with the magnetic field as a function of the magnetization, since the magnetic field is the external field parameter, supported constant by the boundary conditions, while the magnetization is the fluctuating parameter. Therefore, by inverting the magnetic field scaling function, we find the scaling of the magnetization,

$$m_0 = |t|^{\beta_t^C}\ \Xi_{m_0}^{\pm}\left(\frac{h}{|t|^{\gamma_t^C + \beta_t^C}}\right) \text{ with} \tag{8.138}$$

$$\Xi^{\pm}_{m_0}(y) = \Xi^{\pm(-1)}_{h}(y), \tag{8.139}$$

as the dependence on the new scaling parameter

$$y \equiv \frac{h}{|t|^{\gamma_t^C + \beta_t^C}} \tag{8.140}$$

which now contains only the field parameters.

The scaling function (8.139) has two asymptotes:

$$\Xi^{\pm}_{m_0}(y) \propto \underline{\underline{O}}(1) \text{ when } |y| << 1, \tag{8.141}$$

$$\Xi^{\pm}_{m_0}(y) \propto y^{\beta_h^C} \text{ when } |y| >> 1, \tag{8.142}$$

which are obvious from (8.121). However, an easier way to prove these asymptotes is to see what scaling dependencies they generate for magnetization (8.138).

The first asymptote, $|y| << 1$, corresponds to the critical isofield curve $h = 0$. For this case, the scaling function (8.139) provides the asymptote of magnetization (8.138)

$$m_0 \propto \underline{\underline{O}}(1)\,|t|^{\beta_t^C} \propto |t|^{\beta_t^C} \text{ when } h << |t|^{\gamma_t^C + \beta_t^C}, \tag{8.143}$$

which is just the scaling (8.103) of the magnetization along the critical isofield curve.

The second asymptote (8.142) of the scaling function represents the critical isotherm $t = 0$. For magnetization (8.138) in this case, we find

$$m_0 \propto |t|^{\beta_t^C} \left(\frac{h}{|t|^{\gamma_t^C + \beta_t^C}} \right)^{\beta_h^C} \text{ when } h >> |t|^{\gamma_t^C + \beta_t^C}. \tag{8.144}$$

The zero deviation of the temperature from critical $t = 0$, would cause singularity (zero or infinity) in this expression unless the temperature dependence, coming from the asymptote (8.142) of the scaling function, canceled out the previous scaling (8.143). But this is exactly what is happening due to the relationship (8.123) among the critical indices! So, we find

$$m_0 \propto h^{\beta_h^C} \text{ when } h >> |t|^{\gamma_t^C + \beta_t^C}, \tag{8.145}$$

which is just the scaling (8.118) of the magnetization at the critical isotherm.

What we have seen here is the typical example of how the scaling works. The scaling function, depending on one scaling parameter, has two asymptotes. One of them provides the scaling of the corresponding quantity along the isofield curve

$h = 0$. The second asymptote is built in such a way that it cancels out the previous scaling on t and generates the new scaling on h for the critical isotherm.

Differentiating (8.138) with respect to h, we find the susceptibility:

$$\chi \sim \frac{\partial m_0}{\partial h} = |t|^{-\gamma_t^C} \left. \frac{d\Xi_{m_0}^{\pm}(y)}{dy} \right|_{h/|t|^{\gamma_t^C + \beta_t^C}}. \tag{8.146}$$

This expression can also be represented by scaling:

$$\chi \propto |t|^{-\gamma_t^C} \Xi_{\chi}^{\pm} \left(\frac{h}{|t|^{\gamma_t^C + \beta_t^C}} \right), \tag{8.147}$$

where the scaling function has two asymptotes again:

$$\Xi_{\chi}^{\pm}(y) \propto \underline{\underline{O}}(1) \text{ when } |y| << 1, \tag{8.148}$$

$$\Xi_{\chi}^{\pm}(y) \propto y^{\beta_h^C - 1} \text{ when } |y| >> 1. \tag{8.149}$$

To prove these asymptotes valid, we could find the susceptibility by differentiating (8.121) with respect to m_0. However, it is much easier to verify these hypotheses by looking at the scaling they generate.

The first asymptote, $|y| << 1$, provides the scaling along the isofield curve $h = 0$,

$$\chi \propto \frac{\underline{\underline{O}}(1)}{|t|^{\gamma_t^C}} \propto \frac{1}{|t|^{\gamma_t^C}} \text{ when } h << |t|^{\gamma_t^C + \beta_t^C}, \tag{8.150}$$

while the second asymptote, $|y| >> 1$, cancels the previous scaling (8.150) to generate the new scaling along the isotherm:

$$\chi \propto |t|^{-\gamma_t^C} \left(\frac{h}{|t|^{\gamma_t^C + \beta_t^C}} \right)^{\beta_h^C - 1} = \frac{1}{h^{1-\beta_h^C}} = \frac{1}{h^{\gamma_h^C}} \text{ when } h >> |t|^{\gamma_t^C + \beta_t^C}. \tag{8.151}$$

In the vicinity of the critical point, the singular part of the specific Helmholtz energy also exhibits scaling:

$$\frac{F_{singular}^{CE}}{N\mu} \equiv \frac{F^{CE}}{N\mu} + 2A \ln 2 = |t|^{2-\alpha_t^C} \Xi_{F^{CE}}^{\pm} \left(\frac{h}{|t|^{\gamma_t^C + \beta_t^C}} \right) \tag{8.152}$$

with the scaling function having two asymptotes:

$$\Xi^{\pm}_{F^{CE}}(y) \propto \underline{\underline{O}}(1) \text{ when } |y| << 1, \tag{8.153}$$

$$\Xi^{\pm}_{F^{CE}}(y) \propto y^{1+\beta_h^C} \text{ when } |y| >> 1. \tag{8.154}$$

This provides two scaling asymptotes for the Helmholtz energy:

$$\frac{F^{CE}_{singular}}{N\mu} \propto \underline{\underline{O}}(1)\,|t|^{2-\alpha_t^C} \propto |t|^{2-\alpha_t^C} \text{ when } h << |t|^{\gamma_t^C+\beta_t^C}, \tag{8.155}$$

$$\frac{F^{CE}_{singular}}{N\mu} \propto |t|^{2-\alpha_t^C}\left(\frac{h}{|t|^{\gamma_t^C+\beta_t^C}}\right)^{1+\beta_h^C} = h^{1+\beta_h^C} \text{ when } h >> |t|^{\gamma_t^C+\beta_t^C}. \tag{8.156}$$

Scaling functions should not necessarily have only one scaling parameter. For example, in Chap. 6, we obtained the following expression for the correlation function:

$$g(R) \propto \frac{e^{-R/\xi}}{R^{\frac{d-1}{2}}} \text{when} R >> \xi, \tag{8.157}$$

$$g(R) \propto \frac{1}{R^{d-2+\eta^C}} \text{ when } R << \xi \text{ and } d > 2. \tag{8.158}$$

This scaling is represented by the scaling function of two scaling parameters:

$$g(R,h,t) \propto \frac{1}{R^{d-2+\eta^C}}\Xi^{\pm}_g\left(\frac{R}{\xi}, \frac{h}{|t|^{\gamma_t^C+\beta_t^C}}\right), \tag{8.159}$$

where the scaling function is of the order of unity when the first scaling parameter is small,

$$\Xi^{\pm}_g(x_1,x_2) \propto \underline{\underline{O}}(1) \text{ when } 0 < x_1 << 1, \tag{8.160}$$

and decays exponentially when $x_1 >> 1$.

Let us, for example, consider the system in the absence of magnetic field. In accordance with the fluctuation–dissipation theorem, the magnetic susceptibility equals the integral of the correlation function:

$$\chi \propto \int_{-\infty}^{+\infty} d^d\mathbf{R}\; g(\mathbf{R}, h=0, t) \propto \int_{0}^{+\infty} dR \frac{R^{d-1}}{R^{d-2+\eta^{\mathrm{C}}}} \Xi_g^{\pm}(R\,|\,t\,|^{\nu_t^{\mathrm{C}}}, 0). \tag{8.161}$$

Let us perform the change of variable $x = R\,|\,t\,|^{\nu_t^{\mathrm{C}}}$ under the sign of the integral:

$$\chi \propto |\,t\,|^{\nu_t^{\mathrm{C}}(\eta^{\mathrm{C}}-2)} \int_{0}^{+\infty} dx \frac{x^{d-1}}{x^{d-2+\eta^{\mathrm{C}}}} \Xi_g^{\pm}(x,0) \propto |\,t\,|^{\nu_t^{\mathrm{C}}(\eta^{\mathrm{C}}-2)}. \tag{8.162}$$

Comparing this divergence with (8.107), we obtain the relation among the critical indices:

$$\gamma_t^{\mathrm{C}} = \nu_t^{\mathrm{C}}(2-\eta^{\mathrm{C}}). \tag{8.163}$$

The generalization of this equality is the *Fisher inequality* (Fisher 1969):

$$\gamma_t^{\mathrm{C}} \le \nu_t^{\mathrm{C}}(2-\eta^{\mathrm{C}}). \tag{8.164}$$

In conclusion of this section, we should say that although we have considered here only the critical scaling of the Ising model, similar results can be found for the proximity of the spinodal point as well. In particular, dependencies (3.92), (3.115), (3.133), and (6.105) are the scaling functions whose asymptotes allowed us in Chaps. 3 and 6 to find all spinodal indices. In more detail we return to this question in Sect. 8.12.

8.4 Magnetic Systems: Scaling Hypotheses

We have considered the scaling of a ferromagnetic system in the approximation of Landau theory. However, very similar scaling dependencies are valid for more general, nonmean-field case as well since the scaling follows from the most basic assumptions.

When the magnetic field is nonzero, a system of linear size L has two scaling parameters:

$$x \equiv \frac{\xi}{L} \text{ and } y \equiv \frac{h}{|\,t\,|^{\Delta_{h\text{-}t}^{\mathrm{C}}}}, \tag{8.165}$$

where by the subscript "h-t" we have specified that this index Δ belongs to the comparison of h with $|\,t\,|^{\Delta_{h\text{-}t}^{\mathrm{C}}}$ and is called *the critical crossover index* of this comparison.

In the thermodynamic limit $L \to +\infty$, the singular part of the equilibrium Helmholtz energy divided by the total number $N = L^d$ of spins is intensive and can depend, therefore, only on the intensive scaling parameter y:

$$\frac{F^{CE}_{singular}}{L^d} \propto \Xi^{\pm}_{F^{CE}}\left(\frac{h}{|t|^{\Delta^{C}_{h,lt}}}\right) \text{ or } F^{CE}_{singular} \propto L^d \Xi^{\pm}_{F^{CE}}\left(\frac{h}{|t|^{\Delta^{C}_{h,lt}}}\right). \tag{8.166}$$

If we had several extensive parameters, we could consider their combinations. However, in (8.165), we have only one extensive parameter x^{-1} and one intensive parameter *y,* which leaves no alternatives to (8.166).

The multiplier L^d in (8.166) seems to be the inheritance of the extensive scaling parameter *x,* so we can assume that

$$F^{CE}_{singular} \propto \left(\frac{L}{\xi}\right)^d \Xi^{\pm}_{F^{CE}}\left(\frac{h}{|t|^{\Delta^{C}_{h,lt}}}\right). \tag{8.167}$$

Recalling that along the critical isofield curve in the vicinity of the critical point, the correlation length diverges as (6.149),

$$\xi \propto \frac{1}{|t|^{\nu^{C}_{t}}}, \tag{8.168}$$

we obtain

$$F^{CE}_{singular} \propto L^d |t|^{d\nu^{C}_{t}} \Xi^{\pm}_{F^{CE}}\left(\frac{h}{|t|^{\Delta^{C}_{h,lt}}}\right). \tag{8.169}$$

If we assume the asymptote of the scaling function

$$\Xi^{\pm}_{F^{CE}}(y) \propto \underline{\underline{O}}(1) \text{ for } |y| << 1, \tag{8.170}$$

this generates the following asymptote for the singular part of the Helmholtz energy along the critical isofield curve:

$$F^{CE}_{singular} \propto L^d |t|^{d\nu^{C}_{t}} \text{ for } h << |t|^{\Delta^{C}_{h,lt}}. \tag{8.171}$$

Recalling the divergence (8.113),

$$F^{CE}_{singular} \propto L^d |t|^{2-\alpha^{C}_{t}}, \tag{8.172}$$

we obtain *the hyperscaling relation,* containing explicitly the dimension of the model:

$$2 - \alpha^{C}_{t} = d\nu^{C}_{t}, \tag{8.173a}$$

which is a particular case of the Josephson inequality (Josephson 1967a, b):

$$2 - \alpha^{C}_{t} \le d\nu^{C}_{t}. \tag{8.173b}$$

To find the magnetization, we should differentiate the Helmholtz energy with respect to h:

$$m_0 = -\frac{1}{L^d}\frac{\partial F^{CE}}{\partial h} \propto |t|^{d\nu_t^C - \Delta_{h\to t}^C} \left.\frac{d\Xi_{F^{CE}}^{\pm}(y)}{dy}\right|_{h/|t|^{\Delta_{h\to t}^C}}. \tag{8.174}$$

Assuming

$$\frac{d\Xi_{F^{CE}}^{\pm}(y)}{dy} \propto \underline{\underline{O}}(1) \quad \text{for } |y| << 1, \tag{8.175}$$

in the limit $h << |t|^{\Delta_{h\to t}^C}$ of the critical isofield curve, we find

$$m_0 \propto |t|^{d\nu_t^C - \Delta_{h\to t}^C} \text{ for } h << |t|^{\Delta_{h\to t}^C}. \tag{8.176}$$

Comparing this result with scaling (8.103),

$$m_0 \propto |t|^{\beta_t^C} \text{ for } h << |t|^{\Delta_{h\to t}^C}, \tag{8.177}$$

we obtain another relation among the critical indices:

$$\beta_t^C = d\nu_t^C - \Delta_{h\to t}^C. \tag{8.178}$$

The susceptibility is the derivative of the magnetization with respect to h:

$$\chi \propto \frac{\partial m_0}{\partial h} \propto |t|^{d\nu_t^C - 2\Delta_{h\to t}^C} \left.\frac{d^2\Xi_{F^{CE}}^{\pm}(y)}{dy^2}\right|_{h/|t|^{\Delta_{h\to t}^C}}. \tag{8.179}$$

Again, assuming

$$\frac{d^2\Xi_{F^{CE}}^{\pm}(y)}{dy^2} \propto \underline{\underline{O}}(1) \quad \text{for } |y| << 1, \tag{8.180}$$

for the critical isofield curve, we find

$$\chi \propto |t|^{d\nu_t^C - 2\Delta_{h\to t}^C} \text{ for } h << |t|^{\Delta_{h\to t}^C}. \tag{8.181}$$

Comparing this power-law dependence with divergence (8.107),

$$\chi \propto \frac{1}{|t|^{\gamma_t^C}}, \tag{8.182}$$

we find the new relation among the critical indices:

$$-\gamma_t^{\mathrm{C}} = d\nu_t^{\mathrm{C}} - 2\Delta_{h\perp t}^{\mathrm{C}}. \tag{8.183}$$

Excluding $\Delta_{h\perp t}^{\mathrm{C}}$ and the dimensionality d of the system from (8.173), (8.178), and (8.183), we return to the particular case (8.114) of *the Rushbrooke inequality* (Essam and Fisher 1963; Rushbrooke 1963):

$$\alpha_t^{\mathrm{C}} + 2\beta_t^{\mathrm{C}} + \gamma_t^{\mathrm{C}} = 2. \tag{8.184}$$

The scaling hypotheses above should be considered as illustrative rather than rigorous. Even more so, a scaling assumption, which happens to be valid for a particular case, may provide incorrect results when applied in a different way. For example, we based the scaling of the Helmholtz energy on the hypothesis that the Helmholtz energy is an extensive quantity and, therefore, should depend as x^{-d} on the extensive scaling parameter x. However, both the nonspecific magnetization and nonspecific susceptibility are also extensive. If we applied the same scaling hypothesis to these quantities, we would obtain incorrect relations among the critical indices.

Another example is that we have obtained the hyperscaling relation (8.173) for a system of an arbitrary dimensionality. However, above the upper critical dimension, we do not expect this relation to be valid because in this case, the critical indices are determined by the mean-field values.

Therefore, we consider the scaling theory itself as a good illustration of already obtained experimental or exact data rather than the independent technique to find the critical indices. However, as we will see below, some hypotheses of the scaling theory can be justified by the properties of the renormalization group (RG) transformation which provides much more fundamental foundation for this theory.

Above, we have considered the scaling of quantities along the critical isofield curve, $h << |t|^{\Delta_{h\perp t}^{\mathrm{C}}}$ and $|y| << 1$. Let us now turn our attention to the critical isotherm.

The critical isotherm corresponds to the limit $h >> |t|^{\Delta_{h\perp t}^{\mathrm{C}}}$ when $|y| >> 1$. Assuming in this limit the power-law asymptote of the scaling function,

$$\frac{d\Xi_{F^{CE}}^{\pm}(y)}{dy} \propto y^{\kappa_{m_0}} \quad \text{for } |y| >> 1, \tag{8.185}$$

for the asymptote of magnetization (8.174), we find

$$m_0 \propto |t|^{d\nu_t^{\mathrm{C}} - \Delta_{h\perp t}^{\mathrm{C}}} \left(\frac{h}{|t|^{\Delta_{h\perp t}^{\mathrm{C}}}} \right)^{\kappa_{m_0}}. \tag{8.186}$$

On the critical isotherm, the deviation of the temperature from its critical value is zero exactly: $t = 0$. To avoid singularities in (8.186), we expect that asymptote (8.185) should cancel out the previous scaling (8.177) of the critical isofield curve. Besides, we expect the new scaling to be in accordance with (8.118):

$$m_0 \propto h^{\beta_h^{\mathrm{C}}} \text{ for } h >> |t|^{\Delta_{h\perp t}^{\mathrm{C}}}. \tag{8.187}$$

This is possible only when

$$\kappa_{m_0} = \frac{d\nu_t^{\mathrm{C}} - \Delta_{h,\mathrm{C}t}^{\mathrm{C}}}{\Delta_{h,\mathrm{C}t}^{\mathrm{C}}} = \beta_h^{\mathrm{C}}. \tag{8.188}$$

Removing $\Delta_{h,\mathrm{C}t}^{\mathrm{C}}$ and the dimensionality d of the system with the aid of the previously found relations, we return to the particular case (8.123) of *the Griffiths inequality* (Griffiths 1965, 1972):

$$\gamma_t^{\mathrm{C}} = \beta_t^{\mathrm{C}} \left(\frac{1}{\beta_h^{\mathrm{C}}} - 1 \right). \tag{8.189}$$

Summarizing, we expect the magnetization to obey the scaling (Widom 1965a)

$$m_0 = |t|^{\beta_t^{\mathrm{C}}} \, \Xi_{m_0}^{\pm} \left(\frac{h}{|t|^{\Delta_{h,\mathrm{C}t}^{\mathrm{C}}}} \right), \tag{8.190}$$

where two asymptotes of the scaling function,

$$\Xi_{m_0}^{\pm}(y) \propto \underline{\underline{O}}(1) \quad \text{for} \quad |y| << 1, \tag{8.191}$$

$$\Xi_{m_0}^{\pm}(y) \propto y^{\beta_h^{\mathrm{C}}} \quad \text{for} \quad |y| >> 1, \tag{8.192}$$

provide two asymptotes of the magnetization:

$$m_0 \propto |t|^{\beta_t^{\mathrm{C}}} \text{ for } h << |t|^{\Delta_{h,\mathrm{C}t}^{\mathrm{C}}}, \tag{8.193}$$

$$m_0 \propto |t|^{d\nu_t^{\mathrm{C}} - \Delta_{h,\mathrm{C}t}^{\mathrm{C}}} \left(\frac{h}{|t|^{\Delta_{h,\mathrm{C}t}^{\mathrm{C}}}} \right)^{\beta_h^{\mathrm{C}}} \propto h^{\beta_h^{\mathrm{C}}} \quad \text{for} \quad h >> |t|^{\Delta_{h,\mathrm{C}t}^{\mathrm{C}}}. \tag{8.194}$$

Problem 8.4.1

Find the scaling of the susceptibility along the critical isotherm.

Solution: Assuming the power-law asymptote for the scaling function

$$\frac{d^2 \Xi_{F^{CE}}^{\pm}(y)}{dy^2} \propto y^{\kappa_\chi} \text{ for } |y| >> 1, \tag{8.195}$$

for the asymptote of susceptibility (8.179), we obtain

$$\chi \propto |t|^{d\nu_t^{\mathrm{C}} - 2\Delta_{h,\mathrm{C}t}^{\mathrm{C}}} \left(\frac{h}{|t|^{\Delta_{h,\mathrm{C}t}^{\mathrm{C}}}} \right)^{\kappa_\chi}. \tag{8.196}$$

However, we expect this asymptote to be (8.127):

$$\chi \propto \frac{1}{|h|^{\gamma_h^C}} \quad \text{for} \quad h >> |t|^{\Delta_{h,|t}^C} . \tag{8.197}$$

It is possible if only

$$\kappa_\chi = \frac{d\nu_t^C - 2\Delta_{h,|t}^C}{\Delta_{h,|t}^C} = -\gamma_h^C . \tag{8.198}$$

Excluding $\Delta_{h,|t}^C$ and the dimensionality d of the system with the aid of the previously found relations, we return to the trivial relation (8.128), connecting the critical indices of the magnetization and the susceptibility which is the derivative of the magnetization with respect to the field:

$$\gamma_h^C = 1 - \beta_h^C . \tag{8.199}$$

So, the susceptibility obeys the scaling

$$\chi = \frac{1}{|t|^{\gamma_t^C}} \Xi_\chi^{\pm}\left(\frac{h}{|t|^{\Delta_{h,|t}^C}}\right), \tag{8.200}$$

where two asymptotes of the scaling function

$$\Xi_\chi^{\pm}(y) \propto \underline{\underline{O}}(1) \text{ for } |y| << 1, \tag{8.201}$$

$$\Xi_\chi^{\pm}(y) \sim y^{-\gamma_h^C} \text{ for } |y| >> 1, \tag{8.202}$$

provide two asymptotes of the susceptibility:

$$\chi \propto \frac{1}{|t|^{\gamma_t^C}} \quad \text{for} \quad h << |t|^{\Delta_{h,|t}^C}, \tag{8.203}$$

$$\chi \propto \frac{1}{|h|^{\gamma_h^C}} \quad \text{for} \quad h >> |t|^{\Delta_{h,|t}^C} . \tag{8.204}$$

Problem 8.4.2

Find the scaling of the singular part of the Helmholtz energy along the critical isotherm.

Solution: Similar to the previous discussion, we find

$$\kappa_{F^{CE}} = \frac{d\nu_t^{\mathrm{C}}}{\Delta^{\mathrm{C}}_{h\text{-}\perp t}}, \tag{8.205}$$

which provides the following scaling:

$$F^{CE}_{singular} \propto L^d \mid t \mid^{d\nu_t^{\mathrm{C}}} \Xi^{\pm}_{F^{CE}} \left(\frac{h}{\mid t \mid^{\Delta^{\mathrm{C}}_{h\text{-}\perp t}}} \right), \tag{8.206}$$

where two asymptotes of the scaling function are

$$\Xi^{\pm}_{F^{CE}}(y) \propto \underline{\underline{\mathrm{O}}}(1) \quad \text{for} \quad \mid y \mid << 1, \tag{8.207}$$

$$\Xi^{\pm}_{F^{CE}}(y) \propto y^{1+\beta_h^{\mathrm{C}}} \quad \text{for} \quad \mid y \mid >> 1, \tag{8.208}$$

and two asymptotes of the Helmholtz energy are

$$F^{CE}_{singular} \propto L^d \mid t \mid^{d\nu_t^{\mathrm{C}}} \quad \text{for} \quad h << \mid t \mid^{\Delta^{\mathrm{C}}_{h\text{-}\perp t}}, \tag{8.209}$$

$$F^{CE}_{singular} \propto L^d \mid h \mid^{1+\beta_t^{\mathrm{C}}} \quad \text{for} \quad h >> \mid t \mid^{\Delta^{\mathrm{C}}_{h\text{-}\perp t}}. \tag{8.210}$$

8.5 Magnetic Systems: Superseding Correction

In Sect. 8.3, we were not able to build the scaling of the heat capacity along the critical isotherm. Let us return to this question.

To find the heat capacity, we differentiate (8.169) twice with respect to temperature:

$$\begin{aligned} \frac{C}{N} = -\frac{T}{N}\frac{\partial^2 F^{CE}}{\partial T^2} &= -\frac{d\nu_t^{\mathrm{C}}(d\nu_t^{\mathrm{C}}-1)}{T_{\mathrm{C}}} \mid t \mid^{d\nu_t^{\mathrm{C}}-2} \Xi^{\pm}_{F^{CE}}\Big|_{h/\mid t\mid^{\Delta^{\mathrm{C}}_{h\text{-}\perp t}}} \\ &+ \frac{(2d\nu_t^{\mathrm{C}} - \Delta^{\mathrm{C}}_{h\text{-}\perp t} - 1)\Delta^{\mathrm{C}}_{h\text{-}\perp t} h}{T_{\mathrm{C}}} \mid t \mid^{d\nu_t^{\mathrm{C}}-2-\Delta^{\mathrm{C}}_{h\text{-}\perp t}} \frac{d\Xi^{\pm}_{F^{CE}}}{dy}\Big|_{h/\mid t\mid^{\Delta^{\mathrm{C}}_{h\text{-}\perp t}}} \\ &- \frac{(\Delta^{\mathrm{C}}_{h\text{-}\perp t} h)^2}{T_{\mathrm{C}}} \mid t \mid^{d\nu_t^{\mathrm{C}}-2-2\Delta^{\mathrm{C}}_{h\text{-}\perp t}} \frac{d^2\Xi^{\pm}_{F^{CE}}}{dy^2}\Big|_{h/\mid t\mid^{\Delta^{\mathrm{C}}_{h\text{-}\perp t}}}. \end{aligned} \tag{8.211}$$

Considering the critical isotherm, we should substitute asymptotes (8.208, 8.185, and 8.195) into this expression:

$$\frac{C}{N} \propto const_1 \mid t \mid^{d\nu_t^{\mathrm{C}}-2} \left(\frac{h}{\mid t \mid^{\Delta_{h\perp t}^{\mathrm{C}}}} \right)^{1+\beta_h^{\mathrm{C}}} + const_2 \mid t \mid^{d\nu_t^{\mathrm{C}}-2-\Delta_{h\perp t}^{\mathrm{C}}} \left(\frac{h}{\mid t \mid^{\Delta_{h\perp t}^{\mathrm{C}}}} \right)^{\beta_h^{\mathrm{C}}}$$

$$+ const_3 \mid t \mid^{d\nu_t^{\mathrm{C}}-2-2\Delta_{h\perp t}^{\mathrm{C}}} \left(\frac{h}{\mid t \mid^{\Delta_{h\perp t}^{\mathrm{C}}}} \right)^{\beta_h^{\mathrm{C}}-1}. \tag{8.212}$$

We have here three unknown constants of proportionality since the utilized asymptotes are proportionalities but not exact equalities.

Recalling relation (8.188), the first term in the right-hand side of (8.212) provides

$$\frac{C}{N} \propto const \mid t \mid^{-2} h^{1+\beta_h^{\mathrm{C}}}. \tag{8.213}$$

Contrary to our expectations, the temperature dependence has not disappeared and is singular at the critical isotherm $t = 0$. Does it mean that the scaling is not valid for the heat capacity?

To see what has happened, we should return to the example of Landau theory. We consider the simplest form of the equilibrium Helmholtz energy when all critical indices equal their mean-field values:

$$F^{CE} = N\mu(-2A\ln 2 - hm_0 + atm_0{}^2 + bm_0{}^4 + \ldots). \tag{8.214}$$

We consider the system below the critical point when magnetic field is positive or zero. The equation of state

$$0 = -h + 2atm_0 + 4bm_0{}^3 + \ldots \tag{8.215}$$

is a cubic equation. When

$$h > 8b\left(\frac{a}{6b}\right)^{3/2} \mid t \mid^{3/2}, \tag{8.216}$$

it has one real solution

$$m_0 = 2\sqrt{\frac{a}{6b}}\sqrt{\mid t \mid}\cosh\left\{\frac{1}{3}\operatorname{acosh}\left(\frac{1}{8b}\left(\frac{a}{6b}\right)^{-3/2}\frac{h}{\mid t \mid^{3/2}}\right)\right\}. \tag{8.217}$$

When

$$0 \le h < 8b\left(\frac{a}{6b}\right)^{3/2} \mid t \mid^{3/2}, \tag{8.218}$$

there are three possible solutions, but we consider only the stable magnetization

$$m_0 = 2\sqrt{\frac{a}{6b}}\sqrt{|t|}\cos\left\{\frac{1}{3}\operatorname{acos}\left(\frac{1}{8b}\left(\frac{a}{6b}\right)^{-3/2}\frac{h}{|t|^{3/2}}\right)\right\}. \tag{8.219}$$

This is clearly the scaling dependence on the scaling parameter $h/|t|^{\Delta^{C}_{h-t}}$, where the mean-field approach provides the value of the crossover index $\Delta^{C}_{h-t} = 3/2$:

$$m_0 = \sqrt{|t|}\,\Xi^{-}_{m_0}\left(\frac{h}{|t|^{3/2}}\right) \tag{8.220}$$

with the scaling function

$$\Xi^{-}_{m_0}(y) = 2\sqrt{\frac{a}{6b}}\cos\left\{\frac{1}{3}\operatorname{acos}\left(\frac{1}{8b}\left(\frac{a}{6b}\right)^{-3/2} y\right)\right\} \text{ for } y < 8b\left(\frac{a}{6b}\right)^{3/2}, \tag{8.221}$$

$$\Xi^{-}_{m_0}(y) = 2\sqrt{\frac{a}{6b}}\cosh\left\{\frac{1}{3}\operatorname{acosh}\left(\frac{1}{8b}\left(\frac{a}{6b}\right)^{-3/2} y\right)\right\} \text{ for } y > 8b\left(\frac{a}{6b}\right)^{3/2}. \tag{8.222}$$

The scaling function has two asymptotes:

$$\Xi^{-}_{m_0}(y) \to 2\sqrt{\frac{a}{6b}}\frac{\sqrt{3}}{2} = \sqrt{\frac{a}{2b}} \quad \text{for } |y| << 1, \tag{8.223}$$

$$\Xi^{-}_{m_0}(y) \to \frac{1}{(4b)^{1/3}} y^{1/3} \quad \text{for } |y| >> 1, \tag{8.224}$$

providing two asymptotes of the magnetization:

$$m_0 = \sqrt{\frac{a}{2b}}\sqrt{|t|} \text{ for } 0 \le h << |t|^{3/2}, \tag{8.225}$$

$$m_0 = \frac{1}{(4b)^{1/3}} h^{1/3} \text{ for } h >> |t|^{3/2}. \tag{8.226}$$

Here in the inequalities, we no longer pay attention to the constant of proportionality (as well as in all other scaling inequalities in other sections).

Substituting solution (8.220) into (8.214), we see the scaling of the Helmholtz energy:

$$\frac{F^{CE}_{singular}}{N\mu} = |t|^2\,\Xi^{-}_{F^{CE}}\left(\frac{h}{|t|^{3/2}}\right), \text{ where} \tag{8.227}$$

$$\Xi^{-}_{F^{CE}}(y) \equiv -y\Xi^{-}_{m_0}(y) - a\Xi^{-}_{m_0}{}^{2}(y) + b\Xi^{-}_{m_0}{}^{4}(y) + \ldots \tag{8.228}$$

The scaling function has two asymptotes:

$$\Xi^{-}_{F^{CE}}(y) \to -\frac{a^2}{4b} \text{ for } |y| << 1, \tag{8.229}$$

$$\Xi^{-}_{F^{CE}}(y) \to -\frac{3b}{(4b)^{4/3}} y^{4/3} \text{ for } |y| >> 1, \tag{8.230}$$

which provide two asymptotes of the Helmholtz energy:

$$\frac{F^{CE}_{singular}}{N\mu} = -\frac{a^2}{4b}|t|^2 \text{ for } 0 \le h << |t|^{3/2}, \tag{8.231}$$

$$\frac{F^{CE}_{singular}}{N\mu} = -\frac{3b}{(4b)^{4/3}} h^{4/3} \text{ for } h >> |t|^{3/2}. \tag{8.232}$$

Since we intend to investigate the behavior of the heat capacity along the critical isotherm, let us investigate the behavior of the scaling function (8.228) in the proximity of this curve. Considering $h >> |t|^{3/2}$, we first improve the accuracy of asymptote (8.224), adding several *corrections to scaling*:

$$\Xi^{-}_{m_0}(y) \to \frac{1}{(4b)^{1/3}} y^{1/3} + (4b)^{1/3} \frac{a}{6b} y^{-1/3} - \frac{1}{3}(4b)^{5/3}\left(\frac{a}{6b}\right)^3 y^{-5/3} + \ldots \text{ for } |y| >> 1. \tag{8.233}$$

This allows us to improve the accuracy of asymptote (8.230):

$$\Xi^{-}_{F^{CE}}(y) \to -\frac{3b}{(4b)^{4/3}} y^{4/3} - \frac{a}{(4b)^{2/3}} y^{2/3} - \frac{a^2}{6b} - \frac{a(4b)^{2/3}}{3}\left(\frac{a}{6b}\right)^2 y^{-2/3} + \ldots \text{ for } |y| >> 1. \tag{8.234}$$

Also formula for (8.211) requires the knowledge of the first and second derivatives of this scaling function:

$$\frac{d\Xi^{-}_{F^{CE}}}{dy} \to -\frac{4b}{(4b)^{4/3}} y^{1/3} - \frac{2a}{3(4b)^{2/3}} y^{-1/3} + \frac{2a}{9}(4b)^{2/3}\left(\frac{a}{6b}\right)^2 y^{-5/3} + \ldots \text{ for } |y| >> 1. \tag{8.235}$$

$$\frac{d^2\Xi^-_{F^{CE}}}{dy^2} \to -\frac{4b}{3(4b)^{4/3}}\,y^{-2/3} + \frac{2a}{9(4b)^{2/3}}\,y^{-4/3} - \frac{10a}{27}(4b)^{2/3}\left(\frac{a}{6b}\right)^2 y^{-8/3} + \ldots \text{ for } |\,y\,| >> 1. \tag{8.236}$$

Let us now find the heat capacity by differentiating the Helmholtz energy (8.227):

$$\frac{C}{N\mu} = -\frac{T}{N\mu}\frac{\partial^2 F^{CE}}{\partial T^2} = -\frac{2\Xi^-_{F^{CE}}\Big|_{h/|t|^{3/2}}}{T_C} + \frac{9}{4}\frac{|\,t\,|^{-3/2}}{T_C}\,h\,\frac{d\Xi^-_{F^{CE}}}{dy}\Bigg|_{h/|t|^{3/2}} - \frac{9}{4}\frac{|\,t\,|^{-3}}{T_C}\,h^2\,\frac{d^2\Xi^-_{F^{CE}}}{dy^2}\Bigg|_{h/|t|^{3/2}}. \tag{8.237}$$

Substituting asymptotes found above, we group the terms by their powers of the scaling parameter y:

$$\frac{C}{N\mu} = \{6-9+3\}\frac{1}{T_C}\frac{b}{(4b)^{4/3}}\left(\frac{h}{|\,t\,|^{3/2}}\right)^{4/3} + \left\{2-\frac{3}{2}-\frac{1}{2}\right\}\frac{1}{T_C}\frac{a}{(4b)^{2/3}}\left(\frac{h}{|\,t\,|^{3/2}}\right)^{2/3} + \frac{1}{T_C}\frac{a^2}{3b} + \left\{\frac{2}{3}+\frac{1}{2}+\frac{5}{6}\right\}\frac{1}{T_C}\,a(4b)^{2/3}\left(\frac{a}{6b}\right)^2\left(\frac{h}{|\,t\,|^{3/2}}\right)^{-2/3} + \ldots, \tag{8.238}$$

where the leading bracket in front of each group explicitly shows three separate numbers, coming from three different terms of the right-hand side of (8.237).

From this result, we see that the leading scaling term (8.230) indeed provides $C \propto |\,y\,|^{4/3} \propto |\,t\,|^{-2}$ which is singular at the critical isotherm $t = 0$. However, the coefficient $\{6-9+3\}$ at this term is exactly zero! Therefore, the divergence $|\,t\,|^{-2}$ does not affect the heat capacity.

The first correction to the main scaling returns singularity $C \propto y^{2/3} \propto |\,t\,|^{-1}$ again; however, the coefficient $\left\{2-\frac{3}{2}-\frac{1}{2}\right\}$ is zero again!

Only the second correction to the main scaling, which we call *the superseding correction,* provides the nonzero value of the heat capacity, while all further corrections are exactly zero at the critical isotherm $t = 0$:

$$\frac{C}{N\mu} = \frac{1}{T_C}\frac{a^2}{3b}. \tag{8.239}$$

In the result, the heat capacity is constant along the critical isotherm in the vicinity of the critical point which corresponds to zero value of the critical index $\alpha_h^C = 0$.

We see that the leading term of the scaling does not always determine the behavior of the system. Corrections to this term often influence experimental results also. Besides, as it has happened in the example considered above, sometimes the coefficient at the leading term becomes exactly zero. In this case, the superseding correction completely "usurps" the leading role in determining the scaling behavior!

8.6 Crossover Effect of Magnetic Field

In Sect. 8.4 for the magnetization, we have found scaling (8.190–8.194):

$$m_0 = \mid t \mid^{\beta_t^C} \Xi^{\pm}_{m_0}\left(\frac{h}{\mid t \mid^{\Delta^C_{h-lt}}}\right), \tag{8.240}$$

where two asymptotes of the scaling function,

$$\Xi^{\pm}_{m_0}(y) \propto \underline{\underline{O}}(1) \text{ for } \mid y \mid << 1, \tag{8.241}$$

$$\Xi^{\pm}_{m_0}(y) \propto y^{\beta_h^C} \text{ for } \mid y \mid >> 1, \tag{8.242}$$

provide two asymptotes of the magnetization:

$$m_0 \propto \mid t \mid^{\beta_t^C} \text{ for } h << \mid t \mid^{\Delta^C_{h-lt}}, \tag{8.243}$$

$$m_0 \propto h^{\beta_h^C} \text{ for } h >> \mid t \mid^{\Delta^C_{h-lt}}. \tag{8.244}$$

This scaling behavior is called *the crossover effect* which should always be taken into account during experimental or numerical studies. Let a scientist investigate the behavior of a magnetic system in the vicinity of its critical point. The main purpose of this study may be to measure the critical index β_t^C at the binodal curve. For this purpose, the scientist isolates the system from external fields and allows the temperature to tend step by step to its critical value from below.

Far from the critical point, there is no scaling, and the investigator observes some complex behavior, specific for this particular system. However, when the temperature more and more approaches the critical value, the fractality tends to occupy larger and larger scales, leading to the appearance of the scaling when the dependence of the magnetization on temperature transforms into power-law (8.243).

This is what the scientist has wanted to achieve. To find the critical index β_t^C she/he needs only to measure the magnetization m_0 when $\mid t \mid \to 0$. Then the sought critical index would be provided by the slope of the dependence of $\ln m_0$ on $\ln \mid t \mid$.

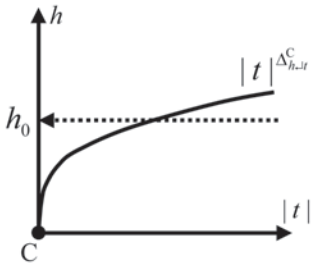

Fig. 8.6 The crossover effect due to the presence of small magnetic field

The more points along this curve the investigator would be able to measure, the more accurate the final value of the critical index would be. However, each unit step of $\ln|t| \Rightarrow \ln|t|-1$ requires to decrease $|t|$ e times: $|t| \Rightarrow |t|/e$. Therefore, the scientist employs the most sensitive equipment capable to perform finest measurements in the close proximity of the critical point. But will the scientist obtain the desired result?

Even if the system has been isolated from external fields, a small but nonzero magnetic field h_0 is always present. So, we actually can talk only about how small its magnitude is, but not about the complete absence of the field.

But the presence of even small field distorts the behavior of the system drastically! Let us look at Fig. 8.6. The small magnetic field h_0 is presented here by the dotted arrow. The scientist believes that when the system tends to the critical point, it follows the abscissa axis of the zero field $h = 0$. However, in reality, the system follows the dotted arrow and finally arrives not at the critical point but at the point with the critical temperature $t = 0$, but nonzero value of the field $h = h_0 \neq 0$.

When $h_0 << |t|^{\Delta^C_{h-lt}}$, i.e., to the right of the curve $h = |t|^{\Delta^C_{h-lt}}$ in Fig. 8.6, the magnetization follows the asymptotic power-law dependence (8.243) on temperature which is singular (zero) at the critical point. However, when the investigator allows the system to tend to the critical point, the system follows the dotted arrow and crosses the curve $h = |t|^{\Delta^C_{h-lt}}$. The corresponding temperature $|t| = h^{1/\Delta^C_{h-lt}}$ is called *the crossover temperature*.

But to the left of this curve, the present nonzero field breaks the singular dependence (8.243) on temperature to generate the new scaling (8.244) when the magnetization tends to a finite value $m_0 \propto h_0^{\beta^C_h}$ instead of the zero value which it would achieve at the critical point. This dependence is presented schematically in Fig. 8.7.

Therefore, preparing the experiment, the scientist should take care not only about how sensitive the equipment is but also about the better isolation from the external field. Otherwise, the crossover effect would break the desired power-law temperature dependence.

Similar to the crossover effect of magnetization, behavior is exhibited by other quantities: Helmholtz energy, susceptibility, and heat capacity. Let us consider, for example, the heat capacity. We expect that, when approaching the critical point, the small but nonzero field should break the temperature divergence $C \propto 1/|t|^{\alpha^C_t}$

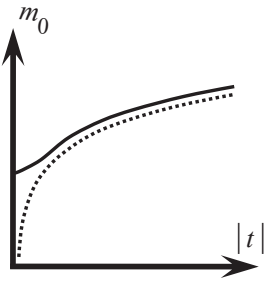

Fig. 8.7 Due to the crossover effect, the magnetization has a nonzero value at the critical temperature

at both sides, $t \to +0$ and $t \to -0$, of the critical point to generate the finite value, depending on the magnetic field:

$$C = |t|^{-\alpha_t^C} \Xi_C^{\pm}\left(\frac{h}{|t|^{\Delta_{h\perp t}^C}}\right), \tag{8.245}$$

where two asymptotes of the scaling function,

$$\Xi_C^{\pm}(y) \propto \underline{\underline{O}}(1) \text{ for } |y| << 1, \tag{8.246}$$

$$\Xi_C^{\pm}(y) \propto y^{-\alpha_h^C} \text{ for } |y| >> 1, \tag{8.247}$$

provide two asymptotes of the heat capacity:

$$C \propto |t|^{-\alpha_t^C} \text{ for } h << |t|^{\Delta_{h\perp t}^C}, \tag{8.248}$$

$$C \propto |t|^{-\alpha_t^C}\left(\frac{h}{|t|^{\Delta_{h\perp t}^C}}\right)^{-\alpha_h^C} \propto h^{-\alpha_h^C} \text{ for } h >> |t|^{\Delta_{h\perp t}^C}. \tag{8.249}$$

We have assumed this scaling to be valid just from the general considerations. But let us look what results this assumption can generate. First, to cancel out the temperature dependence in (8.249), we should assume the following relation among the critical indices:

$$\alpha_t^C = \Delta_{h\perp t}^C \alpha_h^C \tag{8.250}$$

which, with the aid of the relations obtained above, we transform into

$$\frac{\alpha_t^C}{\alpha_h^C} = \frac{\beta_t^C}{\beta_h^C} = \frac{\gamma_t^C}{\gamma_h^C} = \Delta_{h\perp t}^C, \tag{8.251}$$

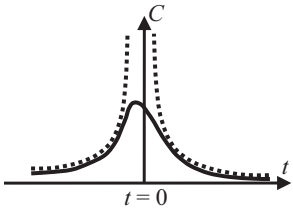

Fig. 8.8 Crossover effect of the heat capacity

$$\alpha_h^{\mathrm{C}} + 2\beta_h^{\mathrm{C}} + \gamma_h^{\mathrm{C}} = 2 / \Delta_{h,t}^{\mathrm{C}}. \tag{8.252}$$

Obviously, the mean-field exponents $\alpha_t^{\mathrm{C}} = 0$, $\alpha_h^{\mathrm{C}} = 0$, $\beta_t^{\mathrm{C}} = 1/2$, $\beta_h^{\mathrm{C}} = 1/3$, $\gamma_t^{\mathrm{C}} = 1$, $\gamma_h^{\mathrm{C}} = 2/3$, and $\Delta_{h,t}^{\mathrm{C}} = 3/2$ obey these relations.

Second, scaling (8.249) tells us that when the system tends to its critical temperature, the temperature divergence (singularity) is substituted by some transient dependence (Fig. 8.8), leading to a finite value of the heat capacity at $t = 0$.We also know this finite value—scaling (8.249) predicts from general considerations that $C \propto h^{-\alpha_h^{\mathrm{C}}}$.

From Fig. 8.8 we see that, theoretically, nothing prevents the point of maximum of the heat capacity to be not exactly at critical temperature $t = 0$. But how far the point of the maximum can go?

Surprisingly, this question is also answered by the scaling itself. Let us suppose that the maximum $C \propto h^{-\alpha_h^{\mathrm{C}}}$ is achieved at point t_0. This maximum has been provided by the maximum of the function $\Xi_C^{\pm}(y)/y^{-\alpha_h^{\mathrm{C}}}$ at some value y_0 of the scaling parameter y. So, by definition, we have

$$y_0 = \frac{h}{|t_0|^{\Delta_{h,t}^{\mathrm{C}}}}. \tag{8.253}$$

Here $|y_0| >> 1$, but y_0 is still a some finite value. This provides the assessment how much the point of the maximum can deflect from $t_{\mathrm{C}} = 0$:

$$|t_0| = \left(\frac{h}{y_0}\right)^{1/\Delta_{h,t}^{\mathrm{C}}} \propto h^{1/\Delta_{h,t}^{\mathrm{C}}}. \tag{8.254}$$

If we decided to find the critical temperature experimentally as the point at which the heat capacity diverges, this expression would give us the possible experimental error present due to the crossover effect.

We should mention here that the presented discussion has been intended only to illustrate the general concepts, following from scaling hypotheses, and should not be considered as rigorous. Each particular system has its own symmetries, positively determined quantities, and model rules, dictating the behavior of the system. For such a system, the presented concepts may illustrate the obtained experimental or numerical results; however, they may also happen to be inapplicable, in which

case the scaling hypotheses should be modified to suite the particular system under consideration.

8.7 Magnetic Systems: Crossover Phenomena

So far for magnetic systems, we have studied the crossover effects caused only by the magnetic field. However, similar phenomena can arise due to many other parameters, for example, weak interactions.

We approximate any real system by a model whose Hamiltonian includes terms which we are holding responsible for the observed behavior. However, any model is just an idealization. The real system may possess more complex interactions that are missed in the model Hamiltonian due to their small amplitude φ. For example, in the Ising model, we may take into account only pair (bi-spin) interactions while the real system may possess very weak but nonzero triple-spin interactions, quadrospin interactions, etc.

These unknown interactions are weak and, far from the critical point, may not be observable experimentally. However, when the system approaches its critical point, the amplitude φ of these interactions may become comparable with the relative deviation of temperature from its critical value, causing the appearance of the new order parameter

$$z = \frac{\varphi}{|t|^{\Delta^{C}_{\varphi\perp t}}}. \tag{8.255}$$

Here we have introduced a new *critical crossover index* $\Delta^{C}_{\varphi\perp t}$ responsible for the comparison of the weak amplitude φ with $|t|^{\Delta^{C}_{\varphi\perp t}}$.

In this case, for an arbitrary quantity *a,* we obtain the scaling

$$a = |t|^{\theta^{C}_{t}} \; \Xi^{\pm}_{a}\left(\frac{\varphi}{|t|^{\Delta^{C}_{\varphi\perp t}}}\right), \tag{8.256}$$

where two asymptotes of the scaling function,

$$\Xi^{\pm}_{a}(z) \propto \underline{\underline{O}}(1) \;\text{ for }\; |z| << 1, \tag{8.257}$$

$$\Xi^{\pm}_{a}(z) \propto z^{\theta^{C}_{\varphi}} \;\text{ for }\; |z| >> 1, \tag{8.258}$$

provide two asymptotes of the scaling:

$$a \propto |t|^{\theta^{C}_{t}} \;\text{ for } \varphi << |t|^{\Delta^{C}_{\varphi\perp t}}, \tag{8.259}$$

$$a \propto |t|^{\theta^{C}_{t}} \left(\frac{\varphi}{|t|^{\Delta^{C}_{\varphi\perp t}}}\right)^{\theta^{C}_{\varphi}} \propto \varphi^{\theta^{C}_{\varphi}} \;\text{ for } \theta^{C}_{\varphi} = \theta^{C}_{t} / \Delta^{C}_{\varphi\perp t} \text{ and } \varphi >> |t|^{\Delta^{C}_{\varphi\perp t}}. \tag{8.260}$$

Here we assume that the temperature dependence is canceled to provide scaling on the amplitude φ with a new critical index θ_{φ}^{C}.

Scaling (8.256–8.260) generates the crossover effect similar to the effect of the small but nonzero magnetic field considered in the previous section. Namely, when the temperature of the system tends to its critical value, the small amplitude φ of unknown interactions breaks the singular (i.e., tending to zero or infinity) temperature dependence to generate the finite value of a depending on the amplitude φ. The temperature $| t |= \varphi^{1/\Delta_{\varphi\perp t}^{C}}$ is, again, called *the crossover temperature*.

Real interactions may not have an amplitude that can be "tuned"; however, in the mathematical model, describing the system, everything is possible. Therefore, the new scaling (8.260) can be considered as a singular power-law dependence again, however in this case, this dependence is on the amplitude φ.

All scaling dependencies considered so far broke the scaling on temperature to generate the new scaling on magnetic field or on amplitudes of weak interactions. However, the reader should not think that this is generally the case. It is also possible for the scaling to transform one scaling dependence on temperature into another scaling dependence also on temperature, changing only the critical index of this dependence.

The typical example is, again, the presence of weak interactions. Let us consider scaling (8.256) when in the limit $| z | >> 1$, the power-law dependence (8.258) does not cancel out the existing temperature power-law dependence:

$$a \propto | t |^{\theta_t^C - \theta_\varphi^C \Delta_{\varphi\perp t}^C} \varphi^{\theta_\varphi^C} \text{ for } \theta_\varphi^C \neq \theta_t^C / \Delta_{\varphi\perp t}^C \text{ and } \varphi >> | t |^{\Delta_{\varphi\perp t}^C}. \tag{8.261}$$

In this case, the presence of unknown weak interactions changes the critical index θ_t^C:

$$\theta_t^C \Rightarrow \theta_t^C - \theta_\varphi^C \Delta_{\varphi\perp t}^C. \tag{8.262}$$

A scientist who does not know that weak interactions are present in the system is observing the change of the temperature power-law dependence from (8.259) to (8.261). She/he is lucky if the scaling (8.259), relevant to the theoretical model, describing the experiment, has been registered first. Otherwise, if only the second scaling (8.261) has been observed, the scientist may blame the mathematical model for crude predictions of the critical index, not knowing that the culprit is not the model.

8.8 Magnetic Systems: The Finite-Size Effect

When we considered the finite-size effect in percolation, we saw that the correlation length of the infinite system, exceeding the size of the finite system, caused the break of the existing power-law dependence on $| p - p_C |$, leading to the finite value (not zero and not infinite) of a quantity at the critical point. But this is exactly the description of a typical crossover effect: Break the singularity on temperature and generate a new scaling. Therefore, we expect the finite-size effect to be the crossover effect as well.

Let us consider the finite-size effect in the case of magnetic systems. First, for simplicity, we consider the critical isofield curve when $h = 0$ strictly. We consider a model of linear size $L = N^{1/d}$ whose behavior deviates from the behavior of the infinite system. To distinguish the quantities belonging to the infinite system from their analogues in the finite system, we will use the superscript "∞."

The scaling behavior of the finite system is built on the base of the scaling parameter

$$x \equiv \frac{\xi^{\infty}}{L}. \tag{8.263}$$

Since we are considering the zero magnetic field, the second scaling parameter $y \equiv h/|t|^{\Delta^{C}_{h,t}}$, is zero and will not participate in the scaling.

The new scaling parameter (8.263) can be transformed into the form identical to already considered scaling parameters. Indeed, substituting into (8.263) the divergence $\xi^{\infty} \propto |t|^{-\nu^{C}_{t}}$ of the correlation length of the infinite system, we find

$$x \equiv \frac{(1/L)}{|t|^{\nu^{C}_{t}}}. \tag{8.264}$$

Introducing the new *critical crossover index*

$$\Delta^{C}_{\frac{1}{L} \perp t} \equiv \nu^{C}_{t}, \tag{8.265}$$

we obtain

$$x \equiv \frac{(1/L)}{|t|^{\Delta^{C}_{\frac{1}{L} \perp t}}}. \tag{8.266}$$

Let us consider the behavior of the extensive quantity A and of the intensive quantity a. For the infinite system in the vicinity of the critical point, we have power-law dependencies

$$A^{\infty} \propto L^{d} |t|^{\Theta^{C}_{t}}, \tag{8.267}$$

$$a^{\infty} \propto |t|^{\theta^{C}_{t}}. \tag{8.268}$$

For the finite system, the scaling dependencies are

$$A \propto L^{d} |t|^{\Theta^{C}_{t}} \Xi^{\pm}_{A}\left(\frac{\xi^{\infty}}{L}\right), \tag{8.269}$$

$$a \sim |t|^{\theta^{C}_{t}} \Xi^{\pm}_{a}\left(\frac{\xi}{L}\right), \tag{8.270}$$

where the scaling functions have asymptotes

$$\Xi_A^{\pm}(x) \propto \underline{\underline{O}}(1),\ \Xi_a^{\pm}(x) \propto \underline{\underline{O}}(1) \text{ for } |x| << 1, \tag{8.271}$$

$$\Xi_A^{\pm}(x) \sim x^{\Theta_t^C/\nu_t^C}, \Xi_a^{\pm}(x) \sim x^{\theta_t^C/\nu_t^C} \text{ for } |x| >> 1, \tag{8.272}$$

providing the scaling

$$A \propto L^d |t|^{\Theta_t^C},\ a \propto |t|^{\theta_t^C} \text{ for } \xi^{\infty} << L, \tag{8.273}$$

$$A \propto L^d |t|^{\Theta_t^C} \left(\frac{1/L}{|t|^{\nu_t^C}}\right)^{\Theta_t^C/\nu_t^C} \propto \left(\frac{1}{L}\right)^{\frac{\Theta_t^C}{\nu_t^C}-d}, \text{ and} \tag{8.274}$$

$$a \propto |t|^{\theta_t^C} \left(\frac{1/L}{|t|^{\nu_t^C}}\right)^{\theta_t^C/\nu_t^C} \propto \left(\frac{1}{L}\right)^{\frac{\theta_t^C}{\nu_t^C}} \text{ for } \xi^{\infty} >> L. \tag{8.275}$$

The singular dependencies on temperature are substituted by some transient dependencies, leading to the finite values, depending on the size of the finite system (Figs. 8.9 and 8.10). Again, the scaling predicts the finite values (8.274 and 8.275), replacing singularities of the quantities at the critical point.

If we decided to measure the critical temperature as the point of singularity, the considered scaling would return the estimate with the accuracy

$$|\Delta t| \propto \frac{1}{L^{1/\nu_t^C}}. \tag{8.276}$$

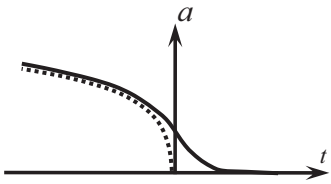

Fig. 8.9 The finite-size effect for the singular temperature dependence tending to zero value at the critical point of the infinite system

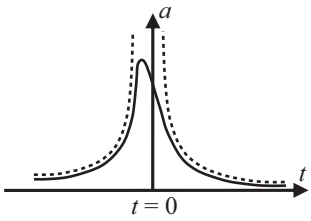

Fig. 8.10 The finite-size effect for the singular temperature dependence diverging at the critical point of the infinite system

8.9 The Illusory Asymmetry of the Temperature

So far, we have considered the crossover phenomena generated by a system, tending to its critical point along the binodal curve.

Far from the critical point, the fractality occupies only the finest scales. The rest of the scales is described by the laws specific for this particular system so that the behavior of the system is not universal. The scaling is also absent.

When the system approaches its critical point, the fractality occupies larger and larger scales, causing the scaling to appear. This scaling manifests itself for a quantity a as a power-law temperature dependence $|t|^{\theta_t^C}$.

Further approach to the critical point makes the temperature comparable with a small but nonzero amplitude φ of some interactions. This amplitude is unknown but is considered to be fixed (to be supported constant while the system tends to its critical point). The presence of this amplitude breaks the temperature scaling, while the value of this amplitude dictates the value of the considered quantity a at the critical point.

Since the majority of the scaling studies is devoted to the crossover phenomena along the binodal curve, it may seem that the temperature plays an asymmetric role in all crossover phenomena; that it is always the temperature scaling that is broken by other field parameters or interaction constants.

However, this impression is not true. The temperature is neither more nor less than any other field parameter or interaction constant. To demonstrate this, we rewrite scaling (8.256) as

$$a = |t|^{\theta_t^C} \Xi_a^{\pm}\left(\frac{\varphi}{|t|^{\Delta_{\varphi\to t}^C}}\right) = \varphi^{\theta_t^C/\Delta_{\varphi\to t}^C}\left[\left(\frac{\varphi}{|t|^{\Delta_{\varphi\to t}^C}}\right)^{-\theta_t^C/\Delta_{\varphi\to t}^C} \Xi_a^{\pm}\left(\frac{\varphi}{|t|^{\Delta_{\varphi\to t}^C}}\right)\right]. \tag{8.277}$$

Inside the square brackets, we see here the new scaling function

$$a = |\varphi|^{\theta_\varphi^C} \Xi_a^{\pm}\left(\frac{t}{|\varphi|^{\Delta_{t\to\varphi}^C}}\right), \text{where } \Delta_{t\to\varphi}^C = 1/\Delta_{\varphi\to t}^C. \tag{8.278}$$

Here the superscript index "±" differentiates functions already not above or below the critical isotherm but the cases $\varphi > 0$ and $\varphi < 0$. Two asymptotes of the scaling function,

$$\Xi_a^{\pm}\left(\frac{t}{|\varphi|^{\Delta_{t\to\varphi}^C}}\right) \propto \underline{\underline{O}}(1) \text{ for } \frac{|t|}{|\varphi|^{\Delta_{t\to\varphi}^C}} << 1, \tag{8.279}$$

$$\Xi_a^{\pm}\left(\frac{t}{|\varphi|^{\Delta_{t\to\varphi}^C}}\right) \propto \left(\frac{|t|}{|\varphi|^{\Delta_{t\to\varphi}^C}}\right)^{\theta_t^C} \text{ for } \frac{|t|}{|\varphi|^{\Delta_{t\to\varphi}^C}} >> 1, \tag{8.280}$$

provide two asymptotes of the scaling:

$$a \propto |\varphi|^{\theta_\varphi^C} \quad \text{for } |t| << |\varphi|^{\Delta_{t\perp\varphi}^C}, \tag{8.281}$$

$$a \propto |\varphi|^{\theta_\varphi^C} \left(\frac{|t|}{|\varphi|^{\Delta_{t\perp\varphi}^C}} \right)^{\theta_t^C} \propto |t|^{\theta_t^C} \quad \text{for } \theta_t^C = \theta_\varphi^C / \Delta_{t\perp\varphi}^C \text{ and } |t| >> |\varphi|^{\Delta_{t\perp\varphi}^C}. \tag{8.282}$$

In this case, instead of fixing $|\varphi|$, we are fixing $|t| \neq 0$ as a small but nonzero deviation from the critical temperature about which the scientist does not know. The scientist assumes that she/he tends the system to its critical point along the critical isotherm $t = 0$ by decreasing the amplitude $|\varphi|$ (for example, by decreasing the magnetic field $|h|$). However, when $|t| \neq 0$ becomes comparable with $|\varphi|^{\Delta_{t\perp\varphi}^C}$, the small but nonzero deviation of the system from its critical temperature breaks the singular scaling on $|\varphi|$ to tend the measured quantity to a finite value, determined by the fixed value of $|t| \neq 0$.

So, any crossover effect has "two sides of a coin." In the above example, the temperature scaling may be considered as broken by the amplitude $|\varphi|$. Or, on the contrary, the scaling on $|\varphi|$ may be considered as broken by the temperature.

We see that the role of the temperature is not special, and the temperature is neither more nor less than just one of many field parameters. In fact, the temperature can disappear from the scaling at all!

To demonstrate this, let us support a system at exactly $t = 0$. In this case, the temperature is always less than all other field parameters or interaction constants and do not participate in scaling. Then we can consider, for example, the crossover effect between the magnetic field and the finite size of the system along the critical isotherm.

The scaling parameter we consider in this case is

$$x \equiv \frac{\xi^\infty}{L} = \frac{(1/L)}{|h|^{\Delta_{\frac{1}{L}\perp h}^C}} \text{ where } \Delta_{\frac{1}{L}\perp h}^C \equiv \nu_h^C. \tag{8.283}$$

We consider an extensive quantity A and an intensive quantity a whose scaling on the magnetic field in the infinite system is provided by

$$A^\infty \propto L^d |h|^{\Theta_h^C}, \tag{8.284}$$

$$a^\infty \propto |h|^{\theta_h^C}. \tag{8.285}$$

For the finite system, we assume that the scaling dependencies are

$$A \propto L^d |h|^{\Theta_h^C} \Xi_A^\pm \left(\frac{\xi^\infty}{L} \right), \tag{8.286}$$

$$a \propto |h|^{\theta_h^C} \Xi_a^{\pm}\left(\frac{\xi^{\infty}}{L}\right), \tag{8.287}$$

where the scaling functions have asymptotes

$$\Xi_A^{\pm}(x) \sim \underline{\underline{O}}(1),\ \Xi_a^{\pm}(x) \sim \underline{\underline{O}}(1) \text{ for } |x| << 1, \tag{8.288}$$

$$\Xi_A^{\pm}(x) \sim x^{\Theta_h^C/\nu_h^C},\ \Xi_a^{\pm}(x) \sim x^{\theta_h^C/\nu_h^C} \text{ for } |x| >> 1, \tag{8.289}$$

providing the scaling

$$A \propto L^d |h|^{\Theta_h^C},\ a \propto |h|^{\theta_h^C} \text{ for } \xi^{\infty} << L, \tag{8.290}$$

$$A \propto L^d |h|^{\Theta_h^C} \left(\frac{1/L}{|h|^{\nu_h^C}}\right)^{\Theta_h^C/\nu_h^C} \propto \left(\frac{1}{L}\right)^{\frac{\Theta_h^C}{\nu_h^C}-d}, \tag{8.291}$$

and

$$a \propto |h|^{\theta_h^C} \left(\frac{1/L}{|h|^{\nu_h^C}}\right)^{\theta_h^C/\nu_h^C} \propto \left(\frac{1}{L}\right)^{\frac{\theta_h^C}{\nu_h^C}} \text{ for } \xi^{\infty} >> L. \tag{8.292}$$

So, we obtain the crossover effect between the magnetic field and the finite size of the system along the critical isotherm when the temperature does not participate in the scaling.

Problem 8.9.1*

Demonstrate how crossover effect (8.261 and 8.262) can change not only the index of the temperature scaling of the heat capacity but also the value of the critical temperature.

Solution: Let us return to scaling (8.278):

$$C = |\varphi|^{\theta_{\varphi}^C} \Xi_C^{\pm}\left(\frac{t}{|\varphi|^{\Delta_{t-|\varphi}^C}}\right). \tag{8.293}$$

When $|t| >> |\varphi|^{\Delta_{t-|\varphi}^C}$, this scaling should provide the usual divergence of the heat capacity:

$$C \propto |t|^{-\alpha}. \tag{8.294}$$

It is possible if

$$\theta_{\varphi}^{C} = -\alpha\,\Delta_{t\perp\varphi}^{C} \text{ and } \Xi_{C}^{\pm}(z) \sim |z|^{-\alpha} \text{ for } |z| >> 1. \tag{8.295}$$

When $|t| << |\varphi|^{\Delta_{t\perp\varphi}^{C}}$, we can no longer assume that the scaling function is of the order of unity. Instead, we should consider the following asymptote:

$$\Xi_{C}^{\pm}(z) \propto |z - z_0|^{-\tilde{\alpha}} \text{ for } |z| << 1. \tag{8.296}$$

For the heat capacity, this assumption provides

$$C \propto |\varphi|^{\theta_{\varphi}^{C}} \left| \frac{t}{|\varphi|^{\Delta_{t\perp\varphi}^{C}}} - z_0 \right|^{-\tilde{\alpha}} = |\varphi|^{(\tilde{\alpha}-\alpha)\Delta_{t\perp\varphi}^{C}} \left| t - z_0 |\varphi|^{\Delta_{t\perp\varphi}^{C}} \right|^{-\tilde{\alpha}}. \tag{8.297}$$

This is the result we have been looking for. First, for the close proximity of the critical point, when the crossover effect $|t| << |\varphi|^{\Delta_{t\perp\varphi}^{C}}$ is in action, the temperature divergence of the heat capacity has a different critical index $\tilde{\alpha}$.

Second, this new scaling chooses the new value of the critical temperature when $t = z_0 |\varphi|^{\Delta_{t\perp\varphi}^{C}}$. Third, it also contains a power-law dependence on φ, but, contrary to our expectations, the index of this dependence is not $\theta_{\varphi}^{C} = -\alpha\,\Delta_{t\perp\varphi}^{C}$ but $(\tilde{\alpha} - \alpha)\Delta_{t\perp\varphi}^{C}$.

All this has happened only because we have assumed that for small values of the scaling parameter the scaling function is no longer of the order of unity. Such dependencies are called *dangerous* and are considered in Sect. 8.11.

8.10 The Formalism of General Homogeneous Functions

The mathematical apparatus, lying in the foundation of scaling, is the formalism of homogeneous functions. *The p^{th}-order general homogeneous function* depending on n variables, $x_1, x_2, \ldots, x_n$, is defined as a function for which the equality

$$f(\lambda^{q_1} x_1, \lambda^{q_2} x_2, \ldots, \lambda^{q_n} x_n) = \lambda^{p} f(x_1, x_2, \ldots, x_n) \tag{8.298}$$

is valid for an arbitrary λ. Further, we assume that this function depends slowly on its arguments when the absolute values of those are much less than unity. In other words, $f(x_1, x_2, \ldots, x_i, \ldots, x_n)$ does not almost depend on x_i when $|x_i| << 1$.

Next, we associate each variable x_i with a particular coupling constant of the system (with a particular field parameter or interaction constant). In accordance with the definition of the general homogeneous function, each coupling constant x_i has its own index q_i. Next, for each x_i, we find x_i^{1/q_i}, and then find the maximum among these quantities: $i^{\max} : \max\limits_{i} x_i^{1/q_i}$.

Choosing $\lambda = x_{i^{\max}}^{-1/q_{i^{\max}}}$, we substitute it into (8.298):

$$f(x_1, x_2, \ldots, x_n) = x_{i^{\max}}^{p/q_{i^{\max}}} f\left(\frac{x_1}{x_{i^{\max}}^{q_1/q_{i^{\max}}}}, \ldots, \frac{x_{i^{\max}}}{x_{i^{\max}}^{q_{i^{\max}}/q_{i^{\max}}}}, \ldots, \frac{x_n}{x_{i^{\max}}^{q_n/q_{i^{\max}}}} \right). \tag{8.299}$$

In the right-hand side of this equality, all arguments for $i \neq i^{\max}$ are less than unity: $\frac{x_i}{x_{i^{\max}}^{q_i/q_{i^{\max}}}} < 1$. Therefore, the function does not depend on them. For $i = i^{\max}$, the argument is exactly unity, so its participation in scaling is also weak. Thereby the scaling of the right-hand side is provided only by the power-law dependence $x_{i^{\max}}^{p/q_{i^{\max}}}$:

$$f(x_1, x_2, \ldots, x_n) \propto x_{i^{\max}}^{p/q_{i^{\max}}} f(0, \ldots, 1, \ldots, 0) \propto x_{i^{\max}}^{p/q_{i^{\max}}} \quad \text{when } x_{i^{\max}}^{1/q_{i^{\max}}} > x_i^{1/q_i} \ \forall\ i \neq i^{\max}. \tag{8.300}$$

And what is even more important is that this scaling is determined by the maximal of quantities x_i^{1/q_i}.

If, during an experiment, we were decreasing the coupling constant $x_{i^{\max}}$, keeping other coupling constants unchanged, sometime the quantity $x_{i^{\max}}^{1/q_{i^{\max}}}$ would no longer be the maximal among x_i^{1/q_i}. Thereby the scaling function f would choose the new "leader" among the coupling constants, providing now the scaling on this variable.

The formalism of general homogeneous functions provides us with a perfect opportunity to look for the relations among the critical indices. Let us consider the magnetization as the scaling function of three arguments:

$$x_1 \equiv |t|,\ x_2 \equiv |h|,\ x_3 \equiv 1/L, \tag{8.301}$$

when initially $i^{\max} = 1$. In other words, we assume that initially

$$|h| << |t|^{\Delta^{\mathrm{C}}_{h\perp t}} \text{ and } 1/L << |t|^{\Delta^{\mathrm{C}}_{\frac{1}{L}\perp t}}, \text{ where } \Delta^{\mathrm{C}}_{h\perp t} = \frac{\beta^{\mathrm{C}}_t}{\beta^{\mathrm{C}}_h} \text{ and } \Delta^{\mathrm{C}}_{\frac{1}{L}\perp t} = \nu^{\mathrm{C}}_t. \tag{8.302}$$

For $i^{\max} = 1$, the scaling function is supposed to provide the scaling on temperature:

$$m_0\left(|t|, |h|, \frac{1}{L}\right) = |t|^{p/q_t}\ \Xi^{\pm}_{m_0}\left(1, \frac{|h|}{|t|^{q_h/q_t}}, \frac{1/L}{|t|^{q_{1/L}/q_t}}\right), \tag{8.303}$$

$$\text{where } \frac{p}{q_t} = \beta_t^{\mathrm{C}}, \frac{q_h}{q_t} = \Delta_{h\downarrow t}^{\mathrm{C}} = \frac{\beta_t^{\mathrm{C}}}{\beta_h^{\mathrm{C}}} \text{ and } \frac{q_{1/L}}{q_t} = \Delta_{\frac{1}{L}\downarrow t}^{\mathrm{C}} = \nu_t^{\mathrm{C}}. \tag{8.304}$$

Next, we assume that during the experiment, the temperature tends to its critical value, so that sometime it happens that

$$|h| >> |t|^{\Delta_{h\downarrow t}^{\mathrm{C}}} \text{ but still } 1/L << |t|^{\Delta_{\frac{1}{L}\downarrow t}^{\mathrm{C}}}. \tag{8.305}$$

Thereby the scaling function transforms into the scaling on magnetic field:

$$m_0\left(|t|, |h|, \frac{1}{L}\right) = |h|^{p/q_h}\, \Xi_{m_0}^{\pm}\left(\frac{|t|}{|h|^{q_t/q_h}}, 1, \frac{1/L}{|h|^{q_{1/L}/q_h}}\right), \tag{8.306}$$

$$\text{where } \frac{p}{q_h} = \beta_h^{\mathrm{C}}. \tag{8.307}$$

When we further tend the temperature to its critical value, it may stop to participate in the scaling, leaving only the crossover effect between the magnetic field and the size of the system:

$$|h| >> |t|^{\Delta_{h\downarrow t}^{\mathrm{C}}} \text{ and } 1/L >> |t|^{\Delta_{\frac{1}{L}\downarrow t}^{\mathrm{C}}}. \tag{8.308}$$

The new scaling parameter is $x \equiv \dfrac{\xi^{\infty}}{L} = \dfrac{(1/\mathrm{L})}{|h|^{\Delta_{\frac{1}{L}\downarrow h}^{\mathrm{C}}}}$ with $\Delta_{\frac{1}{L}\downarrow h}^{\mathrm{C}} \equiv \nu_h^{\mathrm{C}}$, and the scaling function provides

$$m_0\left(|t|, |h|, \frac{1}{L}\right) = |h|^{p/q_h}\, \Xi_{m_0}^{\pm}\left(0, 1, \frac{1/L}{|h|^{q_{1/L}/q_h}}\right), \tag{8.309}$$

$$\text{where } \frac{p}{q_h} = \beta_h^{\mathrm{C}} \text{ and } \frac{q_{1/L}}{q_h} = \nu_h^{\mathrm{C}}. \tag{8.310}$$

Comparing (8.304) and (8.310), we find the relation among the critical indices:

$$\frac{\nu_h^{\mathrm{C}}}{\nu_t^{\mathrm{C}}} = \frac{\beta_h^{\mathrm{C}}}{\beta_t^{\mathrm{C}}}. \tag{8.311}$$

Substituting this equality into (8.251), we find

$$\frac{\alpha_t^{\mathrm{C}}}{\alpha_h^{\mathrm{C}}} = \frac{\beta_t^{\mathrm{C}}}{\beta_h^{\mathrm{C}}} = \frac{\gamma_t^{\mathrm{C}}}{\gamma_h^{\mathrm{C}}} = \frac{\nu_t^{\mathrm{C}}}{\nu_h^{\mathrm{C}}} = \Delta_{h\downarrow t}^{\mathrm{C}}. \tag{8.312}$$

Problem 8.10.1

Prove the relation

$$\frac{\alpha_t^{\mathrm{C}}}{\alpha_h^{\mathrm{C}}} = \frac{\beta_t^{\mathrm{C}}}{\beta_h^{\mathrm{C}}} \tag{8.313}$$

by considering the scaling of the heat capacity.

Solution: For $|h| << |t|^{\Delta_{h\perp t}^{\mathrm{C}}}$ $\left(\text{where } \Delta_{h\perp t}^{\mathrm{C}} = \beta_t^{\mathrm{C}} / \beta_h^{\mathrm{C}}\right)$, we expect that

$$C\left(|t|,|h|\right) = |t|^{p/q_t}\ \Xi_C^{\pm}\left(1, \frac{|h|}{|t|^{q_h/q_t}}\right), \tag{8.314}$$

$$\text{where } \frac{p}{q_t} = -\alpha_t^{\mathrm{C}} \text{ and } \frac{q_h}{q_t} = \Delta_{h\perp t}^{\mathrm{C}} = \frac{\beta_t^{\mathrm{C}}}{\beta_h^{\mathrm{C}}}. \tag{8.315}$$

For $|h| >> |t|^{\Delta_{h\perp t}^{\mathrm{C}}}$:

$$C\left(|t|,|h|\right) = |h|^{p/q_h}\ \Xi_C^{\pm}\left(\frac{|t|}{|h|^{q_t/q_h}}, 1\right), \tag{8.316}$$

$$\text{where } \frac{p}{q_h} = -\alpha_h^{\mathrm{C}}. \tag{8.317}$$

Comparison of (8.315) and (8.317) immediately provides (8.313).

8.11 The Renormalization Group as the Source of Scaling

The scaling behavior appears in the vicinity of the critical point. As we know, the critical point can be the result of the RG transformation only if the initial system was also in the critical state. So, one critical point replaces another along the critical manifold which is the chain of critical states in the space of coupling constants. The critical manifold ends at the critical fixed point which we may consider to be the "capacitor" of the critical scaling behavior.

Besides, since the RG transformation keeps the lattice and the model invariant, it also keeps the critical indices of the system invariant. So, all systems along the critical manifold have the same values of the critical indices. Therefore, to find the scaling behavior of the initial system, there is no need to look for the exact solution of this system. Instead, we may investigate the system at the critical fixed point which is much easier in comparison, as we will see now.

We assume that the RG transforms the vector of coupling constants $\vec{K}$ into the vector $\vec{K}' = \mathrm{RG}(\vec{K})$. The critical fixed point $\vec{K}^{\mathrm{C}}$ of the RG transformation is determined by

$$\vec{K}^{\mathrm{C}} = \mathrm{RG}(\vec{K}^{\mathrm{C}}). \tag{8.318}$$

Considering small deviations of the coupling constants from their values at the fixed point,

$$\vec{K}^{\mathrm{C}} + \vec{k}' = \mathrm{RG}(\vec{K}^{\mathrm{C}} + \vec{k}), \tag{8.319}$$

we linearize the RG transformation in the vicinity of its fixed point by expanding the right-hand side of (8.319):

$$K_i^{\mathrm{C}} + k_i' = K_i^{\mathrm{C}} + \sum_{j=1}^{n} \left.\frac{\partial K_i'}{\partial K_j}\right|_{\vec{K}^{\mathrm{C}}} k_j \tag{8.320}$$

or

$$k_i' = \sum_{j=1}^{n} \left.\frac{\partial K_i'}{\partial K_j}\right|_{\vec{K}^{\mathrm{C}}} k_j, \tag{8.321}$$

where n is the dimensionality of the space of coupling constants.

In Sect. 7.5, when we considered the RG transformation for the ferromagnetic Ising model on triangular lattice, all eigenvalues and eigenvectors of the matrix $\left.\frac{\partial K_i'}{\partial K_j}\right|_{\vec{K}^{\mathrm{C}}}$ happened to be independent. For simplicity, now we also assume that this is the case: the matrix $\left.\frac{\partial K_i'}{\partial K_j}\right|_{\vec{K}^{\mathrm{C}}}$ is symmetric, diagonalizable, and has n independent eigenvalues λ_i and eigenvectors $\vec{\kappa}_i$:

$$\mathrm{RG}(\vec{\kappa}_i) = \lambda_i \vec{\kappa}_i. \tag{8.322}$$

On the basis of these eigenvectors, we introduce coordinates u_i and u_i' to represent vectors $\vec{k}$ and $\vec{k}'$, respectively:

$$\vec{k} = \sum_{i=1}^{n} u_i \vec{\kappa}_i \text{ and } \vec{k}' = \sum_{i=1}^{n} u_i' \vec{\kappa}_i. \tag{8.323}$$

Then from (8.321), we immediately find that each coordinate is transformed independently:

$$u_i' = \lambda_i u_i. \tag{8.324}$$

Obviously, the behavior of the linearized RG transformation in the vicinity of the critical fixed point depends drastically on whether the absolute values of eigenval-

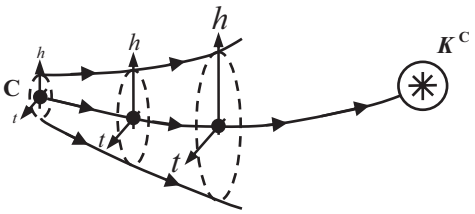

Fig. 8.11 A schematic representation of the behavior of relevant temperature and magnetic field eigenvectors

ues λ_i are more or less than unity. If $|\lambda_i| > 1$, during the chain of the RG transformations, the absolute value of the coordinate u_i will grow so that in the direction of this eigenvector $\vec{\kappa}_i$, the system will move away from the critical point. Such an eigenvalue is called *relevant* since it determines the flow curves of the RG transformation in the vicinity of the critical manifold and thereby influences the scaling.

Since in the direction of the relevant eigenvector $\vec{\kappa}_i$, the system moves away from the critical manifold, this eigenvector cannot be parallel to the critical manifold and is said to form the *codimension* of this manifold. The temperature and magnetic field represent relevant coupling constants of the magnetic systems because, as we have seen, the RG transformation moves these quantities away from their critical values (Fig. 8.11).

On the contrary, the eigenvalue $|\lambda_i| < 1$ is called *irrelevant* because, as we will see later, these eigenvalues do not influence the scaling (with the exception of the so-called dangerous irrelevant eigenvectors which we will also discuss later). During the chain of the RG transformations, the corresponding coordinate u_i disappears. The irrelevant eigenvector $\vec{\kappa}_i$ must, therefore, belong to the critical manifold.

In Fig. 8.11, we considered the flow curves in the space of the coupling constants but drew the eigenvectors in terms of the field parameters, the temperature and magnetic field. We did that out of simplicity, recalling the example of the previous chapter when we considered the ferromagnetic nearest-neighbor (n.n.) Ising model on triangular lattice. It happened that there were two eigenvectors (7.119) parallel to the axes of the space of coupling constants so that the first eigenvector corresponded to the change in K_1 while the second to the change in K_2.

Recalling the definitions (7.95) of the coupling constants,

$$K_1 \equiv \frac{\mu h}{T} \text{ and } K_2 \equiv \frac{J}{T}, \tag{8.325}$$

for small deviations $\vec{k}$ and $\vec{k}'$ in the vicinity of the critical fixed point,

$$K_1^{\mathrm{C}} \equiv 0 \text{ and } K_2 \equiv \frac{J}{T_{\mathrm{C}}} = \frac{1}{4}\ln(2\sqrt{2}+1), \tag{8.326}$$

we find

$$k_1 = \frac{\mu}{T_{\mathrm{C}}} h \text{ and } k_2 = -\frac{J}{T_{\mathrm{C}}} t. \tag{8.327}$$

Therefore, in the case of the example from Chap. 7, the first eigenvector $\vec{\kappa}_1$ and the first coordinate u_1 do correspond to the change of the magnetic field along the critical isotherm, while the second eigenvector $\vec{\kappa}_2$ and the second coordinate u_2 do correspond to the change of the temperature along the critical isofield curve.

For simplicity, in a general case, we may assume similar situation—each coordinate u_i is determined by the deviation of the corresponding field parameter or interaction constant. Returning to the case of the ferromagnetic Ising model, we will consider the first coordinate u_1 to correspond to the magnetic field while the second coordinate u_2 to the temperature.

As we know from Chap. 7, the RG transformation decreases the correlation length b times, i.e., with the scaling factor $r = 1/b$:

$$\xi(|h'|,|t'|) = \xi(|h|,|t|)/b. \tag{8.328}$$

Since the RG transformation keeps both the lattice and the model invariant, here the functional dependence of the correlation length on the values of field parameters is the same for both sides of the equation.

Substituting into (8.328) the connection (8.324) of the new coordinates with the old ones, we obtain

$$\xi(|\lambda_h||h|,|\lambda_t||t|) = \xi(|h|,|t|)/b. \tag{8.329}$$

Next, we consider the critical isofield $h = 0$. In this case, the correlation length diverges as $\xi(|t|,0) \propto |t|^{-\nu_t^{\mathrm{C}}}$. Substituting this scaling into both sides of (8.329), we find the critical index ν_t^{C}:

$$\frac{1}{(|\lambda_t||t|)^{\nu_t^{\mathrm{C}}}} = \frac{1}{b(|t|)^{\nu_t^{\mathrm{C}}}} \quad \text{or} \tag{8.330}$$

$$\nu_t^{\mathrm{C}} = \frac{\ln b}{\ln|\lambda_t|}. \tag{8.331}$$

We have obtained at first sight a strange result—the critical index ν_t^{C} depends on the linear size b of the cell of the RG transformation. The RG transformation is merely a tool, so we have expected that the size of the cell should not influence the found behavior of the system.

How can we exclude b from (8.331)? There is only a single way—to hypothesize that $\ln|\lambda_t|$ is proportional to $\ln b$. This assumption is supported by the fact that the RG transformation is a semigroup.[1] We expect from two consecutive RG transformations with linear cell sizes b_1 and b_2 to be equivalent to the RG transformation with cell size $b_2 b_1$:

[1] The RG transformation is a semigroup since, after we have reduced the number of degrees of freedom in the system, there is no inverse transformation that would restore these degrees of freedom.

$$\mathrm{RG}_{b_2}\mathrm{RG}_{b_1}(\vec{\boldsymbol{K}}) = \mathrm{RG}_{b_2 b_1}(\vec{\boldsymbol{K}}). \tag{8.332}$$

Since the eigenvectors $\vec{\boldsymbol{\kappa}}_i$ depend on the field parameters but not on the cell size, we expect that only the eigenvalues λ_i may depend on b. Performing transformation (8.324) of coordinates twice, we find

$$\lambda_i(b_2)\lambda_i(b_1) = \lambda_i(b_2 b_1). \tag{8.333}$$

But for arbitrary b_1 and b_2, this equality is possible only when

$$\lambda_i(b) = b^{y_i}, \tag{8.334}$$

where y_i are some indices, corresponding each to its own eigenvalue λ_i.

Substituting (8.334) into (8.331), we find

$$\nu_t^{\mathrm{C}} = \frac{1}{y_t}. \tag{8.335}$$

We see that the dependence on the cell size is no longer present in the formula and that the critical index ν_t^{C} is determined by the index y_t, corresponding to the coordinate $u_2 \equiv t$.

Let us now see how the RG transformation determines the scaling of the correlation length. Substituting (8.334) into (8.329), we obtain

$$\xi(b^{y_h}\,|\,h\,|, b^{y_t}\,|\,t\,|) = \xi(|\,h\,|,|\,t\,|)/b. \tag{8.336}$$

After n consecutive RG transformations, this equality transforms into

$$\xi(b^{ny_h}\,|\,h\,|, b^{ny_t}\,|\,t\,|) = \xi(|\,h\,|,|\,t\,|)/b^n \text{ or} \tag{8.337}$$

$$\xi(|\,h\,|,|\,t\,|) = \frac{1}{|\,t\,|^{1/y_t}}(b^{ny_t}\,|\,t\,|)^{1/y_t}\,\xi(b^{ny_h}\,|\,h\,|, b^{ny_t}\,|\,t\,|), \tag{8.338}$$

where the first multiplier of the right-hand side is the scaling $\xi(|\,t\,|,0) \propto |\,t\,|^{-\nu_t^{\mathrm{C}}}$ of the correlation length on the temperature.

So far, we have not specified the value of b. Considering it as a parameter, we choose

$$b = |\,t\,|^{-1/ny_t}. \tag{8.339}$$

In this case, (8.338) transforms into

$$\xi(|\,h\,|,|\,t\,|) = \frac{1}{|\,t\,|^{1/y_t}}\,\xi\left(\frac{|\,h\,|}{|\,t\,|^{y_h/y_t}}, 1\right), \tag{8.340}$$

which is the scaling function, depending on the scaling parameter

$$y \equiv \frac{h}{|t|^{\Delta^{\mathrm{C}}_{h\to t}}} \text{ with } \Delta^{\mathrm{C}}_{h\to t} = \frac{y_h}{y_t}. \tag{8.341}$$

Choosing another value of b for (8.337),

$$b = |h|^{-1/ny_h}, \tag{8.342}$$

we obtain the scaling on magnetic field

$$\xi(|h|,|t|) = \frac{1}{|h|^{1/y_h}} \xi\left(1, \frac{|t|}{|h|^{y_t/y_h}}\right), \tag{8.343}$$

which immediately provides values of the following critical indices

$$\nu^{\mathrm{C}}_h = \frac{1}{y_h} \text{ with } \Delta^{\mathrm{C}}_{t\to h} = \frac{y_t}{y_h}. \tag{8.344}$$

Substituting these indices and (8.335) into (8.312), we find

$$\frac{\alpha^{\mathrm{C}}_t}{\alpha^{\mathrm{C}}_h} = \frac{\beta^{\mathrm{C}}_t}{\beta^{\mathrm{C}}_h} = \frac{\gamma^{\mathrm{C}}_t}{\gamma^{\mathrm{C}}_h} = \frac{\nu^{\mathrm{C}}_t}{\nu^{\mathrm{C}}_h} = \Delta^{\mathrm{C}}_{h\to t} = \frac{y_h}{y_t}. \tag{8.345}$$

Applying relations among the critical indices in the presence of hyperscaling relations, we obtain

$$\nu^{\mathrm{C}}_t = \frac{1}{y_t} \text{ and } \nu^{\mathrm{C}}_h = \frac{1}{y_h}, \tag{8.346}$$

$$\alpha^{\mathrm{C}}_t = 2 - d\nu^{\mathrm{C}}_t = \frac{2y_t - d}{y_t} \text{ and } \alpha^{\mathrm{C}}_h = \frac{2y_t - d}{y_h}, \tag{8.347}$$

$$\beta^{\mathrm{C}}_t = d\nu^{\mathrm{C}}_t - \Delta^{\mathrm{C}}_{h\to t} = \frac{d - y_h}{y_t} \text{ and } \beta^{\mathrm{C}}_h = \frac{d - y_h}{y_h}, \tag{8.348}$$

$$\gamma^{\mathrm{C}}_t = 2\Delta^{\mathrm{C}}_{h\to t} - d\nu^{\mathrm{C}}_t = \frac{2y_h - d}{y_t} \text{ and } \gamma^{\mathrm{C}}_h = \frac{2y_h - d}{y_h}, \tag{8.349}$$

$$\eta^{\mathrm{C}} = 2 - \frac{\gamma^{\mathrm{C}}_t}{\nu^{\mathrm{C}}_t} = 2 + d - 2y_h. \tag{8.350}$$

There is an easy way to verify these expressions: For $d = 4$, they should transform into the mean-field values of the critical indices which we can prove to be true by direct substitution.

Let us consider the RG transformation of an arbitrary intensive quantity a. In comparison with (8.328), we hypothesize that we would find another power-law dependence on b:

$$a(|h'|,|t'|) = a(|h|,|t|)/b^{\kappa}. \tag{8.351}$$

This provides

$$a(b^{ny_h}|h|,b^{ny_t}|t|) = a(|h|,|t|)/b^{n\kappa} \quad \text{and} \tag{8.352}$$

$$a(|h|,|t|) = |t|^{-\kappa/y_t}\,(b^{ny_t}|t|)^{\kappa/y_t}\,a(b^{ny_h}|h|,b^{ny_t}|t|) \quad \text{or} \tag{8.353}$$

$$a(|h|,|t|) = |h|^{-\kappa/y_h}\,(b^{ny_h}|h|)^{\kappa/y_h}\,a(b^{ny_h}|h|,b^{ny_t}|t|). \tag{8.354}$$

Substituting (8.339) and (8.342) into (8.353) and (8.354), respectively, we find the scaling

$$a(|h|,|t|) = |t|^{-\kappa/y_t}\;a\left(\frac{|h|}{|t|^{\Delta^{C}_{h\leftarrow t}}},1\right) \tag{8.355}$$

and

$$a(|h|,|t|) = |h|^{-\kappa/y_h}\;a\left(1,\frac{|t|}{|h|^{\Delta^{C}_{t\leftarrow h}}}\right). \tag{8.356}$$

Defining critical indices for quantity a by

$$a(|h|,|t|) = |t|^{\theta^{C}_{t}}\;a\left(\frac{|h|}{|t|^{\Delta^{C}_{h\leftarrow t}}},1\right), \tag{8.357}$$

$$a(|h|,|t|) = |h|^{\theta^{C}_{h}}\;a\left(1,\frac{|t|}{|h|^{\Delta^{C}_{t\leftarrow h}}}\right), \tag{8.358}$$

by comparison with (8.355) and (8.356), we immediately find

$$\theta^{C}_{t} = -\frac{\kappa}{y_t} \text{ and } \theta^{C}_{h} = -\frac{\kappa}{y_h} \tag{8.359}$$

or

$$\frac{\theta^{C}_{t}}{\theta^{C}_{h}} = \frac{y_h}{y_t} \text{ and } \kappa = -y_t\theta^{C}_{t} = -y_h\theta^{C}_{h}. \tag{8.360}$$

For example, for indices (8.348) of the specific magnetization, these relations provide

$$\beta_t^{\mathrm{C}} = \frac{d - y_h}{y_t} = -\frac{\kappa}{y_t} \text{ and } \beta_h^{\mathrm{C}} = \frac{d - y_h}{y_h} = -\frac{\kappa}{y_h} \text{ or} \tag{8.361}$$

$$\frac{\beta_t^{\mathrm{C}}}{\beta_h^{\mathrm{C}}} = \frac{y_h}{y_t} \text{ and } \kappa = y_h - d. \tag{8.362}$$

So, the specific magnetization transforms as

$$m_0(|h'|,|t'|) = m_0(|h|,|t|)/b^{y_h - d}. \tag{8.363}$$

Problem 8.11.1

Find relations similar to (8.363) for the singular part of the specific Helmholtz energy, specific susceptibility, and specific heat capacity.

Solution: Since all specific quantities $\chi_{specific} \equiv \frac{\chi}{N}$, $f_{singular}^{CE} \equiv \frac{F_{singular}^{CE}}{N}$, and $c_{specific} \equiv \frac{C}{N}$ are intensive parameters, from considerations similar to (8.351–8.363), we obtain

$$f_{singular}^{CE}(|h'|,|t'|) = f_{singular}^{CE}(|h|,|t|)/b^{-d}, \tag{8.364}$$

$$\chi_{specific}(|h'|,|t'|) = \chi_{specific}(|h|,|t|)/b^{2y_h - d}, \tag{8.365}$$

$$c_{specific}(|h'|,|t'|) = c_{specific}(|h|,|t|)/b^{2y_t - d}. \tag{8.366}$$

The last two dependencies are obvious consequences of the first dependence

$$f_{singular}^{CE}(b^{y_h}|h|, b^{y_t}|t|) = f_{singular}^{CE}(|h|,|t|)/b^{-d} \tag{8.367}$$

when we differentiate it twice with respect to the magnetic field or temperature.

If we consider the RG transformation of an arbitrary extensive quantity *A,* we hypothesize the power-law dependence on *b* again:

$$A(|h'|,|t'|) = A(|h|,|t|)/b^{\mathrm{K}}. \tag{8.368}$$

But each extensive quantity is a product of its intensive counterpart and the number of degrees of freedom:

$$A(|h'|,|t'|) = N'a(|h'|,|t'|) \text{ and } A(|h|,|t|) = Na(|h|,|t|), \tag{8.369}$$

where we know that the number of degrees of freedom in a system in transformed as

$$N' = N/b^d. \tag{8.370}$$

Substituting (8.369) and (8.370) into (8.368) and taking into account (8.351), we find

$$\mathrm{K} = \kappa + d. \tag{8.371}$$

For example, utilizing (8.364), for the singular part of the nonspecific Helmholtz energy, we find

$$F^{CE}_{singular}(|h'|,|t'|) = F^{CE}_{singular}(|h|,|t|). \tag{8.372}$$

In other words, the singular part of the Helmholtz energy remains invariant under the RG transformation.

The presence of other field parameters or interaction constants leads to similar formulae. For example, returning to the scaling dependence of the correlation length, we may have

$$\xi(b^{y_h}|h|, b^{y_t}|t|, b^{y_\varphi}|\varphi|, b^{y_\psi}|\psi|) = \xi(|h|,|t|,|\varphi|,|\psi|)/b. \tag{8.373}$$

This assumption, obviously, returns similar relations for the indices, e.g.,

$$\Delta^{\mathrm{C}}_{\varphi\perp\psi} = \frac{y_\varphi}{y_\psi}. \tag{8.374}$$

For example, if we are going to take into account the finite-size effect, we expect to obtain

$$\xi(b^{y_h}|h|, b^{y_t}|t|, b^{y_{1/L}}(1/L)) = \xi(|h|,|t|,(1/L))/b. \tag{8.375}$$

The finite-size effect represents the special case when the value of index $y_{1/L}$ we can foresee from general considerations. Indeed, coarse graining our system, we decrease its linear size b times:

$$L' = L/b. \tag{8.376}$$

This immediately provides

$$(1/L') = b^{y_{1/L}}(1/L) = b(1/L) \tag{8.377}$$

or

$$y_{1/L} = 1. \tag{8.378}$$

Problem 8.11.2

Find relations similar to (8.363) for the correlation function.

Solution: Assuming

$$g(|h'|,|t'|,1/R') = g(|h|,|t|,1/R)/b^{\kappa}, \tag{8.379}$$

in accordance with $R' = R/b$, we find

$$g(b^{ny_h}|h|, b^{ny_t}|t|, b^n/R) = g(|h|,|t|,1/R)/b^{n\kappa}, \tag{8.380}$$

which leads us to scaling

$$g(|h|,|t|,1/R) = R^{\kappa} g\left(\frac{|h|}{(1/R)^{y_h}}, \frac{|t|}{(1/R)^{y_t}}, 1\right). \tag{8.381}$$

Here we expect the scaling parameters to be

$$\frac{|h|}{(1/R)^{y_h}} = \left(\frac{R}{|h|^{-\nu_h^{\mathrm{C}}}}\right)^{y_h} = \left(\frac{R}{\xi}\right)^{1/\nu_h^{\mathrm{C}}}, \tag{8.382}$$

$$\frac{|t|}{(1/R)^{y_t}} = \left(\frac{R}{|t|^{-\nu_t^{\mathrm{C}}}}\right)^{y_t} = \left(\frac{R}{\xi}\right)^{1/\nu_t^{\mathrm{C}}}, \tag{8.383}$$

so we can rewrite scaling (8.381) as

$$g(|h|,|t|,1/R) = R^{\kappa} g\left(\left(\frac{R}{\xi}\right)^{1/\nu_h^{\mathrm{C}}}, \left(\frac{R}{\xi}\right)^{1/\nu_t^{\mathrm{C}}}, 1\right). \tag{8.384}$$

Since for $R << \xi$, we expect to obtain the scaling

$$g \propto \frac{1}{R^{d-2+\eta^{\mathrm{C}}}}, \tag{8.385}$$

which leads us to

$$\kappa = -(d-2+\eta^{\mathrm{C}}). \tag{8.386}$$

Substituting (8.350) into this relation, we obtain

$$\kappa = 2(y_h - d). \tag{8.387}$$

So far for the correlation function, we have considered the single critical index η^{C} which, following the introduced notation, would be better to call η_R^{C}. However, we see that the obtained scaling (8.380):

$$g(b^{ny_h}\,|\,h\,|, b^{ny_t}\,|\,t\,|, b^n / R) = g(|\,h\,|, |\,t\,|, 1/R) / b^{2n(y_h - d)} \tag{8.388}$$

can generate two more scaling dependencies:

$$g(|\,h\,|, |\,t\,|, 1/R) = |\,h\,|^{2(d-y_h)/y_h}\; g\left(1, \frac{|\,t\,|}{|\,h\,|^{y_t/y_h}}, \frac{1/R}{|\,h\,|^{1/y_h}}\right), \tag{8.389}$$

$$g(|\,h\,|, |\,t\,|, 1/R) = |\,t\,|^{2(d-y_h)/y_t}\; g\left(\frac{|\,h\,|}{|\,t\,|^{y_h/y_t}}, 1, \frac{1/R}{|\,t\,|^{1/y_t}}\right), \tag{8.390}$$

which for the critical isotherm and critical isofield curves provide

$$g(|\,h\,|, |\,t\,|, 1/R) = |\,h\,|^{2(d-y_h)/y_h}\; g\left(1, 0, \frac{\xi}{R}\right), \tag{8.391}$$

$$g(|\,h\,|, |\,t\,|, 1/R) = |\,t\,|^{2(d-y_h)/y_t}\; g\left(0, 1, \frac{\xi}{R}\right), \tag{8.392}$$

respectively. This allows us to introduce two more critical indices in the limit $R >> \xi$:

$$g(|\,h\,|, |\,t\,|, 1/R) \propto |\,h\,|^{\eta_h^{\mathrm{C}}} \text{ with } \eta_h^{\mathrm{C}} = 2(d - y_h)/y_h = 2\beta_h^{\mathrm{C}} \tag{8.393}$$

and

$$g(|\,h\,|, |\,t\,|, 1/R) \propto |\,t\,|^{\eta_t^{\mathrm{C}}} \text{ with } \eta_t^{\mathrm{C}} = 2(d - y_h)/y_t = 2\beta_t^{\mathrm{C}}, \tag{8.394}$$

where we explicitly demonstrate only proportionalities of the field parameters of the system. Besides these power-law dependencies, the asymptotes of the scaling function, of course, contain also the dependence exponentially decaying with the increase of R. Both critical indices (8.393 and 8.394) are obvious if we recall the connection between the correlation function and magnetization.

Let us now answer the question why only the relevant eigenvalues influence the scaling of the system while the irrelevant eigenvalues do not participate in the scaling. We assume that in scaling

$$\xi(b^{y_h}\,|\,h\,|, b^{y_t}\,|\,t\,|, b^{y_\varphi}\,|\,\varphi\,|) = \xi(|\,h\,|, |\,t\,|, |\,\varphi\,|)/b \tag{8.395}$$

parameters h and t are relevant as always while an amplitude φ is irrelevant. Substituting (8.339), we generate the scaling on temperature:

$$\xi(|h|,|t|,|\varphi|)=\frac{1}{|t|^{1/y_t}}\xi\left(\frac{|h|}{|t|^{y_h/y_t}},1,\frac{|\varphi|}{|t|^{y_\varphi/y_t}}\right). \tag{8.396}$$

This scaling dependence demonstrates the principal difference between relevant and irrelevant variables. The field parameter h has the eigenvalue whose absolute value is higher than unity: $|\lambda_h|>1$. In accordance with (8.334), this requires that the corresponding index y_h must be positive: $y_h>0$. The corresponding scaling parameter $|y|\equiv\frac{|h|}{|t|^{y_h/y_t}}$ is the ratio of two small quantities and, therefore, can take values from zero, $|y|<<1$, to infinity, $|y|>>1$. These two asymptotes generate two asymptotes of the scaling function, representing diversity of the crossover phenomena we have discussed above.

On the contrary, if the amplitude φ is irrelevant, the absolute value of the corresponding eigenvalue is less than unity, $|\lambda_\varphi|<1$, which, in turn, provides $y_\varphi<0$. In this case, the scaling parameter $z\equiv\frac{|\varphi|}{|t|^{y_\varphi/y_t}}=|\varphi||t|^{|y_\varphi|/y_t}$ is the product of two small quantities and, therefore, is always small by itself, $|z|<<1$. Thereby the scaling parameter z does not participate in the scaling because generally the scaling function does not depend on small parameters.

The exception is the case of the irrelevant amplitude φ when the scaling function does depend on the small scaling parameter z as a power law:

$$\xi(y,1,z)\propto z^\kappa\xi(y,1)\text{ for }|z|<<1. \tag{8.397}$$

Such irrelevant coupling constants are called *dangerous coupling constants*. We have seen an example of the irrelevant dangerous parameter in Problem 8.1.1.

Substituting (8.397) into (8.396), we find

$$\xi(|h|,|t|,|\varphi|)=\frac{1}{|t|^{1/y_t}}(|\varphi||t|^{|y_\varphi|/y_t})^\kappa\xi\left(\frac{|h|}{|t|^{y_h/y_t}},1\right). \tag{8.398}$$

So, the irrelevant dangerous amplitude φ always influences the scaling.

Finally, we should discuss the question about the presence of additional characteristic length (besides the correlation length) in a system in the vicinity of its critical point. To begin the discussion, we should return to the definition of the term "*anomalous dimension.*"

So far, we have discussed two approaches to find the critical indices of a system: The mean-field approach and the RG transformation. It could be demonstrated that the mean-field values of the critical indices can be found just from the dimensional analysis when a single characteristic length in a system is the correlation length.

This hypothesis claims that when a system tends to its critical point, the correlation length diverges, and thereby the fractality occupies all scales, from the lattice constant to the size of the system, forming a "*fluctuation foam*." Fluctuations, occupying all possible scales, begin to dictate the behavior of the system.

But the stochastic behavior of fluctuations is generally universal for an arbitrary system regardless of the nature of this system: thermal, complex, biological, geological, informational, social, etc. The fluctuations suppress the microscopic nature of a system and dictate their own probabilistic tendencies. Therefore, there is no surprise in the fact that in the vicinity of a critical point, the specific for a particular system behavior is substituted by universal power-law dependencies.

This discussion would be perfectly sound if the critical indices were indeed determined by their mean-field values. However, this is not always so. The studies, either experimental, or numerical, or exact, demonstrate that the real critical indices are often very different from the mean-field suggestions. Besides, if we decided to find the nature of these indices with the aid of the dimensional analysis, it happens that the value of an index splits into two parts: the mean-field value and some "addition" called *the anomalous dimension*. While the presence of the mean-field part is explained by the correlation length, the anomalous part has to be determined by the presence of some additional characteristic length besides the correlation length.

This leads to the belief that something of the microscopic properties of the finest scale survives the fluctuations occupying this and larger scales. Some studies suggest that this may be the lattice constant as the representative of the finest scale.

However, we do not share this belief. As we have seen, the process of coarse graining erases all memory in a system about what was the lattice constant of the very initial system. To illustrate this, we may refer to the example of fractals. Let us return to Chap. 1. Comparing parts (a) and (d) of figure given in Problem 1.2.1 of Chap. 1, we see that the dimensionality of the initial branch does not affect the dimension of the developed fractal set. Even more so, nothing of the initial branch survives the process of coarse graining.

But what then determines the fractal dimension? The number of branches K and the scale factor r. In other words, the properties of the generator. We see similar situation in scaling generated by the RG transformation: In accordance with (8.334), the critical index y_i is determined by b as the size of the cell of the RG transformation and by the eigenvalue λ_i of this transformation. Both are the properties of the "RG generator." Therefore, we believe that the additional characteristic length responsible for the appearance of the anomalous dimensions appears not from the properties of the initial system but is determined by the laws of scale invariance.

8.12* Magnetic Systems: Spinodal Scaling

In previous sections, we paid attention mostly to critical phenomena for two reasons. First, initially the scaling was investigated for the proximity of the critical point. Second, the most of studies are devoted to critical phenomena which allow us to present a set of illustrative examples.

However, as we saw in Chap. 6, the correlation length diverges in the vicinity of the spinodal point as well, thereby, providing that the same scales are occupied again by fractal scale invariance. This guarantees that many concepts of critical scaling considered above are applicable to spinodal phenomena as well.

Let us return to the equation of state (8.121):

$$h = 2at^{\gamma_t^{\mathrm{C}}} m_0 + \left(\frac{1}{\beta_h^{\mathrm{C}}} + 1\right) b m_0^{1/\beta_h^{\mathrm{C}}} + \ldots \tag{8.399}$$

To find the spinodal curve, we should investigate when the derivative $\left(\frac{\partial m_0}{\partial h}\right)_t$ is infinite. Differentiating (8.399) and utilizing (8.128) and (8.129), we find:

$$m_{\mathrm{S}} = -\left\{\frac{2a}{\frac{1}{\beta_h^{\mathrm{C}}}\left(\frac{1}{\beta_h^{\mathrm{C}}} + 1\right) b}\right\}^{\frac{\beta_t^{\mathrm{C}}}{\gamma_t^{\mathrm{C}}}} (-t_{\mathrm{S}})^{\beta_t^{\mathrm{C}}} \quad \text{and} \tag{8.400}$$

$$h_{\mathrm{S}} = \frac{1}{\beta_h^{\mathrm{C}}}\left(\frac{1}{\beta_h^{\mathrm{C}}} + 1\right) \gamma_h^{\mathrm{C}} b \left(\frac{2a}{\frac{1}{\beta_h^{\mathrm{C}}}\left(\frac{1}{\beta_h^{\mathrm{C}}} + 1\right) b}\right)^{\frac{1}{\gamma_h^{\mathrm{C}}}} (-t_{\mathrm{S}})^{\frac{\gamma_t^{\mathrm{C}}}{\gamma_h^{\mathrm{C}}}} \tag{8.401}$$

Then, expanding the equation of state (8.399) in the vicinity of the spinodal point, we obtain:

$$\frac{(m_0 - m_{\mathrm{S}})^2}{(-m_{\mathrm{S}})^2} = 2\beta_h^{\mathrm{C}} \frac{-(h - h_{\mathrm{S}})}{h_{\mathrm{S}}} + 2\beta_t^{\mathrm{C}} \frac{-(t - t_{\mathrm{S}})}{(-t_{\mathrm{S}})} + \ldots \tag{8.402}$$

We see that even in the most general case of the equation of state presented by (8.399), the expansion still provides the mean-field values of the spinodal indices: $\beta_t^{\mathrm{S}} = 1/2$ and $\beta_h^{\mathrm{S}} = 1/2$.

Equation (8.402) represents the scaling function of the magnetization:

$$| m_0 - m_{\mathrm{S}} | = | t - t_{\mathrm{S}} |^{\beta_t^{\mathrm{S}}} \sqrt{\frac{2\beta_t^{\mathrm{C}}(-m_{\mathrm{S}})^2}{(-t_{\mathrm{S}})} + \frac{2\beta_h^{\mathrm{C}}(-m_{\mathrm{S}})^2}{h_{\mathrm{S}}} \frac{| h - h_{\mathrm{S}} |}{| t - t_{\mathrm{S}} |^{\Delta_{h \leftrightarrow t}^{\mathrm{S}}}} + \ldots}, \tag{8.403}$$

where $\Delta_{h \leftrightarrow t}^{\mathrm{S}} = 1$.

Differentiating (8.402), we find that the susceptibility,

$$\chi = \beta_h^{\mathrm{C}} \frac{(-m_{\mathrm{S}})^2}{h_{\mathrm{S}}} \frac{1}{-(m_0 - m_{\mathrm{S}})} + \ldots, \tag{8.404}$$

is inversely proportional to the deviation of magnetization from its spinodal value, which provides the following spinodal indices: $\gamma_t^{\mathrm{S}} = \beta_t^{\mathrm{S}} = 1/2$ and $\gamma_h^{\mathrm{S}} = \beta_h^{\mathrm{S}} = 1/2$.

In general case, the RG transformation can be applied in the vicinity of the spinodal point as well as in the vicinity of the critical point. Therefore, the RG will generate the relations among the spinodal indices, similar to (8.345):

$$\frac{\alpha_t^{\mathrm{S}}}{\alpha_h^{\mathrm{S}}} = \frac{\beta_t^{\mathrm{S}}}{\beta_h^{\mathrm{S}}} = \frac{\gamma_t^{\mathrm{S}}}{\gamma_h^{\mathrm{S}}} = \frac{\nu_t^{\mathrm{S}}}{\nu_h^{\mathrm{S}}} = \Delta_{h\text{–}t}^{\mathrm{S}} = \frac{y_h^{\mathrm{S}}}{y_t^{\mathrm{S}}} \tag{8.405}$$

Besides, many other relations, valid for the critical indices, can be proved for the spinodal indices as well (as we, for example, saw in Chap. 6). The reason is again that the divergence of the correlation length, followed by the fractal scale invariance, provides the similarity between critical and spinodal phenomena.

References

Abaimov, S.G.: Statistical Physics of Complex Systems (in Russian), 2nd edn. Synergetics: From Past to Future, vol. **57**. URSS, Moscow (2013)

Balescu, R.: Equilibrium and Nonequilibrium Statistical Mechanics. Wiley, New York (1975)

Brankov, J.G.: Introduction to Finite-Size Scaling. Leuven Notes in Mathematical and Theoretical Physics. Series A: Mathematical Physics, vol. **8**. Leuven University Press, Leuven (1996)

Cardy, J.: Scaling and Renormalization in Statistical Physics. Cambridge University Press, Cambridge (1996)

Domb, C., Green, M.S., Domb, C., Lebowitz, J.L. (eds.): Phase Transitions and Critical Phenomena. Academic, London (1972–2001)

Domb, C., Hunter, D.L.: On the critical behavior of ferromagnets. Proc. Phys. Soc. **86**(5), 1147 (1965)

Essam, J.W.: Percolation theory. Rep. Prog. Phys. **43**(7), 833–912 (1980)

Essam, J.W., Fisher, M.E.: Padé approximant studies of the lattice gas and Ising ferromagnet below the critical point. Chem. Phys. **38**(4), 802 (1963)

Fisher, M.E.: Rigorous inequalities for critical-point correlation exponents. Phys. Rev. **180**(2), 594 (1969)

Goldenfeld, N.: Lectures on Phase Transitions and the Renormalization Group. Perseus, Reading (1992)

Griffiths, R.B.: Ferromagnets and simple fluids near the critical point: Some thermodynamic inequalitites. Chem. Phys. **43**(6), 1958 (1965)

Griffiths, R.B.: Rigorous results and theorems. In: Domb, C., Green, M.S. (eds.) Exact Results. Phase Transitions and Critical Phenomena, vol. **1**, pp. 7–109. Academic, London (1972)

Grimmett, G.R.: Percolation, 2nd edn. Grundlehren der Mathematischen Wissenschaften, vol. 321. Springer, Berlin (1999)

Huang, K.: Statistical Mechanics, 2nd edn. Wiley, New York (1987)

Josephson, B.D.: Inequality for the specific heat: I. Derivation. Proc. Phys. Soc. **92**(2), 269 (1967a)

Josephson, B.D.: Inequality for the specific heat: II. Application to critical phenomena. Proc. Phys. Soc. **92**(2), 276 (1967b)
Kadanoff, L.P.: Spin-spin correlation in the two-dimensional Ising model. Nuovo Cim. **44,** 276 (1966)
Landau, L.D., Lifshitz, E.M.: Statistical Physics, Part 1, 3rd edn. Course of Theoretical Physics, vol. **5**. Pergamon, Oxford (1980)
Ma, S.K.: Modern Theory of Critical Phenomena. Benjamin, Reading (1976)
Patashinskii, A.Z., Pokrovskii, V.L.: Behavior of ordered systems near the transition point. Soviet JETP. **23**(2), 292 (1966)
Pathria, R.K.: Statistical Mechanics, 2nd edn. Butterworth-Heinemann, Oxford (1996)
Rushbrooke, G.S.: On the thermodynamics of the critical region for the Ising problem. Chem. Phys. **39**(3), 842 (1963)
Stanley, H.E.: Introduction to Phase Transitions and Critical Phenomena. Clarendon, Oxford (1971)
Stauffer, D., Aharony, A.: Introduction to Percolation Theory, 2nd edn. Taylor & Francis, London (1994)
Widom, B.: Equation of state in the neighborhood of the critical point. Chem. Phys. **43**(11), 3898 (1965a)
Widom, B.: Surface tension and molecular correlations near the critical point. Chem. Phys. **43**(11), 3892 (1965b)

Index

S. G. Abaimov, *Statistical Physics of Non-Thermal Phase Transitions,*
Springer Series in Synergetics, DOI 10.1007/978-3-319-12469-8